

Studies on Nazarov/ene tandem cyclizations and their application in the total synthesis of (-)-illisimonin A

Von der Naturwissenschaftlichen Fakultät der
Gottfried Wilhelm Leibniz Universität Hannover

zur Erlangung des Grades

Doktorin der Naturwissenschaften (Dr. rer. nat)

genehmigte Dissertation

von

Giada Tedesco, Laurea Magistrale in Chimica (Dott.ssa Mag.)

Università degli Studi dell' Insubria

2023

Referent: Prof. Dr. rer. nat. Markus Kalesse

Korreferent: Prof. Dr. rer. nat. Philipp Heretsch

Korreferent: Prof. Dr. Karl Gademann

Tag der Promotion: 02.06.2023

The experimental and theoretical work reported in this thesis was developed from December 2019 to December 2022 under the supervision of Prof. Dr. rer. nat. Markus Kalesse at the Institute of Organic Chemistry from the Gottfried Wilhelm Leibniz University in Hannover.



Abstract

Keywords:

Nazarov/ene, (-)-illisimonin A, Ti(III)-mediated reductive cyclization, semipinacol rearrangement, White-Chen C–H activation

In the first part of this thesis, the mechanistic insights behind the key step of this total synthesis, the diastereoselective Nazarov/ene tandem cyclization, are unravelled. First, the introduction of an additional methylene in the side chain served the purpose of understanding the connection between the flexibility of the side chain and the feasibility of the desired cyclization. Second, the cyclization in presence of a (*Z*)-substituent at the terminal olefin afforded only products whose double bond occupied the position of the former (*E*)-methyl group, suggesting selective migration of a hydrogen atom from the (*E*)-position. Third, the synthesis of a perdeuterated precursor, bearing a CD₃-substituent in lieu of the (*E*)-methyl group, confirmed the aforementioned migration hypothesis. Finally, crossover experiments outruled the existence of an intermolecular proton/deuterium transfer, confirming a concerted, intramolecular ene-like mechanism.

In the second part, the acquired chemical background for the stereoselective construction of spirocompounds *via* Nazarov/ene cyclizations was transferred to the total synthesis of (-)-illisimonin A, a caged sesquiterpenoid isolated by Ma et al. from the fruits of *Illicium simonsii*, commonly known as star anise. The construction of its unprecedented tricyclo[5.2.1.0^{1,6}]decane skeleton was attempted with an early-stage functionalization strategy and a late-stage parallel approach, in which C-11 functionalization followed one-carbon homologation. While the early-stage plan stranded at an advanced intermediate, the functionalization of the previously homologated spirocycle proved to be successful. A Ti(III)-mediated reductive cyclization of an epoxy-enone, a type III semipinacol rearrangement and a selective deprotection successfully led to a formal synthetic intermediate.

In the third and final act, an enantioenriched cross-conjugated precursor for the key Nazarov/ene cyclization diastereoselectively built the desired stereotriad in the aforementioned spirocompound. In turn, this spiroketone followed the steps of its racemic congener, fruitfully reproducing the optimized synthesis until a second, more advanced, formal intermediate. A carboxylic acid-mediated White-Chen C–H activation gave access to (-)-illisimonin A and concluded this thesis.

Acknowledgements:

Everyone knows how this path has had a different taste for me, and how living so far away from home was always my biggest challenge in my Phd. For this reason, I hereby would like to thank anyone that I encountered on my way that made my steps less harder to make.

First of all, I would like to thank Prof. Kalesse for accepting me in his research group, always making me feel welcome, and always worrying about my well-being. Thank you for accepting my desire to go home, and for always being understandable. Thank you for sharing our success as well as our failure.

I would also like to thank Prof. Heretsch and Prof. Caro for kindly accepting to be my referees, even on such a short notice. Thank you Prof. Heretsch for bringing more nice people into my daily life.

I also would like to thank Linda and Frau Roloff for always being so nice and helpful to me; nice and helpful are also adjectives that perfectly fit the NMR and mass department, for helping with any request I might have had.

And now, as always in this group, I would like to spend a couple of words on each of you, going from lab to lab:

Alex, you were my first friend and I will never forget how I survived the lockdown because of you. Thank you for the trips to IKEA, the nice bike rides, the snowmen and your gym tonics.

Maike, I am just sorry we really tore down our barriers in the very last period. Thanks for our „calm“ breaks, for every wine glass, and for always being there for a nice and deep talk. Thank you for taking care about my introduction of course ;) and thanks for all of the things we found out we have in common.

Simon, thanks for always passing by and greeting me in my own language. You don't know how much familiar sounds were meaning to me.

Morwenna, no words will ever be enough. You were my rock, my sponge, my panda, and so many other things. I will cherish any gym day with you, every weekend, every trip to the panda store, and why not, even every tear. You always were there for me, and even made a huggy person out of me. Thank you so much for being my friend, and because I know we are not gonna lose this. <3

You've arrived at a turning point of my PhD Max, but thank you for always trying to see, and make me see, the bright side of things.

Thank you Cristina for taking care of my gym buddy, and for looking at us suffer with our weights, until you finally joined.

And here comes the most difficult part: my labmates...Daniel, you can't even imagine how much I have learned from you. You made me change my way of seeing myself and my career, you made me a better chemist, and a better cakes eater. Thank you for all of our Skype calls, thank you for always being there for my success and failures, even if you were miles away. Thank you for dancing like a fridge in the lab, thank you for all of the Taylor Swift songs, but also for Mr. Brightside and the Owl city. I look forward to see you again.

Andrea...you imposed your happiness and great mood to me even if I did not want to. You were from the very beginning and still are such a constant presence in my life that I really don't know anymore how I would feel without you. Thank you for running after a violinist (it's a viola!) for me, thanks for always supporting me and making me realize that maybe I am not as stupid as I think to be. You are

basically my private cheerleader and probably one of the best people I have ever known. Thank you for just being the way you are, in spite of me killing your enthusiasm.

Axel, my puppy. You just can't imagine how much I love you. You were my mood booster, my huggy person, my music buddy, my food partner, my labmate. There would be so many things to say that my thesis would not be long enough. Thanks for making me part of your world, for all of the weekends with Tasya, and for being such a good friend. Thank you for being upset at us when we were arguing in the lab.

And of course I am talking about you, Anton. You hit my nerves so much and so many times that I really don't know how we made it. Though, you know you are one of the people I'll miss the most. Thank you for every dinner, every trip to the lake, every sunbath. Thank you for spending nine hours in the sun with me and for (almost) never complaining. Thank you for taking care of me, and for always trying to understand what was wrong with me. Thank you for sometimes leaving me on my own, until I was not upset anymore, and for all of the things that we've already told each other.

Thanks Yannick for all of the things we went through. Thank you for holding me up with minions and food when I was down. Thank you for your Lillet, thank you for all of the late evenings in the lab. Thank you for being so similar to me, for understanding my point of view and for being my motivational coach so many times that I can't even count. Thank you for all the chocolate, the candies and messages on my desk, and for staying even when I was basically shouting at you. Of course, thank you for all of the advice, and for helping me through this writing period.

Thanks Alina for our tandems and for the evenings we spent chatting until your phone turned to sleeping mode. Thank you for being there on one of the most important moments for me, it meant a lot.

Kjeld, the basement will have for ever a memory of us. Thank you for One Hundred and One Dalmatians, and for driving your bike to Mc Donalds in the middle of the night. Thank you for always being so nice to me, in spite of everything.

Christoph. If being away from home was my biggest challenge, you were probably the second. It was so hard to face someone like you. You are so brilliant in everything you do, so enthusiastic and working so hard that any effort I was making seemed nothing to me. I don't know how we made it honestly, but I am so glad we did it together. Thank you for all of the 4-hands reactions, for every stupid toy we got from Woolworth, and for being always in for any proposal. Thank you for everything, and for the best memory book I could ask for.

Thank you Marius for our walks in the park, and because I now eat maracuja because of you. And thank you for Nala. Of course, she was the best part of it ;).

Anna, you are also part of my days. You brought out a shade of me that was buried away. I've loved our time together, and know you're gonna be there tomorrow too. You understand me like you'd known me for years, and are probably one of the few people I could ever live with. And since you know me, you also know how much these words mean for me.

Björn, I will always remember your permanent smile, your good heart, the Opera evenings, and of course our volleyball matches.

Kathy and Dennis, you were one of my latest discoveries, but such a big surprise. I am glad we can keep seeing each other. I enjoyed our weekend in Cologne, every glass of wine, any song from you, Kathy. Dennis, I am glad we got closer at the end. I will always thank Andrea for this. Our evening in Brechts will always be one my best moments in Hannover.

Sinan and Mischa, I did not spend that much time with you, but thanks for being part of my adventure. Mischa, thank you for our nice chats when filling the nitrogen, and for your helpfulness.

From the old members, I would really like to thank Silvia for any series, any movie, any book we are still sharing, and for welcoming me in Hannover.

I would like to thank my friends for staying, even when they were seeing me every six months, or when I did not find the time to text. Thanks Davide for being my best friend, for our Sunday calls, and for any single moment you were there for me. Thank you for sharing this last 8 years with me, and for never stepping back. Francesca, you were there every second of my days, and in every up and down. I am so happy to have you in my life. Silvia, Elena and Francesca, you are my certainties. Time passes, but you never do. Marco, Federico, Laura, Roberta, and Gioele, I am so glad I did not lose you. Robi, our 5-hours calls were always the best.

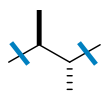
And now, my family. No one could ever understand how much I did miss you. Mum, you are my everything, my rock and my strength. I would have never made it without you. Dad, we are so much alike...You are the one person that gets me the most, and also probably the one person I fight with the most. Thank you for always supporting me. I have kept a picture of us, Bi and Michi, on my night table for three years. You are always gonna be my babies. Thank you for never leaving me alone. Franci and Debora...I know I am on my own in most cases, but I do love you so much. And Alberto is one of the best things in my life. Thank you for understanding me, always. Anny and Guido, you are part of my family too. Thank you for welcoming back home so nicely every time.

Matteo. I would have never made it without you. Thank you for every flight, every call, every text, and every way you kept us alive. Thank you for trying to understand my choice, thank you for making of my battles your battles. Thank you for never giving up on me. Thank you for staying. Thank you for getting us a home, even though my home was always where you were. Thank you because every step I have made in this last years, I owe it to you. You are, truly, the love of my life. I can't wait to be your wife. Perché ho la mano ferma solo se la tieni tu.

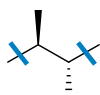
General comments

The structures numbering in this thesis follows an arbitrary choice and does not refer to the official IUPAC-nomenclature.

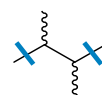
Concerning the stereoconfiguration of the described compounds, the relative and absolute stereoconfiguration are graphically distinguished: bold or hashed bonds represent relative configurations, while solid and hashed wedged bonds indicate the absolute configuration. Unspecified – or unknown – configurations are indicated with wavy bonds. In the case of stereoisomeric mixtures, the configuration of the main stereoisomer is shown if the ratio between the major and the minor stereoisomer is higher than 2:1. Otherwise, the wavy line is used again. This is applied to both enantio- and diastereoisomeric mixtures.



Relative configuration



Absolute configuration



Unspecified configuration

This thesis is organized in three parts, which have been edited following as much as possible a chronological order. However, crossovers among the parts and/or choices made based on the parallel outcome of another experiment were unavoidable. For this reason, the author will give a background – a sort of state of the art – when necessary at the beginning of the sections, or will integrate the work of others to clarify the reasons behind certain synthetic choices. If so, the results and discussion part will follow.

List of abbreviations

Acac	Acetylacetonate
AIBN	Azobisisobutyronitrile
BBN	9-borabicyclo(3.3.1)nonane
BHT	Dibutylhydroxytoluene
BINAP	(2,2'-bis(diphenylphosphino)-1,1'-binaphthyl)
BOM	Benzyloxymethyl-
bp	Boiling point
brsm	Based on recovered starting material
BTTP	(<i>tert</i> -butylimino)tris(pyrrolidino)phosphorane
CAN	Cerium Ammonium Nitrate
Cap	Caprolactamate
cat.	catalytic
CDI	1,1'-carbonyldiimidazole
CoA	Coenzyme A
Cp	Cyclopentadienyl
CSA	Camphorsulfonic acid
<i>m</i> CPBA	<i>meta</i> -chloroperbenzoic acid
CPME	Cyclopentyl methyl ether
Cy	Cyclohexyl-
DBU	1,8-diazabicyclo[5.4.0]undec-7-ene
DCC	<i>N,N'</i> -dicyclohexylcarbodiimide
DCE	Dichloroethane
DET	Diethyltartrate
DFT	Density Functional Theory
DG	Directing Group
DIB	3-amino-(dimethylproylamine)
<i>i</i> BAL-H	Diisobutylaluminium hydride
<i>i</i> PA	<i>N,N</i> -diisopropylamine
<i>i</i> PEA	<i>N,N</i> -diisopropylethylamine
D.I.T.	Digital integration time

4-DMAP	4-dimethylaminopyridine
DMDO	Dimethyldioxirane
DMF	<i>N,N</i> -dimethylformamide
2,2-DMP	2,2-dimethoxypropane
3,5-DMP	3,5-dimethylpyrazole
DMP	Dess–Martin periodinane
DMSO	Dimethylsulfoxide
dppe	1,2-bis(diphenylphosphino)ethane
dppp	1,3-bis(diphenylphosphino)propane
DTBS	Di- <i>tert</i> -butylsilyl-
EC ₅₀	half maximal effective concentration
EDC	1-ethyl-3-(3-dimethylaminopropyl)carbodiimide
equiv.	Equivalents
esp	$\alpha,\alpha,\alpha',\alpha'$ -tetramethyl-1,3-benzenedipropanoic acid
HAT	Hydrogen atom transfer
HFIP	Hexafluoroisopropanol
HMPA	Hexamethylphosphoramide
IBX	Iodoxybenzoic acid
IMes	1,3-bis(2,4,6-trimethylphenyl)-1,3-dihydro-2H-imidazol-2-ylidene
KHMDS	Potassium bis(trimethylsilyl)amide
LA	Lewis Acid
LDA	Lithium diisopropylamide
LiDBB	Lithium 4,4'-di- <i>tert</i> -butylbiphenylide
LiHMDS	Lithium bis(trimethylsilyl)amide
M	Generic metal
MEM	2-methoxyethoxymethyl ether
min	minutes
MNBA	2-methyl-6-nitrobenzoic anhydride
MOM	Methoxymethyl-
MoOPH	Oxidoperoxymolybdenum(pyridine)-(hexamethylphosphoric triamide)
mp	Melting point

MS	Molecular sieves
MTBE	Methyl <i>tert</i> -butyl ether
MVK	Methyl vinyl ketone
NaHMDS	Sodium bis(trimethylsilyl)amide
NBS	<i>N</i> -bromosuccinimide
NCS	<i>N</i> -chlorosuccinimide
NHPI	<i>N</i> -hydroxyphthalimide
NIS	<i>N</i> -iodosuccinimide
NMM	<i>N</i> -methyldmorpholine
NMO	<i>N</i> -methyldmorpholine <i>N</i> -oxide
NMP	<i>N</i> -methyl-2-pyrrolidone
o.n.	overnight
ons	over <i>n</i> steps
PCC	Pyridinium chlorochromate
PDC	Pyridinium dichromate
PDP	[[2-[1-(pyridin-2-ylmethyl)pyrrolidin-2-yl]pyrrolidin-1-yl]methyl]pyridine
PE	Petroleum ether
Phth	Phthaloyl-
PIDA	(Diacetoxyiodo)benzene
pin	pinacol
PMB	<i>p</i> -methoxybenzyl-
PMP	<i>p</i> -methoxyphenyl
PP	pyrophosphate
Ppm	parts per million
PPTS	Pyridinium <i>p</i> -toluenesulfonate
py	Pyridine
R _f	Retention factor
rfx	Reflux
r.t.	Room temperature
SET	Single electron transfer
TBAB	Tetra- <i>n</i> -butylammonium bromide

TBACl	Tetra- <i>n</i> -butylammonium chloride
TBAF	Tetra- <i>n</i> -butylammonium fluoride
TBAI	Tetra- <i>n</i> -butylammonium iodide
TBDPS	<i>tert</i> -butyl-diphenylsilyl-
TBHP	<i>tert</i> -butyl hydroperoxide
TBS	<i>tert</i> -butyl-dimethylsilyl-
TEMPO	2,2,6,6-Tetramethylpiperidin-1-yl)oxyl
TES	Triethylsilyl-
TFA	Trifluoroacetic acid
TFDO	Methyl(trifluoromethyl)dioxirane
TFT	Trifluorotoluene
THF	Tetrahydrofuran
TLC	Thin layer chromatography
TM	Transition metal
TMEDA	<i>N,N,N',N'</i> -tetramethylethylenediamine
TMP	2,2,6,6-tetramethylpiperidine
TMS	Trimethylsilyl-
TosMIC	Toluenesulfonylmethyl isocyanide
TPAP	Tetrapropylammonium perruthenate
TPPB	Tris(pentafluorophenyl)borane
TTMSS	Tris(trimethylsilyl)silane
Δ	Reflux
μW	Microwave

Index

Abstract	ii
Acknowledgements:	iii
General comments	vi
List of abbreviations	vii
Index	xi
Introduction	1
Natural products	1
Terpenoids in total synthesis – state of the art	7
Challenges in total synthesis	34
Illisimonin A	56
Aim of this work and retrosynthetic considerations	60
PART 1: Studies on the Nazarov/ene cyclization	61
(Retro)synthetic background	61
The elongated precursor	63
The functionalized precursor	70
Mechanistic studies: the deuterated precursor	74
PART 2: Studies towards the total synthesis of illisimonin A	79
Alternative approach: early stage functionalization	79
Original approach: late stage functionalization	90
PART 3: The asymmetric total synthesis of (–)-illisimonin A	101
Synthesis of an enantioenriched precursor	101
Conclusions and outlook	111
Experimental section	113
General information	113
Experimental procedures	115
CD spectrum of (–)-illisimonin A	214
Deuteration studies – mass spectra	216
X-ray data	217
References	222
NMR Spectra	232
Curriculum Vitae	454
Scientific Contributions	455

Introduction

Natural products

In the common language the word “natural” has nowadays a positive meaning, opposed to “chemical”, mostly meant as “artificial” or sometimes even “dangerous”. In this sense, people are attracted to products advertised as natural, connecting this term to an old belief according to which everything that is natural is good for our health. This perception is far away from the chemical perspective, in which the term “Natural Product” (NP) refers to molecules produced by any sort of living organism. In this context, the definition possesses a neutral value, and represents a mere description of an objective fact - a scientific observation. But why does this neutral concept still have such a huge impact on today’s research?

As scientists we like numbers: a recent review from Newman and Cragg,¹ part of a long tradition of publications started in 1997, provides an extended overview on newly approved drugs in the last 40 years. In the bar graph in Fig. 1 the almost constant impact of natural products or derivatives of such products on the medicinal field is shown.

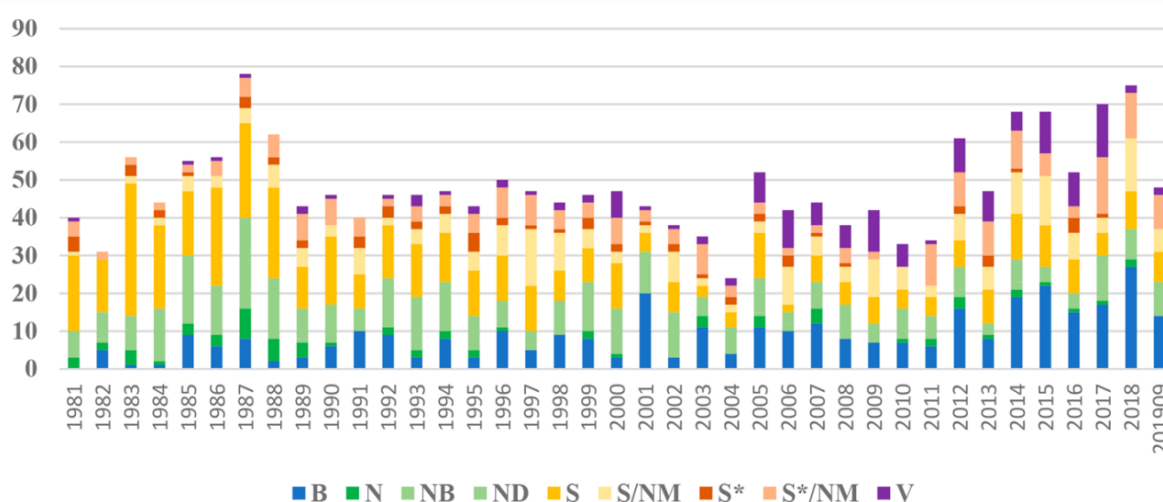


Fig. 1 – Newly approved drugs for the years 1981 – 2019 sorted by source. B = biological macromolecule; N = unaltered natural product; NB = botanical drug (defined mixture); ND = natural product derivative; S = synthetic drug; S* = synthetic drug (NP pharmacophore); /NM = mimic of natural product; V = vaccine. Bar graph from Newman and Cragg.¹

In other words, the wide range of compounds provided by nature is still charming enough from a variety and activity point of view, that the role of natural products in drug discovery survived both the rise of high-throughput screening (HTS) in the mid-80s and the modern combinatorial chemistry era.² One could wonder where this success comes from. First, the variety of sources: NPs, as mentioned, can be produced – and extracted – by any source of living organism. This includes plants, animals, bacteria and fungi. From an historical point of view, plants were the very first exploited for the curative properties of their extracts: earliest traces date back to Mesopotamia (2600 b.C.) and refer to the oils from *Cupressus sempervirens* for the treatment of coughs, cold and inflammation symptoms.³ And here comes into play the second valuable characteristic of NPs: activity. This is commonly found in secondary metabolites, which are produced by any organism to interact with the external environment. While primary metabolites are essential for the proper functioning of the organism itself, secondary metabolites include compounds to defend the organism against predators and pathogens, pigments to attract or discourage other species, hormones or signal molecules. This second

characteristic pre-validates secondary metabolites (*i.e.* NPs) as capable of targeting enzymes or proteins similar to others that they have already met or, in other words, is almost a warranty of activity.⁴

Natural products from plants

Natural products are generally categorized into 4 groups - alkaloids, phenylpropanoids, polyketides, and terpenoids – depending on their biosynthetic origin. Members of all of these classes have been found in plants which, as mentioned, were historically the first organisms recognized and used as sources of natural products. Fig. 2 reports examples of secondary metabolites, as well as their classification and biosynthetic precursor.⁵

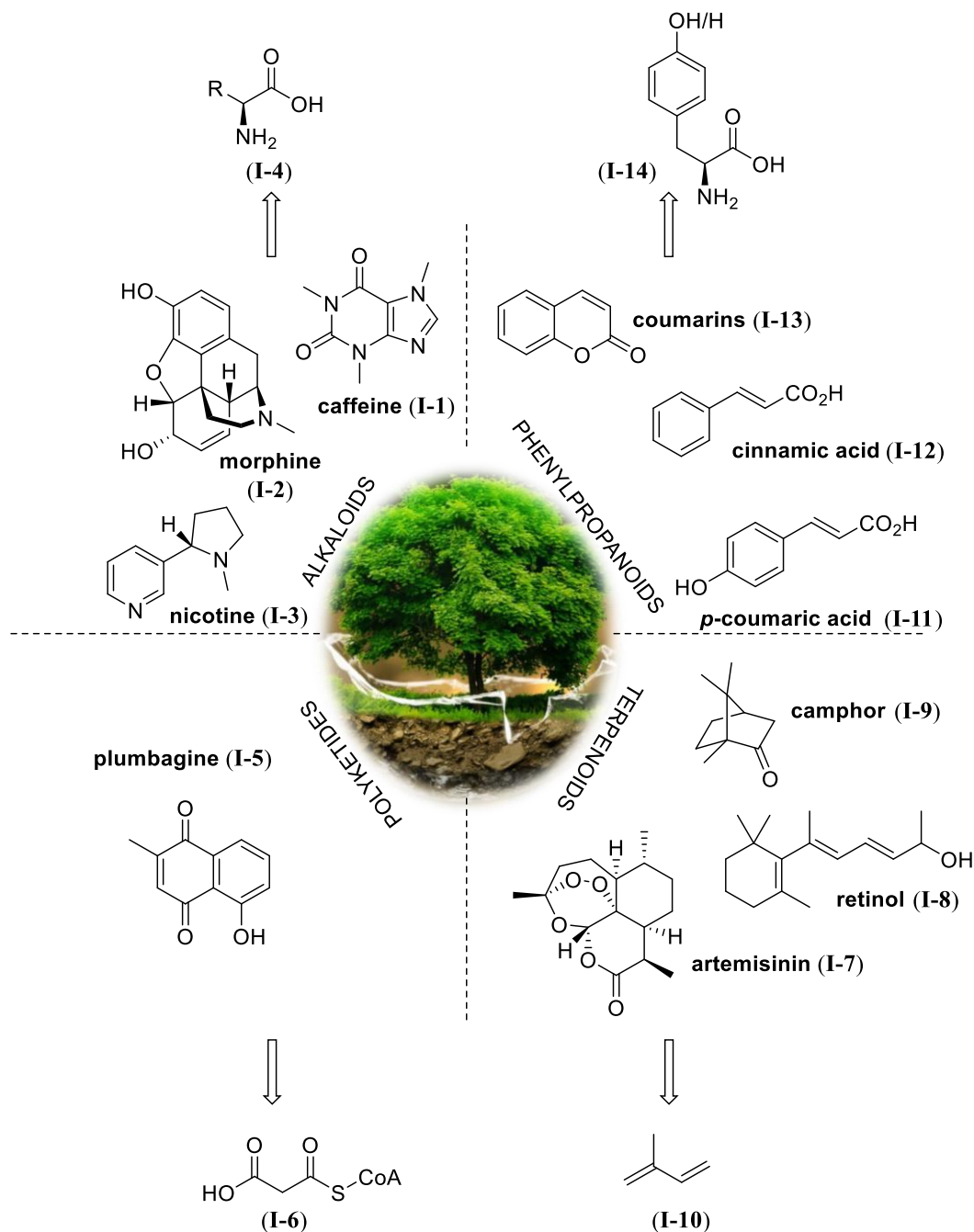


Fig. 2 – Examples of natural products from plants and their categorization.

Alkaloids are generally referred to as nitrogen-containing compounds which were described as

'more or less toxic substances which act primarily on the central nervous system. They have a basic character, contain heterocyclic nitrogen, and are synthesized in plants from amino acids or their immediate derivatives. In most cases they are of limited distribution in the plant kingdom.' (Hegnauer)⁶

However, lots of compounds that historically have been regarded as alkaloids – see the caffeine (**I-1**) case – would have been excluded by this definition. For this reason, compounds in which the nitrogen atom is not part of a ring are today called protoalkaloids, whereas compounds which are not derived from aminoacids and obtain the nitrogen atom from a different pathway are called pseudoalkaloids or Alkaloids *Imperfecta*.⁷ Examples of “true alkaloids” are morphine (**I-2**), already reported in Fig. 2, as well as cocaine (**I-15**) (Fig. 3). Caffeine (**I-1**) (Fig. 2) belongs to the group of pseudoalkaloids; Fig. 3 also reports some protoalkaloids, such as mescaline (**I-16**) and capsaicin (**I-17**).

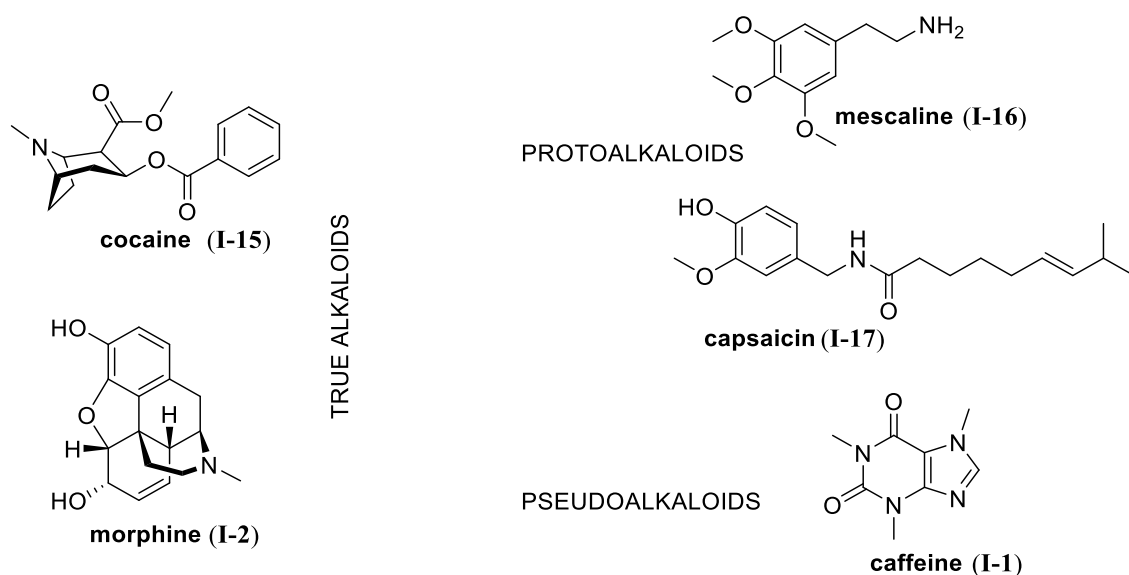


Fig. 3 – Classification of alkaloids and related examples.

Phenylpropanoids include any compounds having a 3-carbon chain attached to a 6-carbon aromatic ring, mostly derived from cinnamic or *p*-coumaric acids (**I-11**), in turn biosynthetically obtained from tyrosine and phenylalanine (**I-14**).⁸ Fig. 4 shows delphinidin (**I-18**) and cyanidin (**I-19**), two flavonoids – a subgroup of phenylpropanoids – responsible for blue and red pigmentation in flowers respectively.

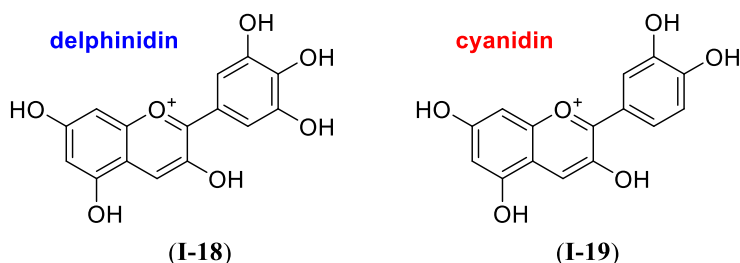


Fig. 4 – Examples of phenylpropanoids.

Closely related to fatty acids, the class of polyketides derives from the acetate-malonate pathway and owes their 1,3-oxo motifs to the reduction of 1,3-dicarbonyl functionalities.⁵ Polyketides have historically been employed as antibiotics: erythromycin (**I-20**) (Fig. 5) the renowned progenitor of macrolides, was extracted from the bacteria *Saccharopolyspora erythraea* in the early 50s.

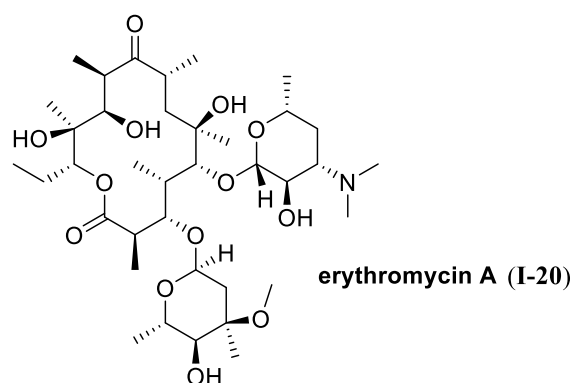


Fig. 5 – Structure of erythromycin.

Finally, terpenes are the most diverse class of natural products, including more than 40.000 compounds produced by plants and fungi but rarely found in bacteria.⁹ The term “terpenoid” or even “isoprenoid” was born to indicate a modified class of terpenes in which various positions bear functional groups and/or are oxidized, in contrast with “pure” terpenes, which are simple hydrocarbons. Today, these terms are often used as synonymous words, and refer to both oxygen-containing or reduced compounds. From a biosynthetic point of view, terpenes follow the so called “biogenetic isoprene rule”, proposed by Leopold Ruzicka¹⁰ (Nobel prize in 1939) on the basis of Wallach’s “isoprene rule”¹¹ according to which terpenes consist of one or more C₅ isoprene units. Starting from this basic idea, the biogenetic isoprene rule describes terpenes as enzymatically cyclized products deriving from ancestral alkene chains, in turn constituted of head-to-tail condensed isoprene monomers.¹²

‘... the leading question was whether the carbon skeletons of the higher terpenes were also composed of isoprene units. For all the compounds we examined, the answer was positive, and thus the original working hypothesis gradually grew into the isoprene rule’. (Ruzicka 1959)¹²

A classification based on the number of isoprene subunits is easily deriving: hemiterpenes (C₅) are made of one subunit, monoterpenes (C₁₀), sesquiterpenes (C₁₅), diterpenes (C₂₀), triterpenes (C₃₀) and tetraterpenes (C₄₀) consist of two, three, four, six and eight units respectively. Polyterpenes, such as rubber, consist of more than 40 carbon atoms.⁵

Hemiterpenoids, found in extracts from the leaves of many trees (conifers, poplars, oaks, and willows to cite some examples) and herbs (e.g., *Hamamelis japonica*)¹³, represent the most simple class of terpenoids from a structural point of view and include the building block isoprene (**I-10**). Tiglic, angelic, isovaleric, and senecioic acids (**I-21** to **23**), along with isoamyl alcohol (**I-24**) are other members of this class.¹⁴

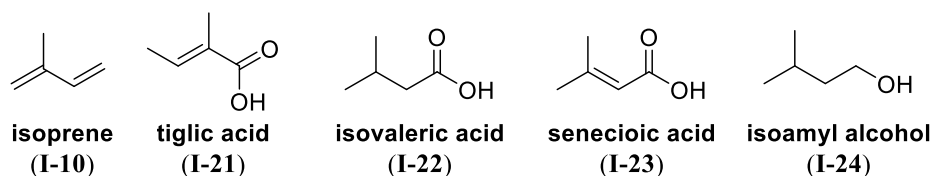


Fig. 6 – Examples of hemiterpenoids.

Monoterpenes are numerous (more than 400 structures) and ubiquitous fragrant molecules extracted from leaves, flowers and fruit of various plants.⁵ This NPs family includes both acyclic and cyclic monoterpenes, which have been extensively employed as starting materials and part of the chiral pool (see paragraph “Terpenoids in total synthesis”), as well as in the food industry. Notable acyclic members are for instance geraniol (**I-25**) and geranial, linalool (**I-26**), citronellol (**I-27**), -al and -one,

nerol (**I-28**) and neral. Carvone (**I-29**), menthol (**I-30**), pulegone (**I-31**) and limonene (**I-32**) belong to the monocyclic family, while nepetalactone (**I-33**) and santonin (**I-34**) possess more than one ring (Fig. 7).

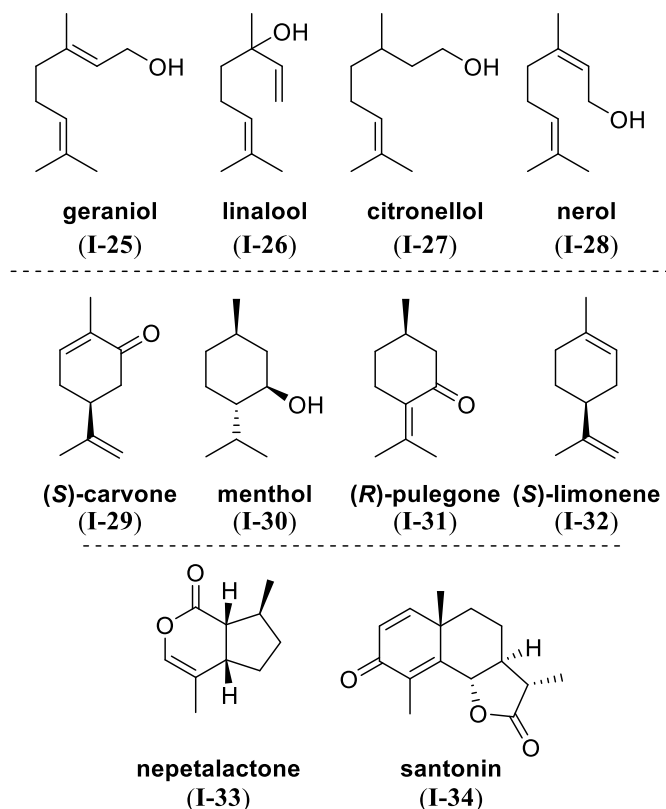


Fig. 7 – Examples of monoterpeneoids categorized by the number of rings.

The scientific community's interest towards sesquiterpenes arises from their roles in biological systems, included the human body.¹⁵ To quote some, antibiotic,¹⁶ antitumor,¹⁷ antiviral,¹⁸ cytotoxic,¹⁹ immunosuppressive,²⁰ phytotoxic,²¹ antifungal²² and hormonal²³ activities have been displayed from several members of this class. Moreover, thousands of different sesquiterpenes, characterized by hundreds of diverse skeletons, have been isolated. This huge diversity allows the research on sesquiterpenes to be always renewing itself. The next paragraph will try to unravel the mysteries of this subclass of terpenes, focusing on synthetic endeavours in this field.

Taxanes, as a class of diterpenes, are characterized by a 6/8/6 ring system and vary in decoration. Taxol (**I-35**) (Fig. 8) is probably the most important member, and one of the first and few diterpenes being commercially available for cancer treatment.

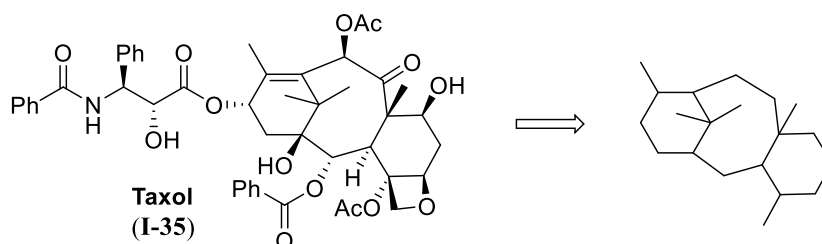
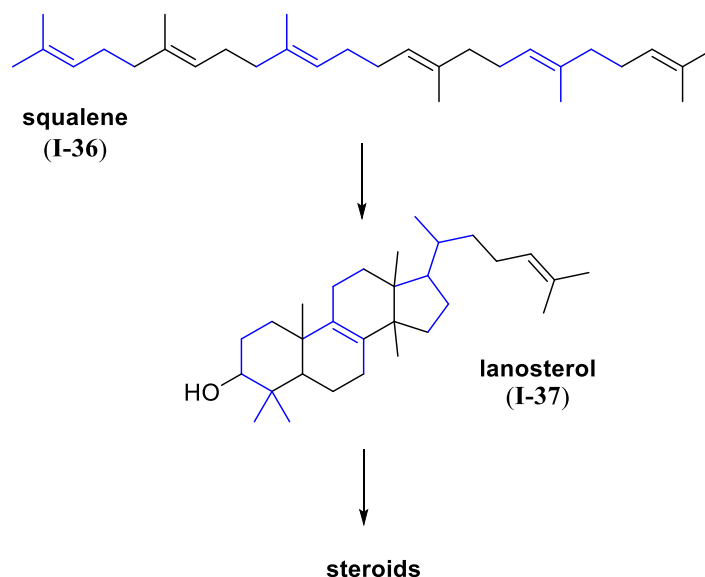


Fig. 8 – Taxol and its 6/8/6 taxane skeleton.

Triterpenes, including squalene (**I-36**), which cyclizes into the signature skeleton of steroids, are the most abundant metabolites besides polysaccharides and are produced by plants, animals and fungi.²⁴



Scheme 1 – Biosynthetic connection among squalene (**I-36**), lanosterol (**I-37**) and steroids; every second isoprene unit is highlighted in blue.

One of the few examples of tetraterpenes are carotenoids, responsible for pigmentation in arthropods and vegetable species as well as acting as antioxidants, attractants, and UV attenuators.⁵ The structure of β -carotene (**I-38**), a renowned member, is reported in Fig. 9

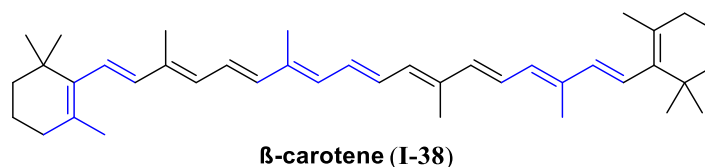


Fig. 9 – Structure of β -carotene; every second isoprene unit is highlighted in blue.

Lastly, as briefly mentioned above, polyterpenes are polymers that find important applications in the rubber industries. Rubber itself, obtained from the homonymous tree, is formed by 4000-5000 isoprene-subunits.²⁵

Terpenoids in total synthesis – state of the art

Terpenoids have always been leaving their footprint in scientific literature, mainly impacting on two types of publications – isolation of new natural products and challenging total syntheses, in which they appear both as targets and/or as starting materials. The purpose of this chapter is to highlight the strong, evergreen influence of this class of natural products on today's research.

In spite of being exploited since the dawn of civilization for its curative extracts, the plant kingdom's creative power is far away to be fully known and understood: new natural products are constantly discovered, belonging either to known classes of compounds or possessing unprecedented structural motifs. By way of explanation, in 2020 a new lignin (**I-39**) characterized by a novel 2,5-dioxane[5.2.2.0^{4,8}] core was isolated from *Eurycoma longifolia*;²⁶ in 2021, illihenin A (**I-40**), a sesquiterpenoid with a cage-like tricyclic [6.2.2.0^{1,5}]dodecane skeleton, was isolated from *Illicium henryi*.²⁷

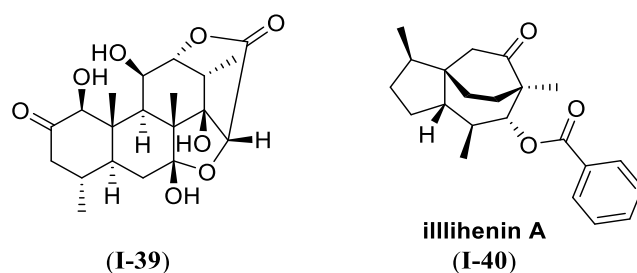
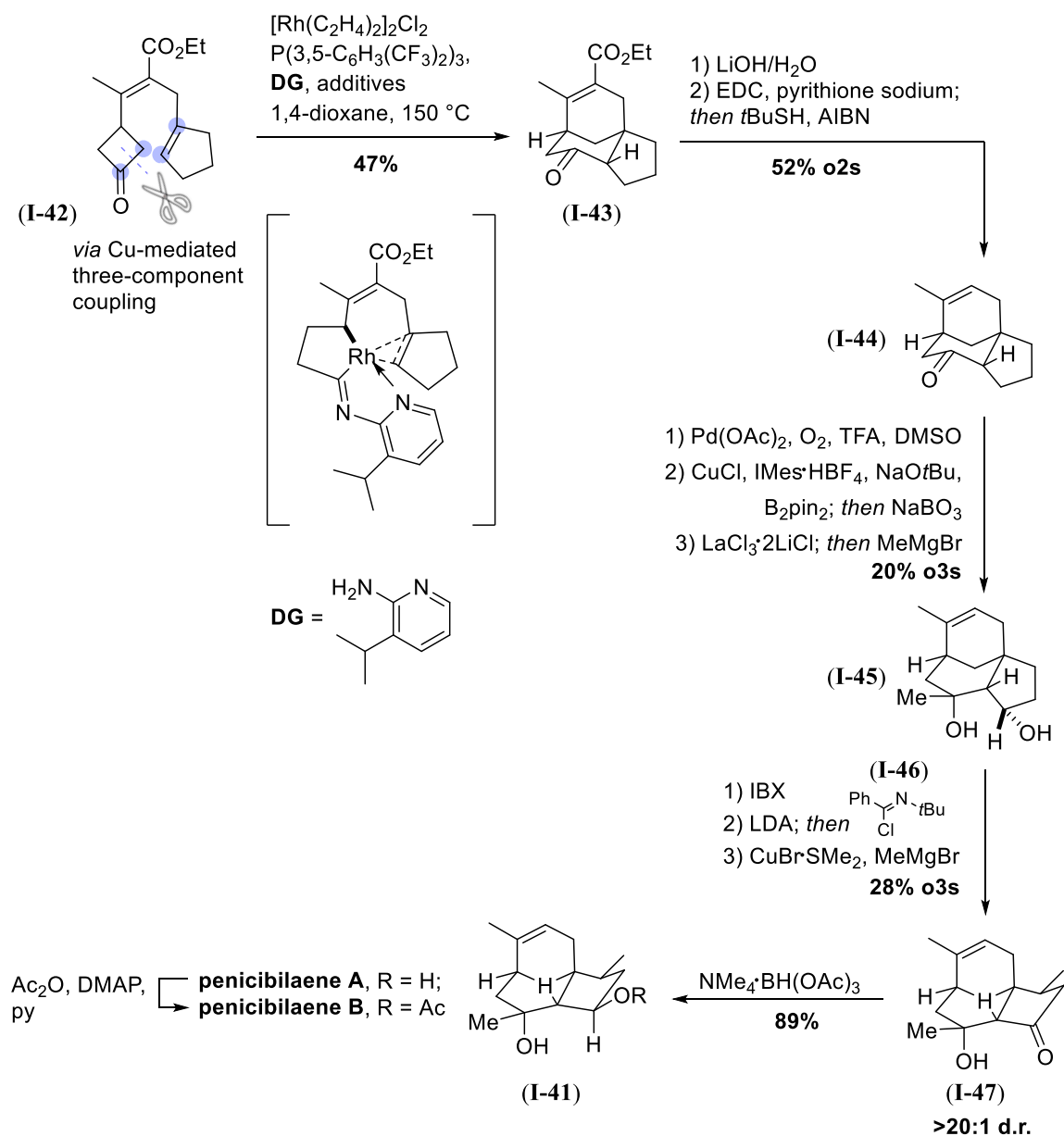


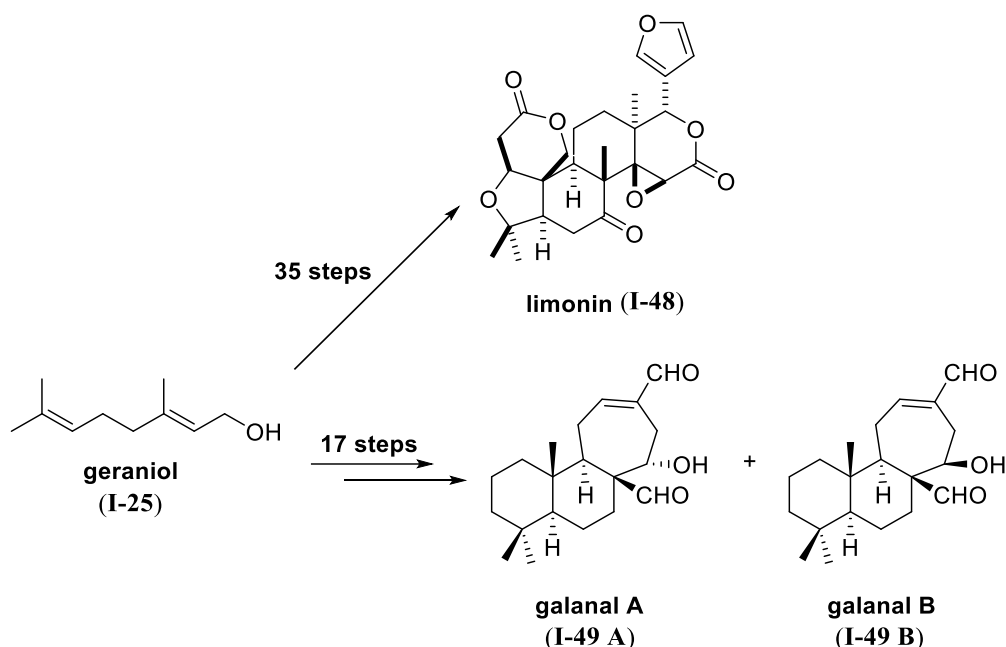
Fig. 10 – Structure of the recently isolated (unnamed) lignin (**I-39**) and illihenin A (**I-40**).

While waiting to witness synthetic efforts towards these newly discovered molecules, other terpenoids have been targeted from organic chemists. One of the latest impressive syntheses in this field was accomplished by Dong and coworkers.²⁸ Although not of plant-origin, sesquiterpenes penicibilaenes A (**I-41A**) and B (**I-41B**) do display activity against plants pathogenic fungi. Their total synthesis was accomplished by employing the so called “cut-and-sew” technique, relying on the construction of the core skeleton *via* C–C activation, followed by a C–H phase, in which unsaturated 2 π -units are inserted and substituents are introduced.²⁹ This approach to terpene-synthesis is an alternative to the bioinspired “two-phase” strategy, pioneered by Baran and coworkers (the synthesis of various eudesmanes³⁰ as well as the synthesis of (–)-taxuyunnanine D,³¹ which will be encountered in the next chapters, took advantage of this technique). In this second approach, an oxidative phase would follow the preliminary cyclase phase. The synthetic key steps are herein summarized (Scheme 2). Rh-catalysed C–C activation of butanone (**I-42**) followed by insertion of the linked 2 π -unit represented the real “cut-and-sew” step and constructed the tricycle[6.3.1.0^{1,5}]dodecane skeleton of penicibilaenes A and B. At this point, basic hydrolysis, followed by Barton's decarboxylation, provided ketone (**I-44**) and initiated the decoration of the core; α,β -desaturation³² was followed by conjugate borylation-oxidation. The resulting secondary alcohol (not shown) was stereospecifically methylated by kelation control, then IBX oxidized the secondary alcohol moiety. A second desaturation with Mukaiyama's method set the stage for diastereoselective copper-mediated 1,4-addition from the convex face. Alcohol directed *syn*-reduction of ketone (**I-47**) afforded penicibilaene A (**I-41A**), and further acylation its congener penicibilaene B (**I-41B**), concluding the total synthesis.



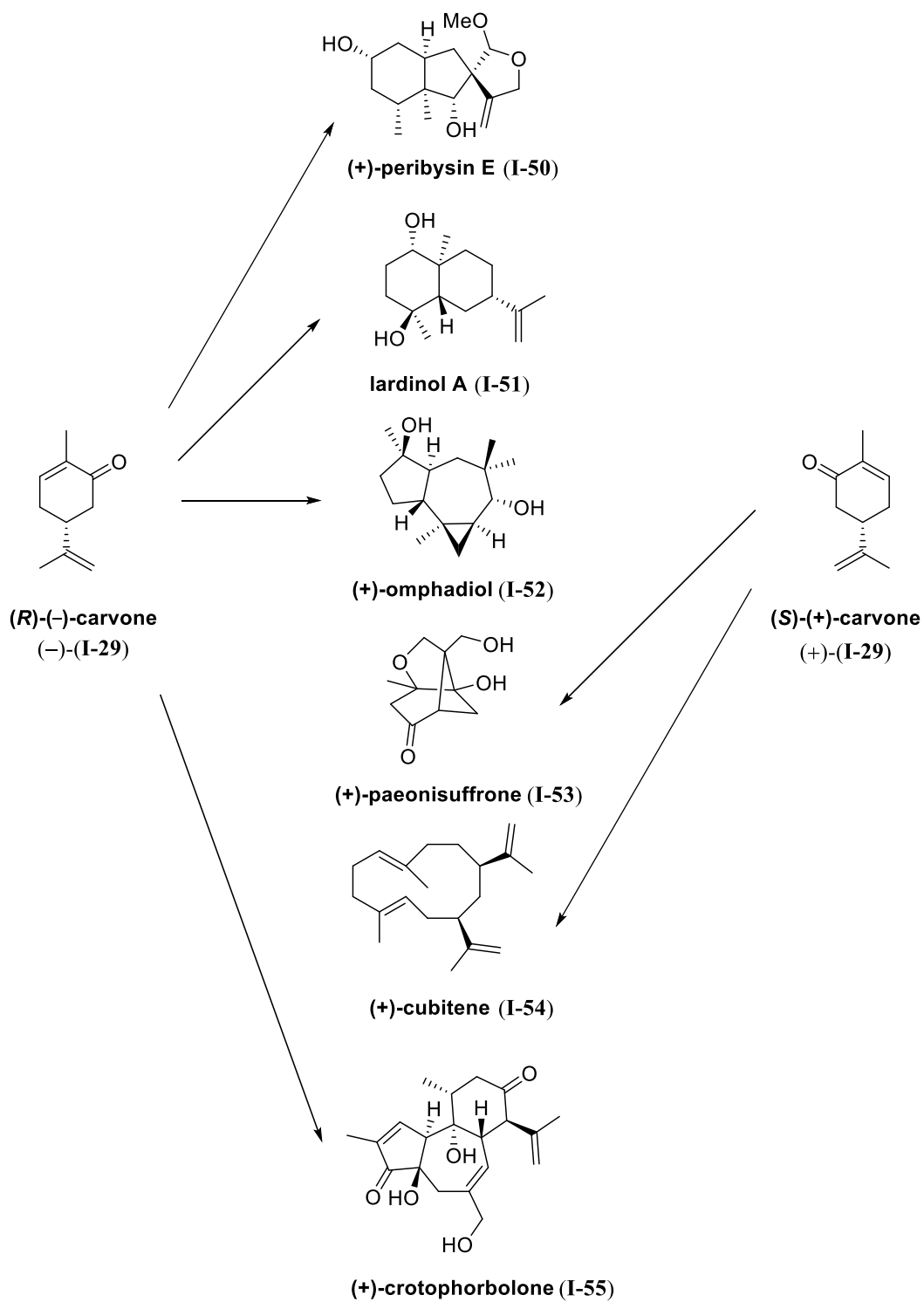
Scheme 2 – Total synthesis of penicibilaenes A and B (**I-41A, B**), through “cut-and-sew” technique; “cut” and “sew” positions are highlighted in the first step.

Apart from being a synthetic target, terpenes are established chiral building blocks, as underlined by several reviews.^{33,34} Monoterpenes (see Fig. 7) are probably the most employed terpenes in total synthesis, because of high abundance and consequent low cost. Moreover, it is intuitive to think that it should be possible to interconvert structures which are biosynthetically related or, more simply said, derive from the same building blocks. This is the reason why the idea of manipulating the structure of one terpene into another preceded the already mentioned biogenetic “isoprene rule”.³³ As an example, 2015 saw the accomplishment of the first total synthesis of (\pm)-limonin (**I-48**), a tetranortriterpenoid, from Yamashita’s research group.³⁵ Geraniol (**I-25**), 173,00€/Kg from Sigma Aldrich, served as the starting material, as shown in Scheme 3. In 2017, Chein and coworkers synthesized the labdane diterpenes galanal A and B (**I-49**),³⁶ also starting from geraniol. This thesis will also take advantage of geraniol (**I-25**) and its low cost for an highly scalable synthesis.



Scheme 3 – Examples of natural products synthesized from geraniol (**I-25**).

Terpene-building blocks are either linear or cyclic, and do or do not possess stereocenters, as already depicted in Fig. 7. Synthesis from terpene-building blocks could consequently present the further warranty of an enantiopure and cheap starting material, part of what is referred to as “chiral pool”, *i.e.* the collection of chiral molecules provided by nature. Carvone (**I-29**) is by far the most frequently exploited monoterpene (Scheme 4). Employed in Diels-Alder reactions for the synthesis of (+)-peribysin E³⁷ (**I-50**) and lairdinol A (**I-51**),³⁸ carvone (**I-29**) was also the designated building block for the synthesis of (+)-paeonisuffrone (**I-53**),³⁹ whose synthesis from Bermejo and coworkers will serve as an inspiration in the next paragraphs. The africanane skeleton of (+)-omphadiol (**I-52**),⁴⁰ extracted from fungal species, was constructed from (–)-carvone (–)-(**I-29**) in 2011. One year later, Lindel’s total synthesis of (+)-cubitene⁴¹ (**I-54**) chose the (+)-enantiomer (+)-(**I-29**) as chiral starting material. (+)-crotophorbolone (**I-55**),⁴² from 2015, was derived from (–)-carvone (–)-(**I-29**). These are only a few examples of the flourishing number of natural products that owe their birth to chiral pool members: as always in this never exhausted field, more examples are about to come.



Scheme 4 – Examples of natural products synthesized from carvone (I-29).

Illicium sesquiterpenes

The genus *Illicium* represents a notable source of diverse sesquiterpenes, often possessing chemically interesting structures and neurotrophic activities.⁴³ Diffused worldwide and recognizable from its characteristic star-shaped fruit, *Illicium* is the only member of the *Illiciaceae* family. Three main groups of *Illicium* sesquiterpenes have been identified in its extracts (Fig. 11): the *seco*-prezizaanes, the anisactones and the *allo*-cedranes.⁴⁴ All presenting a methylcyclopentane subunit, these three classes share a common *gem*-disubstitution, as well as the same fusion bond between the aforementioned 5 membered ring and a 6-, 5- or 6-carbons ring respectively.

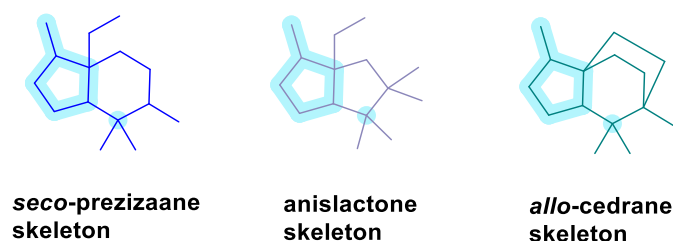


Fig. 11 – Skeletons from the three main sesquiterpene classes of the *Illicium* family. Common features are highlighted.

Seco-prezizaanes

The history of *seco*-prezizaane carbon frameworks begins in the late 60s, when the X-ray crystal structure of anisatin (**I-56**) was obtained from Yamada and coworkers.⁴⁵ After this first milestone was set, over a hundred structures biosynthetically related to anisatin were elucidated, large part of which were possessing a *seco*-prezizaane skeleton, *i.e.* a 5,6-fused system with different oxidation levels,⁴⁶ as shown in Fig. 12.

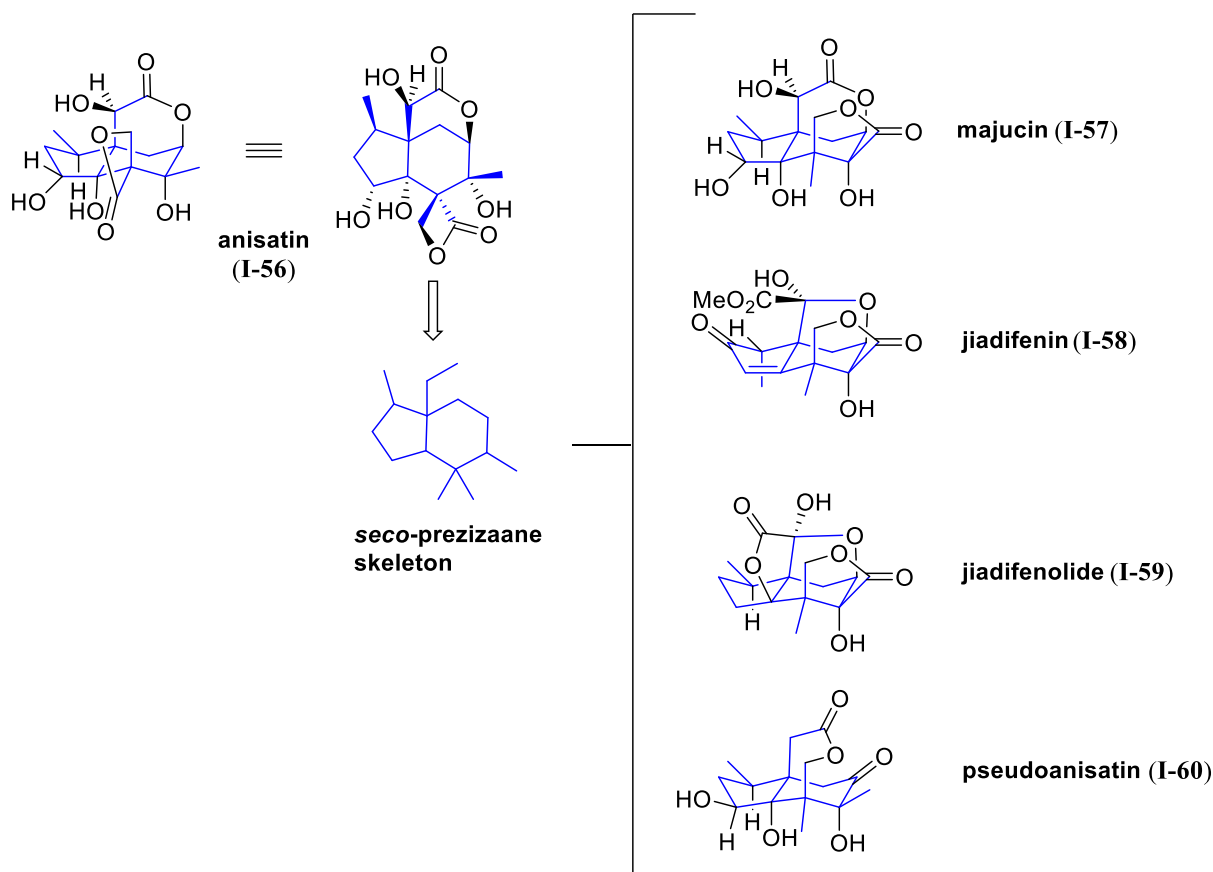
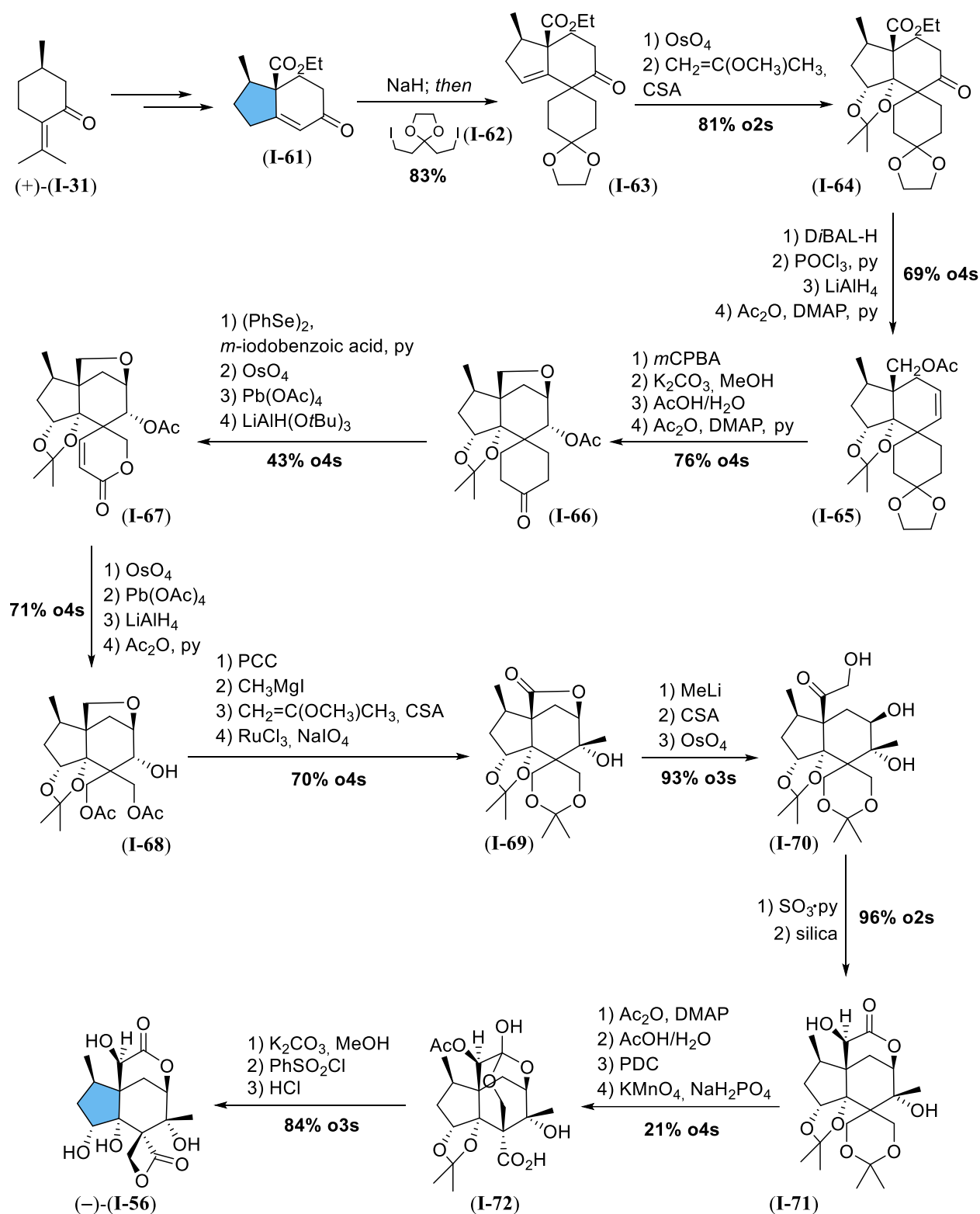


Fig. 12 – Prominent members of the *seco*-prezizaane family; *seco*-prezizaane skeleton is highlighted in blue.

The most prominent members of this class of natural products (Fig. 12) and their impact on synthetic publications will be discussed in this paragraph. In particular, as a link to the subsequent chapter focusing on the construction of 5-membered rings as part of the challenges in total synthesis, a colour code will guide the reader through ring formation in the presented syntheses.



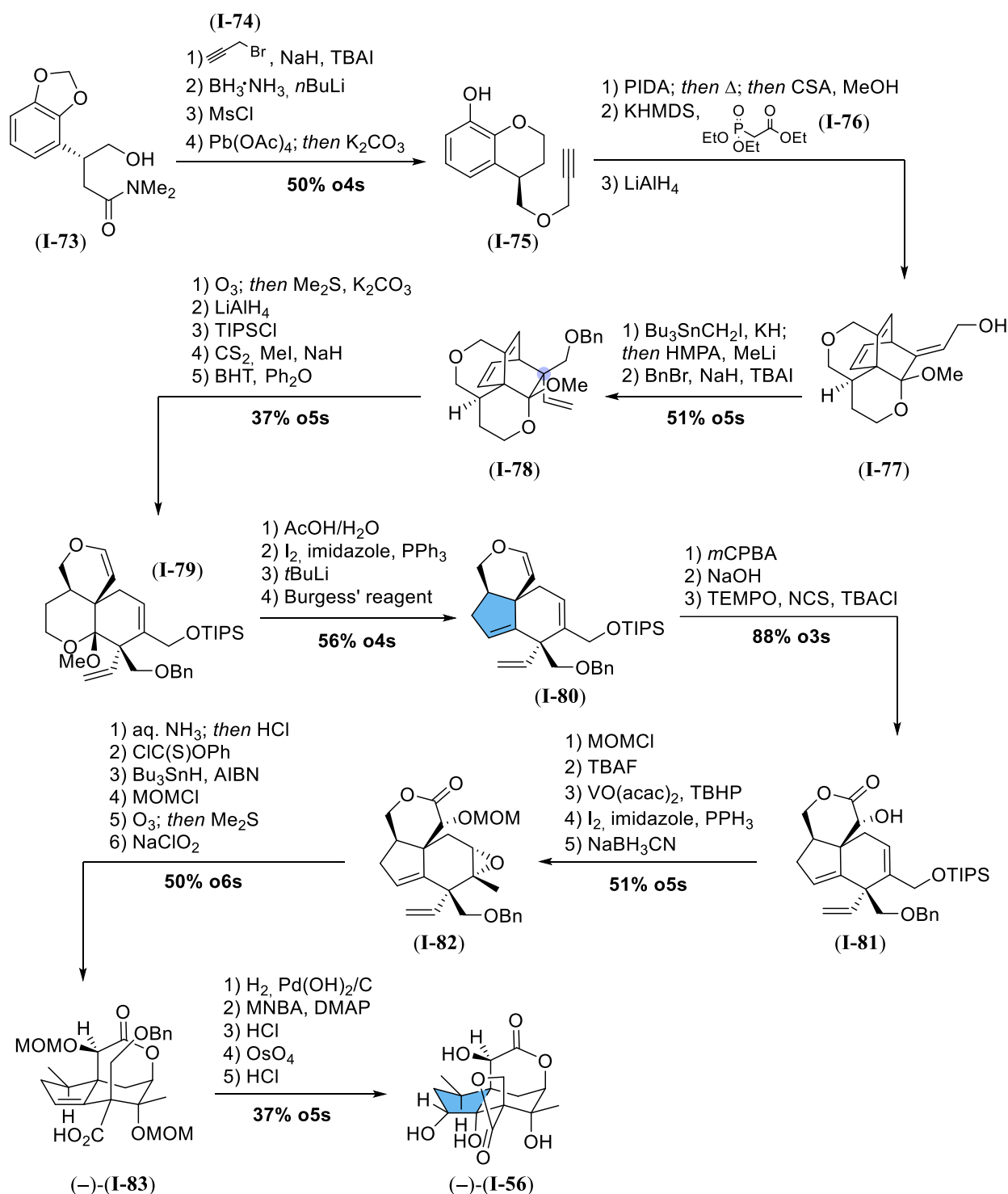
Scheme 5 – First total synthesis of (-)-anisatin (-)-**(I-56)** by Yamada and coworkers.

After the isolation and structure elucidation, Yamada and coworkers concluded their work with the total synthesis of (-)-anisatin (-)-**(I-56)**.⁴⁷ Their ex-chiral pool synthesis (Scheme 5) began with the

conversion of (*R*)-(+)-pulegone (+)-(**I-31**) into bicyclic enone (**I-61**), and was followed by introduction of a synthetic equivalent of the spiro β -lactone onto (**I-61**) thus obtaining (**I-63**). Decoration of the *trans*-fused hydrindan skeleton of (**I-64**), obtained through *cis*-dihydroxylation, employed quite a few synthetic steps, resulting in intermediate (**I-66**). This was the starting point for manipulation of the cyclohexanone ring into the desired 4-membered ring: a geminal bis(hydroxymethyl) group protected as an acetonide as in lactone (**I-69**) served this purpose, preserving the required functionalities during the consequent oxidation steps. Quite interesting is the isomerization of the keto hemiacetal generated from α -hydroxyketone (**I-70**) *via* Parikh-Doering oxidation, that was achieved upon adsorption on silica gel. At this point, the time had come for liberating the future spiro lactone moiety: hydrolysis of acetonide (**I-71**) and consequent 2-steps oxidation sequence provided ortho ester (**I-72**); basic methanolysis, lactonization and acidic liberation of the second acetal moiety afforded (-)-anisatin (-)-(**I-56**).

Although this specific example employs quite old-fashioned chemical transformations, as well as a massive use of protection-deprotection sequences, and doesn't shine for redox efficiency, this groundbreaking work was followed by one and only other accomplished total synthesis of anisatin, proving the challenging nature of this kind of structures.

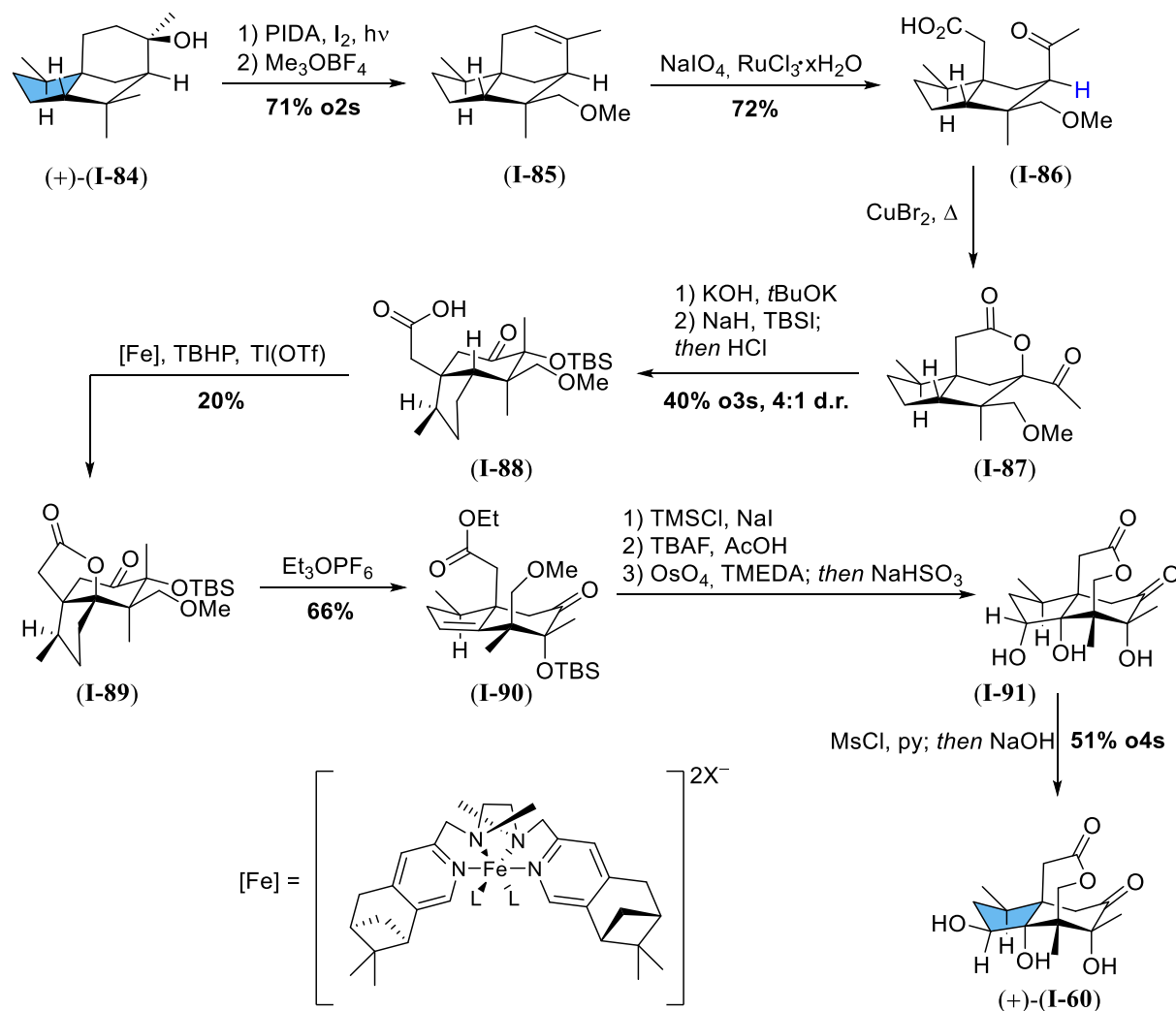
The second contribution belongs to the group of Fukuyama, and dates 2012.⁴⁸ In their approach, enantioenriched amide (**I-73**) was built in three steps involving a diastereoselective Rh-catalyzed 1,4-addition of a known arylboronic acid onto a butenolide counterpart (not shown). Having forged the first of eight contiguous stereocenters, key step of this asymmetric synthesis (Scheme 6) was a dearomatization of the electron-rich core in intermediate (**I-75**) that induced a Diels-Alder reaction. Horner-Wadsworth-Emmons olefination (HWE) olefination and a 2,3-sigmatropic rearrangement, triggered by MeLi in the presence of HMPA, set the second *seco*-preezane stereogenic center, as shown in bis-tetrahydropyran derivative (**I-78**). The construction of the 5-membered ring was the bottleneck of the synthesis, requiring nine additional steps from compound (**I-78**), including a Chugaev elimination, as well as a Barbier-type cyclization. Of interest is the vanadium-catalyzed epoxidation of lactone (**I-81**), followed by reductive removal of the primary alcohol *via* an iodide (see conversion of intermediate (**I-81**) to (**I-82**)). β -lactone formation was achieved with MNBA, while the remaining *cis*-hydroxylation with OsO₄. Global deprotection afforded (-)-anisatin (-)-(**I-56**). Although the efficiency of the reported syntheses of anisatin is questionable, the choice of mentioning these approaches relies on their historical importance, as well as on their difference with the upcoming syntheses. In fact, in seek for a more merciful destiny, other groups targeted the *seco*-preezanes family with a completely different mind setup.



Scheme 6 – Total synthesis of (-)-anisatin (-)-**(I-56)**, by Fukuyama and coworkers.

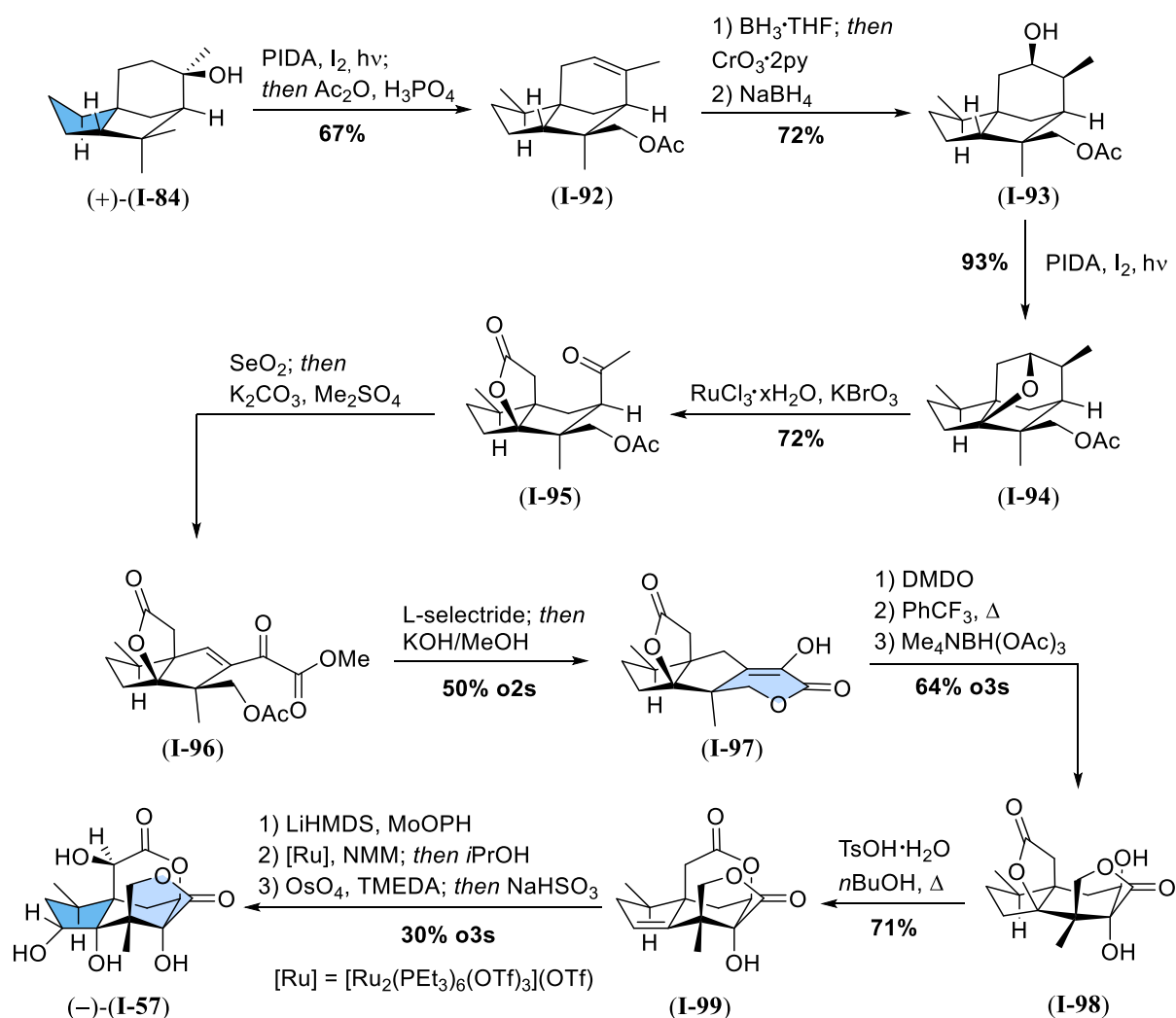
(+)-Pseudoanisatin (+)-**(I-60)** and (-)-majucin (-)-**(I-57)** were for example targeted by Maimone and coworkers in a semisynthetic approach, aiming for the conversion of a pre-existing sesquiterpene into several members of the *Illicium* class.^{49,50} Starting from (+)-cedrol (+)-**(I-84)**, the synthesis of both molecules and related compounds was accomplished in a quite elegant fashion: concerning the semisynthesis of (+)-pseudoanisatin (+)-**(I-60)** (Scheme 7), the starting material was subjected to a hypiodite-mediated CH-activation (Suarez⁵¹), followed by elimination to the olefin-motif in **(I-85)**. Oxidative cleavage set the stage for an intramolecular lactonization, the first of two CH-activations, which resulted in the 5,5-fused cedrane skeleton of lactone **(I-87)**. In order for the desired *seco*-

prezizaane nucleus to be constructed, α -ketol rearrangement was induced in strongly basic conditions, that afforded both lactone hydrolysis and ring shift to intermediate (**I-88**). Carboxylic acid-mediated CH-activation furnished the desired lactone (**I-89**) - this particular transformations will be discussed in a dedicated section – which underwent a transesterification-elimination sequence, resulting in ester (**I-90**), that was converted to the target molecule (+)-(**I-60**) with four additional straightforward steps.



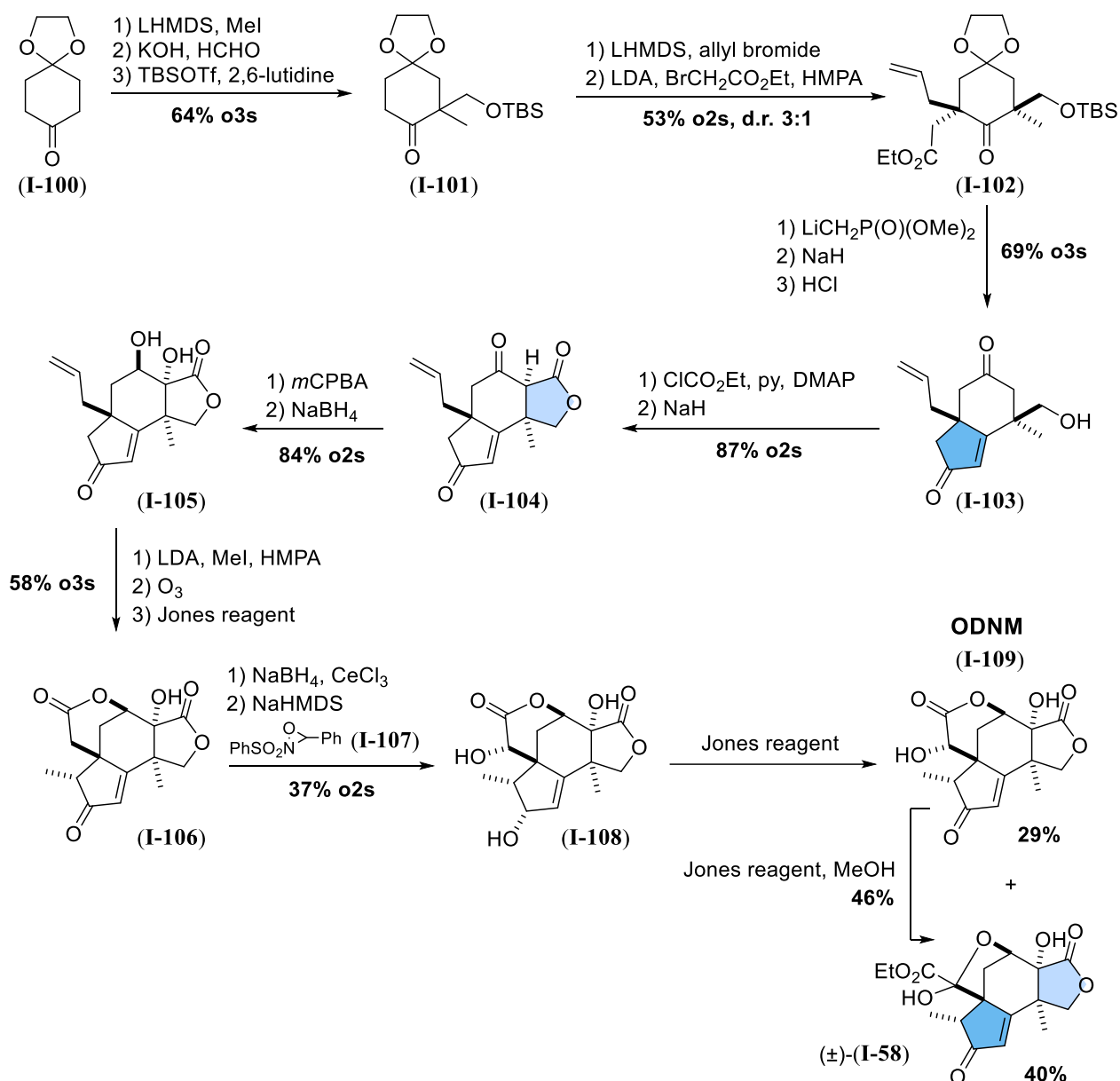
Scheme 7 – Semisynthesis of (+)-pseudoanisatin (+)-(**I-60**) by Maimone and coworkers.

In order to be converted into (–)-majucin (–)-(**I-57**) (Scheme 8), (+)-cedrol (+)-(**I-84**) was subjected to substantially the same C–H functionalization/elimination sequence, affording this time acetate (**I-92**). Straightforward functional group manipulations resulted in secondary alcohol (**I-93**), that subjected to hypiodite photolysis yielded tetrahydrofuran derivative (**I-94**). C–H activation/C–C oxidation sequence inspired from the work of Waegell and coworkers⁵² allowed the formation of keto-lactone (**I-95**), whose extensive oxidation was performed with SeO₂. Lactone (**I-97**) was obtained after L-selectride reduction followed by acetate cleavage/isomerization and underwent ring shift to the 5,6-fused system under thermal treatment. Subsequent reduction to (**I-98**) provided the formal intermediate for (–)-jiadifenolide (–)-(**I-59**) (see Shenvi's⁵³ and Theodorakis's⁵⁴ syntheses, Scheme 18 and 14 respectively) while acidic treatment resulted in translactonization and dehydration to lactone (**I-99**), in turn formal intermediate for (–)-jiadifenin (–)-(**I-58**) and ODNM⁵⁵ – (1R,10S)-2-oxo-3,4-dehydroyneomajucin (**I-109**) (see Scheme 9 and 10). Hydroxylation, epimerization and dihydroxylation furnished targeted (–)-majucin (–)-(**I-57**), underlining the power of Maimone's strategy for the access to various *Illiciums*.



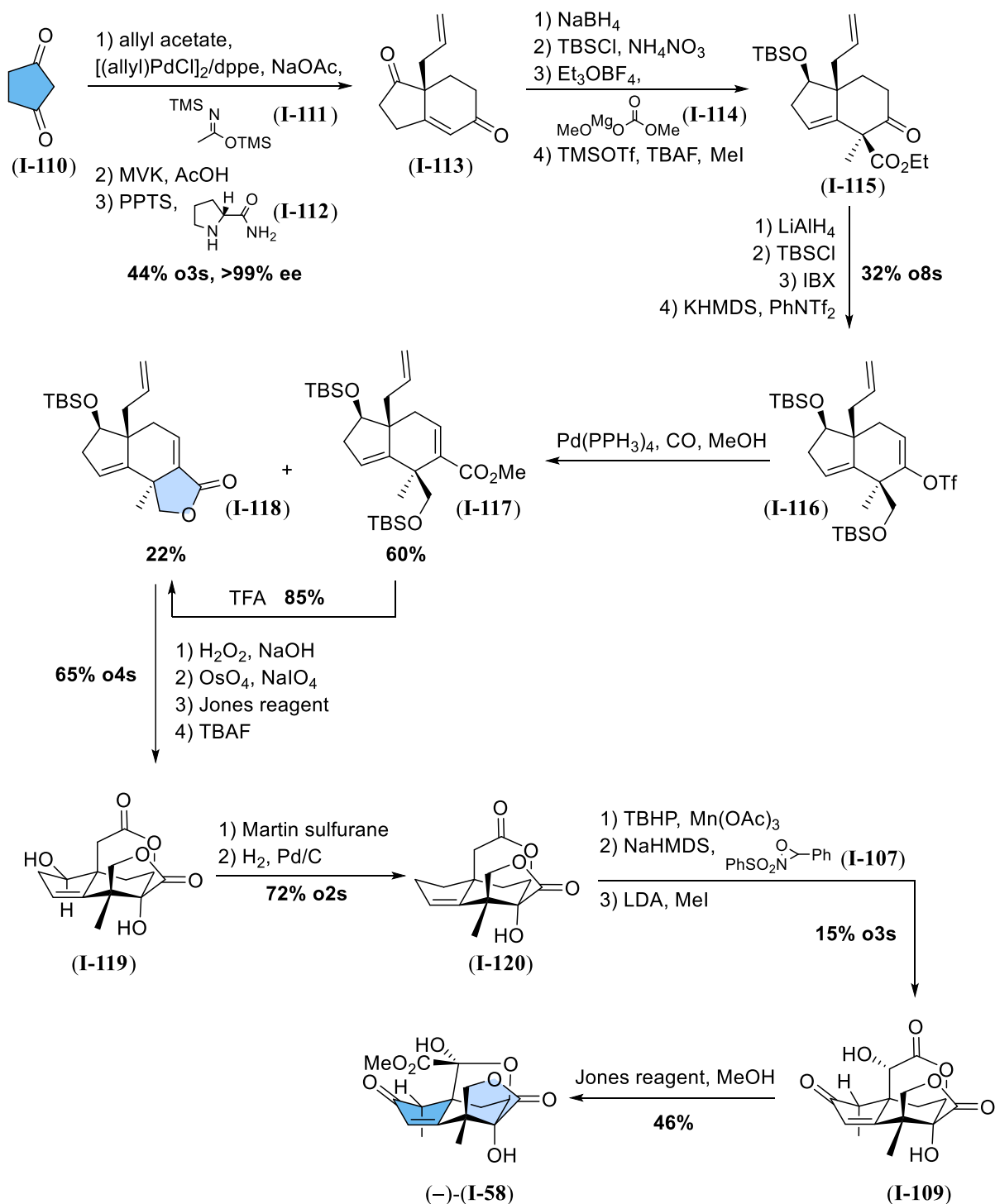
Scheme 8 – Semisynthesis of (-)-majucin (-)-**(I-57)** by Maimone and coworkers.

At the beginning of the current century, jiadifenin (**I-58**) was isolated from *Illicium jiadifengpi* by Fukuyama and coworkers and showed neurotrophic activity.⁵⁶ Due to its interesting structure and properties, it did not take long for the first accomplished total synthesis to be reported: Danishefsky's research group published their synthesis (Scheme 9) of this sesquiterpene in 2004⁵⁷, just two years after its isolation. In their hands, commercially available 1,4-cyclohexanedione monoethylene ketal (**I-100**) was subsequently α -methylated and α -hydroxymethylated, while position α' was subjected to allylation and carboethoxymethylation. Desired diastereoisomer (**I-102**)-derived phosphonate underwent intramolecular HWE, and resulted in cyclopentenone (**I-103**) after deprotection. Carbonylation of the alcohol moiety and basic treatment led to the formation of the new 5-membered-ring, which was in turn α -hydroxylated and reduced to corresponding *trans*-diol (**I-105**). Methylation/oxidative cyclization-sequence produced lacton (**I-106**), which was subjected to Luche reducing conditions and consequent hydroxylation by means of Davis' oxaziridine (**I-107**). Treatment of resulting intermediate (**I-108**) with Jones reagent allowed to isolate a separable mixture of the desired natural product along with C2-oxidized lactone (**I-109**); its prolonged treatment in the same conditions promoted rearrangement of the α -ketolactone to (\pm)-jiadifenin (\pm)-**(I-58)**.



Scheme 9 – Total synthesis of (±)-jiadifenin (±)-**I-58** by Danishefsky and coworkers.

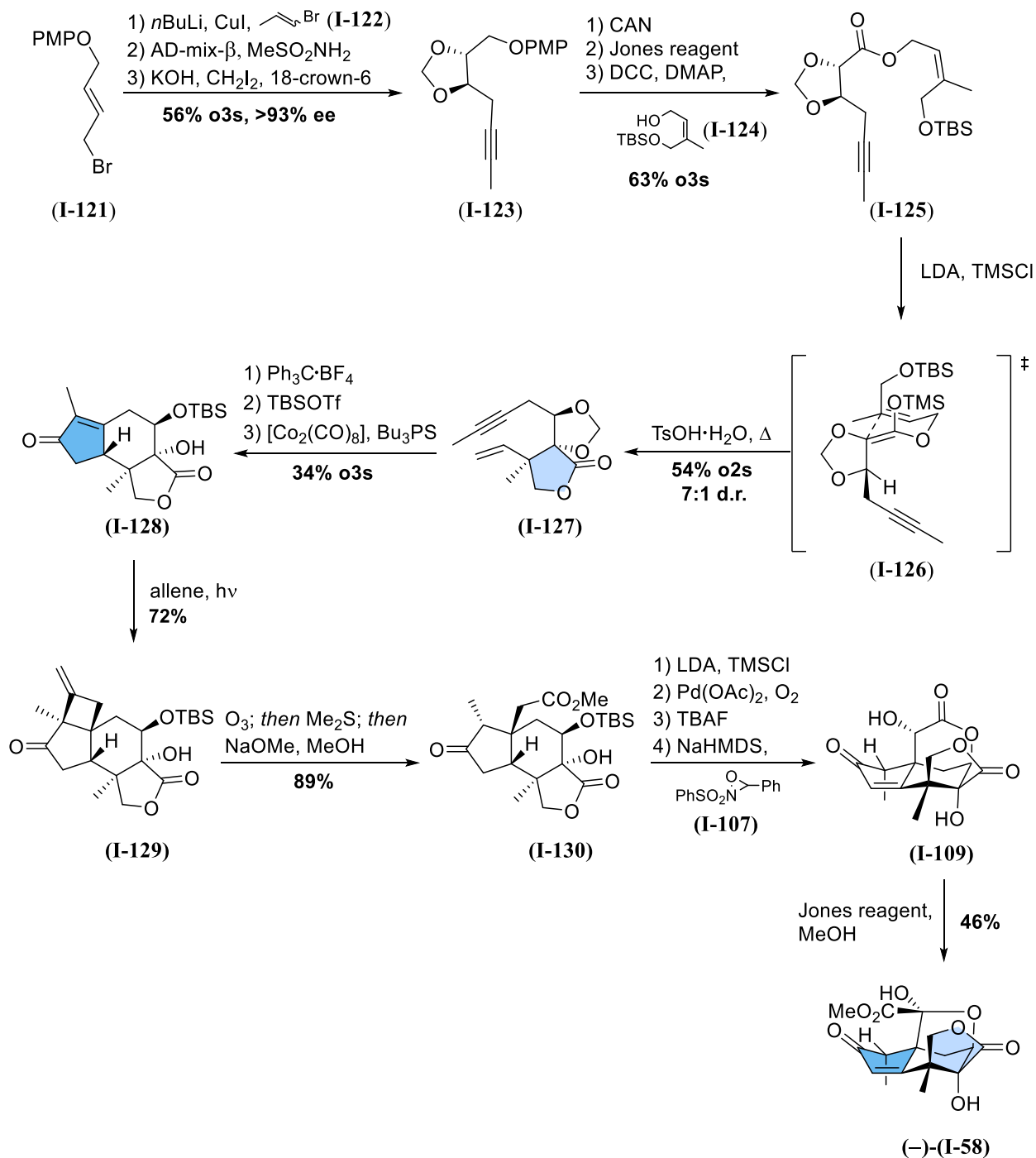
In 2011, Theodorakis and colleagues accomplished the first asymmetric synthesis of (–)-jiadifenin, employing Hajos-Parrish-like diketone (**I-113**) (Scheme 10).⁵⁵ The secondary alcohol resulting from its NaBH₄ reduction was TBS-protected; Stiles-type α-carboxylation⁵⁸ followed. γ-Methylation generated ketone (**I-115**), which was in turn globally reduced, selectively protected and reoxidized, so that triflate (**I-116**) could be employed in a Pd-catalyzed methoxy-carboxylation. Methyl ester (**I-117**) was smoothly converted into lactone (**I-118**), that furnished key intermediate (**I-119**), which will soon be mentioned in the synthesis of jiadifenolide from the same group (Scheme 14).⁵⁴ Martin sulfurane employed on this compound resulted in dehydration; the resulting diene was hydrogenated, oxidated at the remaining allylic position, while hydroxylation occurred at the lactone α-position, resulting in the already mentioned ODNM (**I-109**). Jones oxidation was once again effective for the target molecule to be obtained.



Scheme 10 – Total synthesis of (-)-jiadifenin (-)-**(I-58)** by Theodorakis and coworkers.

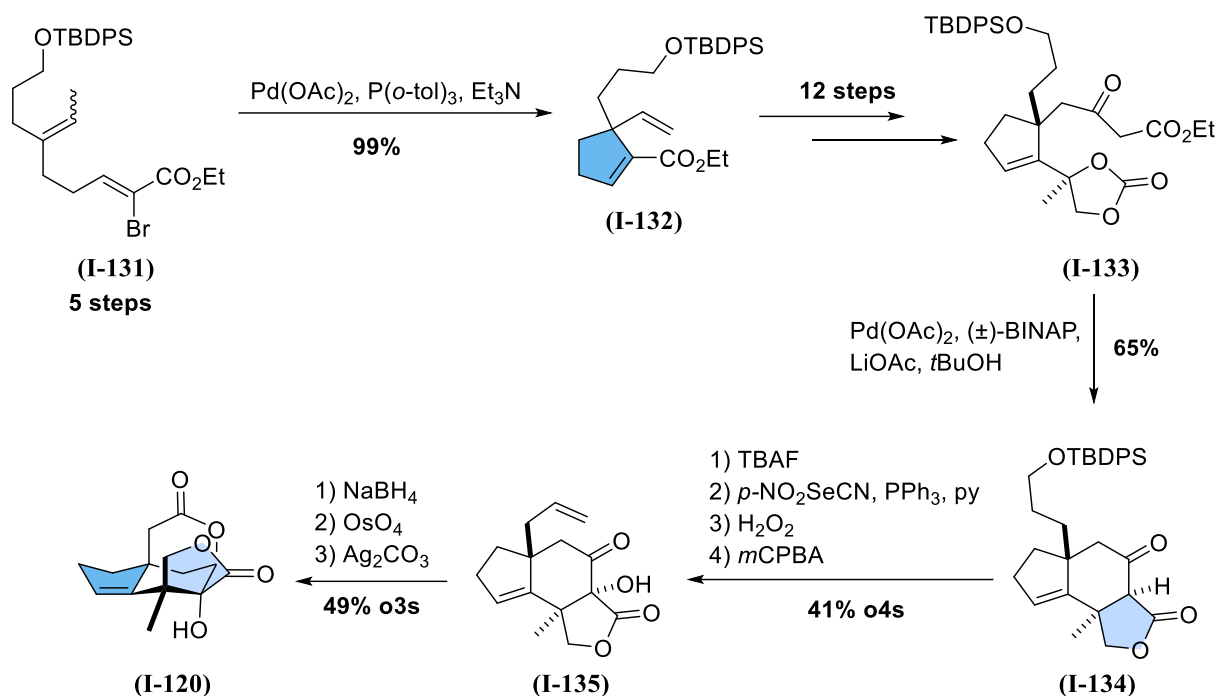
Another synthesis taking advantage of Danishefsky's Jones oxidation/rearrangement sequence is the total synthesis of ODNM (**(I-109)**) and consequently of (-)-jiadifenin (-)-**(I-58)** (Scheme 11) by Zhai's research group.⁵⁹ Enantioenriched internal alkyne (**(I-123)**), obtained by means of a Sharpless dihydroxylation, was converted into ester (**(I-125)**) through coupling of the carboxylic acid resulting from exposure to oxidative conditions with (*Z*)-allylic alcohol (**(I-124)**). The following key step relies on a diastereoselective Claisen-Ireland rearrangement of readily obtained silyl ketene acetal (**(I-126)**). At this point acidic treatment produced the desired γ -lactone moiety in (**(I-127)**). [2+2]-cycloaddition with allene performed on enone (**(I-128)**), in turn obtained *via* Pauson-Khand reaction (see "Construction of 5-membered rings" paragraph), provided cyclobutane-derivative (**(I-129)**) in good yields; oxidative

cleavage to ketoester (**I-130**) set the stage for a two-step Ito-Saegusa desaturation,⁶⁰ and lactonization upon deprotection. Theodorakis' α -oxidation protocol⁵⁵ was employed to obtain ODNM (**I-109**), and consequently (-)-jiadifenin (-)-(**I-58**).



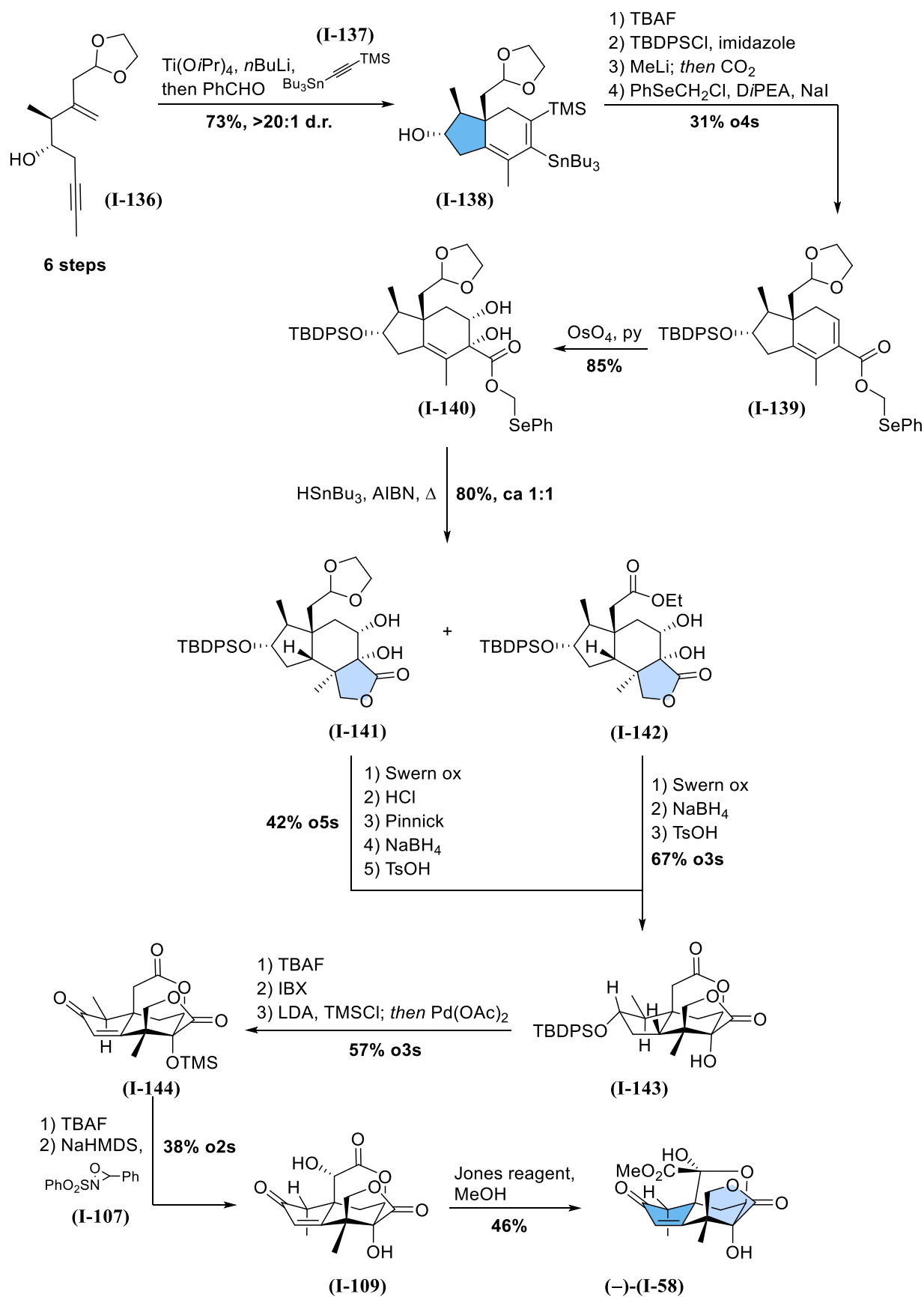
Scheme 11 – Total synthesis of (-)-jiadifenin (-)-(**I-58**) by Zhai and coworkers.

Fukuyama and coworkers accomplished a formal synthesis of (\pm)-jiadifenin (\pm)-(**I-58**) in 2015 (Scheme 12),⁶¹ involving a Heck cyclization for the construction of intermediate (**I-132**), a Tsuji-Trost allylation/lactonization sequence performed on β -ketoester (**I-133**) and an oxidative cyclization to conclude the formal synthesis (intermediate (**I-120**) from Theodorakis' synthesis in Scheme 10).



Scheme 12 – Formal synthesis of (±)-jiadifenin (±)-(I-58) by Fukuyama and coworkers.

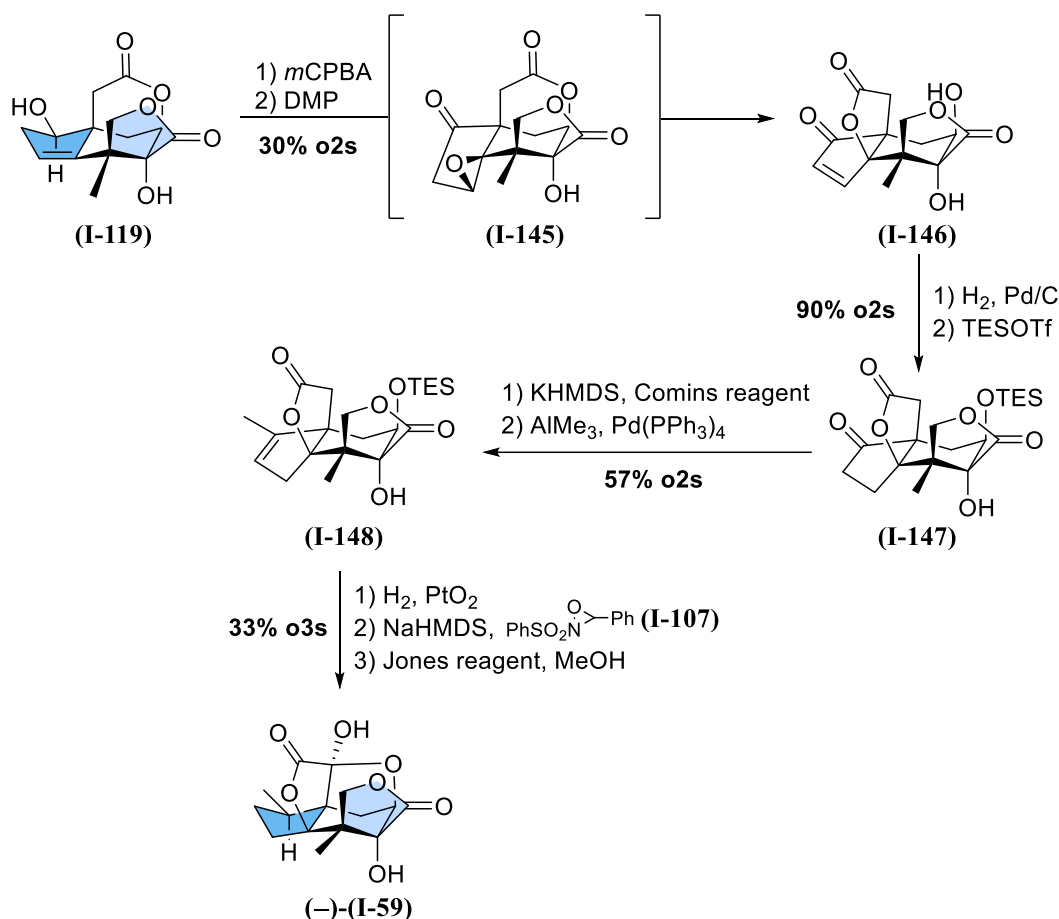
Recently, the asymmetric total synthesis of jiadifenin was reported by Micalizio.⁶² This last synthesis (Scheme 13) relies on the formal [2+2+2] annulation of homopropargyl alcohol (**I-136**), which produced diene (**I-138**) in high yields and diastereoselectivity. Subsequent key step, after straightforward transformations, was a tin-mediated reductive radical cyclization of selenide (**I-140**), which served for the γ -lactone moiety to be installed. Ethylester (**I-142**) was formed in this step along with desired cyclization product (**I-141**), probably deriving from C–H abstraction and subsequent fragmentation. Saegusa protocol was once again employed for desaturation,⁶⁰ and by means of Theodorakis's method⁵⁵ ODNM (**I-109**) was obtained. Jones oxidation yielded the desired product (–)-jiadifenin (–)-(I-58).



Scheme 13 – Total synthesis of (-)-jiadifenin (-)-**(I-58)** by Micalizio and coworkers.

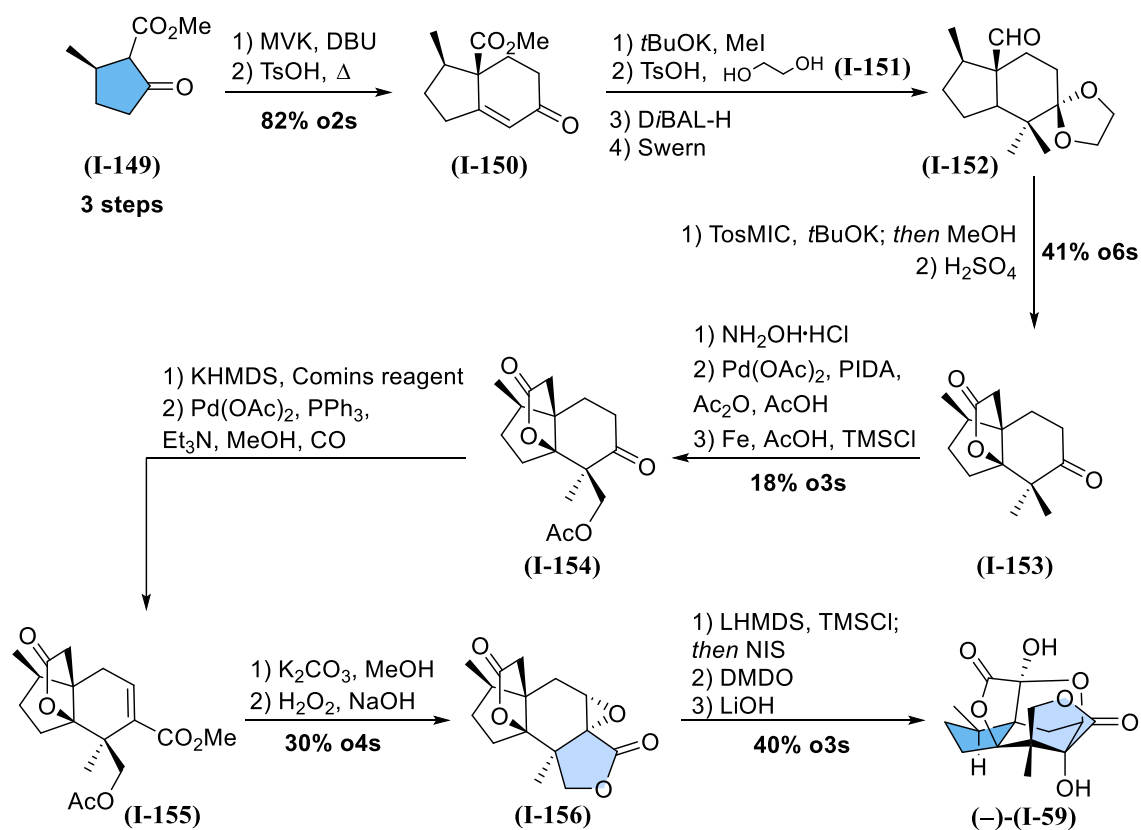
Even though jiadifenin (**(I-58)**) has been the target of many syntheses, the efforts to accomplish its concise synthesis do not compare to those for the synthesis of jiadifenolide (**(I-59)**). With its propellane

core and high neurotrophic activity,⁶³ jiadifenolide was the target molecule for Theodorakis and coworkers already in 2011,⁵⁴ just two years after its isolation.⁶³ They took advantage of intermediate (**I-119**) from their (-)-jiadifenin (-)-(**I-58**) synthesis to construct the propellane core (Scheme 14). First, oxidative treatment of the epoxide derived from known intermediate (**I-119**) resulted in epoxide elimination/translactonization cascade. With these two simple steps, the aforementioned propellane core of (**I-146**) was installed. At this point, Pd-catalyzed cross coupling furnished elongated product (**I-148**), that underwent known transformations to conclude the first total synthesis of (-)-jiadifenolide (-)-(**I-59**). After catalytic hydrogenation, the same intermediate (**I-98**) commented in Maimone's semisynthesis of (-)-majucin (-)-(**I-57**) (Scheme 8) is obtained.



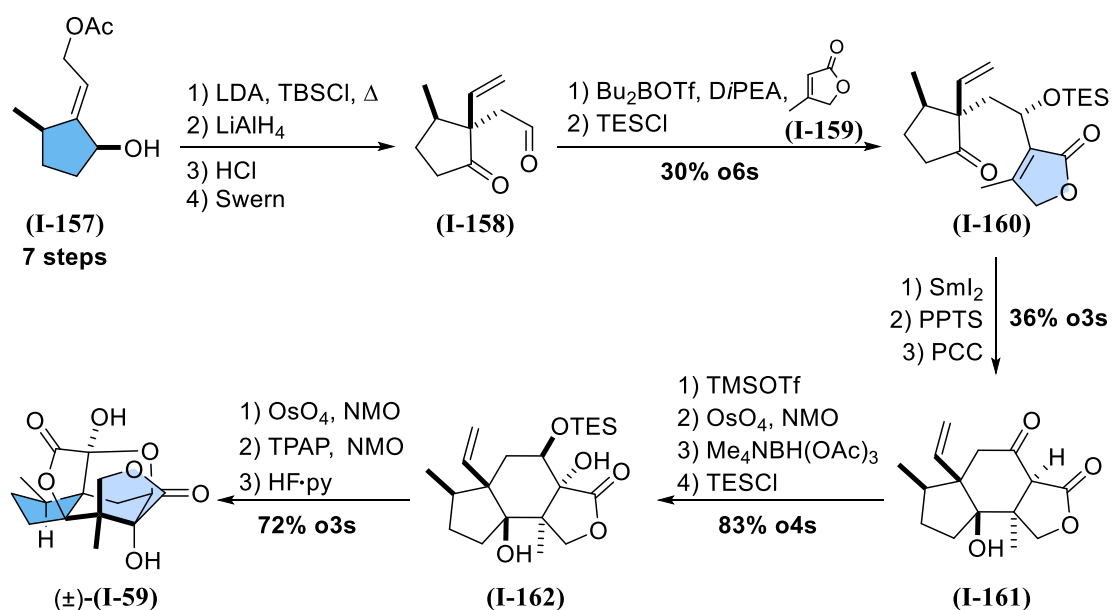
Scheme 14 – Total synthesis of (-)-jiadifenolide (-)-(**I-59**) by Theodorakis and coworkers.

The synthetic community did not have to wait long for the second synthetic effort to be effective: 2014 saw the rise of the *ex*-chiral pool synthesis of (-)-jiadifenolide (-)-(**I-59**) from Sorensen's group.⁶⁴ (*R*)-pulegone (+)-(**I-31**) was converted to enone (**I-150**) by means of a Robinson annulation (Scheme 15), which found precedents in Theodorakis's synthesis of jiadifenin (-)-(**I-58**).⁵⁵ A novel use of TosMIC on intermediate (**I-152**)⁶⁵ granted homologation, and consequent hydrolysis of the nitrile in acidic conditions resulted in direct formation of lactone (**I-153**). The oxime built on its ketone moiety allowed Pd-catalyzed acetoxylation, though in low regioselectivity. In spite of this, monoacetylated product (**I-154**) could be carboxylated *via* Pd-catalyzed cross coupling on the corresponding triflate. The desired lactone moiety was installed after basic treatment of substrate (**I-155**), while oxidation was accomplished through a iodoso-Pummerer rearrangement of epoxide (**I-156**).



Scheme 15 – Total synthesis of (-)-jiadifenolide (-)-(I-59) by Sorensen and coworkers.

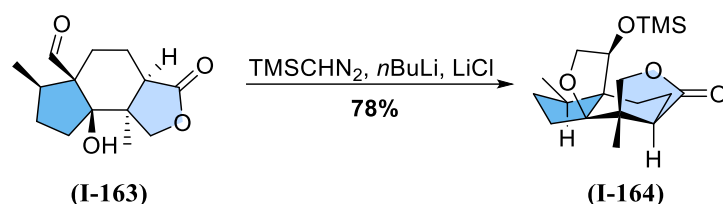
Paterson's approach⁶⁶ followed Sorensen's total synthesis but relied instead first on a Claisen-Ireland rearrangement to set one of the quaternary stereocenters, and later on on a Sml₂-mediated reductive cyclization to β -ketolactone (**I-161**) (Scheme 16). Rubottom-type oxidation and hydroxyl group-directed reduction resulted in α -hydroxylated compound (**I-162**), which could be easily converted into jiadifenolide (\pm)-(I-59) by means of two oxidative steps and a TES-deprotection.



Scheme 16 – Total synthesis of (\pm)-jiadifenolide (\pm)-(I-59) by Paterson and coworkers.

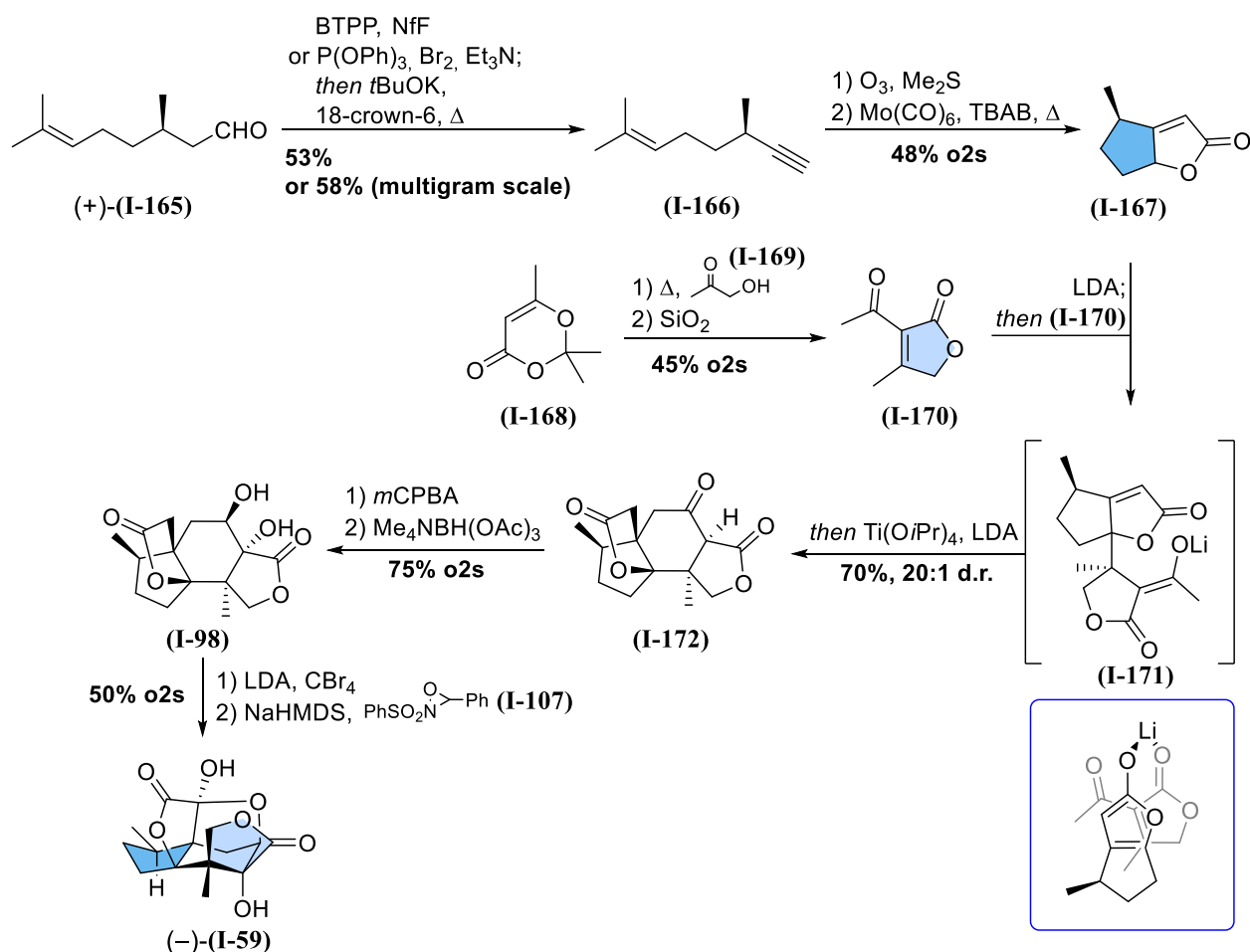
Gademann⁶⁷ and Zhang's⁶⁸ syntheses (formal and total, respectively) do not differ much from Paterson's approach, although one particular transformation is worth mentioning, and was employed

in Zhang's total synthesis. In order to construct the second lactone ring, they performed a [4+1] annulation with TMS-diazomethane (Scheme 17), whose anion is thought to attack the aldehyde in intermediate (**I-163**) thus inducing a Brook rearrangement; subsequent O–H insertion into the proximal tertiary alcohol would then afford intermediate (**I-164**).



Scheme 17 – [4+1] annulation with TMS-diazomethane in Zhang's total synthesis of (–)-jiadifenolide (–)-(**I-59**).

The most impressive total synthesis of (–)-jiadifenolide (–)-(**I-59**) is certainly Shenvi's multigram route,⁵³ in which jiadifenolide was obtained in only eight steps starting from chiral pool material, (+)-citronellal (+)-(**I-165**) (Scheme 18).

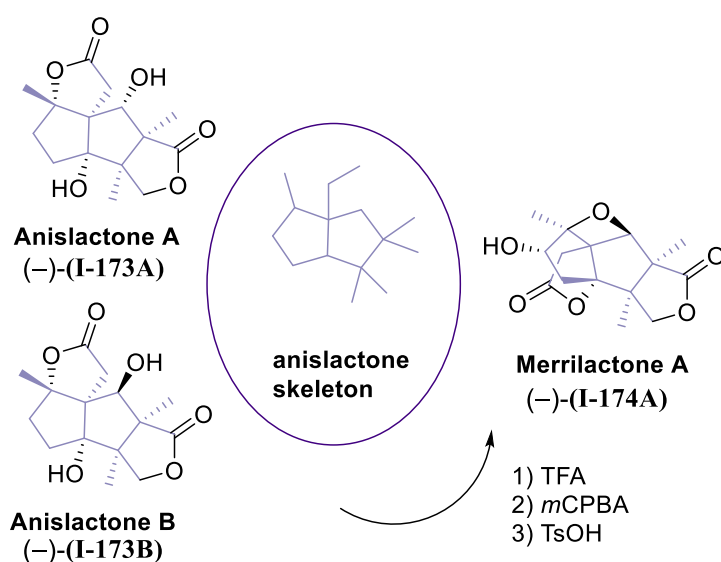


Scheme 18 – Shenvi's multigram total synthesis of (–)-jiadifenolide (–)-(**I-59**). Related intermediate (**I-171**), responsible for the high diastereoselectivity in the butenolide heterodimerization, is highlighted in the blue box.

Key step in this successful approach is the heterodimerization between butenolides (**I-167**) and (**I-170**), which led to di-lactone (**I-172**) in excellent diastereoselectivity which was explained through chelated intermediate (**I-171**). Four more steps, involving enol hydroxylation followed by O–H directed reduction, bromination and an evergreen hydroxylation protocol employing Davis' oxaziridine (**I-107**) yielded (–)-jiadifenolide (–)-(**I-59**) (7% yield over the longest sequence).

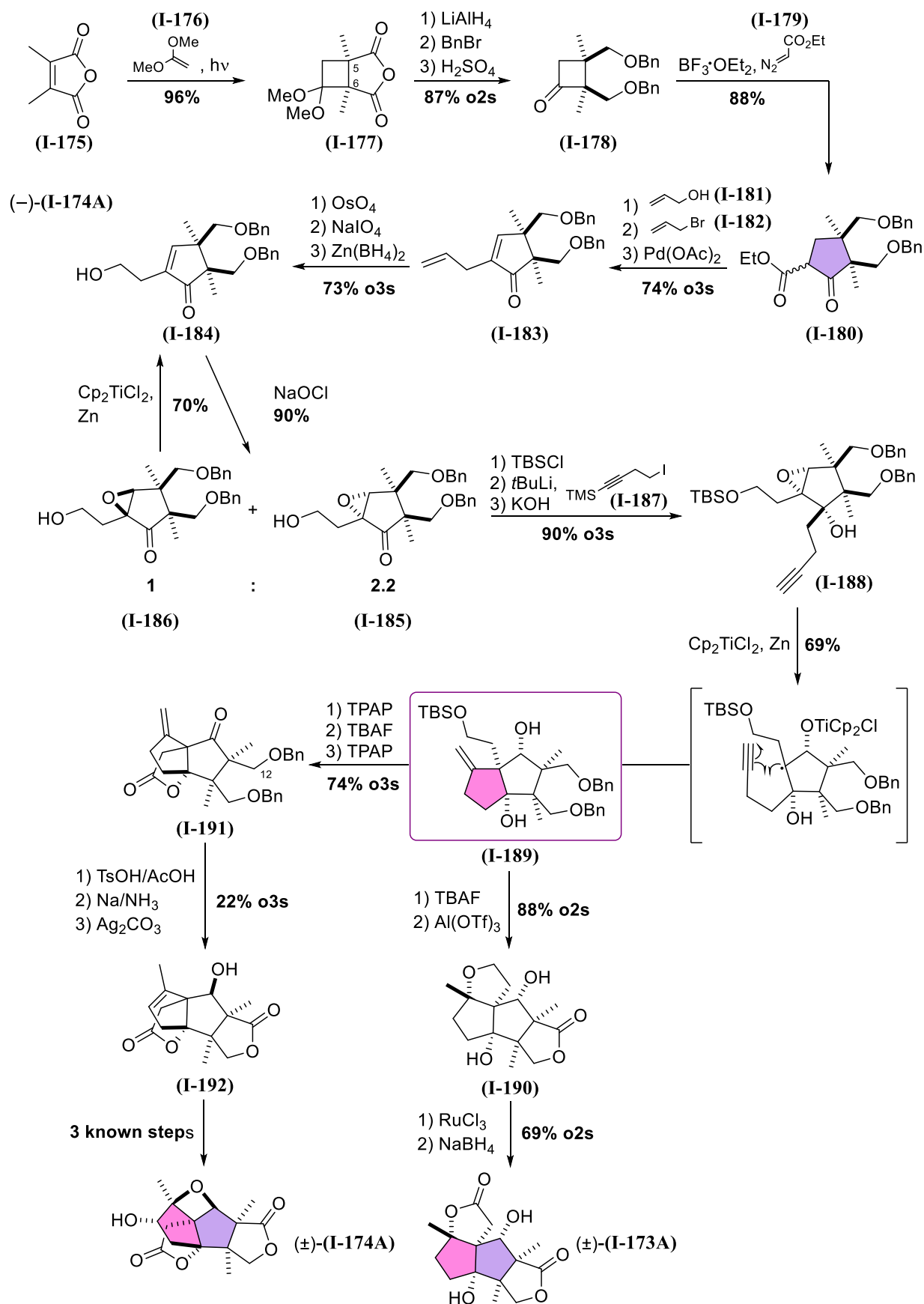
Anisclactones

The anisclactone family, with its 5,5-fused system, does not count as many members as the *secoprezizaane*-type sesquiterpenes, listing only about ten natural products, the most famous being anisclactones A and B (**I-173A** and **I-173B**) – isolated from *Illicium anisatum* by Kouno and coworkers⁶⁹ – and merrilactone A (**I-174A**), found in the pericarps from *Illicium merrilanum* by Fukuyama's research group.⁷⁰ The quite evident connection among these sesquiterpenes was demonstrated by the same research group, that one year later was able to convert anisclactone B (**I-173B**) into merrilactone A (**I-174A**) in three straightforward synthetic steps (Scheme 19).⁷¹



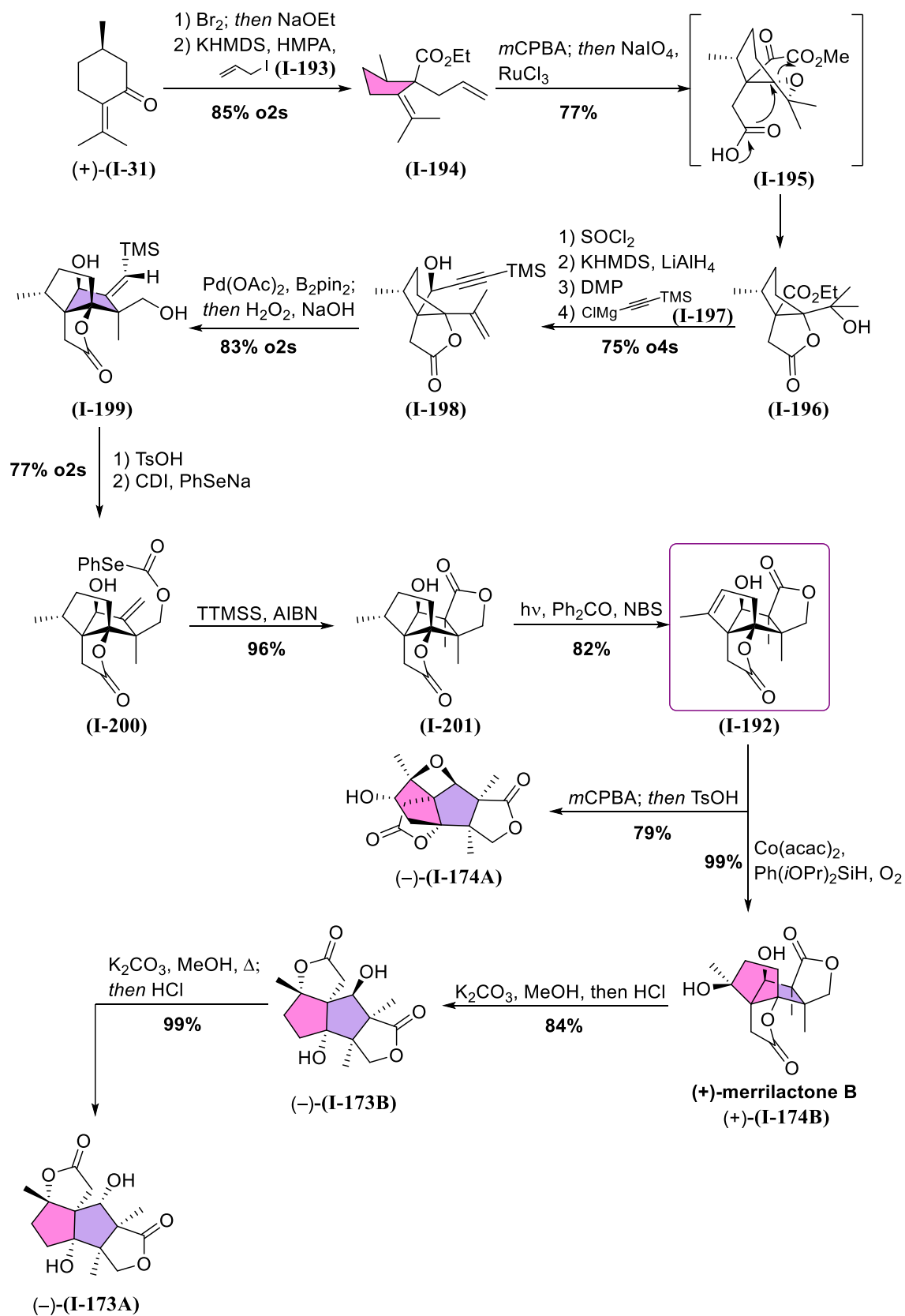
Scheme 19 – Most prominent anisclactones and interconversion of anisclactone B (**I-173B**) into merrilactone A (**I-174A**).

In spite of anisclactone B (**I-173B**) being possibly a biosynthetic intermediate on the way to merrilactone A (**I-174A**),⁷¹ this natural product and its epimer did not capture as much interest as their congener merrilactone A (**I-174A**). A comprehensive synthesis of these sesquiterpenes was published in 2010 by Greaney and coworkers,⁷² and featured a common intermediate with the carbon framework of both anisclactone A (**I-173A**) and merrilactone A (**I-174A**). The synthesis took advantage of a [2+2] photocycloaddition (Scheme 20) to install the *cis* junction at carbons 5 and 6, which was translocated untouched in cyclopentanone (**I-180**), obtained through a Demjanov-Tiffeneau ring expansion. A Tsuji-Trost decarboxylation-dehydrogenation sequence yielded alkene (**I-183**), which was easily converted to primary alcohol (**I-184**). Epoxidation of the enone produced desired and undesired epoxides (**I-185**) and (**I-186**). Both products could conveniently be used; desired epoxide (**I-185**) underwent a 1,2-addition with high diastereoselectivity deriving from the shielding effect of the epoxide itself, while undesired intermediate (**I-186**) could be recycled and reconverted to the correct epoxide by means of a Ti(III)-mediated homolytic cleavage. At this point, the stage was set for a Ti(III)-mediated epoxide cleavage/5-*exo*-*dig* cyclization, whose application will be further discussed in a separate paragraph, and that resulted in the aforementioned common intermediate (**I-189**). The way to (±)-anisclactone A (±)-**I-173A** involved Lewis-acidic conditions to form the tetrahydrofuran ring in (**I-190**), selective oxidations upon deprotection, and final reduction back to the secondary alcohol. Key transformation to (±)-merrilactone A (±)-**I-174A** was the double bond isomerization, carried out under acidic conditions, and a selective Fetizon oxidation targeting C12. Known intermediate (**I-192**)⁷³ concluded the formal synthesis of (±)-merrilactone A (±)-**I-174A**.



Scheme 20 – Comprehensive synthesis of anisactones from Greaney and coworkers; colour code switched to shades of purple for the anisactone family.

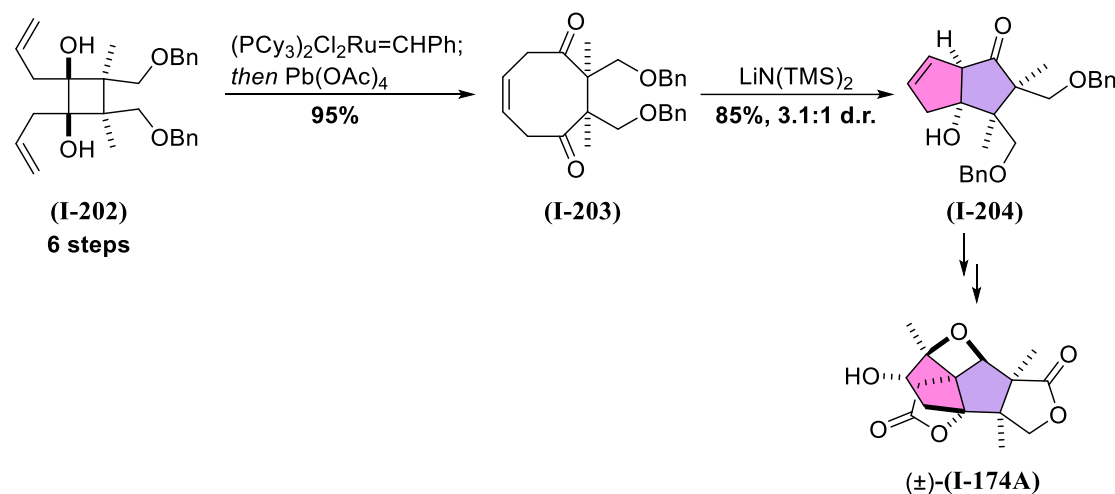
Quite recently, anisactones A and B, as well as merrilactone A, were targeted by Zhang, Zhang and coworkers⁷⁴ in their divergent approach towards Illiciums, summarized in Scheme 21.



Scheme 21 – Comprehensive asymmetric synthesis of anisactones from Zhang, Zhang and coworkers.

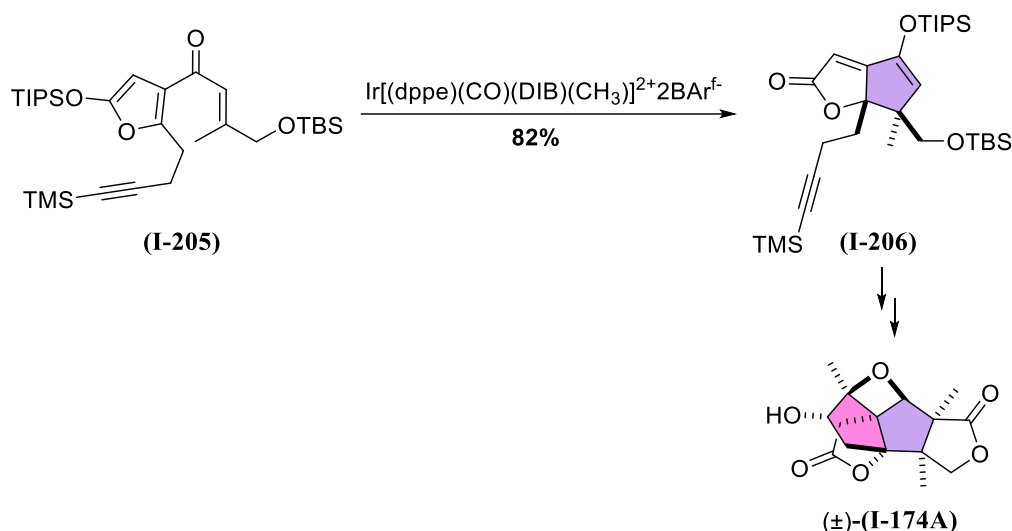
Their strategy (Scheme 21) is based on a mild late stage desaturation, which produced known intermediate (**I-192**),⁷¹ in 12 synthetic steps. With a downhill thermodynamic sequence, trisubstituted alkene (**I-192**) could sequentially be converted into (+)-merrilactone B (+)-(**I-174B**), (-)-anisilactone B (-)-(**I-173B**) and (-)-anisilactone A (-)-(**I-173A**). The total synthesis of (-)-merrilactone A (-)-(**I-174A**) was also accomplished. The starting material for such convenient transformations was synthesized starting from (*R*)-pulegone (+)-(**I-31**), that underwent a Favorskii ring contraction, diastereoselective allylation and regioselective epoxidation to a β -epoxyester. Oxidative cleavage of the terminal double bond of this last intermediate (see carboxylic acid (**I-195**)) triggered epoxide opening and resulted in lactone (**I-196**); exploiting substrate control, the stage was set for a key borylative cyclization, that yielded TMS-alkene (**I-198**). The second lactone ring was readily built *via* 5-*exo*-trig radical cyclization of selenocarbonate (**I-200**). Pivotal desaturation occurred under irradiation with violet LED, in the presence of NBS and benzophenone. Target (-)-merrilactone (-)-(**I-174A**) A was at that point two steps away. Co-catalyzed Mukaiyama hydration was instead successful to convert the common intermediate to (+)-merrilactone B (+)-(**I-174B**), that underwent transesterification in basic conditions resulting in (-)-anisilactone B (-)-(**I-173B**); further treatment with base at higher temperatures epimerized this natural product to (-)-anisilactone A (-)-(**I-173A**).

As already mentioned, merrilactone A (**I-174A**) was way more successful than anisilactones A and B (**I-173A** and **B**), attracting the attention of multiple research groups: similarly to Greaney and coworkers, a [2+2] approach had been employed some years before by Hirma and coworkers⁷⁵ to set the *cis* 5,6-junction. Their key step features a desymmetrization of (**I-203**) *meso*-diketone *via* an aldol reaction, as depicted in Scheme 22:



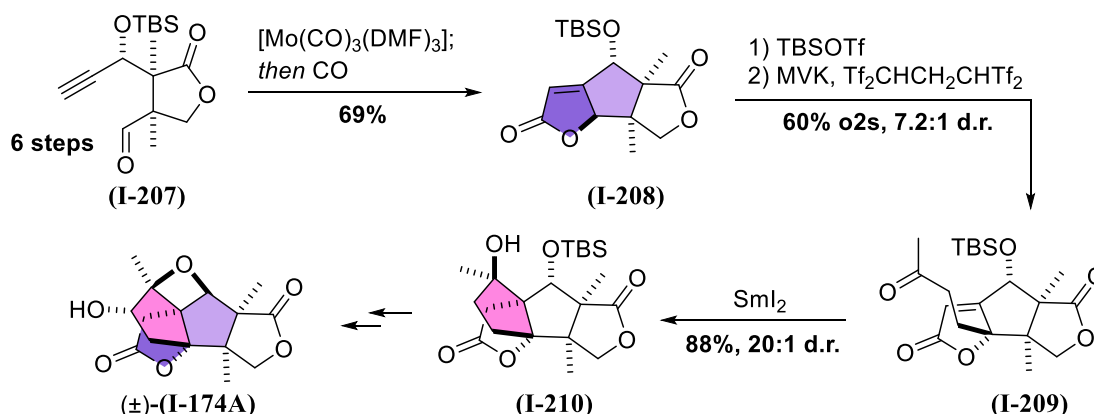
Scheme 22 – Key steps in Hirma and coworkers' approach to (\pm) -merrilactone A $(\pm)\text{-I-174A}$.

Racemic merrilactone A $(\pm)\text{-I-174A}$ was also synthesized in 2008 by Frontier and coworkers⁷⁶ employing the Nazarov cyclization of silyloxyfuran (**I-205**) for the construction of ring B, highlighted in Scheme 23. A more detailed insight into this approach for the construction of 5-membered-rings will be given in the next chapter.



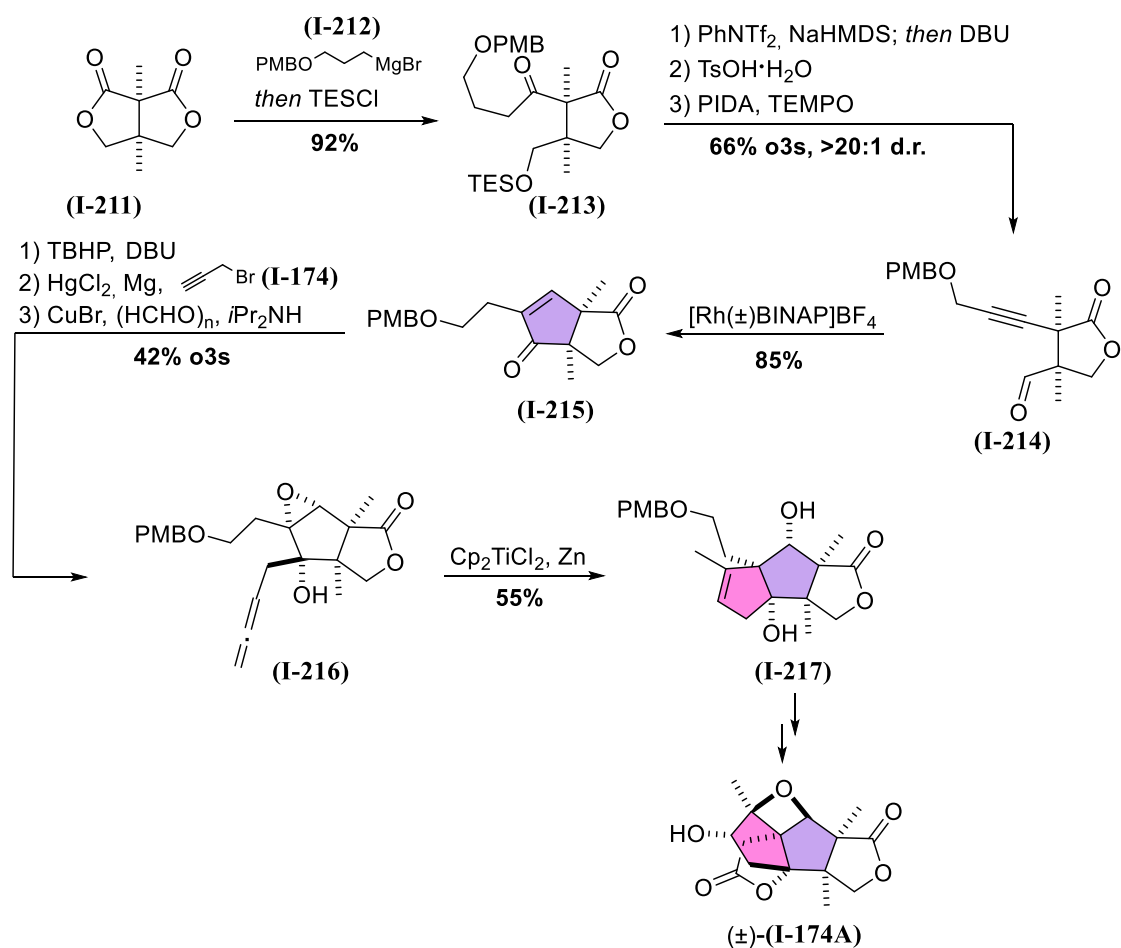
Scheme 23 – Key steps in Frontier and coworkers' approach to (±)-merrilactone A (±)-(I-174A).

The construction of ring B and D (highlighted in light and dark violet respectively, Scheme 24) *via* hetero-Pauson-Khand (**I-207** to **I-208**) was part of the strategy employed by Zhai et al. in their total synthesis of (±)-merrilactone A (±)-(I-174A).⁷⁷ Another strategic crucial point of their approach concerned the formation of ring C, highlighted in pink, that employs a vinylogous Mukaiyama-Michael addition⁷⁸ to install the methylketone moiety, followed by a radical cyclization initiated by SmI_2 for ring closure. In particular, the presence of the bulky protecting group in (I-208) allowed good facial selectivity in the first transformation, which was further implemented in the cyclization step, furnishing tetracycle (I-210) as essentially a single diastereoisomer.



Scheme 24 – Key steps in Zhai and coworkers' approach to (±)-merrilactone A (±)-(I-174A).

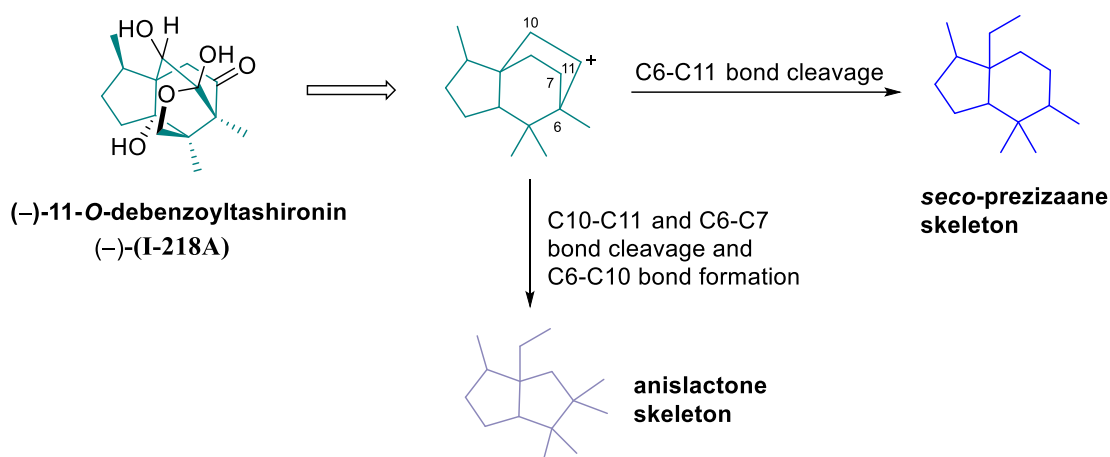
A different strategy was employed by Wang and coworkers in their recent racemic synthesis of merrilactone,⁷⁹ based on desymmetrization of a *meso*-intermediate as in Hirama's synthesis.⁷⁵ This transformation (Scheme 25) smoothly occurred on C_s -symmetric dilactone (I-211) through treatment with an organometallic reagent; dehydration and oxidation of the deprotected alcohol produced intermediate (I-214) that underwent a high yielding intramolecular hydroacylation, resulting in enone (I-215). Ring C, highlighted in pink, was constructed *via* Ti(III) reductive epoxide opening and subsequent 5-*exo*-dig cyclization onto allene (I-216). Desired ABC product (I-217) was then successfully transformed into (±)-merrilactone A (±)-(I-174A).



Scheme 25 – Key steps in Wang and coworkers' approach to (±)-merrilactone A (±-(I-174A)).

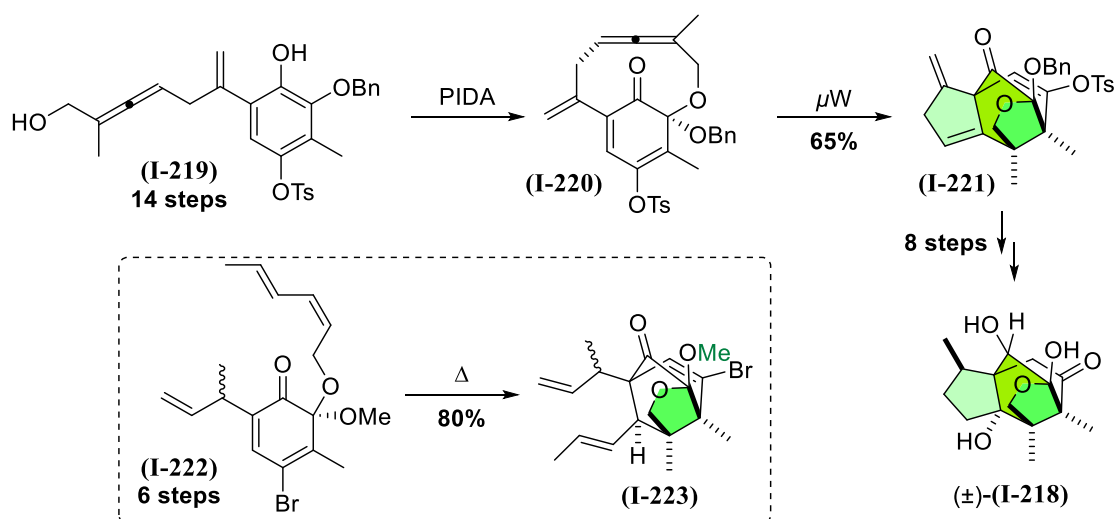
Allo-cedranes

The *allo*-cedrane family does not count as many members as the other two *Illicium*-derived classes and surely cannot brag any renowned sesquiterpene as jiadifenolide (**I-59**) or merrilactone A (**I-174A**), merely counting (-)-11-*O*-debenzoyltashironin (-)-(**I-218**) as most prominent *allo*-cedrane-type natural product. In spite of this, the *allo*-cedrane skeleton maintains its importance, since it is thought to be a key intermediate in the biosynthesis of the other two classes of *Illicium*s. In the paragraph dedicated to the biosynthesis of illisimonin A, a more detailed explanation on how the *allo*-cedrane skeleton would originate such a complex cage-like structure will be given. As for the biosynthetic origin of *seco*-prezizaanes, the *allo*-cedrane cation is supposed to undergo C6-C11 bond cleavage, thus originating *seco*-prezizaane derived compounds. Anisactones would instead be derived from an *allo*-cedrane framework *via* consequent cleavage of the C10-11 and C6-C7 bonds. C6 and C10 would then form the new 5-membered ring, as shown in Scheme 26.⁷¹



Scheme 26 – Biosynthetic relationship between the *allo*-cedrane cation and the other *Illicium*s classes, as well as *allo*-cedranes' most prominent member (-)-11-*O*-debenzoyltashironin (-)-(**I-218**).

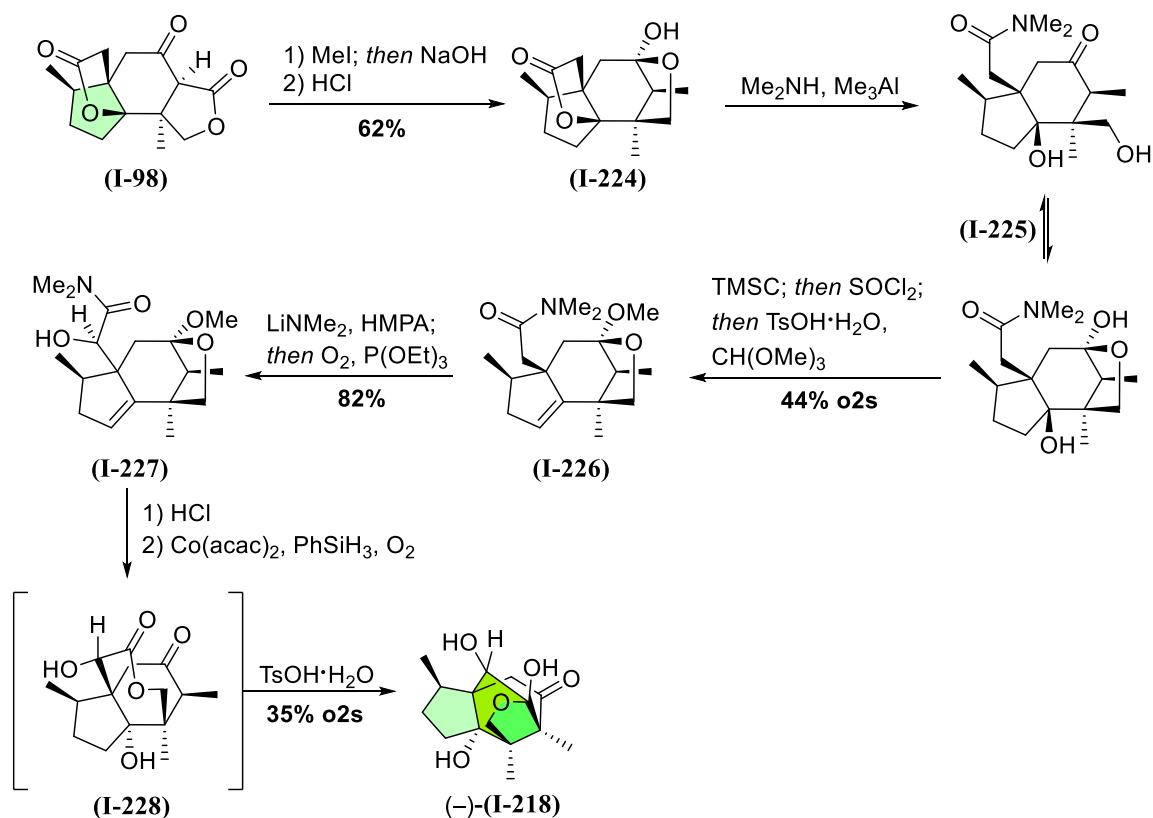
Among the synthetic research dedicated to (\pm)-11-*O*-debenzoyltashironin (\pm)-(**I-218**), Danishefsky and coworkers, who had been involved in the synthesis of other *Illicium* sesquiterpenes,^{57,73} and Mehta's research group targeted the carbon scaffold of this *allo*-cedrane-type sesquiterpene through a Diels-Alder reaction. Their independent approaches are summarized in Scheme 27.



Scheme 27 – Key steps in Danishefsky's, on the top, and Mehta's syntheses, on the bottom, of (\pm)-11-*O*-debenzoyltashironin (\pm)-(**I-218**) and its methyl-ether respectively. Colour code switched to green for *allo*-cedranes.

Danishefsky and coworkers employed an oxidative dearomatization induced by PIDA in order to produce bridging allene (**I-220**), which underwent a transannular Diels-Alder cycloaddition which built in one step the entire tetracyclic skeleton of the natural product. Eight more steps concluded the total synthesis of racemic 11-*O*-debenzoyltashironin (\pm)-(**I-218**).⁸⁰ In a similar approach, Mehta and coworkers cyclized dearomatized intermediate (**I-222**), affording triene (**I-223**) under thermal conditions.⁸¹ However, their synthesis only afforded 11-*O*-methyldebenzoyltashironin (not shown), since the efforts towards demethylation (position highlighted in Scheme 27) were unfruitful.⁸²

The synthesis of the natural enantiomer (-)-(**I-218**) was accomplished in only ten synthetic steps by Shenvi et al. in 2017.⁸³ In this work they took advantage of the butenolide heterodimerization strategy developed a couple of years before in their studies towards the synthesis of (-)-jiadifenolide (-)-(**I-59**),⁵³ and of the same intermediate (**I-98**), obtained in gram-scale (Scheme 28). This dilactone derivative was α -methylated, and ring A was opened in order to perform a decarboxylation, that resulted in ketalization of the liberated primary alcohol moiety. Amidation, dehydration and new ketal formation set the stage for a challenging α -hydroxylation of amide (**I-226**), which occurred with high selectivity, explained through the minimized steric hindrance of the amide enolate when rotating away from the ketal. The carbonyl group protected as ketal was liberated in acidic conditions; the resulting ketoamide was ready to undergo an unusual lactonization, allowed by the proximity between the amide itself and the primary alcohol. Mukaiyama hydration and acidic treatment formed the missing C-C bond, yielding (-)-11-*O*-debenzoyltashironin (-)-(**I-218**).



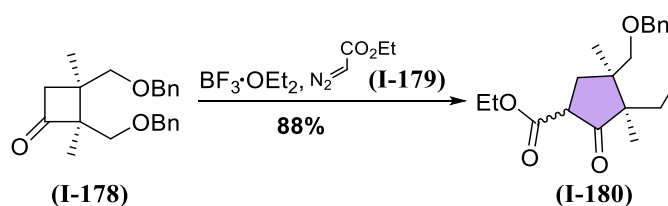
Scheme 28 – Shenvi’s approach to the synthesis of (-)-11-*O*-debenzoyltashironin (-)-(**I-218**) from known intermediate (**I-98**).

Challenges in total synthesis

The previous chapter focused on the synthesis of various *Illiciums* and tried to give an overview on the main challenges that a synthetic chemist faces, with an eye on how such complex structures could be conquered and on which techniques were chosen to answer to a synthetic problem. This is one of the most interesting sides of natural products synthesis, where structural demands translate into a novel problem to be solved and new methodologies to be developed – or old reactions to be reinvented. In this context, the next paragraphs will deal with the synthetic solutions that were found to be decisive while approaching the synthesis of illisimonin A, starting with the construction of 5-membered rings, that was a leitmotiv in the *Illiciums* chapter, and continuing with more specific reaction classes. The purpose is to give the reader a full overview on the chemical transformation that will be encountered along the way, and a background of synthetic examples in which these reactions were successful.

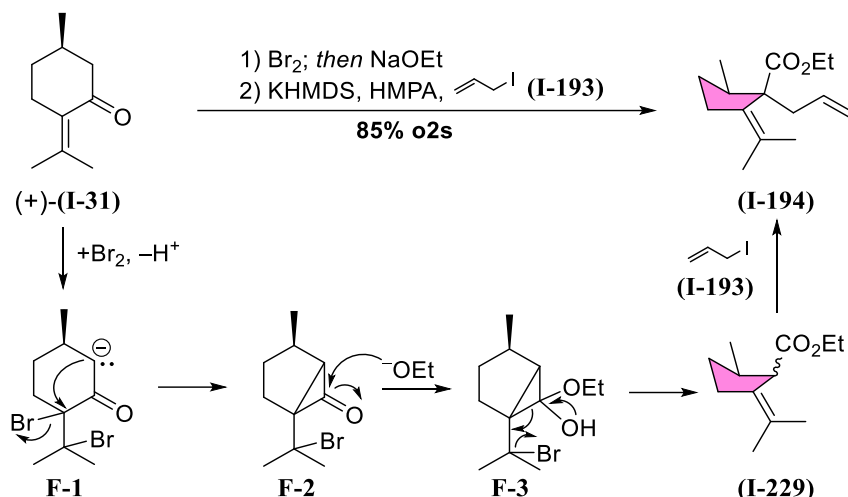
Construction of 5-membered rings

At the dawn of organic chemistry, when the basis of today's organic chemist's basic background were set, 5-membered rings were occupying a place of honour among cycloalkanes. Specifically, when "Baeyer's strain theory" was proposed, Adolf Von Baeyer thought that 5-membered carbon rings were the most stable ones and suffered from poor ring strain, due to the internal angles being close to the ideal 109°. ^{84,85} His theory was though referring to a flat ring, and was proved wrong by experiments on combustion heat, that demonstrated how cyclohexane is the most stable cycloalkane and has no strain; strain energy in cyclopentane is 25 kJ/mol higher. In spite of this difference, 5- and 6-membered rings are both ubiquitous in natural products, the "thermodynamic reign". For this reason, it is not surprising that reactions that are specifically targeting 5-membered rings were developed over the last decades. In the previous chapter, five-membered rings have been constructed with various methods, like the HWE olefination employed in Danishefsky's synthesis of jiadifenin (**I-58**),⁵⁷ or the aldol approach in Hirama's synthesis of merrilactone A (**I-174A**),⁷⁵ or with an Heck-cross coupling in Fukuyama's endeavours on jiadifenin (**I-58**).⁶¹ An interesting hydroacylation resulted in a 5-membered ring in Wang's synthesis of merrilactone A (–)(**I-174A**),⁷⁹ while a Ti-mediated radical cyclization has been successfully used in Greaney's synthesis of anislactones.⁷² All of these methods took advantage of "open intermediates" for building up the desired ring, and featured quite general reactions applied to the synthesis of rings of this specific dimension. It is of course possible to build five-membered rings from other cyclic molecules, *via* ring expansion or contraction. The first is the case for the above mentioned synthesis of various anislactones by Greaney and coworkers,⁷² in which a Demjanov-Tiffeneau rearrangement took place on cyclobutanone-derivative (**I-178**) to yield desired pentanone (**I-180**) (Scheme 29). Effective on various ring dimensions, the reaction consists on a variation of the semipinacol rearrangement, that will be more extensively dealt with in a separate chapter, in which a 2-aminoalcohol is transformed into a diazocompound by treatment with nitrous acid. The presence of this excellent leaving group causes an alkyl residue to 1,2-migrate, resulting in ring enlargement. The driving force of this process is the stabilization of the unstable primary cation generated by nitrogen liberation, as well as the formation of a stable C=O bond. As in semipinacol rearrangements, migration needs antiperiplanarity in between leaving group and migrating residue, and it is generally determined by steric hindrance of the two possible residues.⁸⁶



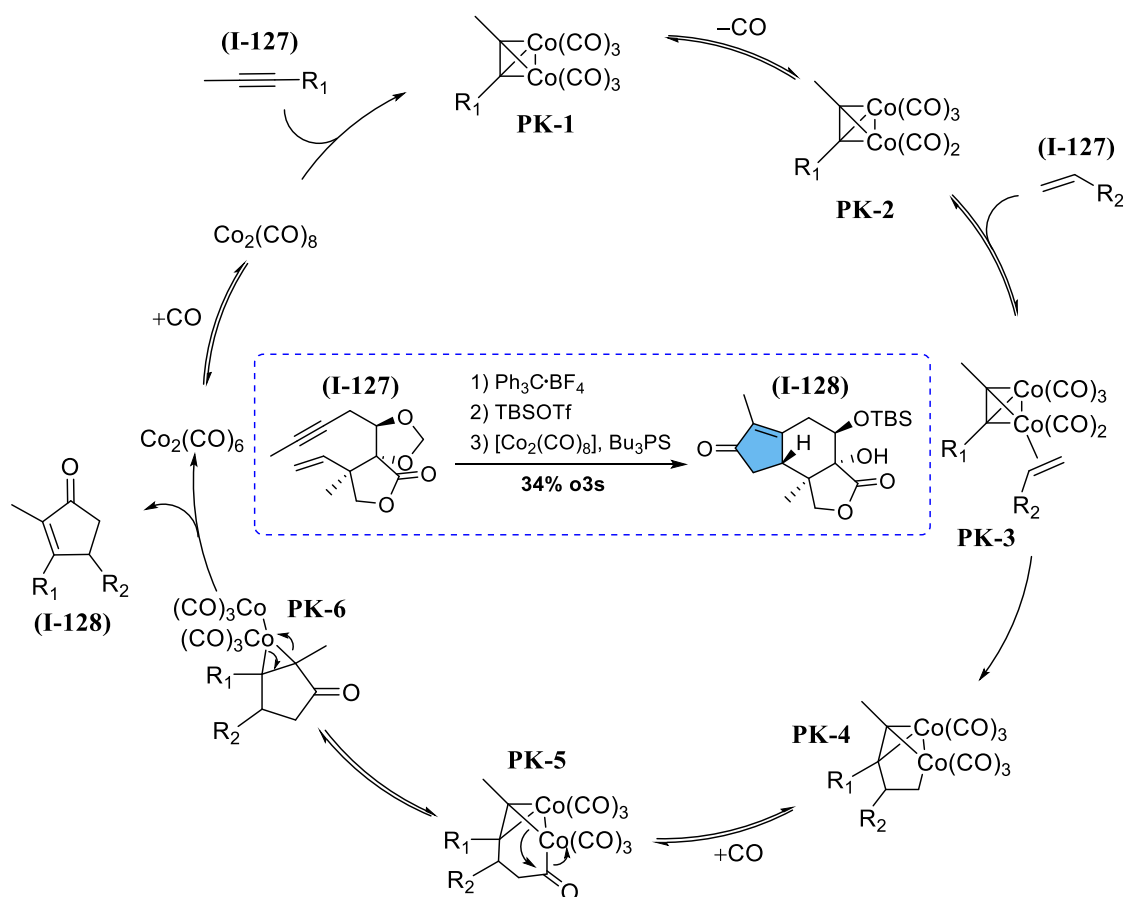
Scheme 29 – Greaney's Demjanov-Tiffeneau ring expansion.

Ring contraction is a valid alternative to ring enlargement, and was for instance employed by Zhang, Zhang and coworkers in their synthesis of merrilactone (Scheme 30).⁶⁸ Favorskii rearrangement is an anionic process in which an α -haloketone, like (*R*)-pulegone (+)-**(I-31)**, is treated under basic conditions to form a cyclopropanone intermediate (F2) that is in turn opened by nucleophilic attack, yielding a carboxylic acid derivative as in the case of reported ethylester (**(I-229)**).



Scheme 30 – Zhang and Zhang’s Favorskii ring contraction.

In the total syntheses of (–)-jiadifenin (–)-**(I-58)** and (±)-merrilactone A (±)-**(I-174A)**,^{59,77} Zhai and coworkers took advantage of the Pauson-Khand reaction (and its hetero-PK variation), that found application also in Shenvi’s multigram synthesis of (–)-jiadifenolide (–)-**(I-59)**.⁵³ This reaction, well known and employed for the formation of 5-membered rings since the 70s, consists of a formal [2+2+1] cycloaddition between an alkene, an alkyne and carbon monoxide in the presence of cobalt octacarbonyl or variations. Mechanistically, as depicted in Scheme 31, the reaction is proposed to start with coordination of the alkyne to the cobalt complex (**(PK-1)**), followed by coordination of the alkene counterpart (**(PK-3)**) promoted by loss of carbon monoxide, and its insertion (**(PK-4)**). At this point, carbon monoxide would insert into the M–C bond (**(PK-5)**), and reductive elimination (**(PK-6)**) would complete the catalytic cycle. Some authors suggest instead that the loss of carbon monoxide would precede the olefin coordination and its insertion.⁸⁷ It is important to underline that, in the mechanism reported in Scheme 31, R_1 and R_2 specifically refer to Zhai’s Pauson-Khand, meaning that the orientation of the substituents does not refer to optimal steric hindrance but takes into consideration the geometrical constraints of the starting material. The alkene and alkyne were reported as separate entities just in order to simplify the drawing.

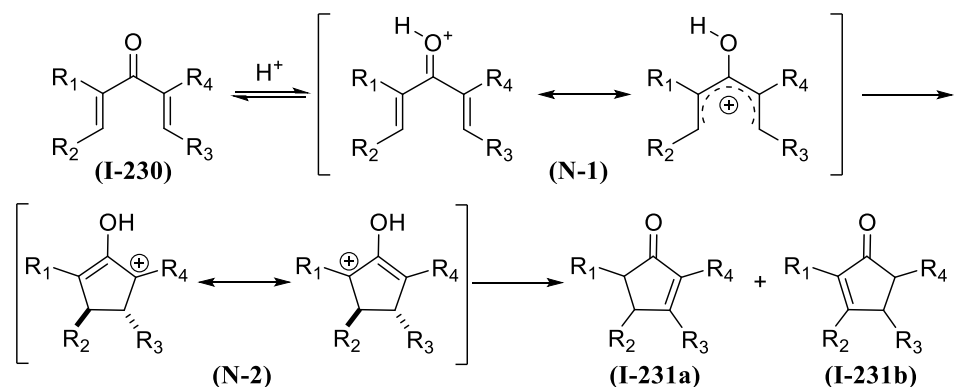


Scheme 31 – Mechanism of the Pauson Khand reaction referring to Zhai's synthesis connectivity.

The last reaction presented in this chapter is the Nazarov cyclization, that was successful in the synthesis of (\pm)-merrilactone A (\pm)-**(I-174A)** by Frontier and coworkers.⁷⁶ Specifically, the next paragraph will focus on this kind of cyclization starting from its discovery, in the 40s, and describing the implementations and/or new variants that were developed over the last decades.

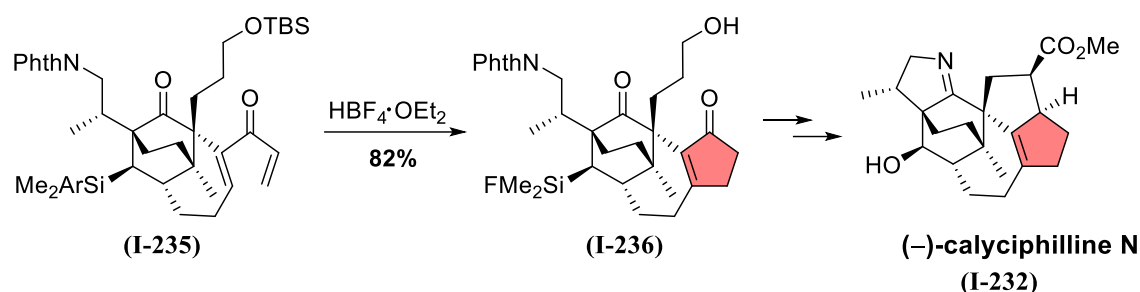
Nazarov cyclizations and interrupted Nazarovs

The first example of Nazarov cyclization was reported in 1941 by the homonym Russian chemist Ivan Nazarov who, while researching on divinylketones, realized that they undergo a cyclization under acidic conditions. The result of this transformation are variously substituted cyclopentenones. The reaction proceeds *via* a 4π -electrocyclization to generate an oxyallyl cation (**N-2**), that is likely to β -eliminate, generating the desired product, as reported in Scheme 32.



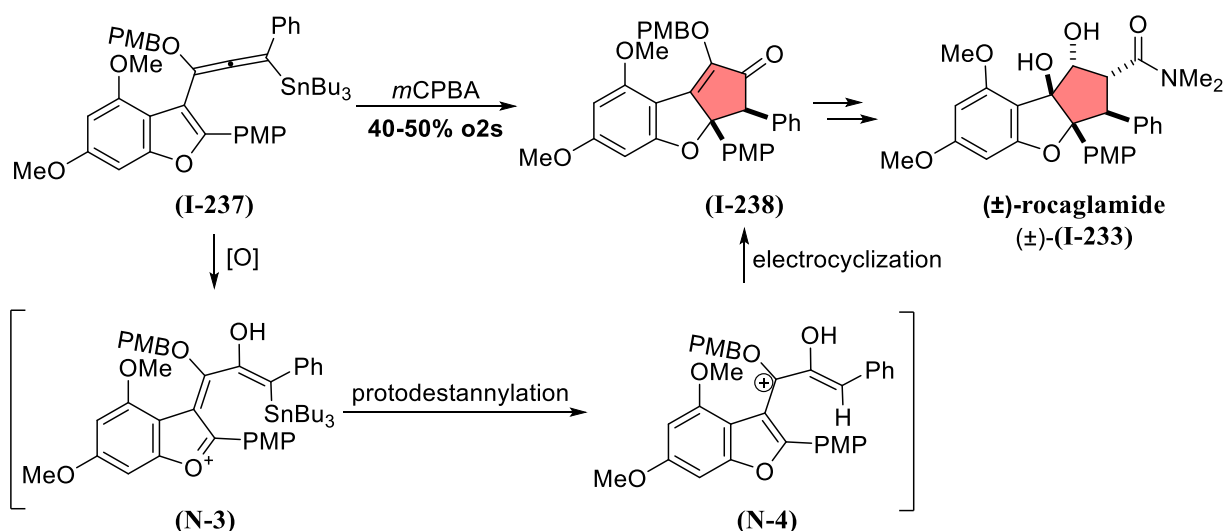
Scheme 32 – Mechanism of the Nazarov cyclization.

Numerous total syntheses took advantage of this cyclization as a key step: for instance, quite recently the synthesis of (-)-calyciphilline N (-)-(**I-232**),⁸⁸ (±)-rocaglamide (±)-(**I-233**),⁸⁹ and (-)-farnesin (-)-(**I-234**)⁹⁰ were reported, in which a Nazarov-cyclization approach was successful for installing the cyclopentenone moiety with high control of the stereochemical outcome due to the pericyclic nature of the Nazarov reaction on one hand, as well as substrate control on the other hand. Specifically, when Smith and coworkers approached the core of (-)-calyciphilline N (-)-(**I-232**),⁸⁸ a *Daphniphyllum* alkaloid, ring E (highlighted in red in Scheme 33) was the perfect target for a classic Nazarov cyclization, that smoothly proceeded by treating the initial dienone with HBF₄·OEt₂.



Scheme 33 – Nazarov key step in the synthesis of (-)-calyciphilline N (-)-(**I-232**). Colour code switched to red for Nazarov-constructed rings.

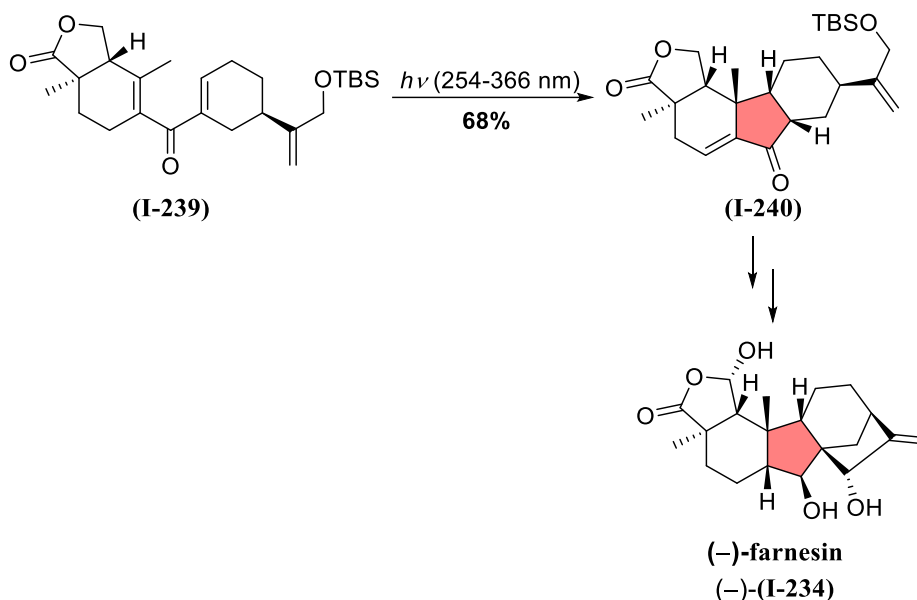
A less classic example is the oxidation-initiated Nazarov cyclization in the synthesis of (±)-rocaglamide (±)-(**I-233**) by Frontier's research group.⁸⁹ After their first generation approach featuring a dienone-like Nazarov failed, they decided to generate the pentadienyl cation *via* oxidation of alkoxyallene (**I-237**), as in Scheme 34. In particular, they found that treating allenylstannane (**I-237**) with *m*CPBA was resulting in oxidation of the allene in the central position or in allene oxide formation; consequent ring-opening revealed the masked pentadienyl cation (**N-3**).⁹¹ At this point, protodestannylation produced less sterically hindered pentadienyl cation (**N-4**). This is the moment in which conrotatory electrocyclization of the enolate occurred, furnishing cyclopentenone (**I-238**). In this particular case, no Lewis acid is promoting the cyclization.



Scheme 34 – Nazarov key step in the synthesis of (±)-rocaglamide (±)-(**I-233**). First step, allene formation, is not shown.

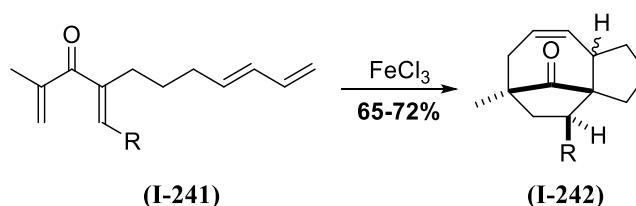
The synthesis of (-)-farnesin (-)-(**I-234**) from Gao and coworkers⁹⁰ represents another case in which no acidic condition is required, but irradiation of initial dienone (**I-239**) is inducing the cyclization (Scheme 35). Unlike the classic acid-promoted ground-state Nazarov reaction, the excited-state

Nazarov reaction promotes disrotatory cyclization, resulting in *syn-syn-syn* skeleton (**I-240**), leading to the correct stereotriad for the targeted natural product.



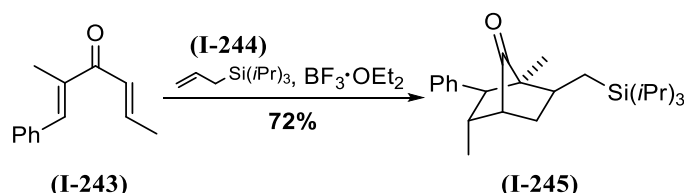
Scheme 35 – Nazarov key step in the synthesis of (-)-farnesin (-)-(I-234).

In the late 90s, the group of West reported that the oxyallyl cation could be trapped by a nucleophile in particular conditions, instead of undergoing the aforementioned β -elimination. They named this variant of the original reaction “interrupted Nazarov”. The first example, reported in Scheme 36, was involving the reaction of a dienone functionalized with a diene moiety (as in (**I-241**)), that behaved as the 4π -counterpart of the oxyallyl cation in a [4+3]-cycloaddition.⁹²



Scheme 36 – Interrupted Nazarov cyclization: Nazarov/[4+3] sequence with a diene from West and coworkers.

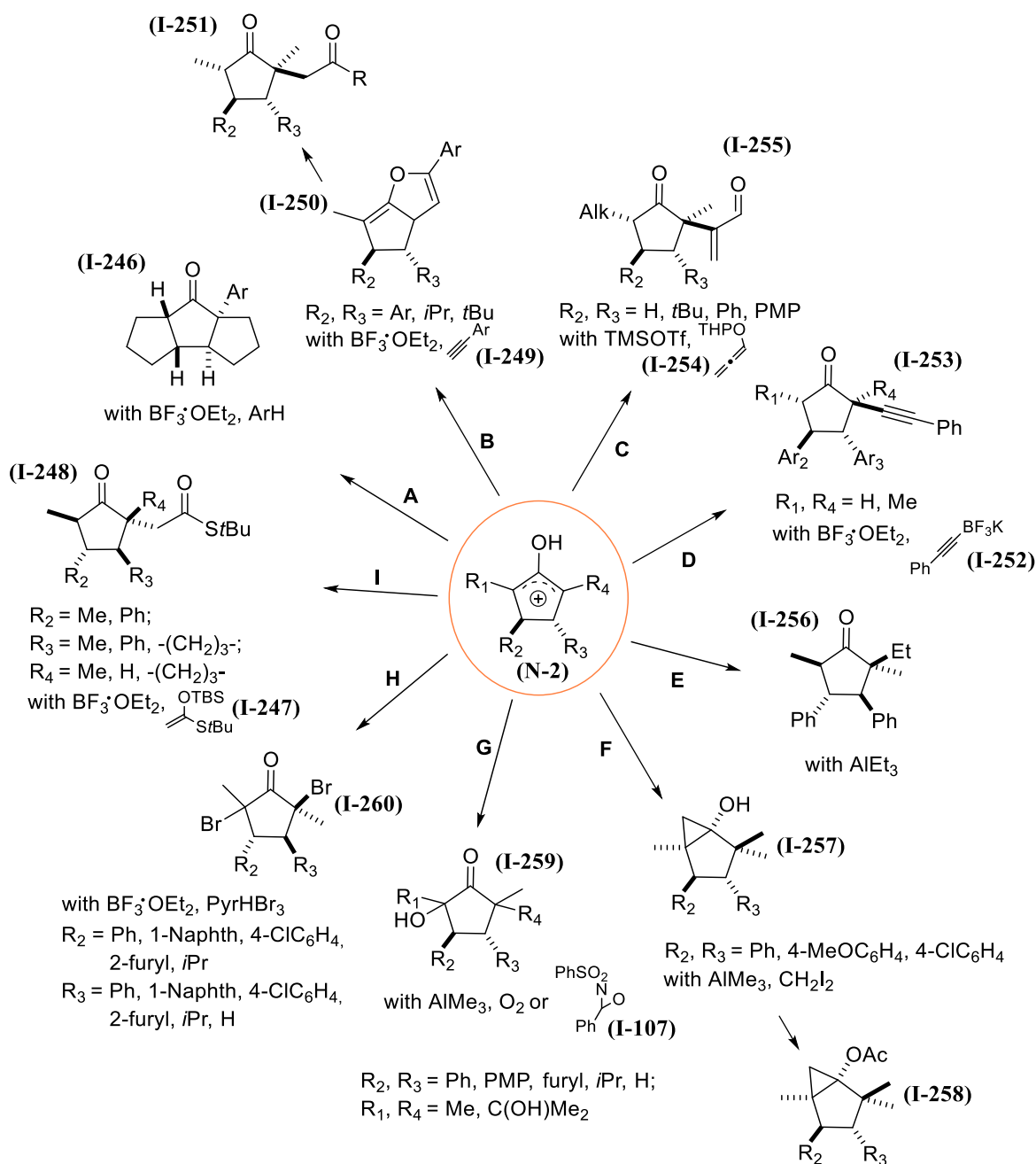
One year later, the same research group observed a [3+2]-termination for a Nazarov cyclization in which the electronrich term was an allylsilane:⁹³



Scheme 37 – Interrupted Nazarov cyclization: Nazarov/[3+2] sequence with allylsilane (**I-244**) from West and coworkers.

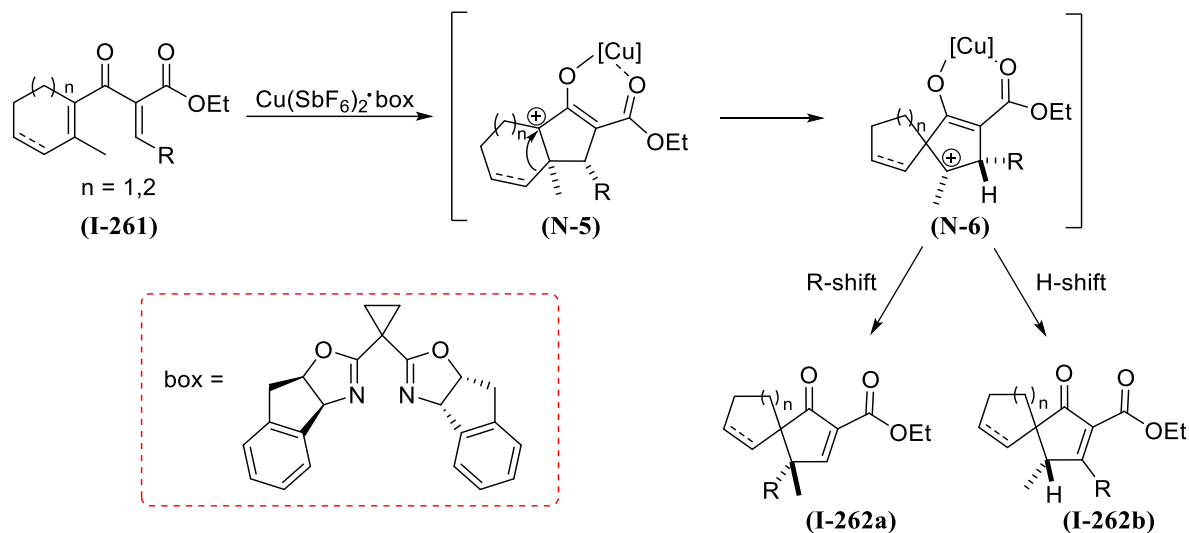
Other nucleophilic counterparts are known to react with Nazarov cations, in what could be defined as an S_N1 -like process.⁹⁴ Specifically, various arenes have been studied from West and coworkers in order to insert an (hetero)aromatic function into the cyclopentanone (Scheme 38, A),⁹⁵ as well as syloxyalkenes (**I-247**), which are able to undergo a Mukaiyama-Michael addition (Scheme 38, I).⁹⁶

Alkynes were found to form an intermediate dihydrofuran (**I-250**), that upon hydrolysis yielded β -diketones like (**I-251**) (Scheme 38, B), namely aldol-like products.⁹⁷ However, an α -alkyne moiety could be introduced by mean of potassium alkynyltrifluoroborates (**I-252**) as reported by Liu and coworkers (Scheme 38, D).⁹⁸ Alcoxyallenes (**I-254**) were able to trap the oxyallyl cation *via anti*-addition, resulting in the formation of “Morita-Baylis-Hillman-like” products (**I-255**) (Scheme 38, C).⁹⁹ The use of organoaluminum compounds (Scheme 38, E) was once again reported by the interrupted Nazarov pioneers – West and coworkers; the intramolecularity of this process allows diastereoselectivity in the transfer of alkyl substituents from the metal to the α -carbon.¹⁰⁰ A Simmons-Smith cyclopropanation was observed in the presence of diiodomethane (Scheme 38, F),¹⁰¹ while the use of oxygen or Davis oxaziridine (**I-107**) or triplet oxygen afforded α -hydroxylated pentanones (**I-259**) (Scheme 38, G).¹⁰² Halogenation could occur in the presence of bromine or pyridinium perbromide (Scheme 38, H).¹⁰³



Scheme 38 – Interrupted Nazarov cyclization: possible nucleophiles to trap the oxyallyl cation (**N-2**).

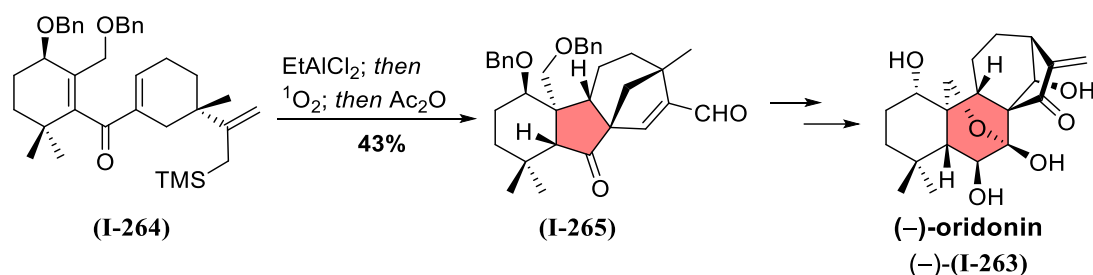
The fourth and last known way of intercepting the oxyallyl cation in a Nazarov cascade is a Wagner-Meerwein rearrangement. The interesting feature of this path, groundbroke by Frontier's research group,¹⁰⁴ is that it opens the way to spiro-pentanones (**I-262**), as depicted in Scheme 39.



Scheme 39 – Interrupted Nazarov cyclization: Wagner-Meerwein rearrangement of the oxyallyl cation.

The employment of Evans' oxazolidinones was reported for asymmetric Nazarov cyclizations by Flynn and coworkers.¹⁰⁵

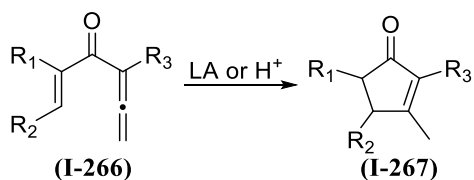
Summarized by choice, the number of terminations available for a Nazarov cyclization is meant to underline the huge potential that this cyclization possesses, counting on paper an infinite variety of possibilities. In spite of this, to this author's knowledge, the synthesis of (–)-oridonin (–)-(**I-263**) is the only reported example in which an interrupted Nazarov cyclization was successfully employed.¹⁰⁶ The key step is hereby reported:



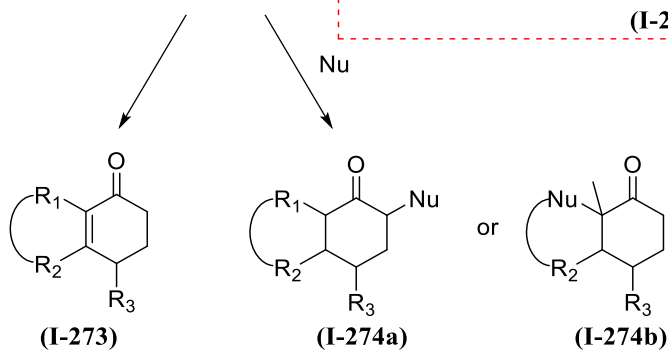
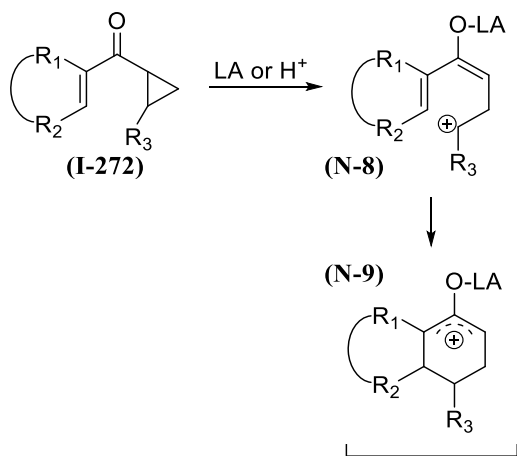
Scheme 40 – Photo-Nazarov cyclization as a key step in the synthesis of (–)-oridonin (–)-(**I-263**).

For the sake of completeness, interrupted Nazarov of allenyl-vinyl ketones (**I-266**), *iso*-, *homo*- and *imino*-Nazarovs (Scheme 41) will be briefly discussed, but a detailed elucidation will not follow, due to their lack of relevance for this thesis. Briefly, while the Nazarov cyclization of allyl vinyl ketones does not need further explanation, *iso*-Nazarov cyclizations are Nazarov cyclizations in which linearly conjugated carbonyl compounds (**I-268**) cyclize in acidic conditions and formation of cyclopentenones (**I-270**) requires migration of an alkyl group.¹⁰⁷ *Homo*-Nazarov cyclizations allow the formation of variously substituted cyclohexanes ((**I-273**) and (**I-274**)), due to the presence of a cyclopropyl substituent at the initial carbonyl group (*i.e.* one more carbon – see intermediate (**I-272**)). In *imino*-Nazarovs, a 1-iminopentadienyl cation (**N-10**) is generated in acidic conditions.⁹⁴

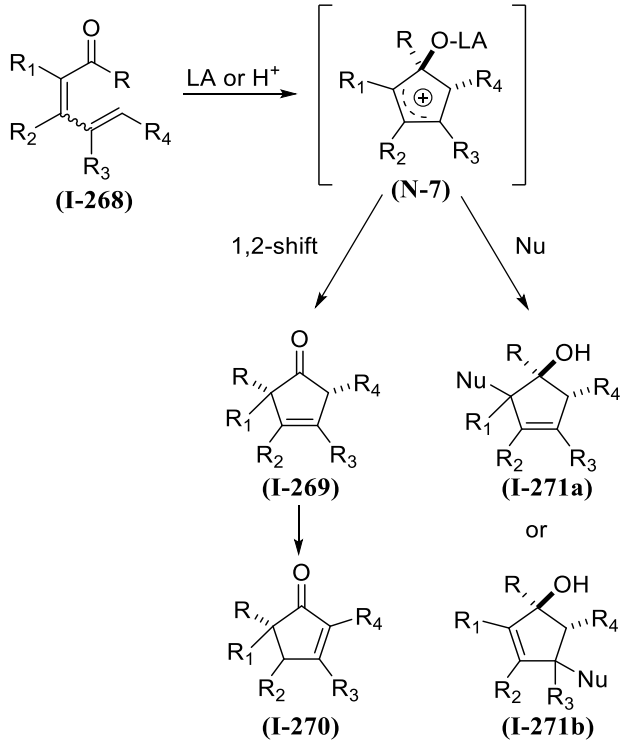
Interrupted Nazarov of allenyl vinyl ketones



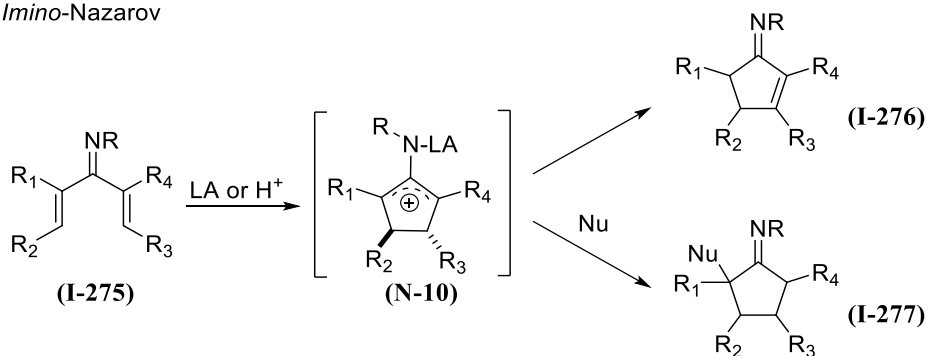
Homo-Nazarov



Iso-Nazarov



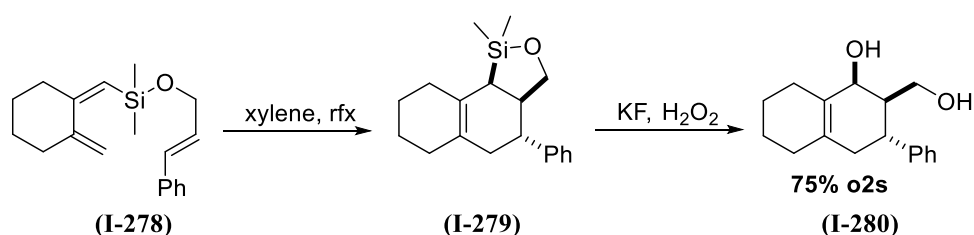
Imino-Nazarov



Scheme 41 – Interrupted Nazarov of allenyl vinyl ketones, *homo*-, *iso*- and *imino*-Nazarovs and their mechanism.

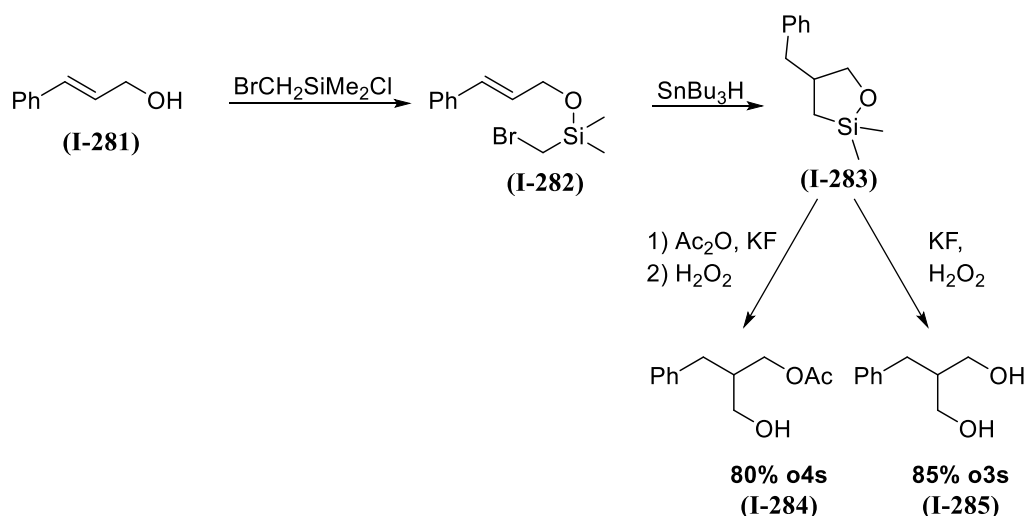
Silicon-tethered reactions

Intramolecular reactions benefit from a huge entropic contribution and are thereby preferred to intermolecular ones, in which success is highly dependent on lots of variables, like (effective) concentration, temperature, pressure etc. In other words, for an intermolecular reaction to be efficient or at least happen, the two reactants have to be brought in close proximity and with the exact geometry. At this point, if the functional groups reactivity is compatible enough, a reaction will occur. In this scenario, it is easy to understand the reason why one of the best ways to facilitate an intermolecular reaction is to make it intramolecular. But how to do so? By tethering the reactants, namely by introducing a linker that is connected to one or both the reacting sites, and that can generally be removed after the desired transformation occurred. Such a tether should obey certain criteria: first, the tethered compound should be readily accessible from cheap, non-toxic materials. Once obtained, it should be easy to handle (for example, moisture and air sensitivity should be avoided) and the tether should survive most reactions without requiring harsh conditions for the removal. Silicon-based tethers positively respond to all of these requirements, and have thus found employment in various synthetic purposes.¹⁰⁸ For example, silicon-tethered Diels-Alder reactions¹⁰⁹ are cycloadditions in which this strategy has been successfully employed:



Scheme 42 – Silicon-tethered Diels-Alder reaction by Sieburth *et al.*

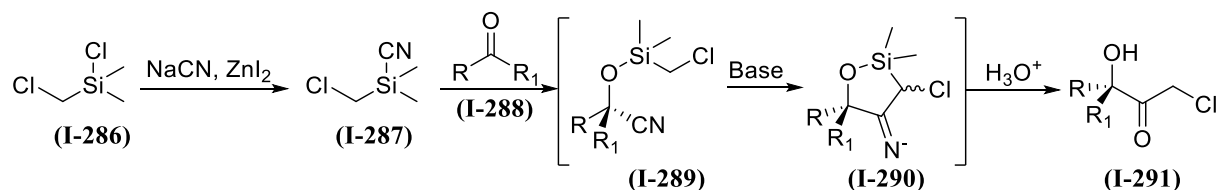
High regio- and stereocontrol was achieved in radical cyclizations through the employment of silicon tethers. An example is reported by Nishiyama and coworkers, in which a (bromomethyl)dimethylsilyl linker was used (see Scheme 43).¹¹⁰ The generated radical underwent a 5-exo-trig cyclization and afforded sila-2-oxacyclopentane (**I-283**) in high yields, that was further functionalized.



Scheme 43 – Silicon-tethered radical cyclization by Nishiyama *et al.*

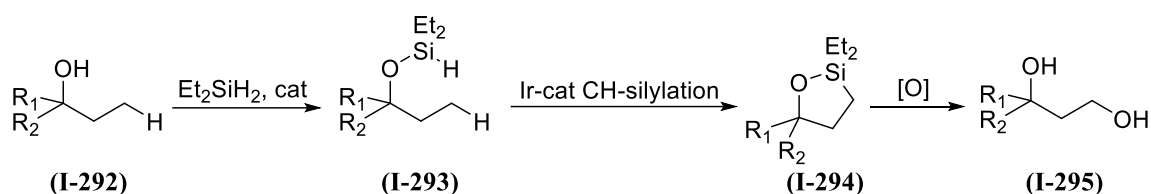
A (halomethyl)dimethylsilyl chain was employed by Zhou and coworkers¹¹¹ to tether the attack onto an electrophilic nitrile group, as shown in Scheme 44. In particular, intermediate (**I-289**), obtained through enantioselective cyanosilylation of a carbonylic compound (**I-288**), was subjected to basic

treatment to allow the formation of siloxacycle (**I-290**), in turn converted into tertiary alcohol (**I-291**) featuring a chloromethylketone moiety.



Scheme 44 –Silicon-tethered nucleophilic addition onto a nitrile by Zhou and coworkers.

Silicon tethers found recent application in C–H functionalization, in which they are employed as ways to reach inert positions. Hartwig and coworkers reported oxidations of unactivated C–H bonds by means of a dehydrogenative cyclization of (hydrido)silyl ether (**I-293**).¹¹² Once again, oxidative cleavage of the silicon-containing ring furnished desired 1,3 diol (**I-295**) (Scheme 45).



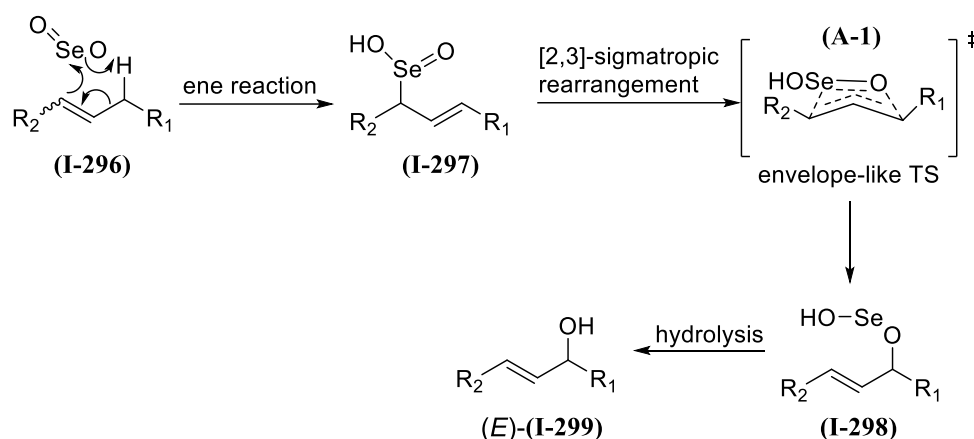
Scheme 45 – Silicon-tethered C–H functionalization by Hartwig and coworkers.

The use of silicon tethers towards the total synthesis of illisimonin A will be reported in due course in this thesis.

Allylic oxidations

As the last example might have suggested, oxidations of unfunctionalized C–H groups are among the most difficult but still crucial transformations in total synthesis, since they not only adjust the oxidation state of a carbon atom, often at a late stage of the sequence, but also introduce an heteroatom in the carbon framework – an alcohol or a ketone – which sets the stage for further functionalization. Allylic oxidations are a special subgroup of C–H oxidations which are generally preferred to other unactivated congeners due to the well known unusual reactivity of C–H functional groups adjacent to double bonds, whose cations or radicals benefit from an increased stabilization. Indeed, it is not surprising that a flourishing number of oxidating reagents have been reported for this purpose. A recent review from Nakada and coworkers¹¹³ categorizes them in Se-based, TM-based and Cr-based.

Selenium dioxide is probably the most famous reagent for allylic oxidations due to high chemoselectivity, low costs and lack of toxicity. It generally results in the formation of allylic alcohols and can be either used in stoichiometric or catalytic amounts; variations, as reported by Barton and coworkers,¹¹⁴ include the use of diphenyldiselenide and iodoxybenzene. Oxidation occurs, according to the mechanism proposed by Sharpless in 1972¹¹⁵ and reported in Scheme 46, *via* ene-reaction of the olefin with selenium dioxide, and consequent 2,3-sigmatropic rearrangement of allylselenenic acid (**I-297**) to the corresponding allylselenite ester (**I-298**), with final hydrolysis to the allylic alcohol. Envelope-like transition state (**A-1**) justifies the *E*-selectivity of this particular oxidation.

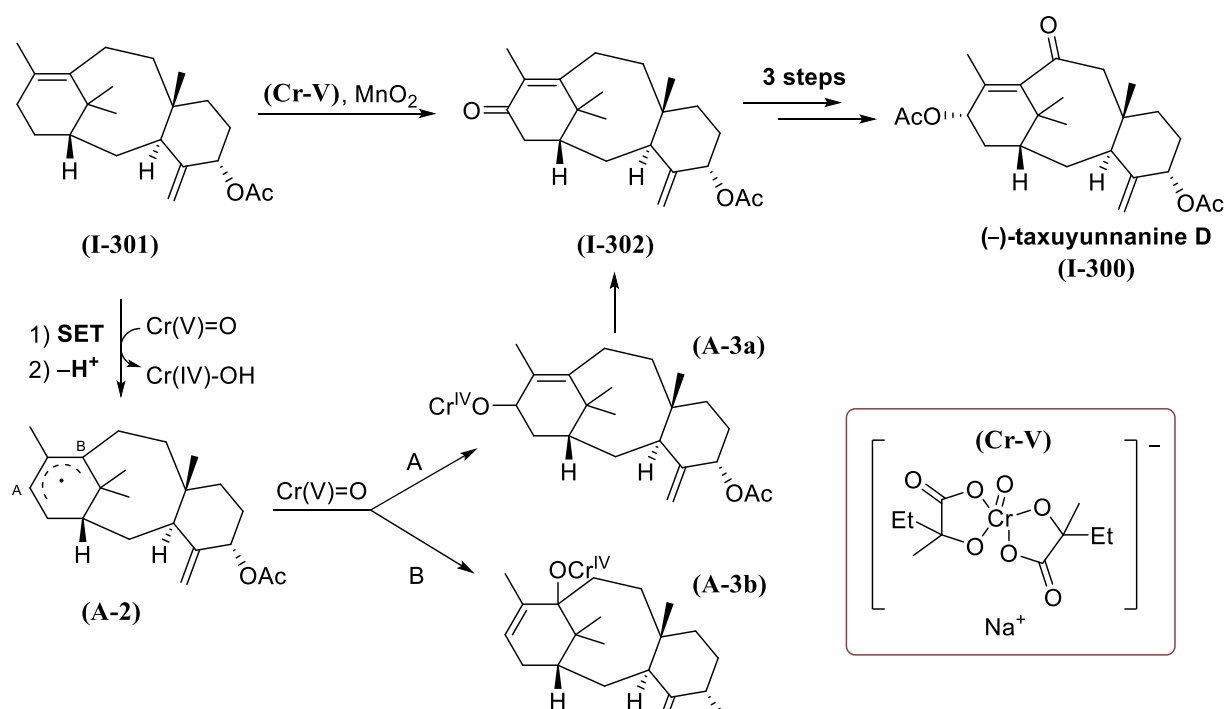


Scheme 46 – Proposed mechanism of the Riley oxidation.

Transition metals employed for allylic oxidations include Pd,¹¹⁶ Mn,⁵⁵ Cu,¹¹⁷ Co,¹¹⁸ Rh¹¹⁹ and Ru.¹²⁰ The use of $\text{Rh}_2(\text{cap})_4$ in the presence of *tert*-butylhydroperoxide (TBHP) as bulk oxidant was introduced by Doyle and coworkers¹¹⁹ to overcome the poor selectivities observed with Wilkinson's catalysis. Among the other dirhodium complexes, Du Bois's catalyst ($\text{Rh}_2(\text{esp})_2$)¹²¹ found application both with TBHP and in aerobic conditions in the presence of *N*-hydroxyphthalimide (NHPI). TBHP served as the oxidant in the presence of Mn(III) or Cu(I) salts: the first is the case of the $\text{Mn}(\text{OAc})_3$ -catalyzed oxidation employed by Theodorakis and coworkers in their already mentioned synthesis of (–)-jiadifenin (–)-**(I-58)**.⁴⁴ CuI and CuBr were instead found to be equally effective in combination with TBHP as shown in the syntheses of (±)-nudenoic acid¹²² and barbaccenic acid¹²³ respectively. Co(II) acetate has been used with the same *t*BuOOH or NHPI combination.¹¹⁸ An allylic oxidation with RuCl_3 and TBHP was reported by Miller and coworkers on steroidal systems,¹²⁰ while Pd served the allylic oxidation purpose supported on carbon (Carreira and coworkers),¹²⁴ as $\text{Pd}(\text{OH})_2$ ¹¹⁶ or $\text{Pd}(\text{OAc})_2$.¹²⁵

In spite of all of these methodologies being available, Cr(VI)-reagents have been occupying a place of honour over the decades for the oxidation of activated methylenes to yield α,β -unsaturated ketones. A few variations are available on this theme, starting from Corey's classics like PCC¹²⁶ and PDC,¹²⁷

moving to chromium trioxide methods, whose history is highly connected to terpenes from 1928¹²⁸ and survives today as CrO₃:3,5-DMP from Salmond and coworkers,¹²⁹ and concluding with “new” variations like Cr(CO)₆ in combination with TBHP (Shing and Jiang, 2000).¹³⁰ While CrO₃:3,5-DMP found application in the *ex*-chiral pool synthesis of (+)-paeonisuffrone (+)-(**I-53**),³⁹ the use of the well known Jones reagent unfolded its full potential in the *Illiciums* chapter. The use of Cr(V) instead, is not so well documented. The best known Cr(V) complexes possess chelating α -hydroxy acids and were at first employed for the oxidation of dialkyl sulphides.¹³¹ Known from the 70s,¹³² they did not find application in total synthesis until 2014, when the synthesis of (-)-taxuyunnanine D (-)-(**I-300**) from Baran and coworkers was published.³¹ In their work, sodium bis(2-hydroxy-2-methyl-butyrato)oxochromate(V) (**Cr-V**) was for the first time successfully employed for an allylic oxidation - with or without MnO₂ - as a co-oxidant. Mechanistically, they proposed that oxidation with Cr(V) started with a SET followed by proton abstraction, that resulted in the formation of a Cr(IV) species and an allyl radical (**A-2**), located either in position A or B (see Scheme 47). Both possible regioisomers could interact with another chromium-oxo species (path A or B), giving birth to two possible intermediates (**A-3a**) and (**A-3b**). The hypothesis that Cr(V) cannot mediate a Babler-Dauben oxidative rearrangement¹³³ on a tertiary allylic alcohol (that would result from Cr-O bond hydrolysis in path B), further supported by experiments on a simpler intermediate, suggested that desired product (**I-302**) derived from the A-located-radical intermediate.

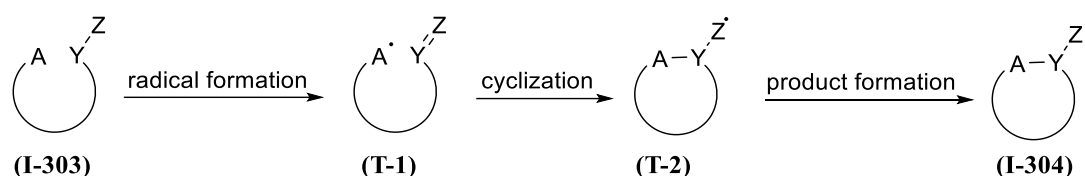


Scheme 47 – Proposed mechanism for the Cr(V) allylic oxidation in the synthesis of (-)-taxuyunnanine D (-)-(**I-300**).

After this groundbreaking application, other natural products syntheses benefited from the use of Cr(V) reagent: the synthesis of ritterazine B by the Reisman group is one of these cases.¹³⁴

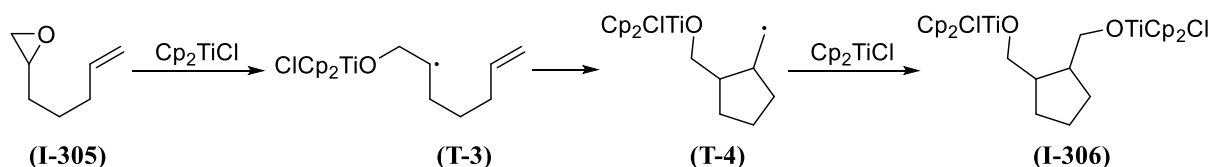
Ti(III)-mediated cyclizations

The employment of radical cyclizations for the synthesis of mono- and polycyclic compounds through C–C bond formation is one of the most diffused methods in total synthesis. The high versatility that characterizes these reactions is related to high functional group tolerance, mild conditions and high regio- and stereoselectivity. Radical cyclizations involve the selective formation of a radical from a suitable precursor (**I-303**), the cyclization itself, in which the radical adds to a multiple bond, and the product formations, in which the radical is either trapped, or a fragmentation occurs, or an electron is transferred (Scheme 48).



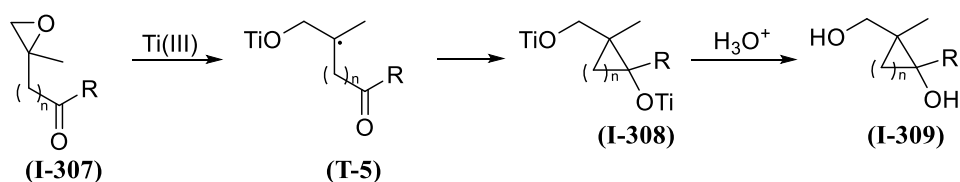
Scheme 48 – General mechanism for a radical cyclization.

Precursors for radical formation involve a broad range of functional groups, such as halides, carbonylic compounds, thioethers, alcohols etc. In 1989, Nugent and coworkers reported the homolytic C–O bond cleavage in epoxides, driven by the strain release in the σ -complex formed after interaction of the epoxide with Cp_2TiCl , which is formed *in situ* through reduction of Cp_2TiCl_2 with Zn powder. The newly formed radical (**T-3**) was, in the original scope, undergoing hexenyl radical *exo*-cyclization resulting in the formation of 5-membered rings, as in Scheme 49.¹³⁵



Scheme 49 – Homolytic cleavage of an epoxide and consequent 5-*exo*-trig cyclization from Nugent and coworkers.

After a decade, the first attack of radicals generated from an epoxy-intermediate to carbonyl groups was observed. Fernández-Mateos' pioneering work involved the treatment of difunctional epoxides (**I-307**) with Ti(III) (Scheme 50) and was completed by the proposal of a mechanism for the formation of 1,3-cycloalkanedioles from epoxyketones.¹³⁶

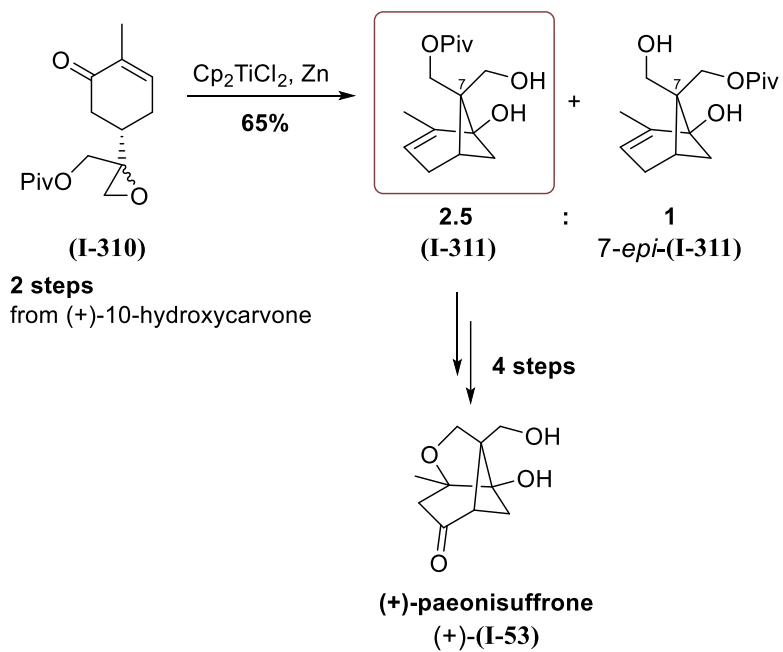


Scheme 50 – Homolytic cleavage of an epoxide and consequent cyclization onto carbonyl acceptors.

One more step was made by Gansäuer and coworkers, who introduced a catalytic version of this method that employs collidine·HCl¹³⁷ as an acid for the protonation of titanocene alcoxides to achieve catalytic turnover.

In spite of their potential, Ti(III)-mediated reductive cyclizations did not find enormous application in NP-synthesis. The total synthesis of (+)-paeonisuffrone (+)-**(I-53)** from Bermejo and coworkers,³⁹ already mentioned because of the *ex*-chiral pool starting material, as well as $\text{Mn}(\text{OAc})_3$ allylic oxidation, represents one of the few examples in which the carbocyclic skeleton of a terpenoid was

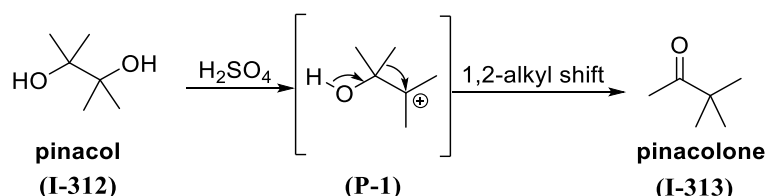
stereoselectively built *via* Cp₂TiCl₂-mediated reductive C–C bond formation. Their total synthesis is summarized in Scheme 51.



Scheme 51 – Pivotal Ti(III)-mediated cyclization in the total synthesis of (+)-paeonisuffrone (+)-I-53 from Bermejo and coworkers.

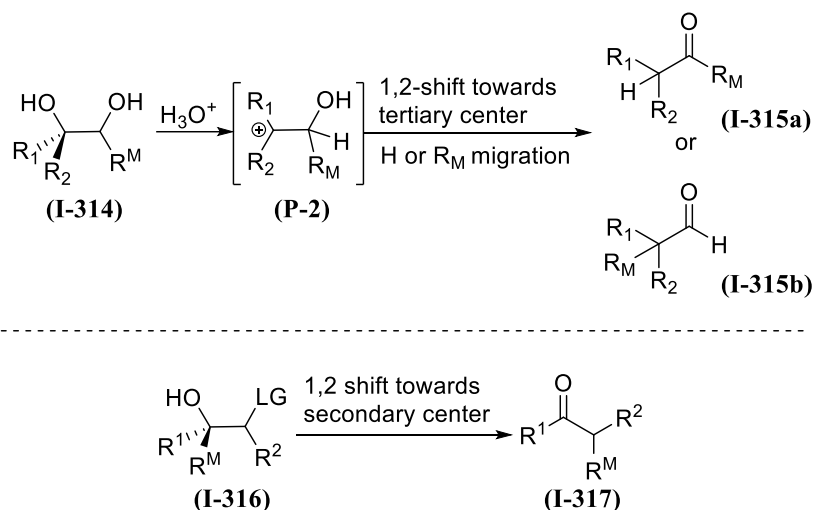
Semipinacol rearrangements

Another reaction which finds application in the formation of 5-membered rings, as the above discussed Ti(III)-mediated reductive cyclization, is the semipinacol rearrangement. The history of (semi)pinacol rearrangements begins almost at the rise of organic chemistry: Wilhelm Rudolph Fittig observed this kind of reaction already in 1860,¹³⁸ roughly thirty years after the first milestone of modern organic chemistry era – the synthesis of urea by Wohler - was set. The original pinacol rearrangement derives its name from pinacol (**I-312**) itself, which undergoes a 1,2-alkyl shift under strongly acidic conditions, yielding pinacolone (**I-313**) (Scheme 52).



Scheme 52 – The original pinacol rearrangement and its mechanism.

The term “semipinacol” (Tiffeneau, 1923)¹³⁹ instead was initially referring to a transformation in which an inverted migration happens in a tertiary-secondary 1,2-diol (**I-316**), in the sense that migration occurs towards the secondary center, unlike in pinacol rearrangements, in which the most stable carbocation (**P-2**) is formed, as in Scheme 53. This unusual behaviour is due to the presence of a good leaving group at the secondary center.



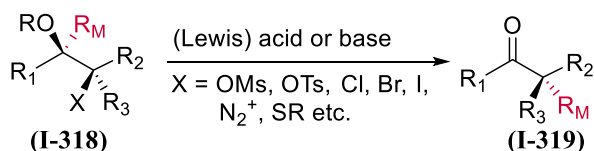
Scheme 53 – Comparison between pinacol (on the top) and semipinacol (at the bottom) rearrangements.

Nowadays, the meaning of this concept has expanded, and the category “semipinacol rearrangements” involves 1,2-migration of C–C or C–H bonds towards an electrophilic carbon centre vicinal to an oxygen-bonded carbon atom.¹⁴⁰ As a result of this transformation, a carbonyl group is formed. This new definition is the reason why, as aforementioned, the Demjanov-Tiffeneau rearrangement can be regarded as a semipinacol rearrangement in which molecular nitrogen acts as the leaving group. This is of course not the only existing variation of this transformation, and a categorization based on the type of electrophilic carbon center has been established. Four types of semipinacol rearrangements have been distinguished (Scheme 54):

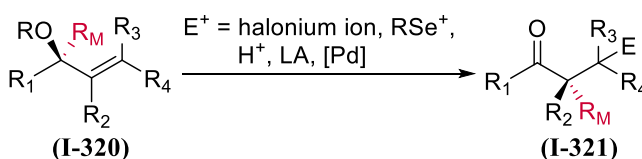
- Type I semipinacol rearrangements are those in which 2-heterosubstituted alcohols (**I-318**) are reacting. The presence of a good leaving group, as in the first definition, is facilitating the process.

- Type II semipinacol rearrangements involve allylic alcohols (**I-320**) and their derivatives. A carbocation is generated through attack of an electrophilic species to the double bond.
- Type III rearrangements see 2,3-epoxyalcohols (**I-322**) as protagonists; acid-promoted epoxide opening is occurring; the reaction is terminated by different kind of migrations: 1,2-, 2,3- and 3,2-migrations are equally possible.
- In Type IV, tertiary α -hydroxyketones or imines (**I-324**) are rearranging. These last transformations are also known as acyloin or α -ketol rearrangements.

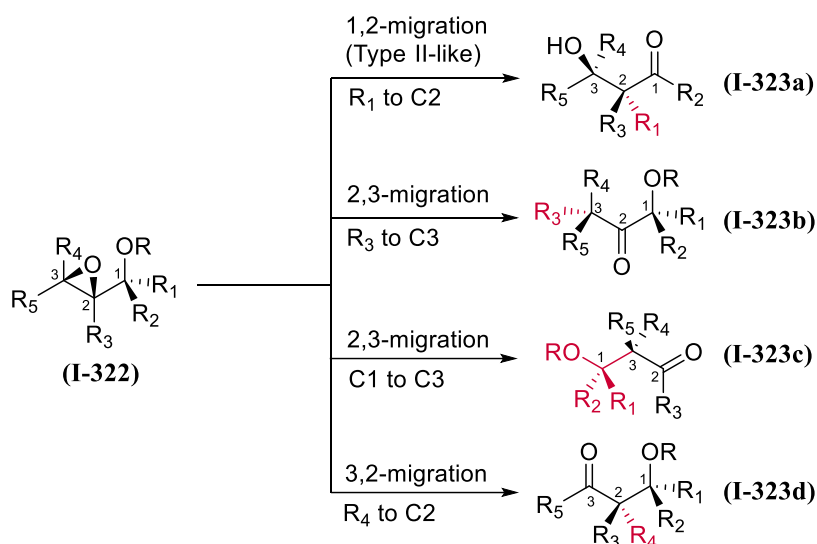
Type I



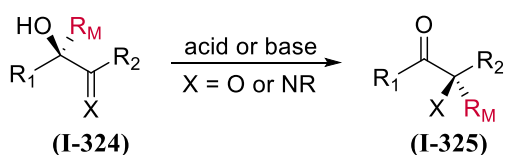
Type II



Type III



Type IV

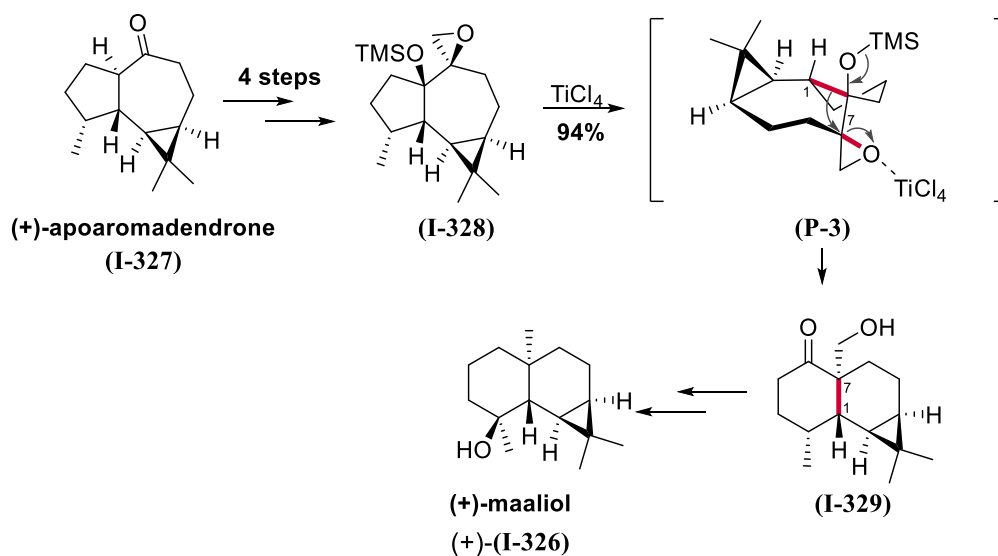


Scheme 54 – Different types of semipinacol rearrangements.

Similarly to the Nazarov cyclization, semipinacol rearrangements include such a broad range of applications, that a comprehensive review is almost impossible. Moreover, some of the examples are not as related to this thesis as Type III. For this reason, this paragraph will mainly focus on the

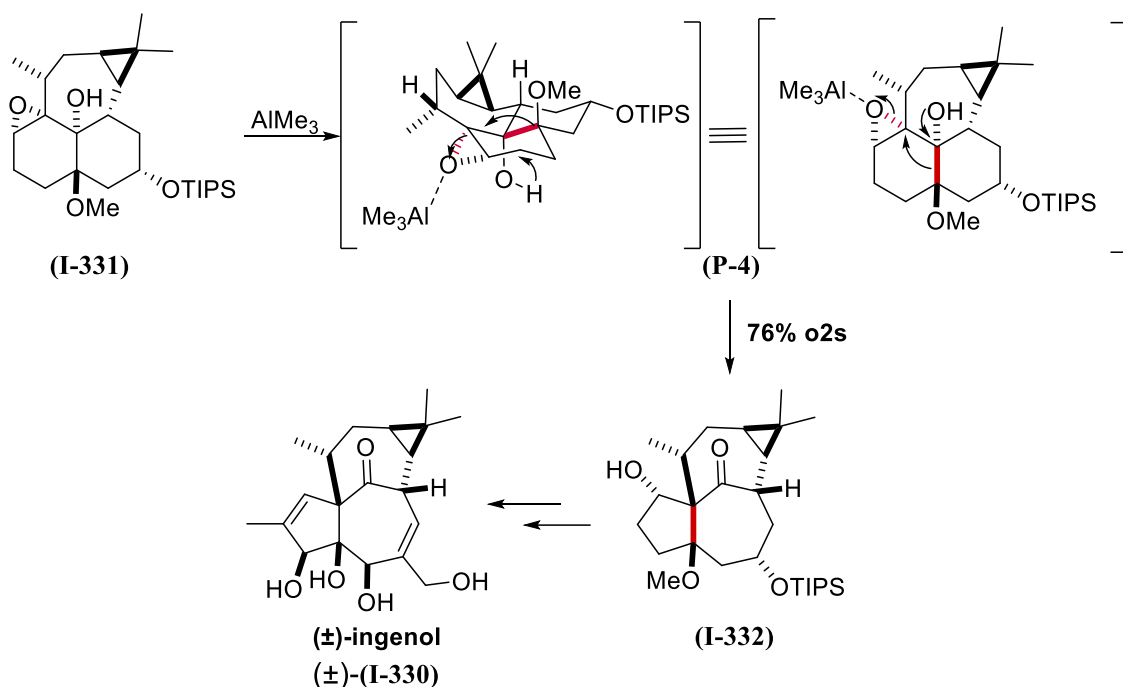
behaviour of epoxides and explicative examples (for further reading, excellent reviews on the topic have been published by Tu and coworkers).^{140,141}

Seminal work on this subclass was done starting from the late 60s,¹⁴² and extensively developed due to the great number of possibilities regarding the nature of the Lewis acids, their employment in either catalytic or stoichiometric amounts and the high stereocontrol. This last feature derives from the migrating group attacking *anti* to the epoxide, generally with stereoretention at the migrating carbon, and results in diastereoselective production of aldol-like products.¹⁴⁰ The possible quaternary nature of the migrating carbon center enhances the applicability of this kind of transformation. Moreover, the use of semipinacol rearrangements in cyclic systems is resulting in either ring expansion or contraction when applied to isolated rings. When starting from isolated bicyclic compounds, spiro systems are formed; spirocompounds are also the result of exendo bond migration in fused systems. The migration of the fusion bond in fused bicyclic systems results in ring enlargement on one ring, and contraction on the other. The synthesis of (+)-maaliol (+)-**(I-326)** (1994) from the sesquiterpene (+)-apoaromadendrone (+)-**(I-327)**¹⁴³ was accomplished by Wijnberg and de Groot by employing a semipinacol strategy, as in Scheme 55: specifically, rearrangement of a 5,7-system (**I-328**) in Lewis acidic conditions yielded the corresponding 6,6-ketone (**I-329**), characterized by the natural product's *trans* junction and in excellent yields.



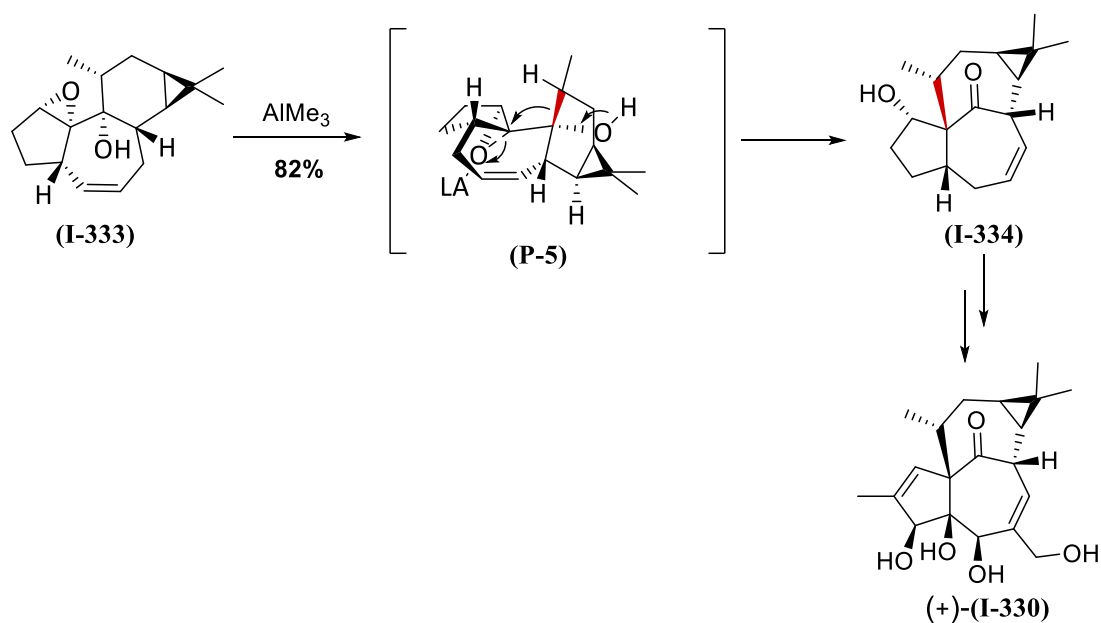
Scheme 55 – Semipinacol rearrangement in the total synthesis of (+)-maaliol (+)-**(I-326)** by Wijnberg and de Groot. Migrating bond is highlighted in red.

The above showed 1,2-migration strategy was proved to be successful when targeting ingenol (**I-330**), a diterpene from the ingenane family. Tanino, Kuwajima and coworkers utilised trimethyl aluminium to initiate fusion bond migration in the initial 6,6-system (**I-331**) (Scheme 56). The result was the formation of the desired tetracyclic scaffold.¹⁴⁴



Scheme 56 – Semipinacol rearrangement in the total synthesis of (\pm) -ingenol (\pm) -**(I-330)** by Tanino, Kuwajima and coworkers. Migrating bond is highlighted in red.

Cha's approach to the ingenol $(+)$ -**(I-330)** core¹⁴⁵ also involved a type III semipinacol rearrangement with 1,2-bond migration **(P-5)**, though applied to a quite different ring system:



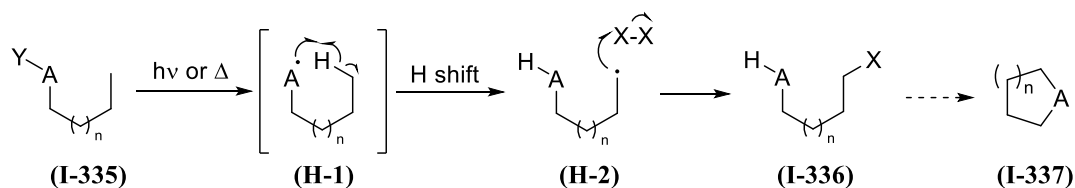
Scheme 57 – Semipinacol rearrangement towards the synthesis of $(+)$ -ingenol $(+)$ -**(I-330)** by Cha and coworkers.

Such a 1,2-migration appears in the total synthesis of illisimonin A by Rychnovsky and Burns.¹⁴⁶ Further details on their approach will be given in the dedicated chapter.

C–H activation

The importance of direct C–H functionalization has been partially outlined in the allylic oxidation chapter. However, as already mentioned, allylic oxidation are a special case of C–H oxidation, in which a functional group acts in the stabilization of resulting intermediates and distinguishes the allylic methylene from other analogous groups in the molecule. This chapter will instead focus on the functionalization of strong, unactivated C–H bonds, and on its growing influence in the synthesis of natural products. Specifically, the conversion of sp^3 C–H bonds into C–O bonds will be described because of its major impact on this thesis.

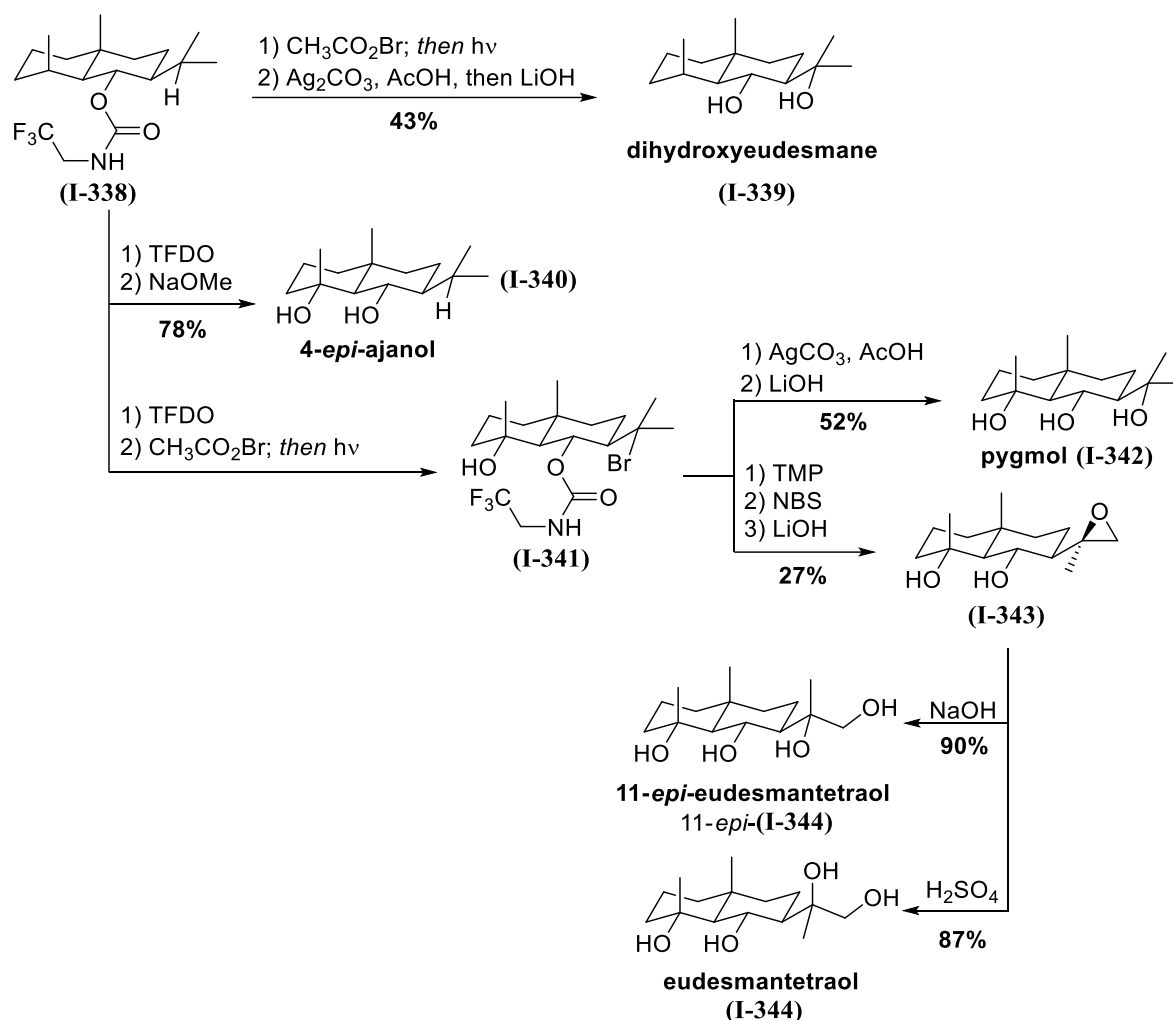
The major problem when thinking of directly functionalize a C–H bond is abundance: organic chemistry is defined as the chemistry of hydrocarbons, and it is not surprising that these kind of bonds are ubiquitous in organic compounds. Consequently, the first question to answer is how to discriminate among the different C–H groups or, in other words, the question is how to selectively activate a specific C–H group. One of the first answers was given by Hofmann, Löffler and Freytag,¹⁴⁷ and relies on a thermolytic or photolytic cleavage of a Y–A bond (both Y and A being heteroatoms), that causes the formation of a radical (**H-1**). This heteroatom-centered radical is in turn extracting an hydrogen atom, generally with a 6-membered TS, and the newly formed C-centered radical (**H-2**) is then intercepted by an halogen atom, as in Scheme 58.



Scheme 58 – General mechanism of Hofmann-Löffler-Freytag (HLF) C–H activation.

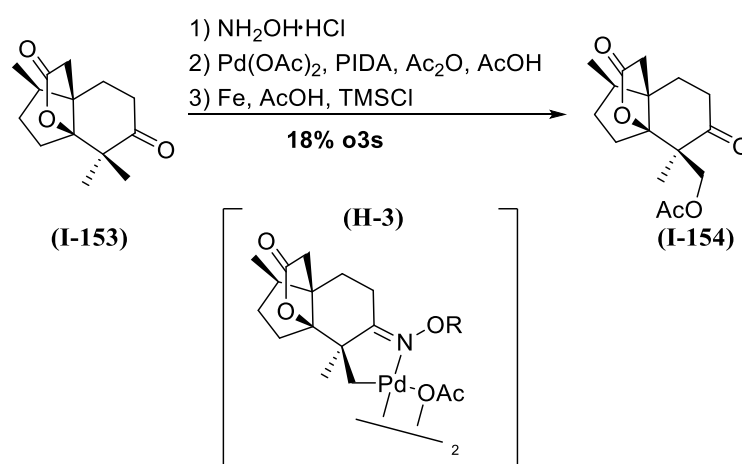
This strategy has been widely applied with rigid substrates, specifically with steroids. Moreover, when A is an oxygen atom, methods have been developed with nitrite esters (Y = NO, Barton's method)¹⁴⁸ or hypochlorites (Y = Cl),¹⁴⁹ in which the intermediates need to be isolated; alternatively alcohols can be transformed *in situ* into hypoiodites (with PIDA) or lead alcoxides (with $Pb(OAc)_4$) to perform the same C–H activation.¹⁴⁷

The use of directing groups is generally a valid alternative to HLF-like C–H activations, since it also allows to reach unfavoured hydrogen atoms. In this context, a methodology was developed and successfully employed in the synthesis of various eudesmanes, a family of terpenes, by Baran and coworkers.³⁰ In this work, the same alcohol could be converted into diverse 1,3-diols through the formation of an intermediate trifluoroethyl carbamate (**I-338**), as in Scheme 59.



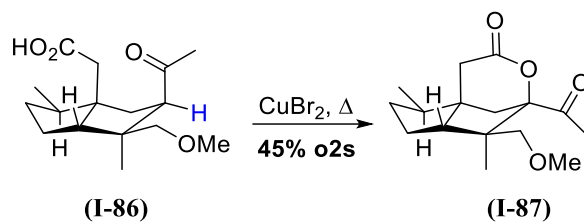
Scheme 59– Synthesis of various eudesmanes by Baran and coworkers.

Directing groups have also been employed in metal-catalyzed C–H activations. In this case, their role is to coordinate the metal and selectively deliver it to the desired C–H group. Most of the directing group are nitrogen-based, as in the case of Sanford-like methodology in the synthesis of (–)-jiadifenolide (–)-(I-59) from the Sorensen group.⁶⁴ Here, an hydroxylamine was built, that in Pd-catalytic conditions directed the metal towards one of the two vicinal methyl groups (Scheme 60), allowing C–O bond formation.



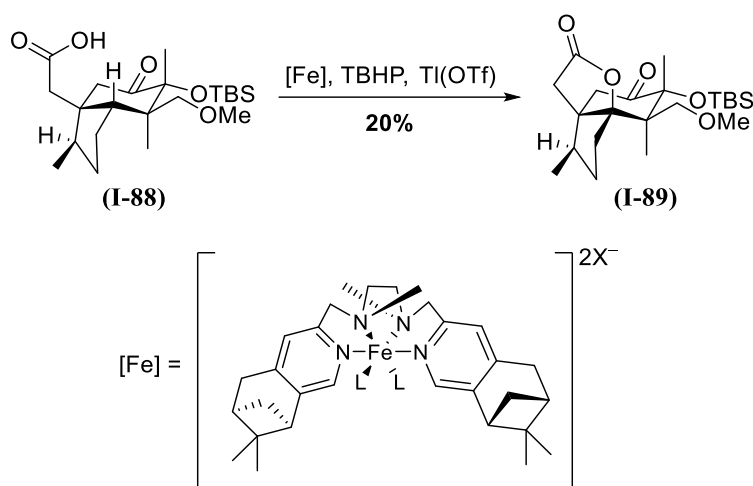
Scheme 60 – Sorensen's use of DG-directed C–H functionalization in the synthesis of (–)-jiadifenolide (–)-(I-59).

The directing-group-strategy is highly diffused but surely has some disadvantages, as the installation and removal of the DG-itself require additional steps. Some directing groups-free methodologies have been briefly mentioned in the *Illicium* sesquiterpenes chapter, as the C–H activation in the presence of CuBr₂ from Maimone and coworkers on the way to (+)-pseudoanisatin (+)-(**I-60**).⁵⁰



Scheme 61 – Maimone’s use of DG-free direct C–H functionalization in the synthesis of (+)-pseudoanisatin (+)-(**I-60**). Activated C–H position highlighted in blue. Second step not shown.

In the same synthesis, the authors took advantage of another C–H activation, that was not as effective as the previous one. In this case, a Fe-catalyzed carboxylic acid-mediated C–H activation was attempted, in the presence of TBHP as bulk oxidant (Scheme 62).



Scheme 62 – Maimone’s use of DG-free direct C–H functionalization in the synthesis of (+)-pseudoanisatin (+)-(**I-60**).

Iron catalysis and *tert*-butylhydroperoxide are the ingredients of probably the most famous C–H activation, the White-Chen oxidation. Published in 2007,¹⁵⁰ their methodology arose from the quest for a metal catalyst that could discriminate among different C–H bonds in a predictable way, based on mere sterics and electronics. Their electrophilic, iron-based, bulky catalyst (Fig. 13) combined with mild oxidative conditions was successfully employed with artemisinin (**I-7**) and other complex molecules, which made of Fe(*S,S*)-PDP (**I-345**) and its enantiomer a quite essential tool for late stage C–H functionalization. A directed variation, taking advantage of the presence of carboxylic moieties, made it possible to use this method for γ -lactones formation. Once again, an example on intricate molecules was reported in the total synthesis of illisimonin A and will be described in due course.

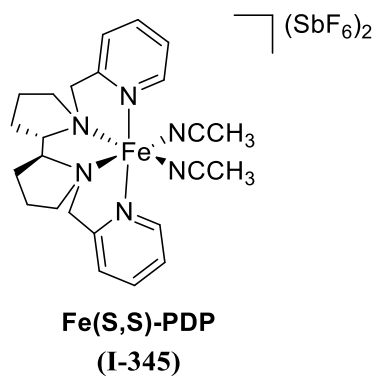


Fig. 13 – The White-Chen catalyst, Fe(S,S)-PDP (I-345).

Illisimonin A

In 2017 the group of Ma and coworkers reported the isolation of a novel sesquiterpenoid from the fruits of *Illicium simonsii*, an evergreen shrub historically known and employed in folk medicine.¹⁵¹ Named illisimonin A (**I-346**) after the genitor species, this NP is characterized by an unprecedented tricyclo[5.2.1.0^{1,6}]decane skeleton, since then referred as illisimonane, that attracted the interest of several research groups,^{146,152} including Kalesse's research group.

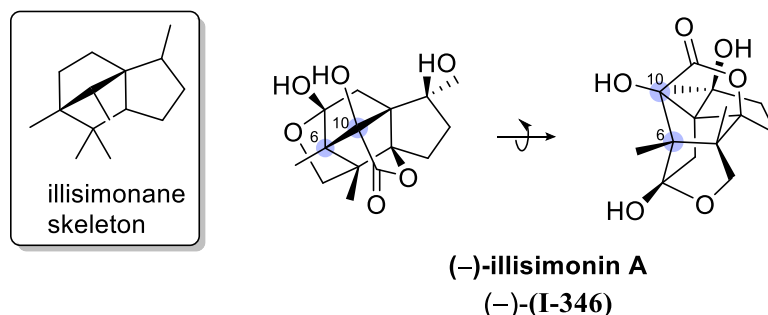


Fig. 14 – (-)-illisimonin A (-)-(**I-346**) and its illisimonane skeleton.

Illisimonin A (**I-346**) possesses in fact a 5/5/5/5/5 pentacyclic scaffold, in which beyond the above mentioned tricyclic decane skeleton (A-C rings, Fig. 15), a norbornane system (BC rings, Fig. 15) and two oxygen-containing rings (lactol D and lactone E, Fig. 15) are present. What is really new about this highly bridged structure is the existence of a C6-C10 bond (highlighted in FIG. 14, numbering from Ma and coworkers), that has never been observed before in other *Illicium* congeners. Moreover, an unstable *trans*-pentalene subunit (AC rings, Fig. 15) is embedded in the core of this molecule; the presence of this subunit was crucial in the synthetic planning behind this thesis, and will be further underlined in due course.

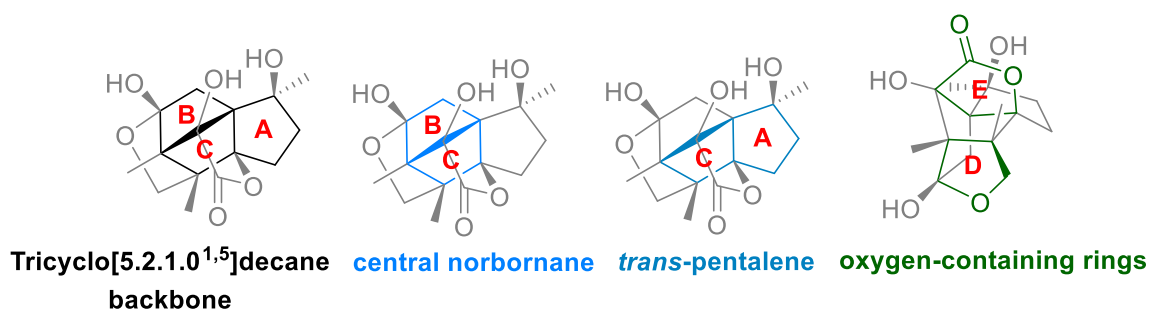


Fig. 15 – (-)-illisimonin A (-)-(**I-346**) ring systems.

From a stereochemical point of view, illisimonin A is equipped with seven contiguous stereogenic centers, all located in the norbornane subunit. Highlighted in FIG. 16 are the three quaternary centers (blue) and the four fully substituted stereocenters (tiffany green).

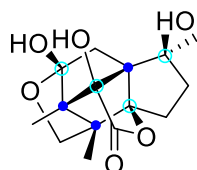
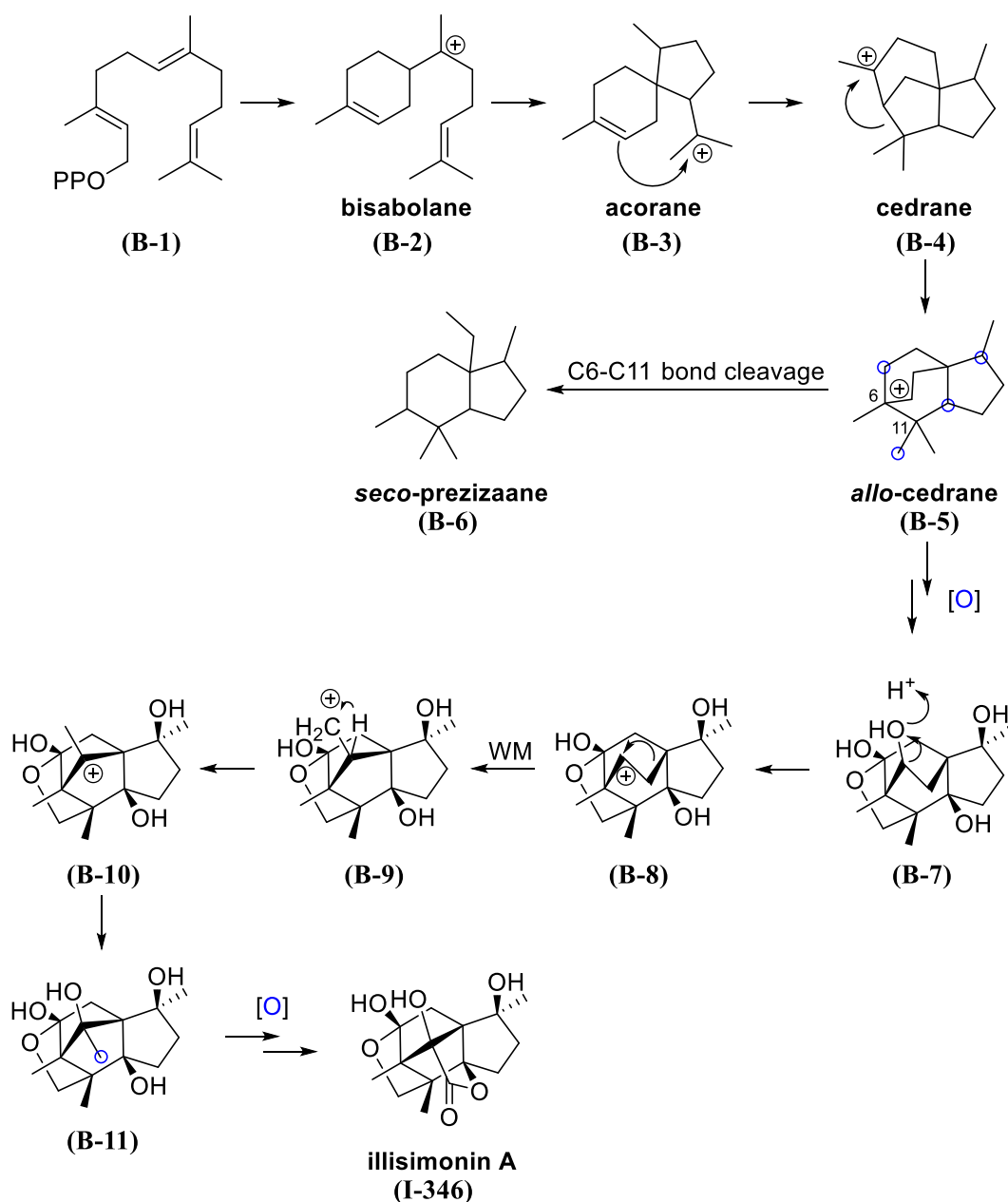


Fig. 16 – Stereogenic centers in (-)-illisimonin A (-)-(**I-346**); quaternary stereocenters are highlighted in blue, while fully substituted stereocenters in tiffany green.

Biosynthetic proposal

A biosynthetic proposal, connecting illisimonin A (**I-346**) to other *Illicium*-sesquiterpenoids, was postulated by Ma and coworkers.¹⁵¹ The illisimonane skeleton would originate from an ancestral 5/6/6 *allo*-cedrane framework (**B-5**), common biogenetic intermediate of the *seco*-prezizaane-type terpenoids (**B-6**) (as already mentioned in the dedicated chapter) through a sequence of oxidations, condensations and skeletal rearrangements (Scheme 63).



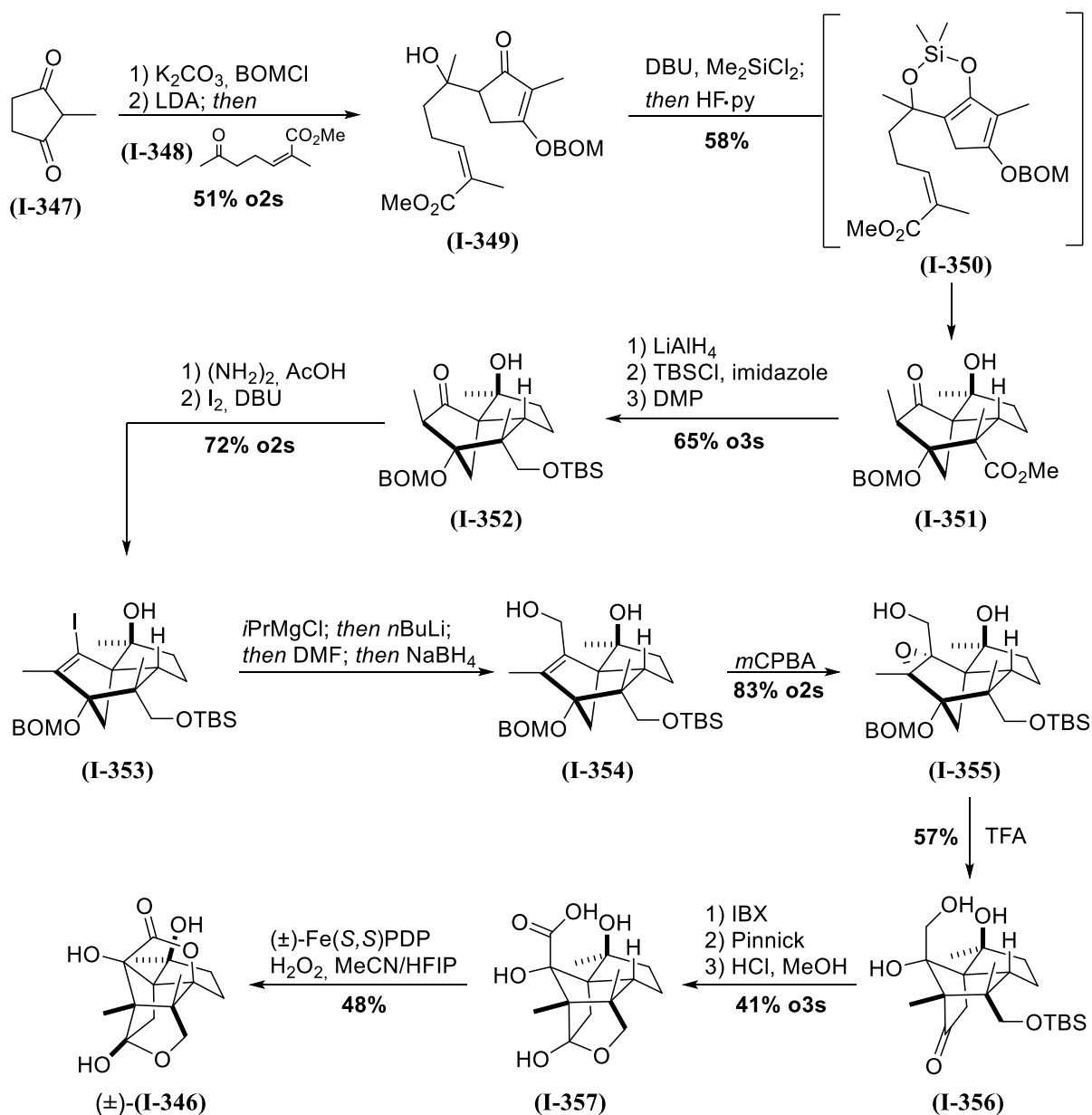
Scheme 63 – Biosynthesis of illisimonin A (**I-346**) proposed by Ma and coworkers. Oxidated positions are highlighted.

In particular, the *allo*-cedrane cation (**B-5**) could either undergo C6-C11 bond cleavage, thus originating *seco*-prezizaane derived compounds (**B-6**), or be subjected to a series of selective oxidations (oxidated positions highlighted in Scheme 63) and a condensation to furnish a highly oxygenated skeleton like (**B-7**). A 1,2-shift of one alkyl substituent would result in unstable primary carbocation (**B-9**), which would then rearrange into more stable carbocation (**B-10**). Water would intercept this cation and after a sequence of selective oxidations illisimonin A (**I-346**) would be

obtained. Given the biogenetic relation with *seco*-prezizaanes and the neuroprotective activities exhibited by this kind of compounds, illisimonin A (**I-346**) possible action against oxygen-glucose deprivation-induced cell injury was also investigated: an EC₅₀ of 27.72 μ M resulted from tests on SH-SY5Y cells.¹⁵¹

Rychnovsky's total synthesis

The total synthesis of (–)-illisimonin A (–)-(I-346) from Rychnovsky and Burns, accomplished in 2019,¹⁴⁶ represents until today the only notable achievement regarding this complex molecule. Their first key step involves an IMDA (intramolecular Diels-Alder reaction) whose diastereofacial selectivity was induced by silacycle templation (see intermediate (I-350)). Further interesting transformations regard the one-carbon elongation, which was achieved through combined Barton¹⁵³/Bouveault¹⁵⁴ chemistry to afford intermediate (I-354) after epoxidation. A semipinacol rearrangement induced by TFA resulted at this point in the strained *trans*-pentalenic intermediate (I-355), that underwent a two-step oxidation, followed by lactolization upon deprotection. To conclude the synthesis, a carboxylic acid-mediated C–H activation was performed by using White-Chen catalyst (I-345) and resulting in the natural product δ -lactone.

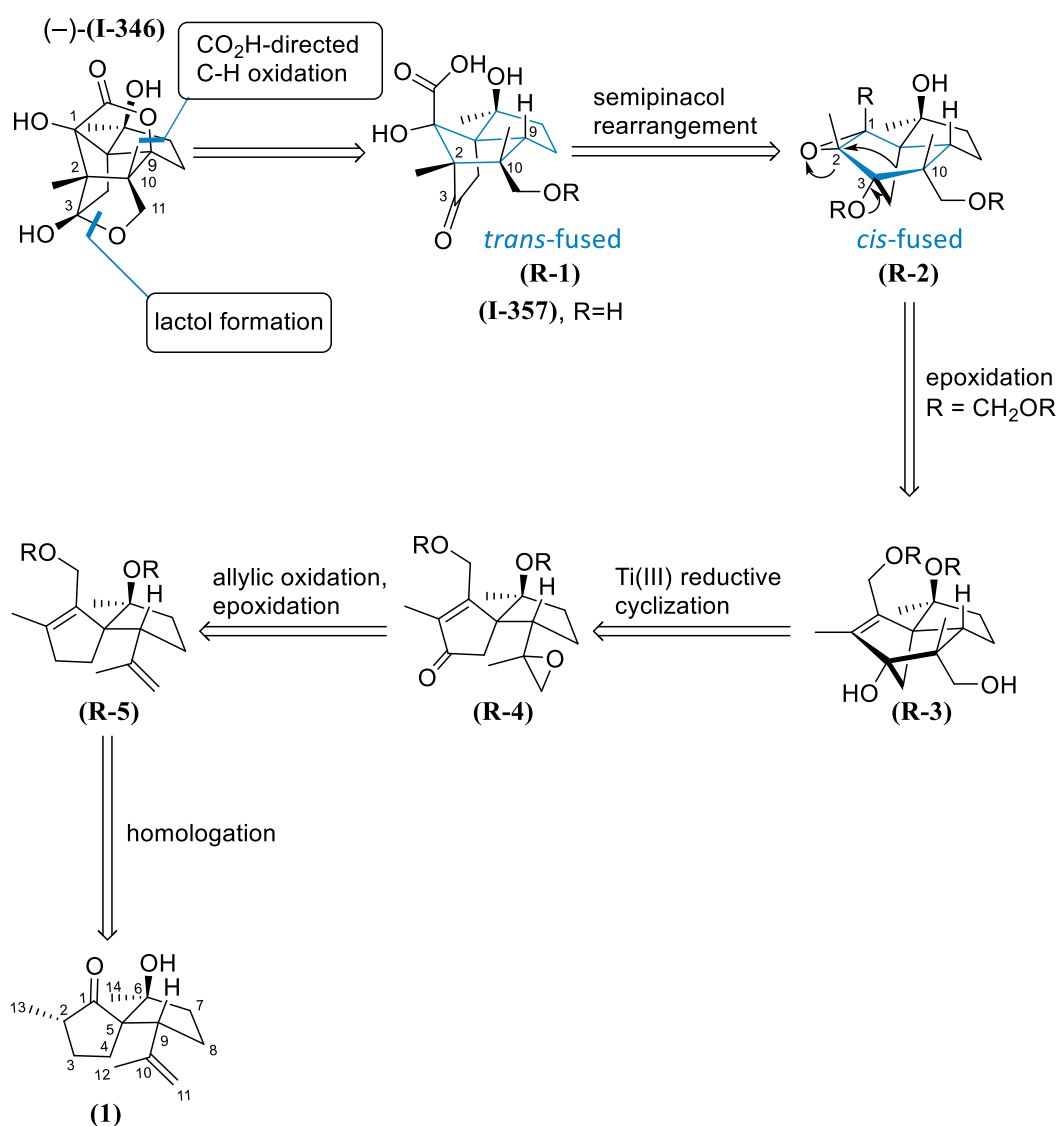


Scheme 64 – Rychnovsky and Burns's total synthesis of (±)-illisimonin A.

The natural enantiomer of the target molecule was obtained through derivatization of alcoholic intermediate (I-354) with (*S*)-1-(1-naphthyl)ethyl isocyanate and separating the diastereomers by silica gel chromatography.

Aim of this work and retrosynthetic considerations

The aim of this work is the total synthesis of (-)-illisimonin A (-)-**(I-346)** *via* an interrupted Nazarov cyclization as the key step for constructing the carbocyclic core. For this purpose, several retrosynthetic approaches were investigated, differing in the stage of functionalization, and will be described in dedicated sections. The successful retrosynthetic approach is presented in Scheme 65, which traces (-)-illisimonin A (-)-**(I-346)** back to carboxylic acid **(R-1)**, thanks to a White-Chen-type carboxylic acid-mediated C-H activation, analogous to Rychnovsky's and Burns's approach.¹⁴⁶ This intermediate could be accessed *via* consecutive oxidations of the primary alcohol moiety in an intermediate containing a *trans*-pentalene subunit (oxidative steps not shown). This unstable structural motif would be in turn obtained by means of a type III-semipinacol rearrangement of an epoxide like **(R-2)**. This transformation would construct the C2-C10 bond through migration of the C10 residue, previously bonded to C3. Such an epoxide would be traced back to a norbornane-derivative like **(R-3)** in which the undesired (*i.e.* *cis*-fused) bond connectivity would be established through a Ti(III)-mediated reductive cyclization of epoxyketone **(R-4)**. The correct oxidation state in this precursor would be obtained through an allylic oxidation of diene **(R-5)**, the homologated derivative of spirocompound **(1)**.

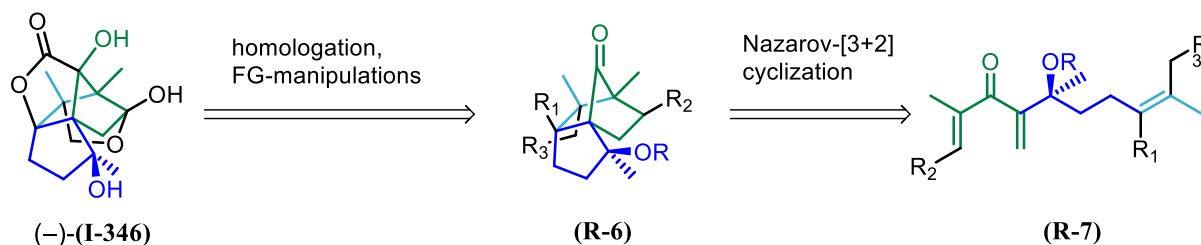


Scheme 65 – Proposed retrosynthetic approach to (-)-illisimonin A (-)-**(I-346)**. Numbering in the structure does not refer to Ma and coworkers¹⁵¹ assignment but refers instead to spirocycle **(1)**, and will be used from now on.

PART 1: Studies on the Nazarov/ene cyclization

(Retro)synthetic background

The proposed retrosynthetic approach entailed from previous experiments carried on in the Kalesse research group starting from 2017. In particular, another retrosynthetic approach was considered when the group turned its attention towards the complex skeleton of illisimonin A (**I-346**). This initial approach was directly aiming for the tricyclic core (**R-6**) embedded in the cage-like structure of illisimonin A (**I-346**), that would have been obtained through a tandem Nazarov/[3+2] reaction, reminiscent of the work described by West and coworkers.⁹³ This alternative approach is reported in Scheme 66.



Scheme 66 – First retrosynthetic approach towards (-)-illisimonin A (-)-**I-346**.

Although quite appealing on paper, this approach was soon realized to be doomed to failure. In particular, Etling, C. realized that, when exposing trienone (\pm)-**(2)** to different Lewis acids, the substrate was showing a strong preference for an alternative reaction pathway, initiating with a Michael-Prins-like cyclization and resulting in different kinds of cyclic products (**(3)** to **(6)**) depending on the employed Lewis acid.

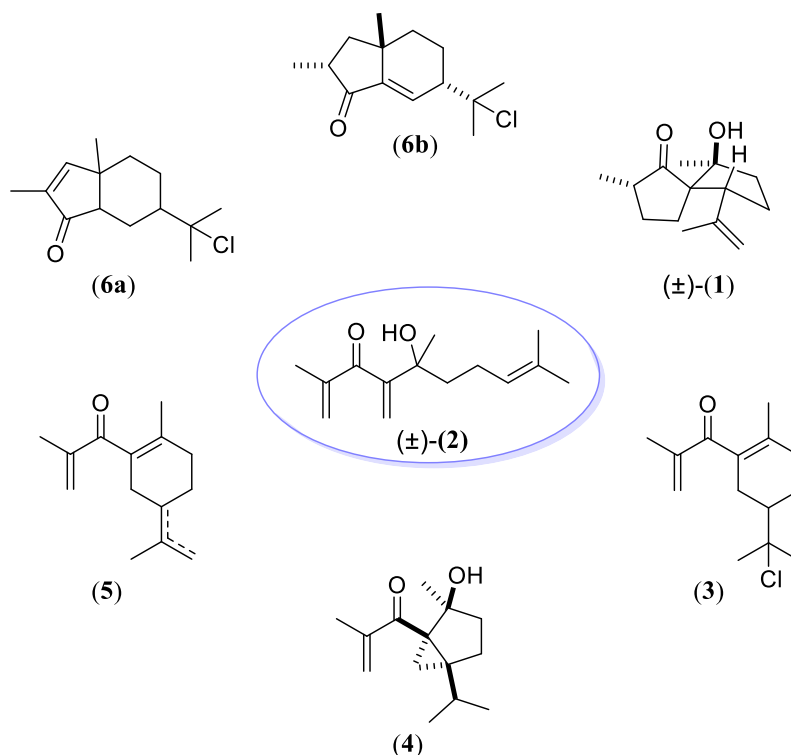
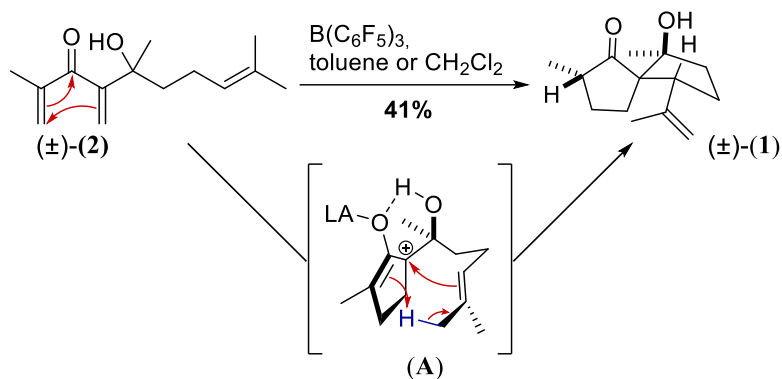


Fig. 17 – Michael-Prins cyclization products of cross-conjugated trienone (\pm)-**(2)**, as well as spirocompound (\pm)-**(1)**.

Instead, a Nazarov cyclization was induced when treating cross conjugated trienone (\pm)-**(2)** with tris(pentafluorophenyl)borane (TPPB), a strong boron-based Lewis acid that had previously been used

in Kalesse's research group in vinylogous Mukaiyama aldol reactions (VMAR).¹⁵⁵ Despite the first successful cyclization, the full cascade to the tricyclic core was never observed. The reaction stopped at a bicyclic compound (\pm)-**(1)**, obtained as a single diastereoisomer (Scheme 67), which was hypothesized and later demonstrated in these studies to be the result of a Nazarov/ene cyclization.



Scheme 67 – Nazarov/ene cyclization of trienone (\pm)-**(2)** and proposed mechanism through intermediate (**A**).

The first part of this thesis will focus on fully understanding the Nazarov/ene cyclization and on testing it on a scope of substrates before its actual application in the total synthesis of (-)-illisimonin A (-)-**(I-346)**. Since the entire scouting was performed on racemic material, for this section the indicator (\pm)- will be omitted.

The elongated precursor

The computational studies reported along with the total synthesis of (-)-illisimonin A (-)-(**I-346**) by Richnovsky and Burns,¹⁴⁶ as well as literature precedents,¹⁵⁶ were a first hint towards understanding the partial cyclization observed for trienone (\pm)-(**2**). In fact, the full cyclization would imply a C2-C10 bond formation (see Fig. 18), resulting in the direct construction of a *trans*-pentalene subunit. Considering that, for the depicted hydrocarbons, the difference in between the desired and undesired connectivity was calculated to be 7.03 kcal/mol, it is not surprising that the full cyclization never occurred.

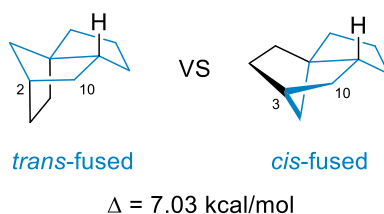


Fig. 18 – Energetic difference between *trans*- and *cis*-pentalene subunits for the depicted simplified hydrocarbon. Numbering follows the retrosynthetic scheme.

At this point, one could wonder if the limited conformational flexibility offered by the three-atom tether that connects oxyallyl cation and interrupting double bond (as in Scheme 67, intermediate (**A**)) could be increased with a longer side chain, lowering the high energetic barrier enough for the desired formal [3+2] cycloaddition to take place. In order to test the validity of this idea, Nazarov precursor (**7**) was designed, elongated by one carbon in the side chain as in Fig. 19.

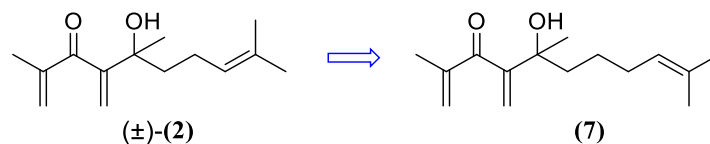
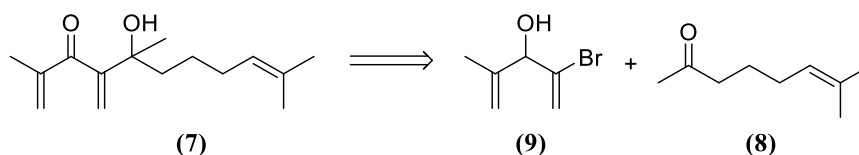


Fig. 19 – Initial Nazarov precursor (\pm)-(**2**) and the new elongated precursor (**7**).

Maintaining the first retrosynthetic strategy applied for “short” precursor (\pm)-(**2**), which will be presented in Part 2, disconnection of compound (**7**) led to methylketone (**8**) and bromoalcohol (**9**), as in Scheme 68. The synthesis of the latter from vinyl bromide (**10**) and methacrolein had been developed by Etling, C. The elongated ketone synthesis will be presented in the discussion part.

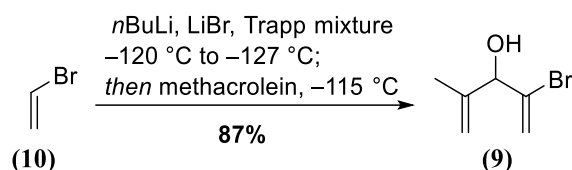


Scheme 68 – Retrosynthetic approach for the synthesis of elongated trienone (**7**).

Once obtained, trienone (**7**) would be subjected to classic spirocyclization conditions as well as further screening for a better understanding of the mechanistic insights behind this transformation.

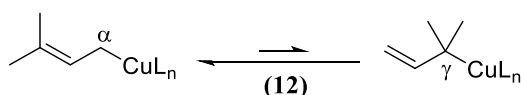
Results and discussion

As already mentioned, the synthesis of bromoalcohol (**11**) had already been developed in the Kalesse research group along with preliminary studies on the original precursor. The synthesis involved the lithiation of vinyl bromide (**10**) at $-120\text{ }^{\circ}\text{C}$ in the presence of lithium bromide, followed by slow addition of methacrolein (Scheme 69). The reaction could be performed on multigram scale, and furnished the desired alcohol in high yields after distillation under reduced pressure.



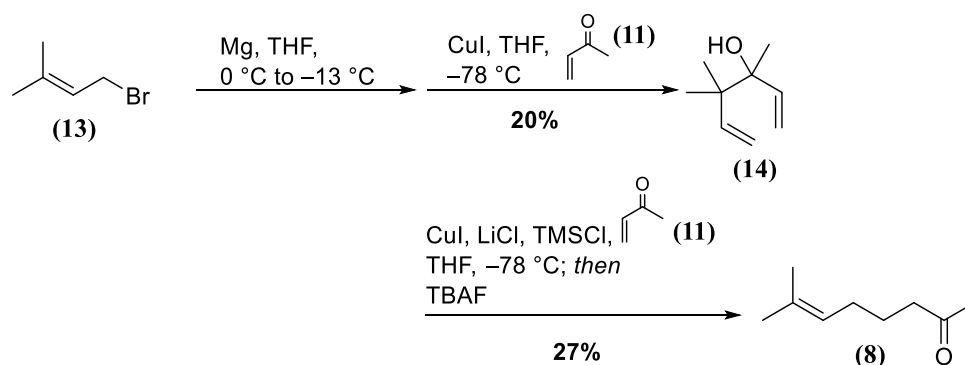
Scheme 69 – Synthesis of bromodienol (**9**) from vinyl bromide (**10**).

Regarding the carbonylic counterpart, the most straightforward idea on paper was a 1,4-addition between methylvinyl ketone (**11**) and a prenyl organometallic reagent (**12**). This strategy would lead to two main issues: first, the choice of the metal counterpart would be crucial for discriminating between the desired 1,4-addition or the concurrent 1,2-addition. Second, the prenyl-type reagents can add either at the α - or γ -site (see Scheme 70 exemplified for prenyl cuprates). An old study from Lipshutz and Hackmann demonstrated *via* NMR experiments that prenyl cuprates are γ -bound species,¹⁵⁷ while the tendency of copper-reagents to undergo 1,4-addition is well documented.¹⁵⁸ However, the nature of the employed enone could likely enable different reactivities.



Scheme 70 – α - or γ -bound prenyl cuprates (**12**) and their equilibrium.

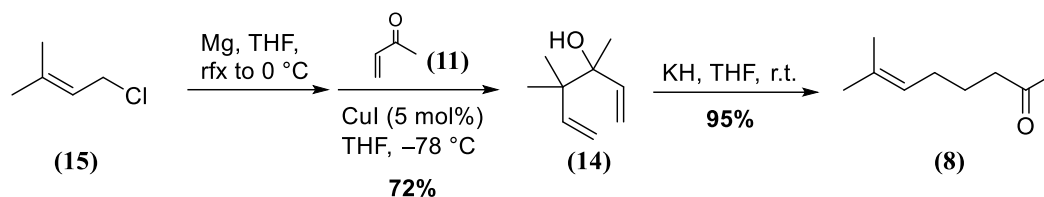
To test whether this chemistry would work on methyl vinyl ketone, a first attempt was made, employing CuI (1.5 equiv.) for the *in situ* production of the copper-reagent from prenylmagnesiumbromide. This approach afforded tertiary alcohol (**14**) due to γ -1,2-addition. This result suggested that the concentration of the active copper species might have been not high enough to favour the desired addition mode. For this reason, an higher excess of copper(I) iodide (3.3 equiv.) was tested. Trimethylsilylchloride, as well as LiCl, were used as additives.¹⁵⁹ The reaction yielded desired ketone (**8**), albeit in poor yields. Both attempts are summarized in Scheme 71.



Scheme 71 – Preliminary synthetic attempts for the synthesis of elongated ketone (**8**).

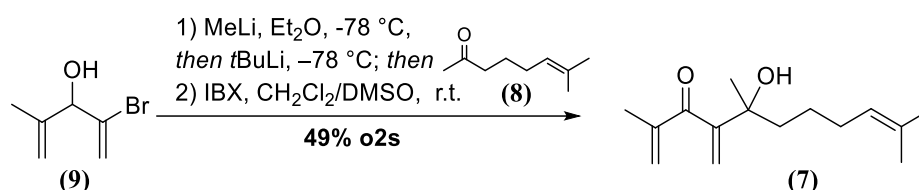
At first, the γ -1,2 addition had appeared as an unfavorable side pathway; however, the observation that desired methyl ketone (**8**) could be on paper be obtained from an oxy-Cope rearrangement of tertiary alcohol (**14**), suggested to further improve the reversed 1,2-addition. The exchange of the

halogen counterpart, and the use of catalytic copper iodide resulted in an increase of the yield to 72%. Treatment of the obtained alcohol (**14**) with potassium hydride¹⁶⁰ furnished the desired ketone (**8**) in 95% yield, as depicted in Scheme 72.



Scheme 72 – Synthesis of elongated ketone (**8**) via oxy-Cope rearrangement of allylvinylalcohol (**14**).

With consistent amounts of compound (**8**) in hands, the deprotonation and lithium-halogen exchange on bromoalcohol (**9**) could be performed, with the same procedure established for the shorter Nazarov precursor. IBX smoothly oxidized the secondary alcohol, furnishing desired trienone (**8**).



Scheme 73 – Synthesis of elongated Nazarov precursor (**7**) via known lithiation chemistry.

A screening of Lewis acids gave a first glance on this new precursor's reactivity. The cyclization attempts are summarized in Table 1.

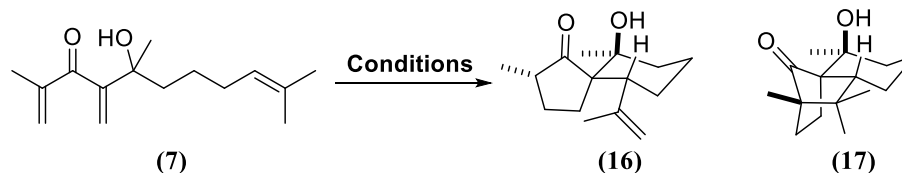


Table 1 – Preliminary screening for the cyclization of elongated trienone (**7**).

Entry	Lewis acid (equiv.)	Conditions	Conc. (M)	Product (Yield ^[a])
1	B(C ₆ F ₅) ₃ (2.5 mol%)	CH ₂ Cl ₂ , 30 °C, 8.5 h	0.02	(16) (77%)
2	FeCl ₃ (1.0 equiv.) ^[b]	CH ₂ Cl ₂ , -30 °C to 30°C, 2 d	0.02	complex mixture
3	BF ₃ ·OEt ₂ (1.1 equiv.) ^[c]	CH ₂ Cl ₂ , -78 °C to -50°C, 2 d	0.02	complex mixture
4	SnCl ₄ (1.1 equiv.) ^[c]	CH ₂ Cl ₂ , -78 °C to 0°C, 2 h	0.02	(16) (25%), (17) (19%)
5	TiCl ₄ (1.1 equiv.)	CH ₂ Cl ₂ , -78 °C, 0.5 h	0.01	decomposition
6	BCl ₃ (1.1 equiv.)	CH ₂ Cl ₂ , -78 °C, 1 d	0.01	complex mixture
7	AlCl ₃ (1.1 equiv.)	CH ₂ Cl ₂ , -78 °C, 1 d	0.01	no reaction ^[b]

[a] Isolated yield. [b] TLC indicated full conversion of starting material, but after workup only starting material could be identified by NMR spectroscopy; [b] *J. Am. Chem. Soc.* **1999**, *121*, 876–877; [c] *Angew. Chem. Int. Ed.* **2000**, *39*, 1970–1973.

Interestingly, during the preliminary screening no cyclization product that could be traced back to the Michael-Prins reaction pathway was observed. Most of the tested conditions resulted either in a complex mixture or in decomposition of the starting material. This behaviour could be explained

referring to the *7-endo-trig* cyclization that would initiate this process, that was thought to occur slower than the corresponding *6-endo* furnishing the Michael-Prins products in Fig. 17. However, treatment of elongated trienone (**7**) with TPPB (Entry 1, Table 1) furnished a 5/6 spirocycle (**16**), whose stereochemistry was reminiscent of predecessor spirocompound (\pm)-(**1**), although in higher yields. Apparently, a positive correlation existed between the chain flexibility and the feasibility of the second cyclization. Moreover, when tin(IV)tetrachloride was employed (Entry 4, Table 1), unprecedented tricyclic compound (**17**) was observed, that was demonstrated to be the result of a Nazarov/[3+2] cascade. This observation suggested that also the full cyclization might benefit from a more flexible side chain. A second screening of conditions followed, aiming for a better understanding of the reaction conditions favouring the [3+2] termination.

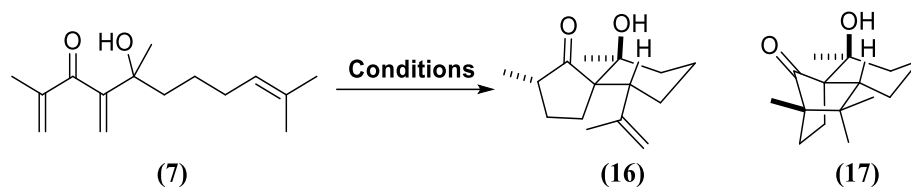


Table 2 – Conditions screening for the full cyclization of elongated trienone (**7**).

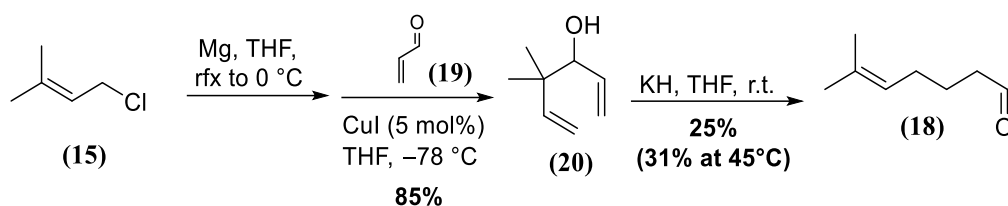
Entry	Lewis acid (equiv.)	Conditions	Conc. (M)	Product (Yield)
1	SnCl ₄ (10 mol%)	CH ₂ Cl ₂ , -78 °C to 0 °C, 4 d	0.01	(16) (21%), (17) (15%), (7) (36%)
2	SnCl ₄ (20 mol%)	CH ₂ Cl ₂ , -78 °C to 0 °C, 2 d	0.01	(16) (26%), (17) (<5%)
3	SnCl ₄ (30 mol%) ^[b]	CH ₂ Cl ₂ , -78 °C to 0 °C, 6 h	0.01	(16) (43%), (17) (1%)
4	SnCl ₄ (1.1 equiv.)	CHCl ₃ , -78 °C to 0 °C, 4 h	0.01	(16) (37%), (17) (<5%)
5	SnCl ₄ (1.1 equiv.)	THF, -78 °C to rt, 2 d	0.01	no reaction
6	SnCl ₄ (1.1 equiv.)	Et ₂ O, -78 °C to rt, 2 d	0.01	uncharacterized product mixture
7	SnCl ₄ (1.1 equiv.)	toluene, -78 °C to 0 °C, 2.5 h	0.01	(16) (45%)

[a] Isolated yield. [b] 0.1 equiv. were added every two hours.

The optimization attempts included both catalytic versions of the successful reaction (Entries 1-3, Table 2) and variations of solvents (Entries 4-7, Table 2). The catalytic use of the Lewis acid resulted in an improvement in the ene-product yields, almost suppressing the [3+2] trapping of the oxyallyl cation. Toluene completely excluded the formation of the fully cyclized product (Entry 7, Table 2). The use of diethyl ether (Entry 6, Table 2) yielded an uncharacterized products mixture, while THF completely inhibited the reaction (Entry 5, Table 2). After these few attempts, it became clear that the partial cyclization involving a postulated ene-like cyclization was the preferred reaction mode of trienones like (**7**) under the investigated conditions.

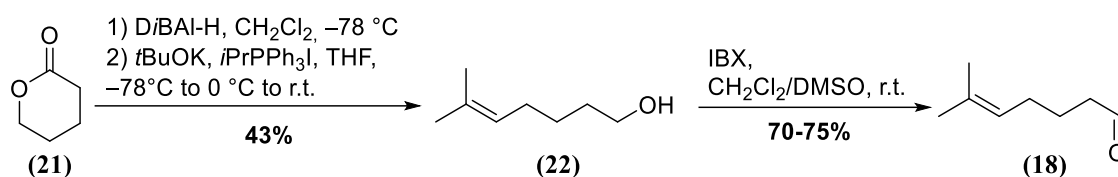
Further insights into this reactivity were gained when designing elongated aldehyde (**18**) (Scheme 74). The synthesis of the secondary alcohol prior to the oxy-Cope rearrangement, analogous to the protocol established for ketone (**8**), worked even better with acrolein, due to the enhanced electrophilicity of

the carbonyl group. However, the consequent rearrangement was not as effective, and the desired aldehyde could be obtained in low yields even at higher temperatures. The observation of a second aldehyde in the proton NMR suggested that secondary alcohol (**20**) would rather undergo acetylene elimination in lieu of the desired rearrangement.



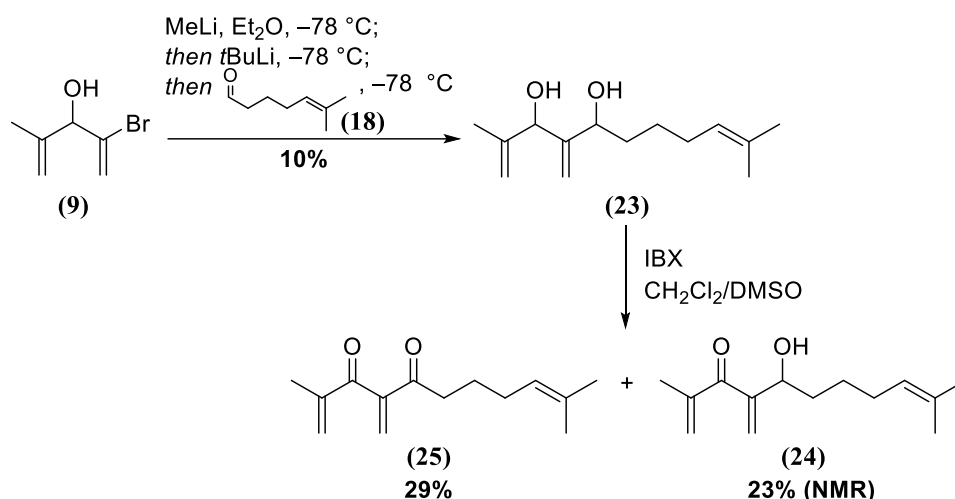
Scheme 74 – Synthesis of elongated aldehyde (**18**) via oxy-Cope rearrangement of secondary alcohol (**20**).

A more scalable procedure was present in literature, in which the reduction of δ -valerolactone (**21**) followed by Wittig olefination of the resulting lactol with isopropyltriphenylphosphonium iodide afforded primary alcohol (**22**),¹⁶¹ as in Scheme 75; consequent IBX oxidation gave desired aldehyde (**18**).



Scheme 75 – Synthesis of elongated aldehyde (**18**) from δ -valerolactone.

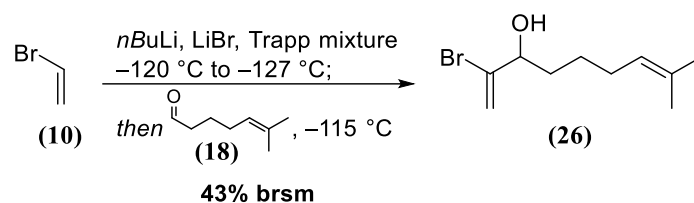
The coupling of aldehyde (**18**) with bromoalcohol (**9**), shown in Scheme 76, was not as effortless as expected: the MeLi/*t*BuLi/electrophile combination that was successful with ketone (**8**) was not effective for elongated aldehyde (**18**). Moreover, it was not possible to discriminate between the two secondary alcohols with the usual oxidative conditions.



Scheme 76 – Synthesis of elongated Nazarov precursor (**24**).

The failure of the first step was posing a surprise, being the electrophile employed the only variation made to the procedure. The overoxidation, on the contrary, was contemplable. A different retrosynthetic cut, which will be encountered in the main synthetic paragraph (Part 2), was considered to circumvent this problem entirely. The use of bromoalcohol (**26**), synthesized as in Scheme 77,

together with a carboxylic acid derivative like (**27**) (see Table 3), would overcome the regioselectivity problems of the first route.



Scheme 77 – Synthesis of vinyl bromide (**26**).

A summary of the conditions tested on bromodienol (**26**) is reported in Table 3:

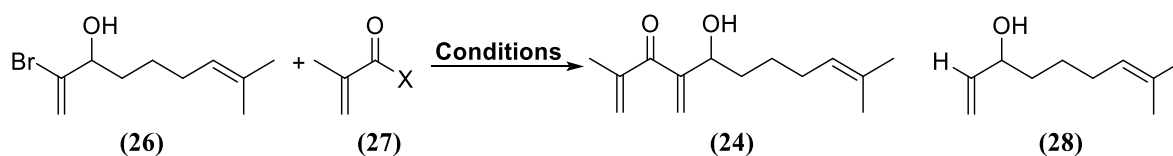


Table 3 – Conditions screening for coupling of bromodienol (**26**) and methacryloyl derivatives (**27**).

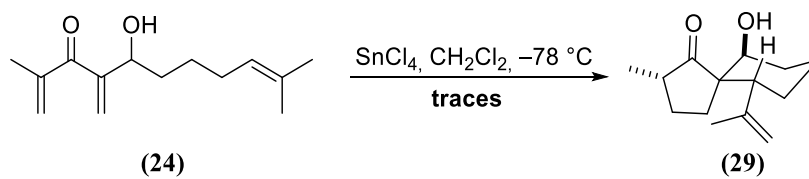
Entry	Conditions ^[b]	Outcome (Yield ^[a])
1	MeLi; then <i>t</i> BuLi (2.2 equiv.), 4 h; then E ⁺ (X = OMe) (1 mmol scale)	(28) (52%)
2	MeLi; then <i>n</i> BuLi (3.5 equiv.), 4 h; then MeOH (0.1 mmol scale)	Br-H exchange (70%) ^[c]
3	MeLi; then <i>n</i> BuLi (3.5 equiv.), 4 h; then E ⁺ (X = OMe) (0.2 mmol scale)	(26) (61%)
4	MeLi; then <i>n</i> BuLi (3.5 equiv.), 22 h ^[c] ; then E ⁺ (X = Cl) (0.2 mmol scale)	Mainly decomposition

[a] Isolated yield; [b] MeLi (1.1 equiv.) and E⁺ (1.2 equiv.) in THF at -78 °C were used in all attempts; [c] Determined by ¹H NMR [c] ¹H NMR of a sample withdrawal quenched with MeOH showed 100% of lithiation.

The first attempt (Entry 1, Table 3) employed methylester (**27**) (X = OMe) as an electrophilic counterpart. However, no traces of desired compound were detected; alcohol (**28**), resulting from simple halogen-metal exchange and quenching with a proton source, was isolated. The low yield posed a doubt on the effective completion of Br/Li-exchange. For this reason, Entry 2 (Table 3) reports an experiment in which the nature of the second base, as well as the equivalents employed, was changed. Quenching with methanol after 4 hours resulted in 70% of Br-H exchange. The same conditions in the presence of the electrophile (Entry 3, Table 3) however, furnished over 60% of recovered starting material. Entry 4 (Table 3) reports a procedure in which lithiation with *n*BuLi prolonged overnight proved to be efficient, but use of methacryloyl chloride (**27**) (X = Cl) as the electrophilic counterpart (Entry 4, Table 3) showed mainly decomposition on TLC.

At this point, no further effort was posed into this direction, supported from the fact that in case of successful cyclization, this would not guarantee any simpler access to the natural product on the long term. As a proof of concept, a cyclization test with tin(IV) tetrachloride (Scheme 78) was performed on impure (**24**). Traces of compound (**29**), as result of a tandem Nazarov/ene cyclization (still an hypothesis until then), were isolated. This gave a further insight on the prominence of this behaviour

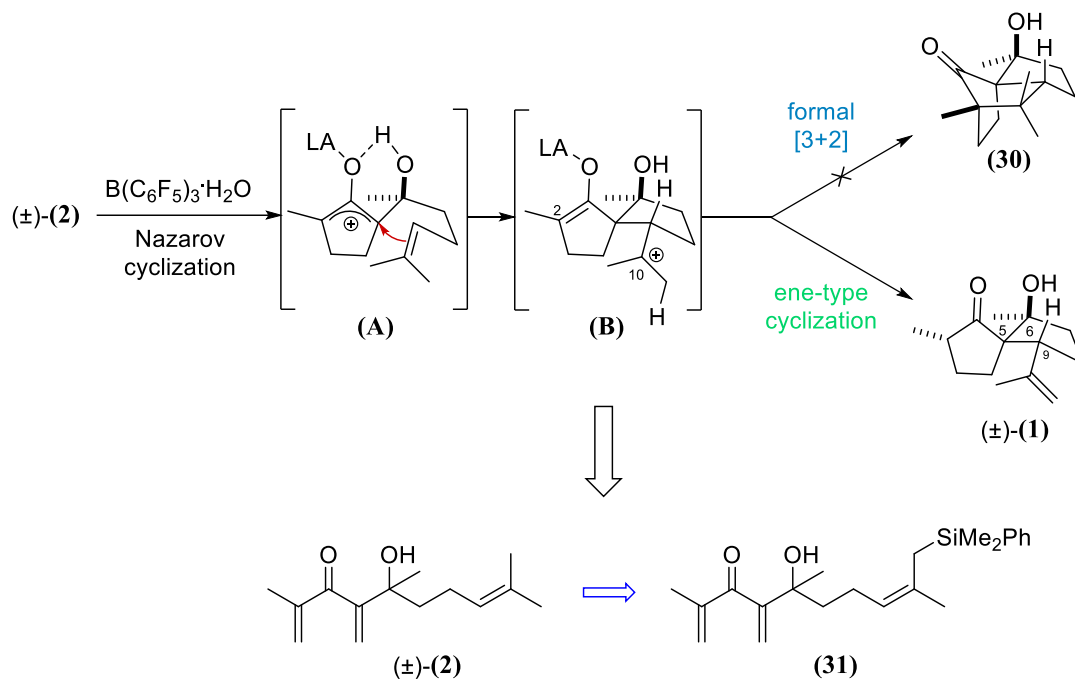
even in the absence of the tertiary alcohol motif. NOE experiments confirmed the relative stereochemistry to be the same for the tertiary alcohol-derivatives.



Scheme 78 – Cyclization of impure compound (24).

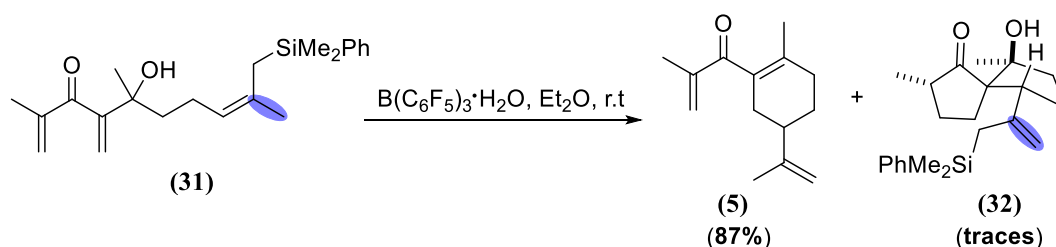
The functionalized precursor

During his studies on the Nazarov cyclization, Etling, C. had designed a silylated trienone (**31**) that, in analogy with the work of West and coworkers on interrupted Nazarov cyclizations with allyl silanes,⁹³ could have been a reasonable option for pushing the substrate to full cyclization. Specifically, the cyclization was at first believed to happen through a cationic intermediate like (**B**), shown in Scheme 79, in analogy with the Prins-like observations; a silicon protecting group was thought to be able to stabilize cationic intermediate (**B**), prolonging its life time enough for the [3+2]-cyclization to occur prior to elimination to ene-like product (\pm)-(**1**). Moreover, the silyl moiety would have constituted a useful handle for further functionalization.



Scheme 79 – Mechanistic hypothesis for the formation of ene-like product (\pm)-(**1**) and consequent design of a silylated precursor (**31**).

However, exposing silylated trienone (**31**) to TPPB in stoichiometric conditions did again not result in the desired outcome, but in monocyclic compound (**5**) (Scheme 80).



Scheme 80 – Cyclization of silylated precursor (**31**).

The formation of compound (**5**) was rationalized through conjugated addition, already encountered during the preliminary studies. In this context, the increased nucleophilicity of the terminal double bond would facilitate the addition to the enone, and result in excellent yields. The observation of spirocycle (**32**), however, was not as straightforward to explain. The idea of a strictly cationic intermediate like (**B**) (Scheme 79) would have been in agreement with a loss of the silicon moiety,¹⁶² which was still present in bicycle (**32**). Moreover, it appeared clearly that the reaction proceeded with selective transposition of the side chain double bond, highlighted in Scheme 80, to the former (*E*-

methyl group position of trienone (**31**). To further support this hypothesis, a new functionalized trienone (**33**) was designed (Fig. 20), in which the (Z)-double bond of the side chain would be equipped with a –OTBS group that, in case of successful cyclization, would represent an handle as useful as the silylated precursor for further synthetic efforts.

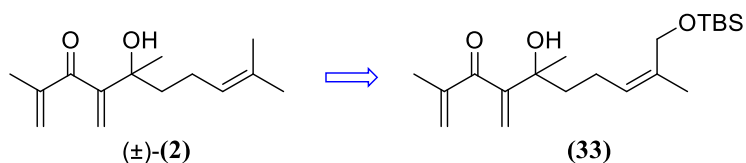
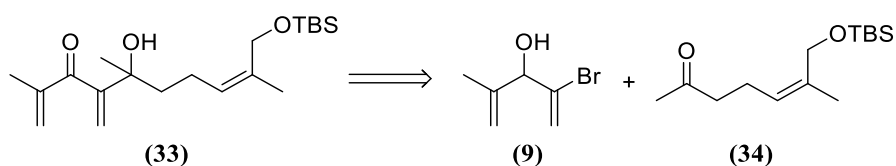


Fig. 20 – Design of a new functionalized precursor (**33**).

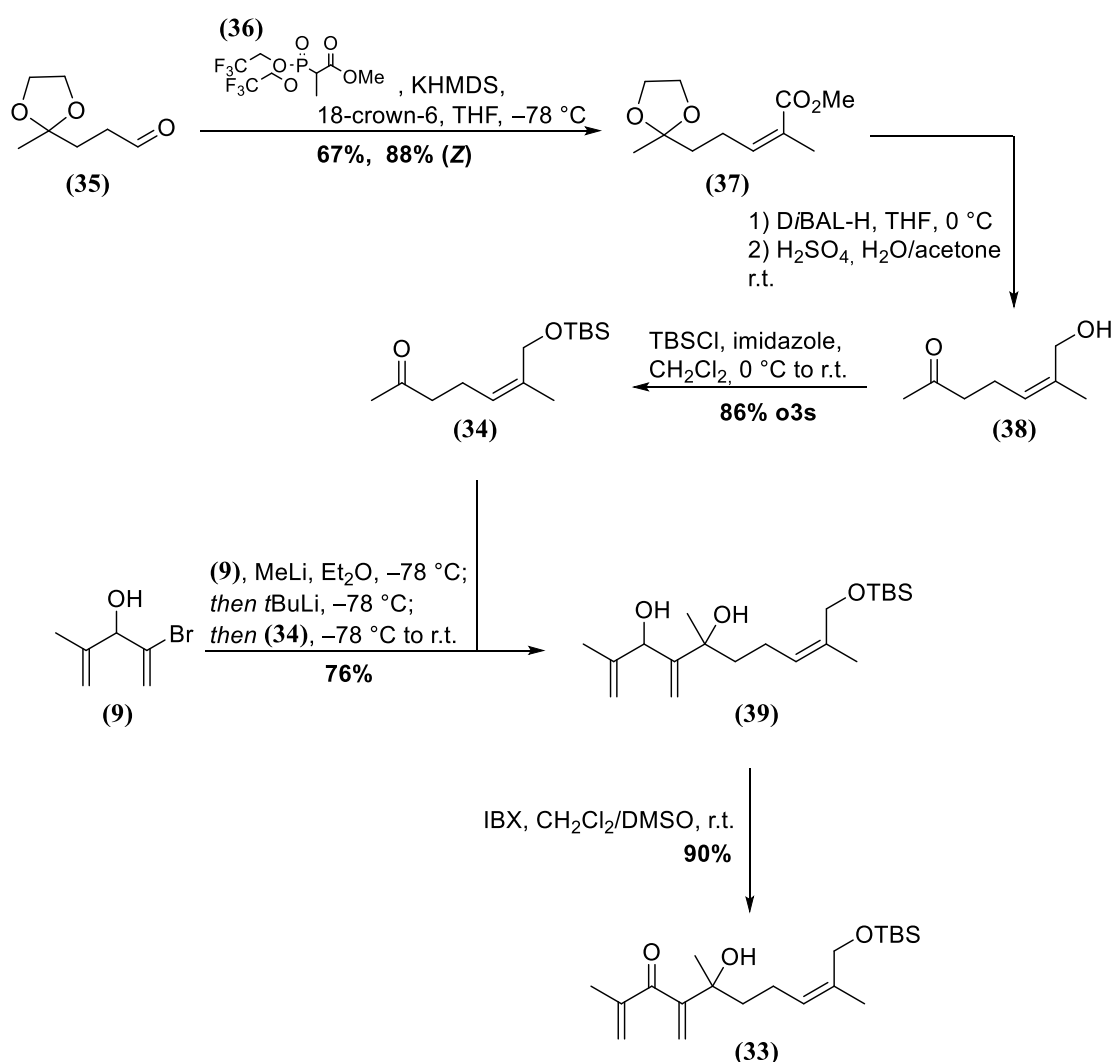
Once again, the most promising retrosynthetic disconnection involved the synthesis of a new carbonylic counterpart, as well as the use of known bromoalcohol (**9**) as shown in Scheme 81.



Scheme 81 – Retrosynthetic approach for the synthesis of functionalized precursor (**33**).

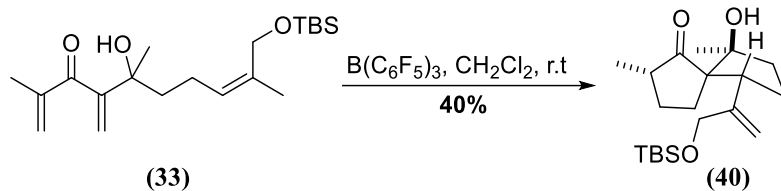
Results and discussion

The synthesis of the functionalized carbonylic compound started from known aldehyde (**35**), which could successfully be synthesized through protected ethyl levulinate, which underwent hydride reduction in accordance with literature conditions.¹⁶³ A Still-Gennari olefination employing methylated phosphonate (**36**), prepared after the protocol from Clausen and coworkers,¹⁶⁴ was successfully performed, yielding desired olefin (*Z*)-(**37**) in 67% yield. Treatment with *D*iBAL-H at 0 °C afforded the corresponding allylic alcohol, whose ketone moiety could be deacetylated and the hydroxyl group TBS-protected to afford the target ketone (**34**) in 86% yields over three steps without any purification of the intermediates.¹⁶³ Coupling with bromodienol (**9**) under the established conditions, followed by IBX oxidation of secondary alcohol (**39**) furnished functionalized Nazarov precursor (**33**), as reported in Scheme 82.



Scheme 82 – Synthetic approach for the synthesis of functionalized precursor (**33**).

Cyclization of compound (**33**), shown in Scheme 83, smoothly occurred with TPPB in catalytic amounts (2.5 mol%) in toluene, with yields comparable to the “short”, unfunctionalized precursor (\pm)-(**2**). Furthermore, the (*Z*)-substituent remained untouched during the cyclization.

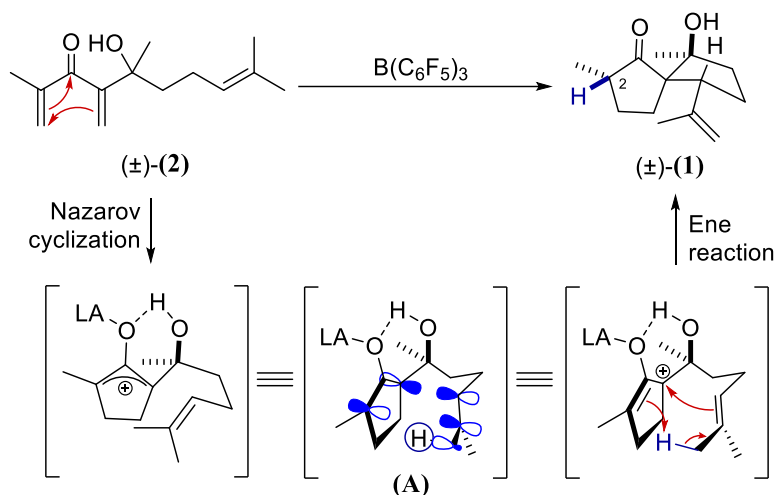


Scheme 83 – Nazarov cyclization of functionalized precursor (33).

This remarkable example demonstrated that, if the electronic properties of the terminal double bond are not strongly modified, the studied Nazarov cyclization can tolerate functional groups at the (Z)-position. The use of this spirocycle in an alternative approach to illisimonin A will be discussed in a dedicated section in Part 2.

Mechanistic studies: the deuterated precursor

The observation of spirocycles like (\pm)-**(1)** in all of the reported experiments, as well as the aforementioned selective transposition of the double bond to the former (*E*)-methyl group position, supported by the very distinct relative stereochemistry at the position 2 in spirocycles (\pm)-**(1)**, **(16)**, **(29)**, **(32)** and **(40)**, gave quite a hint concerning the mechanism involved in this interrupted Nazarov cyclization. Specifically, observations were leading towards a “real” ene-type mechanism, in which the hydrogen bonding between hydroxyl and carbonyl group would guide the attack of the olefin moiety and result in the observed diastereoselectivity (Scheme 84). This hypothesis would correct the mechanistic proposal in Scheme 79 in which intermediate oxyallylcation (**A**) was thought to be converted into ene-product X *via* a strictly cationic intermediate like (**B**).



Scheme 84 – Corrected mechanistic hypothesis for the Nazarov/ene cyclization.

In order to validate this hypothesis, new trienone (**41**) was designed, with a perdeuterated methyl group in the (*E*)-position. The elongated version was chosen due to the better yields observed in the TPPB-initiated cyclization (see Entry 1, Table 1).

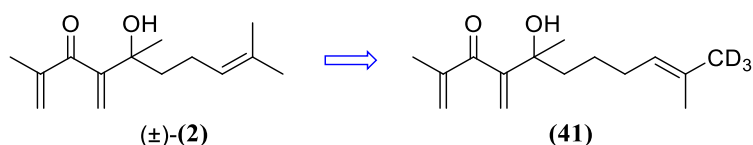
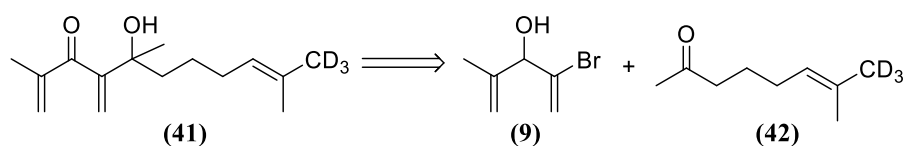


Fig. 21 – Design of a new perdeuterated precursor (**41**).

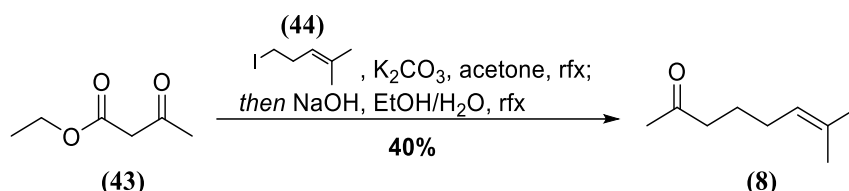
Applying known chemistry, the synthesis of a deuterated trienone would imply focusing the attention on ketone (**42**) (Scheme 85).



Scheme 85 – Retrosynthetic approach for new perdeuterated precursor (**41**).

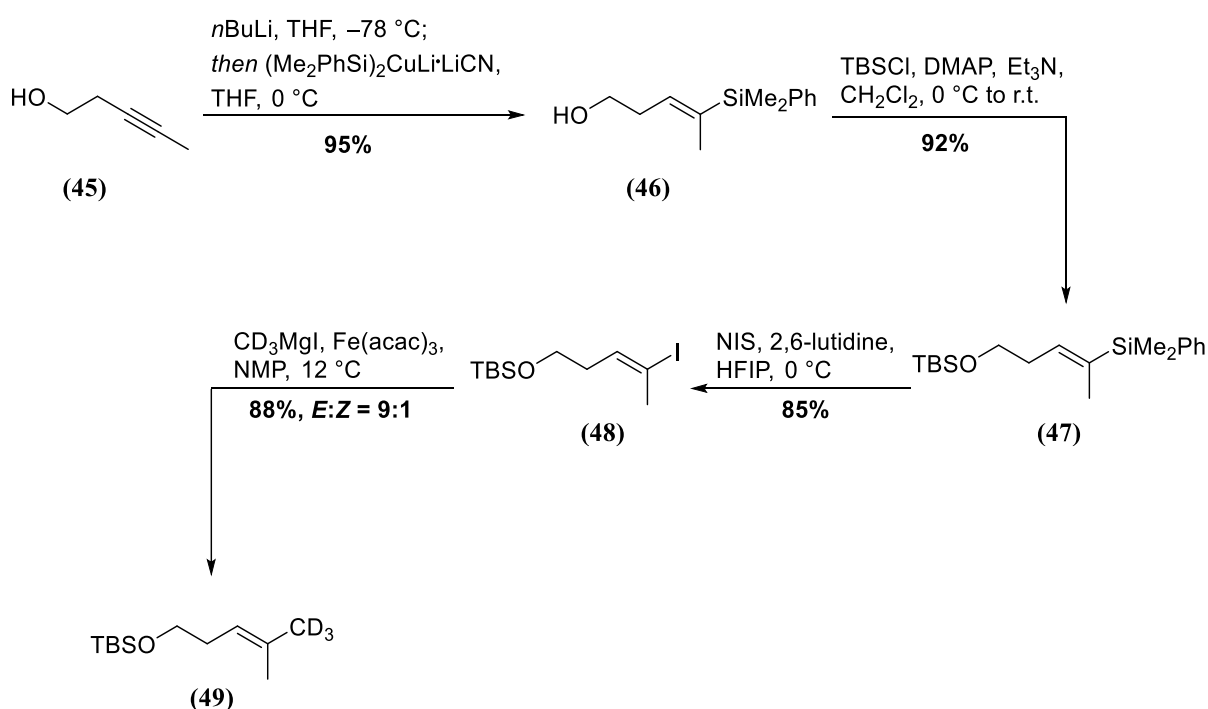
Results and discussion

The biggest challenge associated with the synthesis of perdeuterated ketone (**42**) relied on the selective incorporation of the deuterium atoms into the (*E*)-position, which would be crucial for validating the mechanistic proposal. Specifically, an alternative synthesis of 7-methyloct-6-en-2-one (**8**) had been reported by Tiefenbacher and coworkers,¹⁶⁵ in which the “elongated ketone” had been obtained through an acetoacetic approach, as in Scheme 86. The use of this protocol with the proper homoprenyl halide would probably have guaranteed better chances to obtain higher *E/Z* ratios for aimed ketone (**42**) than the already employed protocol.



Scheme 86 – Tiefenbacher and coworkers’ synthesis of elongated ketone (**8**).

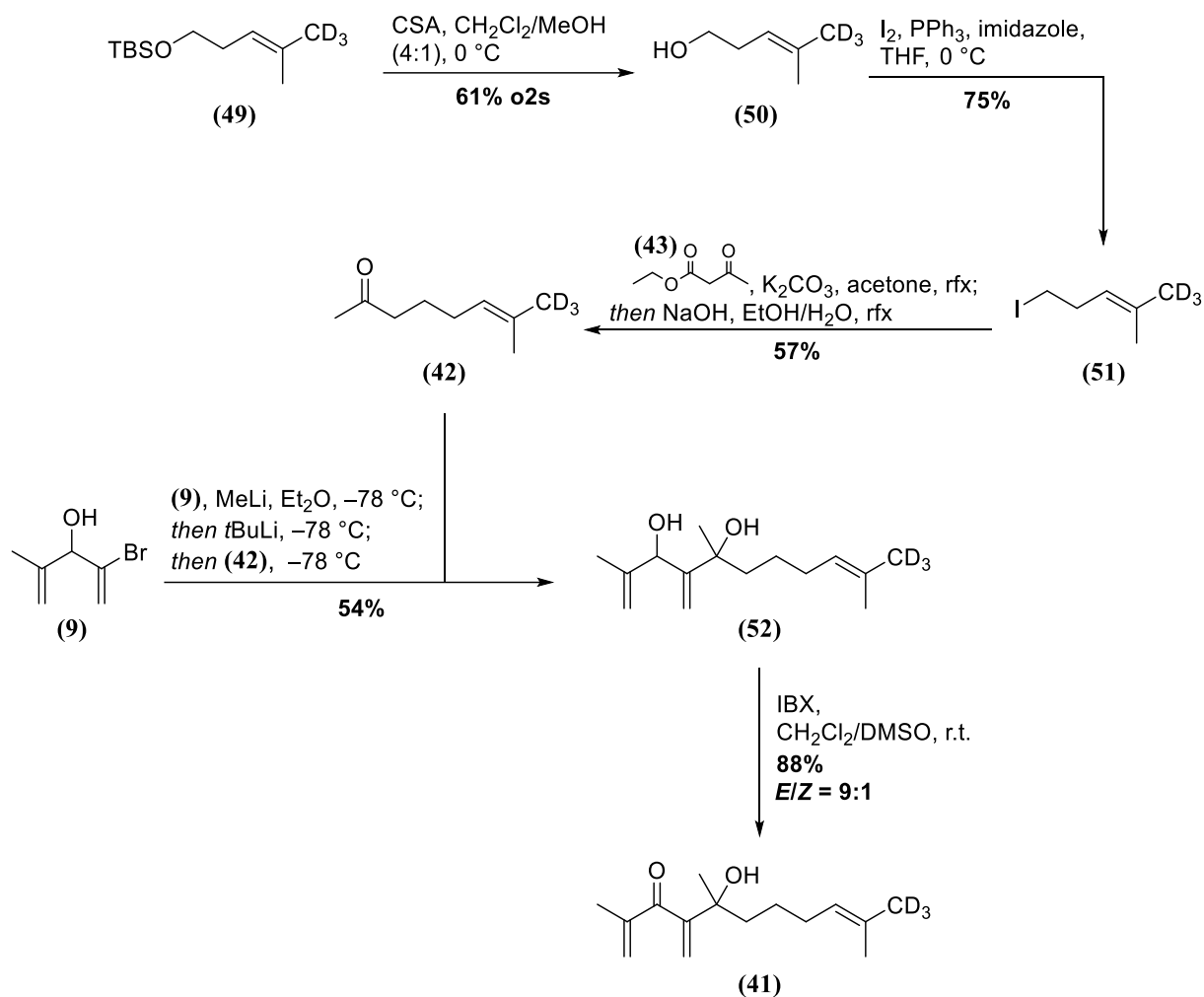
The following experiments were performed in collaboration with Etling, C. who had optimized these reactions on non-deuterated material. Zakarian and coworkers had already reported the synthesis of (*E*)-homoallyl alcohol (**46**), starting from 3-pentyn-1-ol (**45**),¹⁶⁶ the hydroxyl group of this intermediate was protected in standard conditions, to afford TBS-protected vinylsilane (**47**), as depicted in Scheme 87. The conversion of this intermediate into vinyl iodide (**48**) was possible upon treatment with *N*-iodosuccinimide in the presence of 2,6-lutidine. *In situ* prepared trideuteriomethylmagnesiumiodide was used in combination with Fe(acac)₃ (0.25 mol%) to afford (**49**) in good yields, with an *E:Z* ratio of 9:1. An alternative procedure, in which THF was used as a co-solvent (THF:NMP = 5:1), a lower amount of iron catalyst (0.1 mol%) was employed and temperature was maintained at 70 °C overnight, was also unsuccessfully attempted.



Scheme 87 – Synthesis of TBS-protected perdeuterated homoallyl alcohol (**49**).

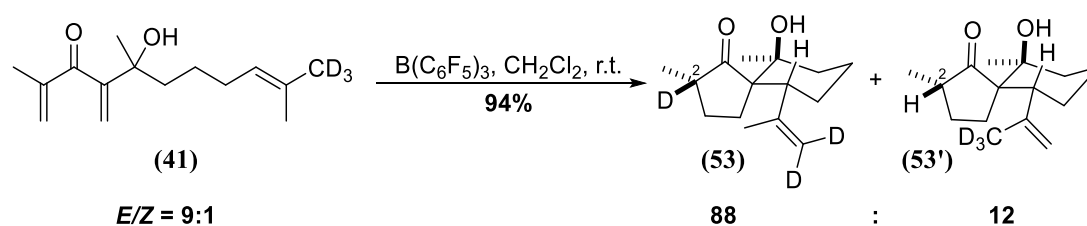
The subsequent operations (Scheme 88) were quite straightforward: removal of the TBS-protecting group in acidic conditions and Appel reaction furnished the substrate for the pivotal acetoacetic step,

that worked even better than the reported procedure,¹⁶⁵ furnishing desired ketone (**42**) in 57% yield. The already mentioned conditions allowed the isolation of perdeuterated Nazarov precursor (**41**) (Scheme 88).



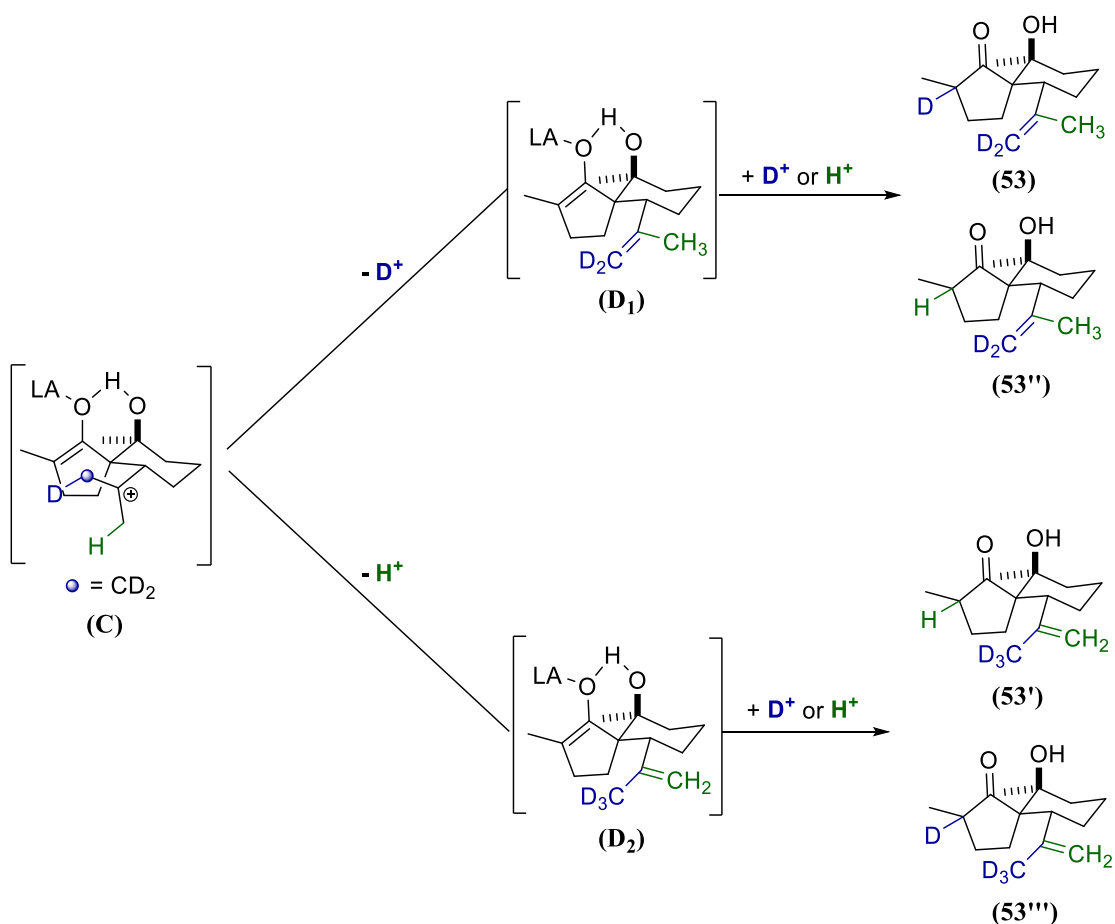
Scheme 88 – Synthesis of perdeuterated Nazarov precursor (**41**).

Cyclization of (**41**) occurred smoothly over three days upon treatment with TPPB in dichloromethane (Scheme 89). The isolated spirocompound (**53**) was easily recognized as deriving from selective incorporation of deuterium at position 2. In fact, proton NMR was lacking the olefinic signals and a sharp singlet took the place of the evergreen doublet belonging to the C-2 methyl group (see experimental part). Moreover, the above mentioned 9:1 ratio in the (*E*)- and (*Z*)-trienone (**41**) mixture was translated almost unaltered in the product composition (88:12 ratio was detected by NMR referring to desired cyclization compound (**53**) and the CD_3 -spirocycle (**53'**) bearing protons at the olefinic and 2 positions).



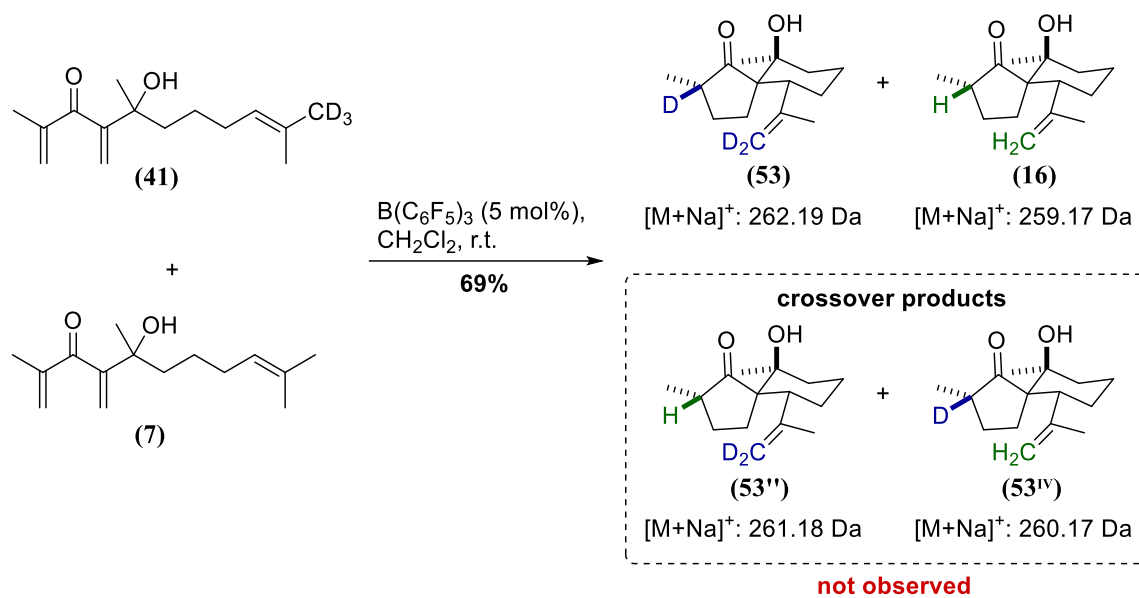
Scheme 89 – Cyclization of perdeuterated Nazarov precursor (**41**).

On the contrary, a stepwise cationic mechanism (E1 elimination of a Prins-like intermediate (**C**), as postulated in Scheme 79, intermediate (**B**)) would have been expected to yield a more or less unselective distribution of deuterium atoms in the product mixture, resulting from an intermediate mixture of alkenes (**D**₁) and (**D**₂). This mixture would in turn derive from intermolecular, casual, proton or deuterium abstraction by a base in the reaction medium, and would undergo subsequent intermolecular protonation/deuteration of (**D**₁) and (**D**₂)'s enol moieties, yielding four different products, as in Scheme 90. Moreover, a weak kinetic isotope effect should operate, favouring proton elimination over deuterium elimination.¹⁶⁷



Scheme 90 – Casual proton/deuteron distribution expected in a stepwise, cationic mechanism.

This experiment indeed confirmed that a concerted ene-type mechanism is operating. To exclude the existence of an intermolecular proton/deuteron transfer as a competing pathway, an equimolar mixture of perdeuterated and non-deuterated precursor ((**41**) and (**7**) respectively) was subjected to a crossover experiment (Scheme 91). Treating the trienones mixture with TPPB (5 mol%) resulted in no detectable crossover products: mass spectrometry (ESI) was employed to confront the isotope distribution in pure samples of (**16**), (**53**) and the product mixture (see experimental section); since no increase in intensity for diagnostic peaks in the reaction mixture was present when comparing to the pure samples, the existence of intermolecular proton/deuteron transfer was ruled out. Moreover, no relevant peak that could correspond to mixed products could be observed.

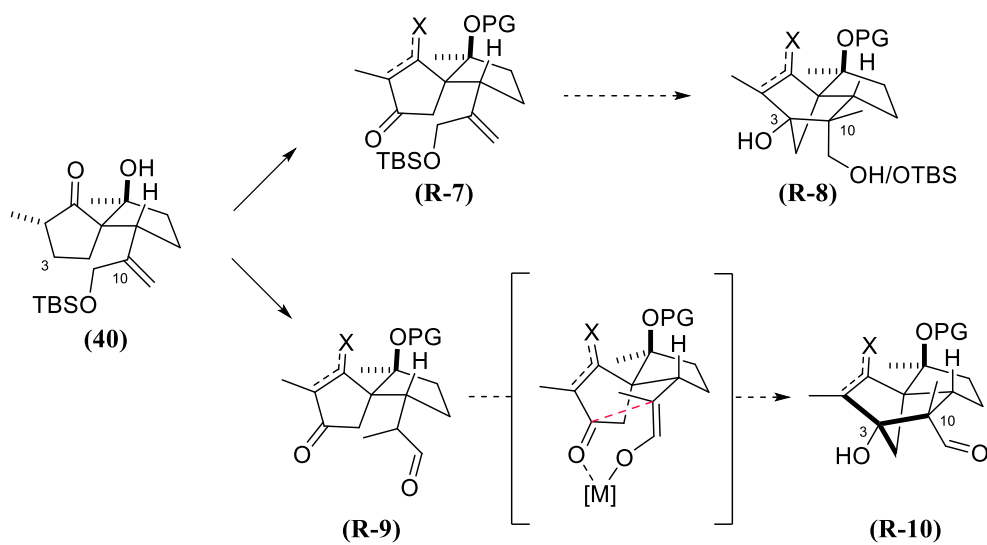


Scheme 91 – Crossover experiment on an equimolar mixture of congeners (7) and (41).

PART 2: Studies towards the total synthesis of illisimonin A

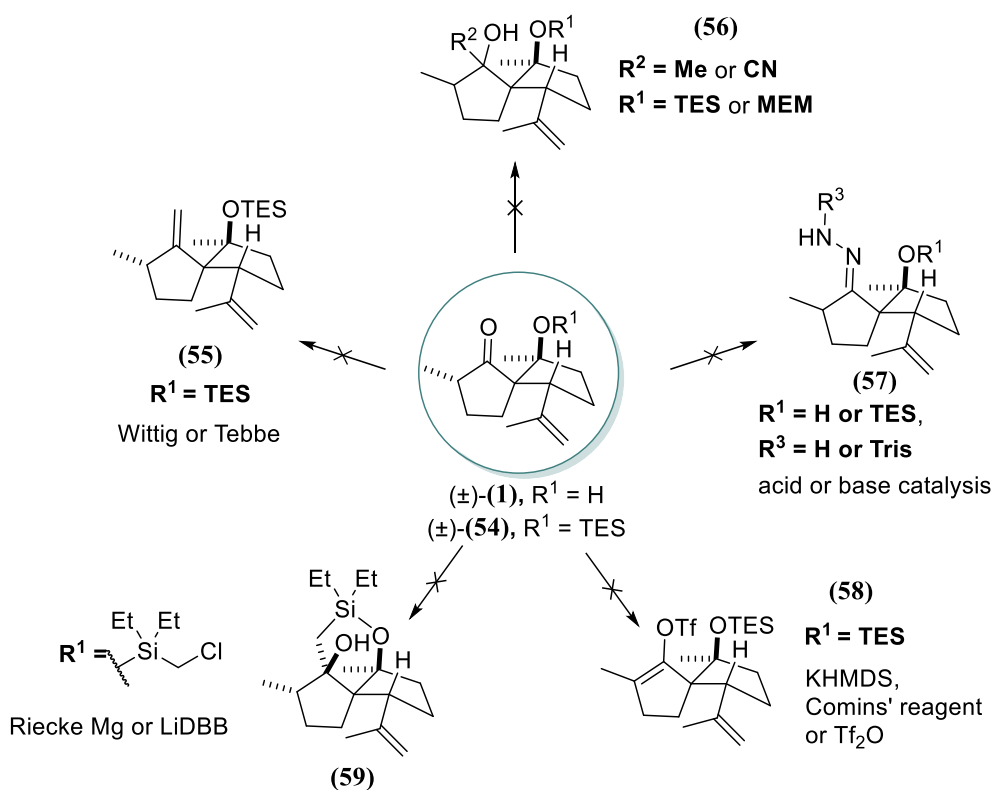
Alternative approach: early stage functionalization

Once the mechanism behind this key step had been fully unraveled, the use of spirocompounds like **(40)** in the total synthesis of (-)-illisimonin A could be evaluated. As already mentioned when dealing with -OTBS cross-conjugated ketone **(33)** in the preliminary Nazarov studies, an early stage-functionalized precursor might have resulted in a useful synthetic intermediate in the total synthesis of illisimonin A (**I-346**). Specifically, the presence of an oxygenated function not only would set the stage for an HAT-like bond formation between C-3 and C-10, but could alternatively be exploited in aldol-type chemistry in case the previous approach would not be successful (Scheme 92).



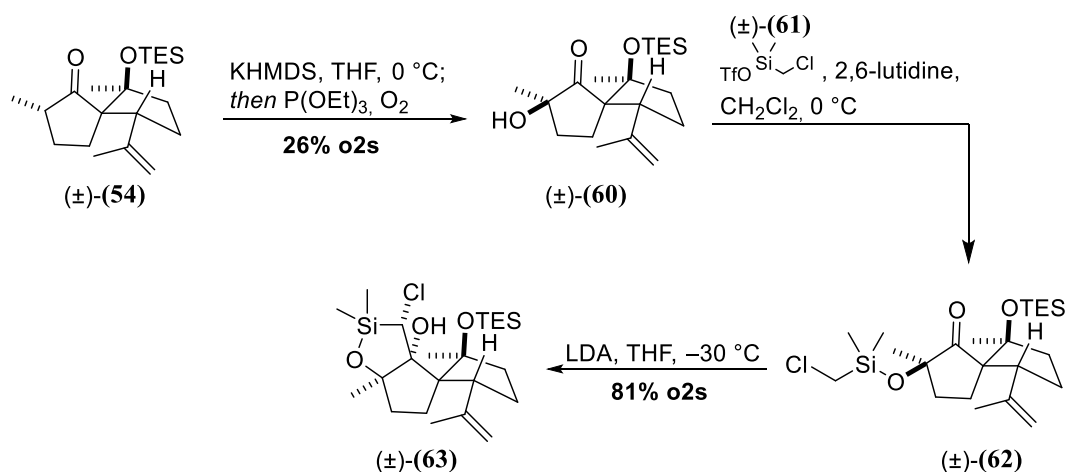
Scheme 92 – Possible HAT or aldol approaches for C3-C10 bond formation.

Preliminary studies by Etling, C., as well as observations made by Rychnovsky and Burns during their synthetic endeavours on illisimonin A (**I-346**),¹⁴⁶ had proved that the one-carbon homologation would have been quite challenging. Specifically, while unprotected spirocycle (\pm)-**(1)** mainly decomposed when subjected to 1,2-addition of organometallic reagents or hydrazine-based homologation strategies,^{153,168} its TES-protected derivative **(54)** was unreactive towards most of the conditions attempted. Unfruitful conditions employed in the Kalesse research group to address the carbonyl moiety, reported in Scheme 93, include 1,2-addition (metal organyls, hydrazine derivatives, or cyanide), olefination, vinyl triflate formation aiming for a subsequent cross-coupling reaction and a silicon-tethered Barbier reaction, using the tertiary alcohol of (\pm)-**(1)** as an anchor.



Scheme 93 – Failed attempts for the homologation of spirocompound (±)-(1) and its TES-protected derivative (±)-(54).

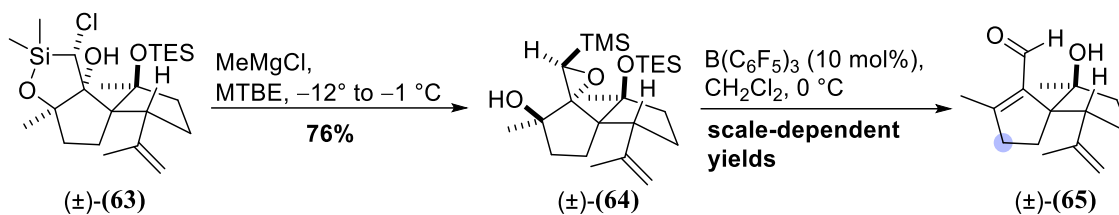
Considering the inertness of both carbon and oxygen atoms in spirocompound (±)-(1) and (±)-(54), homologation of –OTBS functionalized ketone (40) was an urgent discriminant, that would have decided if the pursuing of this strategy would have been valuable. The solution to the homologation problem for non-functionalized spirocompound (±)-(1) had been the α -hydroxylation of spiroketone (±)-(54),⁸³ that delivered the nucleophile to the carbonyl group through the diastereoselective formation of stable oxasilolane (±)-(63) (Scheme 94), in analogy with the work of Zhou and coworkers described in the silicon-tethered reactions section (Scheme 45).¹¹¹



Scheme 94 – Homologation of spirocompound (±)-(54) via α -hydroxylation and Si-tethered 1,2-addition.

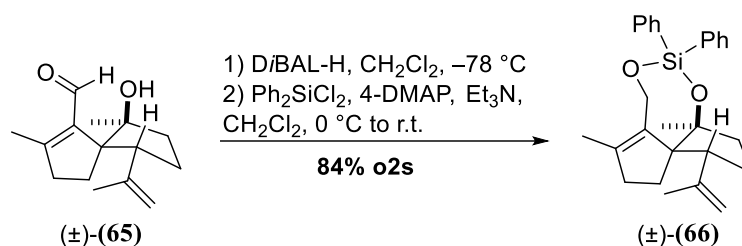
Treatment of silacycle (±)-(63) with MeMgCl (3.0 equiv.) in MTBE at low temperature resulted in the formation of epoxide (±)-(64), which was at this point converted into aldehyde (±)-(65) through

treatment with TPPB. The unsaturation in this last intermediate - or in a derivative – would have served the purpose of facilitating the oxidation at position 3, highlighted in Scheme 95.



Scheme 95 – Rearrangement of oxasilacycle **(±)-(63)** to epoxide **(±)-(64)** and consequent acidic opening.

For chemoselectivity reasons, aldehyde **(±)-(65)** was reduced to the corresponding primary alcohol, as shown in Scheme 96. A stable, bridging, silicon-based protecting group was chosen to prevent reoxidation of the primary alcohol during the above mentioned C-3 oxidation.

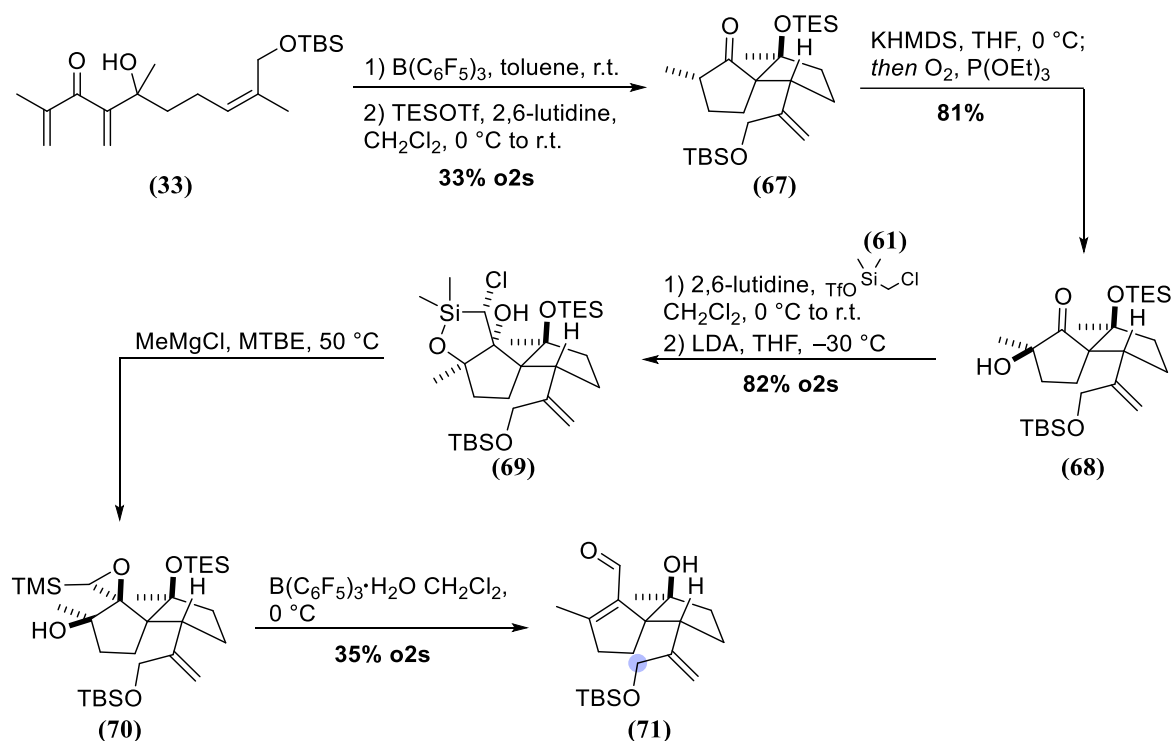


Scheme 96 – Synthesis of protected diol **(±)-(66)**.

Considering these premises, the initial plan was to subject the –OTBS-functionalized spiroketone **(40)** to the same elongation strategy. Synthetic efforts in this direction are reported in the next paragraph.

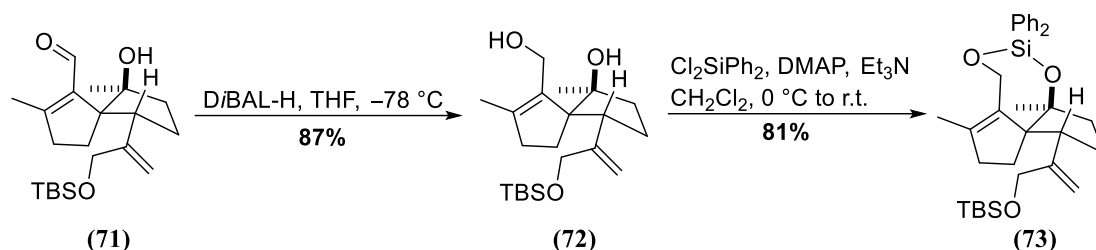
Results and discussion

In analogy with the homologation protocol developed for the unfunctionalized precursor, TES-protected spirocycle (**67**) was deprotonated with KHMDS. Finding precedents in Shenvi's synthesis of (-)-11-O-debenzoyltashironin (-)-(**I-218**) (Scheme 28),⁸³ treatment with triethylphosphite followed by molecular oxygen – compressed air was found to be equally efficient – resulted in diastereoselective α -hydroxylation, as shown in Scheme 97, with yields comparable to the previously reported ones. The silicon tether was smoothly inserted when treating α -hydroxyketone (**68**) with chloromethyldimethylsilyltriflate (**61**), prepared after the procedure reported by Taylor and coworkers,¹⁶⁹ and 2,6-lutidine as the base. Attack of the carbonyl group by the carbon-nucleophile was induced by LDA, which was basic enough to produce α -deprotonation of the chloromethyl moiety. In analogy with the previously observed oxasilolane (\pm)-(**63**), compound (**69**) was obtained as a single diastereoisomer, whose relative stereochemistry was postulated to be the same as in the unfunctionalized case, due to the distance of the –OTBS functionality from the reaction site. Treatment of silacycle (**69**) with MeMgCl, performed at high temperature, resulted in nucleophilic attack of the organometallic species to the electrophilic silicon, with displacement of the chloride caused by the vicinal nucleophilic oxygen, and cleavage of the Si–O bond. Lewis acidic opening of epoxide (**70**) produced α,β -unsaturated aldehyde (**71**), which possessed all of the carbon atoms of the natural product, as well as desired oxidation state at C-11, highlighted in Scheme 97. As in the previously reported preliminary studies, the TES-protecting group was lost during the epoxide opening, while the more stable TBS-group remained untouched.



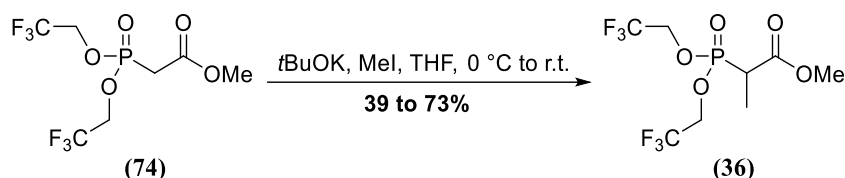
Scheme 97 – Synthesis of functionalized aldehyde (**71**).

Once again, the risk of chemoselectivity problems further in the synthesis suggested the reduction of the aldehyde to be a valid option. Synthesis of diphenylsilyl-protected triol (**73**) is reported in Scheme 98.



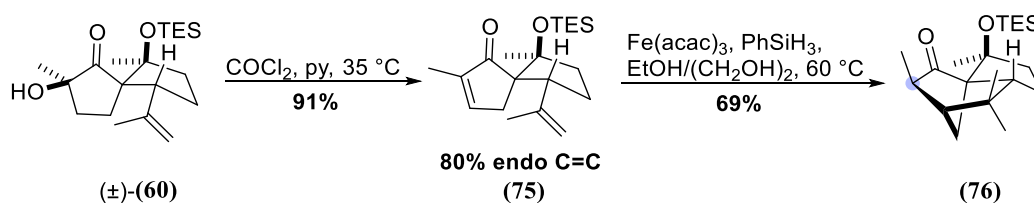
Scheme 98 – Synthesis of diphenylsilyl-protected triol (**73**).

An early deprotection trial was made right after the diphenylsilyl protection, to check if selective deprotection of the TBS-group would be an option later on. A test reaction was performed in which TBAF (1 equiv.) was used at $-40\text{ }^{\circ}\text{C}$. TLC control showed that these conditions were mainly yielding diphenylsilyl deprotection. This observation started to insinuate doubts on the feasibility of this approach. Furthermore, the initial Still-Gennari olefination limited the possibility of a gram-scale synthesis, with methylation of the original Still-Gennari reagent (**74**) (193 € for 5 g by Sigma Aldrich), shown in Scheme 99, featuring a negative correlation between scale and yields. In fact, the same reaction performed on 3 g instead of 1.5 g was causing dropping of the yields from the original 73% to only 39%, and the reaction had to be set on parallel batches of 1.5 g to gather enough material for the entire sequence.



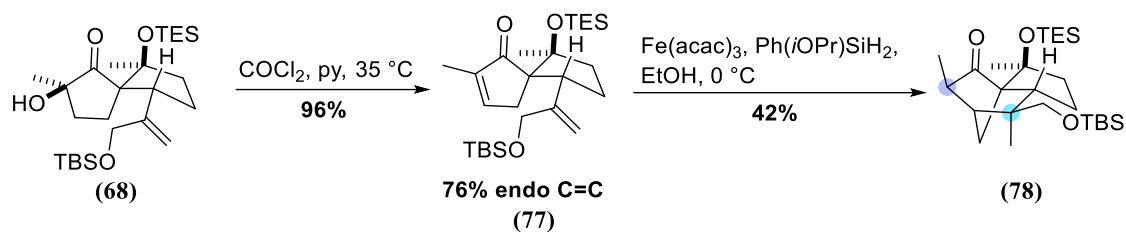
Scheme 99 – Synthesis of functionalized methylated Still-Gennari reagent (**36**).

Moreover, preliminary screenings were made on the envisioned HAT-type cyclization strategy.¹⁷⁰ cyclization on simple enone (**75**), obtained from known α -hydroxylated ketone (**60**) through elimination caused by treatment with phosgene (Scheme 100), had successfully built the desired *cis*-pentalene connectivity, although with the undesired configuration at C-2 (see compound (**76**)).



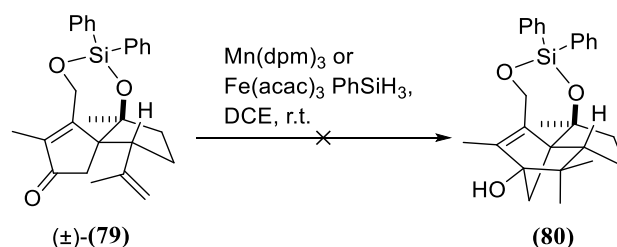
Scheme 100 – HAT-cyclization of dienone (**75**); position 2 is highlighted in norbornane (**76**).

The same stereoconfiguration at C-2, accompanied by the undesired spatial orientation of the OTBS-functionalized methyl group, as depicted in Scheme 101, was observed when translating the same chemical background to functionalized spiroenone (**77**):¹⁷¹



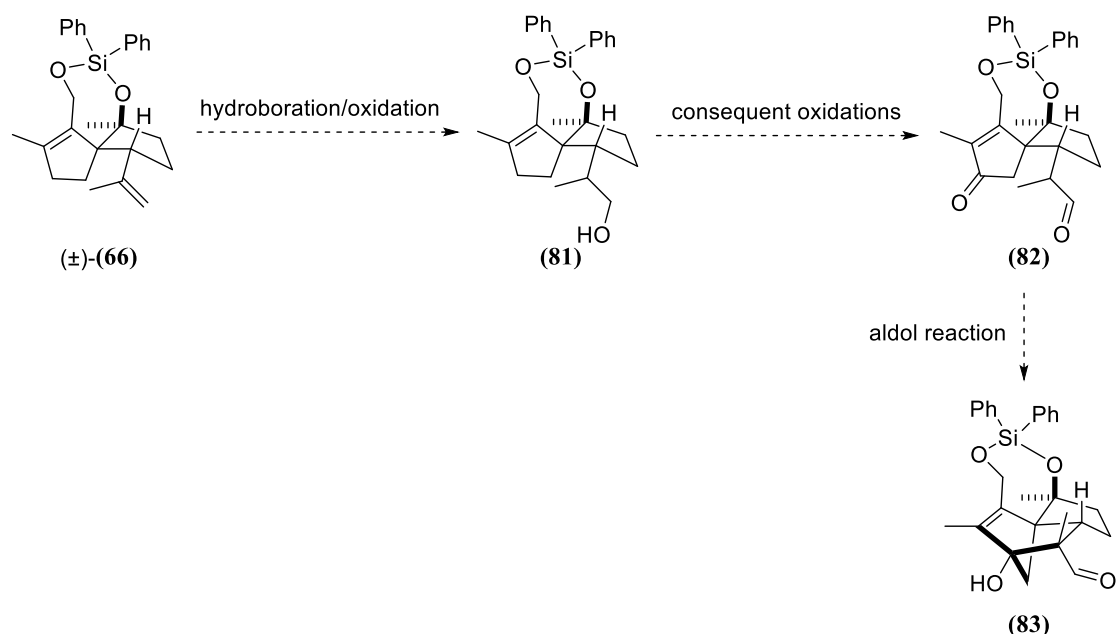
Scheme 101 – HAT-cyclization of functionalized dienone **(77)**. Undesired stereoconfiguration at C-2 and C-10 is highlighted in norbornane **(78)**.

This experiment highlighted the steric demand of the TBS-group and its effect on the desired cyclization: compound **(78)** was obtained as a single diastereomer, with the unwanted stereochemistry confirmed unambiguously by NOE experiments (see experimental part). The final decision concerning the early functionalization strategy was taken after cyclization attempts on enone (\pm)-**(79)** (detailed description on its synthesis will be given in the next chapter): few protocols were known for HAT-like cyclization with ketones as radical acceptors, employing Mn- or Fe-salts.¹⁷² When applied to enone (\pm)-**(79)**, as depicted in Scheme 102, both protocols failed in forming the desired C–C bond. Since the OTBS-functionalization was not thought to dramatically alter the electronic properties of the isopropenyl double bond, and all of the other contra considered, this strategy was soon abandoned.



Scheme 102 – Attempted HAT-cyclization of functionalized dienone (\pm)-**(79)**.

The already mentioned aldol-like approach, in which a metal, as mentioned in Scheme 92, could have been chelated by the two oxygenated functionalities, holding them on the same side during the cyclization, was thought to be a still reasonable option to obtain the desired stereochemistry. Due to the pitfalls in the –OTBS strategy, a new precursor was designed for this chemistry: protected diol (\pm)-**(66)** possessed two double bonds sterically and electronically different enough for regioselective hydroboration-oxidation to occur. The newly formed primary alcohol **(81)** would have delivered the corresponding aldehyde **(82)** after oxidation, as proposed in Scheme 103, leaving the allylic position still available for further functionalization.



Scheme 103 – Aldol approach with late stage functionalization approach on protected diol (±)-(66).

Hydroboration was performed in the presence of Wilkinson's catalyst and pinacol borane. However, even when employing an excess of borane and long reaction times (up to four days, as reported in Table 4), the reaction could not be driven to completion. Moreover, compound (84), formal hydrogenation product of starting diene (±)-(66), was isolated as the main product in the first hydroboration attempt (Entry 1, Table 4).

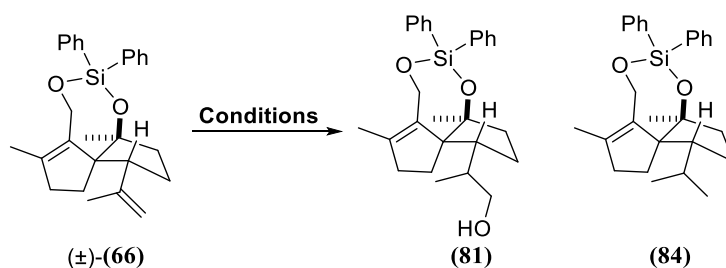


Table 4 – Conditions screening for the hydroboration of (±)-(66).

Entry	Conditions	Product (Yield) ^[a]
1	1) Wilkinson cat. (0.01 equiv.), pinacol borane (1.1 equiv.), CH ₂ Cl ₂ , r.t., 4 days 2) H ₂ O ₂ , NaOH, THF, -20 °C to r.t., 1 h	(81) (<37%), (84) (<63%)
2	1) Wilkinson cat. (0.02 equiv.), pinacol borane (2.2 equiv.), CH ₂ Cl ₂ , r.t., 4 days 2) H ₂ O ₂ , NaOH, THF, -20 °C to r.t., 1 h	(81) (41%), (±)-(66) (46%)

[a] Isolated yield.

With the initial screenings in hand, a first insight on the following transformations was given: oxidation to the corresponding aldehyde was attempted with IBX, which only afforded desired aldehyde (85) in poor yields (Table 5).

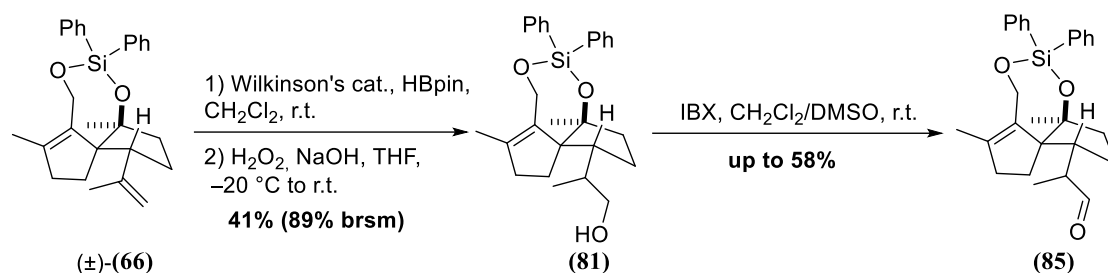
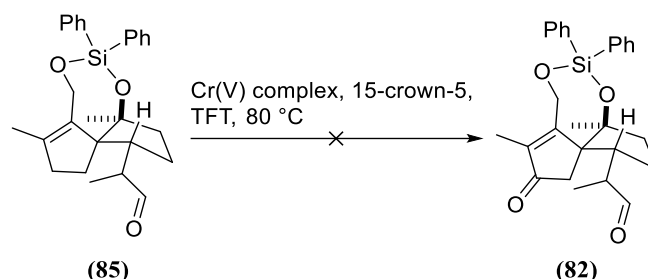


Table 5 – Conditions screening for the oxidation of **(81)**.

Entry	Conditions	Product (Yield) ^[a]
1	IBX (1.1 equiv.), 2 h	(85) (25%)
2	IBX (1.6 equiv.), 3 h ^[b]	(85) (58%)

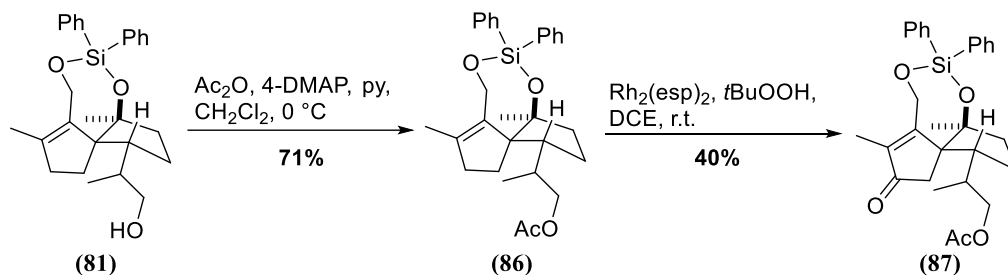
[a] Isolated yield; [b] reaction was stopped as TLC indicated decomposition of the starting material.

Despite these not-encouraging preliminary results, allylic oxidation was also performed with the – up to that point – best conditions found during optimization in the main route (referring to the oxidation of protected diol **(±)**-**(66)**). Unfortunately, decomposition of the starting material occurred, as shown in Scheme 104, which suggested that the installation of the aldehyde at a later stage might have been a more secure alternative.



Scheme 104 – Allylic oxidation attempt for aldehyde **(85)**.

Acetate protection of primary alcohol **(81)** seemed to be a good choice, considering the orthogonality of the diphenylsilyl protecting group and the newly installed ester moiety. Allylic oxidation was performed in milder conditions, reported in Scheme 105, under Rh-catalysis and large excess of TBHP as the oxidant, and yielded desired enone **(87)** in modest yields.



Scheme 105 – Synthesis of triprotected enone **(87)**.

However, deprotection of the primary alcohol moiety proved to be quite challenging, and desired product **(88)** was observed, albeit in traces, only when treating acetate **(87)** with one equivalent of DiBAL-H (Entry 5, Table 6).

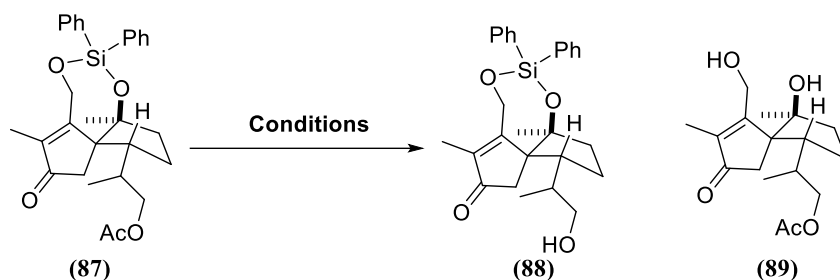
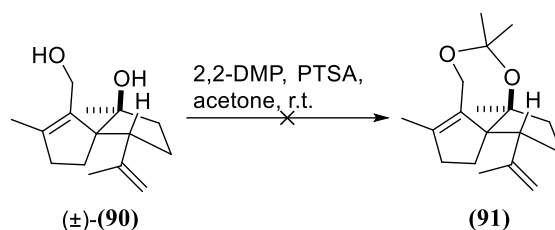


Table 6 – Conditions screening for acetate removal.

Entry	Conditions	Product (Yield) ^[a]
1	K ₂ CO ₃ (1.2 equiv.), THF/MeOH = 1:1, r.t., 2 h	No desired product
2	K ₂ CO ₃ (1.2 equiv.), THF/MeOH = 1:1, 0 °C, 2 h	No desired product
3	NaOH (1 M), THF, 0 °C, 2 h	No desired product
4	LiOH (1.2 equiv.), 1 M in water), MeOH, 0 °C, 2 h	(89) (58%)
5	DiBAL-H (1.0 equiv.), CH ₂ Cl ₂ , -78 °C, 45 min	(88) (traces)

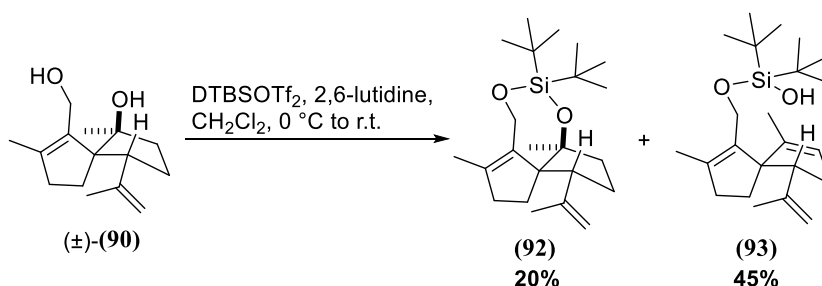
[a] Isolated yield.

Two more alternatives were available at this point: first, the installation of a different protecting group than the bridged diphenylsilyl could have offered a new possibility for selective deprotection. Second, hydroboration at a different stage could overcome the poor yields observed with protected diol (±)-(66) (see Table 4). The use of 2,2-dimethoxypropane in acidic catalysis (10 mol%), as in Scheme 106, did not afford desired ketal (91), resulting instead in decomposition of the starting material.



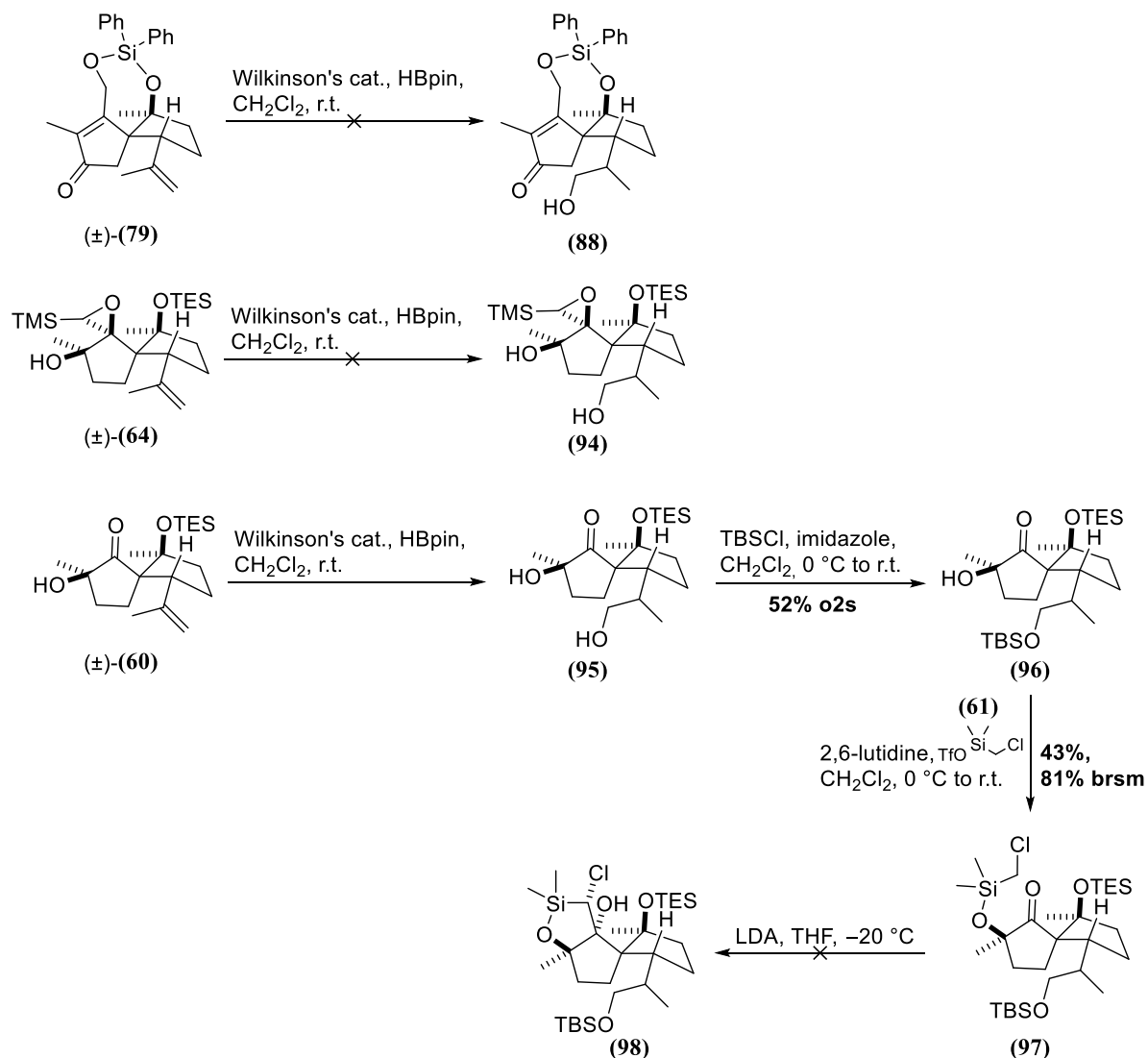
Scheme 106 – Alternative protection attempt for diol (±)-(90): ketal formation

On the contrary, when treating diol (±)-(90) with 1.05 equivalents of di-*tert*-butylsilyl ditriflate (Scheme 107), in the presence of an excess of 2,6-lutidine, a small amount of desired product (92) could be isolated, albeit accompanied by monoprotected byproduct (93) resulting from elimination of the tertiary alcohol.



Scheme 107 – Alternative protection attempt for diol (±)-(90): di-*tert*-butylsilyl-protection

Concerning the alternative substrates for hydroboration, dienone (\pm)-(79), α -hydroxyketone (\pm)-(60) and epoxide (\pm)-(64), were all subjected to the combination of Wilkinson's catalyst and pinacol borane, as depicted in Scheme 108.

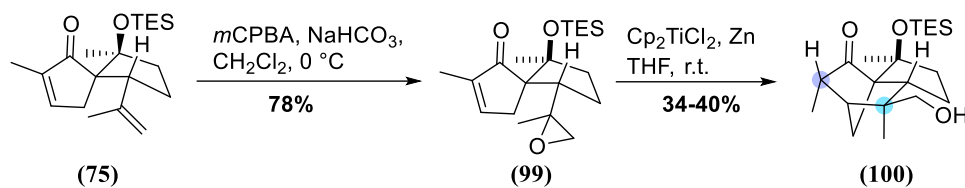


Scheme 108 – Alternative hydroboration substrates, as well as homologation attempts on diprotected triol (96).

No reaction was observed for dienone (\pm)-(79) and epoxide (\pm)-(64), while impure monoprotected triol (95) could be isolated as a result of hydroboration of the olefin in intermediate (\pm)-(60). TBS-protection was successfully performed, yielding α -hydroxyketone (96) in 52% overall yield. The silicon-tether for homologation was installed in the optimized conditions, yielding open-chain silane (97). However, the reaction could not be driven to completion, even when refluxing overnight, possibly for the abovementioned steric demand of the TBS-group; moreover, treatment with LDA for ring closure was also unfruitful, demonstrating the proposed theory.

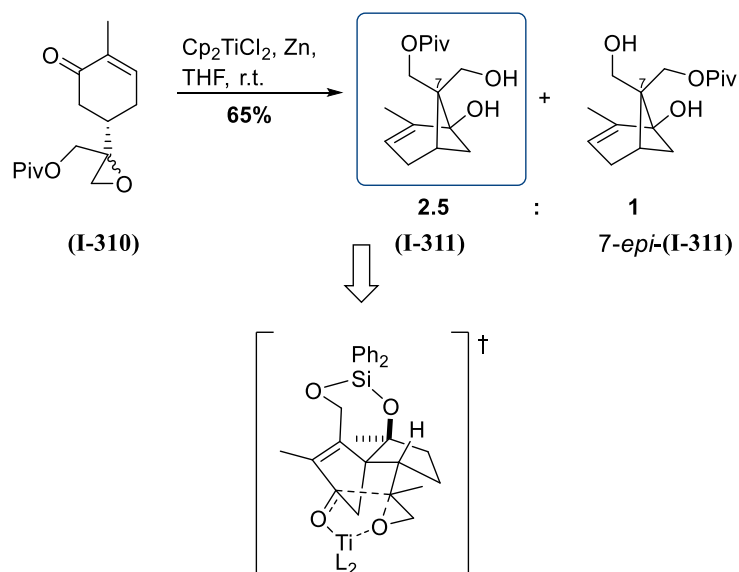
The decision of abandoning the early-functionalization strategy was further supported by the result of one last cyclization trial, on epoxides (99), in which a Ti(III)-mediated strategy was employed. The homolytic C–O bond cleavage in each of the epoxides, caused by interaction with the Ti(III) species, was followed by cyclization onto the enone moiety. Cyclized product (100) was isolated as essentially a single diastereoisomer for both epoxides used individually. The oxidized methyl group was again

pointing in the undesired direction. In this case, stereoconfiguration at C-2 was the desired one, as illustrated in Scheme 109.



Scheme 109 – Ti(III)-mediated cyclization of simple epoxy-enones (**99**). Stereoconfiguration at C-2 and C-10 is highlighted in norbornane (**100**).

Although unsuccessful, this last experiment set the stage for what would become the main cyclization strategy. In fact, the isolation of triol (**100**) suggested that not only the employment of a different cyclization approach for the formation of C3-C10 bond might have been a valid option, but also that the same idea behind the aldol approach – a chelating metal to force the hydroxyl groups-to be *syn*, as shown in Scheme 110 – might have found new applicability. The already mentioned synthesis of (+)-paeonisuffrone (+)-(**I-53**) by Bermejo and coworkers,³⁹ as well as their screening on the pivotal Ti(III) cyclization, represented strong synthetic background in support of this new idea.



Scheme 110 – Ti(III)-mediated cyclization in Bermejo's synthesis of (+)-paeonisuffrone (+)-(**I-53**) and suggested strategy applied to illisimonin A (**I-346**).

Original approach: late stage functionalization

Results and discussion

The first step for testing the envisioned Ti(III)-mediated cyclization was optimizing the allylic oxidation step. In collaboration with Etling, C., catalytic methods based on transition metals and mild oxidants, as reported in Table 7 (Entries 1-7, Table 7) were focused on. Rh-based complexes such as $\text{Rh}_2(\text{cap})_4(\text{MeCN})_2$ or the Du Bois's catalyst ($\text{Rh}_2(\text{esp})_2$) were used in combination with excess TBHP, yielding the desired product in poor yields. Worth mentioning is the method in Entry 3 (Table 7), which was inspired by the allylic oxidation conditions employed with acetate (**86**) in the previous paragraph. *N*-hydroxyphthalimide was employed unfruitfully in an aerobic oxidation of diene (\pm)-(**66**) (Entry 4, Table 7). $\text{Co}(\text{OAc})_2 \cdot 4\text{H}_2\text{O}$, as an alternative to Rh-catalysts, was also proved to be inefficient. The inertness of the allylic position in protected diol (\pm)-(**66**) became evident when focusing the attention on Cr-based reagents. Chromium(VI) oxide and 3,5-dimethylpyrazole (Entry 8, Table 7) were used in large excess to afford only 20% of the desired compound, along with almost equal amounts of starting material. The use of Cr(V) complexes had been reported by Baran and coworkers in their synthesis of (-)-taxuyunnanine D;³¹ variations of this method had also been reported in the Reisman's group.¹³⁴ These conditions were tested both in trifluorotoluene and dichloroethane, in the presence or absence of Mn(IV) oxide as a co-oxidant, without any outstanding result. Lactone (\pm)-(**101**) (Entry 9, Table 7), deriving from deprotection of oxidized diol (\pm)-(**79**), consequent oxidation of the primary alcohol and γ -lactonization, was isolated as a side product when using 25 equivalents of MnO_2 . Portionwise addition of complex (**Cr-V**) (Entry 13, Table 7) did not affect the yield in a positive manner. Soon, the idea of driving the reaction to completion was abandoned, and a recycle-based strategy found application: decreasing the excess of (**Cr-V**) complex down to 2 equivalents (Entry 14, Table 7), minimized decomposition enough to guarantee massive recovery of starting material and a cumulative yield of 48% over four cycles.

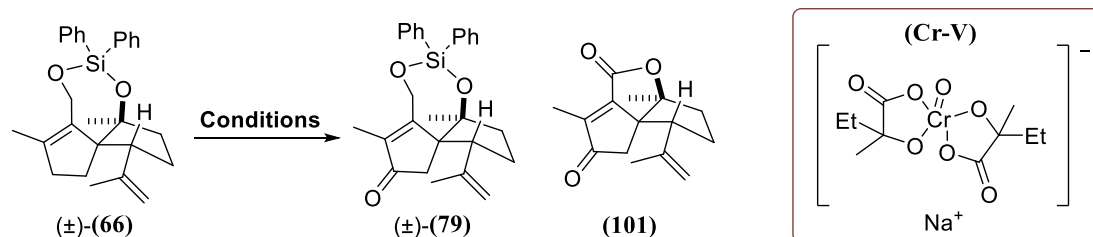


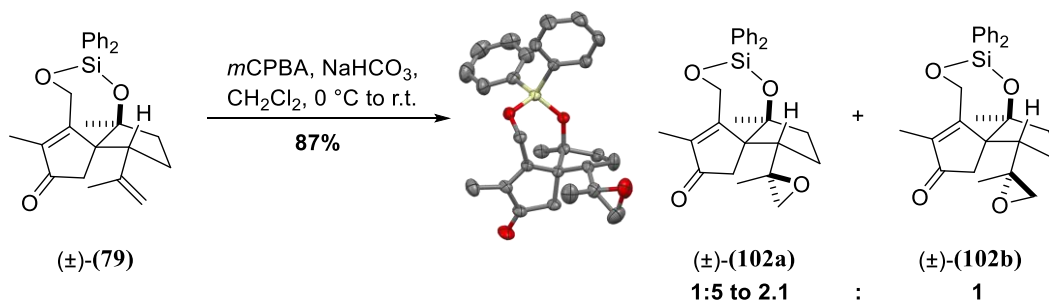
Table 7 – Conditions screening for the allylic oxidation of diene (\pm)-(**66**).

Entry	Conditions	Product (Yield) ^[a]
1	$\text{Rh}_2(\text{cap})_4(\text{MeCN})_2$ (5.0 mol%), <i>t</i> BuOOH (70% in water), DCE, 45 °C, 12 h	(\pm)-(79) (12%)
2	$\text{Rh}_2(\text{cap})_4(\text{MeCN})_2$ (5.0 mol%), <i>t</i> BuOOH (5.5 M in decane), DCE, r.t., 33 h	(\pm)-(79) (25%)
3	$\text{Rh}_2(\text{esp})_2$ (5.0 mol%), <i>t</i> BuOOH (70% in water), DCE, r.t., 6 h	(\pm)-(79) (40%)
4	$\text{Rh}_2(\text{esp})_2$ (0,5 mol%), NHPI (10 mol%), ethyl acetate, air, r.t., 19 h	(\pm)-(79) (17%, 25% brsm)
5	$\text{Mn}(\text{OAc})_3 \cdot 2\text{H}_2\text{O}$ (10 mol%), <i>t</i> BuOOH (5.5 M in decane), 3Å MS, EtOAc, r.t., 24 h ^[d]	(\pm)-(79) (19%)
6	CuI, <i>t</i> BuOOH (5.5 M in decane), MeCN, r.t., 33 h ^[e]	(\pm)-(79) (16%)

7	Co(OAc) ₂ ·4H ₂ O (1.0 mol%), NHPI (10 mol%), tBuOOH (5.5 M in decane), acetone, r.t., 19 h ^[f]	(±)-(79) (31%)
8	CrO ₃ (12 equiv.), 3,5-dimethylpyrazole (12 equiv.), CH ₂ Cl ₂ , -20 to -10 °C ^[l]	(±)-(79) (20%, 26% brsm)
9	Cr(V)-complex (Cr-V) (5.0 equiv.), 15-crown-5 (7.0 equiv.), MnO ₂ (25 equiv.), trifluorotoluene, 80 °C, 36 h	(±)-(79) (31%, 39% brsm), (101) (6%)
10	Cr(V)-complex (Cr-V) (5.0 equiv.), 15-crown-5 (7.0 equiv.), MnO ₂ (10 equiv.), DCE, 80 °C, 2 d	(±)-(79) (36%, 47% brsm)
11	Cr(V)-complex (Cr-V) (5.0 equiv.), 15-crown-5 (7.0 equiv.), MnO ₂ (25 equiv.), trifluorotoluene, 100 °C, 2 d	(±)-(79) (5%)
12	Cr(V)-complex (Cr-V) (5.0 equiv.), 15-crown-5 (7.0 equiv.), trifluorotoluene, 80 °C, 19 h	(±)-(79) (21%, 45% brsm)
13	Cr(V)-complex (Cr-V) ^[b] , 15-crown-5 (7.0 equiv.), trifluorotoluene, 80 °C, 19 h	(±)-(79) (18%, 43% brsm)
14	Cr(V) (2.0 equiv.), 15-crown-5 (3.0 equiv.), trifluorotoluene, 80 °C, 19 h	(±)-(79) (23%, 63% brsm); 48% in 4 cycles ^[c]

[a] Isolated yield; [b] Successive addition of 1.0 equiv./hour; [c] Starting material was recovered by column chromatography and reused for the oxidation; [d] *Chem. Eur. J.* **2013**, *19*, 6398–6408; [h] LIAONING ASYMCHEM - CN110407678, **2019**, A, 0031-0047; [e] *Steroids* **2015**, *94*, 1–6; [f] *J. Org. Chem.* **2005**, *70*, 1597–1604.

Epoxidation of enone (±)-(79) proceeded smoothly upon treatment with *m*CPBA, furnishing a mixture of separable isomers (±)-(102) (d.r. 1.5:1 up to 2.1:1) as depicted in Scheme 111. The structure of the major isomer (±)-(102a) was unambiguously determined *via* X-ray single crystal diffraction.



Scheme 111 – Epoxidation of enone (±)-(79), as well as ORTEP representation of the crystal structure from the major epoxide. Major epoxide co-crystallized with benzene, not shown.

Preliminary screenings on the Ti(III)-mediated reductive cyclization were conducted on each diastereomer (±)-(102) at first (Entries 1 and 2, Table 8). Lately, when the dependence of the d.r. for norbonanes (±)-(103) and (±)-10-*epi*-(103) on the configuration of the pre-existing C-10 stereocenter was outruled, the epoxides were no further separated and were employed in the cyclization as a mixture. The addition of the Ti(III) solution to the epoxides (Entry 3, Table 8), which was thought to favor the desired chelating effect, led mainly to recovery of starting material; the slow, “classic” addition of (±)-(102) to the *in situ* generated Ti-species controlled by syringe pump was also not effective towards the improvement of the d.r. The use of collidine hydrochloride to decrease the amount of titanocene chloride to catalytic,¹³⁷ resulted in the suppression of reactivity. Optimized conditions (Entry 6, Table 8) involved manual addition of the epoxides to the freshly prepared Ti(III)

solution and yielded desired diastereoisomer (\pm)-**(103)** as minor product, with an improved diastereoisomeric ratio of 1:1.4 on large scale.

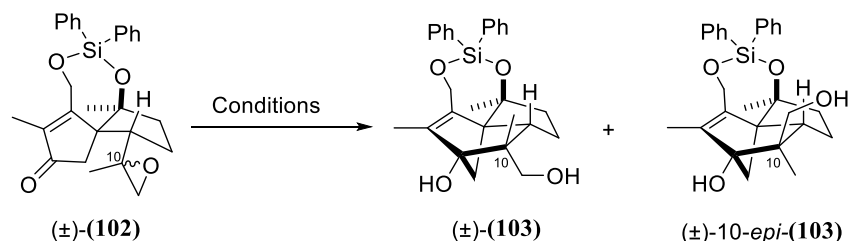
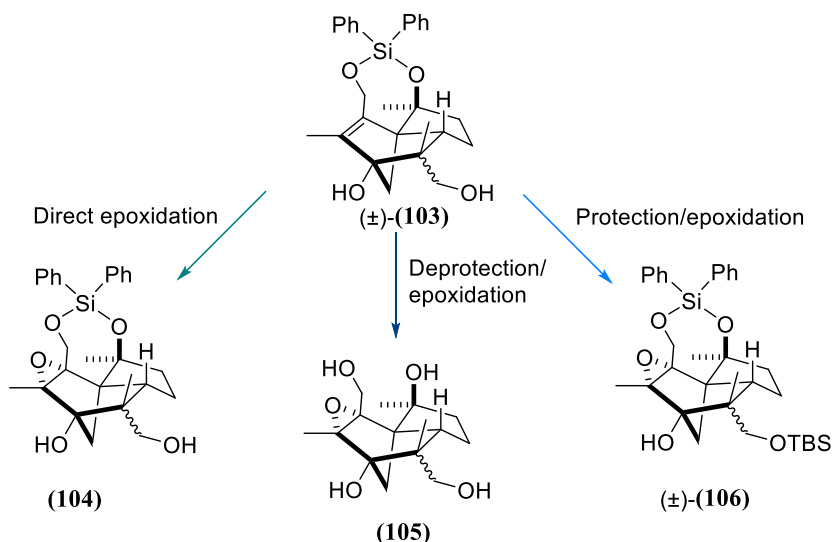


Table 8 – Conditions screening for the Ti(III)-mediated reductive cyclization of epoxyenones (\pm)-**(102)**.

Entry	Conditions ^[b]	Product (Yield) ^{[a],[d]}
1	(\pm)- (102a) , Cp ₂ TiCl ₂ (3.0 equiv.), Zn (9.0 equiv.), 3 h; addition of epoxide solution to Ti(III) solution	(\pm)- (103) (56%), d.r. 1:1.6
2	(\pm)- (102b) , Cp ₂ TiCl ₂ (3.0 equiv.), Zn (9.0 equiv.), 3 h; addition of epoxide solution to Ti(III) solution	(\pm)- (103) (50%), d.r. 1:1.5
3	(\pm)- (102) (2.1:1) ^[c] , Cp ₂ TiCl ₂ (3.0 equiv.), Zn (9.0 equiv.), 24 h; addition of Ti(III) solution to epoxides solution <i>via</i> syringe pump ^[e]	(\pm)- (102) (49%)
4	(\pm)- (102) (2.1:1) ^[c] , Cp ₂ TiCl ₂ (3.0 equiv.), Zn (9.0 equiv.), 5 h; addition of epoxides solution to Ti(III) solution <i>via</i> syringe pump ^[f]	(\pm)- (103) (63%), d.r. 1:1.7
5	(\pm)- (102) (2.1:1) ^[c] , Cp ₂ TiCl ₂ (0.1 equiv.), Zn (3.0 equiv.), collidine·HCl (2.0 equiv.), 24 h; addition of epoxides solution to solution of Ti(III)-complex and collidine·HCl <i>via</i> syringe pump ^[e]	No reaction
6	(\pm)- (102) (2.1:1) ^[c] , Cp ₂ TiCl ₂ (3.0 equiv.), Zn (9.0 equiv.), 1 h; addition of epoxides solution to Ti(III) solution over 30 min	(\pm)- (103) (89%), d.r. 1:1.4 to 1:1.6 ^[g]

[a] Isolated yield; [b] reactions performed at r.t. with degassed THF as solvent; [c] diastereomeric epoxides not separated prior to cyclization; [d] the main isomer was found to be the undesired (\pm)-10-*epi*-**(103)** (see NOE correlations); [e] addition time = 2 h; [f] addition time = 1.5 h; [g] yield and selectivity tended to increase upon scale-up.

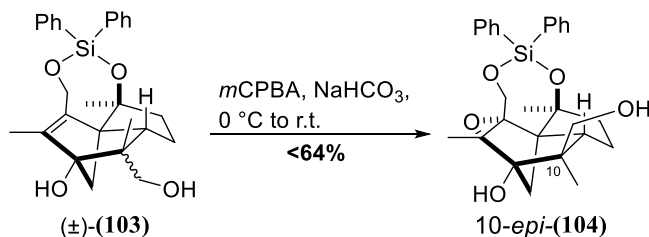
Considering the results of the preliminary studies, the observation of the desired cyclization product (\pm)-**(103)** as the minor diastereomer did not pose a surprise and a 1:1.4 d.r. was considered a sufficient result for being exploited towards the synthetic target. In other words, having established an efficient enough protocol for the synthesis of the *cis*-pentalene skeleton, the next challenge would be inducing the migration of the C3-C10 bond in a semipinacol rearrangement, giving thermodynamic a new, stable carbonyl group in exchange for the *trans*-pentalene strain. Several possibilities were available: first, a direct epoxidation of (\pm)-**(103)** and (\pm)-10-*epi*-**(103)** consequent rearrangement in the absence of further protecting groups. Second, the removal of the diphenylsilyl bridge, consequent formation of epoxides **(105)** and rearrangement in acidic conditions. Third, a “Rychnovky-like” strategy, in which a TBS protection would be performed prior to the core rearrangement. The three options are summarized in Scheme 112.



Scheme 112 – Possible strategies starting from norbornane (±)-(103) and aiming for a type-III semipinacol rearrangement.

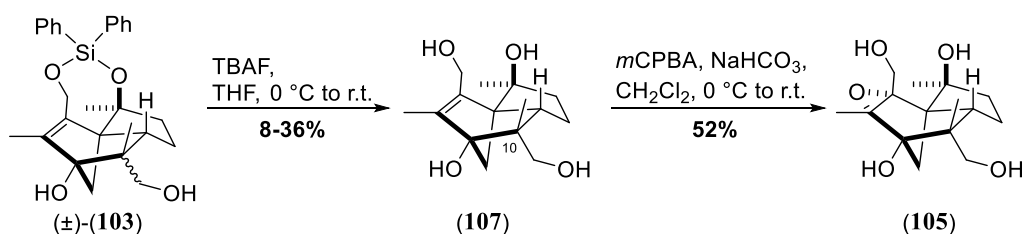
Naturally, the first two options seemed to be more appealing, since they featured less steps and by far better atom economy; for this reason, attention was initially focused on these two approaches.

The direct epoxidation was soon discarded as an option: epoxidation of epimeric mixture (±)-(103) occurred under classic conditions as shown in Scheme 113. However, the only obtained product was one diastereomer, with the undesired configuration at C-10 as confirmed by NOE experiments. The desired isomer could not be isolated.



Scheme 113 – Epoxidation of norbornanes (±)-(103).

Deprotection of diprotected tetraol (±)-(103) occurred upon treatment with TBAF (2.4 equiv.) at room temperature, as reported in Scheme 114. The two separable diastereomers (107) were isolated in 36% and 29-50% for the minor and major one respectively. NOE experiments at the epoxide stage confirmed the less polar isomer (36% yield) to be the desired one. It is worth mentioning that, as one might imagine, the high polarity of these compounds made purification quite a challenge; for this reason yields were varying, and were also found to decrease upon scale up (down to 8% for the desired compound). An alternative deprotection, with *in situ* generation of hydrochloric acid (AcCl/MeOH)¹⁴⁶ was attempted to overcome the negative correlation between yields and scale of the reaction; however, this approach did not afford the desired product. During the first scouting, instability of norbornanes (107) and 10-*epi*-(107) in deuterated chloroform was also highlighted. Epoxidation of the desired diastereoisomer afforded (105) in poor yields but, as expected, electrophilic attack of the peracid occurred from the less hindered face.



Scheme 114 – Synthesis of epoxytetraol (**105**).

At this point, the stage for the semipinacol rearrangement was set. TFA, as in the published synthesis of the natural product,¹⁴⁶ was given a first attempt. However, both the conditions employed (Table 9) - chloroform or hexafluoroisopropanol¹⁷³ as solvents - were not able to induce the rearrangement to *trans*-pentalene (**108**).

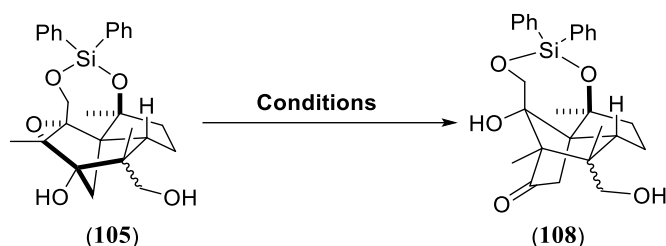
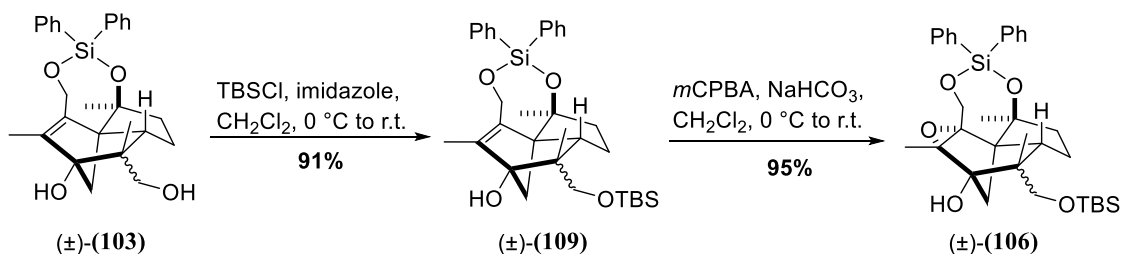


Table 9 – Conditions screening for the semipinacol rearrangement of epoxide (**105**).

Entry	Conditions	Product (Yield)
1	TFA (2.0 equiv.), CHCl ₃ , r.t., 5 days	No reaction
2	TFA (1.0 equiv.), HFIP, r.t., 6 days	No reaction

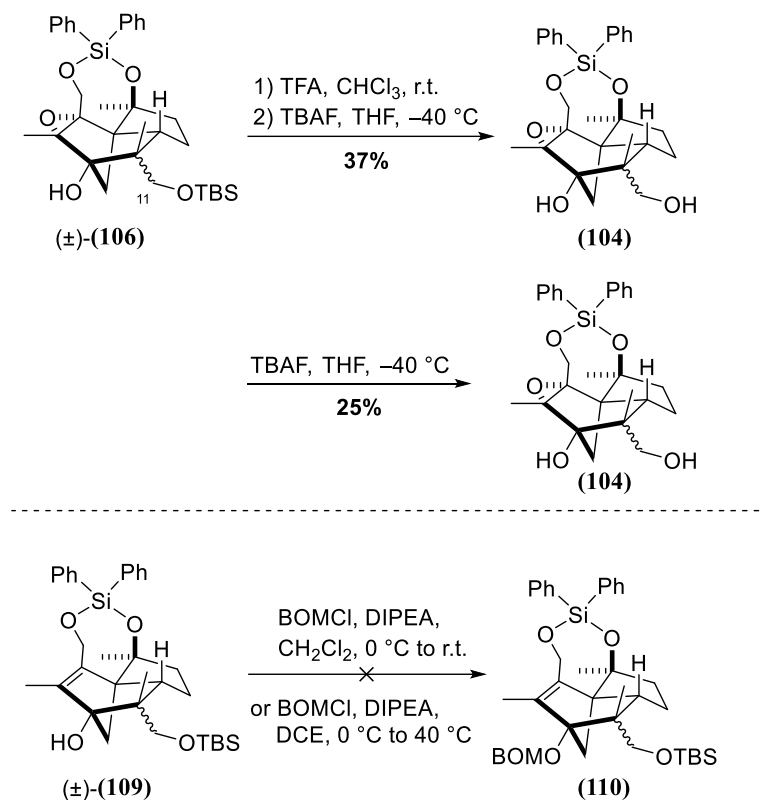
In the meantime, the third alternative was giving better results: TBS protection of epimeric mixture (\pm)-(**103**) occurred in mild conditions, with overnight stirring necessary to force the bulky protecting group underneath the caged molecule. Epoxidation occurred in high yields, but separation of the diastereoisomers was still not possible. The route to epoxide (\pm)-(**106**) is reported in Scheme 115.



Scheme 115 – Synthesis of triprotected epoxytetraol (\pm)-(**106**).

Epoxides (\pm)-(**106**) differed from the reported intermediate (**I-355**) only by the diphenylsilyl protecting group and the lack of the BOM-protection at the carbonyl-group-to-be tertiary alcohol (C-3). The presence of the protecting group was not considered to effect the rearrangement, due to the modest flexibility of the 7-membered ring. On the contrary, the absence of the BOM-protecting group insinuated some doubts, since the semipinacol rearrangement would have resulted in loss of this protecting group in favour of the formation of the carbonyl group. For these reasons, it did not surprise

that TFA, employed in chloroform or HFIP (see Entry 1 and 2, Table 10), was not able to induce the rearrangement (Scheme 116). A BOM protection of the TBS-protected cyclization product (\pm)-**(109)** was also considered, but was not effective, as depicted in Scheme 116, probably due to the tertiary nature of the alcohol at C-3, as well as the bulky, neighbouring TBS group. At this stage, deprotection conditions that might selectively remove the bridging protecting group, leaving the TBS-protected alcohol untouched, were tested. Selective deprotection would be in fact needed for the oxidation steps, in which steric hindrance was not believed to be discriminant enough to favour the formation of the carboxylic acid at the desired position (*i.e.* without concomitant oxidation of the alcoholic function at C-11). Unfortunately, treatment with TBAF at low temperature resulted in low yielding removal of the TBS group (Scheme 116).



Scheme 116 – Deprotection and semipinacol rearrangement attempts on triprotected epoxytetraol (\pm)-**(106)** as well as unfruitful BOM-protection of triprotected tetraol (\pm)-**(109)**.

Since selective deprotection was not possible at this stage in the tested conditions, the quest for appropriate reagent for the semipinacol rearrangement began at this point, moving in the direction of Lewis acids, instead of the unfruitful protic acid strategy. Table 10 shows the tested Lewis acids, as well as the above mentioned TFA-attempts (Entries 1-2, Table 10). BF₃·OEt₂ and SnCl₄ (Entries 5 and 6, Table 10), previously employed in synthetic endeavours from Ogura's and Edge's research groups respectively, were found to be equally efficient in inducing the semipinacol rearrangement, yielding the two separable *trans*-pentalenes in good yields. However, since the desired isomer (\pm)-**(111)** obtained with trifluoroborane was accompanied by visible impurities, tin(IV) tetrachloride resulted to be the best option. Surprisingly, both silyl-protecting groups survived the excess of Lewis acid. The structure of the undesired diastereomer 10-*epi*-**(111)**, obtained in unreproducible yields, was unambiguously determined *via* X-ray single crystal diffraction: ORTEP representation of its crystal structure is hereby reported.¹

¹ 10-*epi*-**(111)** co-crystallized with benzene; disordered benzene is not shown.

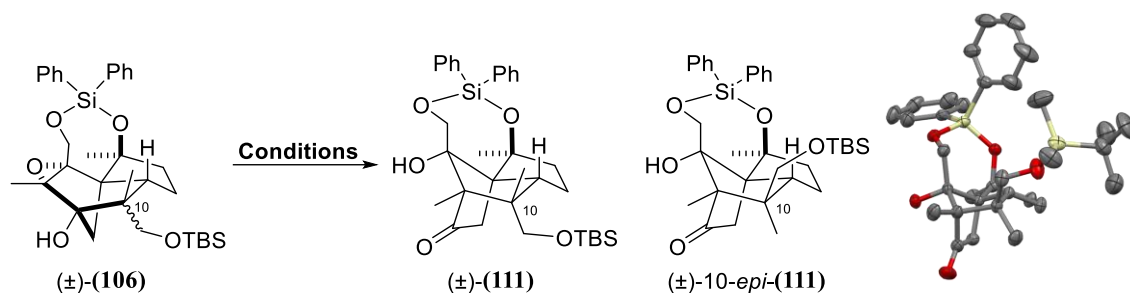
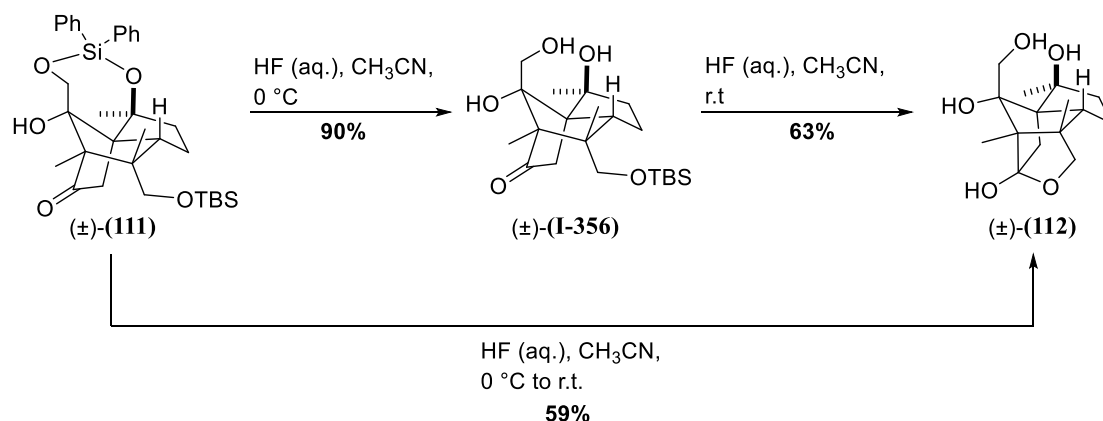


Table 10 – Conditions screening for the semipinacol rearrangement of epoxide **(±)-(106)**.

Entry	Conditions	Product (Yield) ^[a]
1	TFA (0.9 equiv.), CHCl ₃ , r.t.	No reaction
2	TFA (0.9 equiv.), HFIP, r.t.	Decomposition
3	TMSOTf (3.6 equiv.), <i>i</i> Pr ₂ NEt (3.6 equiv.), CH ₂ Cl ₂ , -78 °C ^[b]	Inconclusive NMR data
4	AlMe ₃ (2M in heptane, 2.0 equiv.), CH ₂ Cl ₂ , -78 °C to 0 °C ^[c]	No reaction
5	BF ₃ ·OEt ₂ (2.0 equiv.), CH ₂ Cl ₂ , -78 °C ^[d]	(±)-(111) (<36%)
6	SnCl ₄ (2.0 equiv.), CH ₂ Cl ₂ , -78 °C ^[e]	(±)-(111) 38%

[a] Isolated yield referring to desired isomer **(±)-(111)**; [b] *Org. Lett.* **1999**, *1*, 307–310; [c] *J. Am. Chem. Soc.* **2003**, *125*, 1498–1500; [d] *Org. Lett.* **2020**, *22*, 9234–9238; [e] *J. Org. Chem.* **1993**, *58*, 5944–5951.

Having established reliable and scalable semipinacol conditions, the deprotection could no further be postponed. Due to the rearranged nature of ketone **(±)-(111)**, deprotection with TBAF was given a second try, but soon disappointed the expectations. On the contrary, the use of a 2 M aqueous solution of hydrofluoric acid as a mild deprotecting agent, as in Scheme 117, was an excellent solution to discriminate between the two silicon-based protecting groups: stirring at low temperature yielded the formal intermediate from Rychnovsky's route, TBS-protected alcohol **(±)-(I-356)**. Increasing the temperature to room temperature, together with longer reaction times (up to 10 days) afforded instead lactol **(±)-(112)**, which was believed to be a valid alternative to the above mentioned, published intermediate. Selective oxidation was in fact thought to be possible, due to the stability of the δ -lactol embedded in the cage structure, as well as steric availability of the "other" primary alcohol.



Scheme 117 – Partial and full deprotection of *trans*-pentalene **(±)-(111)**.

Plenty of oxidative conditions for direct conversion of primary alcohols to carboxylic acids were available in literature; attention was at first focused on these methodologies. Most of them employed catalytic amounts of TEMPO (Entries 1 to 3, Table 11), together with a stoichiometric oxidant as trichloroisocyanuric acid, the combination of sodium chlorite and hypochlorite, or even (diacetoxyiodo)benzene. In this last case, ketone (**113**) was observed as main product, along with traces of desired compound (**I-357**), detected *via* mass and NMR spectroscopy. The isolation of C14-ketone (**113**), posed a surprise: on one hand, bond cleavage between C1 and C15 was easy to rationalize in the presence of hypervalent iodine.¹⁷⁴ On the other hand however, fragmentation of the same intermediate had been observed by Rychnovsky and Burns when attempting a semipinacol rearrangement prior to one-carbon-homologation, as depicted in Scheme 118.¹⁴⁶

The use of TCCA (Entry 1, Table 11) and wet NMO (Entry 4, Table 11), both produced an aldehyde (detected by NMR); it must be said at this point that purification or characterization of any of the detected aldehydes was not attempted, since rearrangement of aldehyde (**116**) in acidic conditions had been reported along with the first total synthesis of illisimonin A (**I-346**), as in Scheme 118. The presence of the lactol moiety was not believed to interfere with the depicted α -ketol rearrangement. When the use of PDC in dimethylformamide (Entry 5, Table 11) proved unfruitful too, efforts were moved towards a stepwise oxidation.

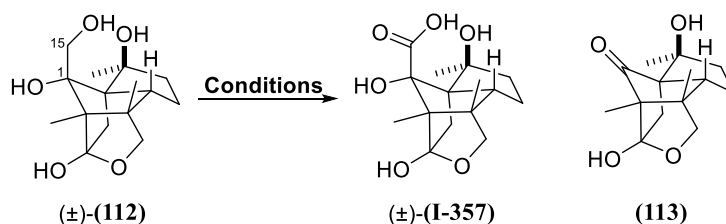
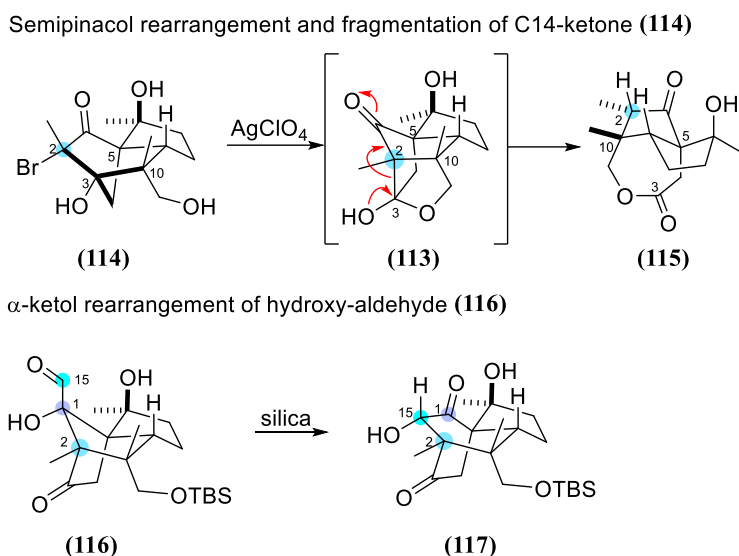


Table 11 – Conditions screening for the oxidation of lactol (±)-(112) in one step.

Entry	Conditions	Product (Yield) ^[a]
1	TEMPO (2.0 mol%), NaHCO ₃ (15% aq.), TCCA (2.0 equiv.), NaBr (0.2 equiv.), acetone, 0 °C to r.t. ^[b]	No desired product
2	TEMPO (7.0 mol%), NaClO ₂ (2.0 equiv.), NaClO (2.0 mol%), phosphate buffer, CH ₃ CN, 35 °C ^[c]	No reaction
3	TEMPO (0.2 equiv.), PIDA (2.5 equiv.), CH ₂ Cl ₂ /H ₂ O, r.t. ^[d]	(113) (68%) + (±)-(I-357) (traces)
4	NMO·H ₂ O (10 equiv.), TPAP (0.1 equiv.), CH ₃ CN, r.t. ^[e]	No desired product
5	PDC (4.0 equiv.), DMF, r.t. ^[f]	No desired product

[a] Isolated yield; [b] *J. Org. Chem.* **2003**, *68*, 4999–5001; [c] *J. Org. Chem.* **1999**, *64*, 2564–2566; [d] *Synthesis* **2015**, *47*, 1016–1023; [e] *Org. Lett.* **2011**, *13*, 4164–4167; [f] *J. Org. Chem.* **1992**, *57*, 8–9.



Scheme 118 – α -ketol rearrangement of aldehyde (**116**) as well as fragmentation of C14-ketone (**114**) observed by Rychnovsky and Burns in their synthesis of illisimonin A (**I-346**).

As mentioned, the main issue in this stepwise oxidation strategy was the presumed instability of the intermediate aldehyde, that was somehow confirmed by the NMR quality of the previous screening (clear, reasonable looking spots on TLC were resulting in low quality NMRs, which made it almost impossible to understand the reaction outcome and consequently to adjust the conditions). The safest strategy would have been employing the IBX/Pinnick combination already reported by Rychnovsky and coworkers¹⁴⁶; however, the very first attempt with these conditions did not afford desired product (\pm)-(**I-357**). Consequently, the oxidation with TEMPO (Entry 1, Table 12) or TPAP (Entry 2, Table 12), and the use of Pinnick conditions for the second oxidation were tested. However, at least on TLC the IBX oxidation looked more reliable, and a quest for alternative conditions for the carboxylic acid formation was initiated (Entries 2-8, Table 12). DMSO, aminosulfonic acid, or hydrogen peroxide were given a chance as scavengers, and the use of other solvents as THF (Entry 4, Table 12), *tert*-butanol/water mixture (Entry 5, Table 12) or acetonitrile (Entry 6, Table 12) was contemplated. Silver- or manganese-based procedures were also unfruitful, causing decomposition of the starting material (Entry 6 and 7, Table 12). On the contrary, the stoichiometric use of TEMPO, accompanied by equal amounts of $\text{Fe}(\text{NO}_3)_3 \cdot 9\text{H}_2\text{O}$ (Entry 9, Table 12), was too mild to induce any reaction. In summary, none of the tested conditions afforded desired carboxylic acid (\pm)-(**I-357**). Moreover, NMR quality was always so low that no real hypothesis on the outcome of the reaction could be postulated. One common trait of the oxidation products was the presence of an ubiquitous signal in the carbon NMR around 110 ppm, compatible with the intact lactol moiety. This result suggested two thoughts: first, the oxidation had occurred – if at all – at the desired position; second, if the lactol moiety, which was the only discriminant compared to the known conditions, was still in place, there shouldn't be reasons speaking against the applicability of the literature known Pinnick conditions. A new try was given to Rychnovsky's protocol (Entry 10, Table 12), with particular attention to the purity of the reagents as well as light exclusion. A compound whose mass and NMRs matched with the reported ones was isolated.

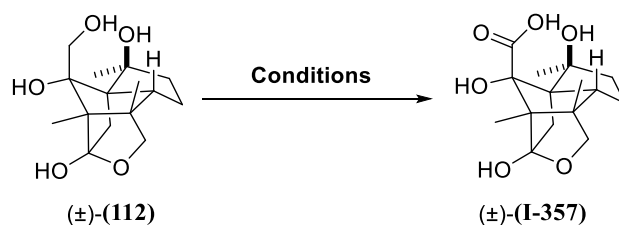


Table 12 – Conditions screening for the oxidation of lactol (±)-(112) in two steps.

Entry	Conditions	Product (Yield) ^[a]
1	1) TEMPO (3 mol%), KBr (5.0 equiv.), NaHCO ₃ (3.8 equiv.), NaOCl (13% wt aq. sol., 1.8 equiv.), CH ₂ Cl ₂ /H ₂ O, 0 °C ^[b] 2) 2-methyl-2-butene (10 equiv.), NaH ₂ PO ₄ (5.5 equiv.), NaClO ₂ (5.5 equiv.), acetone/H ₂ O, r.t.	No desired product
2	1) TPAP (0.1 equiv.), NMO (6.0 equiv.), 4Å MS, CH ₂ Cl ₂ , r.t. 2) 2-methyl-2-butene (10 equiv.), NaH ₂ PO ₄ (5.5 equiv.), NaClO ₂ (5.5 equiv.), acetone/H ₂ O, r.t.	No desired product
3	1) IBX (1.5 equiv.), DMSO, r.t. 2) H ₂ NSO ₃ H, (4.0 equiv.), NaClO ₂ (4.0 equiv.), dioxane/H ₂ O, 0 °C ^[c]	No desired product
4	1) IBX (1.5 equiv.), DMSO, r.t. 2) NaClO ₂ (1.5 equiv.), NaH ₂ PO ₄ (2.2 equiv.), DMSO (3.0 equiv.), THF, 0 °C to r.t. ^[d]	No desired product
5	1) IBX (1.5 equiv.), DMSO, r.t. 2) 2-methyl-2-butene (15 equiv.), NaClO ₂ (3.0 equiv.), NaH ₂ PO ₄ (3.0 equiv.), <i>t</i> BuOH/H ₂ O, 0 °C to r.t. ^[e]	No desired product
6	1) IBX (1.5 equiv.), DMSO, r.t. 2) AgNO ₃ (3.4 equiv.), NaOH (3.1 equiv.), EtOH/H ₂ O, r.t. ^[f]	Decomposition
7	1) IBX (1.5 equiv.), DMSO, r.t. 2) KMnO ₄ (1M in H ₂ O, 10 equiv.), <i>t</i> BuOH/H ₂ O, phosphate buffer, r.t. ^[g]	Decomposition
8	1) IBX (1.5 equiv.), DMSO, r.t. 2) H ₂ O ₂ (30% in water, 1.1 equiv.), NaClO ₂ (0.75 M in water, 1.5 equiv.), NaH ₂ PO ₄ (0.2 M in water, 0.2 equiv.), CH ₃ CN, 0 °C to r.t. ^[h]	No desired product
9	1) IBX (1.5 equiv.), DMSO, r.t. 2) TEMPO (1.0 equiv.), Fe(NO ₃) ₃ ·9H ₂ O (1.0 equiv.), KCl (1.0 equiv.), DCE, r.t. ^[i]	No reaction
10	1) IBX (1.5 equiv.), DMSO, r.t. 2) 2-methyl-2-butene (20 equiv.), NaH ₂ PO ₄ (11 equiv.), NaClO ₂ (11 equiv.), acetone/H ₂ O, r.t.	Impure (±)-(I-357) (<46% o2s)

[a] Isolated yield [b] *J. Org. Chem.* **2007**, *72*, 7034–7037; [c] *Eur. J. Med. Chem.* **2018**, *150*, 829–840; [d] *J. Am. Chem. Soc.* **2022**, *144*, 11574–11579; [e] *Angew. Chem. Int. Ed.* **2021**, *60*, 6938–6942; [f] *J. Med. Chem.* **1995**, *38*, 1922–1927; [g] *J. Am.*

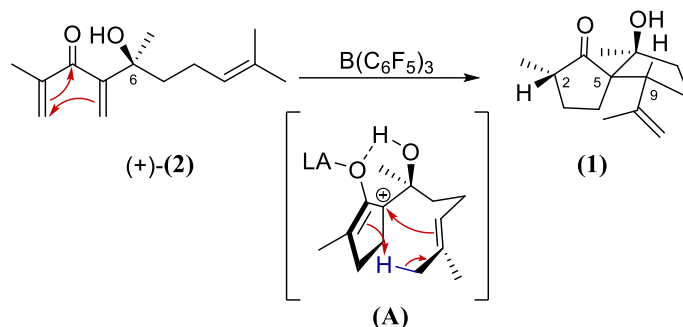
Chem. Soc. **1997**, *119*, 2784–2794; [h] *Chem. Comm.* **2015**, *51*, 9737–9740; [i] LANZHOU UNIVERSITY - CN111004225, **2020**, A, 0060-0062; 0075-0076.

With the racemic route to two formal intermediates fully established and the scarcity of remaining racemic material, attention was moved towards the asymmetric route.

PART 3: The asymmetric total synthesis of (-)-illisimonin A

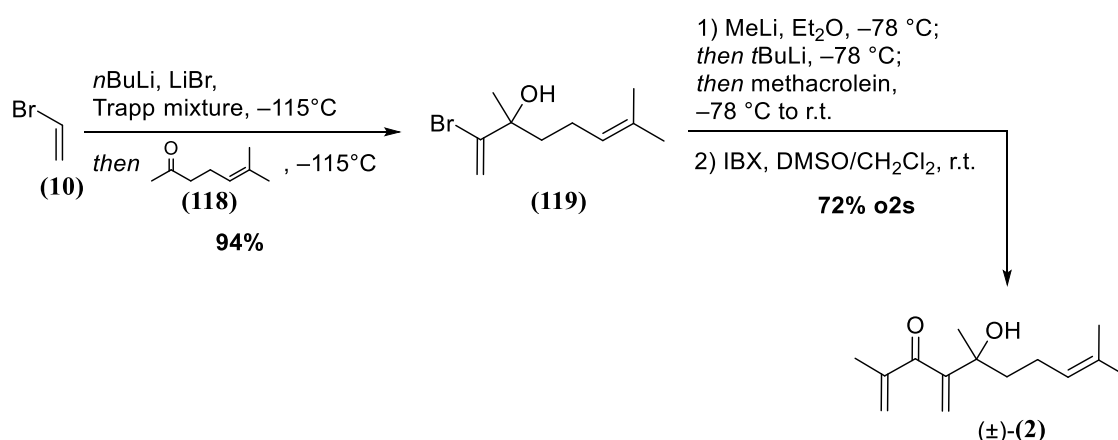
Synthesis of an enantioenriched precursor

The extensive studies on the Nazarov cyclization, reported at the beginning of this thesis, had shown how the spiroketones were obtained as single distereoisomers, independent on chain length, functionalization or β -substituents to the carbonyl group. The diastereoselectivity of this key reaction was thought to derive from hydrogen bonding between carbonyl group and hydroxyl group at C-6, which forced the side of attack of the side chain olefin. Controlling the configuration of this one stereocenter would, in other words, result in a predictable and fixed relative and absolute configuration for the newly formed sterotriad at C-2, C-5 and C-9 as shown in Scheme 119.



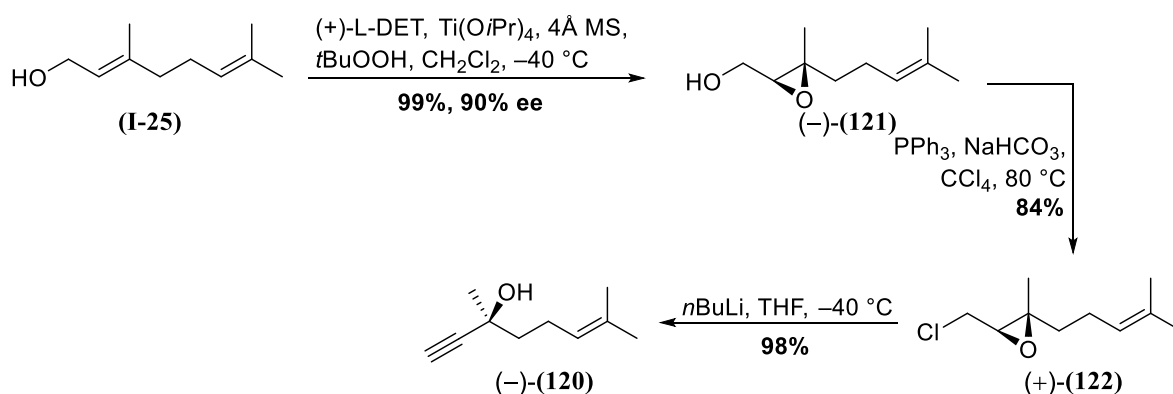
Scheme 119 – Nazarov cyclization of enantioenriched trienone (+)-(2). No indicator for the absolute stereoconfiguration of spiroketone (1) is indicated since this intermediate was TES-protected *in situ* to avoid retro-aldol decomposition that had been observed on large scale for the free spirocompound.

These premises considered, an asymmetric synthesis of (-)-illisimonin A (-)-(I-346) would imply synthesizing enantioenriched trienone (+)-(2). During scale-up for the racemic route, Etling, C. had introduced a different retrosynthetic cut for the synthesis, in which bromoalcohol (9) had been substituted by bromodienol (119), prepared from sulcatone (118) and vinyl bromide (10) with the same, established Li-chemistry. Deprotonation with MeLi, Li-halogen exchange with *t*BuLi and nucleophilic attack of the dianion to methacrolein produced the intermediate alcohol that was oxidized to Nazarov precursor (\pm)-(2) (Scheme 120).



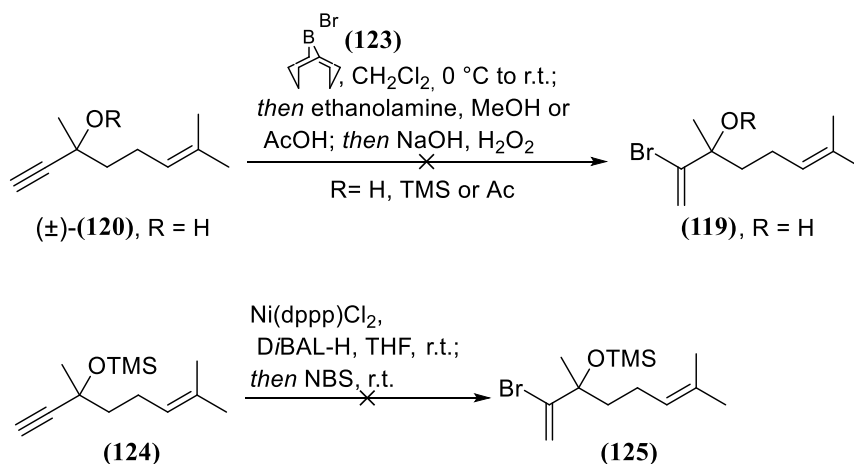
Scheme 120 – Alternative approach to trienone (\pm)-(2).

Efforts for an asymmetric total synthesis were at first addressed to bromoalcohol (119) (scouting on racemic material). The group of Echavarren and coworkers¹⁷⁵ had reported the synthesis of propargylic alcohol (-)-(120) in three steps from geraniol (I-25). Hydrobromination of its racemic congener (\pm)-(120) was not as straightforward as expected (Scheme 121).



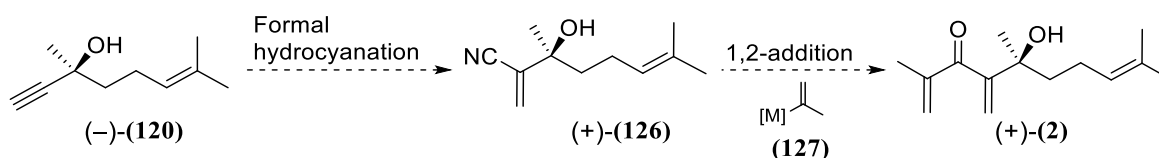
Scheme 121 – Known route to propargylic alcohol (-)-(120) by Echavarren and coworkers.

Experiments in this direction were conducted by Di Marco, A. during the course of her master thesis and Etling, C. Hydrobromination with Markovnikov selectivity was attempted with *B*-Br-9-BBN (123),¹⁷⁶ both on free alcohol (±)-(120) and on the acetate or TMS-protected derivatives, as well as through a Nickel-catalyzed hydroalumination (reported by Hoveyda and coworkers¹⁷⁷), using NBS as brominating reagent, as reported in Scheme 122. Unfortunately, the desired vinyl bromide (±)-(119) (or protected versions) was never observed, and every tested condition led to decomposition of the starting material.



Scheme 122 – Failed attempts towards vinyl bromide (±)-(119) and protected derivatives.

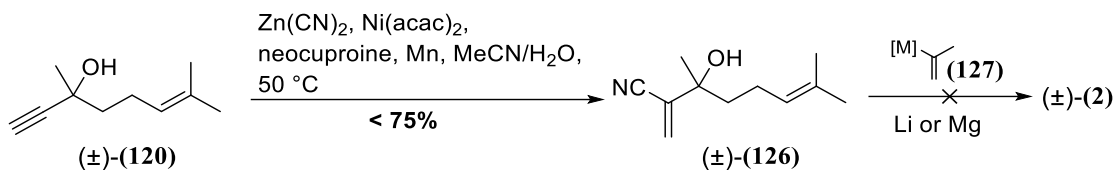
An alternative to this approach was soon found: the hydrocyanation of propargylic alcohol (-)-(120), followed by 1,2-addition of an isopropenyl metalorganic species (127), would have directly delivered the cross-conjugated trienone, with no need of oxidative steps. This new strategy is reported in Scheme 123.



Scheme 123 – Alternative route to enantioenriched trienone (+)-(2).

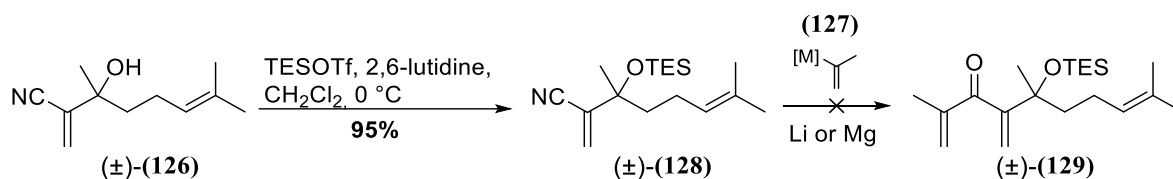
A synthetic protocol by Zhang and coworkers¹⁷⁸ was available, in which a Nickel-catalyzed hydrocyanation with Markovnikov selectivity was performed on a broad scope, including propargylic alcohols. In this approach, Zn(CN)₂ and water were used as cyanide and proton sources respectively, neocuproine as ligand and Mn as reducing agent to reconvert the Ni(II) species into the active Ni(0).

complex. The application of this protocol to propargylic alcohol (\pm)-(120) was successful, as shown in Scheme 124. However, the 1,2-addition on resulting nitrile (\pm)-(126) (Etling, C.) was never observed, both with Li-derivatives or Grignard reagents.



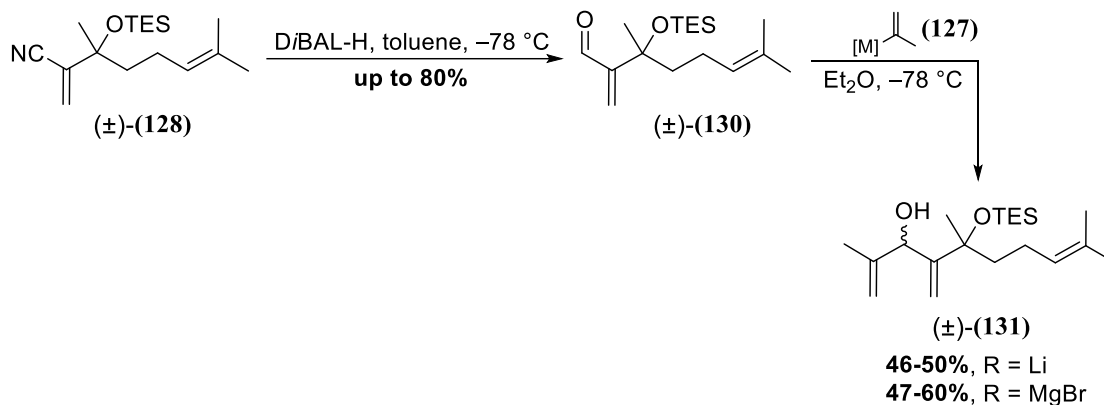
Scheme 124 – Formal hydrocyanation of propargylic alcohol (\pm)-(120) as well as 1,2-addition attempts.

Di Marco, A. focused instead on the 1,2-addition onto protected nitrile (\pm)-(128), depicted in Scheme 125. A TES-protecting group was chosen, since it had to be installed later on in the synthesis. However, treatment of TES-protected nitrile (\pm)-(128) with organometallic reagents (127) resulted in decomposition of the starting material (alkenyl-Li) or in 1,4 addition (Grignard reagent).



Scheme 125 – 1,2-addition attempt on TES-protected nitrile (\pm)-(128).

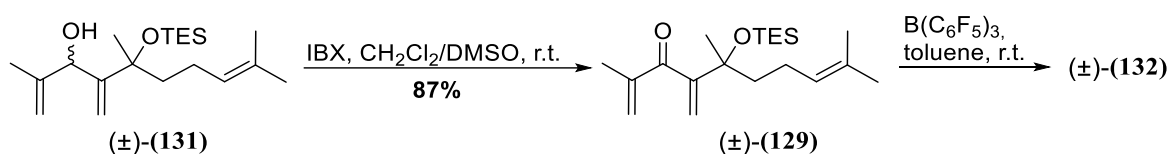
As a consequence, the shortcut to trienone (\pm)-(2) was substituted by reduction to aldehyde prior to 1,2-addition onto nitrile (\pm)-(128), since the increased electrophilicity of the carbonyl group should have favoured 1,2-addition against the competing 1,4 reaction mode. Reduction to aldehyde (\pm)-(130) worked after extensive screening, both on free β -hydroxynitrile (\pm)-(126), and its protected version (\pm)-(128), including Red-Al, NaH/ZnCl₂ and DiBAL-H as reducing agents and different solvent systems. Finally, reduction with DiBAL-H in toluene afforded aldehyde (\pm)-(130) although in not-reproducible yields (Scheme 126). The same problem remained for following 1,2-addition, in which low yields were obtained with both chosen organometallic species, both with direct and reversed addition (for a comprehensive table of tested conditions, see Results and discussion section).



Scheme 126 – Successful 1,2-addition on TES-protected aldehyde (\pm)-(130).

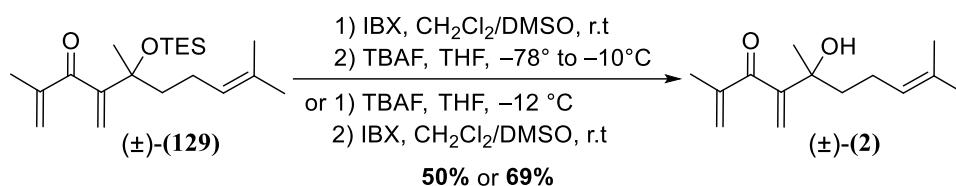
The small amount of obtained material was enough to test the next transformations: oxidation of protected dienol (\pm)-(131) afforded trienone (\pm)-(129) (Scheme 127), which was subjected to the optimized Nazarov conditions. However, although cyclization of protected trienone occurred to deliver

what seemed to be the desired spirocompound, detailed NMR analysis showed that the obtained product was one of its diastereoisomers.² The scarce amount of material, as well as the low quality of the NMRs did not allow full signal assignment; consequently, the attribution of a relative stereoconfiguration *via* NOE analysis was not possible. This disappointing result seemed however to confirm the initial proposal that the hydroxyl group controls the stereochemical outcome of the reaction: the lack of the H-bond donating group, which guaranteed the formation of a rigid and stabilised intermediate, and the hindered TES-group might have forced the cyclization to occur on the opposite face of the molecule.



Scheme 127 – Synthesis and Nazarov cyclization of TES-protected trienone (±)-(129).

For this reason, Di Marco, A. explored deprotection and oxidation conditions (and oxidation-deprotection), obtaining free-Nazarov precursor (±)-(2), shown in Scheme 128.



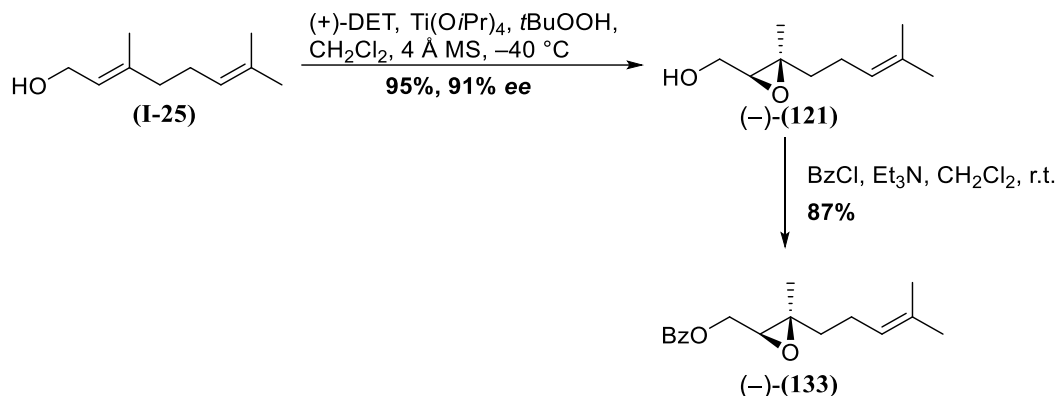
Scheme 128 – Oxidation/deprotection and deprotection/oxidation sequences towards cross-conjugated trienone (±)-(2).

Although with minor changes, this route was ready to be applied to the asymmetric total synthesis of (-)-illisimonin A (-)-(I-346).

² The same signals were present, although shifted to different chemical shifts. R_f was identical, but the spectra could not be superimposed.

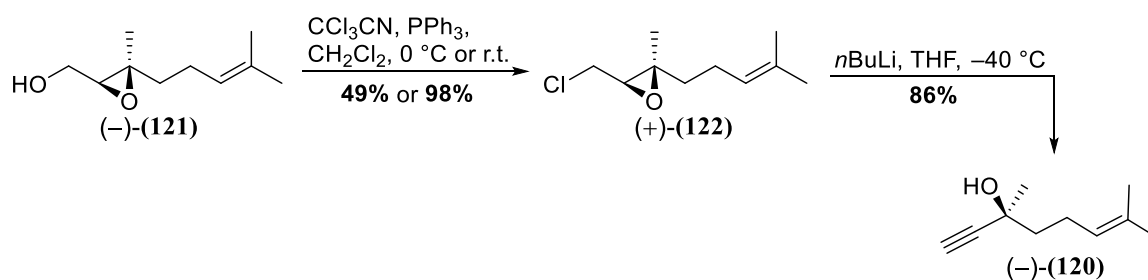
Results and discussion

For the feasibility of a scale-up, some minor issues remained to be taken care of. Sharpless epoxidation of geraniol (**I-25**) could be performed on 50 g scale in high, reproducible yields; determination of the enantiomeric excess was possible through HPLC analysis on chiral stationary phase performed on the corresponding benzoate (**-**)-(133) (Scheme 129).



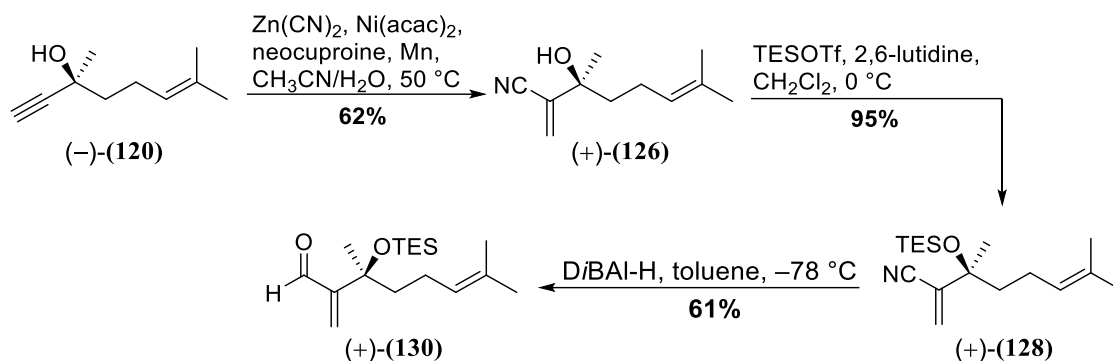
Scheme 129 – Synthesis of (**-**)-2,3-epoxygeraniol (**-**)-(121) and corresponding benzoate (**-**)-(133).

The use of refluxing CCl₄ in the subsequent Appel reaction was not the best option on such a large scale. For this reason, a milder, greener procedure was tested in two temperature variants, with trichloroacetonitrile in dichloromethane, as reported in Scheme 130. When the chlorinated reagent was added dropwise to (**-**)-geraniol epoxide (**-**)-(121) at room temperature, gentle reflux was induced by the exothermic reaction. In this fashion, desired nucleophilic substitution could be scaled up in almost quantitative yields. Double elimination *via* epoxide opening was obtained with *n*BuLi (3.5 equiv.) and afforded almost 40 g of (**-**)-propargylic alcohol (**-**)-(120) in one pot.



Scheme 130 – Synthesis of (**-**)-propargylic alcohol (**-**)-(120).

Reproducibility, that was still an issue during the preliminary studies, was achieved through careful purification of β -hydroxynitrile (+)-126, obtained *via* the optimized formal hydrocyanation strategy, as shown in Scheme 131. Column chromatography, followed by bulb-to-bulb distillation, as well as removal of the residual impurities after TES-protection, were necessary to obtain reproducible yields during the reductive steps. With these few attentions, reduction to α,β -unsaturated aldehyde (+)-130 settled down to 61% yield on 20 g scale.



Scheme 131 – Synthesis of (+)-TES-protected aldehyde (+)-(130).

With a scalable procedure for the synthesis of aldehyde (+)-(130) available, the conditions for the 1,2-addition were given a second glance. At first, due to the commercial availability of the Grignard reagent (0.5 M solution in THF), the use of isopropenyl magnesium bromide was investigated. The use of conditions from Entry 4 (Table 13) on bigger scale gave even better yields (69%). This finding suggested a further screening regarding the employed solvent (Entry 5, Table 13). However, the product obtained *via* Grignard addition was always accompanied by a slight impurity detectable only *via* proton NMR, that made the *in situ* preparation of the lithium reagent look like a still reasonable option. Specifically, when the excess of organometallic reagent employed in the preliminary screenings by Di Marco, A. (Entries 1-4, Table 13) was cut down to 1.5 equivalents (Entry 6, Table 13), desired diol (131) was obtained in high yields and purity, so that it could be employed in the deprotection step without any column chromatography, with overall yield of 80%. Moreover, the addition of the electrophile in diethyl ether solution to the nucleophile, generated *in situ* through lithium-halogen exchange for 2-bromopropene, was applied to over 12 g of aldehyde, with no significant variation in yield or purity (Entry 6, Table 13).

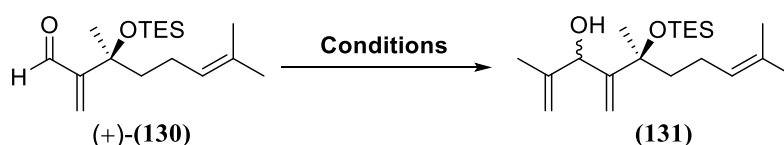
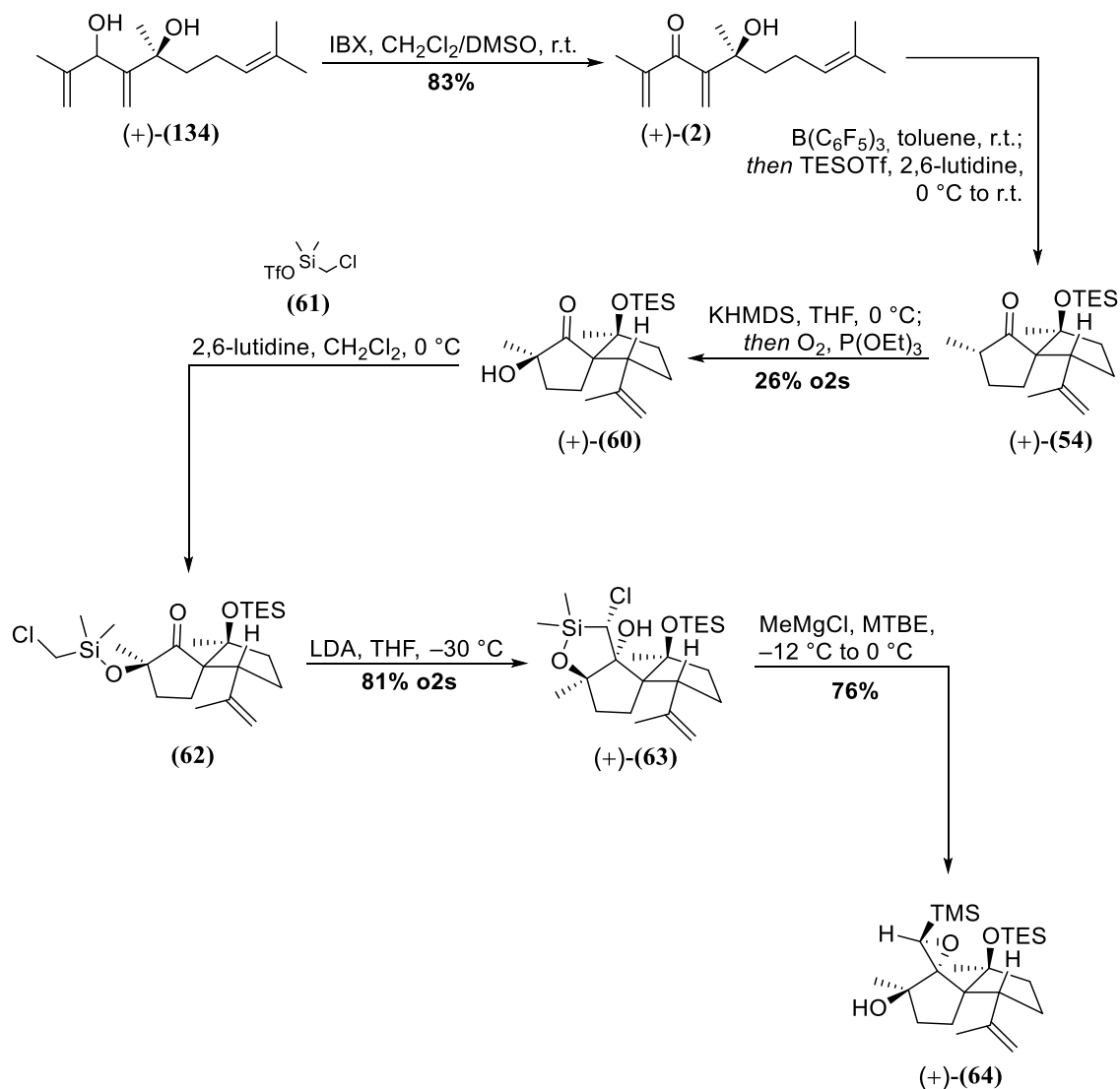


Table 13 – Comprehensive 1,2-addition attempts on enal (+)-(130).

Entry	Conditions	Product (Yield) ^[a]
1	[M] = Li (3.0 equiv.), Et ₂ O, -78 °C, 1 h; addition of [M] to (+)-(130)	(131) (50%)
2	[M] = MgBr (3.0 equiv.), Et ₂ O, -78 °C, 3 h; addition of [M] to (+)-(130)	(131) (60%)
3	[M] = Li (3.0 equiv.), Et ₂ O, -78 °C, 3 h; addition of (+)-(130) to [M]	(131) (46%)
4	[M] = MgBr (3.0 equiv.), Et ₂ O, -78 °C, 3 h; addition of (+)-(130) to [M]	(131) (47%)
5	[M] = MgBr (3.0 equiv.), THF, -78 °C, 2.5 h; addition of (+)-(130) to [M]	(131) (65%)
6	[M] = Li (1.5 equiv.), Et ₂ O, -78 °C, 50 min; addition of [M] to (+)-(130)	(134) (80% o2s)

[a] Isolated yields; [b] Deprotection conditions: TBAF, THF, 0 °C.

Oxidation with IBX proceeded smoothly yielding cross-conjugated ketone (+)-(2) in 83% yields. Nazarov cyclization, α -hydroxylation and homologation to enantioenriched oxasilolane (+)-(63), as well as its rearrangement to (+)-epoxyde (+)-(64) did not suffer from scaling up, as shown in Scheme 132.



Scheme 132 – Asymmetric route to (+)-TMS-epoxide (+)-(64).

However, since the scale-dependency of TPPB-initiated epoxide opening had already been highlighted during the racemic studies (yields were progressively dropping from 64% to 51% when increasing the amount of starting material from 1 g to 3.5 g), further effort was posed in this direction: the use of TFA, HCl, HF and HClO₄ was evaluated concerning protic conditions, while BF₃·OEt₂ was chosen among the Lewis acids (see Table 14). Perchloric acid used in substoichiometric amounts gave the best yields and reproducibility.

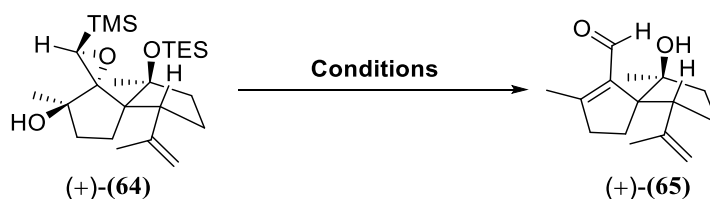
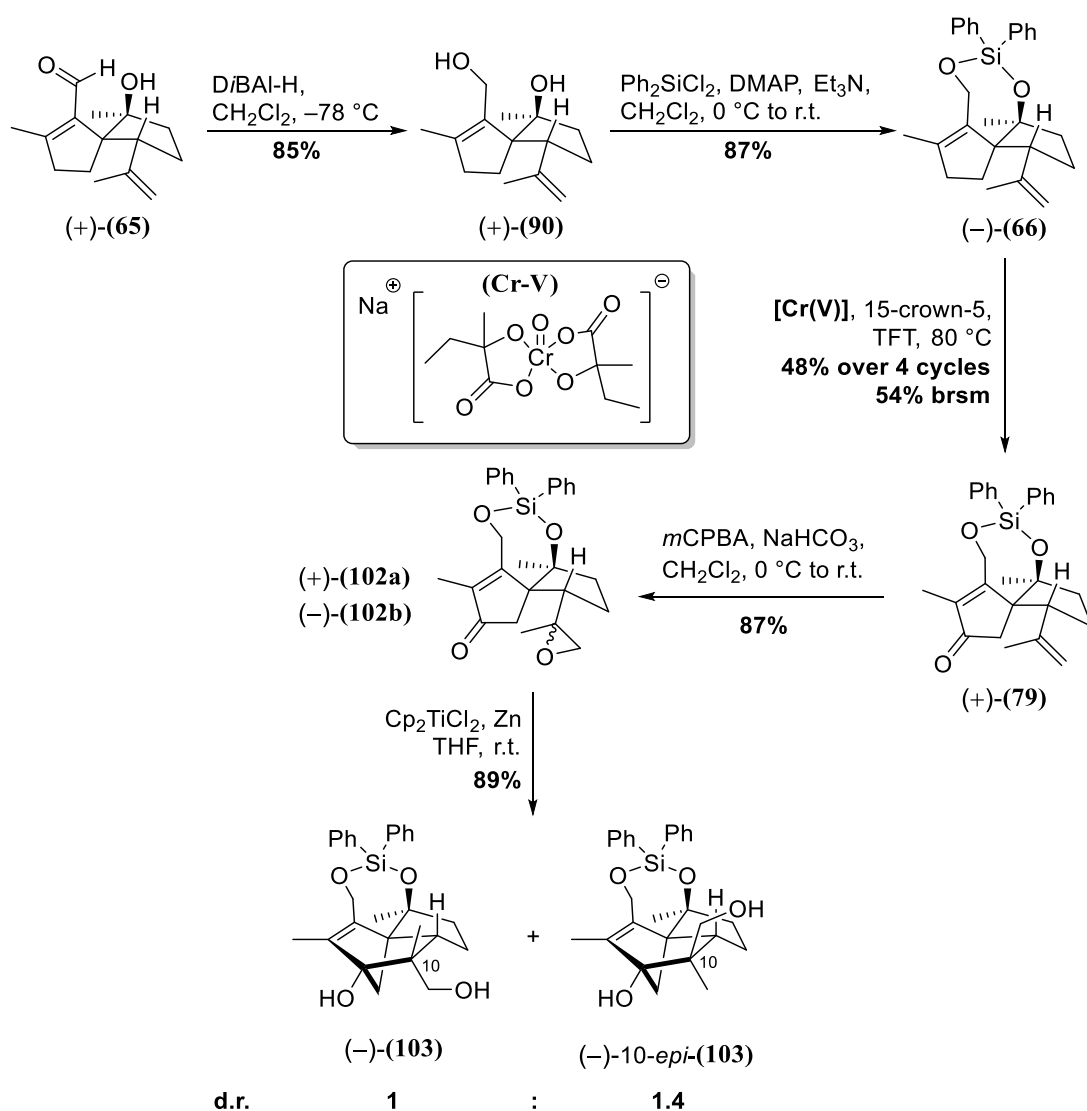


Table 14 – Conditions screening for the opening of (+)-TMS-epoxide (+)-(64).

Entry	Conditions	Product (Yield) ^[a]
1	TFA (1 equiv.), CHCl ₃ , 0 °C	(+)-(65) (<44%)
2	AcCl (1.2 equiv.), MeOH, 0 °C	(+)-(65) (49%)
3	HF (2M in H ₂ O, 3 equiv.), CH ₃ CN, 0 °C	(+)-(65) (31-40%)
4	BF ₃ ·H ₂ O (0.75 equiv.), MeOH, 0 °C	(+)-(65) (18%)
5	HClO ₄ (0.3 equiv.), THF/H ₂ O = 4:1, 0 °C to r.t.	(+)-(65) (79%)

[a] Isolated yield.

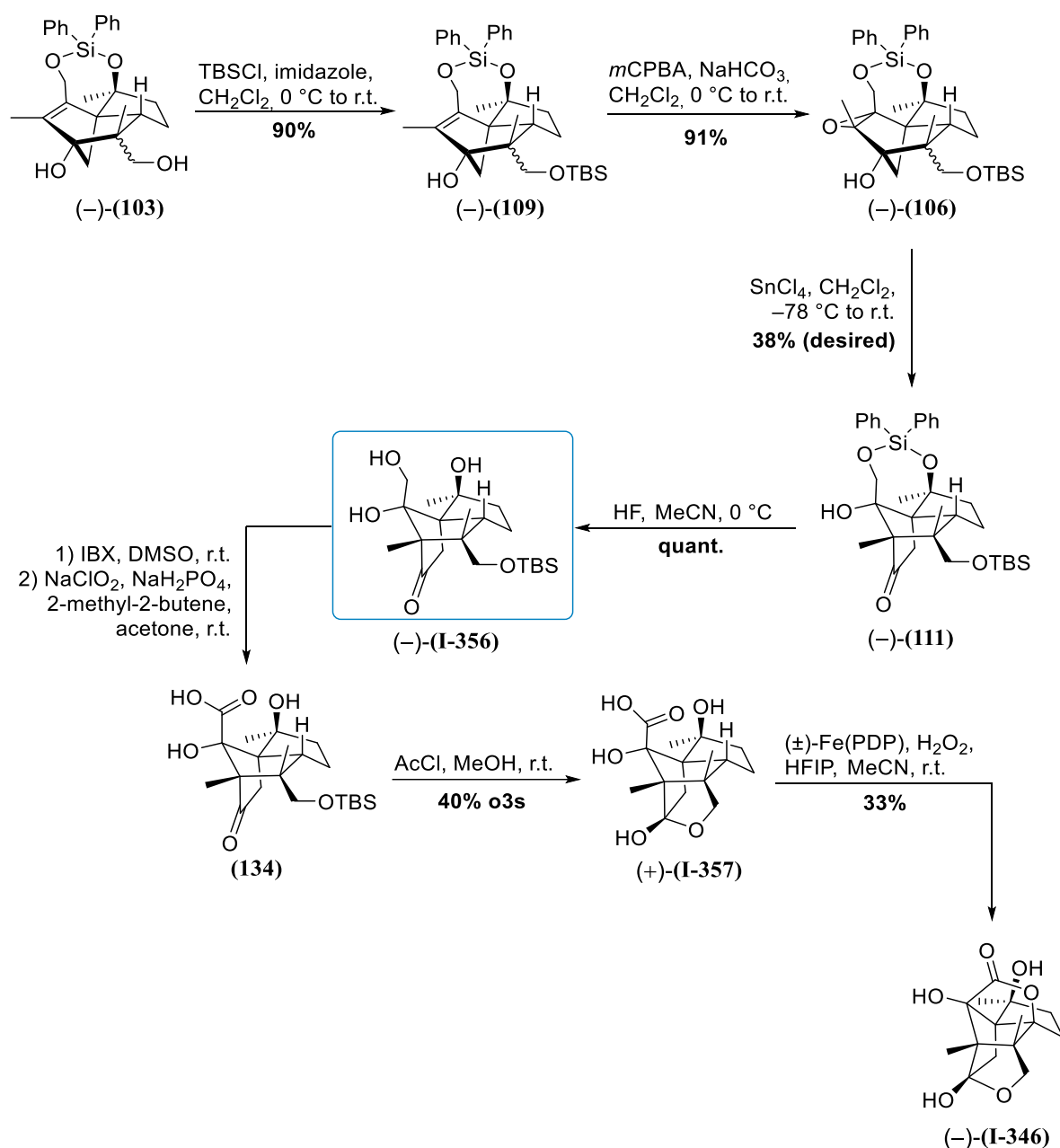
Reduction, protection of the resulting (+)-diol (+)-(90) and allylic oxidation did not require any further optimization; the mixture of epoxides (+)-(102a) and (-)-(102b), obtained through treatment of enantioenriched enone (+)-(79) with *m*CPBA, underwent the key Ti(III)-mediated reductive cyclization affording tricycles (-)-(103) in high yields and diastereoselectivity (Scheme 133).



Scheme 133 – Synthesis of enantioenriched norbornanes (-)-(103).

After TBS-protection, epoxidation and type III semipinacol rearrangement as reported in Scheme 134 and established in the racemic route, selective deprotection furnished Rychnovsky's formal intermediate (-)-(I-356), highlighted in Scheme 134 (164 mg obtained in one pot). A slight modification

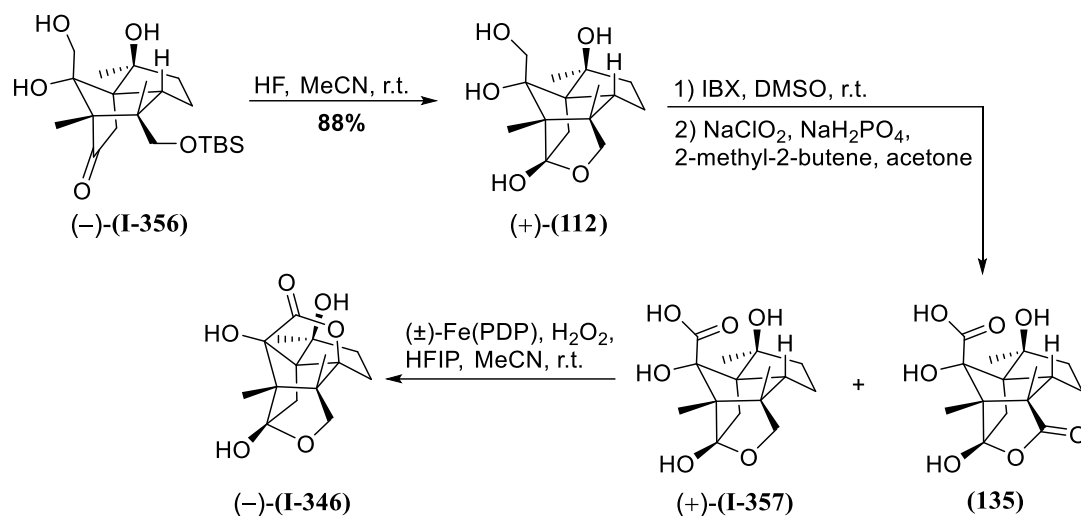
of the reported IBX oxidative conditions concerning low temperature work up was necessary due to the observation of α -ketol rearrangement (as previously commented in Scheme 118), along with the desired aldehyde. Moreover, the addition of sodium chlorite as an aqueous solution during the Pinnick oxidation, performed under strict light exclusion, was necessary to achieve reproducible yields. Carboxylic acid (+)-(I-357) was obtained after acidic deprotection and consequent lactolization of intermediate (134). The asymmetric total synthesis of (-)-illisimonin A (-)-(I-346) was terminated by a White-Chen C–H activation as in the reported synthesis, and yielded 1.6 mg of natural product in overall 0.03% yield over 28 steps.



Scheme 134 – Formal and total synthesis of (-)-illisimonin A (-)-(I-346), endgame. First formal intermediate from Rychnovsky and Burns (-)-(I-356) is highlighted in the box.

Having obtained (-)-illisimonin A (-)-(I-346) in reasonable and comparable yields with respect to the published conditions,¹⁴⁶ and considered the efforts dedicated to the alternative route during the racemic scouting, the “lactol route” was also given a chance. After full deprotection to (+)-lactol (+)-(I-112), the successful conditions found (IBX-Pinnick sequence) were applied to this extremely polar

compound. Desired acid (+)-(**I-357**) was obtained as inseparable mixture with overoxidized lactone (**135**); White-Chen conditions applied to the mixture afforded further 0.8 mg of (-)-illisimonin A (-)-(**I-346**) in 6% unoptimized yield over 3 steps. This result represents a proof of principle for the feasibility of the alternative endgame. Circular dichroism measurements, as well as NMR data, confirmed the nature of the obtained compound, and concluded this thesis.



Scheme 135 – Alternative endgame to (-)-illisimonin A (-)-(**I-346**) via (+)-lactol (+)-(**I-112**).

Conclusions and outlook

This work fully represents the dual relationship between methodology and total synthesis. In the first, methodological part, the joined efforts of this author and Etling, C. explored an unprecedented termination of the Nazarov oxyallyl cation, the ene reaction. Observed for the first time on a simple cross-conjugated trienone, the Nazarov/ene tandem cyclization showed its tolerance to different functional groups (simple methyl groups, silyl-protected oxygen functionalities and silanes, as well as deuterated olefins), while the increase in yield with an elongated precursor suggested a positive correlation between chain flexibility and feasibility of the cyclization itself. Deuteration studies crowned the methodological part of this thesis, fully unravelling the mechanistic insights of this new way to access spirocompounds. The diastereoselectivity of this reaction, ascribed to hydrogen bonding between the carbonyl and β -hydroxyl group, made of this reaction a powerful tool for constructing contiguous quaternary centers.

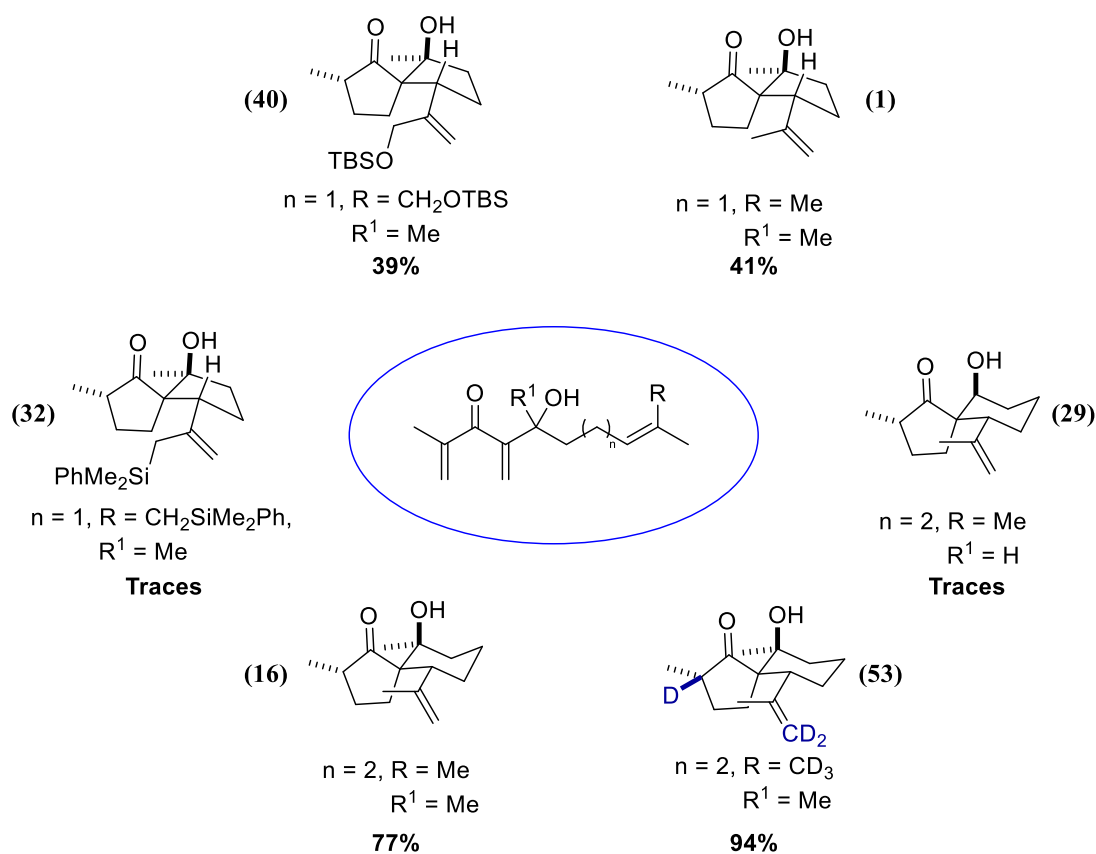
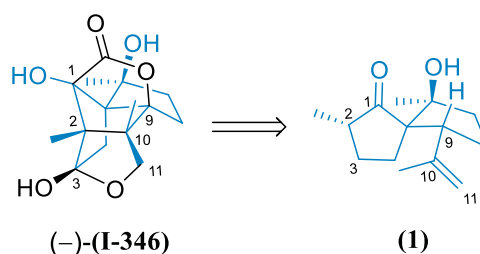


Fig. 21 – Library of synthesized spirocompounds deriving from variously substituted cross-conjugated trienones.

(–)-illisimonin A (–)-(I-346), with its unprecedented tricyclo[5.2.1.0^{1,6}]decane skeleton, represented the perfect way for validating this new reaction sequence, due to the spiro-substructure embedded in its cage-like structure:



Scheme 136 – Spirosubstructure embedded in the cage-like structure of (-)-illimonin A (-)-**(I-346)**.

Spiroketone **(1)**, obtained in 10 steps from geraniol, was successfully converted into (-)-illimonin A (-)-**(I-346)** by means of a one-carbon homologation (C-1), C2–C10 bond formation, and functionalization at C-3, C-9 and C-11. Pivotal transformations in this sequence were a Si-tethered homologation, an allylic oxidation with an unusual Cr(V) complex and a Ti(III)-mediated cyclization to construct the undesired C3–C10 bond. A semipinacol rearrangement afforded the natural product *trans*-pentalene connectivity (C2–C10 bond formation). A carboxylic acid-directed C–H activation resulted in targeted (-)-illimonin A (-)-**(I-346)** in overall 0.03% yield over 28 steps.

Experimental section

General information

Reactions employing air- or moisture-sensitive reagents were performed under argon atmosphere (the use of an inert gas atmosphere will be specified in the following experimental procedures). In these cases, the used glassware was dried by heating with a Bunsen burner or heat-gun under high vacuum prior to use. Air- and moisture-sensitive liquids and solutions were transferred *via* syringe flushed with argon prior to use. All reagents were purchased from commercial suppliers and used without further purification unless otherwise noted. For reagents prepared after literature procedures, possible changes are referred to as "after a (slight) modification of" followed by the actual procedure employed. Stated temperatures, except room temperature (22 to 29 °C), refer to bath temperatures. All reactions were stirred magnetically, unless noted otherwise. In context of work-up, NH₄Cl, NaCl, Na₂S₂O₃, NaHCO₃ and Na/K tartrate refer to the respective saturated aqueous solutions, unless noted otherwise.

Dry solvents Dichloromethane, diisopropylamine and triethylamine were distilled under an inert atmosphere over calcium hydride. Tetrahydrofuran was distilled under inert atmosphere over sodium or, in alternative, it was purchased from Acros Organics (stabilized with BHT and stored over molecular sieves). Diethyl ether (stabilized with BHT and stored over molecular sieves), MTBE (stored over molecular sieves), CPME (stabilized with BHT and stored over molecular sieves) and *n*-pentane (stored over molecular sieves) were purchased from Acros Organics. Benzene was bought from Sigma Aldrich.

Organolithium reagents were purchased from Acros Organics.

Thin layer chromatography All reactions were monitored using pre-coated TLC sheets ALUGRAM® Xtra SIL G/UV₂₅₄ (0.2 mm, silica gel, F₂₅₄, aluminium-backed, MACHEREY-NAGEL) with detection by UV light ($\lambda = 254$ nm) and/or by staining with either acidic vanillin stain, acidic anisaldehyde, basic potassium permanganate or Hanessian's stain.

Flash column chromatography was performed using silica gel (0.04-0.063 mm, 240-400 mesh) obtained from MACHEREY-NAGEL. The applied petroleum ether fraction had a bp of 40–60 °C. The eluent is given in volume ratios (v/v).

NMR experiments were recorded in CDCl₃, C₆D₆ or methanol-*d*₄ purchased from deutero GmbH. The following NMR spectrometers were used: Bruker Ultrashield 400 MHz (ULS400), Bruker Ascend 400 MHz (ASC400), Bruker Ascend 400 MHz with Prodigy BBFO probe head, Bruker Ultrashield 500 MHz with TCI cyro probe head, Bruker Ascend 600 MHz with DUL cryo probe head. The ¹H-NMR spectra were calibrated using the residual solvent peak: $\delta(\text{CDCl}_3) = 7.26$ ppm, $\delta(\text{C}_6\text{D}_6) = 7.16$ ppm, $\delta(\text{CD}_3\text{OD}) = 3.31$ ppm. ¹³C-NMR spectra were calibrated using the solvent's carbon signal: $\delta(\text{CDCl}_3) = 77.16$ ppm, $\delta(\text{C}_6\text{D}_6) = 128.06$ ppm, $\delta(\text{CD}_3\text{OD}) = 49.00$ ppm. The methanol-*d*₄ contained trace amounts of ethanol-*d*₆, as confirmed by deutero GmbH. Chemical shifts δ are given in parts per million (ppm), coupling constants *J* in Hertz (Hz) and multiplicities as follows: s, singlet; d, doublet; t, triplet; q, quartet; quint, quintet; m, multiplet; or combinations of these acronyms. Broad signals will be denoted by addition of the letter "b"; e.g. "broad singlet" is written as "bs". Peak integrals are given as multiples of protons YH, with *Y* being the number of protons belonging to the given signal.

For all substances NOE experiments were performed with, a signal-structure assignment is given. For the assignment of NMR signals to atoms in the structures, NMR active positions are labeled with arabic numbers. Those numbers were assigned arbitrarily and usually do not follow the numbering by the IUPAC system. The atom labels are written in the form "H-x" for proton spectra, where "x" marks the position number. The notation "C-x" is used for carbon spectra. In case of multiplets that consist of

several overlapping proton signals, the “grouped” notation "H-{x, y, ...}" is used, listing the associated positions in brackets.

Signals that belong to heteroatom bound groups that are not part of the actual backbone of a molecule (such as protecting groups), are referred to in the notation "XR", with "X" being the corresponding heteroatom and "R" being the abbreviation for the particular residue/group. If the samples contained a mixture of two inseparable isomers and no complete signal assignment is given, distinguishable signals of the minor isomer are marked with an asterisk. NMR spectra were processed using TopSpin (Bruker) Version 4.1.4 or MestreNova version 6.22.0-7238.

High Resolution Mass Spectra (HRMS) were obtained either using a Q-ToF Premier (Waters), a LCT Premier (Waters) or an Agilent 7890 GC system with a 5977B detector. Both the masses found and the masses calculated are given.

GC/MS (Electron-impact ionization) data was recorded with a GC-system Agilent 6890 coupled with an Agilent 5977B mass-sensitive detector. For EI mass spectra, the fragmentation patterns with relative intensities are given.

Optical rotations were measured with A. Krüss optronic P3000 polarimeter or a Perkin-Elmer 241 polarimeter. Measurements were performed in a cuvette with a cell length of $d = 1$ dm and at wavelength of $\lambda_{\max} = 589.3$ nm (sodium D-line). The solvent used is specified for each substance. Concentrations are given in g/100 mL.

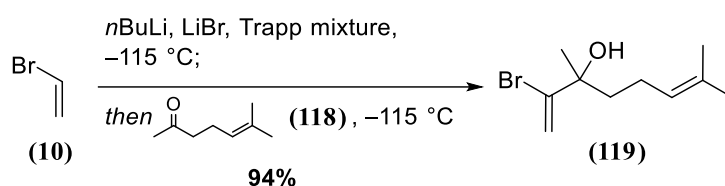
CD spectra were recorded with a Jasco J-815 CD Spectrometer. Range of measurement: 190–400 nm, resolution: 0.2 nm, speed: 50 nm/min, D.I.T. 0.5 s. A Hellma Analytics Suprasil 110-QS quartz cuvette with a thickness of 1 mm and a volume of 350 μ L was used.

Melting points were measured using an OptiMelt MPA 100 (Stanford Research System).

Experimental procedures

PART 1: the original Nazarov cyclization

(±)-2-Bromo-3,7-dimethylocta-1,6-dien-3-ol (**119**)



A solution of vinyl bromide³ (**10**) (23.5 mL, 335 mmol, 2.0 equiv.) and LiBr (7.23 g, 83.2 mmol, 0.5 equiv.)⁴ in Trapp mixture (THF:Et₂O:*n*-pentane = 4:1:1, 160 mL) was placed into a three-neck round-bottom flask equipped with an internal thermometer, a mechanical stirrer with argon inlet and a rubber septum. This flask will be further referred to as "main flask". A Schlenk flask, further referred to as "side flask", was filled with Trapp mixture (240 mL) and both flasks were cooled to -78 °C.⁵ *n*BuLi (2.5 M in hexanes, 100 mL, 250 mmol, 1.5 equiv.) was added to the side flask and the solution was mixed by gently shaking the flask outside the cooling bath for approx. 30 s. Both solutions were cooled to -118 °C and the *n*BuLi solution was transferred to the main flask *via* transfer cannula over 2 h. After complete addition, the side flask was rinsed with Trapp mixture (2x, 10 mL). During the entire addition and reaction the temperature of both main and side flask was maintained between -115 and -112 °C. Stirring in this temperature range was continued for 1 h during which time the formation of a white suspension occurred, indicating the precipitation of 1-bromo-1-lithioethene. Precipitation was accompanied by a swift rise of the main flask temperature which was countered by quick addition of liquid nitrogen to the coolant.

6-Methyl-5-hepten-2-one (**118**) (25.0 mL, 168 mmol, 1.0 equiv.) and Trapp mixture (80 mL) were placed in the side flask and the solution was cooled to -115 °C. The solution was then added to the reaction solution *via* transfer cannula over the course of 40 min, maintaining the temperature between -115 and -112 °C. After complete addition, stirring was continued in this temperature range for 1 h, before a solution of acetic acid (7.5 mL, 131 mmol, 0.8 equiv.) in Trapp mixture (80 mL) was added at -115 °C over 20 min. The solution was allowed to warm to r.t. overnight, was washed with NaHCO₃ (5%, 250 mL) and the aqueous phase was extracted with Et₂O (3x, 250 mL). The combined organic phases were washed with brine (150 mL), dried over MgSO₄ and concentrated under reduced pressure. The resulting bright yellow crude product was purified *via* vacuum distillation to afford bromo alcohol (**119**) (36.6 g, 157 mmol, 94%) as a colorless oil.

b.p.(1 mbar) = 75 °C;

R_f (PE:EtOAc = 10:1, vanillin) = 0.46 (dark blue);

¹H-NMR (400 MHz, CDCl₃): δ(ppm) = 5.93 (d, *J* = 2.0 Hz, 1H), 5.56 (d, *J* = 2.0 Hz, 1H), 5.18–5.11 (m, 1H), 2.11–1.92 (m, 3H), 1.91–1.83 (m, 1H), 1.71–1.63 (m, 4H), 1.62 (s, 3H), 1.44 (s, 3H);

¹³C-NMR (101 MHz, CDCl₃): δ(ppm) = 140.8, 132.9, 123.9, 116.3, 77.1, 40.2, 27.1, 25.9, 22.9, 17.9;

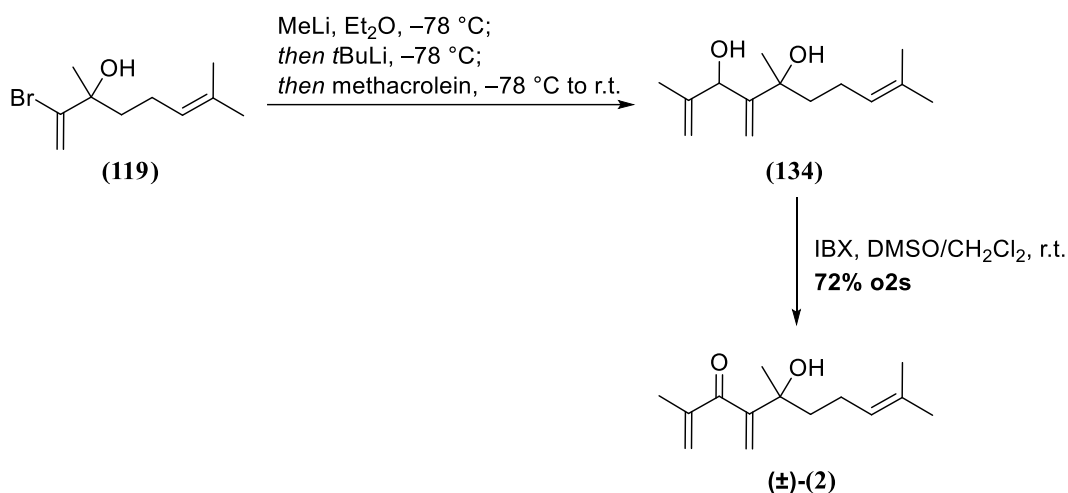
HRMS(CI): Calcd for C₁₀H₁₈OBr [M+H]⁺: 233.0541; found: 233.0536.

³ Vinyl bromide was dried by passing through a nitrogen flushed column filled with anhydrous CaCl₂ and the gas condensed into a Schlenk tube at -78 °C.

⁴ Prior to use, LiBr was molten over a Bunsen burner and poured directly into the empty reaction flask, where it was allowed to return to r.t. under a constant nitrogen stream.

⁵ *n*-Pentane/liquid nitrogen was used as cooling mixture. Controlled cooling was achieved by pouring the liquid nitrogen into a glass tube that was immersed in the pentane.

(±)-5-Hydroxy-2,5,9-trimethyl-4-methylenedeca-1,8-dien-3-one (±)-(2)



MeLi (1.6 M in Et₂O, 200 mL, 320 mmol, 1.0 equiv.) was added at -78 °C to a stirred solution of bromoalcohol (**119**) (74.6 g, 320 mmol, 1.0 equiv.) in dry Et₂O (2.0 L). The addition required 45 min.⁶ Stirring at -78 °C was continued for 60 min and a cooled solution of tBuLi (1.9 M in pentane, 354 mL, 672 mmol, 2.1 equiv.) was added dropwise over the course of 1 h 15 min.⁷ The slightly yellow solution was stirred at -78 °C for 5 h before methacrolein (31.8 mL, 384 mmol, 1.2 equiv.) was added over 20 min and the resulting nearly colorless mixture was allowed to warm to r.t. overnight. MeOH (100 mL) was added slowly and the resulting heterogeneous mixture was poured into a mixture of Na/K tetratate solution and EtOAc (500 mL each). The phases were separated and the aqueous phase was extracted with EtOAc (3x, 500mL). The combined organic layers were washed with brine (500 mL), dried over Na₂SO₄ and concentrated under reduced pressure. The obtained diol (**134**) (yellow oil) was used in the subsequent step without further purification. If desired, a pure diastereomeric mixture of diol (**134**) can be obtained after column chromatography (PE:EtOAc = 5:1 to 2:1); following analytical data were obtained:

R_f (CyH:EtOAc = 5:1; vanillin) = 0.25 (dark blue);

¹H-NMR (400 MHz, CDCl₃): δ(ppm) = 5.19–5.08 (m, 4H), 5.05–5.00 (m, 1H), 4.77–4.72 (m, 1H), 2.82 (bs, 1H), 2.56* (bs, 1H), 2.48 (bs, 1H), 2.32* (bs, 1H), 2.08–1.97 (m, 2H), 1.78–1.63 (m, 2H), 1.71 (s, 3H), 1.68 (s, 3H), 1.60 (s, 3H), 1.40 (s, 3H), 1.38 (s, 3H);

¹³C-NMR (101 MHz, CDCl₃): δ(ppm) = 153.8*, 153.3, 146.5*, 146.1, 132.2, 124.3*, 124.2, 112.7, 112.1*, 111.9, 111.7*, 76.6, 76.4*, 75.63, 75.56*, 42.3, 42.2*, 29.3*, 29.0, 25.8, 23.1, 22.8*, 19.8, 19.6*, 17.86*, 17.84;

HRMS(ESI): Calcd for C₁₄H₂₄O₂Na [M+Na]⁺: 247.1674; found: 247.1674.

The crude diol was dissolved in CH₂Cl₂/DMSO (1:1, 2.0 L) and IBX (108 g, 384 mmol, 1.20 equiv.) was added at 0 °C. The mixture was allowed to warm to r.t.. Stirring was continued for 2 h, the mixture was diluted with water (1 L) and transferred to a separatory funnel. The phases were separated, the aqueous phase extracted with CH₂Cl₂ (5x, 1 L) and the combined organic layers washed with water (2x, 1 L) and brine (1 L). The organic layers were dried over Na₂SO₄ and the solvent was removed under

⁶ Addition *via* transfer cannula directly from the bottle.

⁷ tBuLi was added from a dropping funnel with exterior glass mantle for cooling. The reagent was cooled with dry ice/acetone prior to and during addition.

reduced pressure. The oily residue was purified by column chromatography (PE:EtOAc = 50:1 to 25:1), followed by vacuum distillation to give (±)-(2) (51.3 g, 231 mmol, 72%) as a colorless oil.

b.p.(0.5 mbar) = 91 °C;

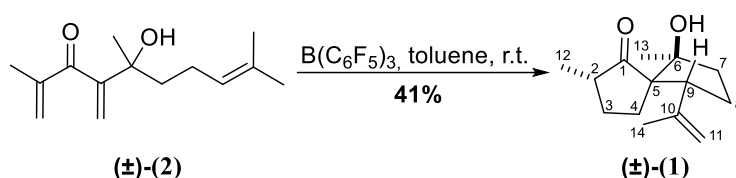
R_f (CyH:EtOAc = 5:1; cerium molybdate) = 0.47 (dark blue);

¹H-NMR (400 MHz, CDCl₃): δ(ppm) = 5.85 – 5.82 (m, 1H), 5.78 (bs, 1H), 5.59 (s, 1H), 5.11 – 5.04 (m, 1H), 3.49 (s, 1H), 2.03 – 1.95 (m, 2H), 1.93 (s, 3H), 1.82 – 1.73 (m, 1H) 1.69–1.61 (m, 4H), 1.56 (s, 3H), 1.38 (s, 3H);

¹³C-NMR (101 MHz, CDCl₃): δ(ppm) = 201.6, 151.7, 144.7, 132.0, 127.9, 124.2, 122.7, 74.8, 41.5, 27.1, 25.8, 23.1, 18.0, 17.8;

HRMS(ESI): Calcd for C₁₄H₂₂O₂Na [M+Na]⁺: 245.1517; found: 245.1517.

Spiro ketone (±)-(1)



$B(C_6F_5)_3$ (5.9 mg, 11.5 μ mol, 5.0 mol%) was added in one portion to a stirred solution of cross-conjugated ketone (±)-(2) (51 mg, 0.23 mmol, 1.0 equiv.) in toluene (23 mL) at r.t. and stirring at this temperature was continued for 36 h. During this time the solution color changed from nearly colorless over bright pink to orange. The mixture was concentrated under reduced pressure and subjected to column chromatography (PE:EtOAc = 99:1 to 19:1) to afford spiro ketone (±)-(1) (21 mg, 94.3 μ mol, 41%).

R_f (PE:EtOAc = 10:1; vanillin) = 0.48 (dark purple);

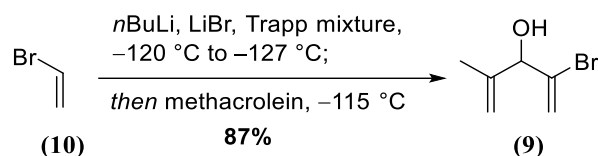
1H -NMR (400 MHz, $CDCl_3$): δ (ppm) = 4.93–4.91 (m, 1H, H-11), 4.78–4.76 (m, 1H, H-11), 4.06 (s, 1H, OH), 3.43 (t, J = 2.8 Hz, 1H, H-9), 2.29–2.18 (m, 1H, H-2), 2.17–2.08 (m, 1H, H-3), 1.93–1.68 (m, 5H, H-{4,7,8}), 1.61 (ddd, J = 13.9, 7.6, 1.7 Hz, 1H, H-4), 1.52 (s, 3H, H-14), 1.47–1.36 (m, 1H, H-3), 1.15 (s, 3H, H-13), 1.07 (d, J = 6.7 Hz, 3H, H-12);

^{13}C -NMR (100 MHz, $CDCl_3$): δ (ppm) = 228.9 (C-1), 144.3 (C-10), 113.2 (C-11), 85.6 (C-6), 63.0 (C-5), 53.2 (C-9), 45.5 (C-2), 37.7 (C-7), 28.5 (C-3), 26.0 (C-4), 25.2 (C-8), 24.5 (C-14), 24.4 (C-13), 13.7 (C-12);

HRMS(ESI): Calcd for $C_{14}H_{22}O_2Na$ $[M+Na]^+$: 245.1517; found: 245.1516.

PART 1: the elongated precursor

2-Bromo-4-methylpenta-1,4-dien-3-ol (**9**)



A solution of vinyl bromide (**10**) (16.0 mL, 223 mmol, 2.3 equiv.) and LiBr (1.69 g, 19.4 mmol, 0.20 equiv.) in 100 mL of Trapp mixture (THF:Et₂O:*n*-pentane = 4:1:1) was placed inside a three-necked round-bottom flask (in the following text referred to as "main flask") equipped with an internal thermometer, a mechanical stirrer with argon inlet and a septum. A second schlenk flask (further referred to as "side flask") was filled with 150 mL of Trapp mixture and both flasks were cooled to $-78\text{ }^\circ\text{C}$.⁸ *n*BuLi (2.5 M in hexanes, 63.0 mL, 158 mmol, 1.6 equiv.) was added to the side flask and the solution was mixed by gently shaking the flask outside the cooling bath for approx. 30 s. Both solutions were cooled to $-115\text{ }^\circ\text{C}$ and the *n*BuLi solution of the side flask was added to reaction solution in the main flask *via* transfer cannula over the course of 1.5 h. After complete addition the side flask was rinsed with 5 mL of Trapp mixture (2x) and the rate of liquid nitrogen addition was increased until a solid bridge of frozen *n*-pentane had formed between the heat exchanger and the main flask, which resulted in a decrease of the reaction temperature to $-127\text{ }^\circ\text{C}$. The addition of nitrogen was stopped until the majority of frozen *n*-pentane had molten; the whole process took approx. 1.5 h during which the temperature of the reaction solution remained below $-112\text{ }^\circ\text{C}$. Trapp mixture (50 mL) and methacrolein (8.0 mL, 97.0 mmol, 1.0 equiv.) were placed inside the side flask and the solution was cooled to $-115\text{ }^\circ\text{C}$. The solution was added to the lithium reagent in the main flask *via* transfer cannula over the course of 15 min, during which time temperature was maintained between -112 and $-117\text{ }^\circ\text{C}$. After complete addition, stirring was continued at $-105\text{ }^\circ\text{C}$ for 2 h, before acetic acid (5.0 mL, 87.0 mmol, 0.90 equiv.) in Trapp mixture (75 mL) was added at $-115\text{ }^\circ\text{C}$ over the course of 20 min. The solution was allowed to warm to r.t., was washed with NaHCO₃ (5%, 200 mL) and brine (200 mL), dried over MgSO₄, filtered and concentrated under reduced pressure. The resulting bright yellow crude mixture was subject to vacuum distillation to afford bromo alcohol (**9**) (15.0 g, 84.5 mmol, 87%) as a colorless oil.

b.p. (10 mbar) = 67–68 °C;

R_f (PE:EtOAc = 10:1; cerium molybdate) = 0.26 (ultramarine);

¹H-NMR (400 MHz, CDCl₃): δ (ppm) 6.01 – 5.98 (m, 1H), 5.68 – 5.65 (m, 1H), 5.19 – 5.16 (m, 1H), 5.08 – 5.06 (m, 1H), 4.60 (d, *J* = 5.8 Hz, 1H), 2.12 (d, *J* = 5.8 Hz, 1H), 1.72 (s, 3H);

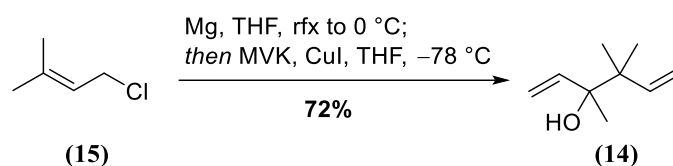
¹³C-NMR (101 MHz, CDCl₃): δ (ppm) = 143.0, 134.6, 118.3, 114.0, 79.4, 18.2;

HRMS(EI): Calcd for C₂H₂Br [M–C₄H₇O]⁺:104.9340; found: 104.9343.⁹

⁸ *n*-Pentane was used as coolant. It was cooled to the appropriate temperature by placing liquid nitrogen inside a large test tube that was immersed in the coolant, which served as "heat exchanger" in order to facilitate controlled cooling of the latter.

⁹ Vinyl bromide radical cation resulting from β -cleavage of (**9**).

3,4,4-trimethylhexa-1,5-dien-3-ol (**14**)



The reaction was conducted after a literature procedure reported by Dubac and coworkers.¹⁰

Mg turnings (3.00 g, 118 mmol, 4.5 equiv.) were suspended in 20 mL of dry THF. Some drops of a prenyl chloride (**15**) (4.8 mL, 39.4 mmol, 1.5 equiv.) 1 M solution in THF were added and the suspension was refluxed until it became slightly dark (approx. 30 min). At this point, 33 mL of THF were added and the mixture was cooled to 0 °C. The remaining prenyl chloride (**15**) solution was added over the course of 2 h. After no starting material was detected through TLC (1 h), the mixture was warmed to r.t.. The freshly prepared prenyl magnesium chloride solution was slowly added (1 h) to a solution of CuI (0.25 g, 1.30 mmol, 5 mol%) and MVK (2.2 mL, 26.4 mmol, 1.0 equiv.) in dry THF (100 mL) previously cooled to -78 °C. The reaction was stirred at -78 °C for 2 h, then quenched with 50 mL of a 9:1 mixture of NH₄Cl and NH₄OH. The layers were separated, and the aqueous phase was extracted with Et₂O (3x, 50 mL). The combined organic layers were dried over Na₂SO₄ and concentrated under reduced pressure. The crude product was subject to column chromatography (PE:EtOAc = 12:1) to afford desired alcohol (**14**) (2.63 g, 18.8 mmol, 72%) as a light yellow oil.

R_f (PE:EtOAc = 95:5; KMnO₄) = 0.33;

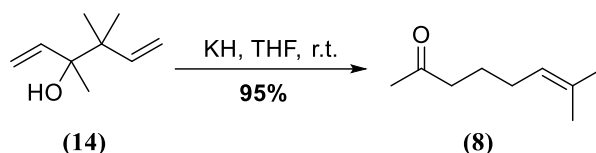
¹H NMR (400 MHz, CDCl₃): δ(ppm) = 6.10 – 5.93 (m, 2H), 5.25 – 5.02 (m, 4H), 1.54 (s, 1H), 1.23 (s, 3H), 1.05 (s, 6H);

¹³C NMR (101 MHz, CDCl₃): δ(ppm) = 144.8, 142.6, 113.7, 112.8, 76.0 (HMBC), 43.6 (HMBC), 23.2, 22.4, 21.6;

HRMS(ESI): Calcd for C₉H₁₆ONa [M+Na]⁺: 163.1099; found: 163.1101.

¹⁰ *J. Organomet. Chem.* **1985**, *281*, 149–162.

7-methyloct-6-en-2-one (**8**)



Prepared after the procedure reported by Nakai and coworkers.¹¹

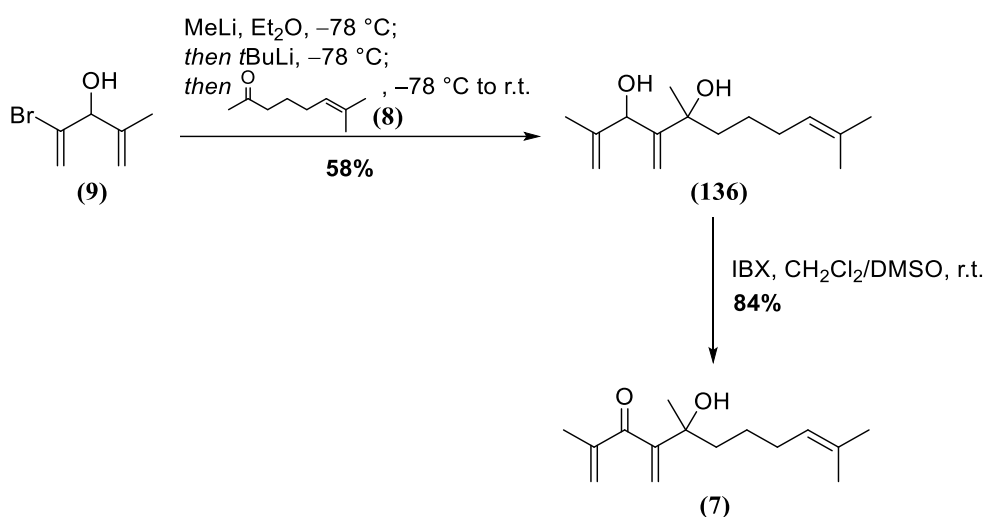
A solution of alcohol (**14**) (2.63 g, 18.8 mmol, 1.0 equiv.) in dry THF (80 mL) was added dropwise to a suspension of KH (25-35% in mineral oil, 5.00 g, 37.5 mmol, 2.0 equiv.) (washed 3x with dry *n*-hexane to remove mineral oil) in dry THF (160 mL). The dark orange solution was stirred at r.t. for 3 h; it was quenched with 50 mL of phosphate buffer (pH 7). The layers were separated and the aqueous phase was extracted with Et₂O (3x, 50 mL). The combined organic layers were washed with brine (50 mL), dried over Na₂SO₄ and concentrated under reduced pressure. The crude ketone (**8**), a brown oil (2.50 g, 17.8 mmol, 95%), was used without any further purification. The analytical data match with the literature reported ones.¹¹

R_f (PE:EtOAc = 95:5; KMnO₄) = 0.38;

¹H NMR (400 MHz, CDCl₃): δ = 5.11–5.05 (m, 1H), 2.41 (t, *J* = 7.4 Hz, 2H), 2.12 (s, 3H), 2.02 – 1.92 (m, 2H), 1.68 (s, 3H), 1.65 – 1.59 (m, 2H), 1.59 (s, 3H).

¹¹ *Tetrahedron* **1993**, *49*, 1025–1042.

5-hydroxy-2,5,10-trimethyl-4-methyleneundeca-1,9-dien-3-one (7)



MeLi (1.6 M in Et₂O, 3.5 mL, 5.63 mmol, 1.1 equiv.) was added dropwise to a solution of bromo alcohol (9) (906 mg, 5.12 mmol, 1.0 equiv.) in dry Et₂O (37 mL) at -78 °C. The solution was stirred at -78 °C for 30 min. At this point tBuLi (1.9 M in pentane, 5.9 mL, 11.3 mmol, 2.2 equiv.) was added dropwise over the course of 1 h. The slightly yellow solution was stirred at -78 °C for 5 h before ketone (8) (861 mg, 6.14 mmol, 1.2 equiv.) was added over 1 h, and the resulting mixture was allowed to warm to r.t. overnight. MeOH (1 mL) was added and the resulting heterogeneous mixture was poured into a mixture of Na/K tetrates solution and EtOAc (50 mL each). The phases were separated and the aqueous phase was extracted with EtOAc (3x, 50 mL). The combined organic layers were washed with brine (50 mL), dried over Na₂SO₄ and concentrated under reduced pressure. The crude mixture was purified *via* column chromatography (PE:EtOAc = 4:1), affording desired diol (136) as a yellow oil (704 mg, 2.95 mmol, 58%). The product was directly used in the subsequent step without detailed characterization.

IBX (1.24 g, 4.44 mmol, 1.5 equiv.) was added in one portion to a solution of diol (136) (0.70 g, 2.96 mmol, 1.0 equiv.) in a 1:1 mixture of CH₂Cl₂/DMSO (26 mL) at r.t.. The reaction was stirred at r.t. for 2 h, then poured into water (30 mL). The phases were separated and the aqueous layer was extracted with CH₂Cl₂ (5x, 25 mL). The combined organic layers were washed with brine (50 mL), dried over Na₂SO₄ and concentrated *under reduced pressure*. The crude product was subjected to column chromatography (PE:EtOAc = 9:1) to afford the desired trienone (7) (0.59 g, 2.48 mmol, 84%) as a yellow oil.

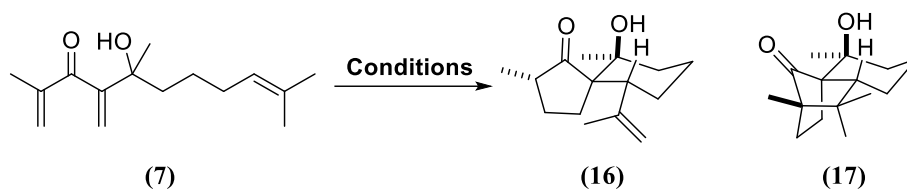
R_f (PE:EtOAc = 4:1; KMnO₄) = 0.46;

¹H NMR (400 MHz, CDCl₃): δ(ppm) = 5.88–5.81 (m, 2H), 5.78 (s, 1H), 5.59 (s, 1H), 5.13–5.04 (m, 1H), 3.50 (bs, 1H), 2.00–1.80 (m, 2H), 1.90 (s, 3H), 1.72–1.70 (m, 1H), 1.67 (s, 3H), 1.62–1.59 (m, 1H), 1.57 (s, 3H), 1.38 (s, 3H), 1.36–1.26 (m, 2H);

¹³C NMR (101 MHz, CDCl₃): δ(ppm) = 201.9, 151.7, 144.7, 131.9, 128.0, 124.5, 122.7, 74.8, 41.4, 28.4, 27.0, 25.8, 24.7, 18.1, 17.8;

HRMS(ESI): Calcd for C₁₅H₂₄O₂Na [M+Na]⁺: 259.1674; found: 259.1679.

Table E1 – Initial Lewis acid screening for cyclization of (7).



Entry	Lewis acid	Conditions	Conc. (M)	Procedure	Product (Yield ^[a])
1	B(C ₆ F ₅) ₃ ·H ₂ O (2.5 mol%)	CH ₂ Cl ₂ , 30 °C, 8.5 h	0.02	A	(16) (77%)
2	FeCl ₃ (1.0 equiv.)	CH ₂ Cl ₂ , -30 °C to 30 °C, 2 d	0.02	A	complex mixture
3	BF ₃ ·OEt ₂ (1.1 equiv.)	CH ₂ Cl ₂ , -78 °C to -50 °C, 2 d	0.02	B	complex mixture
4	SnCl ₄ (1.1 equiv.)	CH ₂ Cl ₂ , -78 °C to 0 °C, 2 h	0.02	B	(16) (25%), (17) (19%)
5	TiCl ₄ (1.1 equiv.)	CH ₂ Cl ₂ , -78 °C, 0.5 h	0.01	B	decomposition
6	BCl ₃ (1.1 equiv.)	CH ₂ Cl ₂ , -78 °C, 1 d	0.01	B	complex mixture
7	AlCl ₃ (1.1 equiv.)	CH ₂ Cl ₂ , -78 °C, 1 d	0.01	A	no reaction ^[b]

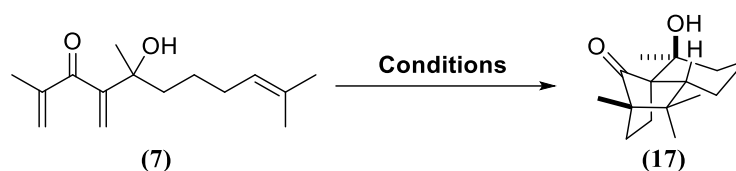
[a] Isolated yield. [b] TLC indicated full conversion of starting material, but after workup only starting material could be identified by NMR spectroscopy.

General procedure A (for Lewis acids handled as solids)

The Lewis acid (equiv. alents given in Table E1) was added in one portion to a stirred solution (concentration in Table E1) of (7) (200 μmol to 300 μmol) in the given solvent at the stated temperature. Reaction progress was monitored by TLC and the solvent was removed under reduced pressure as soon as full conversion of starting material was observed. The resulting crude product was directly purified by column chromatography (PE:EtOAc = 12:1).

General procedure B (for Lewis acids handled as liquids/solutions)

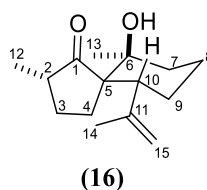
The Lewis acid (equiv. alents given in Table E1) was added dropwise to a stirred solution (concentration in Table E1) of substrate (7) (200 μmol to 300 μmol) in the given solvent at the stated temperature. Reaction progress was monitored by TLC and the reaction was quenched by addition of water as soon as full conversion of starting material was observed. The phases were separated, the aqueous phase extracted three times with CH₂Cl₂. The combined organic layers were dried over Na₂SO₄, filtered and concentrated under reduced pressure. The crude products were purified by column chromatography (usually eluent mixtures of PE:EtOAc = 99:1).

Table E2. Optimization for cyclization of (7) to tricycle (17).

Entry	Lewis acid	Conditions	Conc. (M)	Procedure	Product (Yield) ^[a]
1	SnCl ₄ (10 mol%)	CH ₂ Cl ₂ , -78 °C to 0 °C, 4 d	0.01	B	(16) (21%), (17) (15%), (7) (36%)
2	SnCl ₄ (30 mol%) ^[b]	CH ₂ Cl ₂ , -78 °C to 0 °C, 6 h	0.01	B	(16) (43%), (17) (1%)
3	SnCl ₄ (20 mol%)	CH ₂ Cl ₂ , -78 °C to 0 °C, 2 d	0.01	B	(16) (26%), (17) (<5%)
4	SnCl ₄ (1.1 equiv.)	CHCl ₃ , -78 °C to 0 °C, 4 h	0.01	B	(16) (37%), (17) (<5%)
5	SnCl ₄ (1.1 equiv.)	THF, -78 °C to rt, 2 d	0.01	B	no reaction
6	SnCl ₄ (1.1 equiv.)	Et ₂ O, -78 °C to rt, 2 d	0.01	B	uncharacterized product mixture
7	SnCl ₄ (1.1 equiv.)	toluene, -78 °C to 0 °C, 2.5 h	0.01	B	(16) (45%)

[a] Isolated yield. [b] 0.1 equiv. were added every two hours.

Spiro ketone (16)



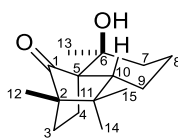
R_f (PE:EtOAc = 12:1; vanillin) = 0.44 (dark purple);

¹H NMR (500 MHz, CDCl₃): δ(ppm) = 4.93–4.91 (m, 1H, H-15), 4.73–4.70 (m, 1H, H-15), 4.56–4.54 (bs, 1H, OH), 2.94 (dd, *J* = 12.9, 2.7 Hz, 1H, H-10), 2.18–2.03 (m, 3H, H-{2,3,4}), 1.88–1.77 (m, 1H, H-8), 1.73–1.68 (m, 1H, H-3), 1.59 (s, 3H, H-14), 1.54–1.41 (m, 5H, H-{7,8,9}), 1.41–1.27 (m, 1H, H-4), 1.03 (d, 3H, *J* = 6.5 Hz, H-12), 1.01 (s, 3H, H-13);

¹³C NMR (126 MHz, CDCl₃): δ(ppm) = 229.6 (C-1), 147.1 (C-11), 114.5 (C-15), 74.4 (C-6), 58.4 (C-5), 46.3 (C-10), 45.7 (C-2), 35.1 (C-7), 28.8 (C-4), 27.62 (C-9), 27.57 (C-13), 25.7 (C-3), 25.0 (C-14), 21.1 (C-8), 13.0 (C-12);

HRMS(ESI): Calcd for C₁₅H₂₄O₂Na [M+Na]⁺: 259.1674; found: 259.1674.

Tricyclic ketone (**17**)



(17)

R_f (PE:EtOAc = 12:1; vanillin) = 0.40 (dark blue);

$^1\text{H NMR}$ (600 MHz, CDCl_3): δ (ppm) = 2.64 (bs, 1H, OH), 2.01 (m, 1H, H-10), 1.92 – 1.83 (m, 2H, H-{3,4}), 1.66 – 1.46 (m, 6H, H-{4,7,8,9}), 1.38 – 1.31 (m, 1H, H-3), 1.28 (s, 3H, H-13), 1.11 – 1.04 (m, 1H, H-7), 0.91 (s, 3H, H-14), 0.83 (s, 3H, H-15), 0.82 (s, 3H, H-12);

$^{13}\text{C NMR}$ (151 MHz, CDCl_3): δ (ppm) = 219.6 (C-1), 71.2 (C-6), 53.1 (C-5), 49.7 (C-2), 43.7 (C-10), 35.5 (C-7), 35.1 (C-11), 29.7 (C-15), 27.3 (C-3), 26.3 (C-13), 21.9 (C-8), 19.7 (C-9), 19.0 (C-4), 18.0 (C-14), 10.5 (C-12);

For the determination of the relative stereochemistry the NMR spectra were measured in C_6D_6 :

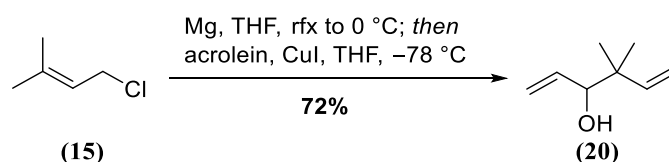
$^1\text{H NMR}$ (500 MHz, C_6D_6): δ (ppm) = 2.76 (bs, 1H, OH), 2.09 (ddd, J = 12.8, 3.9, 2.0 Hz, 1H, H-10), 1.76 (qt, J = 13.3, 4.3 Hz, 1H, H-8), 1.54 – 1.30 (m, 5H, H-{3,4,7,8,9}), 1.27 – 1.23 (m, 1H, H-4), 1.26 (s, 3H, H-13), 1.13 (dd, J = 12.9, 4.0 Hz, 1H, H-9), 1.01 – 0.95 (m, 1H, H-3), 0.88 – 0.81 (m, 1H, H-7), 0.77 (s, 3H, H-12), 0.68 (s, 3H, H-15), 0.61 (s, 3H, H-14);

$^{13}\text{C NMR}$ (126 MHz, C_6D_6): δ (ppm) = 217.9 (C-1), 70.7 (C-6), 53.1 (C-5), 49.5 (C-2), 43.9 (C-10), 35.8 (C-7), 34.9 (C-11), 29.5 (C-15), 27.3 (C-3), 26.3 (C-13), 22.2 (C-8), 19.7 (C-9), 18.9 (C-4), 17.7 (C-14), 10.6 (C-12);

HRMS(ESI): Calcd for $\text{C}_{15}\text{H}_{24}\text{O}_2\text{Na}$ $[\text{M}+\text{Na}]^+$: 259.1674; found: 259.1681.

PART 1: the elongated aldehydic precursor

3,4,4-trimethylhexa-1,5-dien-3-ol (**20**)



Mg turnings (1.50 g, 39.4 mmol, 4.5 equiv.) were suspended in 6.5 mL of dry THF. Some drops of prenyl chloride (**15**) (1.6 mL, 13.1 mmol, 1.5 equiv.) 1 M solution in THF were added and the suspension was refluxed until it became slightly dark (approx. 30 min). At this point, 11 mL of THF were added and the mixture was cooled to 0 °C. The remaining prenyl chloride (**15**) solution was added over the course of 2 h. After no starting material was detected through TLC (1 h), the mixture was warmed to r.t.. The freshly prepared prenyl magnesium chloride solution was slowly added (1 h) to a solution of CuI (83.0 mg, 0.44 mmol, 5.0 mol%) and acrolein (584 μ L, 8.75 mmol, 1.0 equiv.) in dry THF (32 mL) previously cooled to -78 °C. The reaction was stirred at -78 °C for 3 h, then quenched with 50 mL of a 9:1 mixture of NH₄Cl and NH₄OH. The layers were separated, and the aqueous phase was extracted with Et₂O (3x, 50 mL). The combined organic layers were dried over Na₂SO₄ and concentrated under reduced pressure. The crude product was subject to column chromatography (PE:EtOAc = 12:1) to afford desired alcohol (**20**) (936 mg, 7.42 mmol, 85%) as a light yellow oil.

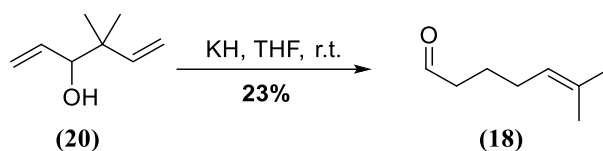
R_f (CH₂Cl₂; KMnO₄) = 0.33;

¹H NMR (400 MHz, CDCl₃): δ (ppm) = 5.94 – 5.80 (m, 2H), 5.25 (dt, J = 17.2, 1.5 Hz, 1H), 5.20 (ddd, J = 10.5, 1.8, 1.1 Hz, 1H), 5.12 (dd, J = 10.8, 1.4 Hz, 1H), 5.08 (dd, J = 17.5, 1.4 Hz, 1H), 3.80 (dt, J = 6.5, 1.2 Hz, 1H), 1.60 (bs, 1H), 1.03 (s, 3H), 1.01 (s, 3H);

¹³C NMR (101 MHz, CDCl₃): δ (ppm) = 145.0, 137.3, 117.0, 114.0, 79.6, 41.5, 23.7, 21.9;

HRMS(ESI): Calcd for C₈H₁₄ONa [M+Na]⁺: 149.0942; found: 149.0945.

6-methylhept-5-enal (**18**)



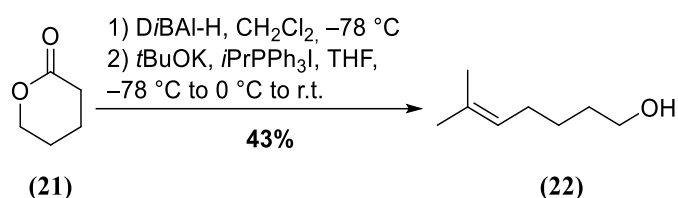
A solution of alcohol (**20**) (936 mg, 7.42 mmol, 1.0 equiv.) in dry THF (30 mL) was added dropwise to a suspension of KH (25-35% in mineral oil, 2.48 g, 18.5 mmol, 2.5 equiv.) (washed 3x with dry *n*-hexane to remove mineral oil) in dry THF (60 mL). The dark orange solution was stirred at r.t. for 24 h; it was quenched with 50 mL of phosphate buffer (pH 7). The layers were separated and the aqueous phase was extracted with Et₂O (3x, 50 mL). The combined organic layers were washed with brine (50 mL), dried over Na₂SO₄ and concentrated under reduced pressure. Column chromatography on silica gel (CH₂Cl₂) afforded aldehyde (**18**) as a colourless oil (219 mg, 1.74 mmol, 23%), whose analytical data match the reported ones.¹²

R_f (CH₂Cl₂; KMnO₄) = 0.55;

¹H NMR (400 MHz, CDCl₃): δ (ppm) = 9.75 (t, J = 1.8 Hz, 1H), 5.08 (t, J = 7.3 Hz, 1H), 2.41 (td, J = 7.3, 1.8 Hz, 2H), 2.03 (q, J = 7.3 Hz, 2H), 1.71 – 1.65 (m, 5H), 1.59 (s, 3H).

¹² Angew. Chem. Int. Ed. **2022**, *61*, e202114235.

6-methylhept-5-en-1-ol (**22**)



(**22**) was prepared after a modification of the protocol by Magauer and coworkers:¹³

DiBAL-H (1 M in hexanes, 24 mL, 24.0 mmol, 1.2 equiv.) was added over a period of 20 min to a solution of δ -valerolactone (**21**) (2.00 g, 20.0 mmol, 1.0 equiv.) in dry CH₂Cl₂ (2.0 mL) under Ar atmosphere. The solution was stirred for 40 min, then quenched with ethyl acetate (5 mL), followed by addition of Na/K tartrate (5 mL). The biphasic mixture was allowed to warm to room temperature. In order to achieve clear phase separation, the mixture was transferred into an Erlenmeyer flask containing a 1:1 mixture of Na/K tartrate and CH₂Cl₂ (50 mL each). After 2h under vigorous stirring, the layers were separated and the aqueous phase extracted with CH₂Cl₂ (3x, 50 mL). The combined organic phases were dried over Na₂SO₄, filtered and concentrated at reduced pressure. The obtained δ -valerolactol was used in the next step without further purification.

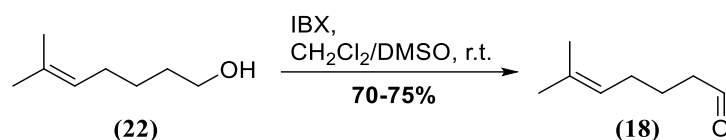
*t*BuOK (2.58 g, 23.0 mmol, 1.15 equiv.) was added to a suspension of isopropyltriphenylphosphonium iodide (9.08 g, 21.0 mmol, 1.05 equiv.) in THF (40 mL) at -78 °C. After 5 min, the mixture was transferred to an ice bath and stirred for further 30 min. A solution of the crude lactol in THF (10 mL) was added dropwise; upon addition the mixture's colour changed from dark red to yellow. After removal of the ice bath, the reaction was stirred at r.t. for 24 h. Water (50 mL) was added; the phases were separated and the aqueous phase was extracted with Et₂O (3x, 75 mL). The combined organic layers were dried over Na₂SO₄, filtered and concentrated at reduced pressure. (**22**) (1.11 g, 8.67 mmol, 43% o2s) was obtained as a pale yellow oil after column chromatography (PE:EA = 4:1). The analytical data match the reported ones.¹³

R_f (PE:EtOAc = 4:1; KMnO₄) = 0.22;

¹H NMR (400 MHz, CDCl₃): δ (ppm) = 5.11 (tt, J = 7.1, 1.3 Hz, 1H), 3.64 (t, J = 6.6 Hz, 2H), 2.00 (q, J = 7.2, 2H), 1.69 (s, 3H), 1.61 (s, 3H), 1.59 – 1.53 (m, 2H), 1.46 – 1.35 (m, 2H).

¹³ *Org. Lett.* **2015**, *17*, 1982–1985.

6-methylhept-5-enal (**18**)

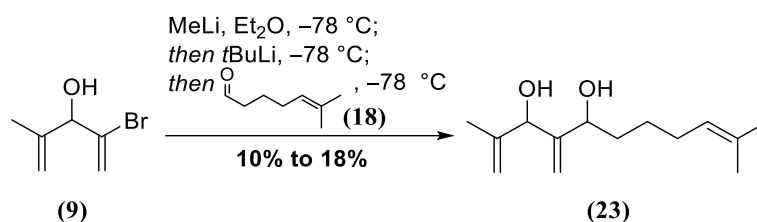


IBX (2.91 g, 10.4 mmol, 1.2 equiv.) was added in one portion to a solution of 6-methylhept-5-en-1-ol (**22**) (1.11 g, 8.62 mmol, 1.0 equiv.) in a 1:1 mixture of CH₂Cl₂/DMSO (74.0 mL). The mixture was stirred at r.t. for 2h, then water (50 mL) was added. The phases were separated and the aqueous phase extracted with CH₂Cl₂ (5x, 50 mL). The combined organic phases were dried over Na₂SO₄, filtered and concentrated at reduced pressure. Crude aldehyde (**18**) was passed over a pad of silica gel and flushed with CH₂Cl₂. After careful evaporation at low temperature due to the volatility of the compound, aldehyde (**18**) was obtained as a colourless oil, used for the next step without further purification. The analytical data match the reported ones.¹²

R_f (PE:EtOAc = 4:1; KMnO₄) = 0.48;

¹H NMR (400 MHz, CDCl₃): δ (ppm) = 9.75 (t, J = 1.8 Hz, 1H), 5.08 (t, J = 7.3 Hz, 1H), 2.41 (td, J = 7.3, 1.8 Hz, 2H), 2.03 (q, J = 7.3 Hz, 2H), 1.71 – 1.65 (m, 5H), 1.59 (s, 3H).

2,10-dimethyl-4-methyleneundeca-1,9-diene-3,5-diol (**23**)



MeLi (1.6 M in Et₂O, 4.9 mL, 7.9 mmol, 1.1 equiv.) was added dropwise to a solution of bromo alcohol (**9**) (1.27 g, 7.18 mmol, 1.0 equiv.) in dry Et₂O (51 mL) at -78 °C. The solution was stirred at -78 °C for 30 min. At this point *t*BuLi (1.9 M in pentane, 8.3 mL, 15.8 mmol, 2.2 equiv.) was added dropwise over the course of 1 h. The slightly yellow solution was stirred at -78 °C for 4 h before half of the solution was added to half of the impure aldehyde (**18**) from the previous reaction (4.31 mmol) previously dissolved in dry Et₂O (1.3 mL) and cooled to -78 °C (Batch 1). Addition took roughly 1 h. A solution of impure aldehyde (**18**) in dry Et₂O (1.3 mL) was added dropwise to the remaining lithiate (Batch 2). Both batches were stirred for 1 h at -78 °C. MeOH (1 mL) was added and the resulting heterogeneous mixtures were poured into a mixture of Na/K tartrate solution and EtOAc (25 mL each). The phases were separated and the aqueous phase was extracted with EtOAc (3x, 25 mL). The combined organic layers were washed with brine (25 mL), dried over Na₂SO₄ and concentrated under reduced pressure. The crude mixtures were purified *via* column chromatography (PE:EtOAc = 99:1 to 4:1 in gradient), affording desired diol (**23**) as a yellow oil (Batch 1: 91.9 mg, 0.41 mmol, 10% o2s; batch 2: 186 mg, 0.83 mmol, 18% o2s).

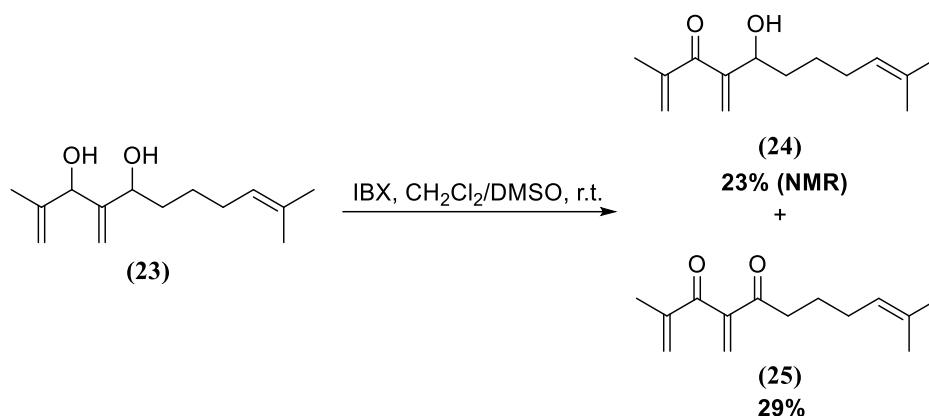
R_f (PE:EtOAc = 9:1; vanillin) = 0.38 (blue-grey);

¹H NMR (400 MHz, CDCl₃): δ(ppm) = 5.21 (d, *J* = 6.7 Hz, 1H), 5.19 (d, *J* = 6.4 Hz, 1H), 5.15 (s, 1H), 5.11 (t, *J* = 7.3 Hz, 1H), 5.00 (d, *J* = 4.3 Hz, 1H), 4.67 (d, *J* = 7.6 Hz, 1H), 4.17 (t, *J* = 6.6 Hz, 1H), 2.06 – 1.96 (m, 2H), 1.94 (bs, 2H), 1.69 (s, 3H), 1.67 (s, 3H), 1.66 – 1.61 (m, 2H), 1.60 (s, 3H), 1.46 – 1.42 (m, 1H), 1.40 – 1.29 (m, 1H);

¹³C NMR (101 MHz, CDCl₃): δ(ppm) = 150.2 (HMBC), 145.9 (HMBC), 132.0 (HMBC), 124.29, 124.2*, 113.1, 112.5*, 112.1, 111.9*, 77.0, 76.9*, 72.9, 72.6*, 35.6, 35.0*, 27.7, 26.1, 25.9*, 25.7, 18.6, 18.4*, 17.7;

HRMS(ESI): Calcd for C₁₄H₂₄NaO₂ [M+Na]⁺: 247.1674; found: 247.1664.

5-hydroxy-2,10-dimethyl-4-methyleneundeca-1,9-dien-3-one (**24**)



IBX (162 mg, 0.58 mmol, 0.95 equiv.) was added in one portion to a solution of diol (**23**) (137 g, 0.61 mmol, 1.0 equiv.) in a 1:1 mixture of CH₂Cl₂/DMSO (5.4 mL) at r.t.. The reaction was stirred at r.t. for 3.5 h, then poured into water (5 mL). The phases were separated and the aqueous layer was extracted with CH₂Cl₂ (5x, 5 mL). The combined organic layers were washed with brine (15 mL), dried over Na₂SO₄ and concentrated under reduced pressure. The crude product was subjected to column chromatography (PE:EtOAc = 10:1) to afford impure desired trienone (**24**) (58.0 mg, 0.26 mmol, 23% estimated *via* NMR) as a yellow oil, as well as dioxidized compound (**25**) (39.1 mg, 0.18 mmol, 29%). Impure trienone (**24**) was used in the next step without further purification and detailed characterization.

(24):

R_f (PE:EtOAc = 3:1; KMnO₄) = 0.39;

¹H NMR (400 MHz, CDCl₃): δ(ppm) = 5.86 (s, 1H), 5.82 (s, 1H), 5.75 (s, 1H), 5.70 (s, 1H), 5.09 (t, *J* = 6.0 Hz, 1H), 4.44 (t, *J* = 7.4 Hz, 1H), 2.80 (bs, 1H), 2.00 (t, *J* = 6.0 Hz, 2H), 1.96 (s, 3H), 1.69 (s, 3H), 1.66 – 1.61 (m, 2H), 1.59 (s, 3H), 1.56 – 1.45 (m, 1H), 1.44 – 1.33 (m, 1H);

HRMS(ESI): Calcd for C₁₄H₂₂O₂Na [M+Na]⁺: 245.1517; found: 245.1522.

(25):

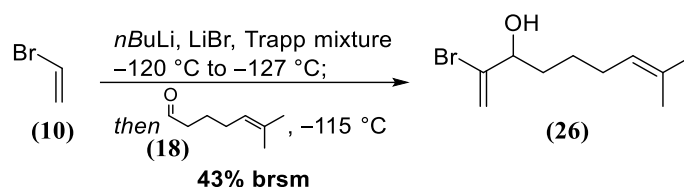
R_f (PE:EtOAc = 3:1; KMnO₄) = 0.49;

¹H NMR (400 MHz, CDCl₃): δ(ppm) = 6.36 (s, 1H), 5.95 (s, 1H), 5.85 (s, 1H), 5.80 (s, 1H), 5.07 (t, *J* = 7.2 Hz, 1H), 2.63 (t, *J* = 7.3 Hz, 2H), 2.03 – 1.98 (m, 2H), 1.97 (s, 3H), 1.68 (s, 3H), 1.68 – 1.61 (m, 2H), 1.58 (s, 3H);

¹³C NMR (101 MHz, CDCl₃): δ(ppm) = 199.3 (HMBC), 197.3 (HMBC), 148.2 (HMBC), 144.9 (HMBC), 132.6, 129.1, 127.6, 123.5, 38.9, 27.2, 25.7, 23.9, 17.7, 17.0.

HRMS(ESI): Calcd for C₁₄H₂₀NaO₂ [M+Na]⁺: 243.1361; found: 243.1359.

2-bromo-8-methylnona-1,7-dien-3-ol (**26**)



A solution of vinyl bromide¹⁴ (**10**) (786 μL , 11.2 mmol, 1.9 equiv.) and LiBr (250 mg, 2.88 mmol, 0.5 equiv.)¹⁵ in Trapp mixture (THF:Et₂O:*n*-pentane = 4:1:1, 10 mL) was placed in a three-neck round-bottom flask equipped with an internal thermometer, a mechanical stirrer with argon inlet and a rubber septum. This flask will be further referred to as "main flask". A Schlenk flask, further referred to as "side flask", was filled with Trapp mixture (7.5 mL) and both flasks were cooled to $-78\text{ }^\circ\text{C}$.¹⁶ $n\text{BuLi}$ (2.5 M in hexanes, 3.2 mL, 8.06 mmol, 1.5 equiv.) was added to the side flask and the solution was mixed by gently shaking the flask outside the cooling bath for approx. 30 s. Both solutions were cooled to $-120\text{ }^\circ\text{C}$ and the $n\text{BuLi}$ solution was added dropwise to the main flask. The the rate of liquid nitrogen addition was increased until a solid bridge of frozen *n*-pentane had formed between the liquid nitrogen vessel and the main flask. This resulted in a decrease of reaction temperature to $-127\text{ }^\circ\text{C}$. The addition of nitrogen was stopped until the majority of frozen coolant had molten and stirring of the cloudy reaction mixture was continued for a total of 2 h, during which time the reaction temperature was maintained between -115 and $-112\text{ }^\circ\text{C}$. Aldehyde (**18**) (729 mg, 5.76 mmol, 1.0 equiv.) and Trapp mixture (2.5 mL) were placed inside the side flask and the solution was cooled to $-115\text{ }^\circ\text{C}$. The solution was then added dropwise to the reaction mixture while the temperature was maintained around $-112\text{ }^\circ\text{C}$. After complete addition, stirring was continued at -115 to $-112\text{ }^\circ\text{C}$ for 2 h, before a solution of acetic acid (4.4 mL, 4.60 mmol, 0.8 equiv.) in Trapp mixture (2.5 mL) was added at $-120\text{ }^\circ\text{C}$ over the course of 20 min. The mixture was allowed to warm to r.t., it was washed with NaHCO_3 (5%, 10 mL) and the aqueous layer extracted with Et₂O (3x, 10 mL). The combined organic layers were washed with brine (7.5 mL), dried over MgSO_4 , filtered and concentrated under reduced pressure. The resulting crude product was subject to column chromatography (PE:EA = 10:1) to afford bromo alcohol (**26**) (467 mg, 2.00 mmol, 43% brsm).

R_f (PE:EtOAc = 4:1, KMnO_4) = 0.49;

¹H-NMR (400 MHz, CDCl_3): δ (ppm) = 5.87 – 5.86 (m, 1H), 5.55 (d, J = 1.9 Hz, 1H), 5.10 (t, J = 7.2 Hz, 1H), 4.08 (q, J = 6.3 Hz, 1H), 2.01 (q, J = 7.3 Hz, 2H), 1.86 (d, J = 6.0 Hz, 1H), 1.69 (s, 3H), 1.67 – 1.62 (m, 2H), 1.60 (s, 3H), 1.44 – 1.30 (m, 2H);

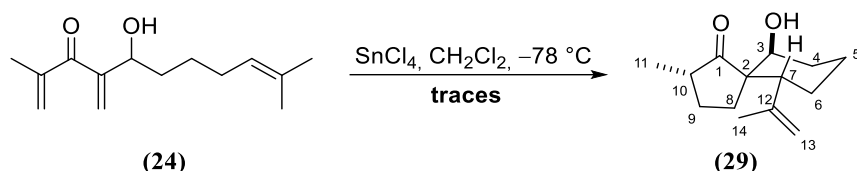
¹³C-NMR (101 MHz, CDCl_3): δ (ppm) = 137.9 (HMBC), 132.5 (HMBC), 124.2, 117.1, 76.2, 35.1, 27.8, 25.9, 25.6, 17.9.

¹⁴ Vinyl bromide was dried by passing through a nitrogen flushed column filled with anhydrous CaCl_2 and the gas condensed into a Schlenk tube at $-78\text{ }^\circ\text{C}$.

¹⁵ Prior to use, LiBr was molten over a Bunsen burner and poured directly into the empty reaction flask, where it was allowed to return to r.t. under a constant nitrogen stream.

¹⁶ *n*-Pentane/liquid nitrogen was used as cooling mixture. Controlled cooling was achieved by pouring the liquid nitrogen into a glass tube that was immersed in the pentane.

Spiroketone (29)



SnCl₄ (1 M in CH₂Cl₂, 1.1 mL, 0.29 mmol, 1.1 equiv.) was added dropwise to a solution of impure trienone (**24**) (58 mg, 0.26 mmol, 1.0 equiv.) in dry CH₂Cl₂ (25 mL) at -78 °C; after complete addition the mixture was stirred at 0 °C for 2 h. Water was added (20 mL), the phases were separated and the aqueous phase extracted with CH₂Cl₂ (3x, 25 mL). The combined organic layers were dried over Na₂SO₄ and concentrated under reduced pressure. The black oily crude was purified *via* column chromatography on silica gel (PE:EA = 12:1) to afford traces of spirocycle (**29**).

R_f (PE:EtOAc = 4:1; vanillin) = 0.48 (pink);

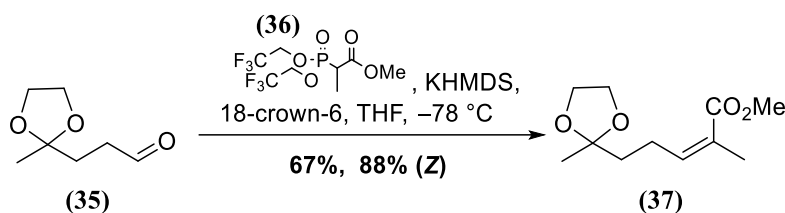
¹H NMR (400 MHz, CDCl₃): δ(ppm) = 4.90 (s, 1H, H-13a), 4.73 – 4.68 (m, 1H, H-13b), 4.23 (bs, 1H, OH), 3.67 (t, *J* = 2.8 Hz, 1H, H-3), 2.83 (dd, *J* = 12.7, 3.0 Hz, 1H, H-7), 2.19 – 2.03 (m, 3H, H-{10, 5a, 9a}), 1.92 – 1.65 (m, 3H-{4a, 5b, 9b}), 1.60 (s, 3H, H-14), 1.55 – 1.42 (m, 3H-{4b, 6}), 1.43 – 1.30 (m, 2H, H-8), 1.07 (d, *J* = 6.5 Hz, 3H, H-11);

¹³C NMR (101 MHz, CDCl₃): δ(ppm) = 228.4 (C-1, HMBC), 147.2 (C-12, HMBC), 114.0 (C-13), 69.3 (C-3), 55.2 (C-2, HMBC), 45.6 (C-10), 43.1 (C-7), 27.9 (C-5), 27.7 (C-8), 27.5 (C-4), 26.0 (C-9), 24.6 (C-14), 19.4 (C-6), 14.0 (C-11);

HRMS(ESI): Calcd for C₁₄H₂₂O₂Na [M+Na]⁺: 245.1517; found: 245.1515.

PART 1: the functionalized precursor

Methyl (Z)-2-methyl-5-(2-methyl-1,3-dioxolan-2-yl)pent-2-enoate (**37**)



After a slight modification of the procedure reported by Clausen and coworkers.¹⁷

Methylated Still-Gennari reagent **(36)**¹⁸ (1.83 g, 5.52 mmol, 0.90 equiv.) was dissolved in dry THF (58 mL) together with 18-crown-6 (13.8 g, 52.0 mmol, 8.5 equiv.). The mixture was cooled to $-78\text{ }^{\circ}\text{C}$ and KHMDS (1.0 M in THF, 6.13 mmol, 2.0 equiv.) was added dropwise. The mixture was stirred for 1 h, before a solution of aldehyde **(35)**¹⁹ (884 mg, 6.13 mmol, 1.0 equiv.) in dry THF (5.0 mL) was added dropwise. The mixture was stirred at $-78\text{ }^{\circ}\text{C}$ for 2 h, then quenched with NH_4Cl (50 mL). The layers were separated and the aqueous phase extracted with EtOAc (3x, 100 mL). The combined organic layers were dried over Na_2SO_4 and concentrated under reduced pressure. The crude product was purified *via* column chromatography (PE:EtOAc = 4:1), affording ester **(37)** as a light yellow oil (792 mg, 3.70 mmol, 67%, 88% Z). The diastomeric ratio was determined *via* NMR (see NMR section).

R_f (PE:EtOAc = 4:1; vanillin) = 0.48 (blue);

$^1\text{H NMR}$ (400 MHz, CDCl_3): δ (ppm) = 5.96 (td, J = 7.4, 1.3 Hz, 1H), 3.97–3.91 (m, 4H), 3.73 (s, 3H), 2.59–2.51 (m, 2H), 1.90–1.88 (3H, m), 1.78–1.72 (m, 2H), 1.33 (s, 3H);

$^{13}\text{C NMR}$ (101 MHz, CDCl_3): δ (ppm) = 168.6, 143.1, 127.0, 109.9, 64.8, 51.4, 38.6, 24.7, 24.0, 20.8;

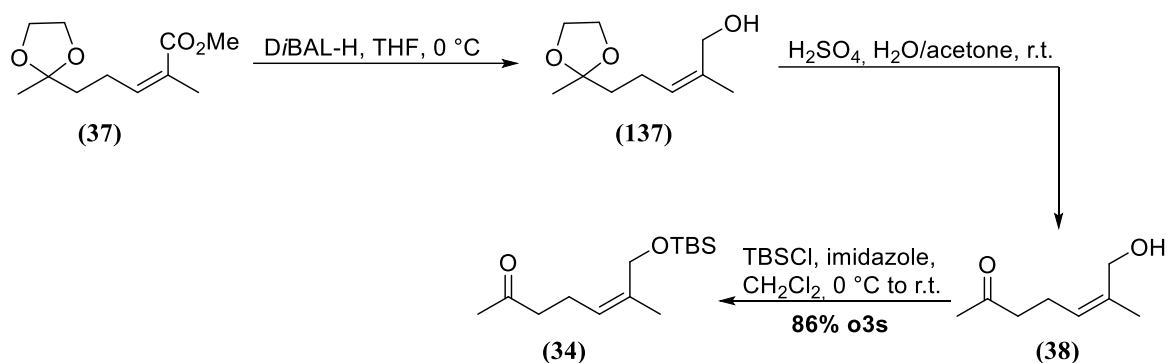
HRMS(ESI): Calcd for $\text{C}_{11}\text{H}_{18}\text{O}_4\text{Na}$ $[\text{M}+\text{Na}]^+$: 237.1103; found: 237.1101.

¹⁷ *J. Med. Chem.* **2013**, *56*, 4071–4081.

¹⁸ Prepared after the same protocol: *J. Med. Chem.* **2013**, *56*, 4071–4081.

¹⁹ Aldehyde **(35)** was prepared according to the procedure reported by Woerpel and coworkers: *Org. Lett.* **2009**, *11*, 507–510.

(Z)-7-((tert-butyldimethylsilyl)oxy)-6-methylhept-5-en-2-one (**34**)



(**137**) was prepared after a modification of the protocol reported by Woerpel and coworkers.¹⁷

DIBAL-H (1 M THF, 12.7 mL, 3.0 equiv.) was added over the course of 15 min to a solution of ester (**37**) (904 mg, 4.22 mmol, 1.0 equiv.) in dry THF (13 mL) at 0 °C. The mixture was stirred at 0 °C for 2.5 h, then it was slowly quenched with EtOAc (2 mL), followed by Na/K tartrate solution (10 mL) and warmed to r.t.. The mixture was transferred to an Erlenmeyer flask, where it was vigorously stirred and diluted with ethyl acetate and Na/K tartrate solution until two distinct layers were formed (ca. 50 mL each). After separation of the layers, the aqueous phase was extracted with ethyl acetate (3x, 75 mL). The combined organic layers were dried over Na₂SO₄ and concentrated under reduced pressure. Crude allylic alcohol (**137**) (787 mg) was used for the next step without purification.

R_f (PE:EtOAc = 7:3; KMnO₄) = 0.14.

(**38**) was prepared after a modification of the protocol reported by Woerpel and coworkers.^[9]

Some drops of concentrated sulfuric acid were added to a solution of ketal (**137**) (779 mg, 4.22 mmol) in a 5:2 acetone/water mixture (42 mL). The reaction was stirred at r.t. for 24 h. It was diluted with CH₂Cl₂ (20 mL) and washed with NaHCO₃ (25 mL). The layers were separated and the aqueous phase was extracted with CH₂Cl₂ (3x, 40 mL). The combined layers were dried over Na₂SO₄ and concentrated under reduced pressure. The crude ketone (**38**) (572 mg) was used for the next step without purification.

R_f (PE:EtOAc = 7:3; KMnO₄) = 0.11.

TBSCl (618 mg, 4.10 mmol, 1.1 equiv.) was added in one portion to a solution of crude allylic alcohol (**38**) (530 mg, 3.73 mmol, 1.0 equiv.) and imidazole (305 mg, 4.47 mmol, 1.2 equiv.) in dry CH₂Cl₂ (14 mL) at 0 °C. The mixture was allowed to warm to r.t. and stirred for 16 h. It was diluted with CH₂Cl₂ and brine. The phases were separated and the aqueous layer was extracted with CH₂Cl₂ (3x, 10 mL). The combined organic layers were dried over Na₂SO₄ and concentrated under reduced pressure. The crude product was purified via column chromatography (PE:EtOAc = 4:1) and afforded desired ketone (**34**) as a light yellow oil (871 mg, 3.39 mmol, 86% o3s).

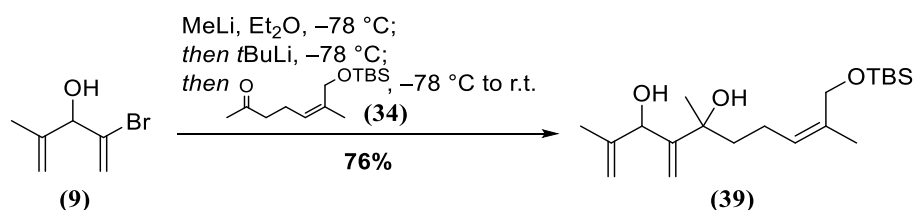
R_f (PE:EtOAc = 7:3; KMnO₄) = 0.61;

¹H NMR (400 MHz, CDCl₃): δ(ppm) = 5.17–5.11 (m, 1H), 4.14 (s, 2H), 2.46 (t, *J* = 7.4 Hz, 2H), 2.29 (q, *J* = 7.2 Hz, 2H), 2.12 (s, 3H), 1.74–1.69 (m, 3H), 0.89 (s, 9H), 0.06 (s, 6H);

¹³C NMR (101 MHz, CDCl₃): δ(ppm) = 208.6, 136.3, 124.6, 61.8, 43.9, 30.1, 26.1, 22.0, 21.3, 18.5, –5.2;

HRMS(ESI): Calcd for C₁₄H₂₈O₂SiNa [M+Na]⁺: 256.1756; found: 256.1758.

(Z)-10-((tert-butyldimethylsilyl)oxy)-2,5,9-trimethyl-4-methylenedeca-1,8-diene-3,5-diol (**39**)



MeLi (1.6 M in Et₂O, 19.0 mL, 30.0 mmol, 1.0 equiv.) was added dropwise to a solution of bromo alcohol (**9**) (5.31 g, 30.0 mmol, 1.0 equiv.) in dry Et₂O (200 mL) at -78 °C. The solution was stirred at -78 °C for 1 h. At this point *t*BuLi (1.9 M in pentane, 32.0 mL, 60.0 mmol, 2.0 equiv.) was added dropwise over the course of 1 h. The slightly yellow solution was stirred at -78 °C for 4 h before ketone (**34**) (4.62 g, 18.0 mmol, 1.0 equiv.) was added dropwise. The resulting mixture was allowed to warm to r.t. overnight. MeOH (10 mL) was added and the resulting heterogeneous mixture was poured into a mixture of Na/K tatrata solution and EtOAc (200 mL each). The phases were separated and the aqueous phase was extracted with EtOAc (3x, 200mL). The combined organic layers were washed with brine (200 mL), dried over Na₂SO₄ and concentrated under reduced pressure. The crude mixture was purified via column chromatography (PE:EtOAc= 9:1 to 4:1, affording the desired diol (**39**) as a yellow oil (4.86 g, 13.7 mmol, 76%).

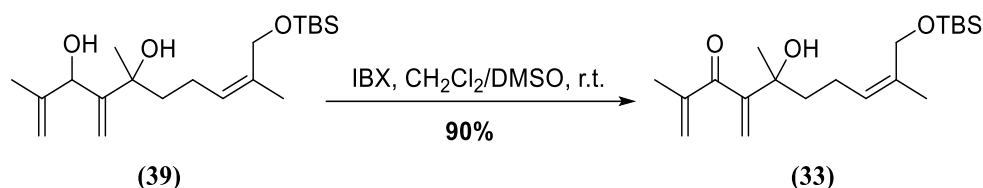
R_f (PE:EtOAc = 4:1, KMnO₄) = 0.44;

¹H NMR (400 MHz, CDCl₃): δ(ppm) = 5.21 (t, *J* = 7.4 Hz, 1H), 5.17 (bs, 1H), 5.14 (d, *J* = 3.3 Hz, 1H), 5.10 (d, *J* = 4.9 Hz, 1H), 5.03 (s, 1H), 4.74 (d, *J* = 11.7 Hz, 1H), 4.14 (s, 2H), 2.52 (bs, 2H), 2.14–2.06 (m, 2H), 1.79–1.66 (m, 2H), 1.73 (s, 3H), 1.71 (s, 3H), 1.39 (d, *J* = 6.4 Hz, 3H), 0.90 (s, 9H), 0.07 (s, 6H);

¹³C NMR (101 MHz, CDCl₃): δ(ppm) = 153.8, 153.3, 146.4, 146.0, 135.2, 135.1, 126.6, 126.6, 112.7, 112.1, 111.9, 111.8, 76.5, 76.3, 75.8, 75.5, 62.0, 61.9, 42.6, 42.3, 29.3, 29.2, 26.1, 22.7, 22.4, 21.4, 19.8, 19.6, 18.6, -5.1;

HRMS(ESI): Calcd for C₂₀H₃₈O₃SiNa [M+Na]⁺: 377.2488; found: 377.2483.

(Z)-10-((tert-butyldimethylsilyl)oxy)-5-hydroxy-2,5,9-trimethyl-4-methylenedeca-1,8-dien-3-one (**33**)



IBX (5.6 mg, 20.1 mmol, 1.5 equiv.) was added in one portion to a solution of diol (**39**) (4.76 g, 13.4 mmol, 1.0 equiv.) in a 1:1 mixture of CH₂Cl₂/DMSO (148 mL) at r.t.. The reaction mixture was stirred at r.t. for 2.5 h, before being poured into water (75 mL). The phases were separated and the aqueous layer was extracted with CH₂Cl₂ (5x, 75 mL). The combined organic layers were washed with brine (50 mL), dried over Na₂SO₄ and concentrated under reduced pressure. The crude product was subjected to column chromatography (PE:EtOAc = 9:1 to 4:1) to afford desired trienone (**33**) (4.13 g, 12.2 mmol, 90%) as a yellow oil.

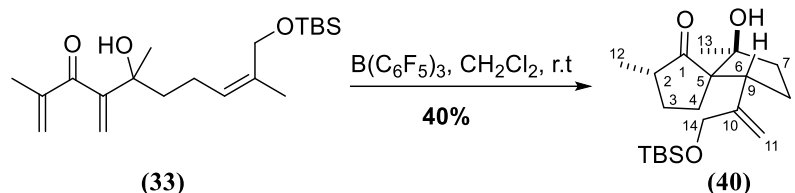
R_f (PE:EtOAc = 4:1 KMnO₄) = 0.62;

¹H-NMR (400 MHz, CDCl₃): δ(ppm) = 5.87 (m, 2H), 5.78 (s, 1H), 5.61 (s, 1H), 5.18 (t, *J* = 7.1 Hz, 1H), 4.14–4.10 (m, 2H), 3.47 (s, 1H), 2.10–2.02 (m, 2H), 1.95 (s, 3H), 1.84–1.74 (m, 1H), 1.72 (s, 3H), 1.69–1.62 (m, 1H), 1.40 (s, 3H), 0.90 (s, 9H), 0.06 (s, 6H);

¹³C-NMR (101MHz, CDCl₃): δ(ppm) = 201.6, 151.6, 144.8, 135.4, 128.0, 126.2, 122.8, 74.7, 61.9, 41.8, 27.2, 26.1, 25.8, 22.7, 21.3, 18.1, -5.1;

HRMS(ESI): Calcd for C₂₀H₃₆O₃SiNa [M+Na]⁺: 375.2331; found: 375.2341

Spiro ketone (40)



$B(C_6F_5)_3$ (150 mg, 0.29 mmol, 2.5 mol%) was added in one portion to a stirred solution of cross-conjugated ketone (33) (4.13 g, 11.7 mmol, 1.0 equiv.) in toluene (688 mL) at r.t. and stirring at this temperature was continued for 72 h. During this time the color changed from slightly yellow to purple. The mixture was concentrated under reduced pressure and subjected to column chromatography (PE:EtOAc = 99:1 to 19:1) to afford spiro ketone (40) (1.65 g, 4.68 mmol, 40%).

R_f (PE:EtOAc = 4:1; vanillin) = 0.48 (purple);

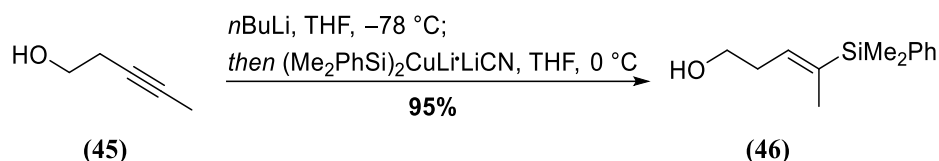
1H -NMR (500 MHz, $CDCl_3$): δ (ppm) = 5.40–5.38 (m, 1H, H-11), 4.99–4.96 (m, 1H, H-11), 4.06 (bs, 1H, OH), 3.87–3.82 (m, 1H, H-14), 3.69–3.63 (m, 1H, H-14), 3.38 (t, J = 9.0 Hz, 1H, H-9), 2.19–2.09 (m, 2H, H-{2,8}), 2.04–1.95 (m, 1H, H-7), 1.93–1.87 (m, 1H, H-8), 1.83–1.69 (m, 3H, H-{7,8}), 1.66–1.60 (m, 1H, H-4), 1.47–1.39 (m, 1H, H-3), 1.18 (s, 3H, H-13), 1.08 (d, J = 6.6 Hz, 3H, H-12), 0.89 (s, 9H, OTBS), 0.03 (s, 3H, OTBS), 0.02 (s, 3H, OTBS);

^{13}C -NMR (126 MHz, $CDCl_3$): δ (ppm) = 228.5 (C-1), 147.1 (C-10), 111.4 (C-11), 85.9 (C-6), 66.2 (C-14), 63.0 (C-5), 48.8 (C-9), 45.7 (C-2), 37.6 (C-7), 28.6 (C-3), 26.1 (C-4), 26.01 (OTBS), 25.7 (C-8), 24.5 (C-13), 18.5 (OTBS), 13.6 (C-12), -5.2 (OTBS), -5.4 (OTBS);

HRMS(ESI): Calcd for $C_{20}H_{36}O_3SiNa$ $[M+Na]^+$: 375.2331; found: 375.2341.

PART 1: the deuterated precursor

(E)-4-(dimethyl(phenyl)silyl)pent-3-en-1-ol (**46**)



The compound was prepared after the protocol reported by Zakarian and coworkers:²⁰

$\text{Me}_2\text{PhSiLi}^{21}$ (0.47 M in THF, 300 mL, 141 mmol, 3.0 equiv.) was added over 30 min to a stirred suspension of CuCN^{22} (6.29 g, 70.3 mmol, 1.5 equiv.) in dry THF (25 mL) in a 1 L Schlenk flask at $0\text{ }^\circ\text{C}$. A second 250 mL Schlenk flask was charged with 3-pentyn-1-ol (**45**) (4.3 mL, 46.8 mmol, 1.0 equiv.) and dry THF (100 mL). The solution was cooled to $-78\text{ }^\circ\text{C}$ and $n\text{BuLi}$ (2.5 M in hexanes, 19.0 mL, 46.8 mmol, 1.0 equiv.) was added over 30 min. After complete addition, both solutions were stirred for 1 h at the stated temperature. The still $-78\text{ }^\circ\text{C}$ cold alkoxide solution was then added to the cuprate solution at $0\text{ }^\circ\text{C}$ over 15 min and stirring at $0\text{ }^\circ\text{C}$ was continued for an additional hour. The reaction mixture was cooled to $-78\text{ }^\circ\text{C}$, NH_4Cl (100 mL) was added, the mixture was diluted with EtOAc and allowed to warm to r.t. The phases were separated, the aqueous phase extracted with EtOAc (3x, 100 mL), combined organic layers washed with brine, dried over Na_2SO_4 and concentrated under reduced pressure. The dark green crude product was purified by column chromatography (PE:EtOAc = 20:1) to afford vinyl silane (**46**) (9.77 g, 44.3 mmol, 95%) as a colorless oil.

R_f (PE:EtOAc = 2:1; vanillin) = 0.65 (blue-grey);

$^1\text{H-NMR}$ (400 MHz, C_6D_6): δ (ppm) = 7.55 – 7.48 (m, 2H), 7.26 – 7.18 (m, 3H), 5.94–5.87 (m, 1H), 3.38 (t, J = 6.7 Hz, 2H), 2.22 (q, J = 6.7 Hz, 2H), 1.65 (s, 3H), 0.93 (bs, 1H), 0.32 (s, 1H);

$^{13}\text{C-NMR}$ (101 MHz, C_6D_6): δ (ppm) = 138.6, 137.8, 137.1, 134.4, 129.3, 128.2, 62.0, 32.5, 15.1, -3.3 ;

HRMS(EI): Calcd for $\text{C}_{12}\text{H}_{17}\text{OSi}$ $[\text{M-Me}]^+$: 205.1049; found: 205.1056.

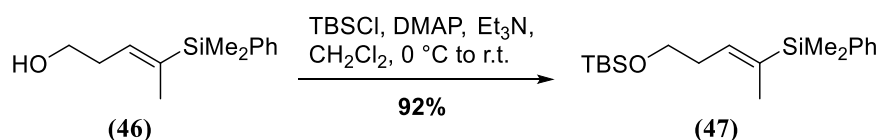
The analytical data are in accordance with the data reported by Zakarian and coworkers.²⁰

²⁰ *J. Am. Chem. Soc.* **2011**, *133*, 10499–10511.

²¹ Me_2PhSiLi was prepared after the protocol of Fleming and coworkers: *J. Chem. Soc. Perkin Trans. 1* **1981**, 2527–2532. For determination of concentration, 0.5 mL of the deep red solution were added to 5 mL of distilled water under stirring at r.t. followed by a few drops of phenolphthalein (0.1% solution in water:EtOH = 1:1) were added. The solution was titrated with HCl (0.05 M) until the pink color vanished. Titration was repeated three times and average concentration determined.

²² CuCN was heated with a heat gun under vacuum prior to use to remove residual water.

O-TBS-(*E*)-4-(dimethyl(phenyl)silyl)pent-3-en-1-ol (**47**)



Et₃N (21.0 mL, 148 mmol, 3.0 equiv.), 4-DMAP (3.01 g, 24.7 mmol, 0.50 equiv.) and TBSCl (9.29 g, 61.7 mmol, 1.3 equiv.) were sequentially added at 0 °C to a stirred solution of alcohol (**46**) (10.9 g, 49.3 mmol, 1.0 equiv.) in dry CH₂Cl₂ (200 mL). Stirring at 0 °C was continued for 2 h, followed by 5.5 h of stirring at r.t. Water was added (150 mL), the phases were separated and the aqueous phase extracted with CH₂Cl₂ (3x, 150 mL). The combined organic layers were washed with brine (300 mL), dried over Na₂SO₄ and the solvent was removed under reduced pressure. After purification by column chromatography (PE:EtOAc = 100:1), TBS-protected alcohol (**47**) (15.2 g, 45.4 mmol, 92%) was obtained as a colorless oil.

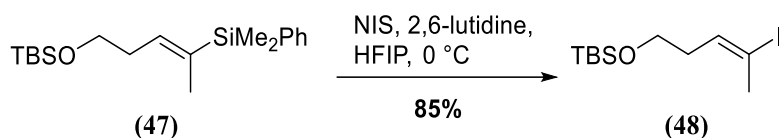
R_f(PE:EtOAc = 100:1; vanillin) = 0.57 (blue-grey);

¹H-NMR (400 MHz, C₆D₆): δ(ppm) = 7.58–7.53 (m, 2H), 7.28–7.18 (m, 3H), 6.04–5.99 (m, 1H), 3.57 (t, *J* = 6.5 Hz, 2H), 2.39–2.33 (m, 2H), 1.71–1.68 (m, 3H), 0.97 (s, 9H), 0.36 (s, 6H), 0.04 (s, 6H);

¹³C-NMR (101 MHz, C₆D₆): δ(ppm) = 138.7, 138.4, 136.3, 134.4, 129.2, 128.1, 62.7, 32.5, 26.1, 18.5, 15.1, -3.2, -5.1;

HRMS(ESI): Calcd for C₁₉H₃₄OSi₂Na [M+Na]⁺: 357.2046; found: 357.2043.

O-TBS-(*E*)-4-iodopent-3-en-1-ol (**48**)



Prepared after a slight modification of the procedure reported by Zakarian and coworkers.²³

NIS (6.82 g, 30.3 mmol, 1.5 equiv.) was added slowly to a well stirred solution of vinyl silane (**47**) (7.00 g, 20.9 mmol, 1.0 equiv.) and 2,6-lutidine (969 μL , 8.37 mmol, 0.40 equiv.) in HFIP (42 mL) at 0 $^\circ\text{C}$. Stirring at 0 $^\circ\text{C}$ was continued for 10 min and the brown reaction mixture was poured into a separatory funnel containing $\text{Na}_2\text{S}_2\text{O}_3$ (50 mL) and CH_2Cl_2 (100 mL). The mixture was shaken until the initially pink color had faded, the phases were separated and the aqueous phase was extracted with CH_2Cl_2 (3x, 100 mL). The combined organic layers were washed with brine (250 mL), dried over Na_2SO_4 and concentrated under reduced pressure. After column chromatography (PE:EtOAc = 200:1), vinyl iodide (**48**) (5.80 g, 17.8 mmol, 85%) was obtained as a colorless oil.

R_f (PE; vanillin) = 0.23 (yellow);

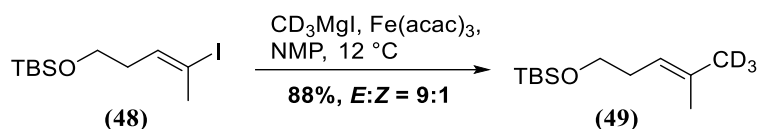
$^1\text{H-NMR}$ (400 MHz, C_6D_6): δ (ppm) = 6.18–6.10 (m, 1H), 3.31 (t, J = 6.5 Hz, 2H), 2.12–2.09 (m, 3H), 1.97–1.91 (m, 2H), 0.94 (s, 9H), 0.01 (s, 6H);

$^{13}\text{C-NMR}$ (101 MHz, C_6D_6): δ (ppm) = 138.1, 95.5, 61.8, 34.3, 27.6, 26.1, 18.4, -5.2;

HRMS(EI): Calcd for $\text{C}_7\text{H}_{14}\text{IOSi}$ [M-tBu] $^+$: 268.9859; found: 268.9865.

²³ *J. Am. Chem. Soc.* **2011**, *133*, 10499–10511.

O-TBS-(*E*)-4-methylpent-3-en-5,5,5-*d*₃-1-ol (**49**)



CD₃I (2.2 mL, 34.5 mmol, 2.0 equiv.) was added dropwise to a stirred suspension of freshly activated magnesium turnings in dry Et₂O (11.5 mL) at 0 °C. Stirring at 0 °C was continued for 1 h, then the grey reaction mixture was stirred at r.t. overnight. A 250 mL Schlenk flask was charged with vinyl iodide (**48**) (5.70 g, 17.5 mmol, 1.0 equiv.), Fe(acac)₃ (1.54 g, 4.37 mmol, 0.25 equiv.) and NMP (85 mL) and the red solution was cooled to 12 °C using a cold water bath. The freshly prepared Grignard solution was added over the course of 30 min and stirring was continued for additional 15 min before NH₄Cl was added and the mixture was allowed to warm to r.t.. After diluting with brine (75 mL), water (75 mL) and EtOAc (100 mL), the phases were separated and the aqueous phase extracted with EtOAc (5x, 150 mL). The combined organic layers were dried over Na₂SO₄ and concentrated under reduced pressure. After purification by column chromatography, (**49**) (3.35 g, 15.5 mmol, 88%, (*E*):(*Z*) = 91:1) was obtained as light yellow oil.

R_f(PE:EtOAc = 100:1; vanillin) = 0.53 (dark purple);

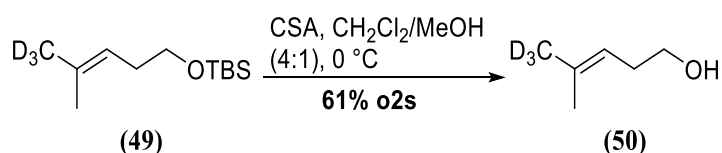
¹H-NMR (400 MHz, CDCl₃): δ(ppm) = 5.11 (t, *J* = 6.6 Hz, 1H), 3.57 (t, *J* = 7.3 Hz, 2H), 2.22 (q, *J* = 7.3 Hz, 2H), 1.69 (s, minor isomer, 3H),²⁴ 1.62 (s, 3H), 0.89 (s, 9H), 0.05 (s, 6H);

¹³C-NMR (101 MHz, CDCl₃): δ(ppm) = 133.5, 120.7, 63.3, 32.1, 26.1, 25.5–24.5 (m, CD₃), 18.5, 17.9, –5.1;

HRMS(EI): Calcd for C₈H₁₄D₃OSi [M-*t*Bu]⁺: 160.1237; found: 160.1239.

²⁴ The methyl signals at 1.69 ppm and 1.62 ppm are the only ones that allow distinction between (*E*)- and (*Z*)-isomer. For all other signals, no difference could be observed in the recorded spectra.

(*E*)-4-Methylpent-3-en-5,5,5-*d*₃-1-ol (**50**)



TBS-protected alcohol (**49**) (3.56 g, 16.4 mmol, 1.0 equiv.) was dissolved in $CH_2Cl_2/MeOH$ (4:1, 80 mL), the solution was cooled to $0\text{ }^\circ\text{C}$ and CSA (457 mg, 1.97 mmol, 0.12 equiv.) was added in one portion. Stirring at $0\text{ }^\circ\text{C}$ was continued for 1 h 15 min and the solution was poured into $NaHCO_3$ (40 mL). The phases were separated, the aqueous phase extracted with CH_2Cl_2 (5x, 50 mL), the combined organic layers washed with brine (150 mL), dried over Na_2SO_4 and concentrated under reduced pressure. Purification by column chromatography (*n*-pentane: Et_2O = 10:1 to 5:1) afforded alcohol (**50**) (64% in Et_2O ,²⁵ 1.82 g, 1.16 mmol, 69%) as a colorless liquid.

R_f (PE: $EtOAc$ = 2:1; vanillin) = 0.46 (dark blue);

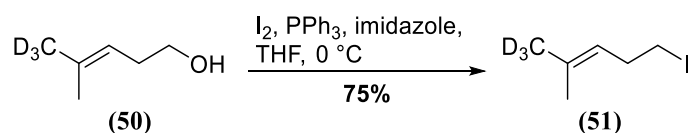
1H -NMR (500 MHz, $CDCl_3$): δ (ppm) = 5.15–5.10 (m, 1H), 3.62 (t, J = 6.6 Hz, 2H), 2.27 (q, J = 6.6 Hz, 2H), 1.73 – 1.72 (m, 3H, (*Z*)-isomer (minor)), 1.66 – 1.64 (m, 3H, (*E*)-isomer (major)), 1.46 (bs, 1H);

^{13}C -NMR (126 MHz, $CDCl_3$): δ (ppm) = 135.3, 120.2, 62.7, 31.7, 25.1 (sep, $J_{C,D}$ = 19.2 Hz), 18.0;

HRMS(EI): Calcd for $C_6H_9D_3O$ [M]⁺: 103.1076; found: 103.1074.

²⁵ The solvent was consciously not removed entirely to avoid substance loss due to the volatility of (**50**). Analytically pure material was obtained after Kugelrohr distillation (100 mbar, $100\text{ }^\circ\text{C}$, ice-cooled receiver) of a small sample.

(*E*)-5-Iodo-2-methylpent-2-ene-1,1,1-*d*₃ (**51**)



Triphenylphosphine (1.91 g, 7.27 mmol, 1.5 equiv.), imidazole (495 mg, 7.27 mmol, 1.5 equiv.) and iodine (1.35 g, 5.33 mmol, 1.1 equiv.) were sequentially added to a stirred solution of alcohol **(50)** (64% in Et₂O, 500 mg, 4.85 mmol, 1.0 equiv.) in dry THF (48 mL) at 0 °C. Stirring at this temperature was continued for 45 min, before Na₂S₂O₃ (40 mL) was added and the mixture was allowed to warm to r.t.. The phases were separated, the aqueous phase extracted with Et₂O (3x, 50 mL), the combined organic layers washed with half-saturated brine (100 mL), dried over Na₂SO₄ and concentrated under reduced pressure. After purification by column chromatography (*n*-pentane:Et₂O = 100:1), iodide **(51)** (777 mg, 3.65 mmol, 75%) was obtained as a colorless oil.

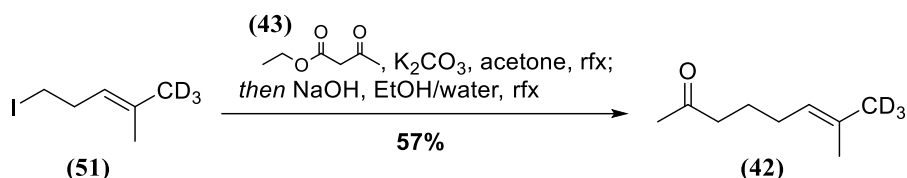
R_f(PE:EtOAc = 100:1; UV, KMnO₄) = 0.60;

¹H-NMR (600 MHz, C₆D₆): δ(ppm) = 4.91–4.87 (m, 1H), 2.70 (t, *J* = 7.3 Hz, 2H), 2.29–2.24 (m, 2H), 1.51–1.50 (m, 3H, (*Z*)-isomer (minor)), 1.34–1.32 (m, 3H (*E*)-isomer (major));

¹³C-NMR (151 MHz, C₆D₆): δ(ppm) = 134.0, 123.6, 32.7, 24.8 (sep, *J*_{C,D} = 19.1 Hz), 17.7, 5.8;

HRMS(EI): Calcd for C₆H₈D₃I [M]⁺: 213.0094; found: 213.0097.

(*E*)-7-methyloct-6-en-2-one-8,8,8-*d*₃ (**42**)



(**42**) was prepared after the protocol by Tiefenbacher and coworkers:²⁶

K₂CO₃ (219 mg, 1.58 mmol, 1.2 equiv.) and iodide (**51**) (281 mg, 1.32 mmol, 1.0 equiv.) were added at r.t. to a stirred solution of ethyl acetoacetate (**43**) (185 μL, 1.45 mmol, 1.1 equiv.) in dry acetone (3.3 mL) and the mixture was stirred under reflux for 16 h. After returning to r.t., solvent was removed under reduced pressure, the residue taken up in EtOH (2.5 mL) and aqueous NaOH (10%, 2.5 mL) was added. The mixture was stirred under reflux for 5 h, allowed to cool to r.t. and extracted with Et₂O (3x, 5 mL). The combined organic layers were dried over Na₂SO₄ and concentrated under reduced pressure. Column chromatography (*n*-pentane:Et₂O = 10:1) afforded methyl ketone (**42**) (107 mg, 0.76 mmol, 57%) as a light yellow oil.

R_f(PE:EtOAc = 7:3; vanillin) = 0.53 (dark turquoise);

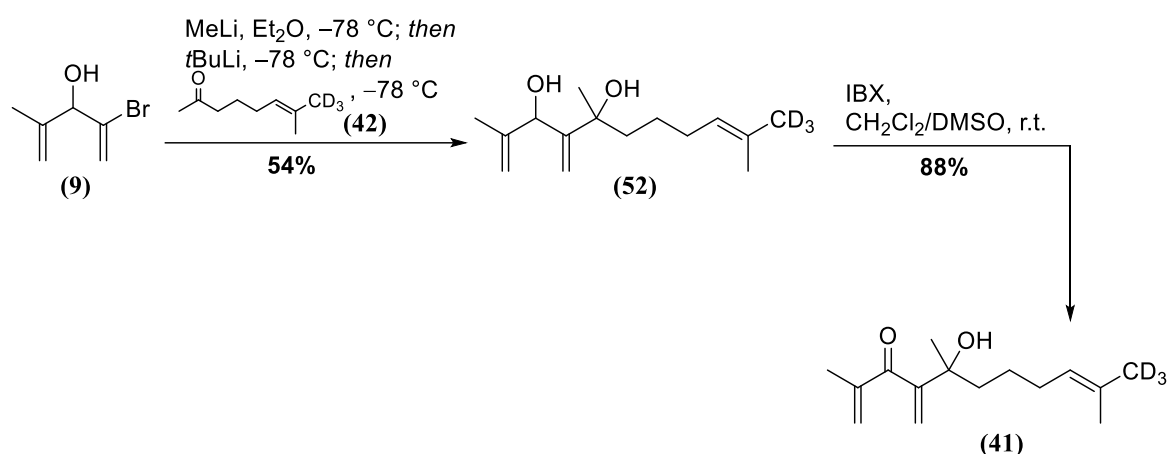
¹H-NMR (600 MHz, CDCl₃): δ(ppm) = 5.07 (t, *J* = 7.2 Hz, 1H), 2.41 (t, *J* = 7.4 Hz, 2H), 2.13 (s, 3H), 1.98 (q, *J* = 7.3 Hz, 2H), 1.66–1.57 (m, 5H);

¹³C-NMR (151 MHz, CDCl₃): δ(ppm) = 209.4, 132.5, 123.8, 43.3, 30.0, 27.5, 25.0 (sep, *J*_{C,D} = 19.2 Hz), 24.1, 17.8;

HRMS(EI): Calcd for C₉H₁₃D₃O [M]⁺: 143.1389; found: 143.1388.

²⁶ *Adv. Synth. Catal.* **2017**, *359*, 1331–1338.

Deuterated cyclization precursor (**41**)



MeLi (1.6 M in Et₂O, 3.5 mL, 2.0 equiv.) was added over 30 min to a stirred solution of bromo alcohol (**9**) (1.00 g, 5.65 mmol, 2.0 equiv.) in dry Et₂O (38 mL) at -78 °C. Stirring at this temperature was continued for 1 h, before tBuLi (1.6 M in pentane, 7.0 mL, 11.3 mmol, 4.0 equiv.) was added over the course of 1 h. The slightly turbid solution was stirred at -78 °C for 4 h and then treated with methyl ketone (**42**) (406 mg, 2.83 mmol, 1.0 equiv.); the addition took 15 min. Stirring at -78 °C was continued for additional 3 h, before NH₄Cl (20 mL) was added, the mixture was allowed to warm to r.t., and diluted with EtOAc. The phases were separated, the aqueous phase extracted with EtOAc (3x, 25 mL) and the combined organic layers were washed with brine (50 mL), dried over Na₂SO₄ and concentrated under reduced pressure. Column chromatography (PE:EtOAc = 10:1 to 5:1) afforded a diastereomeric mixture of diol (**52**) (370 mg, 1.53 mmol, 54%), which was used in the subsequent oxidation without detailed characterization.

Diol (**52**) (85.0 mg, 352 μmol, 1.0 equiv.) was dissolved in CH₂Cl₂/DMSO (1:1, 2.4 mL) and IBX (148 mg, 529 μmol, 1.5 equiv.) was added in one portion at r.t., and the mixture was stirred at this temperature for 2 h. Water (2 mL) was added, the phases separated and the aqueous phase was extracted with CH₂Cl₂ (5x, 3 mL). The combined organic phases were washed with brine (10 mL), dried over Na₂SO₄ and concentrated under reduced pressure. Purification by column chromatography afforded cross-conjugated ketone (**41**) (73.9 mg, 309 μmol, 88%) as a light yellow oil.

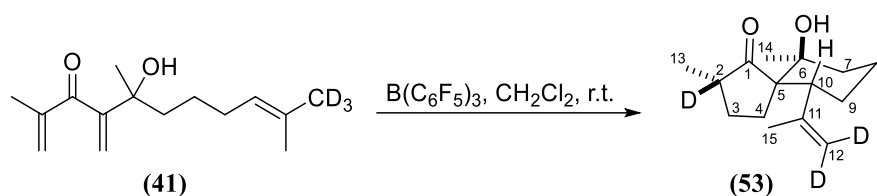
R_f(PE:EtOAc = 5:1; vanillin) = 0.55 (dark blue);

¹H-NMR (600 MHz, CDCl₃): δ(ppm) = 5.85–5.83 (m, 1H), 5.82 (s, 1H), 5.79–5.77 (m, 1H), 5.59 (m, 1H), 5.10–5.05 (m, 1H), 3.45 (bs, 1H), 1.98–1.91 (m, 5H), 1.77–1.70 (m, 1H), 1.68–1.62 (m, 1H), 1.58–1.56 (m, 3H), 1.38 (s, 3H), 1.37–1.25 (m, 2H);

¹³C-NMR (151 MHz, CDCl₃): δ(ppm) = 201.8, 151.7, 144.7, 131.7, 128.0, 124.5, 122.7, 74.8, 41.4, 28.3, 27.0, 25.0 (sep, J_{C,D} = 18.9 Hz), 24.7, 18.1, 17.8;

HRMS(ESI): Calcd for C₁₅H₂₁D₃O₂Na [M+Na]⁺: 262.1862; found: 262.1865.

Deuterated spiroketone (**53**)



$\text{B(C}_6\text{F}_5)_3$ (3.7 mg, 7.30 μmol , 2.5 mol%) was added in one portion to a stirred solution of cross-conjugated ketone (**41**) (70.0 mg, 292 μmol , 1.0 equiv.) in CH_2Cl_2 (17 mL) at r.t. and stirring at this temperature was continued for 72 h. The mixture was concentrated under reduced pressure and subjected to column chromatography (PE:EtOAc = 99:1 to 49:1) to afford spiro ketone (**53**) (65.8 mg, 275 μmol , 94%).

R_f (PE:MTBE = 8:2; vanillin) = 0.43 (deep purple);

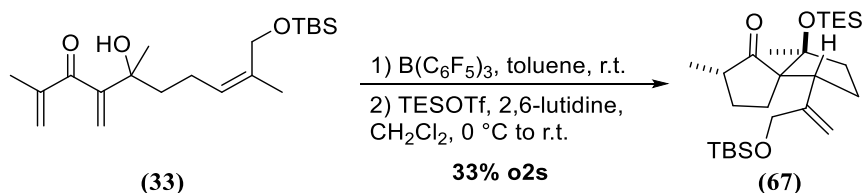
$^1\text{H-NMR}$ (600 MHz, CDCl_3): δ (ppm) = 4.57–4.53 (m, 1H, OH), 2.94 (dd, $J = 12.9, 2.7$ Hz, 1H, H-10), 2.17–2.07 (m, 2H, H-{3,4}), 1.87–1.78 (m, 1H, H-8), 1.73–1.68 (m, 1H, H-4), 1.58 (s, 3H, H-15), 1.54–1.39 (m, 4H, H-{7,8,9}), 1.36–1.27 (m, 2H, H-{3,9}), 1.03 (s, 3H, H-13), 1.01 (s, 3H, H-14);

$^{13}\text{C-NMR}$ (151 MHz, CDCl_3): δ (ppm) = 229.7 (C-1), 146.9 (C-11), 113.9 (p, $J_{\text{C,D}} = 23.6$ Hz, C-12), 74.4 (C-6), 58.4 (C-5), 46.3 (C-10), 45.3 (t, $J_{\text{C,D}} = 18.9$ Hz, C-2), 35.1 (C-7), 28.7 (C-3), 27.61 (C-9), 27.56 (C-14), 25.7 (C-4), 24.9 (C-15), 21.1 (C-8), 12.9 (C-13);

HRMS(ESI): Calcd for $\text{C}_{15}\text{H}_{21}\text{D}_3\text{O}_2\text{Na}$ $[\text{M}+\text{Na}]^+$: 262.1862; found: 262.1863.

PART 2: early stage functionalization

Spiroketone (**67**)



$\text{B}(\text{C}_6\text{F}_5)_3$ (150 mg, 293 μmol , 2.5 mol%) was added in one portion to a stirred solution of cross-conjugated ketone (**33**) (4.13 g, 11.7 mmol, 1.0 equiv.) in toluene (690 mL) at r.t.. After 3 d, the purple reaction mixture was concentrated under reduced pressure and the crude material was purified *via* column chromatography (PE:EtOAc = 99:1 to 19:1) to separate the unprotected spiroketone from the main impurities.

2,6-lutidine (940 μL , 8.13 mmol, 1.5 equiv.) and TESOTf (1.3 mL, 5.69 mmol, 1.05 equiv.) were added successively to a solution of the obtained spiro ketone (1.91 g, 5.42 mmol, 1.0 equiv.) in anhydrous CH_2Cl_2 (50 mL) at 0 °C. The cooling bath was removed and stirring was continued at r.t. for 1 h. Water (25 mL) was added, the phases were separated and the aqueous phase was extracted with CH_2Cl_2 (3x, 25 mL). The combined organic phases were dried over Na_2SO_4 and concentrated under reduced pressure. Purification *via* column chromatography (PE:EtOAc = 49:1) gave TES-protected spiroketone (**67**) (1.84 g, 3.86 mmol, 33% o2s) as a light yellow oil.

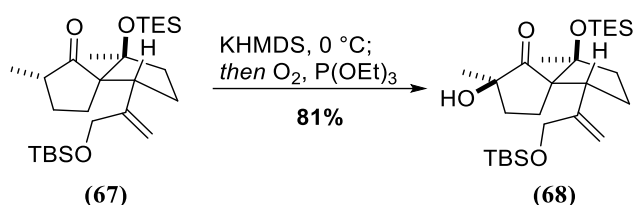
R_f (PE:EtOAc = 4:1; vanillin) = 0.71 (purple).

$^1\text{H-NMR}$ (400 MHz, CDCl_3) δ (ppm) = 5.25 (d, J = 1.8 Hz, 1H), 4.81 (s, 1H), 3.86 (d, J = 15.1 Hz, 1H), 3.75 (d, J = 15.0 Hz, 1H), 3.03 (dd, J = 11.6, 7.8 Hz, 1H), 2.11–1.78 (m, 5H), 1.72–1.61 (m, 2H), 1.53–1.41 (m, 2H), 1.30 (s, 3H), 1.11 (d, J = 6.9 Hz, 3H), 0.92 (t, J = 8.0 Hz, 9H), 0.89 (s, 9H), 0.55 (q, J = 7.9 Hz, 6H), 0.03 (s, 3H), 0.02 (s, 3H).

$^{13}\text{C-NMR}$ (101 MHz, CDCl_3) δ (ppm) = 222.7, 149.2, 110.2, 86.7, 66.6, 64.8, 46.5, 44.3, 40.4, 28.90, 28.88, 28.8, 26.3, 26.1, 18.6, 14.1, 7.1, 6.6, -5.3.

HRMS(ESI): Calcd for $\text{C}_{26}\text{H}_{50}\text{O}_3\text{Si}_2\text{Na}$ $[\text{M}+\text{Na}]^+$: 489.3196; found: 489.3192.

α -Hydroxy ketone (**68**)



A solution of (**67**) (500 mg, 1.07 mmol, 1.0 equiv.) in anhydrous THF (0.5 mL) was cooled to 0 °C and KHMDS (1.0 M in THF, 2.1 mL, 2.15 mmol, 2.0 equiv.) was added dropwise. The yellow solution was stirred at 0 °C for 1 h. P(OEt)₃ (350 μ L, 2.15 mmol, 2.0 equiv.) was added and pressured air was bubbled through the solution. Upon exposure to oxygen, the solution gradually got darker, with a dark orange solution usually indicating completion of the reaction. After exposure to the air stream for 10 min, aqueous NH₄Cl (2 mL) was added and the mixture was diluted with MTBE (4 mL). The phases were separated, the aqueous phase extracted with MTBE (3x, 5 mL) and the combined organic phases were washed with brine (5 mL), dried over Na₂SO₄ and concentrated under reduced pressure. Purification *via* column chromatography (PE:EtOAc = 11:1) gave α -hydroxy ketone (**68**) (412 mg, 0.85 mmol, 79%) as a light yellow oil.

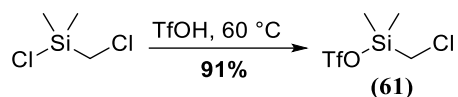
R_f (PE:EtOAc = 2.5:1; vanillin) = 0.69 (blue).

¹H-NMR (400MHz, CDCl₃): δ (ppm) = 5.32 (q, J = 1.8 Hz, 1H), 4.87 (s, 1H), 3.88 (d, J = 4.8 Hz, 2H), 2.97 (dd, J = 11.0, 8.1 Hz, 1H), 2.12 (td, J = 11.7, 7.0 Hz, 1H), 1.93–1.84 (m, 2H), 1.84–1.77 (m, 2H), 1.77–1.65 (m, 2H), 1.65–1.59 (m, 1H), 1.28 (d, J = 2.8 Hz, 6H), 0.91 (t, J = 6.0 Hz, 9H), 0.89 (s, 9H), 0.54 (q, J = 7.9 Hz, 6H), 0.03 (s, 6H).

¹³C-NMR (101 MHz, CDCl₃): δ (ppm) = 221.6, 148.9, 110.7, 86.0, 76.8, 66.3, 63.4, 46.9, 40.0, 34.7, 29.0, 26.2, 26.1, 25.4, 22.7, 18.5, 7.1, 6.5, –5.24, –5.26.

HRMS(ESI): Calcd for C₂₆H₅₀O₄SiNa [M+Na]⁺: 505.3145; found: 505.3135.

(Chloromethyl)dimethylsilyl trifluoromethanesulfonate (**61**)



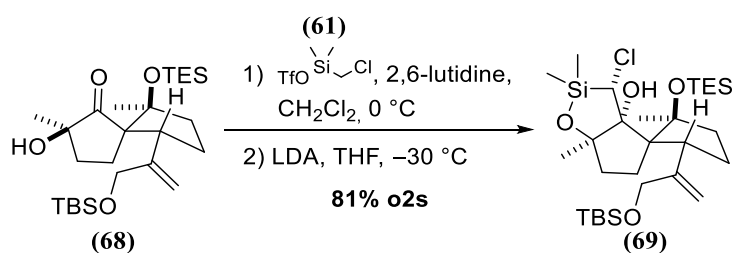
A flame-dried 50 mL Schlenk tube capped with a rubber septum was charged under argon with triflic acid (6.6 mL, 74.8 mmol, 1.0 equiv.). Chloro(chloromethyl)dimethylsilane (10.0 mL, 74.8 mmol, 1.0 equiv.) was added carefully over 5 min at r.t. and the rubber septum was replaced by a glass stopper. The colorless mixture was stirred at 60 °C for 13 h, was allowed to cool to r.t. and the glass stopper was replaced with an argon-flushed flame-dried distillation apparatus. Distillation from the reaction flask delivered (chloromethyl)dimethylsilyl trifluoromethanesulfonate (**61**) (17.4 g, 17.4 mmol, 91%) as a colorless liquid.

b.p. (22 mbar) = 64–65 °C.

¹H-NMR (400 MHz, C₆D₆): δ(ppm) = 2.39 (s, 2H), 0.09 (s, 6H).

¹³C-NMR (101 MHz, C₆D₆): δ(ppm) = 118.9 (q, *J* = 317.5 Hz), 27.0, –3.6.

TBS-protected oxasilolane (**69**)



2,6-Lutidine (395 μL , 3.42 mmol, 4.0 equiv.) was added to a stirred solution of hydroxy ketone (**68**) (412 mg, 0.85 mmol, 1.0 equiv.) in anhydrous CH_2Cl_2 (4.3 mL) at $0\text{ }^\circ\text{C}$, followed by dropwise addition of silyl triflate (**61**) (438 g, 1.70 mmol, 2.0 equiv.). The solution was allowed to warm to r.t. and stirring was continued for 2.5 h. Water (5 mL) was added under vigorous stirring, the phases were separated and the aqueous phase was extracted with CH_2Cl_2 (3x, 5 mL). The combined organic phases were washed with brine (10 mL), dried over Na_2SO_4 and concentrated under reduced pressure. The oily residue was coevaporated with benzene three times and dried under high vacuum overnight. The so obtained crude silyl ether was used in the subsequent step without further purification.²⁷

$^1\text{H-NMR}$ (400 MHz, CDCl_3): δ (ppm) = 5.35 (d, J = 1.4 Hz, 1H), 4.88 (s, 1H), 3.97 – 3.84 (m, 2H), 2.90 (m, 1H), 2.83 (s, 1H), 2.77 (s, 1H), 2.21 (m, 1H), 1.98 – 1.86 (m, 2H), 1.85 – 1.79 (m, 2H), 1.74 – 1.66 (m, 2H), 1.59 – 1.55 (m, 1H), 1.32 (s, 3H), 1.28 (s, 3H), 0.97 – 0.90 (m, 18H), 0.55 (q, J = 7.9 Hz, 6H), 0.29 (d, J = 6.3 Hz, 3H), 0.24 (s, 3H), 0.07 (d, J = 2.6 Hz, 6H);

$^{13}\text{C-NMR}$ (101 MHz, CDCl_3): δ (ppm) = 219.2, 149.0, 111.1, 85.9, 80.0, 66.4, 62.8, 47.2, 39.6, 37.0, 31.4, 31.0, 29.4, 26.2, 26.1, 25.2, 22.7, 18.5, 7.1, 6.5, -0.8, -1.2, -5.2.

HRMS(ESI): Calcd for $\text{C}_{29}\text{H}_{57}\text{O}_4\text{NaSi}_3\text{Cl}$ [$\text{M}+\text{Na}$] $^+$: 611.3151; found: 611.3141.

The crude silyl ether was dissolved in anhydrous THF (4.3 mL) and the colorless solution was cooled to $-30\text{ }^\circ\text{C}$. Freshly prepared LDA solution (1M in THF, 2.55 mL, 2.6 mmol, 3.0 equiv.) was added dropwise over 5 min at $-30\text{ }^\circ\text{C}$ and stirring at this temperature was continued for 3.5 h. NH_4Cl (50 mL) was added at $-30\text{ }^\circ\text{C}$ and the mixture was allowed to warm to r.t. under vigorous stirring. The phases were separated and the aqueous phase was extracted with MTBE (3x, 5 mL). The combined organic phases were washed with brine (10 mL), dried over Na_2SO_4 and concentrated under reduced pressure. After purification by column chromatography (PE:EtOAc = 10.5:1), oxasilolane (**69**) (412 mg, 0.70 mmol, 81% o2s) was obtained as an off-white solid.

R_f (PE:MTBE = 4:1; vanillin) = 0.58 (violet);

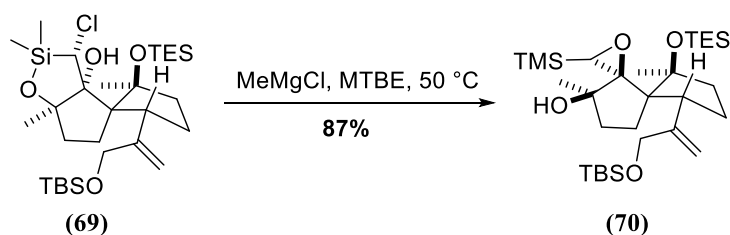
$^1\text{H-NMR}$ (400 MHz, CDCl_3): δ (ppm) = 5.27 (s, 2H), 4.88 (s, 1H), 4.39 (d, J = 15.6 Hz, 1H), 4.06 (d, J = 15.4 Hz, 1H), 3.70 (s, 1H), 3.47 (t, J = 9.5 Hz, 1H), 2.07 – 1.96 (m, 1H), 1.91 – 1.82 (m, 1H), 1.79 – 1.67 (m, 4H), 1.65 – 1.57 (m, 2H), 1.52 (s, 3H), 1.40 (s, 3H), 1.00 (t, J = 7.9 Hz, 9H), 0.93 (s, 9H), 0.71 (q, J = 7.7 Hz, 6H), 0.30 (s, 3H), 0.22 (s, 3H), 0.09 (s, 6H);

$^{13}\text{C-NMR}$ (101 MHz, CDCl_3): δ (ppm) = 152.1, 108.4, 91.1, 89.2, 87.8, 66.0, 64.8, 52.3, 44.3, 38.9, 37.6, 30.7, 28.3, 26.1, 24.7, 24.5, 18.6, 7.2, 6.6, -1.0, -1.2, -5.1, -5.2;

HRMS(ESI): Calcd for $\text{C}_{29}\text{H}_{57}\text{O}_4\text{NaSi}_3\text{Cl}$ [$\text{M}+\text{Na}$] $^+$: 611.3151; found: 611.3152.

²⁷ An analytically pure sample could be obtained *via* column chromatography (PE:EA = 15:1).

TBS-protected TMS-epoxide (**70**)



Oxasilolane (**69**) (404 mg, 0.68 mmol, 1.0 equiv.) was dissolved in anhydrous MTBE (6.8 mL) and heated to 50 °C. MeMgCl (3.0 M, 685 μ L, 3.0 equiv.) was quickly added. Stirring of the white turbid mixture was continued at the stated temperature for 5 min. The reaction was quenched by careful addition of NH₄Cl (10 mL) until no further gas development was observed. The mixture was allowed to cool to r.t., the phases were separated and the aqueous phase was extracted with MTBE (3x, 10 mL). The combined organic phases were concentrated under reduced pressure and column chromatography (PE:EtOAc = 10:1) gave TBS-protected TMS epoxide (**70**) (338 mg, 0.59 mmol, 87%) as a sticky colorless oil.

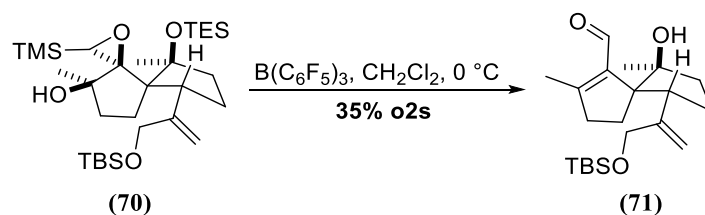
R_f(PE:EtOAc = 4:1; vanillin) = 0.52 (purple);

¹H-NMR (400 MHz, CDCl₃): δ (ppm) = δ 5.33 (s, 1H), 5.00 (s, 1H), 4.14 – 3.97 (m, 2H), 2.52 (t, *J* = 9.4 Hz, 1H), 2.04 – 1.96 (m, 1H), 1.90 (s, 1H), 1.87 – 1.77 (m, 2H), 1.68 – 1.61 (m, 2H), 1.57 – 1.51 (m, 3H), 1.28 (s, 3H), 1.01 (s, 3H), 0.97 (t, *J* = 7.9 Hz, 9H), 0.91 (s, 9H), 0.71 – 0.59 (m, 6H), 0.23 (s, 9H), 0.09 – 0.04 (2s, 6H);

¹³C-NMR (101 MHz, CDCl₃): δ (ppm) = 149.9, 109.6, 85.9, 81.8, 67.1, 57.7, 53.6, 46.4, 39.7, 38.2, 29.5, 27.3, 27.1, 26.1, 22.2, 18.6, 7.4, 7.2, 6.9, -0.6, -2.2, -5.1, -5.2;

HRMS(ESI): Calcd for C₃₀H₆₀O₄NaSi₃ [M+Na]⁺: 591.3697; found: 591.3693.

TBS-protected enal (**71**)



$B(C_6F_5)_3$ (15.2 mg, 0.03 mmol, 5.0 mol%) was added in one portion to a solution of TBS-protected epoxide (**70**) (338 mg, 0.59 mmol, 1.0 equiv.) in CH_2Cl_2 (5.9 mL) at $0\text{ }^\circ\text{C}$. The resulting red mixture was stirred at $0\text{ }^\circ\text{C}$ for 2 days. $NaHCO_3$ (5 mL) was added and the mixture was allowed to warm to r.t.; the phases were separated and the aqueous phase was extracted with MTBE (3x, 5 mL). The combined organic layers were washed with brine (10 mL), dried over Na_2SO_4 and concentrated under reduced pressure. Column chromatography (PE:EtOAc = 4:1) gave TBS-protected enal (**71**) (87.9 mg, 0.24 mmol, 41%).

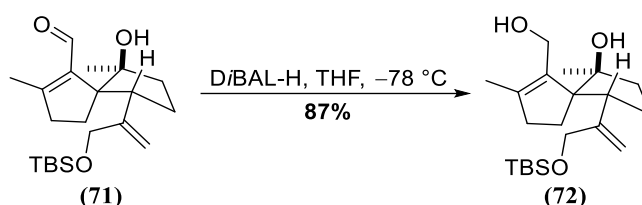
R_f (PE:EtOAc = 4:1; vanillin) = 0.22 (purple);

$^1\text{H-NMR}$ (400 MHz, $CDCl_3$): δ (ppm) = 10.03 (s, 1H), 5.33 (s, 1H), 4.93 (s, 1H), 4.32 (s, 1H), 3.84 (pd, 2H), 3.58 (t, $J = 8.8$ Hz, 1H), 2.56 – 2.32 (m, 2H), 2.21 (s, 3H), 1.98 – 1.86 (m, 2H), 1.84 – 1.69 (m, 3H), 1.54 – 1.47 (m, 1H), 1.12 (s, 3H), 0.88 (s, 9H), 0.01 (s, 6H);

$^{13}\text{C-NMR}$ (101 MHz, $CDCl_3$): δ (ppm) = 192.1, 170.3, 148.5, 138.0, 110.0, 85.2, 67.8, 66.1, 44.0, 38.9, 37.5, 27.6, 26.1, 24.9, 22.9, 18.7, 15.7, -5.26, -5.29;

HRMS(ESI): Calcd for $C_{21}H_{36}O_3NaSi$ [$M+Na$] $^+$: 387.2331; found: 387.2326.

Mono-TBS-protected triol (**72**)



DiBAL-H (1 M in THF, 0.5 mL, 0.50 mmol, 2.2 equiv.) was added dropwise to a solution of TBS-protected enal (**71**) (82.9 mg, 0.23 mmol, 1.0 equiv.) in dry THF (2.3 mL) at $-78\text{ }^\circ\text{C}$. The resulting mixture was stirred at the stated temperature for 1.5 h. Na/K tartrate (2.5 mL) was added and the mixture was allowed to warm to r.t.; the phases were separated and the aqueous phase was extracted with MTBE (3x, 2.5 mL). The combined organic phases were washed with brine (5 mL), dried over Na_2SO_4 and concentrated under reduced pressure. The obtained white solid (73.6 mg, 0.20 mmol, 87%) was used in the next step without further purification.

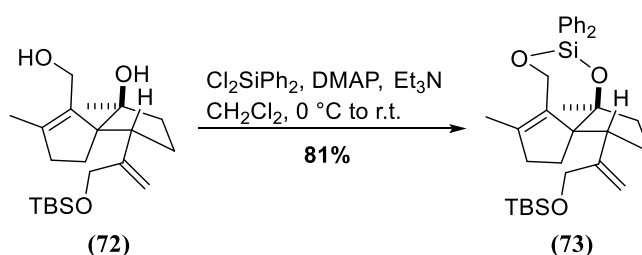
R_f (PE:EtOAc = 4:1; vanillin) = 0.13 (purple);

$^1\text{H-NMR}$ (400 MHz, CDCl_3): δ (ppm) = 5.27 (s, 1H), 4.90 (s, 1H), 4.28 (d, J = 11.6 Hz, 1H), 4.01 (d, J = 11.3 Hz, 1H), 3.88 (d, J = 14.3 Hz, 1H), 3.78 (d, J = 14.9 Hz, 1H), 3.25 (t, J = 8.8 Hz, 1H), 3.06 (bs, 2H), 2.29 – 2.22 (m, 1H), 2.13 – 2.07 (m, 1H), 1.89 – 1.81 (m, 3H), 1.84 (s, 3H), 1.80 – 1.76 (m, 1H), 1.73 – 1.66 (m, 1H), 1.41 – 1.32 (m, 1H), 1.17 (s, 3H), 0.88 (s, 9H), 0.01 (s, 3H), 0.00 (s, 3H);

$^{13}\text{C-NMR}$ (101 MHz, CDCl_3): δ (ppm) = 149.1, 144.0, 135.2, 109.4, 85.2, 68.2, 66.0, 56.1, 44.4, 37.2, 36.3, 27.4, 26.1, 24.3, 23.0, 18.6, 14.7, -5.2, -5.4;

HRMS(ESI): Calcd for $\text{C}_{21}\text{H}_{38}\text{O}_3\text{NaSi}$ $[\text{M}+\text{Na}]^+$: 389.2488; found: 389.2490.

Diphenylsilyl- TBS-protected triol (**73**)



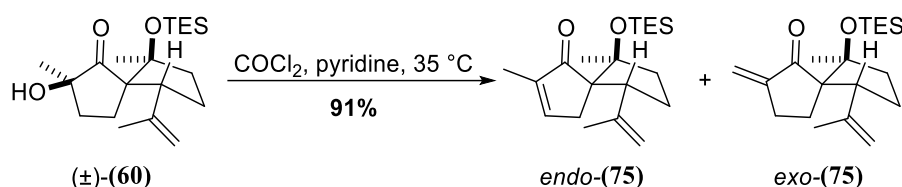
Triethylamine (100 μL , 0.73 mmol, 4.0 equiv.) and DMAP (22.0 mg, 0.18 mmol, 1.0 equiv.) were sequentially added to a solution of TBS-protected triol (**72**) (64.7 mg, 0.18 mmol, 1.0 equiv.) in dry CH_2Cl_2 (1.70 mL) at $0\text{ }^\circ\text{C}$. The resulting mixture was stirred at the stated temperature for 10 min before diphenylsilylchloride (41.0 μL , 0.20 mmol, 1.1 equiv.) was added dropwise. The mixture was stirred at r.t. for 1h. Water (2.0 mL) was added and the phases were separated; the aqueous phase was extracted with CH_2Cl_2 (3x, 2.5 mL). The combined organic phases were washed with brine (5.0 mL), dried over Na_2SO_4 and concentrated under reduced pressure. Column chromatography (PE:EA = 15:1) afforded a white, sticky solid (79.7 mg, 0.15 mmol, 81%) that was dried under high vacuum to remove the residual diphenylsilane. Impure triprotected triol (**73**) was not extensively characterized.

R_f (PE:EtOAc = 4:1; vanillin) = 0.70 (blue);

$^1\text{H-NMR}$ (400 MHz, CDCl_3): δ (ppm) = 7.65 (td, J = 8.1, 1.6 Hz, 4H), 7.41 – 7.33 (m, 6H), 5.30 (s, 1H), 4.97 (s, 1H), 4.54 (d, J = 12.3 Hz, 1H), 4.22 (d, J = 12.0 Hz, 1H), 3.89 (d, J = 14.6 Hz, 1H), 3.74 (d, J = 14.6 Hz, 1H), 3.41 (t, J = 8.8 Hz, 1H), 2.30 – 2.19 (m, 1H), 2.19 – 2.16 (m, 1H), 2.12 – 2.05 (m, 2H), 1.91 (s, 3H), 1.89 – 1.81 (m, 2H), 1.57 – 1.41 (m, 1H), 1.36 – 1.30 (m, 1H), 1.09 (s, 3H), 0.85 (s, 9H), -0.02 (s, 3H), -0.03 (s, 3H);

HRMS(ESI): Calcd for $\text{C}_{33}\text{H}_{46}\text{O}_3\text{NaSi}_2$ $[\text{M}+\text{Na}]^+$: 569.2883; found: 569.2904.

Enone (75)



α -hydroxy ketone $(\pm)\text{-}(\mathbf{60})$ (1.96 g, 5.55 mmol, 1.0 equiv.) was dissolved in anhydrous pyridine (110 mL) and the solution was heated to 35 °C. Phosgene (15 wt% in toluene, 40.0 mL, 56.0 mmol, 10 equiv.) was added quickly *via* dropping funnel. After 16 h, the brown heterogeneous mixture was cooled to 0 °C and water (50 mL) was added carefully. The mixture was diluted with MTBE (100 mL), the phases were separated and the aqueous phase was extracted with MTBE (3x, 50 mL). The combined organic phases were washed with brine (100 mL), dried over Na_2SO_4 and concentrated under reduced pressure (60 °C water bath temperature to remove residual pyridine). Purification *via* column chromatography (PE:EtOAc = 100:1) gave a mixture of desired enone *endo*- $(\mathbf{75})$ and its double bond isomer *exo*- $(\mathbf{75})$ (*endo*:*exo* = 5:1, 1.69 g, 5.04 mmol, 91%) as a light yellow oil.

An analytically pure sample of *endo*- $(\mathbf{75})$ was obtained by preparative TLC (50.0 mg sample, plate size: 20x10 cm, eluent: PE:EtOAc = 200:1, run 5x).

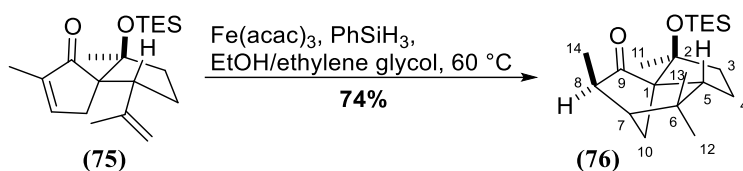
R_f (PE:EtOAc = 25:1; vanillin) = 0.66 (dark-purple).

$^1\text{H-NMR}$ (400 MHz, CDCl_3): δ (ppm) = 7.15–7.12 (m, 1H), 4.80–4.77 (m, 1H), 4.67–4.64 (m, 1H), 3.49 (t, J = 8.0 Hz, 1H), 2.34 (dq, J = 18.9, 2.5 Hz, 1H), 2.17–2.09 (m, 1H), 2.00–1.89 (m, 2H), 1.77–1.66 (m, 5H), 1.49 (s, 3H), 1.14 (s, 3H), 0.94 (t, J = 7.9 Hz, 9H), 0.60–0.53 (6H, m).

$^{13}\text{C-NMR}$ (101 MHz, CDCl_3): δ (ppm) = 208.9, 153.8, 146.8, 142.3, 111.2, 86.3, 63.6, 49.2, 39.7, 33.6, 25.5, 23.9, 23.7, 10.7, 7.2, 6.8.

HRMS(ESI): Calcd for $\text{C}_{20}\text{H}_{34}\text{O}_2\text{SiNa}$ [$\text{M}+\text{Na}$] $^+$: 357.2226; found: 357.2225.

Fe(acac)₃-mediated cyclization of enone (**75**)



Tricyclic (**76**) was synthesized according to the protocol by Baran and co-workers.²⁸

PhSiH₃ (1.5 mL, 12.3 mmol, 2.5 equiv.) was added at r.t. to a stirred solution of enone (**75**) (*endo:exo* = 5:1, 1.65 g, 4.92 mmol, 1.0 equiv.) and Fe(acac)₃ (434 mg, 1.23 mmol, 0.25 equiv.) in EtOH/ethylene glycol (5:1, 96 mL) and the reaction mixture was heated to 60 °C.²⁹ After 4 h, the mixture was allowed to cool to r.t. and was diluted with brine (100 mL). The phases were separated, the aqueous phase was extracted with MTBE (5x, 100 mL) and the combined organic phases were dried over Na₂SO₄ and concentrated under reduced pressure. Purification *via* column chromatography (PE:EtOAc = 200:1 to 100:1) gave tricyclic (**76**) (1.22 g, 3.63 mmol, 74%) as a light yellow oil.

R_f (PE:EtOAc = 25:1; vanillin) = 0.62 (red).

¹H-NMR (400 MHz, CDCl₃): δ(ppm) = 2.27 (ddq, *J* = 7.4, 4.2, 1.2 Hz, 1H, H-8), 2.15 (ddd, *J* = 10.8, 4.6, 2.0 Hz, 1H, H-5), 2.04–2.01 (m, 1H, H-7), 1.94–1.83 (m, 1H, H-4a), 1.77–1.72 (m, 3H, H-{3,10b}), 1.63–1.58 (m, 1H, H-4b), 1.37–1.32 (m, 1H, H-10a), 1.31 (s, 3H, H-11), 1.23 (d, *J* = 7.4 Hz, 3H, CH₃-14), 1.14 (s, 3H, CH₃-13), 1.07 (s, 3H, CH₃-12), 0.97 (t, *J* = 7.9 Hz, 9H, OTES), 0.71–0.53 (m, 6H, OTES).

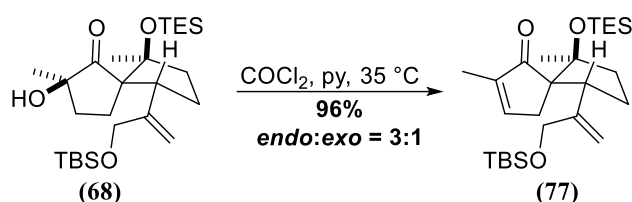
¹³C-NMR (101 MHz, CDCl₃): δ(ppm) = 216.0 (C-9), 81.1 (C-2), 74.4 (C-1), 55.0 (C-5), 52.8 (C-8), 51.5 (C-7), 42.39, 42.38 (C-{3,6}), 40.8 (C-10), 29.6 (C-13), 29.1 (C-12), 23.7 (C-11), 22.5 (C-4), 13.6 (C-14), 7.3 (OTES), 6.9 (OTES).

HRMS(ESI): Calcd for C₂₀H₃₆O₂SiNa [M+Na]⁺: 359.2382; found: 359.2383.

²⁸ *J. Am. Chem. Soc.* **2017**, *139*, 2484–2503.

²⁹ The reaction flask should be only loosely closed to allow evolving hydrogen gas to escape.

Enone (77)



α -Hydroxy ketone (**68**) (76.7 mg, 157 μmol , 1.0 equiv.) was dissolved in anhydrous pyridine (3.2 mL) and heated to 35 $^\circ\text{C}$. After 10 min, phosgene (15 wt% in toluene, 170 μL , 1.57 mmol, 10 equiv.) was added quickly. After 29 h, the mixture was cooled to 0 $^\circ\text{C}$, and water (5 mL) was added under vigorous stirring. The phases were separated and the aqueous phase was extracted with MTBE (3x, 10 mL). The combined organic phases were washed with brine (10 mL), dried over Na_2SO_4 and concentrated under reduced pressure. Purification *via* column chromatography (PE:EtOAc = 11:1) gave enone (**77**) (*endo:exo* = 3:1, 68.7 mg, 0.15 mmol, 96%) as a colorless oil.

Analytical data (main isomer):

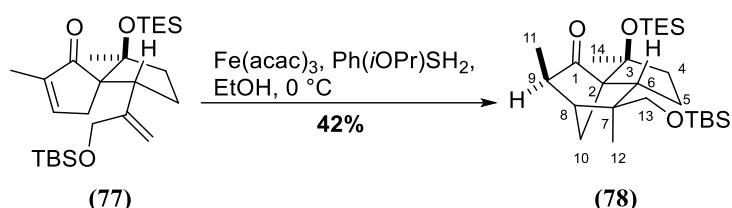
R_f (PE:EtOAc = 4:1; vanillin) = 0.77 (blue).

$^1\text{H-NMR}$ (400 MHz, CDCl_3): δ (ppm) = 7.14 (bs, 1H), 5.27–5.26 (m, 1H), 5.29–4.82 (m, 1H), 3.83 (d, J = 15.4 Hz, 1H), 3.59 (d, J = 15.6 Hz, 1H), 3.41 (t, J = 9.0 Hz, 1H), 2.39 (dt, J = 18.9, 2.5 Hz, 1H), 2.12 (d, J = 18.9 Hz, 1H), 2.01–1.87 (m, 2H), 1.85–1.76 (m, 1H), 1.74–1.73 (m, 4H), 1.15 (s, 3H), 0.93 (t, J = 7.9 Hz, 9H), 0.86 (s, 9H), 0.56 (qd, J = 7.9, 1.7 Hz, 6H), –0.02 (s, 3H), –0.02 (s, 3H).

$^{13}\text{C-NMR}$ (101 MHz, CDCl_3): δ (ppm) = 208.7, 154.0, 149.5, 142.2, 108.4, 86.5, 65.9, 63.8, 45.0, 39.6, 33.6, 26.1, 25.6, 23.7, 18.5, 10.7, 7.3, 6.8, –5.33, –5.37.

HRMS(ESI): Calcd for $\text{C}_{26}\text{H}_{48}\text{O}_3\text{Si}_2\text{Na}$ $[\text{M}+\text{Na}]^+$: 487.3040; found: 487.3046.

Tricycle (78)



Cyclization of enone (77) was performed according to a procedure by Pronin and co-workers.³⁰

PhSi(*i*OPr)₂³¹ (11.0 mg, 66.1 μmol, 3.2 equiv.) was added dropwise to a degassed mixture of enone (77) (9.5 mg, 20.4 μmol, 1.0 equiv) and Fe(acac)₃ (4.0 mg, 11.3 μmol, 0.6 equiv) in degassed anhydrous EtOH (300 μL)³² at 0 °C. After 4 h, degassed NaHCO₃ (200 μL) was added, and the mixture was diluted with water and brine (200 μL each). The aqueous phase was extracted with Et₂O (3x, 2 mL). The combined organic phases were washed with brine (2 mL), dried over Na₂SO₄ and concentrated under reduced pressure. Purification by column chromatography (PE:EtOAc = 15:1) gave tricycle (78) (4.4 mg, 9.4 μmol, 46%) as a colorless oil.

R_f (PE:EtOAc = 4:1; vanillin) = 0.64 (blue).

¹H-NMR (500 MHz, CDCl₃): δ(ppm) = 3.46 (d, *J* = 10.0 Hz, 1H, H-13a), 3.35 (d, *J* = 9.9 Hz, 1H, H-13b), 2.37–2.34 (m, 2H, H-{8,9}), 2.07–2.04 (m, 1H, H-6), 1.90–1.87 (m, 1H, H-4a), 1.86–1.79 (m, 3H, H-{5a,10a,10b}), 1.74–1.68 (m, 1H, H-4b), 1.41 (d, *J* = 10.0 Hz, 1H, H-5b), 1.29 (s, 3H, CH₃-14), 1.26 (s, 3H, CH₃-11), 1.13 (s, 3H, CH₃-12), 0.97 (t, *J* = 7.9 Hz, 9H, OTES), 0.88 (s, 9H, OTBS), 0.60 (q, *J* = 7.9 Hz, 6H, OTES), 0.02 (s, 3H, OTBS), 0.01 (s, 3H, OTBS).

¹³C-NMR (126 MHz, CDCl₃) δ(ppm) = 216.3 (C-1), 81.1 (C-3), 73.6 (C-2), 70.3 (C-13), 52.5 (C-9), 51.0 (C-6), 48.4 (C-8), 48.3 (C-7), 42.2 (C-4), 40.3 (C-10), 25.9 (OTBS), 24.0 (C-12), 23.6 (C-14), 22.2 (C-5), 18.3 (OTBS), 12.4 (C-11), 7.2 (OTES), 6.8 (OTES), –5.4 (OTBS), –5.6 (OTBS).

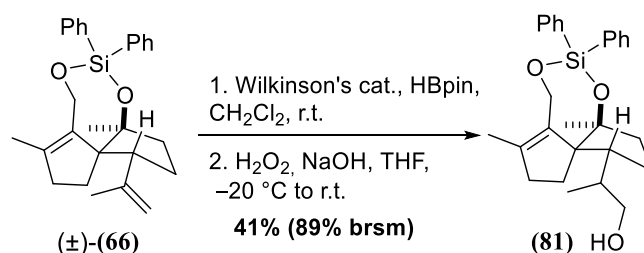
HRMS(ESI): Calcd for C₂₆H₅₀O₃Si₂Na [M+Na]⁺: 489.3196; found: 489.3201.

³⁰ *J. Am. Chem. Soc.* **2015**, *137*, 15410–15413.

³¹ Reagent prepared according to the procedure reported by Yamada and co-workers: *Chem. Lett.* **2006**, *35*, 714–715.

³² Solvent was degassed *via* freeze-pump-thaw technique. The starting material and Fe(acac)₃ were evacuated and flushed with Ar (3x) before the degassed solvent was added. The so obtained mixture was further degassed through bubbling of Ar through a needle, leaving a second, shorter needle as a way out.

Diphenylsilyl-protected triol (**81**)



Pinacol borane (315 μ L, 2.17 mmol, 2.2 equiv.) was added to a solution of diphenylsilyl-protected diol (\pm)-(**66**) (412 mg, 0.99 mmol, 1.0 equiv.) and Wilkinson's catalyst (18.3 mg, 19.8 μ mol, 2.0 mol%) in dry CH₂Cl₂ (580 μ L) at r.t. The resulting mixture was stirred at the stated temperature for 3 days before the solvent was evaporated. The crude intermediate was purified *via* column chromatography (PE:EA = 12:1) to remove the excess of pinacol borane and the residual starting material (188 mg, 0.46 mmol, 46%), then dissolved in THF (2.2 mL) and cooled to -20 °C. A pre-mixed solution of NaOH/H₂O₂³³ was carefully added; the mixture was warmed to r.t. and stirred for 1 h. Na₂S₂O₃ (2.0 mL) was carefully added at 0 °C; after vigorous stirring at r.t. the phases were separated. The aqueous phase was extracted with MTBE (3x, 2.5 mL). The combined organic phases were dried over Na₂SO₄ and concentrated under reduced pressure, affording impure diprotected triol (**81**) (177 mg, 0.41 mmol, 89% brsm) as a colorless oil.

R_f(PE:EtOAc = 4:1; vanillin) = 0.23 (pink);

¹H-NMR (400 MHz, CDCl₃): δ (ppm) = 7.64 (dd, J = 7.9, 1.6 Hz, 2H), 7.61 – 7.59 (dd, J = 8.0, 1.4 Hz, 2H), 7.42 – 7.33 (m, 4H), 7.32 – 7.26 (m, 2H), 4.53 (d, J = 12.2 Hz, 1H), 4.12 (d, J = 12.3 Hz, 1H), 3.68 (dd, J = 10.6, 3.4 Hz, 1H), 3.39 (dd, J = 10.6, 7.1 Hz, 1H), 3.21 (s, 1H), 2.52 (q, J = 9.4 Hz, 1H), 2.35 – 2.13 (m, 2H), 2.19 – 2.15 (m, 1H), 1.93 – 1.80 (m, 2H), 1.90 (s, 3H), 1.79 – 1.74 (m, 1H), 1.60 – 1.57 (m, 1H, HSQC, HMBC), 1.42 – 1.32 (m, 2H), 1.05 (s, 3H), 0.74 (d, J = 6.7 Hz, 3H);

¹³C-NMR (101 MHz, CDCl₃): 134.9, 134.8, 134.5, 130.1, 130.0, 128.1, 127.9, 127.7, 91.4, 68.2, 56.8, 42.8, 39.4, 38.1, 36.4, 27.2, 25.0, 24.7, 22.4, 15.1, 14.7;

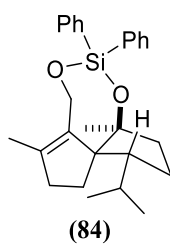
¹H-NMR (400 MHz, C₆D₆): δ (ppm) = 7.91 (dd, J = 23.1, 9.5 Hz, 4H), 7.28 – 7.16 (m, 6H), 4.56 (d, J = 12.2 Hz, 1H), 4.28 (d, J = 11.7 Hz, 1H), 3.47 (dd, J = 10.3, 3.4 Hz, 1H), 3.19 (dd, J = 10.3, 6.8 Hz, 1H), 2.79 – 2.68 (m, 1H), 2.25 – 2.16 (m, 1H), 2.11 – 2.04 (m, 1H), 2.02 – 1.95 (m, 2H), 1.70 (s, 3H), 1.66 – 1.58 (m, 2H), 1.43 – 1.38 (m, 1H), 1.24 – 1.10 (m, 2H), 1.09 (s, 3H), 0.71 (d, J = 6.8 Hz, 3H);

¹³C-NMR (101 MHz, C₆D₆): 141.8, 136.9, 136.1, 135.5, 135.34, 135.25, 130.4, 130.2, 128.6, 128.2, 128.0, 91.4, 69.1, 67.8, 56.7, 43.2, 39.5, 38.3, 36.4, 27.4, 27.3, 22.5, 15.2, 14.4;

HRMS(ESI): Calcd for C₂₇H₃₄O₃NaSi [M+Na]⁺: 457.2175; found: 457.2191.

³³ 340 μ L of H₂O₂ (30% in water, 11.0 mmol, 25.0 equiv.) were added dropwise to 2M NaOH (2.20 mL, 4.40 mmol, 10 equiv.) at 0 °C.

Compound (84)

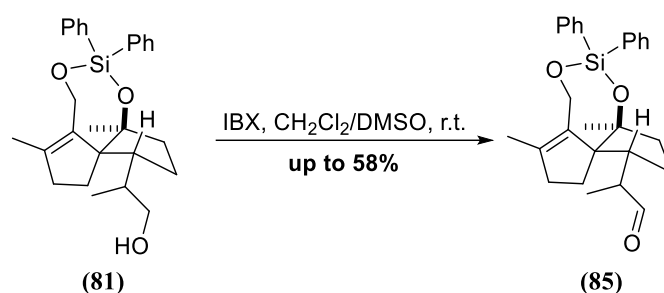


R_f (PE:EtOAc = 4:1; vanillin) = 0.71 (blue);

$^1\text{H-NMR}$ (400 MHz, CDCl_3): δ (ppm) = 7.69 – 7.63 (m, 2H), 7.63 – 7.56 (m, 2H), 7.43 – 7.35 (m, 4H), 7.31 – 7.27 (m, 2H), 4.51 (d, J = 12.2 Hz, 1H), 4.14 (d, J = 11.6 Hz, 1H), 2.38 – 2.26 (m, 2H), 2.23 – 2.18 (m, 2H), 1.94 – 1.83 (m, 2H), 1.89 (s, 3H), 1.74 (td, J = 12.8, 6.3 Hz, 1H), 1.28 (s, 3H), 1.02 (s, 3H), 0.90 (d, J = 6.4 Hz, 3H), 0.65 (d, J = 6.6 Hz, 3H);

HRMS(ESI): Calcd for $\text{C}_{27}\text{H}_{34}\text{O}_2\text{NaSi}$ $[\text{M}+\text{Na}]^+$: 441.2226; found: 441.2232.

Aldehyde (**85**)



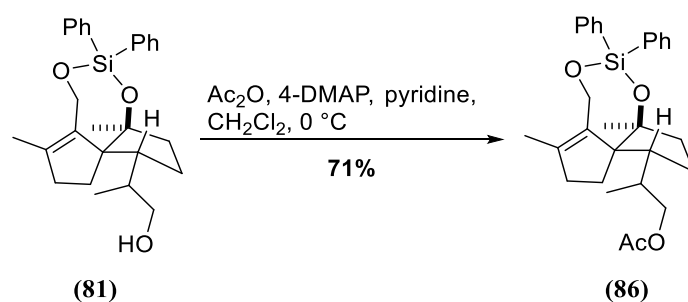
IBX (14.2 mg, 50.6 μmol , 1.1 equiv.) was added in one portion to a solution of diprotected triol (**81**) (20.0 mg, 46.0 μmol , 1.0 equiv.) in a 1:1 mixture CH₂Cl₂/DMSO (400 μL) at r.t.. The heterogeneous mixture was stirred for 2.5 h before additional 6.4 mg of IBX (23.0 μmol , 0.5 equiv.) were added. After one hour, TLC showed traces of decomposition and the reaction was quenched with water (1 mL) although not completed. The phases were separated and the aqueous phase extracted with CH₂Cl₂ (5x, 1 mL); the combined organic layers were washed with brine (5 mL), dried over Na₂SO₄ and concentrated. Column chromatography (PE:EA = 9.5:1) afforded desired aldehyde (**85**) (11.6 mg, 27.0 μmol , 58%) that was used in the consequent oxidation without detailed characterization.

R_f (PE:EtOAc = 4:1; vanillin) = 0.46 (pink-brownish);

¹H-NMR (400 MHz, CDCl₃): δ (ppm) = 9.57 (d, J = 3.4 Hz, 1H), 7.62 (ddd, J = 16.7, 8.0, 1.5 Hz, 4H), 7.44 – 7.35 (m, 4H), 7.32 – 7.29 (m, 2H), 4.55 (d, J = 12.4 Hz, 1H), 4.12 (d, J = 12.2 Hz, 1H), 2.86 (q, J = 9.4 Hz, 1H), 2.37 – 2.30 (m, 2H), 2.28 – 2.17 (m, 2H), 1.98 – 1.91 (m, 1H), 1.91 (s, 3H), 1.84 – 1.76 (m, 2H), 1.50 – 1.38 (m, 2H), 1.07 (s, 3H), 0.86 (d, J = 6.9 Hz, 3H);

HRMS(ESI): Calcd for C₂₇H₃₂O₃NaSi [M+Na]⁺: 455.2018; found: 455.2014.

Diphenylsilyl-protected acetate (**86**)



DMAP (3.0 mg, 25.0 μmol , 10 mol%), pyridine (60 μL , 0.75 mmol, 3.0 equiv.) and Ac_2O (35 μL , 0.38 mmol, 1.5 equiv.) were sequentially added to a stirred solution of alcohol (**81**) (108 mg, 0.25 mmol, 1.0 equiv.) in dry CH_2Cl_2 (2.5 mL) at 0 $^\circ\text{C}$. After 1h, the reaction was quenched with water (2.0 mL); the phases were separated and the aqueous phase was extracted with CH_2Cl_2 (3x, 2.5 mL). The combined organic phases were washed with brine (5.0 mL), dried over Na_2SO_4 and concentrated under reduced pressure. Column chromatography (PE:EA =20:1) afforded acetate (**86**) (84 mg, 0.18 mmol, 71%).

R_f (PE:EtOAc = 4:1; vanillin) = 0.46 (pink);

$^1\text{H-NMR}$ (400 MHz, CDCl_3): δ (ppm) = 7.65 – 7.59 (m, 4H), 7.43 – 7.29 (m, 6H), 4.52 (d, J = 12.2 Hz, 1H), 4.14 – 4.09 (m, 2H), 3.89 (dd, J = 10.7, 6.5 Hz, 1H), 2.68 – 2.55 (m, 1H), 2.37 – 2.29 (m, 1H), 2.26 – 2.14 (m, 2H), 1.98 (s, 3H), 1.90 (s, 3H), 1.88 – 1.84 (m, 2H), 1.80 – 1.70 (s, 2H), 1.45 – 1.33 (s, 2H), 1.04 (s, 3H), 0.73 (d, J = 6.8 Hz, 3H);

$^{13}\text{C-NMR}$ (101 MHz, CDCl_3): δ (ppm) = 171.6, 142.6, 136.1, 135.3, 134.88, 134.86, 134.8, 130.1, 130.0, 127.9, 127.7, 91.3, 69.6, 68.8, 56.7, 42.9, 38.0, 36.4, 36.3, 27.2, 27.1, 22.4, 21.1, 15.6, 14.7;

HRMS(ESI): Calcd for $\text{C}_{29}\text{H}_{36}\text{O}_5\text{NaSi}$ [$\text{M}+\text{Na}$] $^+$: 499.2281; found: 499.2268.

Acetate protected enone (**87**)



*t*BuOOH (70% in water, 2.3 mL, 1.70 mmol, 100 equiv.) was added over 6 h *via* syringe pump to a solution of triprotected triol (**86**) (80 mg, 0.17 mmol, 1.0 equiv.) and Du Bois's catalyst (6.3 mg, 8.50 μmol , 5.0 mol%) in DCE (3.3 mL) at r.t.; the green solution turned slightly blue upon addition. The mixture was quenched with $\text{Na}_2\text{S}_2\text{O}_3$ (3 mL). The phases were separated and the aqueous phase extracted with CH_2Cl_2 (3x, 5mL); the combined organic layers were dried over Na_2SO_4 and concentrated under reduced pressure. Column chromatography (PE:EA = 5:1) afforded desired enone (**87**) (34 mg, 68.5 μmol , 40%).

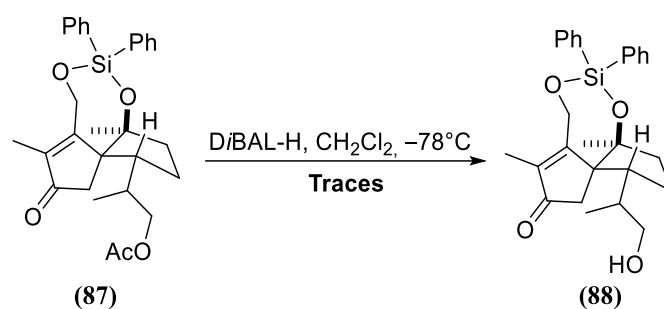
R_f (PE:EtOAc = 4:1; KMnO_4) = 0.23;

$^1\text{H-NMR}$ (400 MHz, C_6D_6): δ (ppm) = 7.83 – 7.80 (m, 2H), 7.75 – 7.72 (m, 2H), 7.23– 7.18 (m, 3H), 7.15 – 7.10 (m, 3H), 4.48 (d, J = 12.1 Hz, 1H), 4.42 (d, J = 12.2 Hz, 1H), 3.95 (dd, J = 10.9, 3.2 Hz, 1H), 3.84 (dd, J = 10.9, 5.4 Hz, 1H), 2.93 – 2.84 (m, 1H), 2.18 – 2.05 (m, 2H), 1.87 – 1.82 (m, 1H), 1.80 (s, 3H), 1.75 – 1.70 (m, 1H), 1.71 (s, 3H), 1.34 – 1.16 (mz, 4H), 1.06 – 0.96 (m, 1H), 0.90 (s, 3H), 0.46 (d, J = 6.8 Hz, 3H);

$^{13}\text{C-NMR}$ (101 MHz, C_6D_6): δ (ppm) = 205.5, 170.2, 166.7, 142.3, 135.2, 135.0, 134.5, 134.0, 130.8, 130.7, 90.3, 68.6, 62.6, 56.5, 43.4, 40.9, 39.1, 36.4, 27.4, 21.4, 20.5, 16.3, 8.2;

HRMS(ESI): Calcd for $\text{C}_{29}\text{H}_{36}\text{O}_5\text{NaSi}$ [$\text{M}+\text{Na}$] $^+$: 513.2073; found: 513.2064.

Deprotected enone (**88**)



DIBAL-H (1 M in CH₂Cl₂, 38.3 μL, 38.3 μmol, 1.0 equiv.) was added dropwise to a solution of triprotected enone (**87**) (18.8 mg, 38.3 μmol, 1.0 equiv.) in dry CH₂Cl₂ (380 μL) at -78 °C. The mixture was stirred for 45 min at -78 °C before MeOH (1 mL) was added. The mixture was diluted with ethyl acetate (5 mL) and Na/K tartrate (5 mL) before it was warmed to room temperature. The phases were separated and the aqueous phase extracted with CH₂Cl₂ (3x, 5mL); the combined organic layers were dried over Na₂SO₄ and concentrated under reduced pressure. Preparative TLC (PE:EA = 1:1) afforded traces of desired enone (**88**).

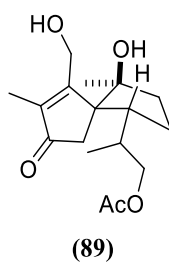
R_f (PE:EtOAc = 1:1; KMnO₄) = 0.10;

¹H-NMR (600 MHz, CDCl₃): δ(ppm) = 7.70 – 7.54 (d, *J* = 95.0 Hz, 4H), 7.50 – 7.26 (m, 6H), 4.73 (d, *J* = 12.3 Hz, 1H), 4.55 (d, *J* = 12.3 Hz, 1H), 3.68 (dd, *J* = 10.5, 3.3 Hz, 1H), 3.45 (dd, *J* = 10.6, 6.4 Hz, 1H), 2.96 – 2.85 (m, 1H), 2.43 (d, *J* = 18.6 Hz, 1H), 2.36 – 2.29 (m, 1H), 2.29 – 2.22 (m, 1H), 2.02 (d, *J* = 18.8 Hz, 1H), 1.93 (s, 3H), 1.77 – 1.71 (m, 1H), 1.65 – 1.63 (m, 1H), 1.46 – 1.42 (m, 1H), 1.01 (s, 3H), 0.70 (d, *J* = 6.7 Hz, 3H);

¹³C-NMR (151 MHz, CDCl₃): δ(ppm) = 207.8, 168.7, 142.0, 134.9, 134.7, 133.8, 133.4, 130.7, 130.6, 128.1, 128.0, 90.2, 67.6, 62.9, 56.8, 43.5, 41.5, 41.3, 39.4, 29.2, 21.7, 16.1, 8.4;

HRMS(ESI): Calcd for C₂₇H₃₂O₄NaSi [M+Na]⁺: 471.1968; found: 471.1957.

Deprotected enone (**89**)



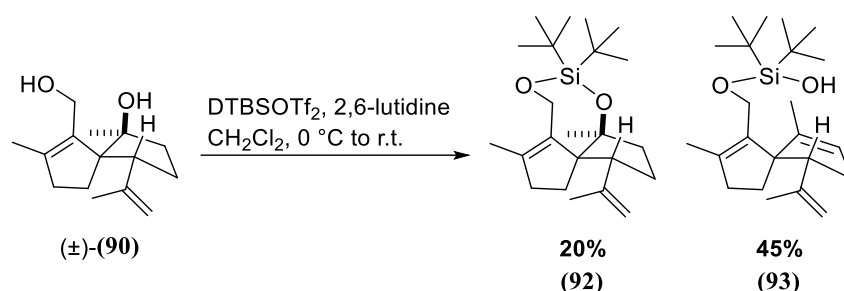
R_f (PE:EtOAc = 1:1; KMnO_4) = 0.03;

$^1\text{H-NMR}$ (400 MHz, CDCl_3): δ (ppm) = 4.42 (s, 2H), 4.11 (dd, J = 10.8, 3.6 Hz, 1H), 3.87 (dd, J = 10.9, 6.8 Hz, 1H), 2.83 (q, J = 9.9 Hz, 1H), 2.34 (d, J = 18.6 Hz, 1H), 2.23 – 2.10 (m, 1H), 2.06 (s, 3H), 1.99 (d, J = 18.5 Hz, 1H), 1.95 – 1.87 (m, 1H), 1.86 (s, 3H), 1.81 – 1.75 (m, 1H), 1.72 – 1.63 (m, 1H), 1.48 – 1.35 (m, 1H), 1.09 (s, 3H), 0.72 (d, J = 6.7 Hz, 3H);

$^{13}\text{C-NMR}$ (101 MHz, CDCl_3): δ (ppm) = 207.3, 171.4, 170.6, 141.9, 86.2, 68.9, 61.6, 56.8, 43.5, 40.8, 38.9, 36.3, 27.1, 21.9, 21.1, 16.4, 8.4;

HRMS(ESI): Calcd for $\text{C}_{17}\text{H}_{26}\text{O}_5\text{Na}$ $[\text{M}+\text{Na}]^+$: 333.1678; found: 333.1673.

Di-*tert*-butylsilyl-protected diol (**92**)



DTBSOTf₂ (15 μ L, 44.4 μ mol, 1.1 equiv.) was added dropwise to a solution of diol (\pm)-**(90)** (10.0 mg, 42.3 μ mol, 1.0 equiv.) and 2,6-lutidine (15 μ L, 127 μ mol, 3.0 equiv.) in dry CH₂Cl₂ (420 μ L) at 0 °C. The resulting mixture was stirred at r.t. overnight before it was diluted with CH₂Cl₂ (1.0 mL) and water (1.0 mL) was added. The phases were separated; the aqueous phase was extracted with CH₂Cl₂ (3x, 1.5 mL). The combined organic phases were dried over Na₂SO₄ and concentrated under reduced pressure. Column chromatography (PE:EA = 19:1) afforded desired product **(92)** (3.2 mg, 8.5 μ mol, 20%) along with elimination product **(93)** (7.2 mg, 19.1 μ mol, 45%).

Di-*tert*-butyldiphenylsilyl protected diol (**92**)

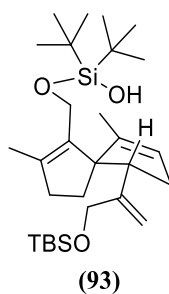
R_f(PE:EtOAc = 6:1; vanillin) = 0.56 (blue);

¹H-NMR (400 MHz, CDCl₃): δ (ppm) = 4.84 (s, 1H), 4.68 (s, 1H), 4.59 (d, J = 12.7 Hz, 1H), 4.31 (d, J = 12.6 Hz, 1H), 3.39 – 3.27 (m, 1H), 2.34 (dt, J = 17.6, 8.8 Hz, 1H), 2.09 (dd, J = 16.5, 10.1 Hz, 1H), 1.96 – 1.81 (m, 4H), 1.79 (s, 3H), 1.73 – 1.64 (m, 1H), 1.60 (s, 3H), 1.40 (dd, J = 13.7, 7.9 Hz, 1H), 1.31 (s, 3H), 1.03 (s, 9H), 0.97 (s, 9H);

¹³C-NMR (101 MHz, CDCl₃): δ (ppm) = 146.9, 142.0, 111.7, 90.7, 69.5, 59.7, 47.7, 39.5, 36.6, 28.74, 28.66, 28.5, 27.7, 27.6, 25.7, 24.3, 22.1, 20.7, 14.8;

HRMS(ESI): Calcd for C₂₃H₄₀O₂NaSi [M+Na]⁺: 399.2695; found: 399.2676.

Di-*tert*-butyldiphenylsilyl mono-protected diol (**93**)



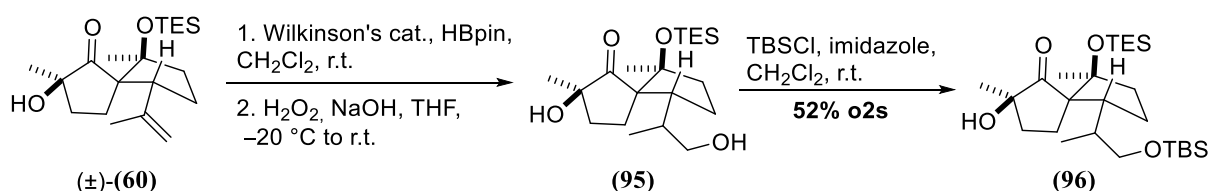
R_f (PE:EtOAc = 6:1; vanillin) = 0.48 (blue);

$^1\text{H-NMR}$ (400 MHz, CDCl_3): δ (ppm) = 5.31 (s, 1H), 4.81 (s, 1H), 4.76 (s, 1H), 4.38 (d, J = 11.4 Hz, 1H), 4.18 (d, J = 11.5 Hz, 1H), 3.08 (t, J = 8.1 Hz, 1H), 2.28 (d, J = 8.1 Hz, 2H), 2.21 (t, J = 7.5 Hz, 2H), 1.98 – 1.90 (m, 1H), 1.76 (s, 3H), 1.66 (s, 3H), 1.53 – 1.45 (m, 2H), 1.49 (s, 3H), 1.03 (s, 9H), 1.01 (s, 9H);

$^{13}\text{C-NMR}$ (101 MHz, CDCl_3): δ (ppm) = 147.9, 146.2, 139.3, 137.3, 123.0, 111.1, 68.7, 57.9, 52.9, 37.4, 34.6, 28.4, 27.7, 27.6, 27.4, 22.9, 20.9, 14.9, 13.7;

HRMS(ESI): Calcd for $\text{C}_{23}\text{H}_{40}\text{O}_2\text{NaSi}$ $[\text{M}+\text{Na}]^+$: 399.2695; found: 399.2702.

Diprotected triol (**96**)



A solution of α -hydroxyketone (\pm)-(**60**) (50 mg, 0.14 mmol, 1.0 equiv.) in dry CH_2Cl_2 (300 μL) was added to Wilkinson's catalyst (1.3 mg, 1.40 μmol , 1.0 mol%) at r.t. followed by neat pinacol borane (23 μL , 0.16 mmol, 1.1 equiv.). The mixture was stirred at r.t. for 20 h, when the same amounts of catalyst and pinacol borane were added. The mixture was stirred for further 6 h, before the solvent was removed under reduced pressure, since no further conversion was observed. The crude intermediate was dissolved in THF (700 μL) and cooled to -20°C . 1.0 mL of a stock solution of aq. NaOH/ H_2O_2 ³⁴ were carefully added. The mixture was stirred at r.t. before $\text{Na}_2\text{S}_2\text{O}_3$ (2 mL) was carefully added at 0°C . The mixture was diluted with MTBE (2.0 mL) and warmed to r.t.. The phases were separated and the aqueous phase extracted with MTBE (3x, 2.0 mL); the combined organic layers were dried over Na_2SO_4 and concentrated. Impure TES-protected triol (**95**) was obtained after column chromatography (PE:EA = 2.3:1) and used in the next step without further purification.

Crude alcohol (**95**) (49 mg, 0.13 mmol, 1.0 equiv.) was dissolved in dry CH_2Cl_2 (520 μL) and the resulting solution cooled to 0°C . Imidazole (11 mg, 0.16 mmol, 1.2 equiv.) was added in one portion, followed by TBSCl (22 mg, 0.15 mmol, 1.1 equiv.). The mixture was stirred at r.t. for 18 h; brine (2.5 mL) was added after dilution with CH_2Cl_2 (3.0 mL). The phases were separated and the aqueous phase extracted with CH_2Cl_2 (3x, 2.5 mL); the combined organic layers were dried over Na_2SO_4 and concentrated. Pure diprotected triol (**96**) (35 mg, 72.0 μmol) was obtained after column chromatography (PE:EA = 4:1) in 52% yield from α -hydroxyketone (\pm)-(**60**).

R_f (PE:EtOAc = 4:1; vanillin) = 0.52 (blue);

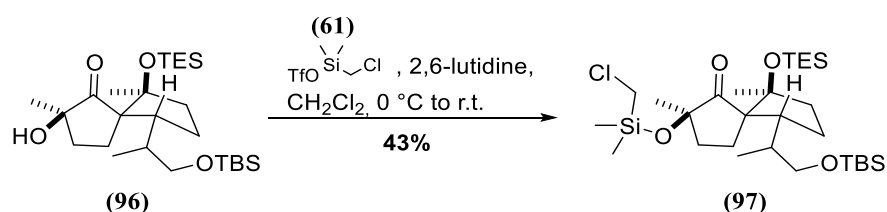
¹H-NMR (400 MHz, CDCl_3): δ (ppm) = 3.56 (dd, J = 9.7, 3.8 Hz, 1H), 3.37 (dd, J = 9.7, 6.9 Hz, 1H), 2.46 (dt, J = 10.9, 8.2 Hz, 1H), 2.08 – 2.01 (m, 2H), 1.97 – 1.91 (m, 3H), 1.89 – 1.81 (m, 2H), 1.67 – 1.62 (m, 1H), 1.58 (s, 1H), 1.53 – 1.43 (m, 1H), 1.29 (s, 3H), 1.26 (s, 3H), 0.96 – 0.85 (m, 21H), 0.54 (q, J = 7.9 Hz, 6H), 0.02 (s, 6H);

¹³C-NMR (101 MHz, CDCl_3): δ (ppm) = 221.2, 86.5, 76.6, 66.8, 63.5, 48.0, 40.2, 37.1, 34.7, 27.0, 26.1, 24.5, 23.1, 18.5, 18.0, 7.1, 6.5, -5.3;

HRMS(ESI): Calcd for $\text{C}_{26}\text{H}_{52}\text{O}_4\text{NaSi}_2$ [$\text{M}+\text{Na}$]⁺: 507.3302; found: 507.3298.

³⁴ The solution was prepared by mixing 2 mL of NaOH (2 M aq. sol.) with 4 mL of H_2O_2 at 0°C .

Chloromethyldimethylsilyl functionalized α -hydroxyketone (**97**)



2,6-lutidine (30 μL , 263 μmol , 4.0 equiv.) and chloromethyldimethylsilyltriflate (34 mg, 132 μmol , 2.0 equiv.) were sequentially added to a solution of α -hydroxyketone (**96**) (32 mg, 65.8 μmol , 1.0 equiv.) in dry CH_2Cl_2 (330 μL) at $0\text{ }^\circ\text{C}$. The mixture was stirred at r.t. for 2 h, when the same amounts of 2,6-lutidine and triflate were added. The mixture was stirred for further 16 h, before water (2.5 mL) was added; it was then diluted with CH_2Cl_2 (2.0 mL), the phases were separated and the aqueous phase extracted with CH_2Cl_2 (3x, 2.5 mL); the combined organic layers were washed with brine (5.0 mL), dried over Na_2SO_4 and concentrated under reduced pressure. Column chromatography (PE:EA = 12:1) afforded pure functionalized hydroxyketone (**97**) (17 mg, 28.0 μmol , 81% brsm).

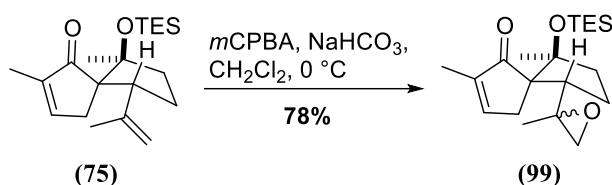
R_f (PE:EtOAc = 4:1; vanillin) = 0.74 (pink);

$^1\text{H-NMR}$ (400 MHz, CDCl_3): δ (ppm) = 3.55 (dd, J = 9.7, 3.8 Hz, 1H), 3.36 (dd, J = 9.7, 7.2 Hz, 1H), 2.79 (d, J = 4.8 Hz, 2H), 2.39 – 2.30 (m, 1H), 2.08 – 1.77 (m, 5H), 1.68 – 1.59 (m, 1H), 1.52 – 1.45 (m, 1H), 1.31 (s, 3H), 1.22 (s, 3H), 0.92 – 0.87 (m, 21H), 0.52 (q, J = 7.9 Hz, 6H), 0.24 (d, J = 7.8 Hz, 6H), 0.02 (s, 6H);

$^{13}\text{C-NMR}$ (101 MHz, CDCl_3): δ (ppm) = 218.7, 86.5, 79.5, 66.6, 62.9, 48.1, 40.0, 37.3, 36.8, 31.3, 29.9, 26.7, 26.3, 26.1, 24.5, 22.7, 18.5, 18.3, 7.1, 6.5, -0.9, -5.2;

HRMS(ESI): Calcd for $\text{C}_{29}\text{H}_{57}\text{O}_4\text{NaClSi}_3$ [$\text{M}+\text{Na}$] $^+$: 613.3307; found: 613.3300.

Epoxyenones (**99**)



NaHCO₃ (62.3 mg, 741 μmol, 2.0 equiv.) and *m*CPBA (75% in water, 128 mg, 556 μmol, 1.5 equiv.) were added to a stirred solution of enone (**75**) (*endo:exo* = 5:1, 124 mg, 371 μmol, 1.0 equiv.) in CH₂Cl₂ (4.0 mL) at 0 °C. After 15 h, Na₂S₂O₃ (2 mL) and NaHCO₃ (2 mL) were added. The mixture was diluted with CH₂Cl₂ (5 mL), and stirred vigorously until two clear phases were obtained. The phases were separated and the aqueous phase was extracted with CH₂Cl₂ (3x, 5 mL). The combined organic phases were washed with NaHCO₃ (15 mL) and brine (15 mL), dried over Na₂SO₄ and concentrated under reduced pressure. Purification *via* column chromatography (PE:EtOAc = 25:1 to 10:1) gave epoxyenone (**99a**) (60.5 mg, 173 μmol, 47%) as a colorless oil and (**99b**) (40.3 mg, 115 μmol, 31%) as a white solid.

The relative configuration of the epoxides could not be determined. When trying the Ti-mediated reductive cyclization, the diastereomers were distinguished by their *R_f*-values:

Analytical data for (**99a**):³⁵

R_f (PE:EtOAc = 10:1; vanillin) = 0.42 (bright-green).

¹H-NMR (400 MHz, CDCl₃): δ(ppm) = 7.22–7.17 (m, 1H), 3.40 (t, *J* = 8.8 Hz, 1H), 2.89–2.80 (m, 1H), 2.50 (d, *J* = 4.8 Hz, 1H), 2.35 (d, *J* = 4.8 Hz, 1H), 2.22–2.13 (m, 1H), 1.80–1.76 (m, 3H), 1.75–1.59 (m, 3H), 1.38–1.29 (m, 1H), 1.07 (s, 3H), 0.97 (s, 3H), 0.93 (t, *J* = 7.9 Hz, 9H), 0.60–0.52 (m, 6H).

¹³C-NMR (101 MHz, CDCl₃): δ(ppm) = 207.9, 153.6, 142.5, 87.1, 63.8, 56.8, 51.4, 46.0, 39.6, 34.6, 22.3, 22.0, 20.8, 10.7, 7.3, 6.8.

HRMS(ESI): Calcd for [M+Na]⁺: C₂₀H₃₄O₃SiNa: 373.2175; found: 373.2184.

Analytical data for (**99b**):

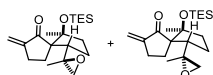
R_f (PE:EtOAc = 10:1; vanillin) = 0.32 (dark-green).

¹H-NMR (400 MHz, CDCl₃): δ(ppm) = 7.19–7.15 (m, 1H), 3.22 (t, *J* = 9.1 Hz, 1H), 2.76–2.66 (m, 1H), 2.59 (d, *J* = 4.4 Hz, 1H), 2.47 (d, *J* = 4.4 Hz, 1H), 2.25–2.16 (m, 1H), 1.98–1.85 (m, 2H), 1.80–1.72 (m, 3H), 1.67–1.57 (m, 1H), 1.36–1.27 (m, 1H), 1.13 (s, 6H), 0.92 (t, *J* = 7.9 Hz, 9H), 0.60–0.49 (m, 6H).

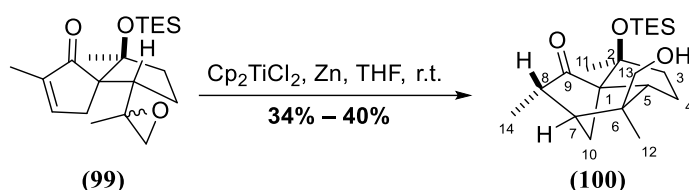
¹³C-NMR (101 MHz, CDCl₃): δ(ppm) = 208.4, 153.6, 142.0, 86.6, 63.3, 57.7, 52.0, 46.5, 39.6, 33.7, 23.2, 23.1, 22.8, 10.7, 7.2, 6.7;

HRMS(ESI): Calcd for [M+Na]⁺: C₂₀H₃₄O₃SiNa: 373.2175; found: 373.2169.

³⁵ Epoxide (**99a**) was obtained as an inseparable mixture with two other compounds which we identified as the epoxides of *exo*-(**75**):



Tricycle (100)



The cyclization of (**99**) was performed according to a variation of the procedure published by Bermejo and co-workers.³⁶

Degassed³⁷ THF (2.5 mL) was added at r.t. to a mixture of Cp_2TiCl_2 (59.7 mg, 240 μmol , 3.0 equiv.) and Zn powder (47.0 mg, 719 μmol , 9.0 equiv.). After 70 min, a solution of epoxide (**99a**) (28.0 mg, 79.9 μmol , 1.0 equiv.) in degassed³⁷ THF (2.5 mL) was added dropwise at r.t. over 5 min. After 45 min, the reaction was quenched by addition of aqueous NaH_2PO_4 (10 wt%, 1 mL) and brine (1 mL). The mixture was stirred vigorously for 30 min, was diluted with MTBE (5 mL), the phases were separated and the aqueous phase was extracted with MTBE (3x, 5 mL). The combined organic phases were washed with brine (10 mL), dried over Na_2SO_4 and concentrated under reduced pressure. Purification by column chromatography (PE:EtOAc = 10:1) gave cyclized product (**100**) (9.5 mg, 26.9 μmol , 34%) as a colorless oil.

R_f (PE:EtOAc =2:1; vanillin) = 0.64 (turquoise).

¹H-NMR (600 MHz, C_6D_6): δ (ppm) = 3.09 (d, J = 10.4 Hz, 1H, H-13a), 3.02 (d, J = 10.4 Hz, 1H, H-13b), 2.19 (dq, J = 7.4, 3.6 Hz, 1H, H-8), 2.13–2.08 (m, 1H, H-5), 1.92–1.81 (m, 1H, H-4a), 1.72 (m, 2H, H-{3a,7}), 1.55–1.45 (m, 2H, H-{3b,4b}), 1.35–1.32 (m, 1H, H-10a), 1.31–1.27 (m, 1H, H-10b), 1.29 (s, 3H, CH_3 -11), 1.15 (t, J = 7.9 Hz, 9H, OTES), 1.01 (d, J = 7.4 Hz, 3H, CH_3 -14), 1.00 (s, 3H, CH_3 -12), 0.88–0.80 (m, 3H, OTES), 0.76–0.69 (m, 3H, OTES).

¹³C-NMR (151MHz, C_6D_6): δ (ppm) = 212.6 (C-9), 80.7 (C-2), 73.0 (C-1), 69.3 (C-13), 49.0 (C-7), 48.6 (C-5), 47.0 (C-6), 43.6 (C-8), 42.4 (C-3), 36.0 (C-10), 23.2 (C-11), 22.0 (C-12), 21.8 (C-4), 14.9 (C-14), 7.6 (OTES), 7.3 (OTES).

HRMS(ESI): Calcd for $\text{C}_{20}\text{H}_{36}\text{O}_3\text{SiNa}$ [$\text{M}+\text{Na}$]⁺: 375.2331; found: 375.2339.

The same procedure was applied to epoxide (**99b**) (18.0 mg, 51.3 μmol , 1.0 equiv) yielding cyclization product (**100**) (7.3 mg, 20.7 μmol , 40%) as a colorless oil.

The cyclization of both epoxide diastereomers (**99a**) and (**99b**) afforded the same product (**100**).

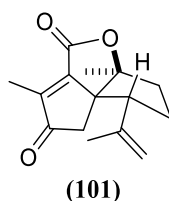
³⁶ *Tetrahedron* **2006**, *62*, 8933–8942.

³⁷ The freeze-pump-thaw technique was used.

PART 2: original approach

This section will report the analytics of racemic compounds which were only isolated during the preliminary racemic scouting of the route. For all of the other compounds, complete analytics and procedures will be found in Part 3.

Lactone (101)



Appearance: colorless oil.

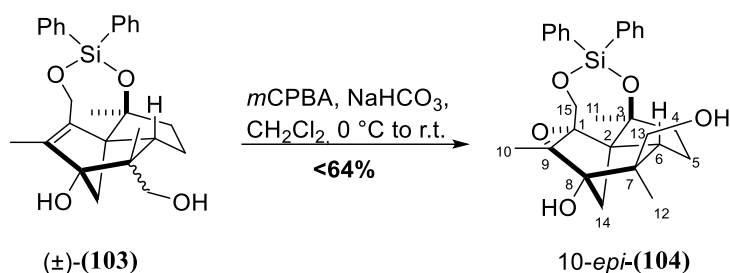
R_f (PE:EtOAc = 5:1; vanillin) = 0.42 (dark-green).

¹H-NMR (400 MHz, CDCl₃): δ (ppm) = 4.98–4.94 (m, 1H), 4.75–4.70 (m, 1H), 2.85 (dd, J = 11.8, 5.8 Hz, 1H), 2.59 (d, J = 18.0 Hz, 1H), 2.33 (ddd, J = 14.9, 10.1, 8.2 Hz, 1H), 2.22 (d, J = 18.0 Hz, 1H), 2.07–1.96 (m, 2H), 2.04 (s, 3H), 1.89–1.77 (m, 1H), 1.58 (s, 3H), 1.33 (s, 3H).

¹³C-NMR (101 MHz, CDCl₃): δ (ppm) = 208.4, 164.8, 160.5, 143.9, 142.7, 114.7, 98.5, 60.9, 53.4, 40.6, 36.8, 30.0, 23.4, 22.5, 9.1.

HRMS(ESI): Calcd for C₁₅H₁₈O₃Na [M+Na]⁺ = 269.1154; found: 269.1159.

Diphenylsilyl-protected epoxide 10-*epi*-(**104**)



*m*CPBA (75% wt. in water, 7.4 mg, 32.1 μmol , 1.5 equiv.) was added in one portion to a mixture of norbornane (±)-(103) (9.6 mg, 21.4 μmol , 1.0 equiv.) and NaHCO_3 (5.4 mg, 64.2 μmol , 3.0 equiv.) in dry CH_2Cl_2 (460 μL) at 0 $^\circ\text{C}$. The mixture was stirred at r.t. for 24 h, before $\text{Na}_2\text{S}_2\text{O}_3$ (2.5 mL) was added at 0 $^\circ\text{C}$. The mixture was diluted with CH_2Cl_2 (2.0 mL), the phases were separated and the aqueous phase extracted with CH_2Cl_2 (3x, 2.5 mL); the combined organic layers were washed with brine (5.0 mL), dried over Na_2SO_4 and concentrated under reduced pressure. Column chromatography (PE:EA = 2.3:1) afforded slightly impure epoxide 10-*epi*-(104) (6.3 mg, 13.6 μmol , 64%) as a white residue.

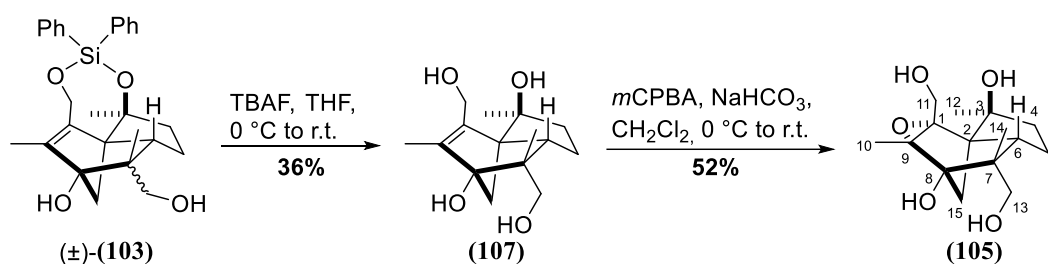
R_f (CH_2Cl_2 :MeOH = 9:1; vanillin) = 0.48 (pink);

$^1\text{H-NMR}$ (400 MHz, CDCl_3): δ (ppm) = 7.68 (dd, J = 8.0, 1.5 Hz, 2H, - SiPh_2), 7.61 (dd, J = 8.0, 1.6 Hz, 2H, - SiPh_2), 7.45 – 7.32 (m, 6H, - SiPh_2), 4.27 (d, J = 12.5 Hz, 1H, H-15a), 3.71 (d, J = 12.5 Hz, 1H, H-15b), 3.62 (d, J = 7.6 Hz, 1H, H-13a), 3.49 (d, J = 7.6 Hz, 1H, H-13b), 3.12 (bs, 1H, OH), 2.49 – 2.38 (m, 1H, H-6), 2.15 (d, J = 9.6 Hz, 1H, H-14a), 2.11 – 2.06 (m, 1H, H-5a), 2.02 – 1.93 (m, 1H, H-4a), 1.96 – 1.93 (m, 2H, H-{4b, 5b}), 1.48 (d, J = 9.8 Hz, 1H, H-14b), 1.27 (s, 3H, H-11), 1.23 (s, 3H, H-10), 1.04 (s, 3H, H-12);

$^{13}\text{C-NMR}$ (101 MHz, CDCl_3): δ (ppm) = 134.8, 134.5, 134.3, 133.6, 130.5, 130.5, 128.0, 128.0, 92.8, 88.7, 85.5, 82.5, 79.1, 62.3, 61.8, 51.9, 51.1, 42.7, 39.0, 25.3, 21.7, 14.9, 14.0;

HRMS(ESI): Calcd for $\text{C}_{27}\text{H}_{32}\text{O}_5\text{NaSi}$ [$\text{M}+\text{Na}$] $^+$: 487.1917; found: 487.1916.

Epoxide (104)



TBAF (1 M in THF, 200 μ L, 200 μ mol, 2.4 equiv.) was added dropwise to a solution of norbornane (±)- **103** (38.4 mg, 85.6 μ mol, 1.0 equiv.) in dry THF (1.7 mL) at 0 °C. The mixture was stirred at r.t. for 24 h, before Na₂S₂O₃ (2.5 mL) was added at 0 °C. The mixture was stirred at 0 °C for 10 min, then at r.t. for further 3 h. Phosphate buffer (pH 7, 2.0 mL) was slowly added, the phases were separated and the aqueous phase extracted with ethyl acetate (3x, 2.5 mL); the combined organic layers were dried over Na₂SO₄ and concentrated under reduced pressure. Column chromatography (PE:EA = 1:1.5) afforded impure tetraol **107** – desired isomer – (8.3 mg, 30.9 μ mol, 36%) as a white residue. Extensive characterization, as well as determination of the relative stereochemistry, was performed after further purification at the epoxide stage. Undesired isomer was always obtained as a mixture with a major impurity and in unreproducible yields.

R_f (PE:EA = 1:1.5; Hanessian's stain) = 0.13;

¹H-NMR (600 MHz, MeOD): δ (ppm) = 4.58 (s, 1H), 4.33 (d, J = 13.7 Hz, 1H), 4.17 (d, J = 13.0 Hz, 1H), 3.91 (d, J = 11.0 Hz, 1H), 3.67 (d, J = 11.0 Hz, 1H), 2.25 (t, J = 7.5 Hz, 1H), 2.22 – 2.17 (m, 1H), 2.05 – 2.00 (m, 1H), 1.98 – 1.95 (m, 1H), 1.90 – 1.84 (m, 2H), 1.78 (d, J = 7.7 Hz, 1H), 1.74 (s, 1H), 1.64 – 1.59 (m, 2H), 1.31 (s, 3H), 1.20 (s, 3H), 0.96 (s, 3H);

HRMS(ESI): Calcd for C₁₅H₂₄O₄NaSi [M+Na]⁺: 291.1572; found: 291.1567.

*m*CPBA (75% wt. in water, 12 mg, 48.2 μ mol, 2.0 equiv.) was added in one portion to a mixture of norbornane **107** (6.5 mg, 24.2 μ mol, 1.0 equiv.) and NaHCO₃ (6.1 mg, 72.6 μ mol, 3.0 equiv.) in dry CH₂Cl₂ (590 μ L) at 0 °C. The mixture was stirred at r.t. for 1.5 h, before Na₂S₂O₃ (1 mL) was added at 0 °C. The mixture was diluted with CH₂Cl₂ (1 mL), the phases were separated and the aqueous phase extracted with CH₂Cl₂ (3x, 1 mL); the combined organic layers were dried over Na₂SO₄ and concentrated under reduced pressure. Column chromatography (CH₂Cl₂:MeOH = 9:1) afforded pure epoxide **104** (3.6 mg, 12.7 μ mol, 52%) as a white solid.

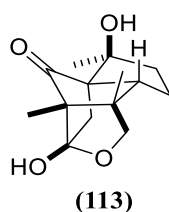
R_f (CH₂Cl₂:MeOH = 85:15; Hanessian's stain) = 0.62;

¹H-NMR (600 MHz, CDCl₃): δ (ppm) = 4.13 (d, J = 11.5 Hz, 1H, H-11a), 3.69 (d, J = 8.7 Hz, 1H, H-13a), 3.51 (d, J = 8.7 Hz, 1H, H-13b), 3.38 (dd, J = 11.5, 0.8 Hz, 1H, H-11b), 2.87 (ddd, J = 11.8, 8.1, 2.5 Hz, 1H, H-6), 2.31 (d, J = 13.1 Hz, 1H, H-15a), 2.14 - 2.10 (m, 1H, H-4a), 1.99 - 1.96 (m, 1H, H-4b), 1.80 (d, J = 13.0 Hz, 1H, H-15b), 1.68 - 1.62 (m, 1H, H-5a), 1.58 - 1.51 (m, 1H, H-5b), 1.30 (s, 3H, H-12), 0.98 (s, 3H, H-14), 0.85 (s, 3H, H-10);

¹³C-NMR (151 MHz, CDCl₃): δ (ppm) = 111.5 (C-8), 84.3 (C-1, C-9), 76.4 (C-3), 70.2 (C-7), 62.6 (C-2, C-7), 60.2 (C-11), 53.3 (C-6), 44.8 (C-4), 43.4 (C-15), 25.1 (C-12), 21.9 (C-14), 18.7 (C-5), 5.8 (C-10);

HRMS(ESI): Calcd for C₁₅H₂₄O₅NaSi [M+Na]⁺: 307.1521; found: 307.1524.

Lactone (113)



R_f (CH₂Cl₂:MeOH = 4:1; Hanessian's) = 0.53.

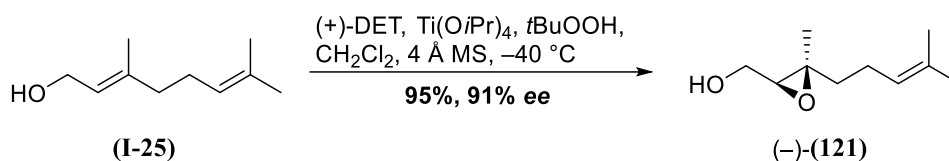
¹H-NMR (400 MHz, MeOD): δ (ppm) = 3.82 (d, J = 8.6 Hz, 1H), 3.59 (d, J = 8.6 Hz, 1H), 2.90 (t, J = 9.0 Hz, 1H), 2.16 (d, J = 13.3 Hz, 1H), 2.14 – 2.06 (m, 1H), 2.07 – 1.99 (m, 1H), 1.96 (dd, J = 13.4, 1.8 Hz, 1H), 1.76 – 1.65 (m, 2H), 1.26 (s, 3H), 1.02 (s, 3H), 0.87 (s, 3H);

¹³C-NMR (101 MHz, MeOD): δ (ppm) = 210.5, 107.5, 75.2, 70.7, 64.6, 61.4, 54.8, 54.5, 45.4, 42.5, 24.59, 21.5, 19.0, 4.67;

HRMS(ESI): Calcd for C₁₄H₂₀O₄Na [M+Na]⁺ = 275.1259; found: 275.1249.

PART 3: asymmetric total synthesis

(2S,3S)-2,3-Epoxy geraniol (-)-(121)



(-)-(121) was synthesized according to the procedure published by Echavarren and co-workers.³⁸

A 2 L three-necked flask, equipped with an overhead stirrer with inert gas inlet, dropping funnel and thermometer, was charged under argon with 4 Å MS (25.0 g) and anhydrous CH₂Cl₂ (500 mL). The stirred mixture was cooled to -20 °C (internal temperature), before (+)-DET (7.8 mL, 45.4 mmol, 14 mol%) and Ti(OiPr)₄ (9.0 mL, 30.5 mmol, 9.4 mol%) were added. *t*BuOOH (4.64 M in CH₂Cl₂, 238 mL, 1.10 mol, 3.4 equiv.) was added *via* dropping funnel over 30 min, maintaining the internal temperature below -20 °C. The dropping funnel was rinsed with anhydrous CH₂Cl₂ (20.0 mL) and stirring at -20 °C was continued for 30 min. The mixture was cooled to -40 °C and a solution of geraniol (**I-25**) (50.0 g, 324 mmol, 1.0 equiv.) in anhydrous CH₂Cl₂ (50.0 mL) was added over 2 h *via* dropping funnel. After complete addition, the dropping funnel was rinsed with anhydrous CH₂Cl₂ (20.0 mL) and stirring at -40 °C was continued for 40 min. Water (200 mL) was added at -40 °C under vigorous stirring and the mixture was allowed to warm to r.t.. 100 mL of an aqueous solution containing 30% NaOH and 5% NaCl were added and the mixture was stirred vigorously at r.t. for 45 min; phase separation was obtained after addition of a small volume of MeOH (approx. 5.0 mL). The phases were separated and the white aqueous phase was extracted with CH₂Cl₂ (3x, 200 mL). The combined organic phases were dried over Na₂SO₄, filtered over Celite[®] and concentrated under reduced pressure. The crude product was dried with a rotary evaporator to remove the majority of excess *t*BuOOH.³⁹ Distillation under reduced pressure gave epoxy geraniol (-)-(121) (52.3 g, 307 mmol, 95%, 91% ee) as a colorless oil.

b.p.(1.3 mbar) = 97 °C.

R_f (PE:EtOAc = 4:1; vanillin) = 0.20 (dark blue).

¹H-NMR (400 MHz, CDCl₃): δ(ppm) = 5.11–5.04 (m, 1H), 3.86–3.76 (m, 1H), 3.73–3.63 (m, 1H), 2.97 (dd, *J* = 6.7, 4.3 Hz, 1H), 2.13–2.03 (m, 2H), 1.94–1.86 (m, 1H), 1.72–1.63 (m, 4H), 1.60 (s, 3H), 1.51–1.42 (m, 1H), 1.29 (s, 3H).

¹³C-NMR (101 MHz, CDCl₃): δ(ppm) = 132.2, 123.4, 63.2, 61.5, 61.3, 38.6, 25.7, 23.8, 17.7, 16.8.

HRMS(ESI): Calcd for C₁₀H₁₈O₂Na [M+Na]⁺: 193.1204; found: 193.1209.

[α]_D²² = -4.8 (*c* = 1.7, CHCl₃).

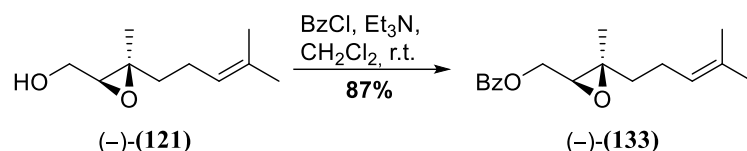
The obtained analytical data match the data reported by Mohapatra and co-workers.⁴⁰

³⁸ *ChemMedChem* **2016**, *11*, 1003–1007.

³⁹ Extended evaporation times were necessary to remove the majority of *t*BuOOH.

⁴⁰ *Eur. J. Org. Chem.* **2007**, *2007*, 5059–5063.

The enantiomeric excess was determined by chiral HPLC after formation of the corresponding benzoate:



Et₃N (48.8 μ L, 350 μ mol, 1.8 equiv.) and benzoyl chloride were added sequentially at r.t. to a stirred solution of epoxy geraniol (-)-(121) (34.0 mg, 200 μ mol, 1.0 equiv.) in anhydrous CH₂Cl₂ (1.0 mL). Stirring at r.t. was continued for 5.5 h, the mixture was diluted with MTBE and washed with aqueous NaOH (1 M, 3x, 1.0 mL), NaHCO₃ (3x, 1.0 mL) and brine (1x, 1.0 mL). The organic phase was dried over Na₂SO₄ and concentrated under reduced pressure. Purification by column chromatography (PE:EtOAc = 25:1) afforded benzoate (-)-(133) (47.5 mg, 173 μ mol, 87%) as a colorless oil.

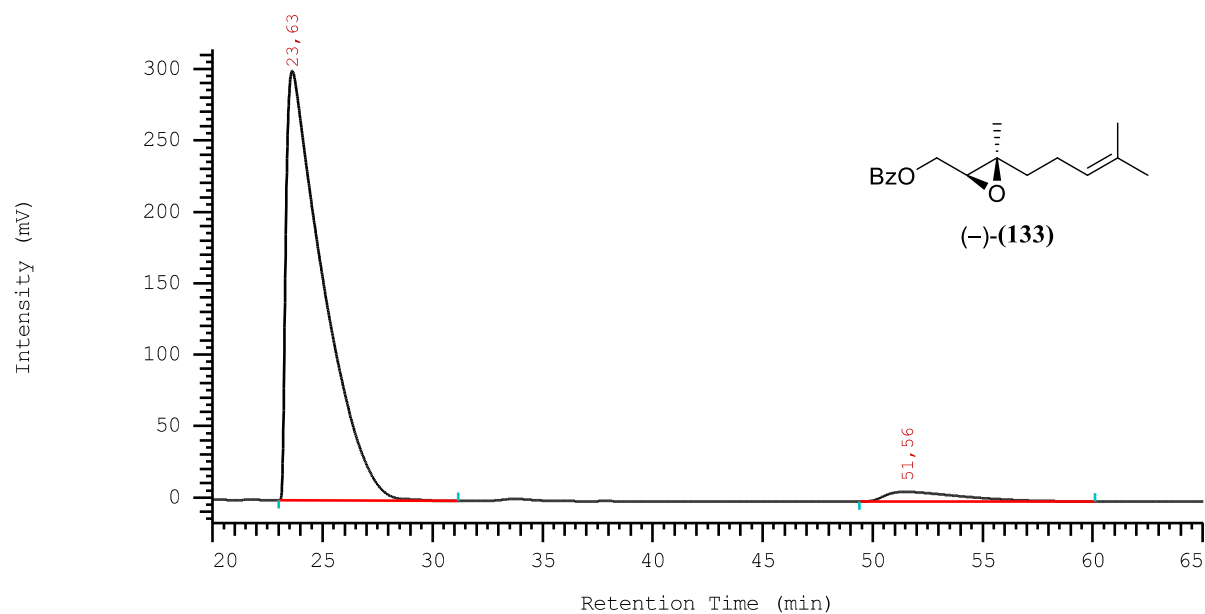
R_f (PE:EtOAc = 10:1; vanillin) = 0.57 (dark blue).

¹H-NMR (400 MHz, CDCl₃): δ (ppm) = 8.08 (d, J = 7.3 Hz, 2H), 7.57 (t, J = 7.3 Hz, 1H), 7.45 (t, J = 7.7 Hz, 2H), 5.13–5.05 (m, 1H), 4.57 (dd, J = 12.1, 4.3 Hz 1H), 4.29 (dd, J = 12.1, 6.7 Hz, 1H), 3.14 (dd, J = 6.8, 4.2 Hz, 1H), 2.21–2.02 (m, 2H), 1.77–1.68 (m, 1H), 1.66 (s, 3H), 1.61 (s, 3H), 1.56–1.46 (m, 1H), 1.38 (s, 3H).

¹³C-NMR (101 MHz, CDCl₃): δ (ppm) = 166.6, 133.3, 132.4, 129.93, 129.88, 128.5, 123.3, 64.1, 60.8, 59.9, 38.5, 25.8, 23.8, 17.8, 17.1.

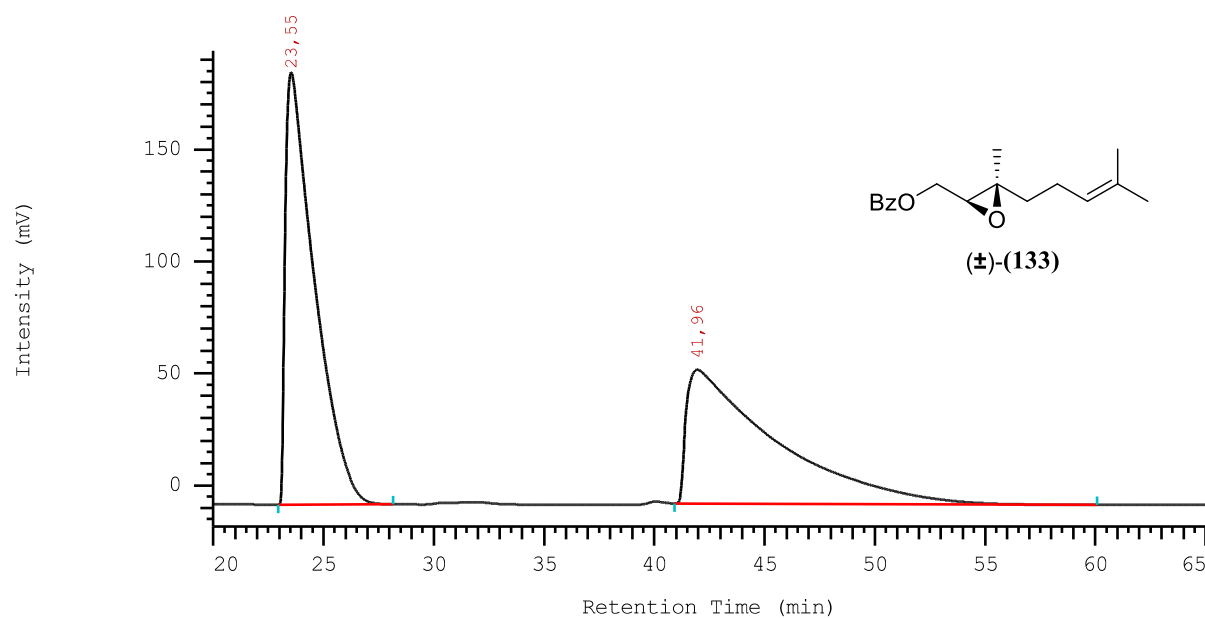
HRMS(ESI): Calcd for C₁₇H₂₂O₃Na [M+Na]⁺: 297.1467; found: 297.1457.

$[\alpha]_{\text{D}}^{22}$ = -13.0 (c = 2.2, CHCl₃).



No.	RT	Area	Conc 1	BC
1	23,63	35011225	95,487	BB
2	51,56	1654714	4,513	MC
			100,000	

Figure H1. Chromatogram of enantioenriched epoxy geraniol benzoate (-)-(133).



No.	RT	Area	Conc 1	BC
1	23,55	17641064	51,386	MC
2	41,96	16689500	48,614	MC
			100,000	

Figure H2. Chromatogram of racemic epoxy geraniol benzoate (±)-(133).

HPLC setup:

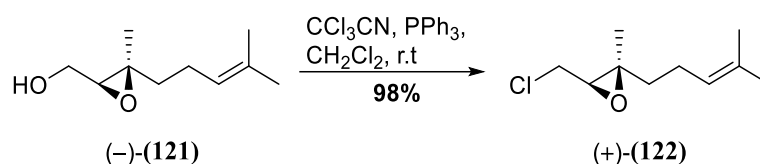
Merck/Hitachi La Chrome®-HPLC-system with L-7150 pump, L-7200 autosampler and L-7400-UV-detector

Column: Daicel Chiracel® OD-H (250 mm x 4.6 mm)

Eluent: *n*-Hexane:*iso*-propanol = 200:1

Flow rate: 0.5 mL/min

(2*S*,3*R*)-3-(Chloromethyl)-2-methyl-2-(4-methylpent-3-en-1-yl)oxirane (+)-(122)



(+)-(122) was synthesized after a modification of the procedure published by Chavasiri and co-workers.⁴¹

A 1 L two-necked flask equipped with a reflux condenser and a rubber septum was charged under argon with PPh₃ (95.2 g, 363 mmol, 1.2 equiv.), epoxy geraniol (-)-(121) (51.5 g, 302 mmol, 1.0 equiv.) and anhydrous CH₂Cl₂ (300 mL). Trichloroacetonitrile (36.4 mL, 363 mmol, 1.2 equiv.) was added carefully at r.t.. The addition rate was adjusted so that the reaction mixture maintained a gentle reflux. The amber reaction mixture was stirred at r.t. for additional 40 min, water (200 mL) was added and the mixture stirred vigorously for 15 min. The phases were separated and the aqueous phase was extracted with CH₂Cl₂ (3x, 200 mL). The combined organic phases were dried over Na₂SO₄ and concentrated under reduced pressure. The crude product was applied on silica and purified by column chromatography (PE:EtOAc = 25:1) to afford epoxy chloride (+)-(122) (55.7 g, 295 mmol, 98%) as a light yellow oil.

R_f (PE:EtOAc = 10:1; vanillin) = 0.60 (grey-blue).

¹H-NMR (400 MHz, CDCl₃): δ (ppm) = 5.12–5.06 (m, 1H), 3.69 (dd, J = 11.4, 5.9 Hz, 1H), 3.44 (dd, J = 11.4, 7.2 Hz, 1H), 3.03 (dd, J = 7.1, 5.9 Hz, 1H), 2.14–2.06 (m, 2H), 1.76–1.65 (m, 4H), 1.61 (s, 3H), 1.50–1.41 (m, 1H), 1.32 (s, 3H).

¹³C-NMR (101 MHz, CDCl₃): δ (ppm) = 132.4, 123.3, 62.3, 61.7, 42.4, 38.4, 25.8, 23.9, 17.8, 16.4.

HRMS(CI): Calcd for C₁₀H₁₈OCl [M+H]⁺: 189.1046; found: 189.1039.

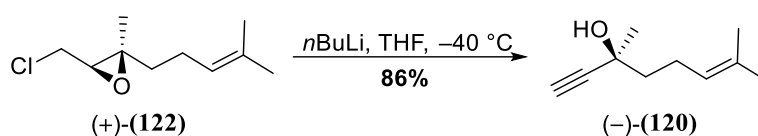
$[\alpha]_D^{22}$ = +12.2 (c = 5.3, CHCl₃).

The obtained analytical data match the data reported by Mohapatra and co-workers.⁴²

⁴¹ *Tetrahedron Lett.* **2006**, *47*, 6821–6823.

⁴² *Eur. J. Org. Chem.* **2007**, *2007*, 5059–5063.

(S)-3,7-Dimethyloct-6-en-1-yn-3-ol (-)-(120)



(-)-(120) was synthesized according to the procedure published by Echavarren and co-workers.⁴³

*n*BuLi (2.5 M in hexanes, 413 mL, 1.03 mol, 3.5 equiv.) was added over 1.5 h to a stirred solution of epoxy chloride (+)-(122) (55.7 g, 295 mmol, 1.0 equiv.) in anhydrous THF (420 mL) at $-40\text{ }^\circ\text{C}$. The solution turned deep brown upon addition of the organolithium reagent. After complete addition stirring at $-40\text{ }^\circ\text{C}$ was continued for 2 h, before NH_4Cl (100 mL) was added and the mixture was allowed to warm to r.t. under vigorous stirring. The phases were separated and the aqueous phase was extracted with Et_2O (3x, 100 mL). The combined organic phases were washed with brine (200 mL), dried over Na_2SO_4 and concentrated under reduced pressure to afford a dark-brown oil. After purification by vacuum distillation propargylic alcohol (-)-(120) (38.5 g, 252 mmol, 86%) was obtained as a colorless oil.

b.p. (40 mbar) = $103\text{ }^\circ\text{C}$.

R_f (PE:EtOAc = 10:1; vanillin) = 0.36 (blue).

¹H-NMR (400 MHz, CDCl_3): δ (ppm) = 5.21–5.12 (m, 1H), 2.46 (s, 1H), 2.36–2.24 (m, 1H), 2.24–2.12 (m, 1H), 1.97 (bs, 1H), 1.74–1.67 (m, 2H), 1.70 (s, 3H), 1.66 (s, 3H), 1.50 (s, 3H).

¹³C-NMR (101 MHz, CDCl_3): δ (ppm) = 132.7, 123.8, 87.7, 71.6, 68.4, 43.3, 29.9, 25.8, 23.7, 17.8.

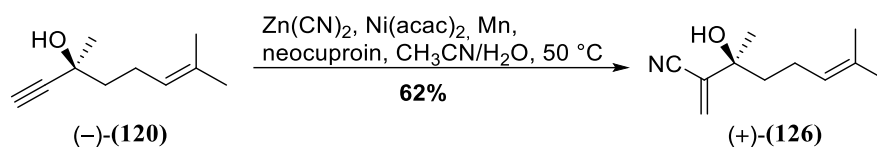
HRMS(CI): Calcd for $\text{C}_{10}\text{H}_{17}\text{O}$ $[\text{M}+\text{H}]^+$: 153.1279; found: 153.1284.

$[\alpha]_{\text{D}}^{22} = -12.9$ ($c = 2.9$, CHCl_3).

The obtained analytical data match the data reported by Mohapatra and co-workers.⁴²

⁴³ *ChemMedChem* 2016, 11, 1003–1007.

β -hydroxy acrylonitrile (+)-(126)



(+)-(126) was synthesized after a variation of the protocol published by Liu and co-workers.⁴⁴

Ni(acac)₂ (6.41 g, 25.0 mmol, 0.1 equiv.), neocuproin (6.24 g, 30.0 mmol, 0.12 equiv.), Zn(CN)₂ (23.5 g, 200 mmol, 0.8 equiv.) and Mn (6.86 g, 125 mmol, 0.5 equiv.) were placed in a Schlenk flask with a rubber septum and the flask was evacuated and backfilled with argon three times. Degassed⁴⁵ MeCN (1.0 L) was added and the green-grey suspension was stirred at r.t. for 20 min. Propargyl alcohol (-)-(120) (38.0 g, 250 mmol, 1.0 equiv.) was added, followed by degassed⁴⁴ water (210 mL). The septum was replaced by a glass stopper, the reaction mixture was heated to 50 °C and stirred for 16 h. The mixture was allowed to cool to r.t., water and MTBE (500 mL each) were added and the mixture was filtered over Celite[®]. The phases were separated and the aqueous phase was extracted with MTBE (3x, 250 mL). The combined organic phases were washed with water and brine, dried over Na₂SO₄ and concentrated under reduced pressure. The crude product was purified by column chromatography (PE:EtOAc = 25:1 to 20:1 to 15:1 to 10:1), followed by bulb-to-bulb distillation (0.4 mbar, 120–130 °C) to give β -hydroxy acrylonitrile (+)-(122) (27.7 g, 155 mmol, 62%) as a light yellow oil.

R_f (PE:EtOAc = 5:1; vanillin) = 0.37 (purple).

¹H-NMR (400 MHz, CDCl₃): δ (ppm) = 6.09 (d, J = 0.6 Hz, 1H), 6.00 (s, 1H), 5.18–5.11 (m, 1H), 2.15–1.96 (m, 2H), 1.89–1.80 (m, 2H) 1.74 (ddd, J = 14.2, 9.0, 7.3 Hz, 1H), 1.71–1.67 (m, 3H), 1.61 (s, 3H), 1.44 (s, 3H).

¹³C-NMR (101 MHz, CDCl₃): δ (ppm) = 133.5, 130.6, 128.9, 123.4, 117.8, 74.6, 40.4, 27.9, 25.8, 22.6, 17.9.

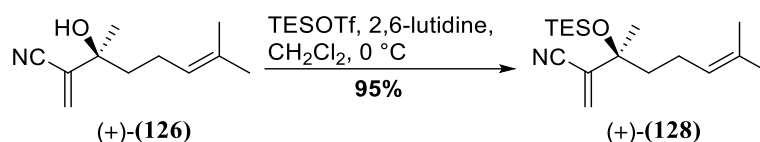
HRMS(ESI): Calcd for C₁₁H₁₇NONa [M+Na]⁺: 202.1208; found: 202.1201.

$[\alpha]_D^{24}$ = +0.9 (c = 30.0, CHCl₃).

⁴⁴ *J. Am. Chem. Soc.* **2018**, *140*, 7385–7389.

⁴⁵ Degassed by sonication under argon for 30 min.

TES-protected β -hydroxy acrylonitrile (+)-(128)



β -hydroxy acrylonitrile (+)-(126) (26.7 g, 149 mmol, 1.0 equiv.) and 2,6-lutidine (34.5 mL, 297 mmol, 2.0 equiv.) were dissolved under argon in anhydrous CH_2Cl_2 (500 mL). The solution was cooled to 0 °C and TESOTf (40.5 mL, 179 mmol, 1.2 equiv.) was added over 1 h *via* syringe pump. After complete addition, stirring at 0 °C was continued for 25 min, before water (250 mL) was added and the mixture allowed to warm to r.t. under vigorous stirring. The phases were separated and the aqueous phase extracted with CH_2Cl_2 (3x, 200 mL). The combined organic phases were washed with water (2x, 250 mL) and brine (250 mL), dried over Na_2SO_4 and concentrated under reduced pressure. Purification *via* column chromatography (PE:EtOAc = 100:1 to 50:1) gave TES-protected β -hydroxy acrylonitrile (+)-(128) (41.3 g, 141 mmol, 95%) as a yellow oil.

R_f (PE:EtOAc = 25:1; vanillin) = 0.60 (dark-blue).

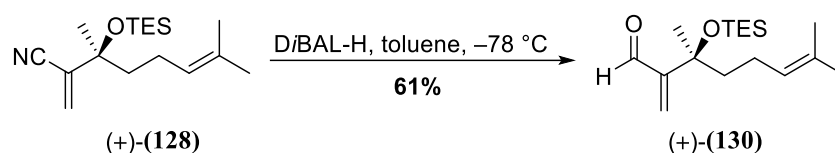
$^1\text{H-NMR}$ (400MHz, CDCl_3): δ (ppm) = 6.04–6.02 (m, 1H), 5.95–5.94 (m, 1H), 5.11–5.04 (m, 1H), 2.07–1.95 (m, 1H), 1.93–1.81 (m, 1H), 1.80–1.71 (m, 1H), 1.67 (s, 3H), 1.64–1.55 (m, 1H), 1.59 (s, 3H), 1.48 (s, 3H), 0.97 (t, J = 7.9 Hz, 9H), 0.64 (q, J = 7.9 Hz, 6H).

$^{13}\text{C-NMR}$ (101MHz, CDCl_3): δ (ppm) = 132.0, 130.8, 128.8, 123.5, 118.0, 76.1, 42.0, 27.9, 25.7, 22.4, 17.6, 7.1, 6.7.

HRMS(ESI): Calcd for $\text{C}_{17}\text{H}_{31}\text{NOSiNa}$ $[\text{M}+\text{Na}]^+$: 316.2073; found: 326.2082.

$[\alpha]_{\text{D}}^{24} = +0.3$ (c = 24.2, CHCl_3).

Aldehyde (+)-(130)



DiBAL-H (1.0 M in toluene, 81.0 mL, 81.0 mmol, 1.2 equiv.) was added over 30 min to a stirred solution of TES-protected β -hydroxy acrylonitrile (+)-(130) (19.8 g, 67.6 mmol, 1.0 equiv.) in anhydrous toluene (675 mL) at $-78\text{ }^\circ\text{C}$. Stirring at $-78\text{ }^\circ\text{C}$ was continued for 3 h. The reaction was then quenched at $-78\text{ }^\circ\text{C}$ by slow addition of MeOH (16.0 mL). Na/K tartrate (1.4 L) was added at $-78\text{ }^\circ\text{C}$, the mixture was diluted with MTBE (0.5 L) and allowed to warm to r.t. under vigorous stirring. After 1 h, the phases were separated and the aqueous phase was extracted with MTBE (3x, 300 mL). The combined organic phases were washed with brine (400 mL), dried over Na_2SO_4 and concentrated under reduced pressure. Purification by column chromatography (PE:EtOAc = 200:1 to 6:1) gave aldehyde (+)-(130) (12.3 g, 41.5 mmol, 61%) as a light yellow oil.

R_f (PE:EtOAc = 25:1; vanillin) = 0.61 (purple).

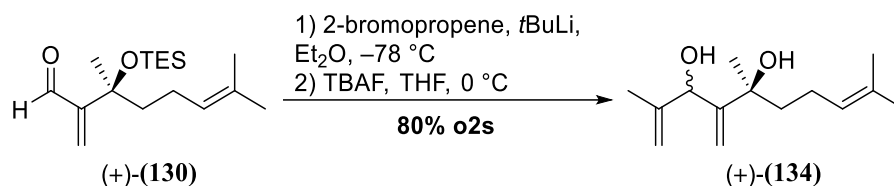
$^1\text{H-NMR}$ (400 MHz, C_6D_6): δ (ppm) = 9.33 (s, 1H), 6.44 (d, $J = 1.9\text{ Hz}$, 1H), 5.49 (d, $J = 1.9\text{ Hz}$, 1H), 5.22–5.15 (m, 1H), 2.31 (ddd, $J = 13.4, 11.7, 5.1\text{ Hz}$, 1H), 2.21–2.09 (m, 1H), 1.85–1.73 (m, 1H), 1.67–1.58 (m, 1H), 1.63–1.61 (m, 3H), 1.55 (s, 3H), 1.48 (s, 3H), 0.97 (t, $J = 7.9\text{ Hz}$, 9H), 0.58 (q, $J = 7.9\text{ Hz}$, 6H).

$^{13}\text{C-NMR}$ (101 MHz, C_6D_6): δ (ppm) = 192.6, 155.7, 135.3, 131.2, 124.9, 76.9, 41.3, 28.5, 25.8, 23.4, 17.7, 7.4, 7.3.

HRMS(ESI): Calcd for $\text{C}_{17}\text{H}_{32}\text{O}_2\text{SiNa}$ [$\text{M}+\text{Na}$] $^+$: 319.2069; found: 319.2078.

$[\alpha]_{\text{D}}^{22} = +17.9$ ($c = 5.2$, CHCl_3).

Diol (+)-(134)



A 1 L Schlenk flask was charged under argon with Et₂O (95 mL) and 2-bromopropene (7.43 g, 61.4 mmol, 1.5 equiv.). The solution was cooled to -78 °C and *t*BuLi (1.9 M in pentane, 63.0 mL, 120 mmol, 2.9 equiv.) was added dropwise over 50 min. After 4 h, a -78 °C cold solution of aldehyde (+)-(130) (12.1 g, 40.9 mmol, 1.0 equiv.) in anhydrous Et₂O (200 mL) was added from a second Schlenk flask *via* transfer cannula over 40 min. The resulting orange solution was stirred at -78 °C for additional 50 min. NH₄Cl (100 mL) was added and the mixture allowed to warm to r.t. under vigorous stirring. The phases were separated and the aqueous phase was extracted with Et₂O (3x, 100 mL). The combined organic phases were washed with brine (100 mL), dried over Na₂SO₄ and concentrated under reduced pressure. The so obtained mono-TES-protected diol was used in the subsequent deprotection without further purification.

The mono-TES-protected diol was dissolved in THF (400 mL), cooled to 0 °C and TBAF (1.0 M in THF, 49.1 mL, 49.1 mmol, 1.2 equiv) was added dropwise over 25 min. Stirring at 0 °C was continued for 1 h, before NH₄Cl (100 mL) was added and the mixture was allowed to warm to r.t.. The phases were separated and the aqueous phase was extracted with EtOAc (3x, 100 mL). The combined organic phases were washed with brine, dried over Na₂SO₄ and concentrated under reduced pressure. Purification by column chromatography (PE:EtOAc = 4:1) gave diol (+)-(134) (7.32 g, 32.6 mmol, 80%, d.r. 4:1) as a pale yellow oil that solidified in the freezer.

R_f (PE:EtOAc = 5:1; vanillin) = 0.21 (dark blue).

¹H-NMR (400 MHz, CDCl₃): δ(ppm) = 5.19–5.16 (m, 1H), 5.15–5.14 (m, 1H), 5.14–5.08 (m, 2H), 5.04–5.00 (m, 1H), 4.75 (bs, 1H), 4.74* (bs, 1H), 2.38 (bs, 2H), 2.08–1.97 (m, 2H), 1.78–1.63 (m, 2H), 1.72–1.70 (m, 3H), 1.69–1.67 (m, 3H), 1.62–1.59 (m, 3H), 1.40* (s, 3H), 1.39 (s, 3H).

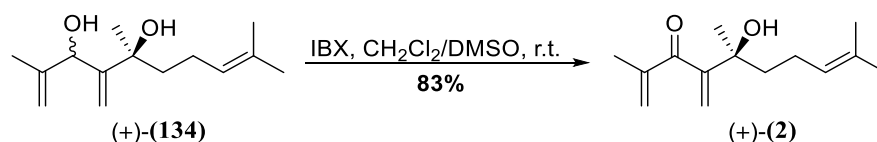
¹³C-NMR (101 MHz, CDCl₃): δ(ppm) = 153.8, 153.3*, 146.5, 146.1*, 132.2, 124.3, 124.2*, 112.7*, 112.1, 111.9*, 111.7, 76.6*, 76.4, 75.63*, 75.56, 42.3*, 42.2, 29.3, 29.0*, 25.8, 23.1*, 22.8, 19.8*, 19.6, 17.9, 17.8*.⁴⁶

HRMS(ESI): Calcd for C₁₄H₂₄O₂Na [M+Na]⁺: 247.1674; found: 247.1674.

[α]_D²² = +8.0 (*c* = 1.0, CHCl₃).

⁴⁶ No distinction between major and minor diastereomer possible for signals at 132.2 ppm and 25.8 ppm.

Cross-conjugated ketone (+)-(2)



IBX (10.8 g, 38.6 mmol, 1.2 equiv.) was added in one portion to a stirred solution of diol (+)-(134) (7.21 g, 32.1 mmol, 1.0 equiv.) in CH_2Cl_2 :DMSO (1:1, 130 mL) and the mixture was stirred at r.t. for 2 h. Water (130 mL) was added under vigorous stirring and the mixture was diluted with CH_2Cl_2 (100 mL). The phases were separated and the aqueous phase was extracted with CH_2Cl_2 (5x, 100 mL). The combined organic phases were washed with water (2x, 300 mL) and brine (300 mL), dried over Na_2SO_4 and concentrated under reduced pressure. Purification *via* column chromatography (PE:EtOAc = 25:1 to 10:1) gave cross-conjugated ketone (+)-(2) (5.95 g, 26.8 mmol, 83%) as a light yellow oil.

b.p. (0.5 mbar) = 91 °C.

R_f (PE:EtOAc = 9:1; vanillin) = 0.44 (turquoise).

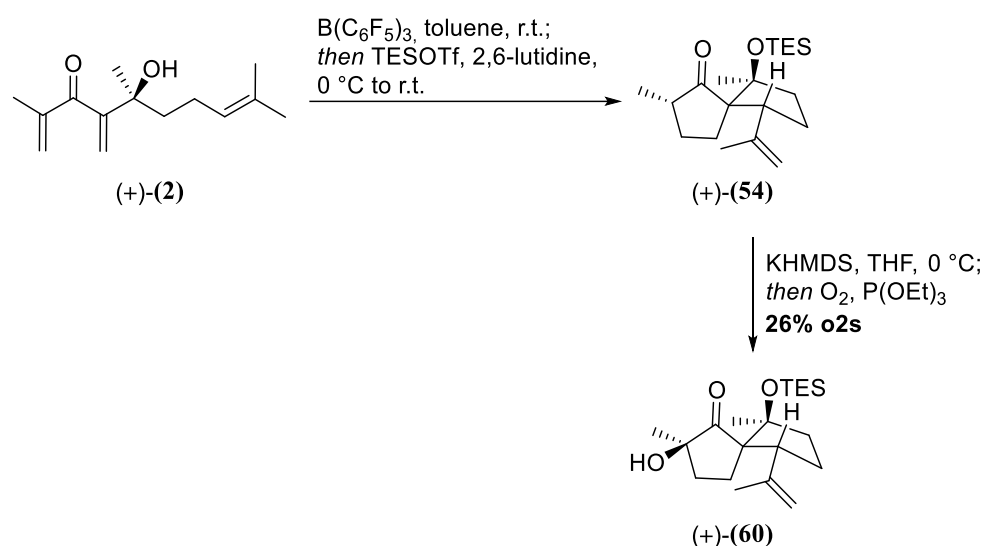
$^1\text{H-NMR}$ (400 MHz, CDCl_3): δ (ppm) = 5.85–5.82 (m, 2H), 5.78 (bs, 1H), 5.59 (s, 1H), 5.11–5.04 (m, 1H), 3.49 (s, 1H), 2.03–1.95 (m, 2H), 1.93 (s, 3H), 1.82–1.73 (m, 1H), 1.69–1.61 (m, 4H), 1.56 (s, 3H), 1.38 (s, 3H).

$^{13}\text{C-NMR}$ (101 MHz, CDCl_3): δ (ppm) = 201.6, 151.7, 144.7, 132.0, 127.9, 124.2, 122.7, 74.8, 41.5, 27.1, 25.8, 23.1, 18.0, 17.8.

HRMS(ESI): Calcd for $\text{C}_{14}\text{H}_{22}\text{O}_2\text{Na}$ $[\text{M}+\text{Na}]^+$: 245.1517; found: 245.1517.

$[\alpha]_{\text{D}}^{22} = +6.0$ ($c = 1.3$, CHCl_3).

α -Hydroxy ketone (+)-(60)



$B(C_6F_5)_3$ (341 mg, 668 μ mol, 2.5 mol%) was added in one portion to a stirred solution of cross-conjugated ketone (+)-(2) (5.92 g, 26.7 mmol, 1.0 equiv.) in toluene (270 mL) at r.t. and stirring at this temperature was continued for 24 h. During this time the solution color changed from nearly colorless over bright pink to orange. The reaction mixture was cooled to 0 °C and 2,6-lutidine (12.5 mL, 108 mmol, 4.0 equiv.) and TESOTf (12.0 mL, 53.2 mmol, 2.0 equiv.) were added successively. The cooling bath was removed and stirring was continued at r.t. for 3 h. Water (200 mL) was added, the phases were separated and the aqueous phase was extracted with EtOAc (3x, 150 mL). Combined organic phases were washed with brine (200 mL), dried over Na_2SO_4 and concentrated under reduced pressure. The crude product purified by column chromatography (PE:EtOAc = 20:1) to separate protected spiro ketone (+)-(54) from the main impurities. Impure (+)-(54) (4.32 g) was obtained as a yellow oil and was used in the following α -oxidation without further purification.

Analytical data of spiro ketone (+)-(54)⁴⁷:

R_f (PE:EtOAc = 9:1; vanillin) = 0.48 (purple).

¹H-NMR (400 MHz, $CDCl_3$): δ (ppm) = 4.78 (s, 1H), 4.63 (s, 1H), 3.21 (dd, J = 11.4, 7.9 Hz, 1H), 2.13–1.95 (m, 3H), 1.93–1.82 (m, 1H), 1.81–1.72 (m, 1H), 1.69–1.60 (m, 2H), 1.59–1.48 (m, 5H), 1.29 (s, 3H), 1.11 (d, J = 6.8 Hz, 3H), 0.92 (t, J = 7.9 Hz, 9H), 0.54 (q, J = 7.9 Hz, 6H).

¹³C-NMR (101 MHz, $CDCl_3$): δ (ppm) = 222.8, 146.1, 113.3, 86.2, 63.8, 51.6, 44.2, 40.4, 28.9, 28.1, 27.8, 26.2, 22.4, 14.1, 7.1, 6.6.

HRMS(ESI): Calcd for $C_{20}H_{36}O_2SiNa$ [$M+Na$]⁺: 359.2382; found: 359.2386.

$[\alpha]_D^{26} = +68.2$ (c = 1.1, $CHCl_3$).

⁴⁷ An analytically pure sample of (+)-(54) was obtained by successive Nazarov cyclization and TES protection with intermediate purification of the unprotected spiro ketone by column chromatography after the protocol described earlier. TES protection was conducted as follows: A solution of the unprotected spiro ketone (1.78 g, 8.01 mmol, 1.0 equiv) in anhydrous CH_2Cl_2 (5.0 mL) was added dropwise to a stirred solution of 2,6-lutidine (2.8 mL, 24.0 mmol, 3.0 equiv) and TESOTf (2.7 mL, 12.0 mmol, 1.5 equiv) in anhydrous CH_2Cl_2 (75 mL) at 0 °C. After complete addition, the solution was allowed to warm to r.t. and stirring was continued for 2.5 h. Water (50 mL) was added, the phases were separated and the aqueous phase was extracted with CH_2Cl_2 (3x). The combined organic phases were washed with brine, dried over Na_2SO_4 and concentrated under reduced pressure. Column chromatography (PE:EtOAc = 200:1 to 100:1) gave TES protected spiro ketone (+)-(54) (2.39 g, 7.10 mmol, 89%) as a light yellow oil.

A solution of purified (+)-**(54)** (4.31 g, 12.8 mmol, 1.0 equiv.) in anhydrous THF (6.5 mL) was placed in a 100 mL Schlenk tube, the solution was cooled to 0 °C and KHMDS (1.0 M in THF, 26.0 mL, 26.0 mmol, 2.0 equiv.)⁴⁸ was added under vigorous stirring over 20 min. The yellow solution was stirred at 0 °C for 1 h. P(OEt)₃ (4.4 mL, 25.6 mmol, 2.0 equiv.) was added and pressured air was bubbled through the solution. Upon exposure to oxygen, the solution gradually became darker, with a dark orange solution usually indicating completion of the reaction. After exposure to the air stream for 15 min, NH₄Cl (20 mL) was added and the mixture was diluted with MTBE (25 mL). The phases were separated, the aqueous phase extracted with MTBE (5x, 25 mL) and the combined organic phases were washed with brine (50 mL), dried over Na₂SO₄ and concentrated under reduced pressure. Purification *via* column chromatography (PE:EtOAc = 15:1) gave α -hydroxy ketone (+)-**(60)** (2.60 g, 7.37 mmol, 28% over two steps) as a light yellow oil that solidified in the freezer.

R_f (PE:EtOAc = 4:1; vanillin) = 0.66 (purple).

¹H-NMR (400 MHz, CDCl₃): δ (ppm) = 4.90–4.86 (m, 1H), 4.72–4.69 (m, 1H), 3.14 (dd, *J* = 10.8, 8.2 Hz, 1H), 2.22–2.12 (m, 1H), 1.95–1.73 (m, 5H), 1.72–1.53 (m, 2H), 1.66 (s, 3H), 1.28 (s, 6H), 0.91 (t, *J* = 7.9 Hz, 9H), 0.54 (q, *J* = 7.9 Hz, 6H).

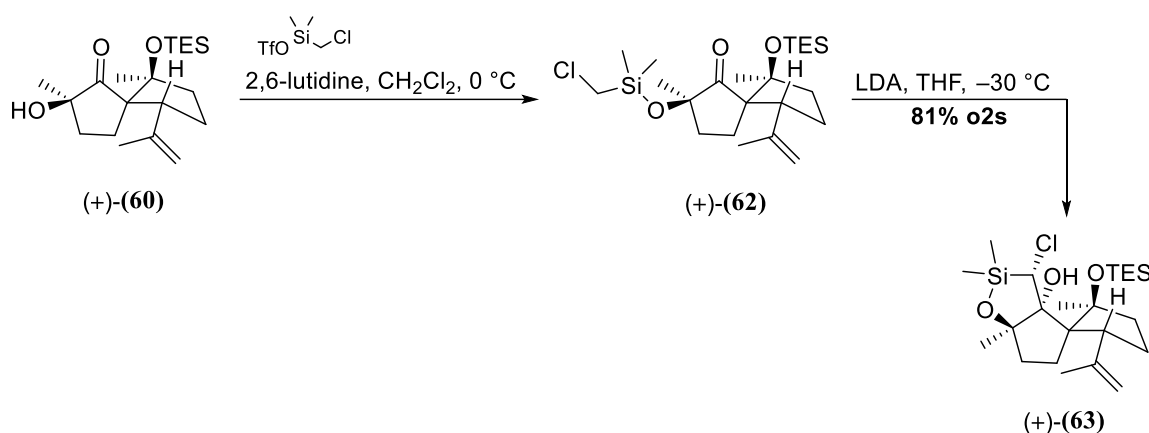
¹³C-NMR (101 MHz, CDCl₃): δ (ppm) = 221.8, 145.2, 114.0, 85.7, 76.7, 63.5, 51.9, 39.9, 34.7, 27.8, 26.0, 24.8, 22.9, 22.8, 7.0, 6.4.

HRMS(ESI): Calcd for C₂₀H₃₆O₃SiNa [M+Na]⁺: 375.2331; found: 375.2330.

$[\alpha]_D^{26}$ = +39.1 (*c* = 1.3, CHCl₃).

⁴⁸ KHMDS (1 M in THF) was freshly prepared prior to use: 5.19 g of KHMDS were dissolved in 26.0 mL of anhydrous THF.

Oxasilolane (+)-(63)



2,6-Lutidine (6.2 mL, 53.9 mmol, 4.0 equiv.) was added to a stirred solution of hydroxy ketone (+)-(60) (4.75 g, 13.5 mmol, 1.0 equiv.) in anhydrous CH₂Cl₂ (68 mL) at 0 °C, followed by dropwise addition of silyl triflate (61) (6.92 g, 26.9 mmol, 2.0 equiv.) over 15 min. The solution was allowed to warm to r.t. and stirring was continued for 30 min. Water (35 mL) was added under vigorous stirring, the phases were separated and the aqueous phase was extracted with CH₂Cl₂ (3x, 50 mL). The combined organic phases were washed with brine (50 mL), dried over Na₂SO₄ and concentrated under reduced pressure. The oily residue was coevaporated with anhydrous benzene three times and dried under fine vacuum overnight. The so obtained crude silyl ether (+)-(62) was used in the subsequent step without further purification.

Analytical data of silyl ether (+)-(62):⁴⁹

R_f (PE:EtOAc = 25:1; vanillin) = 0.68 (dark purple).

¹H-NMR (400 MHz, C₆D₆): δ (ppm) = 4.88–4.85 (m, 1H), 4.80–4.77 (m, 1H), 3.30–3.23 (m, 1H), 2.87–2.79 (m, 2H), 2.36–2.24 (m, 1H), 1.84–1.61 (m, 5H), 1.58–1.55 (m, 3H), 1.46–1.35 (m, 2H), 1.34 (s, 3H), 1.02–1.00 (m, 3H), 0.97 (t, J = 7.9 Hz, 9H), 0.57–0.50 (m, 6H), 0.37 (s, 3H), 0.35 (s, 3H).

¹³C-NMR (101 MHz, C₆D₆): δ (ppm) = 218.6, 145.4, 114.4, 85.7, 80.0, 63.0, 52.3, 39.6, 37.4, 31.4, 28.1, 26.0, 24.9, 23.0, 22.7, 7.2, 6.7, –0.7.

HRMS(ESI): Calcd for C₂₃H₄₃ClO₃Si₂Na [M+Na]⁺: 481.2337; found: 481.2341.

Crude silyl ether (+)-(62) was dissolved in anhydrous THF (68 mL) and the colorless solution was cooled to –30 °C. A freshly prepared LDA solution (1.0 M in THF, 40.0 mL, 40.0 mmol, 3.0 equiv.) was added dropwise over 5 min at –30 °C and stirring at this temperature was continued for 3.5 h. NH₄Cl (50 mL) was added at –30 °C and the mixture was allowed to warm to r.t. under vigorous stirring. The phases were separated and the aqueous phase was extracted with MTBE (3x, 50 mL). The combined organic phases were washed with brine (50 mL), dried over Na₂SO₄ and concentrated under reduced pressure. After purification by column chromatography (PE:EtOAc = 100:1), oxasilolane (+)-(63) (5.02 g, 10.9 mmol, 81% o2s) was obtained as an off-white solid.

⁴⁹ Pure samples of (+)-(62) were obtained by column chromatography (PE:EtOAc = 250:1 to 100:1). Silyl ether (+)-(62) was only isolated and characterized for reaction optimization during the racemic scouting of the synthesis. For the asymmetric synthesis, only the two-step procedure described here was used. Therefore the optical rotation of (+)-(62) was not determined.

R_f (PE:EtOAc = 50:1; vanillin) = 0.41 (purple).

$^1\text{H-NMR}$ (400 MHz, CDCl_3): δ (ppm) = 5.23–5.20 (m, 1H, H-12a), 4.87–4.84 (m, 1H, H-12b), 4.86 (s, 1H, OH), 4.13 (s, 1H, H-1), 3.85 (t, J = 8.7 Hz, 1H, H-10), 1.89–1.86 (m, 3H, CH_3 -17), 1.85–1.52 (m, 8H, H-{4,5,8,9}), 1.51 (s, 3H, CH_3 -16), 1.38 (s, 3H, CH_3 -15), 1.00 (t, J = 7.9 Hz, 9H, OTES, CH_3), 0.72 (q, J = 7.9 Hz, 6H, OTES, CH_2), 0.31 (s, 3H, CH_3 -14), 0.24 (s, 3H, CH_3 -13).

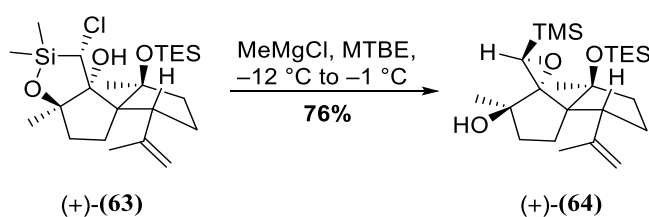
$^{13}\text{C-NMR}$ (100 MHz, CDCl_3): δ (ppm) = 148.5 (C-11), 114.9 (C-12), 91.4 (C-3), 89.0 (C-7), 88.3 (C-2), 64.3 (C-6), 51.1 (C-1), 49.3 (C-10), 39.2 (C-4), 38.2 (C-8), 28.0 (C-5), 27.4 (C-9), 24.8 (C-16), 24.6 (C-15), 21.8 (C-17), 7.2 (OTES), 6.6 (OTES), -1.1 (C-14), -1.5 (C-13).

HRMS(ESI): Calcd for $\text{C}_{23}\text{H}_{43}\text{ClO}_3\text{Si}_2\text{Na}$ $[\text{M}+\text{Na}]^+$: 481.2337; found: 481.2338.

m.p.(CH_2Cl_2) = 45–47 °C.

$[\alpha]_{\text{D}}^{26} = +13.9$ (c = 1.7, CHCl_3).

Trimethylsilyl epoxide (+)-(64)



A 100 mL two-neck flask, equipped with a stir bar, an internal thermometer and a "fake-Schlenk head",⁵⁰ was charged with oxasilolane (+)-(63) (2.00 g, 4.36 mmol, 1.0 equiv.) and anhydrous MTBE (43 mL). The colorless solution was cooled with an acetone-ice bath under vigorous stirring until the internal temperature reached $-12\text{ }^\circ\text{C}$. MeMgCl (3.0 M, 4.4 mL, 3.0 equiv.) was added quickly over 15 s. Addition of the nucleophile was accompanied by a swift gas evolution, a rise in internal temperature to $-1\text{ }^\circ\text{C}$, as well as the formation of a turbid reaction mixture. Stirring was continued under cooling for 15 min. The reaction was quenched by careful addition of NH_4Cl (10 mL) until no further gas evolution was observed. The mixture was allowed to warm to r.t., the phases were separated and the aqueous phase was extracted with MTBE (3x, 10 mL). The combined organic phases were concentrated under reduced pressure and column chromatography (PE:EtOAc = 25:1 to 11:1) gave TMS epoxide (+)-(64) (1.45 g, 3.30 mmol, 76%) as a sticky colorless oil.

R_f (PE:EtOAc = 25:1; vanillin) = 0.33 (dark blue).

$^1\text{H-NMR}$ (400 MHz, C_6D_6): δ (ppm) = 4.99–4.93 (m, 2H, CH_2 -12), 2.81 (t, J = 9.4 Hz, 1H, H-10), 2.12–2.00 (m, 2H, H-{4a,5a}), 2.07 (s, 1H, H-1), 2.00–1.90 (m, 1H, H-8a), 1.77 (s, 3H, CH_3 -15), 1.67–1.52 (m, 2H, H-{5b,9a}), 1.51–1.33 (m, 3H, H-{4b,8b,9b}), 1.20 (s, 3H, CH_3 -14), 1.13 (s, 3H, CH_3 -13), 1.08 (t, J = 7.9 Hz, 9H, OTES, CH_3), 0.90 (bs, 1H, OH), 0.79–0.69 (m, 6H, OTES, CH_2), 0.21 (s, 9H, TMS).

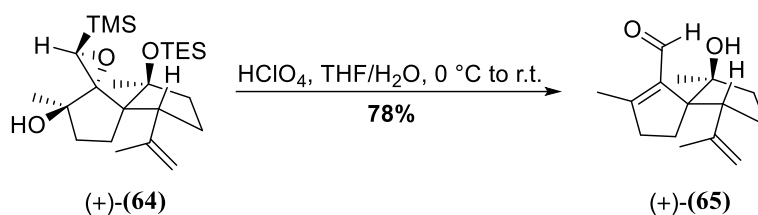
$^{13}\text{C-NMR}$ (101 MHz, C_6D_6): δ (ppm) = 146.7 (C-11), 112.7 (C-12), 86.1 (C-7), 83.4 (C-2), 81.0 (C-3), 57.9 (C-6), 53.9 (C-1), 50.6 (C-10), 40.0 (C-8), 38.7 (C-4), 29.0 (C-5), 27.2 (C-14), 27.1 (C-9), 24.6 (C-15), 22.9 (C-13), 7.6 (OTES), 7.3 (OTES), -0.6 (TMS).

HRMS(ESI): Calcd for $\text{C}_{24}\text{H}_{46}\text{O}_3\text{Si}_2\text{Na}$ $[\text{M}+\text{Na}]^+$: 461.2883; found: 461.2885.

$[\alpha]_{\text{D}}^{26} = +31.6$ (c = 1.1, CHCl_3).

⁵⁰ Y-shaped two-neck adapter where the joint of the straight neck is equipped with a rubber septum and the bend neck is equipped with an inert gas inlet.

Aldehyde (+)-(65)



To a solution of TMS epoxide (+)-(64) (1.11 g, 2.50 mmol, 1.0 equiv.) in a 4:1 mixture of THF:water (25 mL) was added HClO₄ (42.6 μL, 750 μmol, 0.3 equiv.) dropwise at 0 °C. After 30 min at 0 °C, the solution was allowed to warm to r.t. and stirred for 24 h. The slightly yellow reaction was quenched with NaHCO₃ (10 mL) and the phases were separated. The aqueous phase was extracted with MTBE (3x, 20 mL) and the combined organic phases were washed with brine (20 mL), dried over Na₂SO₄ and all volatiles were removed under reduced pressure. Column chromatography (PE:EtOAc = 4:1) gave aldehyde (+)-(65) (458 mg, 1.95 mmol, 78%) as a sticky colorless oil that crystallized in the freezer to give a yellow solid.

R_f (PE:EtOAc = 2:1; vanillin) = 0.47 (dark-blue).

¹H-NMR (400 MHz, C₆D₆): δ(ppm) = 9.76 (s, 1H), 4.95–4.91 (m, 1H), 4.79–4.76 (m, 1H), 4.36 (bs, 1H), 3.91–3.83 (m, 1H), 2.00–1.73 (m, 4H), 1.70–1.57 (m, 3H), 1.57–1.54 (m, 3H), 1.50–1.46 (m, 3H), 1.16–1.09 (m, 1H), 1.08 (s, 3H).

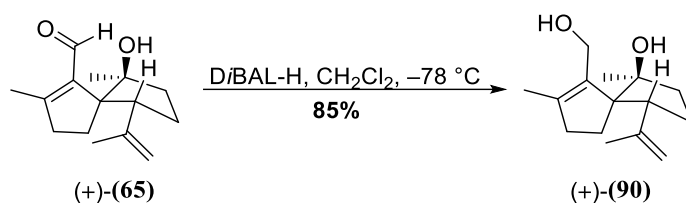
¹³C-NMR (101 MHz, C₆D₆): δ(ppm) = 191.8, 167.4, 146.3, 138.4, 112.4, 84.8, 68.0, 47.9, 38.3, 37.9, 27.5, 25.2, 24.6, 23.1, 14.8.

HRMS(ESI): Calcd for C₁₅H₂₂O₂Na [M+Na]⁺: 257.1517; found: 257.1515.

m.p. (CH₂Cl₂) = 74–77 °C.

[α]_D²⁴ = +104.7 (c = 1.3, CHCl₃).

Diol (+)-**(90)**



DiBAL-H (1.0 M in THF, 7.5 mL, 7.50 mmol, 2.0 equiv.) was added dropwise to a stirred solution of aldehyde (+)-**(65)** (870 mg, 3.71 mmol, 1.0 equiv.) in anhydrous THF (37 mL) at $-78\text{ }^\circ\text{C}$. Stirring was continued at this temperature for 45 min and Na/K tartrate (40 mL) was added. The mixture was allowed to warm to r.t.. The phases were separated and the aqueous phase was extracted with MTBE (3x, 30 mL). The combined organic phases were washed with brine (40 mL), dried over Na_2SO_4 and concentrated under reduced pressure. Purification by column chromatography (PE:EtOAc = 2:1) gave diol (+)-**(90)** (740 mg, 3.13 mmol, 84%) as a white solid.

R_f (PE:EtOAc = 2:1; vanillin) = 0.19 (dark-purple).

$^1\text{H-NMR}$ (400 MHz, CDCl_3): δ (ppm) = 4.86 (s, 1H), 4.70 (s, 1H), 4.31 (d, $J = 11.4\text{ Hz}$, 1H), 4.04 (d, $J = 11.4\text{ Hz}$, 1H), 3.28–3.19 (m, 1H), 2.43 (bs, 2H), 2.34–2.22 (m, 1H), 2.18–2.07 (m, 1H), 1.91–1.62 (m, 5H), 1.82 (s, 3H), 1.55 (s, 3H), 1.41–1.32 (s, 1H), 1.18 (s, 3H).

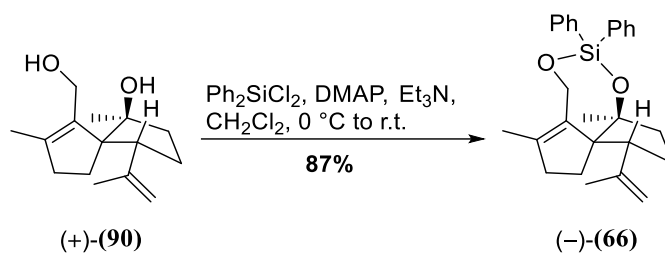
$^{13}\text{C-NMR}$ (101 MHz, CDCl_3): δ (ppm) = 146.6, 143.7, 135.3, 111.6, 85.1, 68.2, 56.2, 48.0, 37.2, 36.3, 27.5, 24.6, 24.4, 23.0, 14.7.

HRMS(ESI): Calcd for $\text{C}_{15}\text{H}_{24}\text{O}_2\text{Na}$ $[\text{M}+\text{Na}]^+$: 259.1674; found: 259.1676.

m.p. (CH_2Cl_2) = 103–106 $^\circ\text{C}$.

$[\alpha]_{\text{D}}^{29} = +125.4$ ($c = 1.2$, CHCl_3).

Diphenyl silyl protected diol (-)-(66)



Diol (+)-(90) (740 mg, 3.13 mmol, 1.0 equiv.) was dissolved in anhydrous CH_2Cl_2 (31 mL) and the solution was cooled to $0\text{ }^\circ\text{C}$. 4-DMAP (383 mg, 3.13 mmol, 1.0 equiv.), Et_3N (1.7 mL, 12.5 mmol, 4.0 equiv.) and Ph_2SiCl_2 (725 μL , 3.44 mmol, 1.1 equiv.) were added successively and the turbid reaction mixture was allowed to warm to r.t.. Stirring at r.t. was continued for 4 h, before the reaction was quenched by addition of water (20 mL), and the mixture was diluted with CH_2Cl_2 (20 mL). The phases were separated and the aqueous phase extracted with CH_2Cl_2 (3x, 20 mL). The combined organic phases were washed with brine (25 mL), dried over Na_2SO_4 and concentrated under reduced pressure. Purification by column chromatography (PE:EtOAc = 19:1) afforded protected diol (-)-(66) (1.18 g, 2.83 mmol, 91%) as a white solid.

R_f (PE:EtOAc = 25:1; vanillin) = 0.57 (dark blue).

$^1\text{H-NMR}$ (400 MHz, CDCl_3): δ (ppm) = 7.68–7.60 (m, 4H), 7.44–7.28 (m, 6H), 4.89–4.85 (m, 1H), 4.78–4.74 (m, 1H), 4.56 (d, $J = 12.3$ Hz, 1H), 4.21 (d, $J = 12.3$ Hz, 1H), 3.40–3.33 (m, 1H), 2.31–2.10 (m, 2H), 2.07–1.93 (m, 2H), 1.90–1.88 (m, 3H), 1.85–1.75 (m, 3H), 1.54–1.52 (m, 3H), 1.39 (ddd, $J = 13.6, 8.8, 2.8$ Hz, 1H), 1.07 (s, 3H).

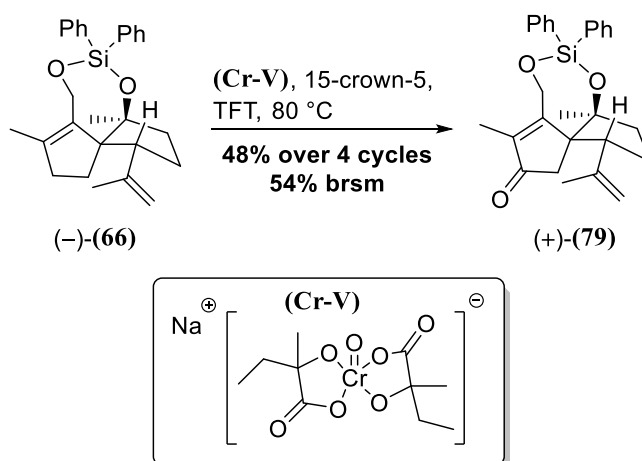
$^{13}\text{C-NMR}$ (101 MHz, CDCl_3): δ (ppm) = 146.9, 143.5, 135.3, 135.1, 134.90, 134.88, 134.7, 130.1, 130.0, 127.9, 127.7, 111.6, 91.2, 69.4, 56.9, 48.2, 38.2, 36.3, 27.6, 24.6, 24.4, 22.9, 14.7.

HRMS(ESI): Calcd for $\text{C}_{27}\text{H}_{32}\text{O}_2\text{SiNa}$ [$\text{M}+\text{Na}$] $^+$: 439.2062; found: 439.2065.

m.p. (CH_2Cl_2) = 56–60 $^\circ\text{C}$.

$[\alpha]_{\text{D}}^{28} = -15.2$ ($c = 2.3, \text{CHCl}_3$).

Enone (+)-(79)



The allylic oxidation of (-)-(66) was performed according to a modification of the procedure described by Baran and co-workers.⁵¹

Sodium bis(2-hydroxy-2-methyl-butyrato)oxochromate(V) (2.15 g, 6.67 mmol, 2.0 equiv.) was added in one portion to a solution of protected diol (-)-(66) (1.39 g, 3.35 mmol, 1.0 equiv.) and 15-crown-5 (2.0 mL, 10.1 mmol, 3.0 equiv.) in anhydrous trifluorotoluene (20 mL) at r.t.. The mixture was heated to 80 °C in a sealed Schlenk tube for 24 h. After cooling to r.t., the reaction mixture was applied on silica and the crude material was purified *via* column chromatography (PE:EtOAc = 15:1) to give enone (+)-(79) (318 mg, 0.74 mmol, 22%) as a white solid. The recovered starting material (899 mg, 2.16 mmol, 65%) was recycled for further oxidations, affording in total 713 mg (1.66 mmol, 48% over 4 cycles) of enone (+)-(79).

R_f (PE:EtOAc = 4:1; vanillin) = 0.60 (light blue).

¹H-NMR (400 MHz, CDCl₃): δ (ppm) = 7.73–7.67 (m, 2H), 7.64–7.60 (m, 2H), 7.51–7.46 (m, 1H), 7.40–7.38 (m, 3H), 7.36–7.30 (m, 2H), 4.94 (d, J = 1.4 Hz, 1H), 4.79 (s, 1H), 4.77 (d, J = 12.3 Hz, 1H), 4.61 (d, J = 12.3 Hz, 1H), 3.66 (t, J = 8.8 Hz, 1H), 2.45 (d, J = 18.8 Hz, 1H), 2.22–2.07 (m, 2H), 1.96 (d, J = 18.8 Hz, 1H), 1.92 (s, 3H), 1.88–1.73 (m, 2H), 1.51 (s, 3H), 1.07 (s, 3H).

¹³C-NMR (100 MHz, CDCl₃): δ (ppm) = 207.9, 167.1, 144.4, 142.4, 134.9, 134.7, 133.8, 133.3, 130.7, 130.6, 128.1, 127.9, 113.4, 89.9, 63.3, 56.9, 48.4, 41.4, 39.4, 25.1, 24.8, 22.4, 8.4.

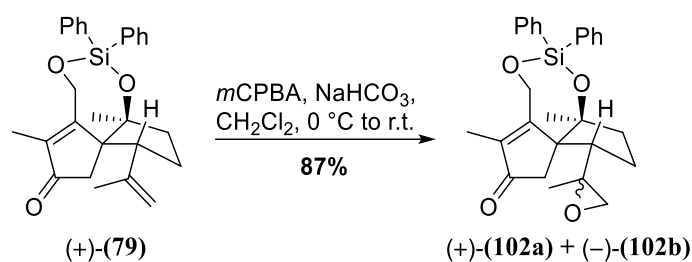
HRMS(ESI): Calcd for C₂₇H₃₀O₃SiNa [M+Na]⁺: 453.1862; found: 453.1868.

m.p. (CH₂Cl₂) = 127 °C.

$[\alpha]_D^{27}$ = +14.2 (c = 1.3, CHCl₃).

⁵¹ *J. Am. Chem. Soc.* **2014**, *136*, 4909–4912.

Epoxides (+)-(102a) and (-)-(102b)

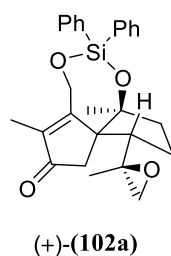


*m*CPBA (70% in water, 705 mg, 3.07 mmol, 1.5 equiv.) was added in one portion to a suspension of enone (+)-(79) (880 mg, 2.04 mmol, 1.0 equiv.) and NaHCO₃ (515 mg, 6.13 mmol, 3.0 equiv.) in CH₂Cl₂ (40 mL) at 0 °C. The mixture was allowed to warm to r.t. and stirred for 15 h. It was then cooled to 0 °C and quenched by addition of Na₂S₂O₃ (20 mL) and NaHCO₃ (20 mL). The phases were separated and the aqueous phase was extracted with CH₂Cl₂ (3x, 40 mL). The combined organic phases were washed with brine (25 mL), dried over Na₂SO₄ and concentrated under reduced pressure. Purification *via* column chromatography (PE:EtOAc = 4:1) gave a 2.1:1 mixture of epoxides (+)-(102a) and (-)-(102b) (797 mg, 1.78 mmol, 87%) as a white solid.

m.p.(CH₂Cl₂) = 115–150 °C (mixture of diastereomers).

The diastereomers were not separated for the subsequent Ti-mediated cyclization. They can however be separated by column chromatography to give pure epoxides (+)-(102a) and (-)-(102b). The relative stereoconfiguration of the major isomer (+)-(102a) was determined *via* x-ray single crystal diffraction.

Major diastereomer (+)-(102a):



R_f (PE:EtOAc = 7:3; vanillin) = 0.16 (light blue).

¹H-NMR (400 MHz, CDCl₃): δ(ppm) = 7.71–7.64 (m, 2H), 7.62–7.56 2(m, 2H), 7.50–7.45 (m, 1H), 7.44–7.37 (m, 3H), 7.36–7.29 (m, 2H), 4.78 (d, *J* = 12.3 Hz, 1H), 4.56 (d, *J* = 12.3 Hz, 1H), 3.44 (t, *J* = 9.2 Hz, 1H), 2.77 (d, *J* = 4.1 Hz, 1H), 2.60 (d, *J* = 18.9 Hz, 1H), 2.53 (d, *J* = 4.2 Hz, 1H), 2.24–2.11 (m, 1H), 2.10–1.99 (m, 2H), 1.96 (s, 3H), 1.73–1.63 (m, 1H), 1.47–1.35 (m, 1H), 1.09 (s, 3H), 1.01 (s, 3H).

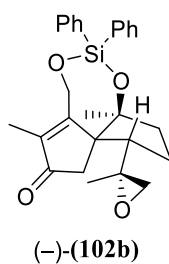
¹³C-NMR (101 MHz, CDCl₃): δ(ppm) = 207.3, 167.0, 142.8, 134.8, 134.7, 133.6, 133.1, 130.7, 130.6, 128.2, 128.0, 90.3, 62.6, 57.0, 56.5, 51.1, 45.7, 42.0, 39.2, 23.2, 22.5, 21.4, 8.4.

HRMS(ESI): Calcd for C₂₇H₃₀O₄SiNa [M+Na]⁺: 469.1811; found: 469.1809.

m.p. (CH₂Cl₂) = 146–149 °C.

[α]_D²⁷ = +5.6 (*c* = 1.0, CHCl₃).

Minor diastereomer (-)-(102b):



R_f (PE:EtOAc = 7:3; vanillin) = 0.23 (green).

$^1\text{H-NMR}$ (400 MHz, CDCl_3): δ (ppm) = 7.71–7.65 (m, 2H), 7.61–7.55 (m, 2H), 7.50–7.45 (m, 1H), 7.44–7.37 (m, 3H), 7.35–7.29 (m, 2H), 4.82 (d, $J = 12.2$ Hz, 1H), 4.55 (d, $J = 12.2$ Hz, 1H), 3.44 (t, $J = 9.3$ Hz, 1H), 2.98 (d, $J = 19.3$ Hz, 1H), 2.54 (d, $J = 4.6$ Hz, 1H), 2.33 (d, $J = 4.6$ Hz, 1H), 2.09–1.99 (m, 2H), 1.97 (s, 3H), 1.95–1.85 (m, 1H), 1.75–1.65 (m, 1H), 1.56–1.44 (m, 1H), 1.06 (s, 3H), 0.97 (s, 3H).

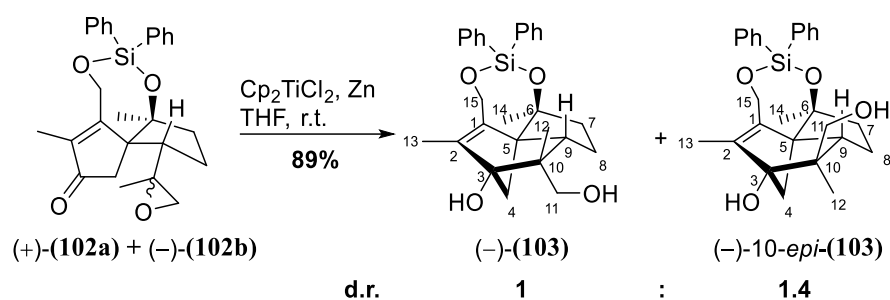
$^{13}\text{C-NMR}$ (101 MHz, CDCl_3): δ (ppm) = 207.6, 166.8, 142.9, 134.7, 134.6, 133.6, 133.2, 130.53, 130.47, 128.0, 127.8, 90.5, 62.9, 56.6, 55.9, 51.0, 44.6, 42.3, 38.8, 22.0, 21.1, 21.0, 8.3.

HRMS(ESI): Calcd for $\text{C}_{27}\text{H}_{30}\text{O}_4\text{SiNa}$ $[\text{M}+\text{Na}]^+$: 469.1811; found: 469.1806.

m.p. (CH_2Cl_2) = 136–139 °C.

$[\alpha]_{\text{D}}^{28} = -4.3$ ($c = 1.5$, CHCl_3).

Tricycle (-)-(103)



For the reductive cyclization of (+)-(102a) and (-)-(102b), a variation of the procedure published by Bermejo and co-workers was used.⁵²

Degassed⁵³ THF (60 mL) was added to Zn powder (815 mg, 12.5 mmol, 9.0 equiv.) and Cp₂TiCl₂ (1.00 g, 4.02 mmol, 3.0 equiv.) under an argon atmosphere. The green mixture was stirred at r.t. for 1 h, before a solution of epoxides (102) (619 mg, 1.38 mmol, 1.0 equiv.) in degassed⁵³ THF (43 mL) was added dropwise over 0.5 h. The brown reaction mixture was stirred at r.t. for 1 h, before aqueous NaH₂PO₄ (10%, 30 mL) and brine (20 mL) were added. The phases were separated and the aqueous phase was extracted with EtOAc (3x, 50 mL). The collected organic phases were dried over Na₂SO₄ and concentrated under reduced pressure. Purification by column chromatography (PE:EtOAc = 7:3) afforded a 1:1.4⁵⁴ mixture of norbornanes (-)-(103) and (-)-10-*epi*-(103) (554 mg, 1.23 mmol, 89%) as a white solid.

R_f (PE:EtOAc = 7:3; vanillin) = 0.09 (dark blue).

¹H-NMR (400 MHz, C₆D₆): δ(ppm) = 7.96–7.90 (m, 2H, M+m Ph₂Si), 7.88–7.82 (m, 2H, M+m Ph₂Si), 7.23–7.17 (m, 6H, M+m Ph₂Si), 4.59 (d, *J* = 14.5 Hz, 1H, H-15a), 4.57 (d, *J* = 14.5 Hz, 1H, H-15a)*, 4.49–4.41 (m, 1H, M+m H-15b), 3.73 (d, *J* = 10.6 Hz, 1H, H-11a)*, 3.40 (d, *J* = 10.5 Hz, 1H, H-11b)*, 2.88 (d, *J* = 9.8 Hz, 1H, H-11a), 2.75 (d, *J* = 9.8 Hz, 1H, H-11b), 2.60 (bs, 1H, OH)*, 2.16–2.07 (m, 2H, M+m H-7a, H-9*), 2.03–1.83 (m, 1H, M+m H-8a), 1.75 (dd, *J* = 11.0, 5.5 Hz, 1H, H-9), 1.67–1.54 (m, 1H, M+m H-7b, HSQC), 1.63–1.61 (m, 3H, CH₃-13), 1.60–1.58 (m, 3H, CH₃-13)*, 1.55–1.47 (m, 1H, H-8b, HSQC), 1.50 (d, *J* = 7.7 Hz, 1H, H-4a)*, 1.44 (s, 2H, CH₂-4), 1.38–1.35 (m, 1H, H-4b)*, 1.34 (s, 3H, CH₃-14)*, 1.33–1.26 (m, 1H, H-8b, HSQC)*, 1.32 (s, 3H, CH₃-14), 1.16 (s, 3H, CH₃-12), 0.85 (s, 3H, CH₃-12)*.

¹³C-NMR (101 MHz, C₆D₆): δ(ppm) = 142.0 (C-2)*, 141.4 (C-2), 138.6 (C-1)*, 138.5 (C-1), 135.60 (Ph₂Si)*, 135.56 (Ph₂Si), 135.43 (Ph₂Si)*, 135.41 (Ph₂Si), 135.2 (M+m Ph₂Si), 134.6 (Ph₂Si), 134.5 (Ph₂Si)*, 130.6 (Ph₂Si)*, 130.5 (Ph₂Si), 130.4 (M+m Ph₂Si), 128.2 (Ph₂Si), 128.1 (Ph₂Si)*, 90.5 (C-3)*, 89.8 (C-3), 83.8 (C-6), 83.5 (C-6)*, 72.2 (C-11), 70.5 (C-11)*, 66.7 (C-5), 66.0 (C-5)*, 58.9 (C-15)*, 58.8 (C-15), 55.9 (C-9)*, 53.7 (C-4)*, 53.2 (C-4), 52.4 (C-9), 48.6 (C-10), 46.2 (C-10)*, 43.71 (C-7)*, 43.66 (C-7), 25.53 (C-14)*, 25.50 (C-14), 22.4 (C-8), 22.3 (C-12)*, 20.7 (C-8)*, 18.2 (C-12), 10.9 (C-13)*, 10.3 (C-13).⁵⁵

HRMS(ESI): Calcd for C₂₇H₃₂O₄NaSi [M+Na]⁺: 471.1968; found: 471.1979.

⁵² *Tetrahedron* **2006**, *62*, 8933–8942.

⁵³ The freeze-pump-thaw technique was used.

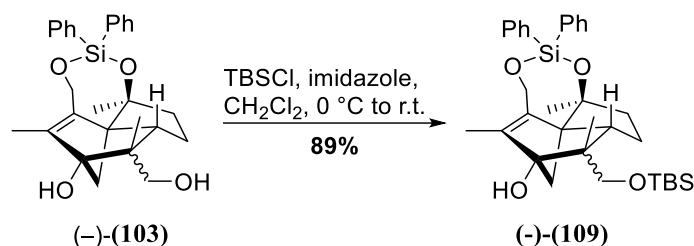
⁵⁴ During the investigations, fluctuations of the d.r. between 1:1.4 and 1:1.6 were observed.

⁵⁵ For the ¹³C-spectrum of (-)-(103) (diastereomeric mixture) in C₆D₆ only seven carbon environments per diastereomer could be distinguished for the Ph₂Si-protecting group. We contribute this either to strong overlapping of the phenyl signals, or the respective signals lying under the solvent signal. The circumstance could not be unambiguously clarified by HSQC and HMBC analysis. ¹H-NMR and mass spectrometry however strongly confirm the identity of the substance.

m.p. (CH₂Cl₂) = 43–50 °C.

[α]_D²⁸ = –35.0 (*c* = 1.2, CHCl₃).

Tri-protected tetraol (-)-(109)



TBSCl (514 mg, 3.41 mmol, 2.2 equiv.) was added to a solution of norbornanes (-)-(103) (680 mg, 1.52 mmol, 1.0 equiv.) and imidazole (310 mg, 4.55 mmol, 3.0 equiv.) in anhydrous CH_2Cl_2 (15.0 mL) at 0 °C. The mixture was stirred at r.t. for 13 h, brine (10 mL) was added and the phases were separated. The aqueous phase was extracted with CH_2Cl_2 (3x, 10 mL). The combined organic phases were dried over Na_2SO_4 and concentrated under reduced pressure. Purification by column chromatography (PE:EtOAc = 20:1) gave TBS-protected product (-)-(109) (768 mg, 1.36 mmol, 89%) as a white solid.

R_f (PE:EtOAc = 7:3; vanillin) = 0.63 (blue).

$^1\text{H-NMR}$ (400 MHz, CDCl_3): δ (ppm) = 7.77–7.66 (m, 2H, M+m), 7.63–7.55 (m, 2H, M+m), 7.44–7.28 (m, 6H, M+m), 4.83 (s, 1H)*, 4.65 (d, J = 14.5 Hz, 1H, M+m), 4.48 (dd, J = 14.5, 8.8 Hz, 1H, M+m), 4.06 (d, J = 10.0 Hz, 1H)*, 3.72 (d, J = 9.9 Hz, 1H)*, 3.31 (d, J = 9.3 Hz, 1H), 3.08 (d, J = 9.5 Hz, 2H), 2.11–2.10 (m, 1H, M+m), 2.01–1.81 (m, 2H, M+m), 1.76–1.72 (m, 2H, M+m), 1.73 (s, 3H, M+m), 1.61–1.44 (m, 2H, M+m), 1.32 (s, 3H, M+m), 1.21 (s, 3H), 0.94–0.87 (m, 9H, M+m), 0.93 (s, 3H)*, 0.17–0.08 (m, 6H), 0.04 (d, J = 11.4 Hz, 6H)*;

$^{13}\text{C-NMR}$ (101 MHz, CDCl_3):⁵⁶ δ (ppm) = 142.8*, 141.7, 138.1, 137.8*, 135.0, 134.8*, 134.7, 134.00, 133.97, 130.3, 130.20, 130.16, 127.87*, 127.85, 90.3*, 89.7, 83.7, 83.4*, 72.8, 71.5*, 66.3*, 65.6, 58.9, 58.8, 55.5*, 53.8*, 52.7, 51.9, 48.4, 45.4*, 43.60, 43.57, 26.03, 25.95, 25.8, 25.4*, 22.7*, 22.1, 20.2*, 18.7, 18.3, 18.2, 11.0*, 10.5, -5.3, -5.51, -5.53, -5.6.

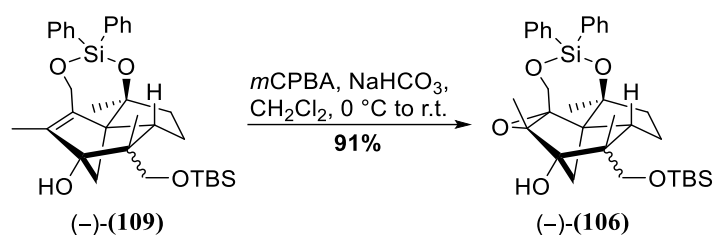
HRMS(ESI): Calcd for $\text{C}_{33}\text{H}_{46}\text{O}_4\text{NaSi}_2$ $[\text{M}+\text{Na}]^+$: 585.2832; found: 585.2833.

m.p.(CH_2Cl_2) = 35–38 °C.

$[\alpha]_{\text{D}}^{28}$ = -25.7 (c = 1.1, CHCl_3).

⁵⁶ Only the signals that could be unambiguously associated to the minor isomer are marked with an asterisk.

Epoxides (-)-(106)



*m*CPBA (70% in water, 670 mg, 2.72 mmol, 2.0 equiv.) was added in one portion to a suspension of allylic alcohols (-)-(109) (860 mg, 1.36 mmol, 1.0 equiv.) and NaHCO₃ (343 mg, 4.08 mmol, 3.0 equiv.) in CH₂Cl₂ (27 mL) at 0 °C. The mixture was allowed to warm to r.t. and stirred for 2 h. The reaction was quenched by addition of Na₂S₂O₃ (10 mL) and NaHCO₃ (10 mL) at 0 °C, the phases were separated and the aqueous phase was extracted with CH₂Cl₂ (3x, 20 mL). The combined organic phases were washed with brine (20 mL), dried over Na₂SO₄ and concentrated under reduced pressure. Purification *via* column chromatography (PE:EtOAc = 10:1) gave epoxides (-)-(106) (mixture of C-10 epimers, d.r. 1.5:1) (741 mg, 1.28 mmol, 94%) as a white solid.

R_f (PE:EtOAc = 4:1; vanillin) = 0.39 (dark-pink).

¹H-NMR (400 MHz, CDCl₃): δ(ppm) = 7.74–7.70 (m, 2H), 7.66–7.60 (m, 2H), 7.46–7.30 (m, 6H), 4.55* (s, 1H), 4.55–4.50 (m, 1H), 4.05* (d, *J* = 10.0 Hz, 1H), 3.74–3.68 (m, 1H), 3.56* (d, *J* = 10.0 Hz, 1H), 3.44 (d, *J* = 10.0 Hz, 1H), 3.40 (d, *J* = 10.0 Hz, 1H), 2.59 (s, 1H), 2.34–2.26* (m, 1H), 2.10–1.93 (m, 4H (major) + 2H (minor))⁵⁷, 1.88–1.70 (m, 2H (major) + 3H (minor))¹⁰, 1.47 (s, 3H), 1.44* (s, 1H), 1.28–1.24* (m, 1H, HSQC), 1.27* (s, 3H), 1.25 (s, 3H), 1.16–1.13 (m, 1H, HSQC), 1.15 (s, 3H), 1.11* (s, 3H), 0.92* (s, 9H), 0.91 (s, 9H), 0.113* (s, 3H), 0.108* (s, 3H), 0.07 (s, 3H), 0.04 (s, 3H);

¹³C-NMR (100 MHz, CDCl₃): δ(ppm) = 135.06, 135.02*, 134.91*, 134.90, 134.1*, 134.0, 133.8, 133.7*, 130.44, 130.38, 130.34*, 128.0, 127.81, 127.79*, 87.6*, 87.0, 83.9, 83.7*, 71.15*, 71.08, 65.0, 64.1*, 63.8, 63.5*, 62.5*, 62.0, 60.2*, 60.1, 54.1*, 49.4, 49.2, 45.6*, 43.0, 42.7*, 36.7*, 36.0, 26.0, 25.9*, 24.4*, 24.3, 23.9*, 21.9, 20.3*, 19.4, 18.22*, 18.20, 12.4*, 11.4, -5.4, -5.51, -5.53*, -5.6*;

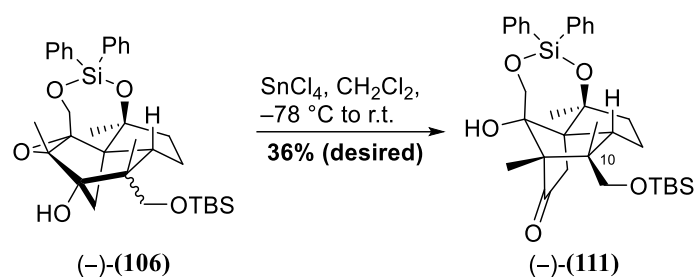
HRMS(ESI): Calcd for C₃₃H₄₆O₅NaSi₂ [M+Na]⁺: 601.2782; found: 601.2789.

m.p.(CH₂Cl₂) = 45–50 °C.

[α]_D²⁸ = -29.4 (*c* = 1.0, CHCl₃).

⁵⁷ This multiplet is comprised of signals of major and minor diastereomer. The number of protons that we interpreted belong to the respective diastereomer is specified in the parentheses.

Rearranged product (-)-(111)



SnCl_4 (1.0 M in CH_2Cl_2 , 2.1 mL, 2.14 mmol, 2.0 equiv.) was added dropwise to a solution of epoxy alcohols (-)-(106) (619 mg, 1.07 mmol, 1.0 equiv.) in anhydrous dichloromethane (10 mL) at $-78\text{ }^\circ\text{C}$. After 5 h, the reaction was quenched with water (5 mL) and allowed to warm to r.t.. The phases were separated and the aqueous phase was extracted CH_2Cl_2 (3x, 10 mL). The combined organic phases were dried over Na_2SO_4 and concentrated under reduced pressure. Purification *via* column chromatography (PE:EtOAc = 19:1) gave rearranged product (-)-(111) (222 mg, 0.38 mmol, 36% desired diastereomer) as a white solid.

R_f (PE:EtOAc = 5:1; vanillin) = 0.50 (dark pink);

$^1\text{H-NMR}$ (600 MHz, C_6D_6): δ (ppm) = 7.84–7.81 (m, 2H, SiPh₂), 7.74–7.70 (m, 2H, SiPh₂), 7.20–7.13 (m, 6H, SiPh₂), 4.59 (d, J = 11.7 Hz, 1H, H-15a), 3.48 (d, J = 11.7 Hz, 1H, H-15b), 3.38 (d, J = 10.0 Hz, 1H, H-11a), 3.31 (d, J = 10.0 Hz, 1H, H-11b), 3.15–3.09 (m, 1H, H-9), 2.97 (s, 1H, OH), 2.49 (dd, J = 17.4, 1.9 Hz, 1H, H-4b), 2.33 (ddd, J = 14.6, 9.1, 5.6 Hz, 1H, H-7a), 1.89–1.83 (m, 1H, H-8a), 1.84 (d, J = 17.4 Hz, 1H, H-4a), 1.72 (ddd, J = 14.4, 11.2, 3.3 Hz, 1H, H-7b), 1.42 (dq, J = 11.9, 5.9 Hz, 1H, H-8b), 1.031 (s, 3H, CH₃-13), 1.027 (s, 3H, CH₃-14), 0.95 (s, 9H, OTBS), 0.85 (s, 3H, CH₃-12), 0.03 (s, 3H, OTBS), 0.01 (s, 3H, OTBS);

$^{13}\text{C-NMR}$ (101 MHz, C_6D_6): δ (ppm) = 209.9 (C-3), 135.1 (SiPh₂), 134.9 (SiPh₂), 134.3 (SiPh₂), 133.8 (SiPh₂), 130.9 (SiPh₂), 130.7 (SiPh₂), 128.4 (HMBC, SiPh₂)⁵⁸, 128.3 (HMBC, SiPh₂)⁵⁹, 85.7 (C-1), 81.3 (C-6), 69.5 (C-2), 66.7 (C-11), 64.7 (C-5), 62.7 (C-15), 52.6 (C-9), 45.9 (C-7), 39.9 (C-4), 39.2 (C-10), 26.1 (OTBS), 25.0 (C-14), 23.6 (C-12), 19.8 (C-8), 18.4 (OTBS), 6.8 (C-13), -5.6 (OTBS), -5.7 (OTBS).

HRMS(ESI): Calcd for $\text{C}_{33}\text{H}_{46}\text{O}_5\text{NaSi}_2$ $[\text{M}+\text{Na}]^+$: 601.2782; found: 601.2780.

m.p. (CH_2Cl_2) = 159 $^\circ\text{C}$.

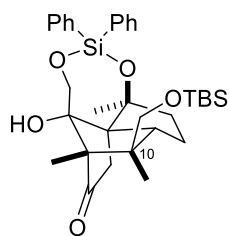
$[\alpha]_{\text{D}}^{29} = -101.1$ (c = 0.9, CHCl_3).

For the experiment outlined above, the undesired diastereomer (-)-10-*epi*-(111) was not isolated. During the racemic scouting of the sequence it was isolated and characterized. 10-*epi*-(111) was usually obtained in 21% yield alongside the desired product. Its relative stereoconfiguration was determined by X-ray crystallography.

Analytical data for (\pm)-10-*epi*-(111):

⁵⁸ Signal underneath the solvent signal.

⁵⁹ For these signals originating from the TBS methyl groups we observed an unusual multiplet-like shape with four peaks in the area between -5.5 ppm and -5.7 ppm.



10-*epi*-(111)

R_f (PE:EtOAc, vanillin) = 0.42 (bright pink).

$^1\text{H-NMR}$ (400 MHz, C_6D_6): δ (ppm) = 7.83–7.79 (m, 2H), 7.74–7.69 (m, 2H), 7.26–7.11 (m, 6H), 4.74 (d, J = 11.6 Hz, 1H), 3.53 (d, J = 11.6 Hz, 1H), 3.42–3.34 (m, 1H), 3.21 (d, J = 9.6 Hz, 1H), 3.09 (d, J = 9.6 Hz, 1H), 3.08 (s, 1H, OH), 2.49 (dd, J = 17.3, 1.9 Hz, 1H), 2.38–2.28 (m, 1H), 1.78 (d, J = 17.3 Hz, 1H), 1.77–1.67 (m, 2H), 1.35–1.23 (m, 1H), 1.05 (s, 3H), 0.95 (s, 3H), 0.90 (s, 9H), 0.83 (s, 3H), –0.15 (s, 6H).

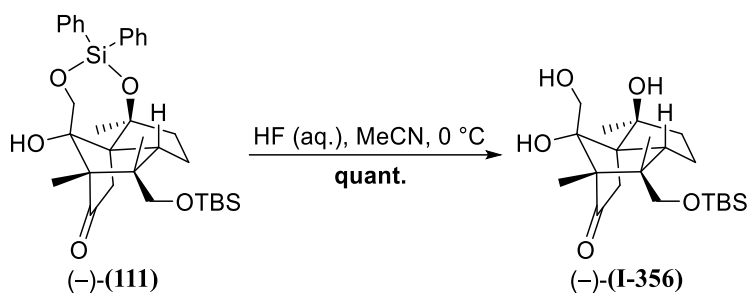
$^{13}\text{C-NMR}$ (101 MHz, C_6D_6): δ (ppm) = 209.5, 135.2, 134.9, 134.4, 133.8, 130.8, 130.7, 128.4, 85.5, 81.6, 70.6, 69.1, 64.3, 63.0, 49.5, 45.9, 39.7, 39.2, 26.1, 24.9, 19.9, 18.4, 17.4, 5.2, –5.5, –5.7.⁶⁰

HRMS(ESI): Calcd for $\text{C}_{33}\text{H}_{46}\text{O}_5\text{NaSi}_2$ $[\text{M}+\text{Na}]^+$: 601.2782; found: 601.2803.

m.p. (CH_2Cl_2) = 158–160 °C.

⁶⁰ A total of seven carbon environments belonging to the Ph_2Si -protecting group could be identified in the $^{13}\text{C-NMR}$ spectrum. HSQC and HMBC spectra of 10-*epi*-(111) may suggest that the missing signal lies underneath the solvent signal around 128.3 ppm.

Mono-TBS-protected tetraol (-)-(I-356)



Tri-protected tetraol (-)-(111) (238 mg, 411 μmol , 1.0 equiv.) was dissolved in MeCN (7.5 mL). HF (2.0 M in water, 820 μL , 1.65 mmol, 4.0 equiv.) was added at 0 $^\circ\text{C}$. Stirring at 0 $^\circ\text{C}$ was continued for 14 h, before NaHCO_3 (5 mL) and EtOAc (5 mL) were added and the mixture was allowed to warm to r.t.. The phases were separated and the aqueous phase extracted with EtOAc (4x, 10 mL). The combined organic phases were dried over Na_2SO_4 and concentrated under reduced pressure. Purification by column chromatography (PE:EtOAc = 1:1 to 1:1.5) gave mono-TBS-protected tetraol (-)-(I-356) (164 mg, 411 μmol , quant.) as a white solid.

Analytical data are in accordance with the data reported by Rychnovsky and Burns.⁶¹

R_f (PE:EtOAc = 1:1; vanillin) = 0.57 (red).

$^1\text{H-NMR}$ (400 MHz, CDCl_3): δ (ppm) = 4.39 (d, J = 12.1 Hz, 1H), 4.22 (bs, 1H), 3.38–3.30 (m, 1H), 3.21 (d, J = 10.0 Hz, 1H), 3.12 (d, J = 10.0 Hz, 1H), 2.91 (ddd, J = 12.0, 8.2, 1.6 Hz, 1H), 2.57 (bs, 1H), 2.52 (dd, J = 17.5, 1.6 Hz, 1H), 2.18–2.08 (m, 1H), 2.09 (d, J = 17.5 Hz, 1H), 1.96 (ddd, J = 14.8, 9.0, 5.8 Hz, 1H), 1.84–1.74 (m, 1H), 1.52 (dq, J = 12.0, 5.8 Hz, 1H), 1.35 (s, 3H), 1.00 (s, 3H), 0.88 (s, 3H), 0.85 (s, 9H), -0.026 (s, 3H), -0.034 (s, 3H).

$^{13}\text{C-NMR}$ (101 MHz, CDCl_3): δ (ppm) = 213.5, 84.1, 76.6, 69.7, 66.0, 63.1, 60.6, 51.5, 45.1, 39.5, 39.4, 25.9, 25.0, 23.5, 19.6, 18.2, 6.4, -5.6, -5.7.

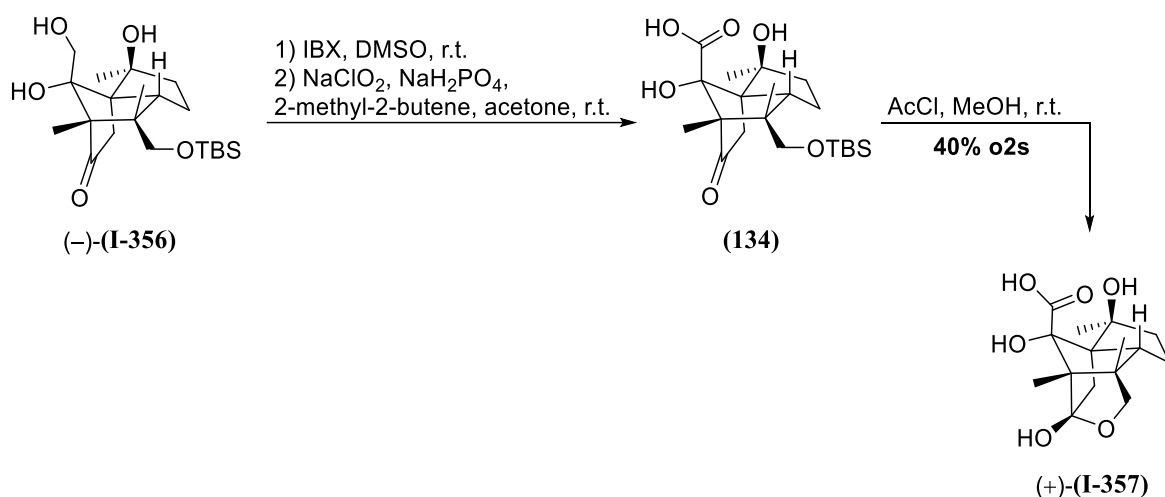
HRMS(ESI): Calcd for $\text{C}_{21}\text{H}_{38}\text{O}_5\text{SiNa}$ [$\text{M}+\text{Na}$] $^+$: 421.2386; found: 421.2383.

m.p. (CH_2Cl_2) = 71–79 $^\circ\text{C}$.

$[\alpha]_{\text{D}}^{25}$ = -14.9 (c = 1.3, CHCl_3).

⁶¹ *J. Am. Chem. Soc.* **2019**, *141*, 13295–13300.

Synthesis of carboxylic acid (+)-(I-357)



A slight variation of the procedure published by Burns and Rychnovsky was used for the synthesis of (+)-(I-357).⁶¹

IBX (75.3 mg, 269 μmol, 5.5 equiv.) was added in one portion to a stirred solution of Rychnovsky's intermediate (-)-(I-356) (19.5 mg, 48.9 μmol, 1.0 equiv.) in anhydrous DMSO (325 μL) at r.t.. The walls of the flask were rinsed with CH₂Cl₂ (100 μL) to ensure that all starting material was inside the reaction mixture and stirring at r.t. was continued for 5 h 45 min. Water (1 mL) was added and the mixture was stirred vigorously for 5 min to achieve precipitation of IBX residues. The mixture was filtered over a fine sintered glass frit and the filter cake was washed with cold CH₂Cl₂ (3x, 1 mL). The phases were separated and the aqueous phase was extracted with cold CH₂Cl₂ (2x, 2 mL). The combined organic phases were washed with water (2 mL) and the resulting aqueous phase was back extracted with cold CH₂Cl₂ (2x, 2 mL). The washing and back extraction procedure was repeated with NaHCO₃/Na₂S₂O₃ (4 mL), and the combined organic phases were dried over Na₂SO₄ and concentrated under reduced pressure (rotavap bath temperature: 0 °C). The so obtained crude aldehyde was dried under vacuum for 30 min prior to the subsequent Pinnick oxidation.

The light-yellow residue was dissolved in acetone (548 μL), 2-methyl-2-butene (104 μL, 978 μmol, 20 equiv.) and NaH₂PO₄ (2.0 M in water, 269 μL, 538 μmol, 11 equiv.) were added at r.t. and the colorless solution was stirred at r.t. for 5 min. NaClO₂ (2.15 M in water, 273 μL, 587 μmol, 12 equiv.) was added at r.t. and the mixture was stirred vigorously for 45 min. The light-yellow solution was cooled to 0 °C, and pH 2.5 buffer⁶² (1 mL) was added. The mixture was diluted with EtOAc (2 mL), the phases were separated and the aqueous phase was extracted with EtOAc (5x, 1 mL). The combined organic phases were dried over Na₂SO₄ and concentrated under reduced pressure. Purification *via* preparative thin-layer chromatography (plate size: 20x10 cm, eluent: EtOAc + 0.5% formic acid)⁶³ gave impure carboxylic acid (134) (14.8 mg) that was used in the subsequent deprotection without detailed characterization.

Acetyl chloride (25.6 μL, 359 μmol, 7.3 equiv.) was added to stirred MeOH (640 μL) at r.t. and the solution was stirred at this temperature for 30 min. The solution was then added to carboxylic acid (134) (14.8 mg) and the mixture was stirred at r.t. for 4.5 h. The light-yellow solution was diluted with MeOH (1 mL) and then concentrated under reduced pressure (rotavap bath temperature: 30 °C). Purification *via* preparative thin-layer chromatography (plate size: 10x10 cm, eluent: CH₂Cl₂:MeOH =

⁶² Prepared as described by Burns and Rychnovsky: *J. Am. Chem. Soc.* **2019**, *141*, 13295–13300.

⁶³ After preparative TLC, the product was eluted from the detached silica using EtOAc containing 0.5% of formic acid.

5:1 + 0.5% formic acid) afforded pure acid (+)-(I-357) (5.9 mg, 19.8 μmol , 40%)⁶⁴ as a colorless residue.⁶⁵

Analytical data are in accordance with the data reported by Rychnovsky and Burns.⁶⁶

R_f (EtOAc + 0.5% formic acid, Hanessian's) = 0.34.

¹H-NMR (600 MHz, CD₃OD): δ (ppm) = 3.65 (d, J = 8.5 Hz, 1H), 3.48 (d, J = 8.5 Hz, 1H), 3.12–3.07 (m, 1H), 2.41 (dd, J = 12.9, 2.3 Hz, 1H), 2.08 (ddd, J = 14.5, 11.0, 3.5 Hz, 1H), 2.00 (ddd, J = 14.5, 8.9, 6.0 Hz, 1H), 1.78 (d, J = 12.9 Hz, 1H), 1.65–1.57 (m, 1H), 1.57–1.50 (m, 1H), 1.30 (s, 3H), 1.08 (s, 3H), 1.00 (s, 3H).

¹³C-NMR (151 MHz, CD₃OD): δ (ppm) = 176.2, 111.8, 86.6, 77.0, 70.5, 66.2, 63.9, 54.1, 45.5, 45.1, 44.6, 24.6, 20.7, 19.4, 7.0.

HRMS(ESI): Calcd for C₁₅H₂₁O₆ [M-H]⁻: 297.1338; found: 297.1333.

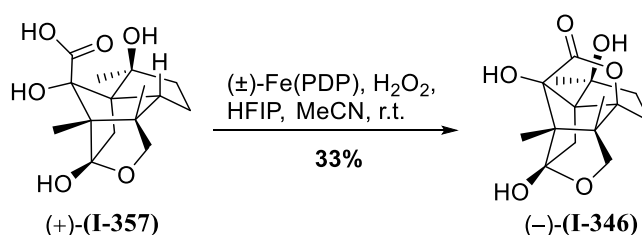
$[\alpha]_D^{23}$ = +4.5 (c = 0.1, MeOH).

⁶⁴ After preparative TLC, the product was eluted from the detached silica using EtOAc containing 0.5% of formic acid. Slow elution of acid (+)-(I-357) in this eluent made it necessary to repeat the washing procedure several times. For the scale described, a total of 30 mL of eluent for isolation of (+)-(I-357) was used.

⁶⁵ For the scale described we deemed it inaccurate to specify the physical appearance (solid, oil, etc.) for the obtained product. The product was usually obtained as a film covering the walls of the flask it was collected in; therefore, we suggest the formulation "residue" as a compromise.

⁶⁶ *J. Am. Chem. Soc.* **2019**, *141*, 13295–13300.

(-)-illisimonin A (-)-(**I-346**)



(-)-illisimonin A (-)-(**I-346**) was prepared after the protocol by Burns and Rychnovsky.⁶⁷

Acid (+)-(**I-357**) (4.9 mg, 16.4 μmol , 1.0 equiv.) was coevaporated three times with HFIP:MeCN (3:1, 0.5 mL), before it was dissolved in HFIP (125 μL).

Racemic White's catalyst was prepared by mixing equal amounts of (+)-Fe(*R,R*)PDP and (-)-Fe(*S,S*)PDP. Two stock solutions were prepared:

H₂O₂ (30 wt% in water, 20 μL) + MeCN (552 μL)

(\pm)-Fe(PDP) (16.9 mg) + MeCN (477 μL)

110 μL of both solutions were added simultaneously *via* syringe pump over 45 min to the stirred solution of (+)-(**I-357**) in HFIP at r.t.. After complete addition, *i*PrOH (500 μL) was added and the mixture was concentrated under reduced pressure. After purification by preparative thin-layer chromatography (plate size: 5x10 cm, eluent: EtOAc, run 3x), (-)-illisimonin A (-)-(**I-346**) (1.6 mg, 5.40 μmol , 33%) was obtained as a colorless residue.

Analytical data are in accordance with the literature.⁶⁷

R_f (EtOAc, Hanessian's) = 0.33.

¹H NMR (600 MHz, CD₃OD): δ (ppm) = 3.79 (d, J = 10.1 Hz, 1H), 3.55 (d, J = 10.1 Hz, 1H), 2.37 (d app. t, J = 14.2, 8.6 Hz, 1H), 2.31 (d, J = 14.3 Hz, 1H), 2.25 (ddd, J = 14.0, 10.6, 3.2 Hz, 1H), 2.02 (ddd, J = 14.3, 10.4, 8.5 Hz, 1H), 1.98 (d, J = 14.3 Hz, 1H), 1.91 (ddd, J = 14.3, 8.9, 3.1 Hz, 1H), 1.27 (s, 3H), 1.03 (s, 3H), 0.91 (s, 3H).

¹³C-NMR (151 MHz, CD₃OD): δ (ppm) = 177.6, 111.5, 104.9, 88.4, 76.7, 71.0, 69.7, 63.9, 52.8, 46.5, 39.1, 28.1, 23.1, 16.7, 5.9.

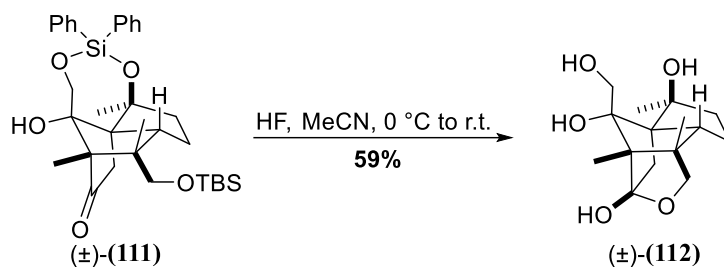
HRMS(ESI): Calcd for C₁₅H₂₀O₆Na [M+Na]⁺: 319.1158; found: 319.1160.

$[\alpha]_D^{29} = -11.9$ (c = 0.3, MeOH).

⁶⁷ *J. Am. Chem. Soc.* **2019**, *141*, 13295–13300.

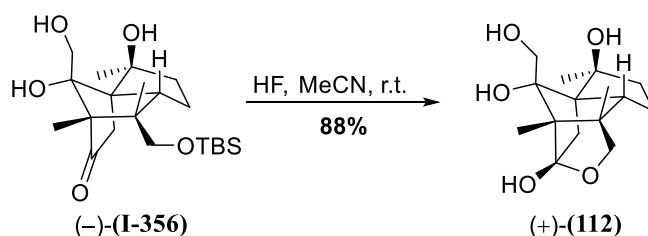
Lactol (**112**)

*Procedure A*⁶⁸ — starting from tri-protected tetraol (±)-(**111**)



HF (2.0 M in water, 760 μL , 1.52 mmol, 4.0 equiv.) was added dropwise to a stirred solution of ketone (±)-(**111**) (220 mg, 380 μmol , 1.0 equiv.) in acetonitrile (7.2 mL) at 0 $^\circ\text{C}$. The mixture was stirred at 0 $^\circ\text{C}$ for 2 h, then warmed to r.t. and stirred for 7 d. The reaction was quenched with NaHCO_3 (2.5 mL), the phases were separated and the aqueous phase was extracted with EtOAc (4x, 10 mL). The combined organic phases were dried over Na_2SO_4 and concentrated under reduced pressure. Purification *via* column chromatography (EtOAc:PE = 1.5:1 to 2.5:1) gave lactol (±)-(**112**) (63.3 mg, 0.22 mmol, 59%) as a white solid.

Procedure B — starting from mono-protected tetraol (-)-(**I-356**)



HF (2.0 M in water, 100 μL , 200 μmol , 4.0 equiv.) was added in one portion to a stirred solution of ketone (-)-(**I-356**) (20.0 mg, 50.2 μmol , 1.0 equiv.) in acetonitrile (1.0 mL) at r.t.. After 5 d, the reaction was quenched by addition of NaHCO_3 (1 mL) and the mixture was diluted with EtOAc (5 mL). The phases were separated and the aqueous phase was extracted with EtOAc (5x, 2 mL). The combined organic phases were dried over Na_2SO_4 and concentrated under reduced pressure. Purification *via* column chromatography (EtOAc) gave lactol (+)-(**112**) (12.6 mg, 44.3 μmol , 88%) as a white solid.

R_f (EtOAc; vanillin) = 0.24 (dark-blue).

$^1\text{H-NMR}$ (400 MHz, CD_3OD): δ (ppm) = 4.09 (d, J = 11.5 Hz, 1H), 3.62 (d, J = 8.4 Hz, 1H), 3.44 (d, J = 8.5 Hz, 1H), 3.35 (d, J = 11.5 Hz, 1H), 2.94–2.82 (m, 1H), 2.36 (dd, J = 12.7, 2.3 Hz, 1H), 2.11–1.93 (m, 2H), 1.72 (d, J = 12.7 Hz, 1H), 1.66–1.45 (m, 2H), 1.27 (s, 3H), 0.98 (s, 3H), 0.83 (s, 3H).

$^{13}\text{C-NMR}$ (101 MHz, CD_3OD): δ (ppm) = 113.0, 85.5, 76.3, 70.5, 64.1, 63.8, 61.2, 54.4, 44.53, 44.47, 44.4, 24.7, 21.7, 19.4, 6.3;

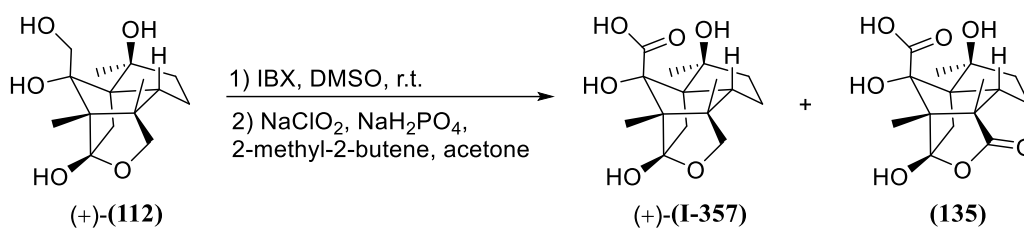
HRMS(ESI): Calcd for $\text{C}_{15}\text{H}_{24}\text{O}_5\text{Na}$ $[\text{M}+\text{Na}]^+$: 307.1521; found: 307.1523.

m.p. (CH_2Cl_2) = 147–149 $^\circ\text{C}$.

$[\alpha]_{\text{D}}^{25}$ = +6.1 (c = 0.6, MeOH).

⁶⁸ Procedure A was performed on racemic material.

Carboxylic acid (+)-(I-357) from lactol (+)-(112)



IBX (33.8 mg, 84.4 μ mol, 2.0 equiv.) was added to a solution of lactol (+)-(112) (12.0 mg, 42.2 μ mol, 1.0 equiv.) in DMSO (420 μ L) at r.t. After 19 h, water (1 mL) was added, the white residues were filtered off and washed with CH₂Cl₂ (2 mL). The phases were separated and the aqueous phase was extracted with CH₂Cl₂ (3x, 1 mL). The combined organic phases were dried over Na₂SO₄ and concentrated under reduced pressure. The crude material was used in the next reaction without further purification.

The residue was dissolved in acetone (183 μ L) and 2-methyl-2-butene (89.4 μ L, 844 μ mol, 20 equiv.) and NaH₂PO₄ (2 M in water, 232 μ L, 464 μ mol, 11 equiv.) were added under stirring at r.t.. After 5 min, NaClO₂ (2 M in water, 232 μ L, 464 μ mol, 11 equiv.) was added and the mixture was stirred vigorously for 50 min. HCl (1 M in water, 2 mL) was added and the mixture diluted with EtOAc (2 mL). The phases were separated and the aqueous phase was extracted with EtOAc (5x, 2 mL). The combined organic phases were dried over Na₂SO₄ and concentrated under reduced pressure. After purification *via* preparative thin-layer chromatography (plate size: 10x10 cm, eluent: EtOAc + 0.5% formic acid), an inseparable mixture of desired carboxylic acid (+)-(I-357) and overoxidized product (135) ((+)-(I-357):(135) = 1:1, 3.0 mg) was obtained as a colorless residue.

Analytical data for (135).⁶⁹

R_f (EtOAc, Hanessian's) = 0.33.

¹H-NMR (600 MHz, CD₃OD): δ (ppm) = 3.25–3.18 (m, 1H), 2.57 (dd, *J* = 13.3, 1.7 Hz, 1H), 2.12–1.93 (m, 2H), 1.95 (d, *J* = 13.3 Hz, 1H), 1.80–1.70 (m, 1H), 1.32–1.26 (m, 1H, HSQC), 1.292 (s, 3H), 1.285 (s, 3H), 1.05 (s, 3H).

¹³C-NMR (151 MHz, CD₃OD): δ (ppm) = 179.7, 175.6, 111.9, 86.6, 76.1, 70.6, 66.4, 52.5, 51.7, 45.2, 41.8, 24.6, 20.8, 17.7, 7.0.

HRMS(ESI): Calcd for C₁₅H₁₉O₇ [M-H]⁻: 311.1131; found: 311.1140.

⁶⁹ The NMR data of (135) was obtained from the impure mixture described above using 2D-NMR experiments for signal assignment.

White-Chen oxidation of the mixture of (+)-(**I-357**) and (**135**)

The reaction was performed after the protocol by Burns and Rychnovsky.⁷⁰

The mixture of (+)-(**I-357**) and (**135**) was azeotroped three times with HFIP:MeCN (3:1, 0.5 mL) before it was dissolved in HFIP (85 μ L).

Racemic White's catalyst was prepared by mixing equal amounts of (+)-Fe(*R,R*)PDP and (–)-Fe(*S,S*)PDP. Two stock solutions were prepared:

H₂O₂ (30 wt% in water, 20 μ L) + MeCN (552 μ L)

(\pm)-Fe(PDP) (16.9 mg) + MeCN (477 μ L)

50 μ L of both solutions were added simultaneously *via* syringe pump to the stirred solution of (+)-(**I-357**) and (**135**) in HFIP at r.t. over 45 min. After complete addition, MeOH (100 μ L) was added and the mixture was concentrated under reduced pressure. After purification *via* preparative thin-layer chromatography (plate size: 5x10 cm, eluent: EtOAc, run 2x), (–)-illisimonin A (–)-(**I-346**) (0.8 mg, 2.7 μ mol, 6% o3s) was obtained as a colorless residue.

⁷⁰ *J. Am. Chem. Soc.* **2019**, *141*, 13295–13300.

NMR data of (-)-illisimonin A (-)-(**I-346**)

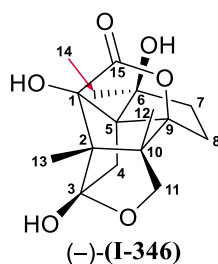


Table E3. Comparison of the obtained ¹H-NMR data with reported data.

Position	Isolation (Qu and co-workers) ⁷¹	Synthetic (Burns and Rychnovsky) ⁷²	Synthetic (this work)
	¹ H NMR (500 MHz, CD ₃ OD)	¹ H NMR (500 MHz, CD ₃ OD)	¹ H NMR (600 MHz, CD ₃ OD)
11α	3.79 (d, <i>J</i> = 10.0 Hz, 1H)	3.79 (d, <i>J</i> = 10.1 Hz, 1H)	3.79 (d, <i>J</i> = 10.1 Hz, 1H)
11β	3.55 (d, <i>J</i> = 10.0 Hz, 1H)	3.55 (d, <i>J</i> = 10.1 Hz, 1H)	3.55 (d, <i>J</i> = 10.1 Hz, 1H)
7β	2.36 (ddd, <i>J</i> = 14.0, 8.5, 8.5 Hz, 1H)	2.37 (d app. t, <i>J</i> = 14.2, 8.7 Hz, 1H)	2.37 (d app. t, <i>J</i> = 14.2, 8.6 Hz, 1H)
4β	2.30 (d, <i>J</i> = 14.5 Hz, 1H)	2.31 (d, <i>J</i> = 14.3 Hz, 1H)	2.31 (d, <i>J</i> = 14.3 Hz, 1H)
7α	2.25 (ddd, <i>J</i> = 14.0, 10.5, 3.5 Hz, 1H)	2.25 (ddd, <i>J</i> = 14.0, 10.6, 3.3 Hz, 1H)	2.25 (ddd, <i>J</i> = 14.0, 10.6, 3.2 Hz, 1H)
8α	2.03 (ddd, <i>J</i> = 14.5, 10.5, 8.5 Hz, 1H)	2.02 (ddd, <i>J</i> = 14.3, 10.3, 8.5 Hz, 1H)	2.02 (ddd, <i>J</i> = 14.3, 10.4, 8.5 Hz, 1H)
4α	1.97 (d, <i>J</i> = 14.5 Hz, 1H)	1.97 (d, <i>J</i> = 14.3 Hz, 1H)	1.98 (d, <i>J</i> = 14.3 Hz, 1H)
8β	1.91 (ddd, <i>J</i> = 14.5, 8.5, 3.5 Hz, 1H)	1.91 (ddd, <i>J</i> = 14.3, 8.9, 3.1 Hz, 1H)	1.91 (ddd, <i>J</i> = 14.3, 8.9, 3.1 Hz, 1H)
14	1.27 (s, 3H)	1.27 (s, 3H)	1.27 (s, 3H)
12	1.03 (s, 3H)	1.03 (s, 3H)	1.03 (s, 3H)
13	0.91 (s, 3H)	0.91 (s, 3H)	0.91 (s, 3H)

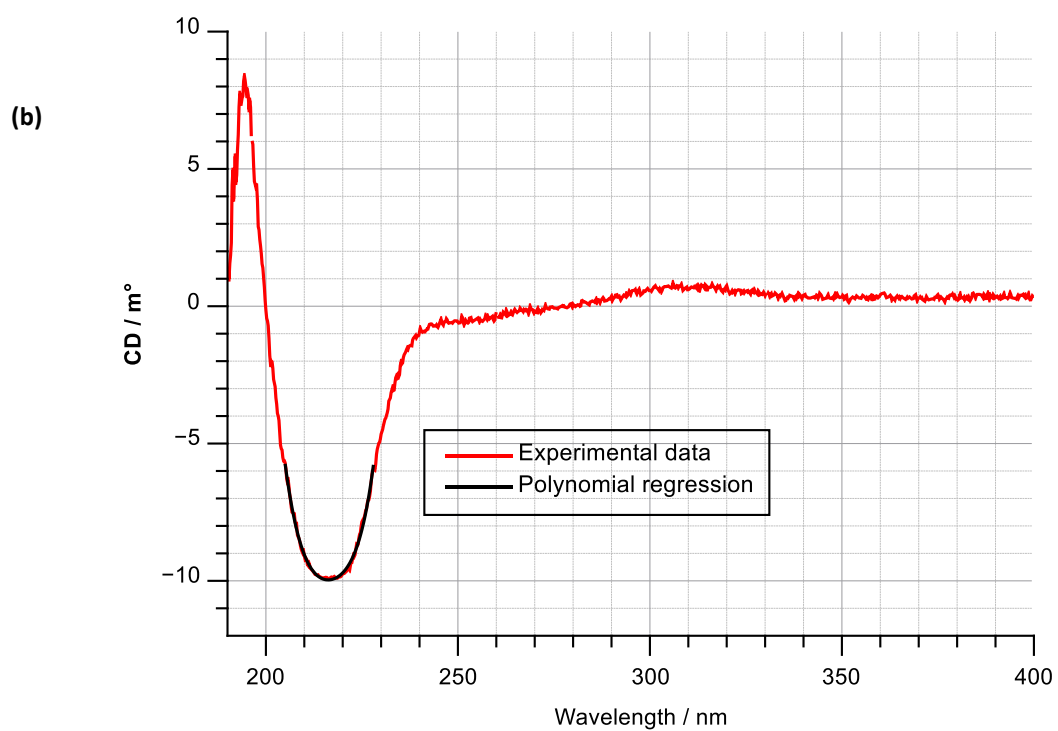
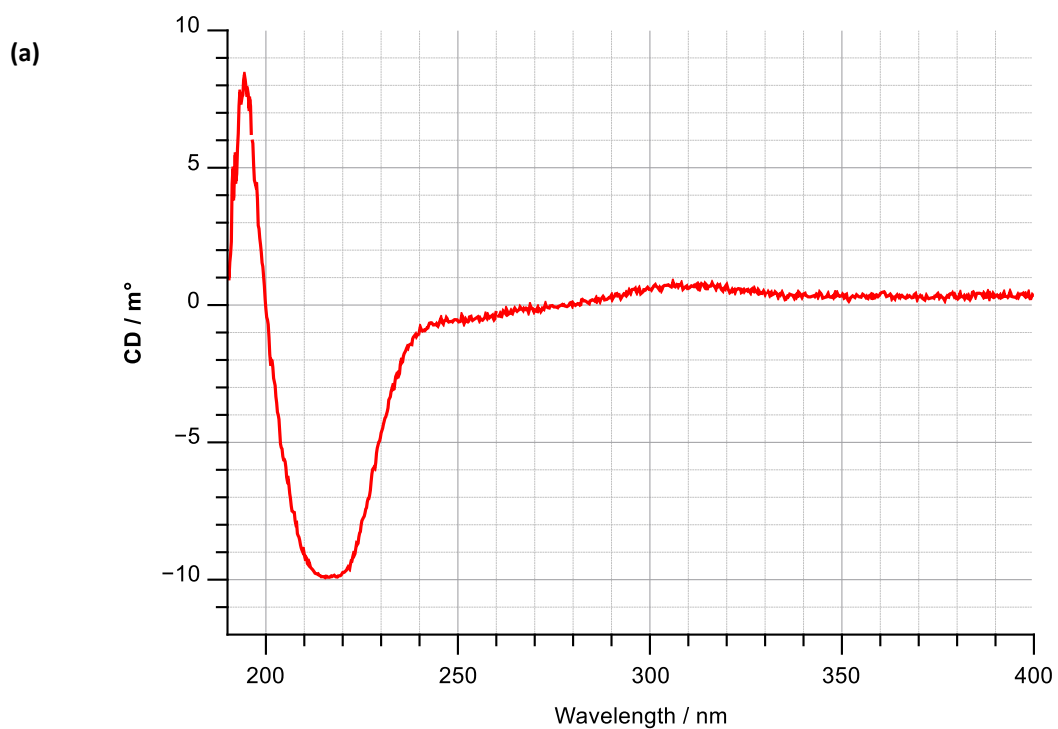
⁷¹ *Org. Lett.* **2017**, *19*, 6160–6163.

⁷² *J. Am. Chem. Soc.* **2019**, *141*, 13295–13300.

Table E4. Comparison of the obtained ^{13}C -NMR data with reported data.

Position	Isolation (Qu and co-workers) ⁷¹ ^{13}C NMR (126 MHz, CD_3OD)	Synthetic (Burns and Rychnovsky) ⁷² ^{13}C NMR (151 MHz, CD_3OD)	Synthetic (this work) ^{13}C NMR (151 MHz, CD_3OD)
15	177.6	177.6	177.6
3	111.5	111.5	111.5
9	104.9	104.9	104.9
1	88.4	88.4	88.4
6	76.7	76.7	76.7
5	71.0	71.0	71.0
11	69.7	69.7	69.7
2	63.9	63.9	63.9
10	52.8	52.8	52.8
7	46.5	46.5	46.5
4	39.0	39.1	39.1
14	28.1	28.1	28.1
8	23.1	23.1	23.1
12	16.7	16.7	16.7
13	6.0	5.9	5.9

CD spectrum of (-)-illisimonin A



CD spectrum of synthetic (-)-illisimonin A (-)-**(I-346)**. (a) Plain spectrum; (b) experimental data superimposed with polynomial function fit to the minimum region.

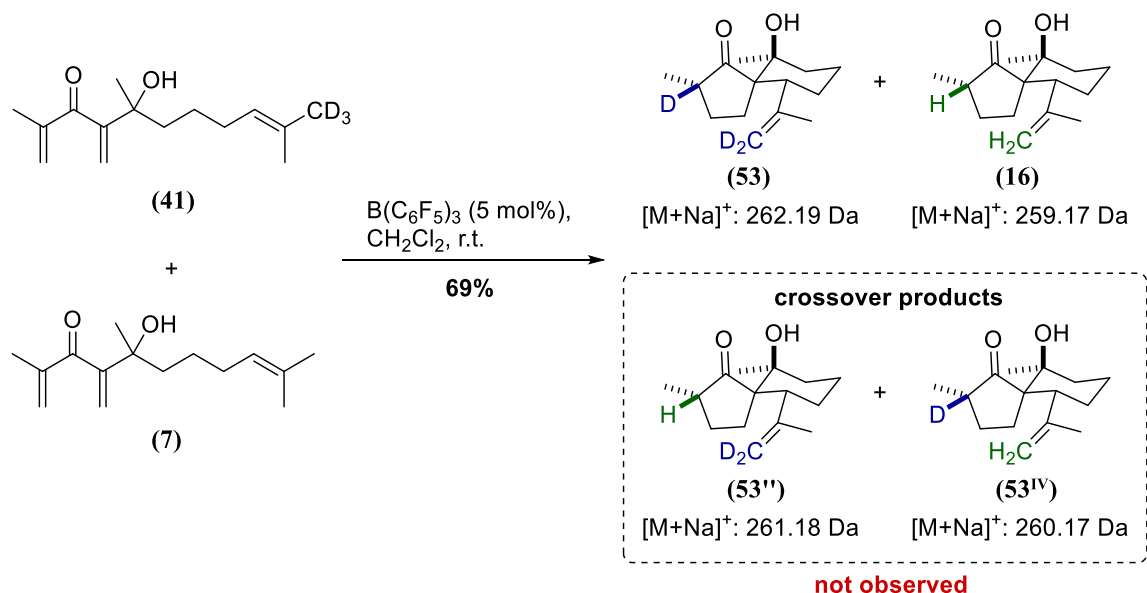
The minimum was determined by polynomial regression of the area between 205 nm and 228 nm. The following function was fit to the data (coefficients rounded to the second decimal):

$$y = 1.69 \cdot 10^{-3} + 7.98 \cdot 10^{-2} \cdot x + 5.27 \cdot x^2 - 9.69 \cdot 10^{-2} \cdot x^3 + 6.68 \cdot 10^{-4} \cdot x^4 - 2.05 \cdot 10^{-6} \cdot x^5 + 2.36 \cdot 10^{-9} \cdot x^6$$

The local minimum in the area between 205 nm and 228 nm was determined to be 216.2 nm. This value is in accordance with the value of 216.5 nm reported by Ma and co-workers.¹⁵¹

Deuteration studies – mass spectra

The constitution of the product mixture obtained from crossover experiment reported in Scheme 137 (ex Scheme 91) was analysed by mass spectrometry (ESI) and the isotope distribution of the compounds in the mixture was compared to the distribution in samples of pure **(16)** and **(53)** (Figure D1). No relevant difference in isotope distribution was observed between the samples obtained from cyclization of **(7)** and **(41)**, individually or in mixture (compare Figure D1 (A)/(C) and (B)), demonstrating that no crossover of deuterium or hydrogen atoms had occurred.



Scheme 137 – Proton/deuteron crossover experiment on an equimolar mixture of congeners **(7)** and **(41)** to exclude intermolecular proton/deuteron transfer during the observed interrupted Nazarov cyclizations. Possible reaction products with calculated masses for the sodium adducts for analysis by mass spectrometry (ESI).

Occurrence of crossed product **(53'V)** for example, would have contributed to the 260.15 Da peak of **(16)**, corresponding to the exchange of one atom by 2H , ^{13}C or ^{17}O in the cross experiment's mass spectrum, and would have thereby resulted in an increased intensity of the peak itself. Since no increase in intensity was observed, the formation of crossed product **(53'V)** during the experiment was ruled out. Additionally, no relevant peak that could correspond to mixed product **(53'')** (261.18 Da) could be found in the measured mass spectra.⁷³

⁷³ The peak at 261.1 Da was ruled out, as its occurrence in all mass spectra suggests that it belongs to background noise.

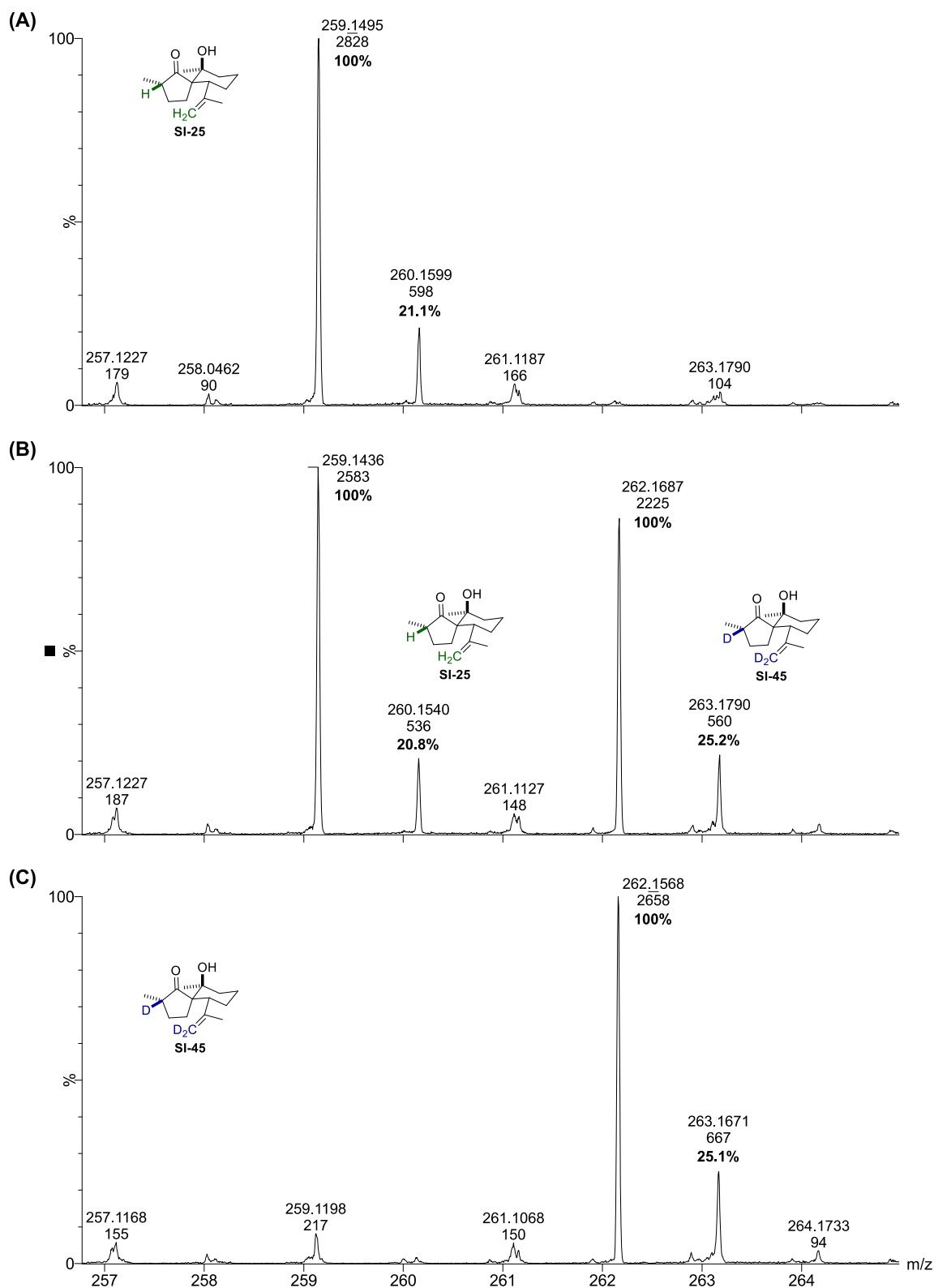


Figure D1. Comparison of isotope distribution in the mass spectra (ESI) of pure compounds **SI-25** and **SI-45** ((**A**) and (**C**)) with the isotope distribution of the product mixture obtained from the cross experiment ((**B**)). Intensities are given as percentage of the most intense peak. The depicted peaks correspond to the sodium adducts of the substances. The mass spectra were measured low resolved.

X-ray data

Single-crystal X-ray crystallography was performed with a Bruker SMART X2S diffractometer. Structures were solved using SHELXT 2014/5 (Sheldrick, 2014). Structures were refined using SHELXL2018/3 (Sheldrick, 2018).

All crystal structures were obtained from racemic intermediates that were obtained during the initial scouting of the reaction sequence.

Epoxide (\pm)-(102a)

Chemical formula	$C_{33}H_{36}O_4Si (C_6H_6)^{74}$
Molecular weight	524.94 g/mol ((102a) + C_6H_6)
Temperature	200 K
Radiation	MoK α (0.71073 Å)
Crystal size	0.600 x 0.49 x 0.46
Crystal system	triclinic
Space group	P-1
Unit cell dimensions	a = 11.074(12) Å α = 76.63(5)° b = 11.380(14) Å β = 76.53(3)° c = 12.423(19) Å γ = 80.99°
Volume	1447 Å ³
Z	2
Density (calculated)	1.205 g/cm ³
Absorption coefficient	0.12 mm ⁻¹
F(000)	560
Theta range for data collection	2.2° to 23.1°
Index ranges	-13 ≤ h ≤ 13, -12 ≤ k ≤ 14, -13 ≤ l ≤ 15
Reflections collected	10144
Independent reflections	5673 [R _{int} = 0.090]
Absorption correction	multi-scan, SADABS-2016/2 - Bruker AXS area detector scaling and absorption correction
Max. and min. transmission	0.95 and 0.25
Refinement method	Full-matrix least-squares on F ²

⁷⁴ Epoxide (\pm)-(102a) co-crystallized with benzene. Disordered benzene not shown in ORTEP for the sake of clarity.

Refinement program	SHELXL-2018/3 (Sheldrick, 2018)
Data / restraints / parameters	5673 / 354 / 401
Goodness-of-fit on F^2	0.97
Final R indices [$I > 2\sigma(I)$]	$R_1 = 0.0825$, $wR_2 = 0.1958$
Final R indices [all data]	$R_1 = 0.1324$, $wR_2 = 0.2280$
H atom treatment	constrained
Largest diff. peak and hole	0.438 and -0.572 \AA^3

(±)-10-*epi*-(111)

Chemical formula	$C_{2.51}H_{3.35}O_{0.32}Si_{0.13}^{75}$
Molecular weight	42.31 g/mol
Temperature	200 K
Radiation	MoK α (0.71073 Å)
Crystal size	0.84 x 0.73 x 0.19
Crystal system	monoclinic
Space group	$P2_1/c$
Unit cell dimensions	$a = 19.8948 \text{ \AA}$ $\alpha = 90^\circ$ $b = 10.4978 \text{ \AA}$ $\beta = 108.347$ $c = 18.9207 \text{ \AA}$ $\gamma = 90^\circ$
Volume	3750.7 Å ³
Z	62
Density (calculated)	1.161 g/cm ³
Absorption coefficient	0.14 mm ⁻¹
F(000)	1414
Theta range for data collection	2.2° to 27.1°
Index ranges	$-25 \leq h \leq 20$, $-13 \leq k \leq 12$, $-22 \leq l \leq 23$
Reflections collected	29795
Independent reflections	8530 [$R_{int} = 0.0.81$]
Absorption correction	multi-scan, SADABS-2016/2 - Bruker AXS area detector scaling and absorption correction
Max. and min. transmission	0.97 and 0.51
Refinement method	Full-matrix least-squares on F^2
Refinement program	SHELXL-2018/3 (Sheldrick, 2018)
Data / restraints / parameters	8530 / 348 / 482
Goodness-of-fit on F^2	1.03
Final R indices [$I > 2\sigma(I)$]	$R_1 = 0.0635$, $wR_2 = 0.1523$
Final R indices [all data]	$R_1 = 0.0873$, $wR_2 = 0.1678$

⁷⁵ Rearrangement product (±)-10-*epi*-(102a) co-crystallized with benzene. Disordered benzene not shown in ORTEP for the sake of clarity. The reason for the unrealistic calculated chemical formula as well as molecular weight still needs to be found.

H atom treatment

mixture of independent and constrained refinement

Largest diff. peak and hole

0.609 and -0.306 \AA^3

References

- ¹ Newman, D. J., Cragg, G. M. (2020). Natural Products as Sources of New Drugs over the Nearly Four Decades from 01/1981 to 09/2019. *J. Nat. Prod.* **2020**, *83*, 770–803.
- ² Li, F., Wang, Y., Li, D., Chen, Y., Ping Dou, Q. (2019). Are we seeing a resurgence in the use of natural products for new drug discovery? *Expert Opin. Drug Discov.* **2019**, *14*, 417–420.
- ³ Dias, D. A., Urban, S., Roessner, U. (2012). A Historical Overview of Natural Products in Drug Discovery. *Metabolites* **2012**, *2*, 303–336.
- ⁴ Wang, S., Dong, G., Sheng, C. (2019). Structural Simplification of Natural Products. *Chem.Rev.* **2019**, *119*, 4180–4220.
- ⁵ Osbourn, A. E., Lanzotti, V. (2009). Plant-derived Natural Product - Synthesis, function and applications. *Springer Ed.* **2009**.
- ⁶ Waller, G. R., Nowacki, E.K., (1978), *Alkaloids biology and metabolism in plants*, Springer Ed. **1978**.
- ⁷ Waterman, P.G., (1998), *Chapter 14 - Alkaloids chemosystematics. The alkaloids: chemistry and biology.* Academic press **1998**, *50*, 537–565.
- ⁸ Seigler, D.S. (1998). *Phenylpropanoids. In: Plant Secondary Metabolism.* Springer Ed. **1998**, 106–129.
- ⁹ Janzen, D. (1981). *Secondary Plant Products.* Springer Ed. **1981**.
- ¹⁰ Ruzicka, L. (1953). The isoprene rule and the biogenesis of terpenic compounds. *Experientia* **1953**, *9*, 357–367.
- ¹¹ Wallach, O. (1887) Zur Kenntniss der Terpene und ätherischen Oele. *Eur JOC* **2019**, *238*, 78–89.
- ¹² Hillier, S. G., Lathe, R. (2019). Terpenes, hormones and life: isoprene rule revisited. *J. Endocrinol.* **2019**, *242*, R9–R22.
- ¹³ Ludwiczuk, A., Skalicka-Woźniak, K., Georgiev, M.I. (2017) *Chapter 11 – Terpenoids. Pharmacognosy*, Academic Press **2017**, 233–266.
- ¹⁴ Delgoda, R. (2016). *Pharmacognosy: Fundamentals, applications and strategies.* Academic Press **2016**.
- ¹⁵ Chappell, J., Coates, R.M. (2010). *Sesquiterpenes, Comprehensive Natural Products II.* Elsevier **2010**, 609–641.
- ¹⁶ Lin, X., Cane, D. E. (2009). Biosynthesis of the Sesquiterpene Antibiotic Albaflavenone in *Streptomyces coelicolor*. Mechanism and Stereochemistry of the Enzymatic Formation of Epi-isozizaene. *J. Am. Chem. Soc.* **2009**, *131*, 6332–6333.
- ¹⁷ Li, Q., Wang, Z., Xie, Y., Hu, H. (2020). Antitumor activity and mechanism of costunolide and dehydrocostus lactone: Two natural sesquiterpene lactones from the Asteraceae family. *Biomed. Pharmacother.* **2020**, *125*, 109955.
- ¹⁸ Shang, S., Zhao, W., Tang, J., Xu, X., Sun, H., Pu, J., Liu, Z., Miao, M., Chen, Y., Yang, G. (2016). Antiviral sesquiterpenes from leaves of *Nicotiana tabacum*. *Fitoterapia* **2016**, *109*, 1–4.
- ¹⁹ Choi, S.Z., Choi, S.U., Lee, K.R. (2005). Cytotoxic sesquiterpene lactones from *Saussurea calcicola*. *Arc. Pharm. Res.* **2005**, *28*, 1142–1146.
- ²⁰ Yuan, P., Wang, X., Jin, B., Yang, Y., Chen, K., Jia, Q., Li, Y. (2016). Sesquiterpenes with immunosuppressive effect from the stems of *Solanum torvum*. *Phytochem. Lett.* **2016**, *17*, 126–130.

-
- ²¹ Ballio, A., Castiglione Morelli, M. A., Evidente, A., Graniti, A., Randazzo, G., Sparapano, L. (1991). Seiricardine A, A phytotoxic sesquiterpene from three Seiridium species pathogenic for cypress. *Phytochem.* **1991**, *30*, 131–136.
- ²² Portillo, A., Vila, R., Freixa, B., Ferro, E., Parella, T., Casanova, J., Cañigüeral, S. (2005). Antifungal sesquiterpene from the root of *Vernonanthura tweedieana*. *J. Ethnopharmacol.* **2005**, *97*, 4917, 126–52.
- ²³ Singh, M. M., Agnihotri, A., Garg, S. N., Agarwal, S. K., Gupta, D. N., Keshri, G., Kamboj, V. P. (1988). Antifertility and Hormonal Properties of Certain Carotane Sesquiterpenes of *Ferula jaeschkeana*. *Planta Med.* **1988**, *54*, 492–494.
- ²⁴ Blundell, R., Azzopardi, J., Briffa, J., Rasul, A., Vargas-de la Cruz, C., Shah, M. A. (2020). Chapter 13 - Analysis of pentaterpenoids. *Recent Advances in Natural Products Analysis*. Elsevier **2020**, 457–475.
- ²⁵ Dewick, P. M. (2002) *Medicinal natural products: a biosynthetic approach*, 2nd edn. Wiley **2002**.
- ²⁶ Yang, W., Shao, X., Deng, F., Hu, L., Xiong, Y., Huang, X., Fan, C., Jiang, R., Ye, W., Wang, Y. (2020). Unprecedented Quassinoids from *Eurycoma longifolia*: Biogenetic Evidence and Antifeedant Effects. *J. Nat. Prod.* **2020**, *83*, 1674–1683.
- ²⁷ Yong, J., Li, W., Wang, X., Su, G., Li, M., Zhang, J., Jia, H., Li, Y., Wang, R., Gan, M., Ma, S. (2021). Illihenin A: An Antiviral Sesquiterpenoid with a Cage-like Tricyclo[6.2.2.0^{1,5}]dodecane Skeleton from *Illicium henryi*. *J. Org. Chem.* **2021**, *86*, 2017–2022.
- ²⁸ Xue, Y., Dong, G. (2021). Total Synthesis of Penicibilaenes via C–C Activation-Enabled Skeleton Deconstruction and Desaturation Relay-Mediated C–H Functionalization. *J. Am. Chem. Soc.* **2021**, *143*, 8272–8277.
- ²⁹ [a] Murakami, M., Ishida, N. (2016). Potential of Metal-Catalyzed C–C Single Bond Cleavage for Organic Synthesis. *J. Am. Chem. Soc.* **2016**, *138*, 13759–13769. [b] Wang, B., Perea, M. A., Sarpong, R. (2020). Transition Metal-Mediated C–C Single Bond Cleavage: Making the Cut in Total Synthesis. *Angew. Chem., Int. Ed.* **2020**, *59*, 18898–18919.
- ³⁰ Chen, K., Baran, P. S. (2009). Total Synthesis of Eudesmane Terpenes by Site-Selective C–H Oxidations. *Nature* **2009**, *459*, 824–828.
- ³¹ Wilde, N. C., Isomura, M., Mendoza, A., Baran, P. S. (2014). Two Phase Synthesis of (–)-Taxuyunnanin D. *J. Am. Chem. Soc.* **2014**, *136*, 4909–4912.
- ³² Diao, T., Stahl, S. S. (2011). Synthesis of Cyclic Enones via Direct Palladium-Catalyzed Aerobic Dehydrogenation of Ketones. *J. Am. Chem. Soc.* **2011**, *133*, 14566–14569.
- ³³ Brill, Z. G., Condakes, M. L., Ting, C. P., Maimone, T. J. (2017). Navigating the Chiral Pool in the Total Synthesis of Complex Terpene Natural Products. *Chem. Rev.* **2017**, *117*, 11753–11795.
- ³⁴ Gaich, T., Mulzer, J. (2012). Chiral Pool Synthesis: Starting from Terpenes. *Comprehensive Chirality* **2012**, *2*, 163–206.
- ³⁵ Yamashita, S., Naruko, A., Nakazawa, Y., Zhao, L., Hayashi, Y., Hiramata, M. (2015). *Angew. Chem. Int. Ed.* **2015**, *54*, 8538–8541.
- ³⁶ Lin, S., Chein, R. (2017). Total Synthesis of the Labdane Diterpenes Galanal A and B from Geraniol. *J. Org. Chem.* **2017**, *82*, 1575–1583.
- ³⁷ Angeles, A. R., Waters, S. P., Danishefsky S. J. (2008). Total Syntheses of (+)- and (–)-Peribysin E. *J. Am. Chem. Soc.* **2008**, *130*, 13765–13770.

- ³⁸ Pardeshi, S. G., Ward, D. E. (2008). Enantiospecific Total Synthesis of Lairdinol A. *J. Org. Chem.* **2008**, *73*, 1071–1076.
- ³⁹ Martín-Rodríguez, M., Galán-Fernández, R., Marcos-Escribano, A., Bermejo, F. A. (2009). Ti(III)-Promoted Radical Cyclization of Epoxy Enones. Total Synthesis of (+)-Paeonisuffrone. *J. Org. Chem.* **2009**, *74*, 1798–1801.
- ⁴⁰ Liu, G., Romo, D. (2011). Total Synthesis of (+)-Omphadiol. *Angew. Chem. Int. Ed.* **2011**, *50*, 7537–7540.
- ⁴¹ Simon, K., Wefer, J., Schöttner, E., Lindel, T. (2012). Enantioselective Total Synthesis of the Diterpene (+)-Cubitene. *Angew. Chem. Int. Ed.* **2012**, *51*, 10889–10892.
- ⁴² Asaba, T., Katoh, Y., Urabe, D., Inoue, M. (2015). Total Synthesis of Crotophorbolone. *Angew. Chem., Int. Ed.* **2015**, *54*, 14457–14461.
- ⁴³ Fukuyama, Y., Huang, J. (2005). *Chemistry and neurotrophic activity of seco-prezizaane- and anisactone-type sesquiterpenes from Illicium species. Studies in Natural Products Chemistry.* Elsevier **2005**, 32L, 395–427.
- ⁴⁴ Trzoss, L., Xu, J., Lacoske, M. H., Mobley, W. C., Theodorakis, E. A. (2013). Illicium Sesquiterpenes: Divergent Synthetic Strategy and Neurotrophic Activity Studies. *Chem. Eur. J.* **2013**, *19*, 6398–6408.
- ⁴⁵ Yamada, K., Takada, S., Nakamura, S., Hirata, Y. (1968). The structures of anisatin and neoanisatin: Toxic sesquiterpenes from *Illicium Anisatum* L. *Tetrahedron* **1968**, *24*, 199–229.
- ⁴⁶ Condakes, M. L., Novaes, L. F. T., Maimone, T. J. (2018). Contemporary Synthetic Strategies toward seco-Prezizaane Sesquiterpenes From *Illicium* Species. *J. Org. Chem.* **2018**, *83*, 14843–14852.
- ⁴⁷ Niwa, H., Nisiwaki, M., Tsukada, I., Ishigaki, T., Ito, S., Wakamatsu, K., Mori, T., Ikagawa, M., Yamada, K. (1980). Stereocontrolled Total Synthesis of (–)-Anisatin: a Neurotoxic Sesquiterpenoid Possessing a Novel Spiro β -Lactone. *J. Am. Chem. Soc.* **1990**, *112*, 9001–9003.
- ⁴⁸ Ogura, A., Yamada, K., Yokoshima, S., Fukuyama, T. (2012). Total Synthesis of (–)-Anisatin. *Org. Lett.* **2012**, *14*, 1632–1635.
- ⁴⁹ Condakes, M. L., Hung, K., Harwood, S. J., Maimone, T. J. (2017). Total Syntheses of (–)-Majucin and (–)-Jiadifenoxolane A, Complex Majucin-Type *Illicium* Sesquiterpenes. *J. Am. Chem. Soc.* **2017**, *139*, 17783–17786.
- ⁵⁰ Hung, K., Condakes, M. L., Morikawa, T., Maimone, T. J. (2016). Oxidative Entry into the *Illicium* Sesquiterpenes: Enantiospecific Synthesis of (+)-Pseudoanisatin. *J. Am. Chem. Soc.* **2016**, *138*, 16616–16619.
- ⁵¹ Dorta, R. L., Francisco, C. G., Freire, R., Suárez, E. (1988). Intramolecular hydrogen abstraction. The use of organoselenium reagents for the generation of alkoxy radicals. *Tetrahedron Lett.* **1988**, *29*, 5429–5432.
- ⁵² [a] Tenaglia A., Terranova E., Waegell B. (1989). Ruthenium-catalyzed C–H bond activation oxidation of bridged bicyclic and tricyclic alkanes. *Tetrahedron Lett.* **1989**, *30*, 5271–5274. [b] Tenaglia A., Terranova E., Waegell B. (1992). Ruthenium-catalyzed carbon-hydrogen bond activation. Oxyfunctionalization of nonactivated carbon-hydrogen bonds in the cedrane series with ruthenium tetroxide generated in situ. *J. Org. Chem.* **1992**, *57*, 5523–5528.
- ⁵³ Lu, H. H., Martinez, M., Shenvi, R. An eight-step gram-scale synthesis of (–)-jiadifenolide. *Nature Chem* **2015**, *7*, 604–607.
- ⁵⁴ Xu, J., Trzoss, L., Chang, W. K., Theodorakis, E. A. (2011). Enantioselective Total Synthesis of (–)-Jiadifenolide. *Angew. Chem. Int. Ed.* **2011**, *50*, 3672–3676.
- ⁵⁵ Trzoss, L., Xu, J., Lacoske, M. H., Mobley, W. C., Theodorakis, E. A. (2011). Enantioselective Synthesis of (–)-Jiadifenin, a Potent Neurotrophic Modulator. *Org. Lett.* **2011**, *13*, 4554–4557.

-
- ⁵⁶ Yokoyama, R., Huang, J., Yang, C., Fukuyama, Y. (2002). New seco-Prezizaane-Type Sesquiterpenes, Jiadifenin with Neurotrophic Activity and 1,2-Dehydroneomajucin from *Illicium jiadifengpi*. *J. Nat. Prod.* **2002**, *65*, 527–531.
- ⁵⁷ Shin Cho, Y., Carcache, D. A., Tian, Y., Li, Y., Danishefsky, S. J. (2004). Total Synthesis of (±)-Jiadifenin, a Non-peptidyl Neurotrophic Modulator. *J. Am. Chem. Soc.* **2004**, *126*, 14358–14359.
- ⁵⁸ Finkbeiner, H. L., Stiles, M. (1963). Chelation as a Driving Force in Organic Reactions. Synthesis of α -Nitro Acids by Control of the Carboxylation-Decarboxylation Equilibrium. *J. Am. Chem. Soc.* **1963**, *85*, 616–622.
- ⁵⁹ Yang, Y., Fu, X., Chen, J., Zhai, H. (2012). Total Synthesis of (-)-Jiadifenin. *Angew. Chem. Int. Ed.* **2012**, *51*, 9825–9828.
- ⁶⁰ Ito, Y., Hirao, T., Saegusa, T. (1978). Synthesis of α,β -Unsaturated Carbonyl Compounds by Palladium(II)-Catalyzed Dehydrosilylation of Silyl Enol Ethers. *J. Org. Chem.* **1978**, *43*, 1011–1013.
- ⁶¹ Harada, K., Imai, A., Uto, K., Carter, R. G., Kubo, M., Hioki, H., Fukuyama, Y. (2015). Synthesis of jiadifenin using Mizoroki–Heck and Tsuji–Trost reactions. *Tetrahedron* **2015**, *71*, 2199–2209.
- ⁶² Cheng, X., Micalizio, G. C. (2016). Synthesis of Neurotrophic Seco-prezizaane Sesquiterpenes (1R,10S)-2-oxo-3,4-dehydroneomajucin, (2S)-hydroxy-3,4-dehydroneomajucin, and (-)-jiadifenin. *J. Am. Chem. Soc.* **2016**, *138*, 1150–1153.
- ⁶³ Kubo, M., Okada, C., Huang, J. M., Harada, K., Hioki, H., Fukuyama, Y. (2009). Novel pentacyclic seco-prezizaane-type sesquiterpenoids with neurotrophic properties from *Illicium jiadifengpi*. *Org. Lett.* **2009**, *11*, 5190–5193.
- ⁶⁴ Siler, D. A., Mighion, J. D., Sorensen, E. J. (2014). An Enantiospecific Synthesis of Jiadifenolide. *Angew. Chem. Int. Ed.* **2014**, *53*, 5332–5335.
- ⁶⁵ Van Leusen, A. M., Oomkes, P. G. (1980). One-Step Conversion of Aldehydes to Nitriles. Introduction of a One-Carbon Unit. *Synth. Commun.* **1980**, *10*, 399–403.
- ⁶⁶ Paterson, I., Xuan, M., Dalby, S. M. (2014). Total Synthesis of Jiadifenolide. *Angew. Chem. Int. Ed.* **2014**, *53*, 7286–7289.
- ⁶⁷ Gomes, J., Daepfen, C., Liffert, R., Roesslein, J., Kaufmann, E., Heikinheim, A., Neuburger, M., Gademann, K. (2016). Formal Total Synthesis of (-)-Jiadifenolide and Synthetic Studies toward seco-Prezizaane-Type Sesquiterpenes. *J. Org. Chem.* **2016**, *81*, 11017–11034.
- ⁶⁸ Shen Y., Li L., Pan Z., Wang Y., Li J., Wang K., Wang X., Zhang Y., Hu T., Zhang Y. (2015). Protecting-Group-Free Total Synthesis of (-)-Jiadifenolide: Development of a [4 + 1] Annulation toward Multisubstituted Tetrahydrofurans. *Org. Lett.* **2015**, *17*, 5480–5463.
- ⁶⁹ Kouno, I., Mori, K., Kawano, N., Sato, S. (1989). Structure of anisactone A; a new skeletal type of sesquiterpene from the pericarps of *Illicium anisatum*. *Tetrahedron Lett.* **1989**, *30*, 7451–7452.
- ⁷⁰ Huang, J., Yokoyama, R., Yang, C., Fukuyama, Y. (2000). Merrilactone A, a novel neurotrophic sesquiterpene dilactone from *Illicium merrillianum*. *Tetrahedron Lett.* **2000**, *41*, 6111–6114.
- ⁷¹ Huang, J., Yang, C., Tanaka, M., Fukuyama, Y. (2001). Structures of merrilactones B and C, novel anisactone-type sesquiterpenes from *Illicium merrillianum*, and chemical conversion of anisactone B to merrilactone A. *Tetrahedron* **2001**, *57*, 4691–4698.
- ⁷² Shi, L., Meyer, K., Greaney, M. F. (2010). Synthesis of (±)-Merrilactone A and (±)-Anisactone A. *Angew. Chem. Int. Ed.* **2010**, *49*, 9250–9253.
- ⁷³ Birman, V. B., Danishefsky, S. J. (2002). The Total Synthesis of (±)-Merrilactone A. *J. Am. Chem. Soc.* **2002**, *124*, 2080–2081.

-
- ⁷⁴ Shen, Y., Li, L., Xiao, X., Yang, S., Hua, Y., Wang, Y., Zhang, Y., Zhang, Y. (2021). Site-Specific Photochemical Desaturation Enables Divergent Syntheses of Illicium Sesquiterpenes. *J. Am. Chem. Soc.* **2021**, *143*, 3256–3263.
- ⁷⁵ Inoue, M., Sato, T., Hiramata, M. (2003). Total Synthesis of Merrillactone A. *J. Am. Chem. Soc.* **2003**, *125*, 10772–10773.
- ⁷⁶ He, W., Huang, J., Sun, X., Frontier, A. J. (2008). Total Synthesis of (±)-Merrillactone A. *J. Am. Chem. Soc.* **2008**, *130*, 300–308.
- ⁷⁷ Chen, J., Gao, P., Yu, F., Yang, Y., Zhu, S., Zhai, H. (2012). Total Synthesis of (±)-Merrillactone A. *Angew. Chem. Int. Ed.* **2012**, *51*, 5897–5899.
- ⁷⁸ Takahashi, A., Yanai, H., Zhang, M., Sonoda, T., Mishima, M., Taguchi, T. (2010). J. Org. Chem. 2010, *75*, 1259. Highly Effective Vinylogous Mukaiyama–Michael Reaction Catalyzed by Silyl Methide Species Generated from 1,1,3,3-Tetrakis(trifluoromethanesulfonyl)propane. *J. Org. Chem.* **2010**, *75*, 1259–1265.
- ⁷⁹ Liu, W., Wang, B. (2018). Synthesis of (±)-Merrillactone A by a Desymmetrization Strategy. *Eur. J. Chem.* **2018**, *24*, 16511–16515.
- ⁸⁰ Cook, S. P., Polara, A., Danishefsky, S. J. (2006). The Total Synthesis of (±)-11-O-Debenzoyltashironin. *J. Am. Chem. Soc.* **2006**, *128*, 16440–16441.
- ⁸¹ Mehta, G., Maity, P. (2011). Towards the total synthesis of tashironin related allo-cedrane natural products: further exploitation of the oxidative dearomatization-IMDA-RCM triad based strategy. *Tetrahedron Lett.* **2011**, *52*, 1753–1756.
- ⁸² Mehta, G., Maity, P. (2011). A total synthesis of 11-O-methyldebenzoyltashironin. *Tetrahedron Lett.* **2011**, *52*, 1749–1752.
- ⁸³ Ohtawa, M., Krambis, M. J., Cerne, R., Schkeryantz, J. M., Witkin, J. M., Shenvi, R. A. (2017). Synthesis of (–)-11-O-Debenzoyltashironin: Neurotrophic Sesquiterpenes Cause Hyperexcitation. *J. Am. Chem. Soc.* **2017**, *139*, 9637–9644.
- ⁸⁴ Baeyer, A. *Chem. Ber.* **1885**, *18*, 2269.
- ⁸⁵ Wiberg, K. B. (1986). The Concept of Strain in Organic Chemistry. *Angew. Chem. Int. Ed. Engl.* **1986**, *25*, 312–322.
- ⁸⁶ Kohlbacher, S. M., Ionasz, V., Ielo, L., Pace, V. (2019). The synthetic versatility of the Tiffeneau–Demjanov chemistry in homologation tactics. *Monatsh Chem* **2019**, *150*, 2011–2019.
- ⁸⁷ Gimbert, Y., Lesage, D., Milet, A., Fournier, F., Greene, A. E., Tabet, J. (2003). On Early Events in the Pauson–Khand Reaction. *Org. Lett.* **2003**, *5*, 4073–4075.
- ⁸⁸ Shvartsbart, A., Smith, A. B. (2014). Total Synthesis of (–)-Calyciphylline N. *J. Am. Chem. Soc.* **2014**, *136*, 870–873.
- ⁸⁹ Malona, J. A., Cariou, K., Spencer, W. T., Frontier, A. J. (2012). Total Synthesis of (±)-Rocaglamide via Oxidation-Initiated Nazarov Cyclization. *J. Org. Chem.* **2012**, *77*, 1891–1908.
- ⁹⁰ Que, Y., Shao, H., He, H., Gao, S. (2020). Total Synthesis of Farnesin through an Excited-State Nazarov Reaction. *Angew. Chem. Int. Ed.* **2020**, *59*, 7444–7449.
- ⁹¹ Wenz, D. R., Read de Alaniz, J. (2014). The Nazarov Cyclization: A Valuable Method to Synthesize Fully Substituted Carbon Stereocenters. *Eur. J. Org. Chem.* **2014**, *2015*, 23–37.

-
- ⁹² Wang, Y., Arif, A. M., West, F. G. (1999). A Novel Cycloisomerization of Tetraenones: 4+3 Trapping of the Nazarov Oxyallyl Intermediate. *J. Am. Chem. Soc.* **1999**, *121*, 876–877.
- ⁹³ Giese, S., Kastrup, L., Stiens, D., West, F. G. (2000). Intermolecular Trapping of the Nazarov Intermediate: Domino Electrocyclization/[3+2] Cycloadditions with Allylsilanes. *Angew. Chem. Int. Ed.* **2000**, *39*, 1970–1973.
- ⁹⁴ Yadikov, A. V., Shirinian, V. Z. (2019). Recent Advances in the Interrupted Nazarov Reaction. *Adv. Synth. Catal.* **2020**, *362*, 702–723.
- ⁹⁵ Rieder, C. J., Fradette, R. J., West, F. G. (2008). Construction of aryl-substituted triquinanes through the interrupted Nazarov reaction. *Chem. Commun.*, **2008**, 1572–1574.
- ⁹⁶ Wu, Y., McDonald, R., West, F. G. (2011). Homologous Mukaiyama Reactions via Trapping of the Nazarov Intermediate with Silyloxyalkenes. *Org. Lett.* **2011**, *13*, 3584–3587.
- ⁹⁷ Wu, Y., West, F. G. (2014). Formal Homologous Aldol Reactions: Interrupting the Nazarov Cyclization via Carboalkoxylation of Alkynes. *Org. Lett.* **2014**, *16*, 2534–2537.
- ⁹⁸ William, R., Wang, S., Mallick, A., Liu, X. (2016). Interrupting Nazarov Reaction with Different Trapping Modality: Utilizing Potassium Alkynyltrifluoroborate as a σ -Nucleophile. *Org. Lett.* **2016**, *18*, 4458–4461.
- ⁹⁹ Wu, Y., Lin, R., West, F. G. (2017). Intercepting the Nazarov Oxyallyl Intermediate with α -Formyl-vinyl Anion Equivalents to Access Formal Morita–Baylis–Hillman Alkylation Products. *Synlett* **2017**, *28*, 1486–1490.
- ¹⁰⁰ Kwon, Y., McDonald, R., West, F. G. (2013). Organoaluminum-Mediated Interrupted Nazarov Reaction. *Angew. Chem. Int. Ed.* **2013**, *52*, 8616–8619.
- ¹⁰¹ Gelozia, S., Kwon, Y., McDonald, R., West, F. G. (2018). One-Pot Generation of Bicyclo[3.1.0]hexanols and Cyclohexanones by Double Interrupted Nazarov Reactions. *Chem. Eur. J.* **2018**, *24*, 6052–6056.
- ¹⁰² Kwon, Y., Scadeng, O., McDonald, R., West, F. G. (2014). α -Hydroxycyclopentanones via one-pot oxidation of the trimethylaluminum-mediated Nazarov reaction with triplet oxygen. *Chem. Commun.*, **2014**, *50*, 5558–5560.
- ¹⁰³ Schatz, D. J., Kwon, Y., Scully, T. W., West, F. G. (2016). Interrupting the Nazarov Cyclization with Bromine. *J. Org. Chem.* **2016**, *81*, 12494–12498.
- ¹⁰⁴ Huang, J., Leboeuf, D., Frontier, A. J. (2011). Understanding the Fate of the Oxyallyl Cation following Nazarov Electrocyclization: Sequential Wagner–Meerwein Migrations and the Synthesis of Spirocyclic Cyclopentenones. *J. Am. Chem. Soc.* **2011**, *133*, 6307–6317.
- ¹⁰⁵ Kerr, D. J., Miletic, M., Chaplin, J. H., White, J. M., Flynn, B. L. (2012). Oxazolidinone-Promoted, Torquoselective Nazarov Cyclizations. *Org. Lett.* **2012**, *14*, 1732–1735.
- ¹⁰⁶ Kong, L., Su, F., Yu, H., Jiang, Z., Lu, Y., Luo, T. (2019). Total Synthesis of (–)-Oridonin: An Interrupted Nazarov Approach. *J. Am. Chem. Soc.* **2019**, *141*, 20048–20052.
- ¹⁰⁷ Riveira, M. J., Marsilia, L. A., Mischne, M. P. (2017). The iso-Nazarov reaction. *Org. Biomol. Chem.* **2017**, *15*, 9255–9274.
- ¹⁰⁸ Bols, M. (1995). Silicon-Tethered Reactions. *Chem. Rev.* **1995**, *95*, 1253–1277.
- ¹⁰⁹ Sieburth, S. M., Fensterbank, L. (1992). An Intramolecular Diels–Alder Reaction of Vinylsilanes. *J. Org. Chem.* **1992**, *57*, 5279–5281.
- ¹¹⁰ Nishiyama, H., Kitajima, T., Matsumoto, M., Itoh, K. Silylmethyl radical cyclization: new stereoselective method for 1,3-diol synthesis from allylic alcohols. *J. Org. Chem.* **1984**, *49*, 2298–2300.

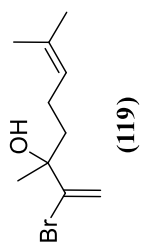
-
- ¹¹¹ Zeng, X., Zhou, J. (2016). Me₂(CH₂Cl)SiCN: Bifunctional Cyanating Reagent for the Synthesis of Tertiary Alcohols with a Chloromethyl Ketone Moiety via Ketone Cyanosilylation. *J. Am. Chem. Soc.* **2016**, *138*, 8730–8733.
- ¹¹² Simmons, E. M., Hartwig, J. F. (2012). Catalytic functionalization of unactivated primary C–H bonds directed by an alcohol. *Nature* **2012**, *483*, 70–73.
- ¹¹³ Nakamura, A., Nakada, M. (2013). Allylic Oxidations in Natural Product Synthesis. *Synthesis* **2013**, *45*, 1421–1451.
- ¹¹⁴ Barton, D. H. R., Crich, D. (1985). Oxydation of Olefins with 2-Pyridineseleninic Anhydride. *Tetrahedron* **1985**, *41*, 4359–4364.
- ¹¹⁵ Sharpless, K. B., Lauer, R. F. (1972). Selenium Dioxide Oxidation of Olefins. Evidence for the Intermediacy of Allylseleninic Acids. *J. Am. Chem. Soc.* **1972**, *94*, 7154.
- ¹¹⁶ Yu, J., Corey, E. J. (2002). Diverse Pathways for the Palladium(II)-Mediated Oxidation of Olefins by tert-Butylhydroperoxide. *Org. Lett.* **2002**, *4*, 2727–2730.
- ¹¹⁷ Salvador, J. A. R., Sáe Melo, M. L., Campos Neves, A. S. (1997). Copper-catalysed allylic oxidation of Δ^5 -steroids by t-butyl hydroperoxide. *Tetrahedron Lett.* **1997**, *38*, 119–122.
- ¹¹⁸ Toyota, M., Asano, T., Ihara, M. (2005). Total Synthesis of Serofenic Acids A and B Employing Tin-Free Homoallyl–Homoallyl Radical Rearrangement. *Org. Lett.* **2005**, *7*, 3929–3932.
- ¹¹⁹ Catino, A. J., Forslund, R. E., Doyle, M. P. (2004). Dirhodium(II) Caprolactamate: An Exceptional Catalyst for Allylic Oxidation. *J. Am. Chem. Soc.* **2004**, *126*, 13622–13623.
- ¹²⁰ Miller, R. A., Li, W., Humphrey, G. R. (1996). A ruthenium catalyzed oxidation of steroidal alkenes to enones. *Tetrahedron Lett.* **1996**, *37*, 3429–3432.
- ¹²¹ Wang, Y., Kuanga, Y., Wang, Y. (2015). Rh₂(esp)₂-catalyzed allylic and benzylic oxidations. *Chem. Commun.* **2015**, *51*, 5852–5855.
- ¹²² Ho, T., Su, C. (2000). Total Synthesis of (±)-Nudenoic Acid. *J. Org. Chem.* **2000**, *65*, 3566–3568.
- ¹²³ Patin, A., Kanazawa, A., Philouze, C., Greene, A. E., Muri, E., Barreiro, E., Costa, P. C. C. (2003). Highly Stereocontrolled Synthesis of Natural Barbacenic Acid, Novel Bisnorditerpene from *Barbacenia flava*. *J. Org. Chem.* **2003**, *68*, 3831–3837.
- ¹²⁴ Jeker, O. F., Carreira, E. M. (2012). Total Synthesis and Stereochemical Reassignment of (±)-Indoxamycin B. *Angew. Chem. Int. Ed.* **2012**, *51*, 3474–3477.
- ¹²⁵ Chen, M. S., White, M. C. (2004). A Sulfoxide-Promoted, Catalytic Method for the Regioselective Synthesis of Allylic Acetates from Monosubstituted Olefins via C–H Oxidation. *J. Am. Chem. Soc.* **2004**, *126*, 1346–1347.
- ¹²⁶ Corey, E. J., Suggs, J. W. (1975). Pyridinium Chlorochromate. An Efficient Reagent for Oxidation of Primary and Secondary Alcohols to Carbonyl Compounds. *Tetrahedron Lett.* **1975**, *16*, 2647–2650.
- ¹²⁷ Schmidt, G., Corey, E. J. (1979). Useful procedures for the oxidation of alcohols involving pyridinium dichromate in aprotic media. *Tetrahedron Lett.* **1979**, *20*, 399–402.
- ¹²⁸ Treibs, W., Schmidt, H. (1928). Über die Oxydation reaktionsfähiger Methylengruppen. *Ber. Dtsch. Chem. Ges.* **1928**, *61*, 459–465.
- ¹²⁹ Salmond, W. G., Barta, M. A., Havens, J. L. (1978). Allylic Oxidation with 3,5-Dimethylpyrazole. Chromium Trioxide Complex. Steroidal Δ^5 -7-Ketones. *J. Org. Chem.* **1978**, *43*, 2057–2059.
- ¹³⁰ Shing, T. K. M., Jiang, Q. (2000). Total Synthesis of (±)-Quassin. *J. Org. Chem.* **2000**, *65*, 7059–7069.

-
- ¹³¹ Ganesan, T. K., Rajagopal, S., Bharathy, J. B. (2000). Comparative Study of Chromium(V) and Chromium(VI) Oxidation of Dialkyl Sulfides. *Tetrahedron* **2000**, *56*, 5885–5892.
- ¹³² Srinivasan, V., Roček, J. (1974). Formation of a Long-Lived Chromium(V) Intermediate in the Chromic Acid Oxidation of Oxalic Acid. *J. Am. Chem. Soc.* **1974**, *96*, 127–133.
- ¹³³ [a] Babler, J. H., Coghlan, M. J. (1976). A Facile Method for the Bishomologation of Ketones to α,β -Unsaturated Aldehydes: Application to the Synthesis of the Cyclohexanoid Components of the Boll Weevil Sex Attractant. *Synth. Commun.* **1976**, *6*, 7, 469–474. [b] Dauben, W. G., Michno, D. M. Direct oxidation of tertiary allylic alcohols. A simple and effective method for alkylative carbonyl transposition. *J. Org. Chem.* **1977**, *42*, 682–685.
- ¹³⁴ Nakayama, Y., Maser, M. R., Okita, T., Dubrovskiy, A. V., Campbell, T. L., Reisman, S. E. (2021). Total Synthesis of Ritterazine B. *J. Am. Chem. Soc.* **2021**, *143*, 4187–4192.
- ¹³⁵ RajanBabu, T. V., Nugent, W. A. (1989). Intermolecular addition of epoxides to activated olefins: a new reaction. *J. Am. Chem. Soc.* **1989**, *111*, 4525–4527.
- ¹³⁶ Fernández-Mateos, A., Martín de la Nava, E., Pascual Coca, G., Ramos Silvo, A., Rubio González, R. (1999). Radicals from Epoxides. Intramolecular Addition to Aldehyde and Ketone Carbonyls. *Org. Lett.* **1999**, *1*, 607–610.
- ¹³⁷ Gansäuer, A., Bluhm, H. (2000). Reagent-Controlled Transition-Metal-Catalyzed Radical Reactions. *Chem. Rev.* **2000**, *100*, 2771–2788.
- ¹³⁸ Fittig, R. (1860). Ueber einige Derivate des Acetons. *Justus Liebigs Ann. Chem.* **1860**, *114*, 54–63.
- ¹³⁹ Tiffeneau, M., Levy, J. (1923). Pinacolic and semi-pinacolic transpositions. Comparative migratory tendencies of different radicals. *Compt. Rend.* **1923**, *176*, 312–314.
- ¹⁴⁰ Song, Z., Fan, C., Tu, Y. (2011). Semipinacol Rearrangement in Natural Product Synthesis. *Chem. Rev.* **2011**, *111*, 7523–7556.
- ¹⁴¹ Zhang, X., Li, B., Wang, S., Zhang, K., Zhang F., Tu, Y. (2021). Recent development and applications of semipinacol rearrangement reactions. *Chem. Sci.*, **2021**, *12*, 9262–9274.
- ¹⁴² Cheer, C. J., Johnson, C. R. (1968). The Stereoselective Rearrangements of Conformationally Mobile Epoxides. *J. Am. Chem. Soc.* **1968**, *90*, 178–183.
- ¹⁴³ Gijzen, H. J. M., Wijnberg, J. B.P.A., Ravenswaay, C., Groot, A. (1994). Rearrangement reactions of aromadendrane derivatives. The synthesis of (+)-maaliol, starting from natural (+)-aromadendrene. *Tetrahedron* **1994**, *50*, 4733–4744.
- ¹⁴⁴ Tanino, K., Onuki, K., Asano, K., Miyashita, M., Nakamura, T., Takahashi, Y., Kuwajima, I. (2003). Total Synthesis of Ingenol. *J. Am. Chem. Soc.* **2003**, *125*, 1498–1500.
- ¹⁴⁵ Epstein, O. L., Cha, J. K. (2004). Rapid Access to the “in,out”-Tetracyclic Core of Ingenol. *Angew. Chem. Int. Ed.* **2004**, *44*, 121–123.
- ¹⁴⁶ Burns, A. S., Rychnovsky, S. D. (2019). Total Synthesis and Structure Revision of (–)-Illisimonin A, a Neuroprotective Sesquiterpenoid from the Fruits of *Illicium simonsii*. *J. Am. Chem. Soc.* **2019**, *141*, 13295–13300.
- ¹⁴⁷ Qiu, Y., Gao, S. (2016). Trends in Applying C–H Oxidation to Total Synthesis of Natural Products. *Nat. Prod. Rep.* **2016**, *33*, 562–581.
- ¹⁴⁸ Barton, D. H. R., Beaton, J. M., Geller, L. E., Pechet, M. M. (1961). A New Photochemical Reaction. *J. Am. Chem. Soc.* **1961**, *83*, 4076–4083.

-
- ¹⁴⁹ Walling, C., Padwa, A. (1961). Intramolecular Chlorination with Long Chain Hypochlorites. *J. Am. Chem. Soc.* **1961**, *83*, 2207–2208.
- ¹⁵⁰ Chen, M., White, M. C. (2007). A Predictably Selective Aliphatic C–H Oxidation Reaction for Complex Molecule Synthesis. *Science* **2007**, *318*, 783–787.
- ¹⁵¹ Ma, S., Li, M., Lin, M., Li, L., Liu, Y., Qu, J., Li, Y., Wang, X., Wang, R., Xu, S., Hou, Q., Yu, S. (2017). Illisimonin A, a Caged Sesquiterpenoid with a Tricyclo[5.2.1.0^{1,6}]decane Skeleton from the Fruits of *Illicium simonsii*. *Org. Lett.* **2017**, *19*, 6160–6163.
- ¹⁵² Suzuki, T., Nagahama, R., Fariz, M. A., Yukutake, Y., Ikeuchi, K., Tanino, K. (2021). Synthesis of Illisimonin a Skeleton by Intramolecular Diels–Alder Reaction of Ortho-Benzoquinones and Biomimetic Skeletal Rearrangement of Allo-Cedranes. *Organics* **2021**, *2*, 306–312.
- ¹⁵³ Barton, D. H. R., O'Brien, R. E., Sternhell, S. (1962). A New Reaction of Hydrazones. *J. Chem. Soc.* **1962**, 470–477.
- ¹⁵⁴ Bouveault, L. (1904). Methods of Preparation of Saturated Aldehydes of the Aliphatic Series. *Bull. Soc. Chim. Fr.* **1904**, *31*, 1306–1322.
- ¹⁵⁵ [a] Hassfeld, J., Eggert, U., Kalesse, M. (2005). Synthesis of the C1-C17 Macrolactone of Tedanolide. *Synthesis* **2005**, *7*, 1183–1199. [b] Liesener, F. P., Janssen, U., Kalesse, M. (2006). Synthesis of the Northern Hemisphere of Amphidinolide H2. *Synthesis* **2006**, *15*, 2590–2602.
- ¹⁵⁶ Allinger, N. L., Hirsch, J. A., Miller, M. A., Tyminski, I. J., Van Catledge, F. A. (1968). Conformational Analysis. LX. Improved Calculations of Structures and Energies of Hydrocarbons by Westheimer Method. *J. Am. Chem. Soc.* **1968**, *90*, 1199–1210.
- ¹⁵⁷ Lipshutz, B. H., Hackmann, C. (1994). Conjugate Addition Reactions of Allylic Copper Species Derived from Grignard Reagents: Synthetic and Spectroscopic Aspects. *J. Org. Chem.* **1994**, *59*, 7437–7444.
- ¹⁵⁸ Lipshutz, B. H., Sengupta, S. (1992). Organocopper Reagents: Substitution, Conjugate Addition, Carbo/Metallo-cupration, and Other Reactions. *Organic reactions*, Wiley **1992**, *41*.
- ¹⁵⁹ Lipshutz, B. H., Dimock, S. H., James, B. (1993). The role of trimethylsilyl chloride in Gilman cuprate 1,4-addition reactions. *J. Am. Chem. Soc.* **1993**, *115*, 9283–9284.
- ¹⁶⁰ Wei, S., Tomooka, K., Nakai, T. (1993). Acyclic diastereocontrol and asymmetric transmission via anionic oxy-Cope rearrangement. Synthesis of key precursors of (+)-faranal and (–)-antirhine. *Tetrahedron* **1993**, *49*, 1025–1042.
- ¹⁶¹ Speck, K., Karaghiosoff, K., Magauer, T. (2015). Sequential O–H/C–H Bond Insertion of Phenols Initiated by the Gold(I)-Catalyzed Cyclization of 1-Bromo-1,5-enynes. *Org. Lett.* **2015**, *17*, 1982–1985.
- ¹⁶² Hosomi, A. (1988). Characteristics in the reactions of allylsilanes and their applications to versatile synthetic equivalents. *Acc. Chem. Res.* **1988**, *21*, 200–206.
- ¹⁶³ Ramirez, A. P., Thomas, A. M., Woerpel, K. A. (2009). Preparation of Bicyclic 1,2,4-Trioxanes from γ,δ -Unsaturated Ketones. *Org. Lett.* **2009**, *11*, 507–510.
- ¹⁶⁴ Risgaard, R., Nielsen, S. D., Hansen, K. B., Jensen, C. M., Nielsen, B., Traynelis, S. F., Clausen, R. P. (2013). Development of 2'-Substituted (2S,1'R,2'S)-2-(Carboxycyclopropyl)glycine Analogues as Potent N-Methyl-d-aspartic Acid Receptor Agonists. *J. Med. Chem.* **2013**, *56*, 4071–4081.
- ¹⁶⁵ Catti, L., Pöthig, A., Tiefenbacher, K. (2017). Host-Catalyzed Cyclodehydration–Rearrangement Cascade Reaction of Unsaturated Tertiary Alcohols. *Adv. Synth. Catal.* **2017**, *359*, 1331–1338.

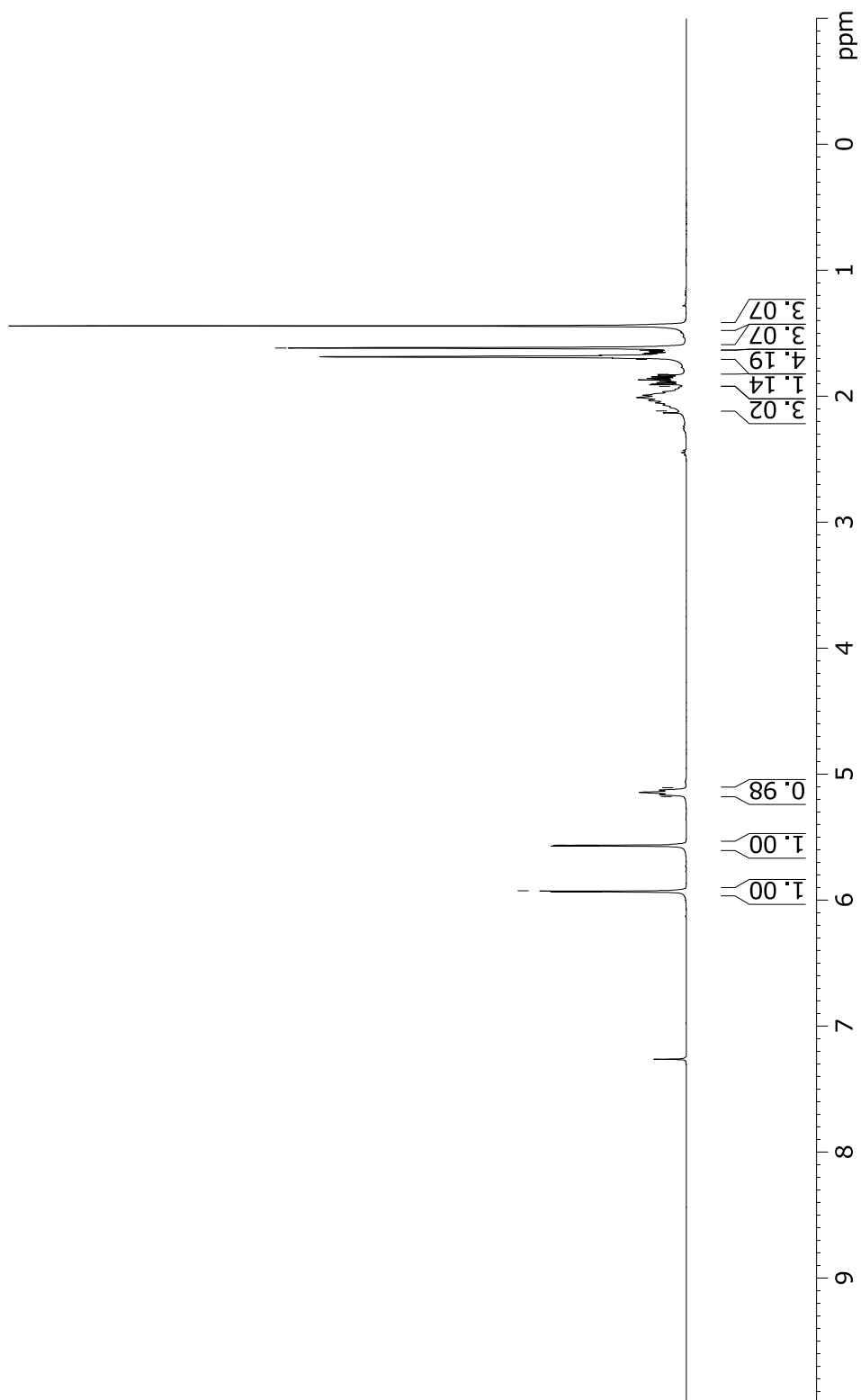
-
- ¹⁶⁶ Araoz, R., Servent, D., Molgoí, J., Iorga, B. I., Fruchart-Gaillard, C., Benoit, E., Gu, Z., Stivala, C., Zakarian, A. (2011). Total synthesis of pinnatoxins A and G and revision of the mode of action of pinnatoxin A. *J. Am. Chem. Soc.* **2011**, *133*, 10499–10511.
- ¹⁶⁷ Creary, X., Casingal, V. P., Leahy, C. E. (1993). Solvolytic elimination reactions. Stepwise or concerted? *J. Am. Chem. Soc.* **1993**, *115*, 1734–1738.
- ¹⁶⁸ Shapiro, R. H., Heath, M. J. (1967). Tosylhydrazones. V. Reaction of Tosylhydrazones with Alkylolithium Reagents. A New Olefin Synthesis. *J. Am. Chem. Soc.* **1967**, *89*, 5734–5735.
- ¹⁶⁹ Bassindale, A. R., Borbaruah, M., Glynn, S. J., Parker, D. J., Taylor, P. G. (2001). Modelling nucleophilic substitution at silicon in solution, using hypervalent silicon compounds based on 2-pyridones. *J. Chem. Soc., Perkin Trans. 2*, **1999**, 2099–2109.
- ¹⁷⁰ Lo, J. C., Kim, D., Pan, C., Edwards, J. T., Yabe, Y., Gui, J., Qin, T., Gutierrez, S., Giacoboni, J., Smith, M. W., Holland, P. L., Baran, P. S. (2017). Fe-Catalyzed C–C Bond Construction from Olefins via Radicals. *J. Am. Chem. Soc.* **2017**, *139*, 2484–2503.
- ¹⁷¹ George, D. T., Kuenstner, E. J., Pronin, S. V. (2015). A Concise Approach to Paxilline Indole Diterpenes. *J. Am. Chem. Soc.* **2015**, *137*, 15410–15413.
- ¹⁷² Saladrigas, M., Bosch, C., Saborit, G. V., Bonjoch, J., Bradshaw, B. (2017). Radical Cyclization of Alkene-Tethered Ketones Initiated by Hydrogen-Atom Transfer. *Angew. Chem. Int. Ed.* **2018**, *57*, 182–186.
- ¹⁷³ Alekseychuk, M., Adrian, S., Heinze, R. C., Heretsch, P. (2022). Biogenesis-Inspired, Divergent Synthesis of Spirochensilide A, Spirochensilide B, and Abifarine B Employing a Radical-Polar Crossover Rearrangement Strategy. *J. Am. Chem. Soc.* **2022**, *144*, 11574–11579.
- ¹⁷⁴ Heinze, R. C., Heretsch, P. (2019). Translation of a Polar Biogenesis Proposal into a Radical Synthetic Approach: Synthesis of Pleurocin A/Matsutakone and Pleurocin B. *J. Am. Chem. Soc.* **2019**, *141*, 1222–1226.
- ¹⁷⁵ López-Suárez, L., Riesgo, L., Bravo, F., Ransom, T. T., Beutler, J. A., Echavarren, A. M. (2016). Synthesis and Biological Evaluation of New (–)-Englerin Analogues. *ChemMedChem* **2016**, *11*, 1003–1007.
- ¹⁷⁶ White, J. D., Kuntiyong, P., Tae, H. L. (2006). Total Synthesis of Phorboxazole A. 1. Preparation of Four Subunits. *Org. Lett.* **2006**, *8*, 6039–6042.
- ¹⁷⁷ Gao, F., Hoveyda, A. H. (2010). α -Selective Ni-Catalyzed Hydroalumination of Aryl- and Alkyl-Substituted Terminal Alkynes: Practical Syntheses of Internal Vinyl Aluminums, Halides, or Boronates. *J. Am. Chem. Soc.* **2010**, *132*, 10961–10963.
- ¹⁷⁸ Zhang, X., Xie, X., Liu, Y. (2018). Nickel-Catalyzed Highly Regioselective Hydrocyanation of Terminal Alkynes with Zn(CN)₂ Using Water as the Hydrogen Source. *J. Am. Chem. Soc.* **2018**, *140*, 7385–7389.

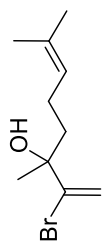
NMR Spectra



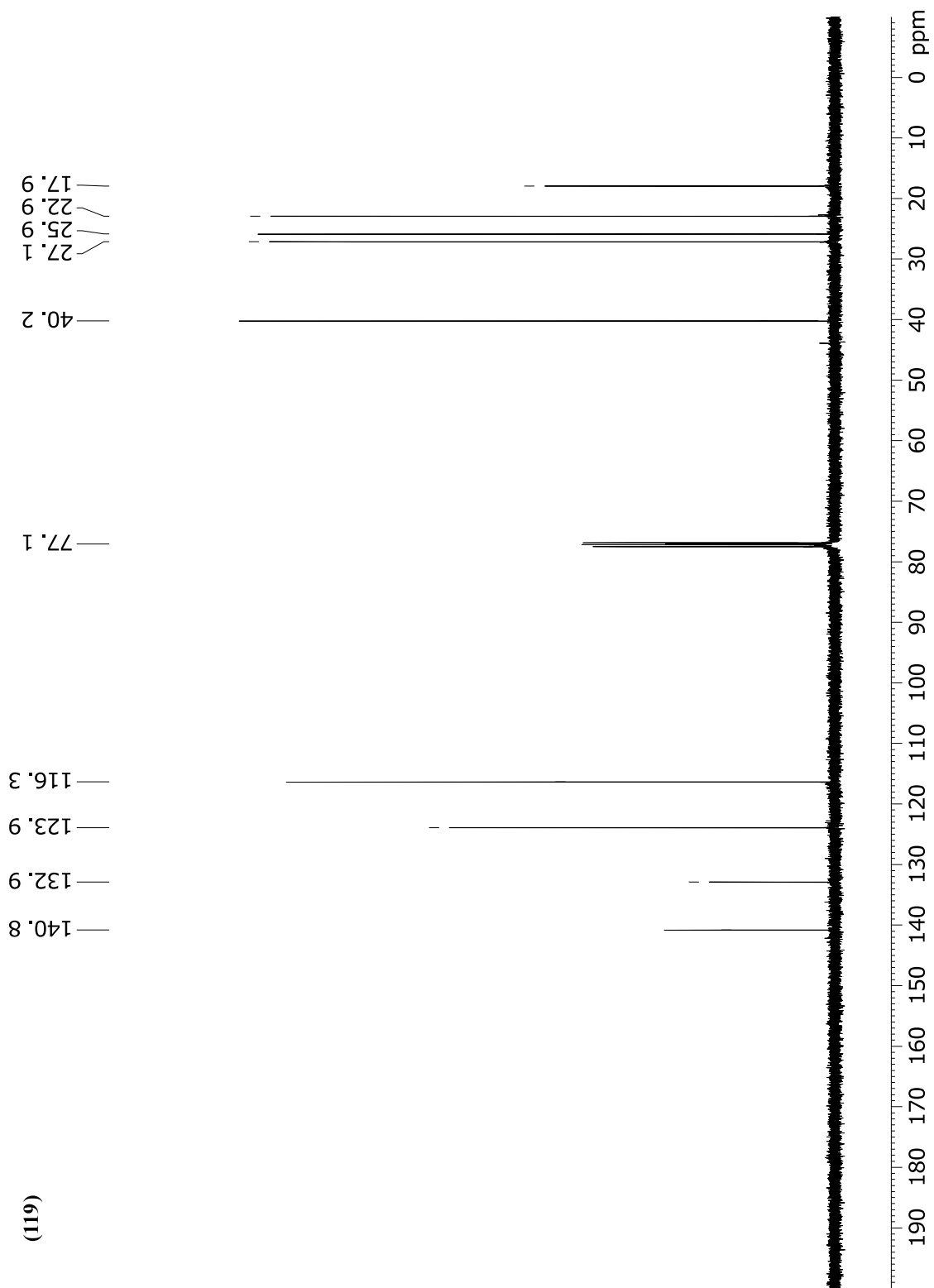
2.12
1.92
1.91
1.83
1.71
1.64
1.62
1.44

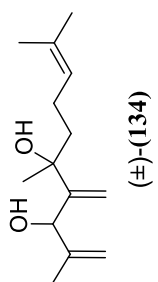
5.93
5.93
5.57
5.56
5.18
5.11





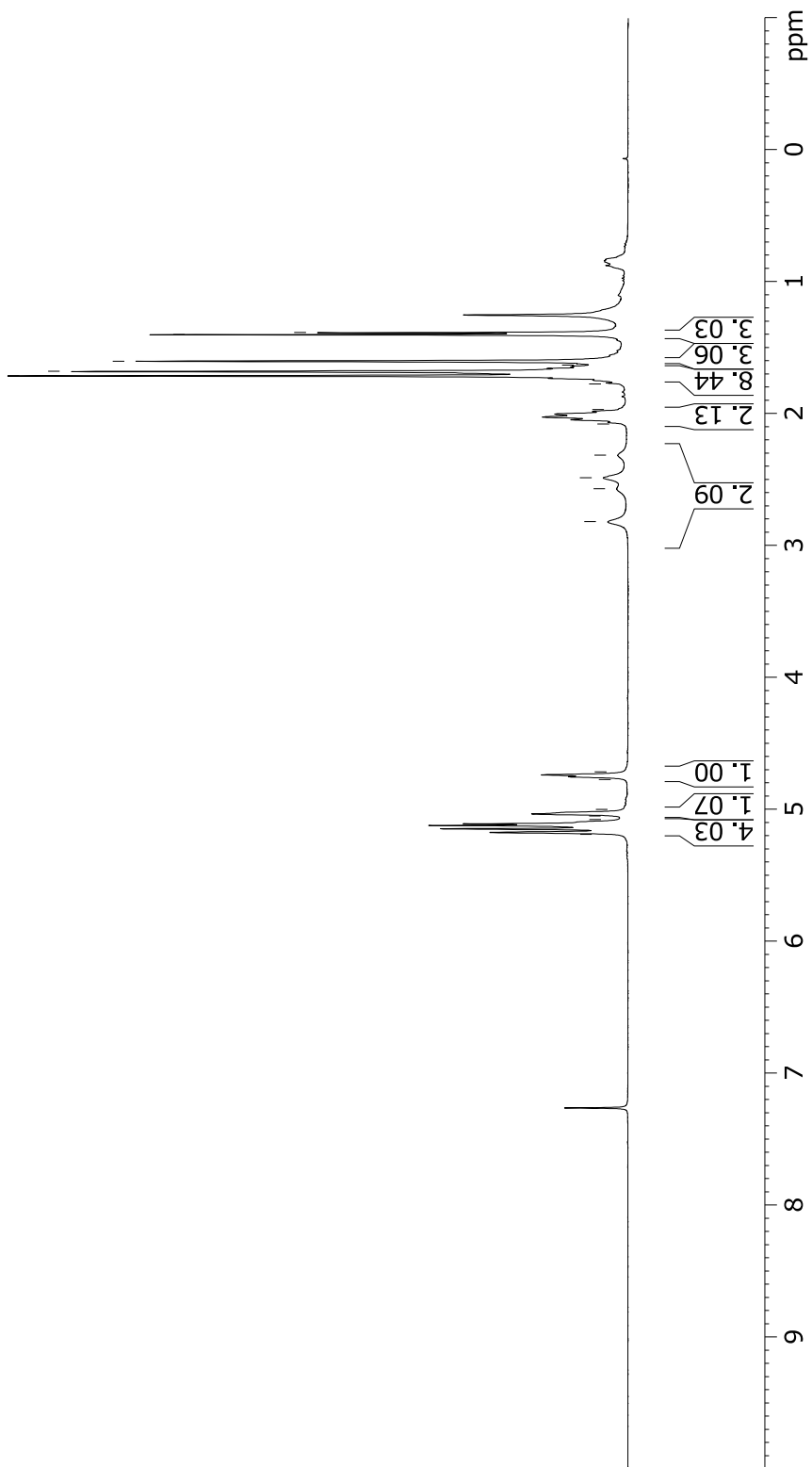
(119)

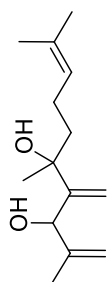




2.82
 2.57
 2.49
 2.32
 2.08
 1.97
 1.78
 1.71
 1.68
 1.63
 1.60
 1.40
 1.39

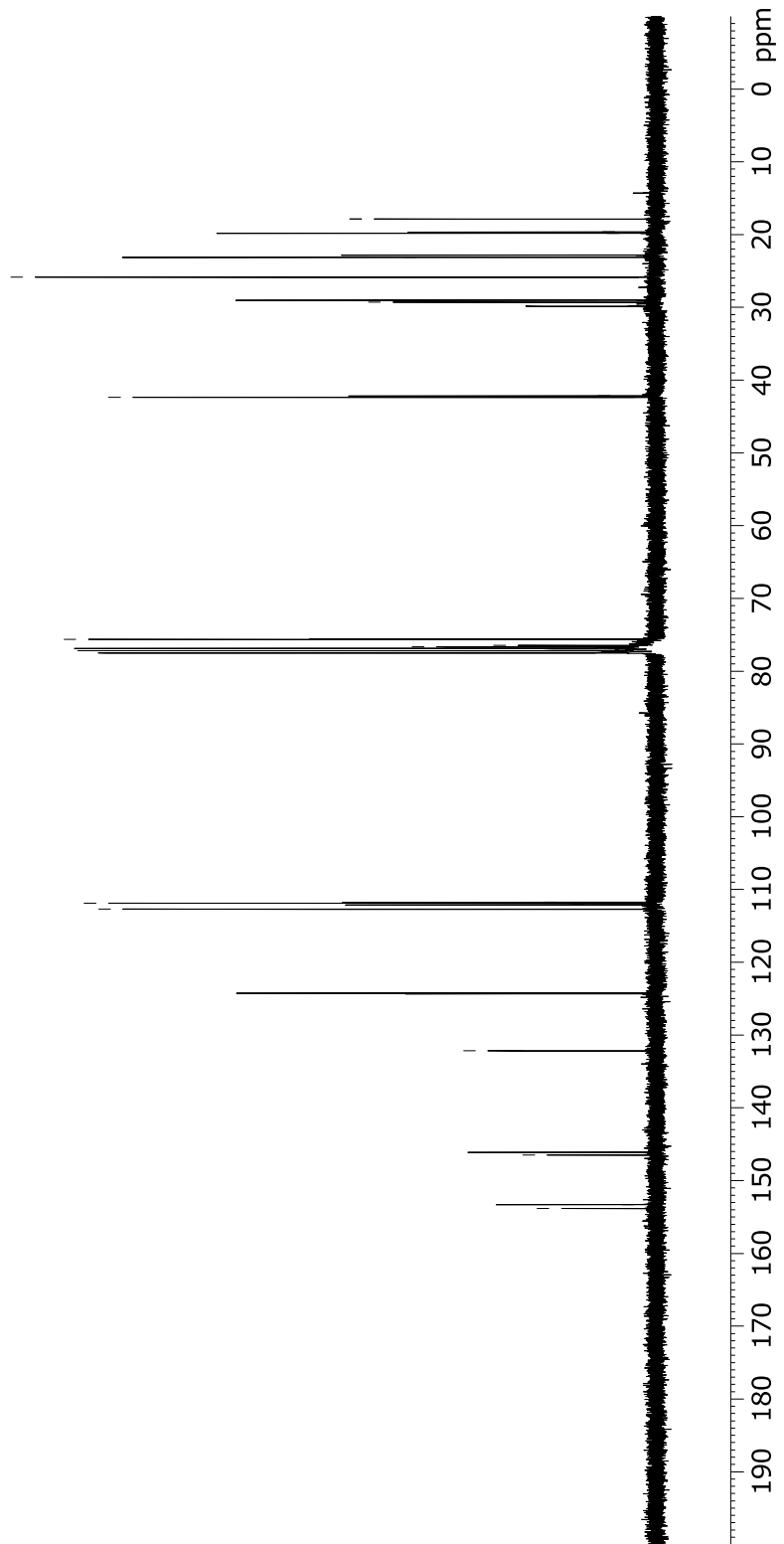
5.19
 5.08
 5.05
 5.00
 4.77
 4.72

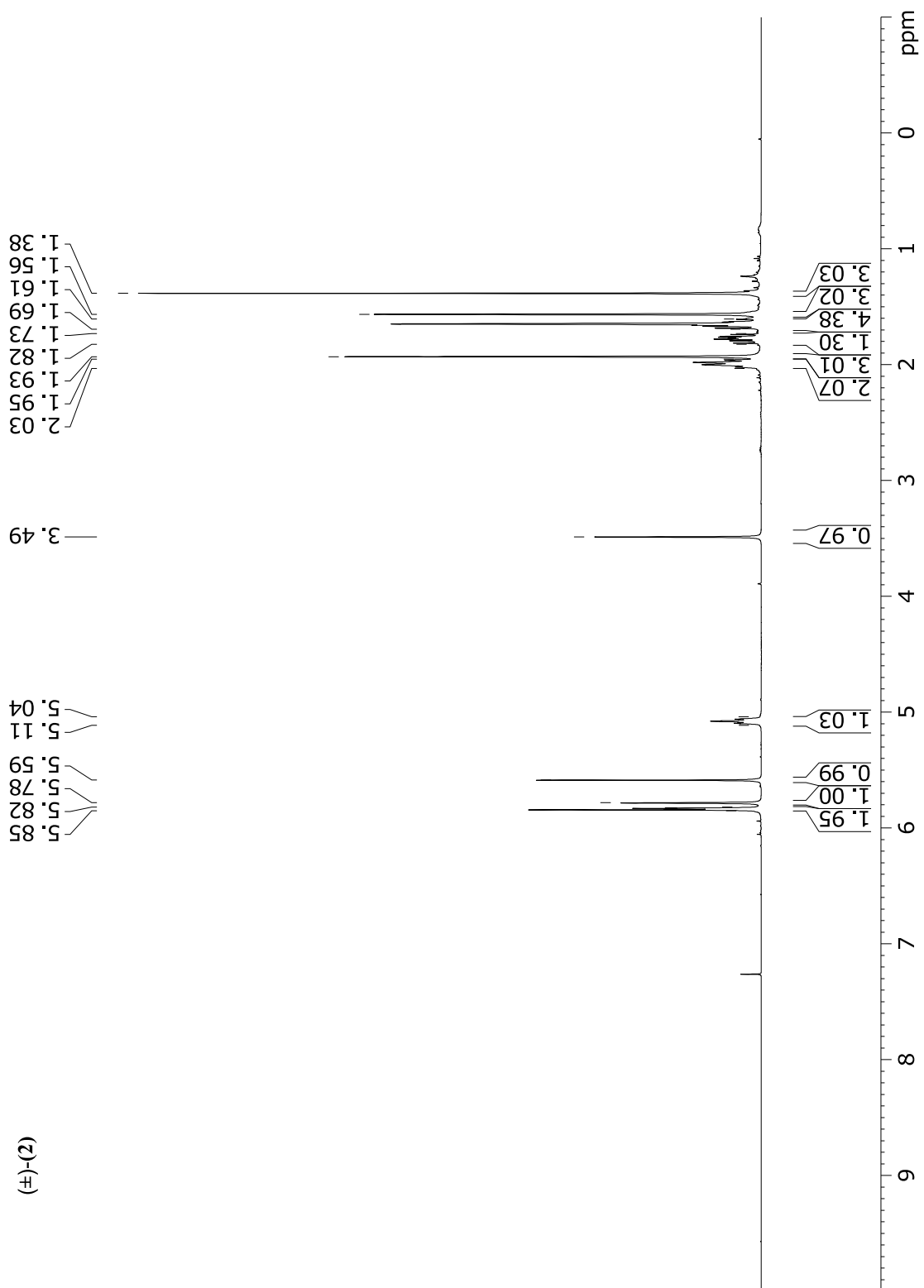
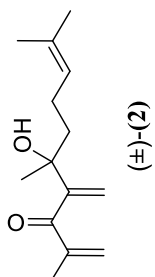


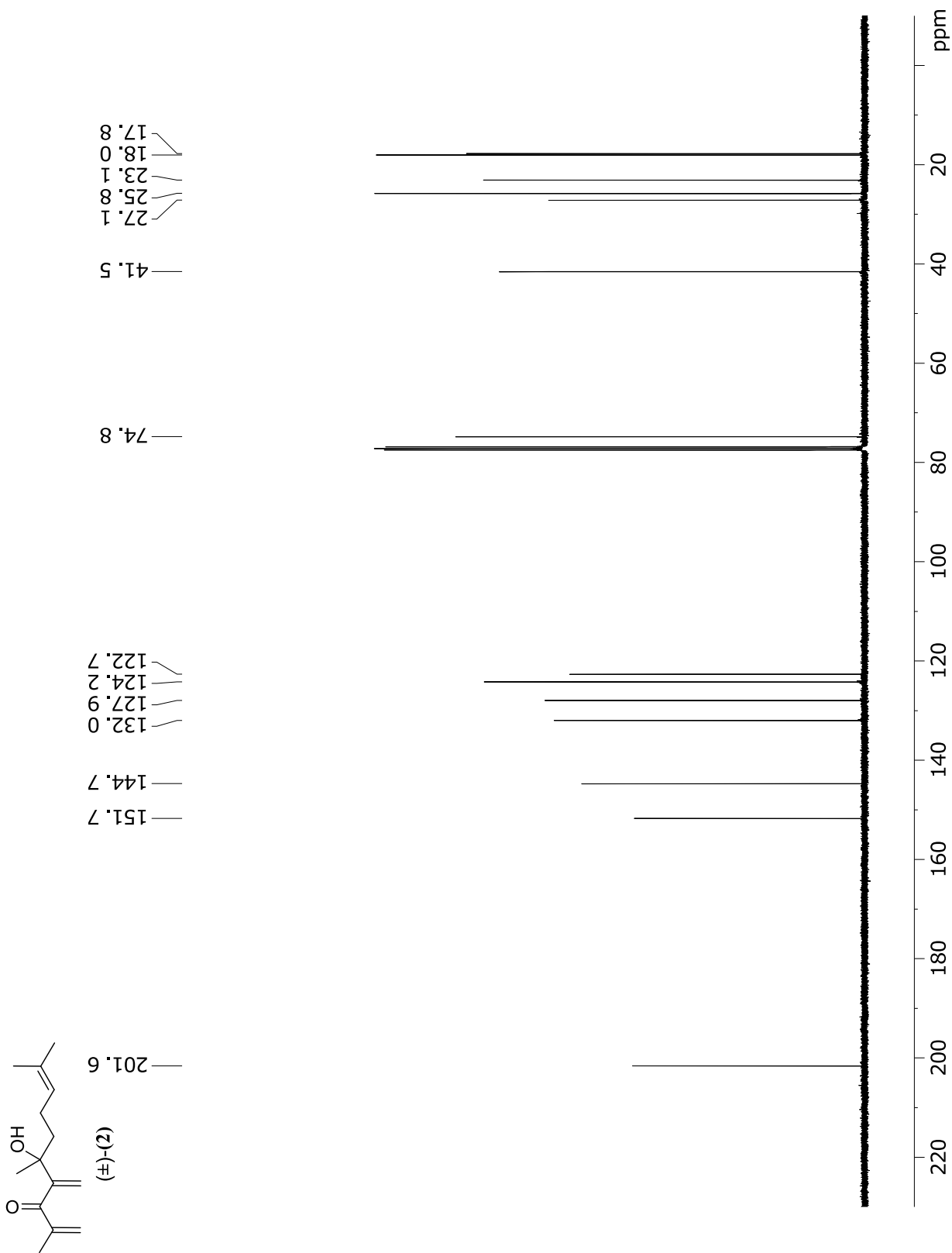


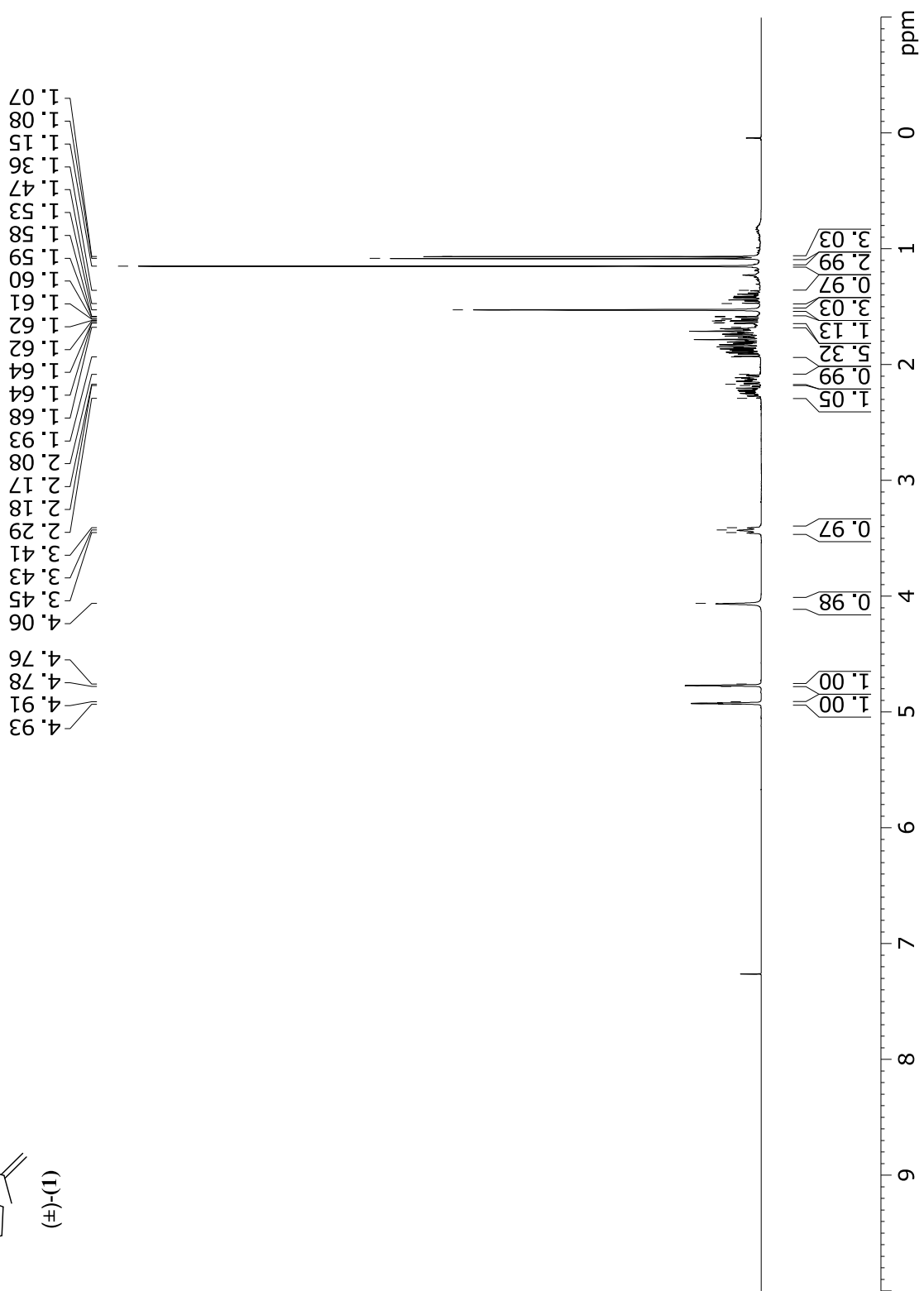
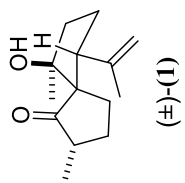
(±)-(134)

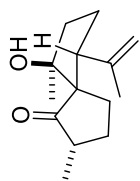
- 153.8
- 153.3
- 146.5
- 146.1
- 132.2
- 124.3
- 124.2
- 112.7
- 112.1
- 111.9
- 111.7
- 76.6
- 76.4
- 75.6
- 75.6
- 75.6
- 42.3
- 42.2
- 29.3
- 29.0
- 25.8
- 23.1
- 22.8
- 19.8
- 19.8
- 19.6
- 17.9
- 17.8











— 228.9

— 144.3

— 113.2

— 85.6

— 63.0

— 53.2

— 45.5

— 37.7

— 28.5

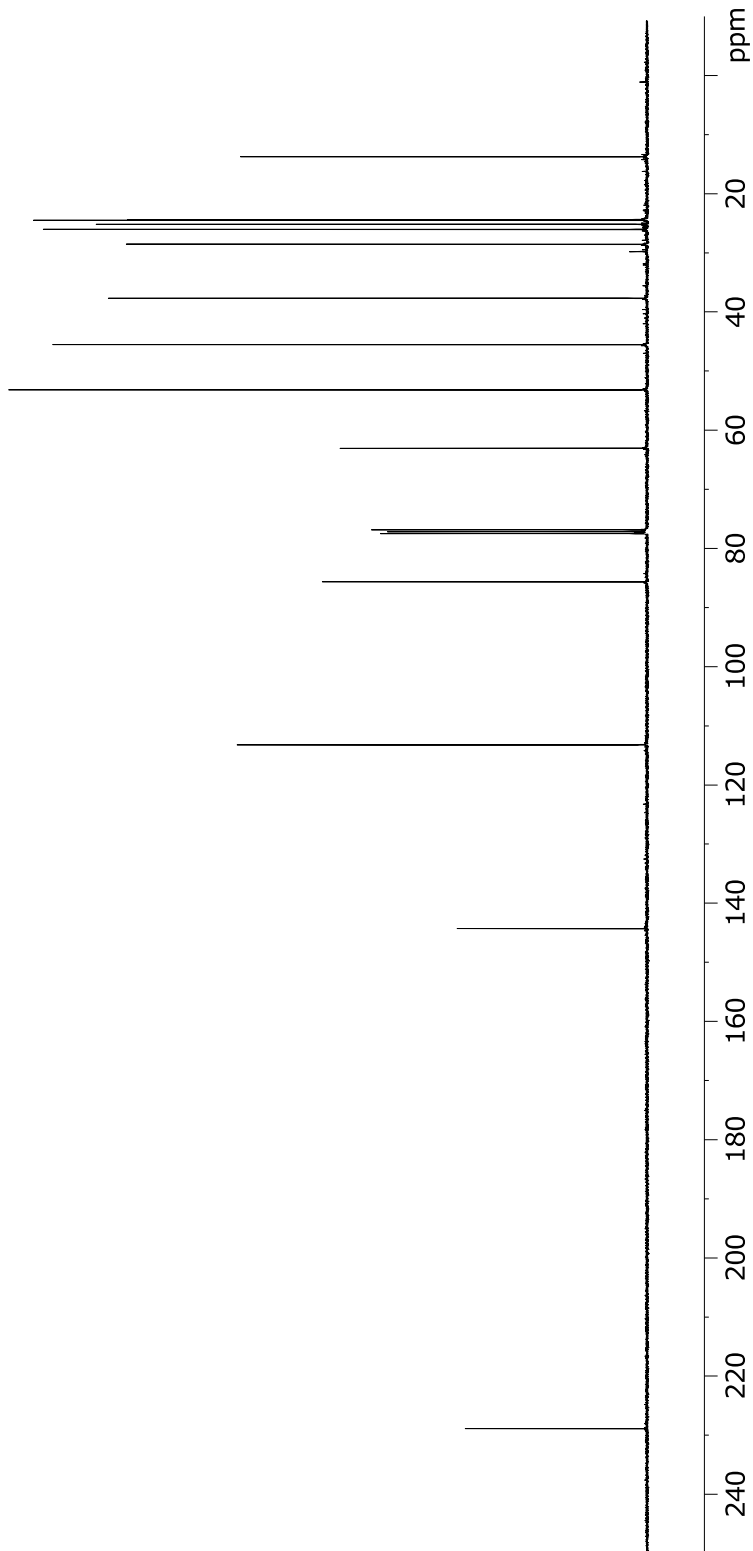
— 26.0

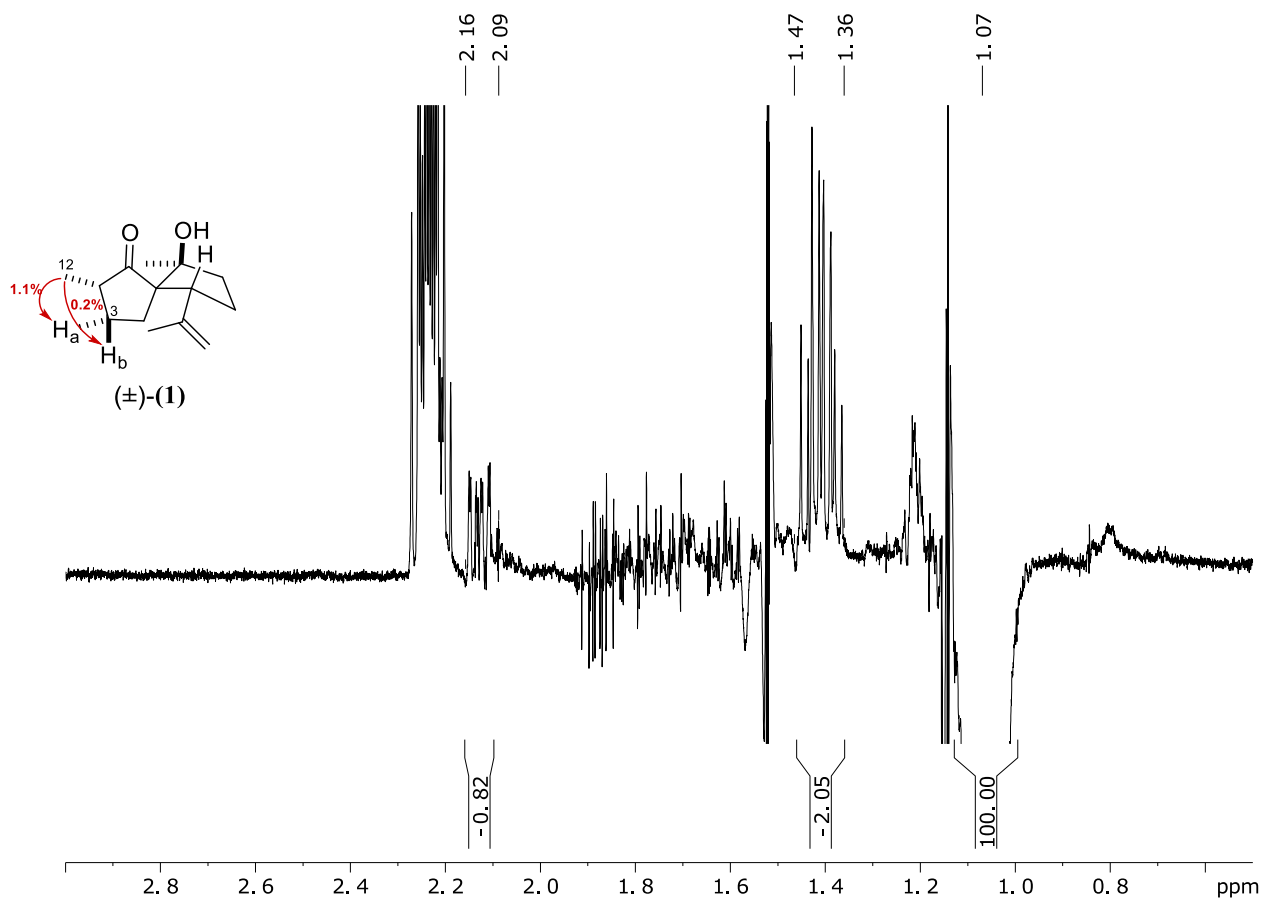
— 25.2

— 24.5

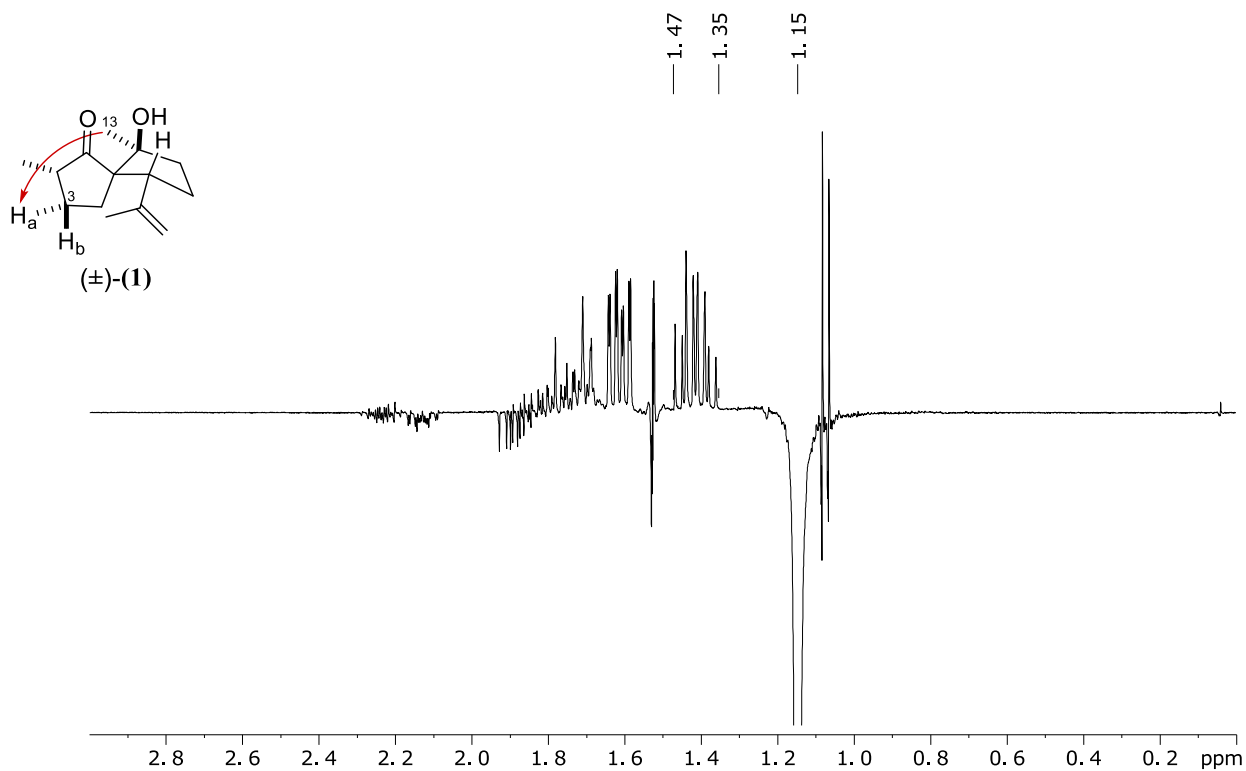
— 24.4

— 13.7

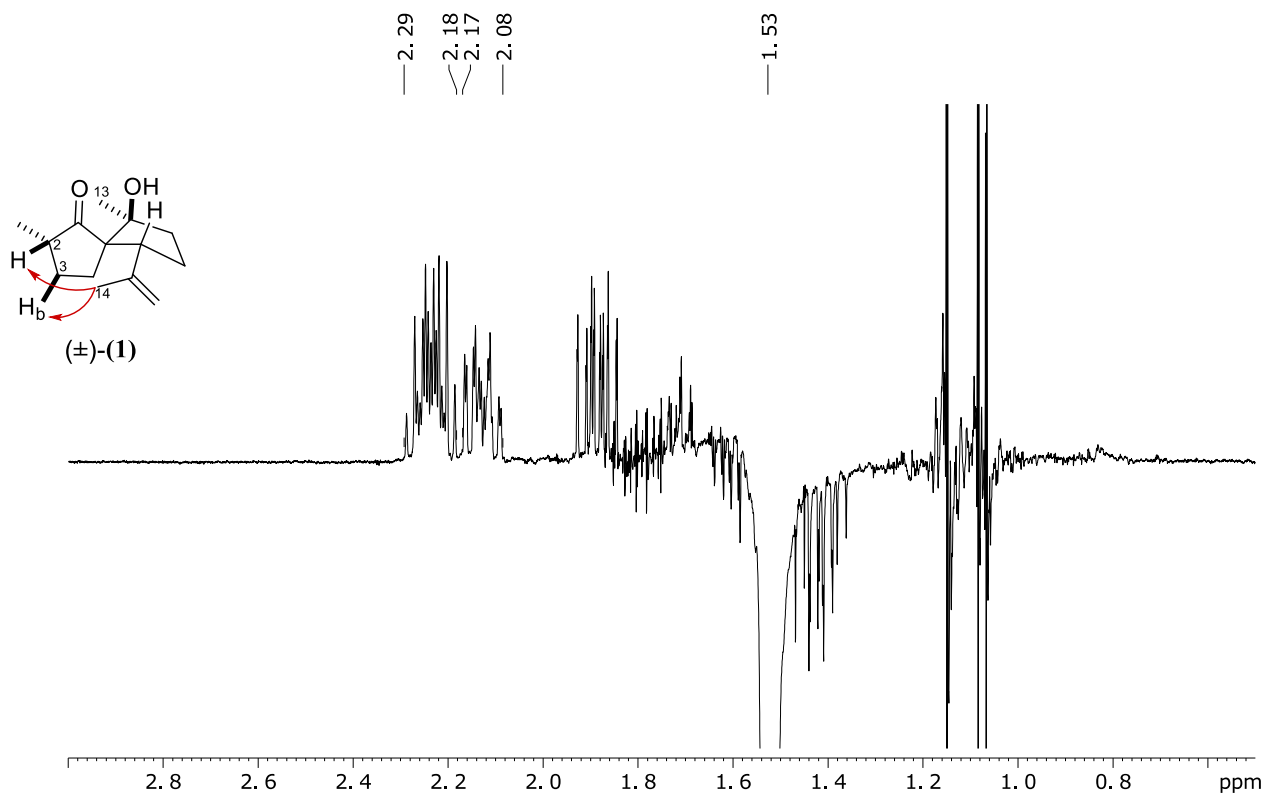




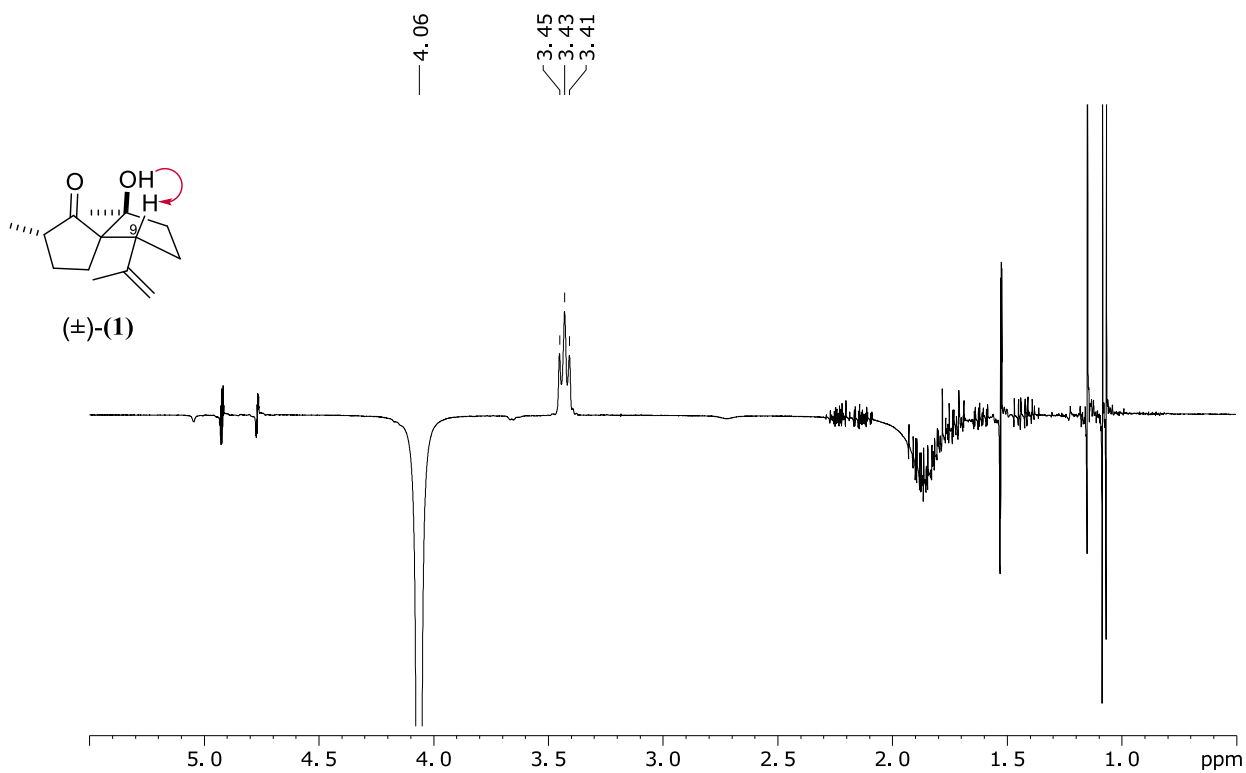
NOE response of (\pm) -**1** after irradiation at 1.07 ppm (CH_3 -12); NOE intensity quantified by integration to unambiguously distinguish between *syn*- and *anti*-aligned proton of CH_2 -3; spectrum measured in $CDCl_3$ at 400 MHz.



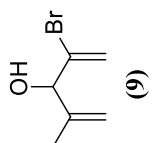
NOE response of (\pm) -**1** after irradiation at 1.15 ppm (CH_3 -13); spectrum measured in $CDCl_3$ at 400 MHz.



NOE response of (\pm) -**1** after irradiation at 1.53 ppm (CH₃-14); spectrum measured in CDCl₃ at 400 MHz.



NOE response of (\pm) -**1** after irradiation at 4.06 ppm (OH); spectrum measured in CDCl₃ at 400 MHz.



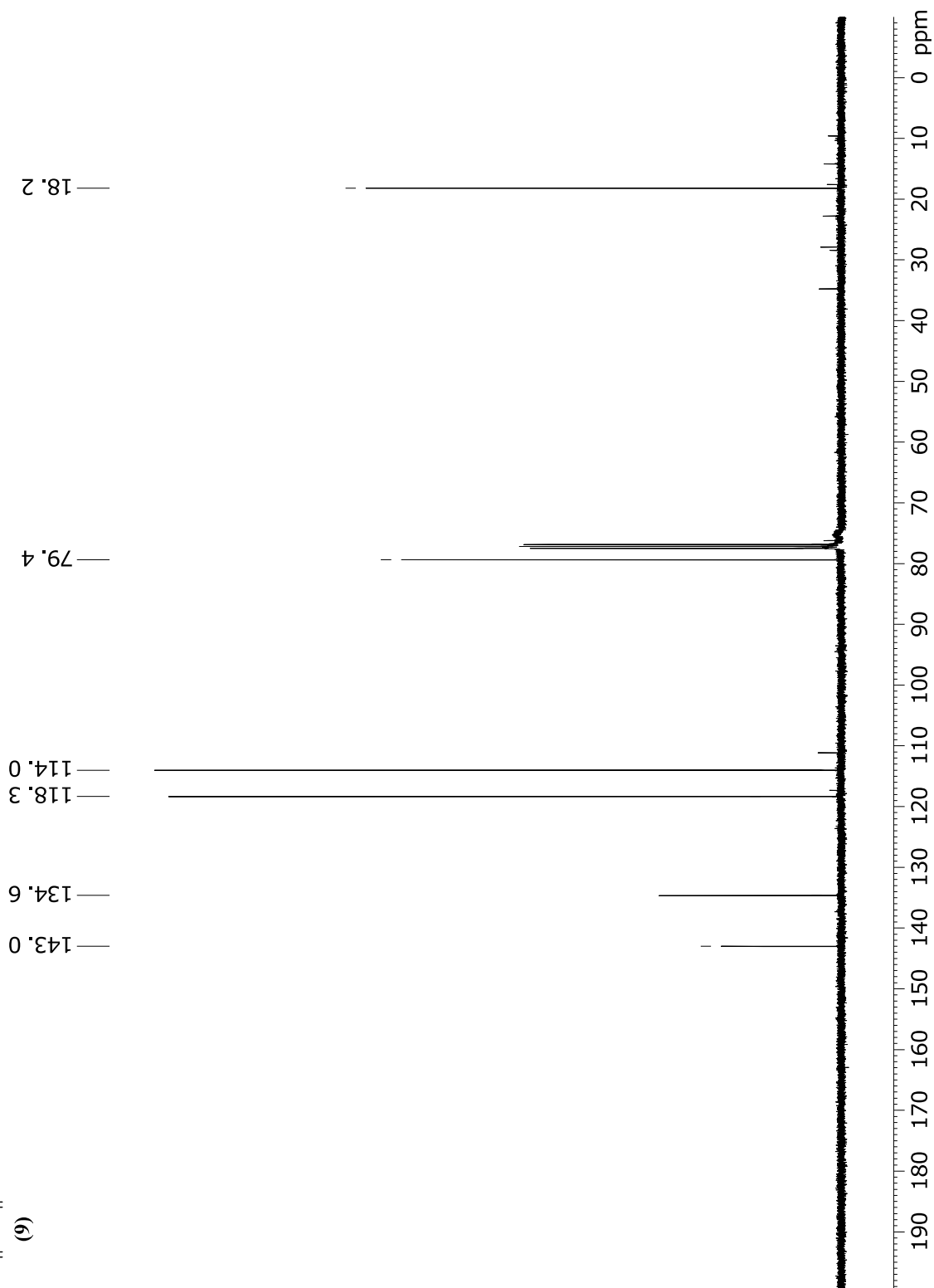
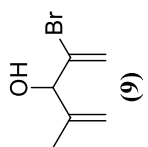
1.72
2.13
2.11

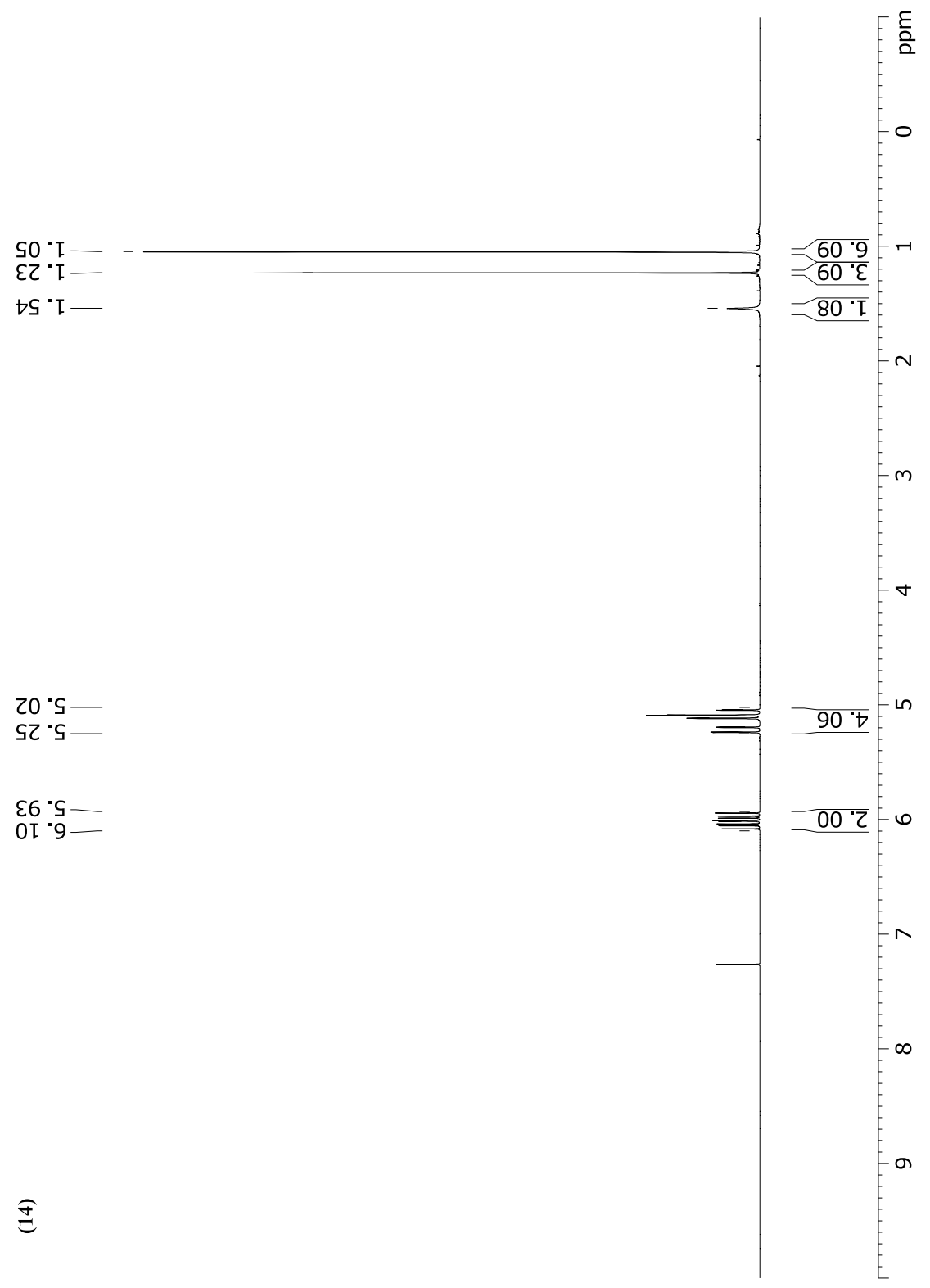
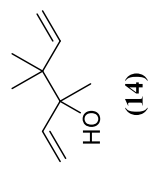
4.59
4.60
5.06
5.08
5.16
5.19
5.65
5.68
5.98
6.01

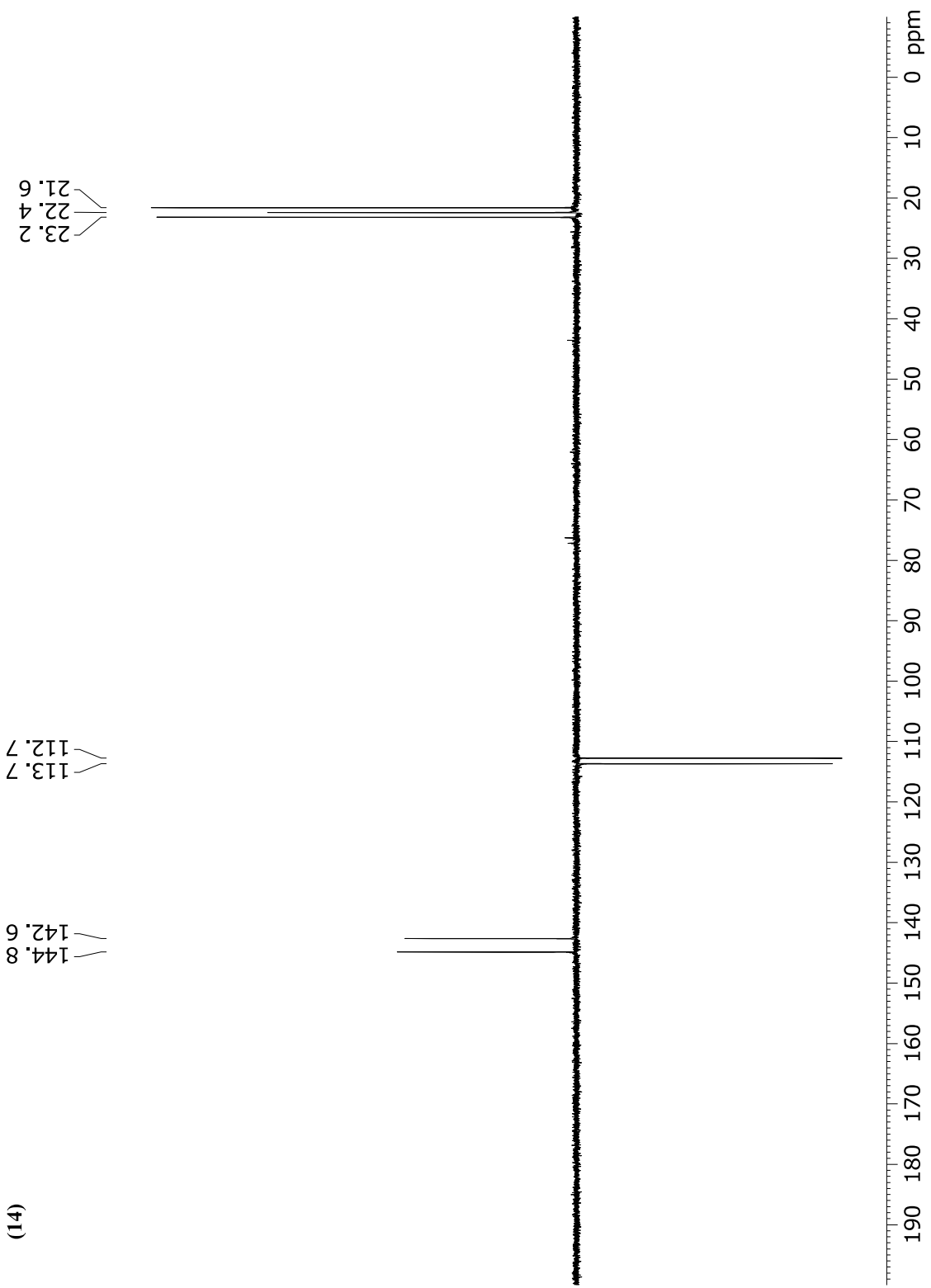
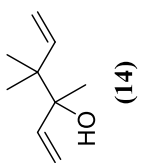
3.13
0.95

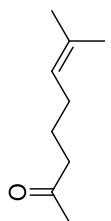
0.96
1.01
1.00
0.99
1.00



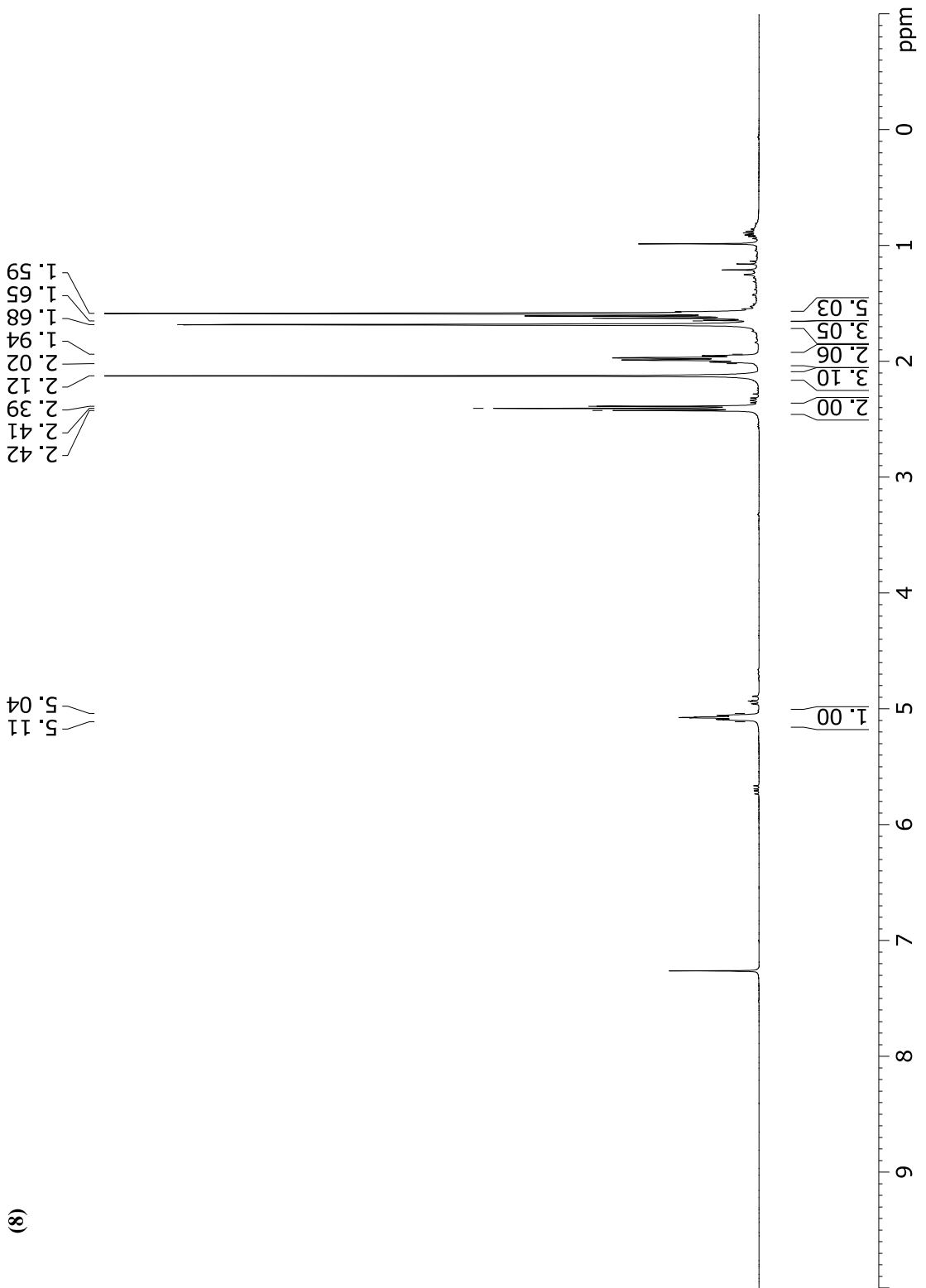


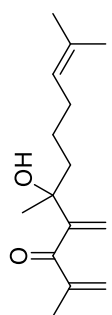




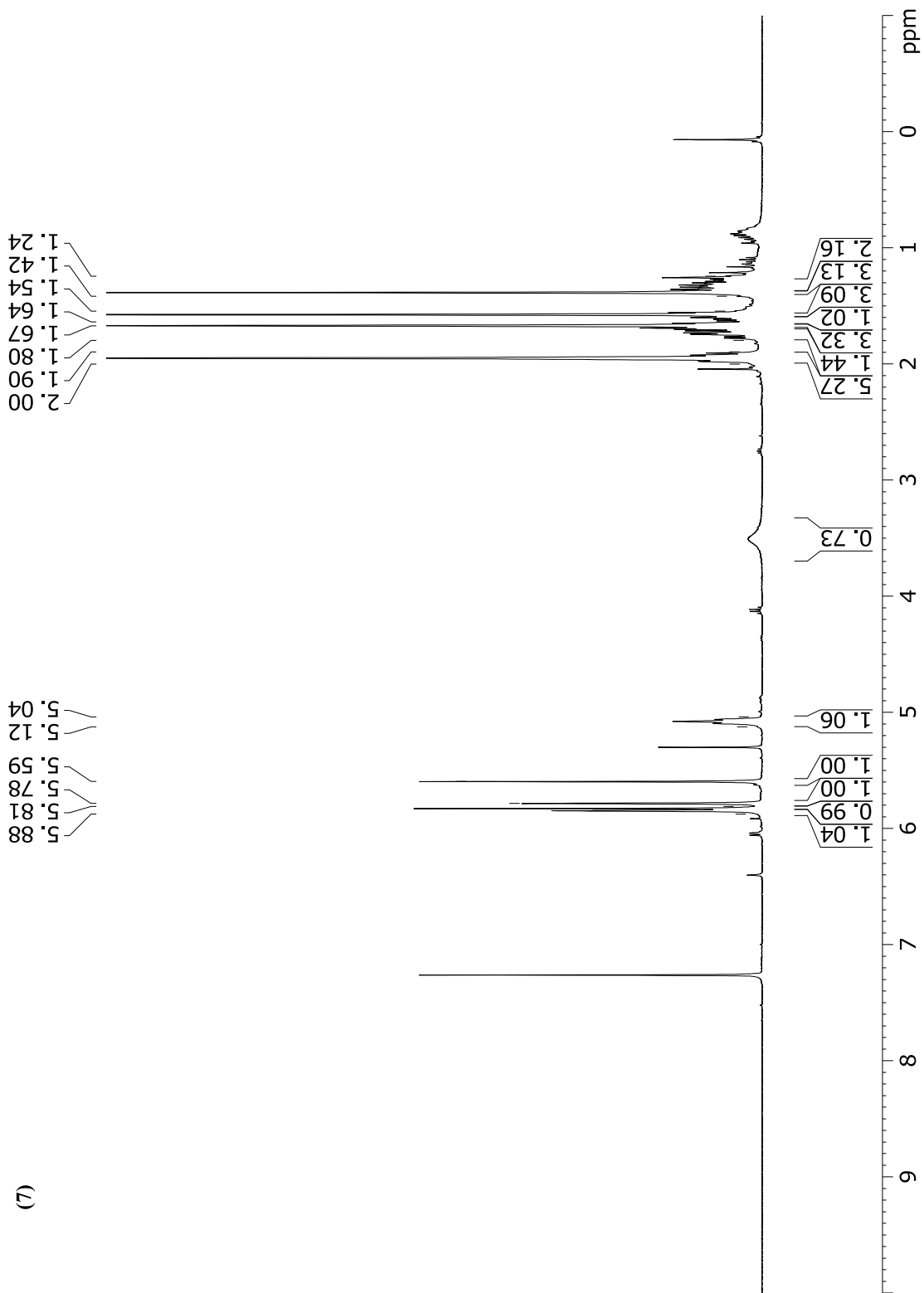


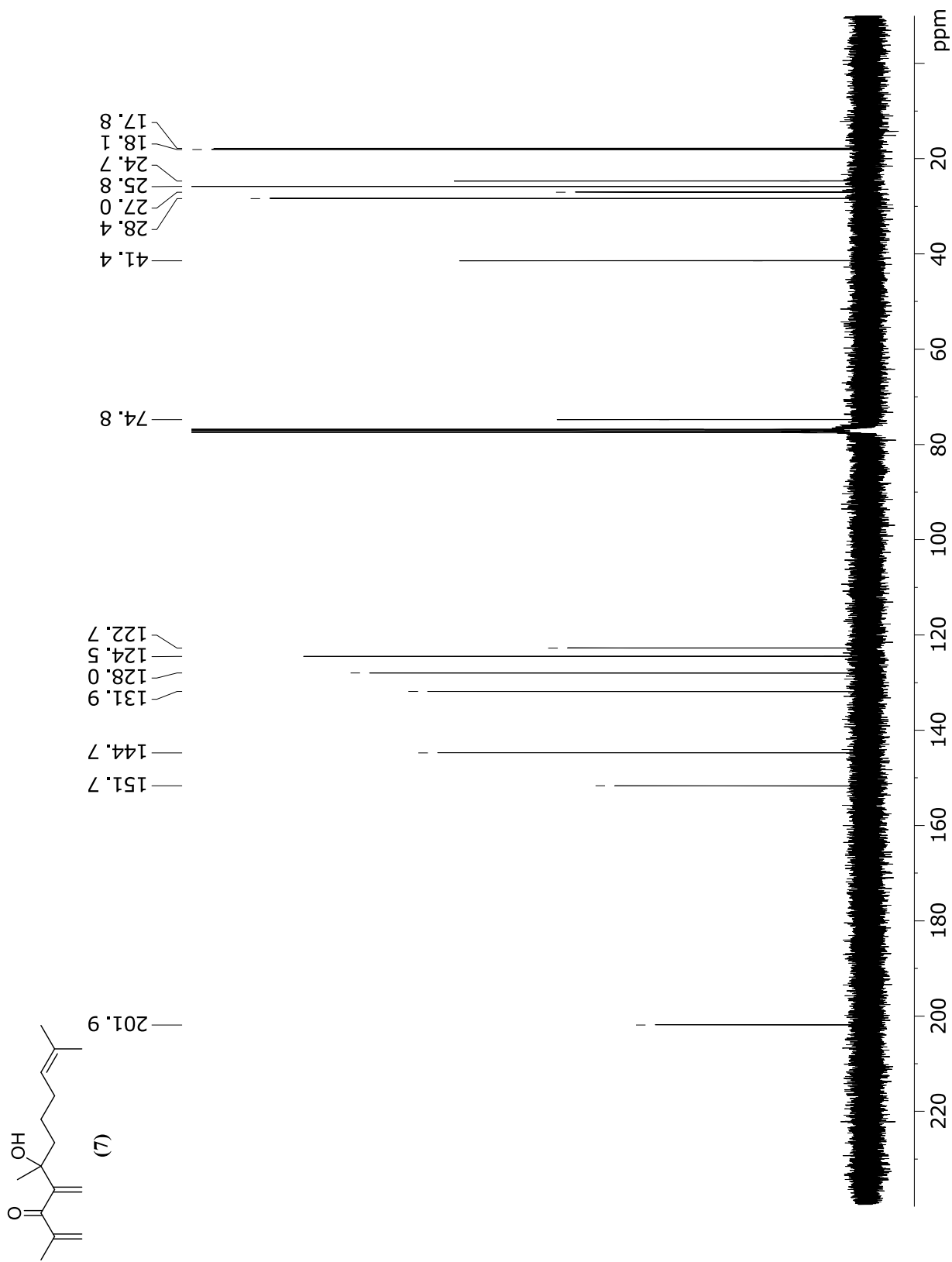
(8)

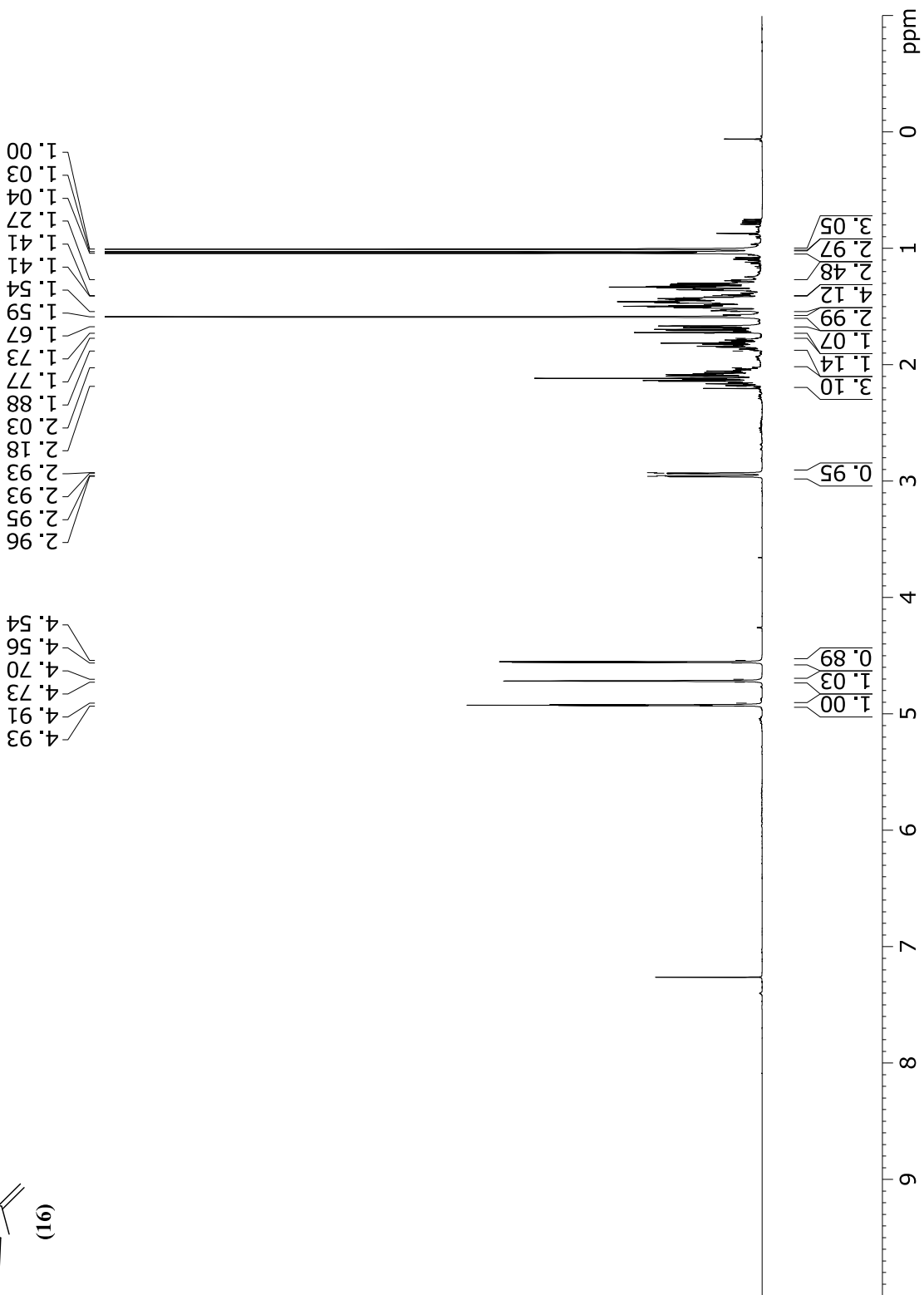
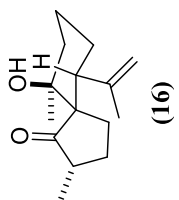


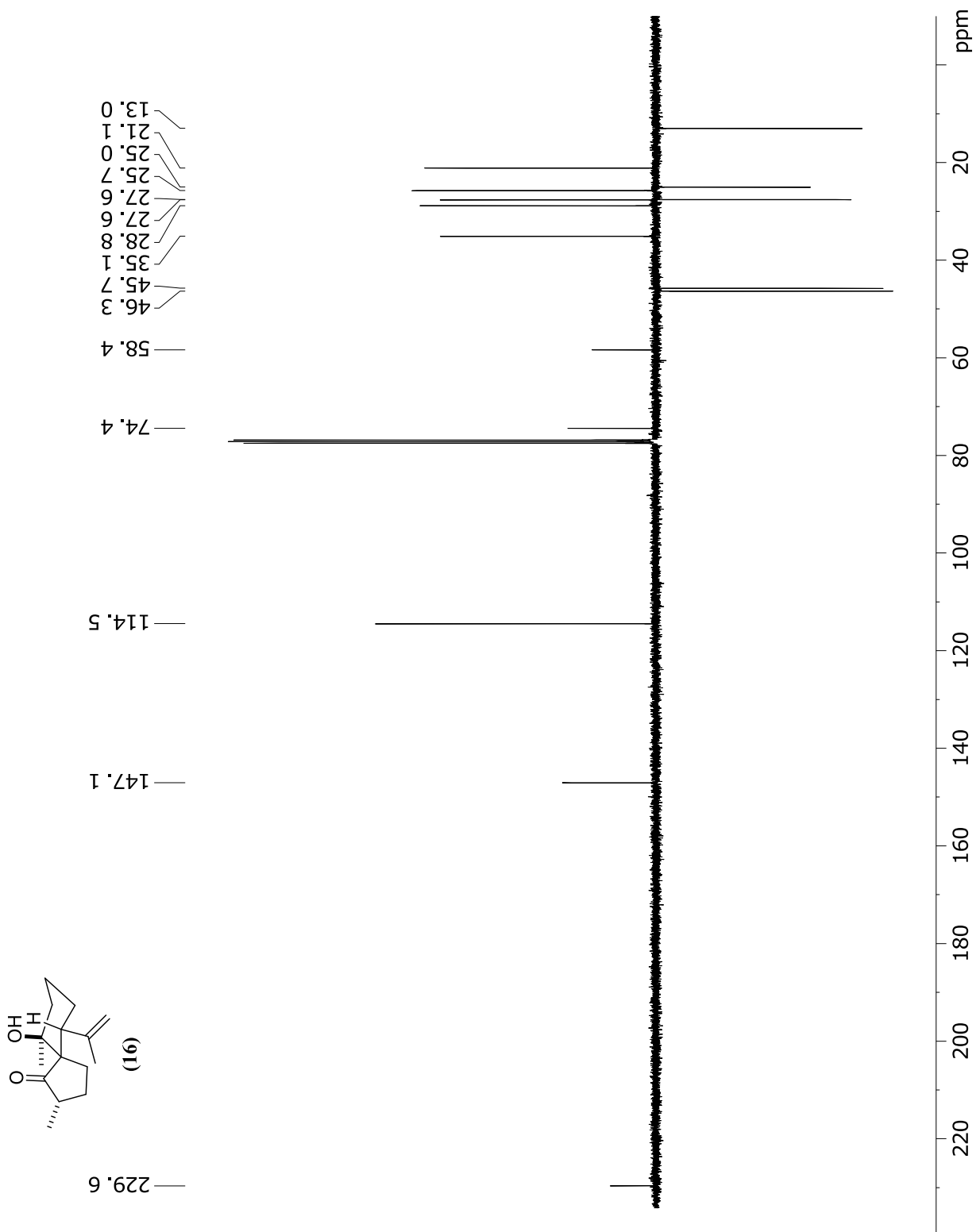


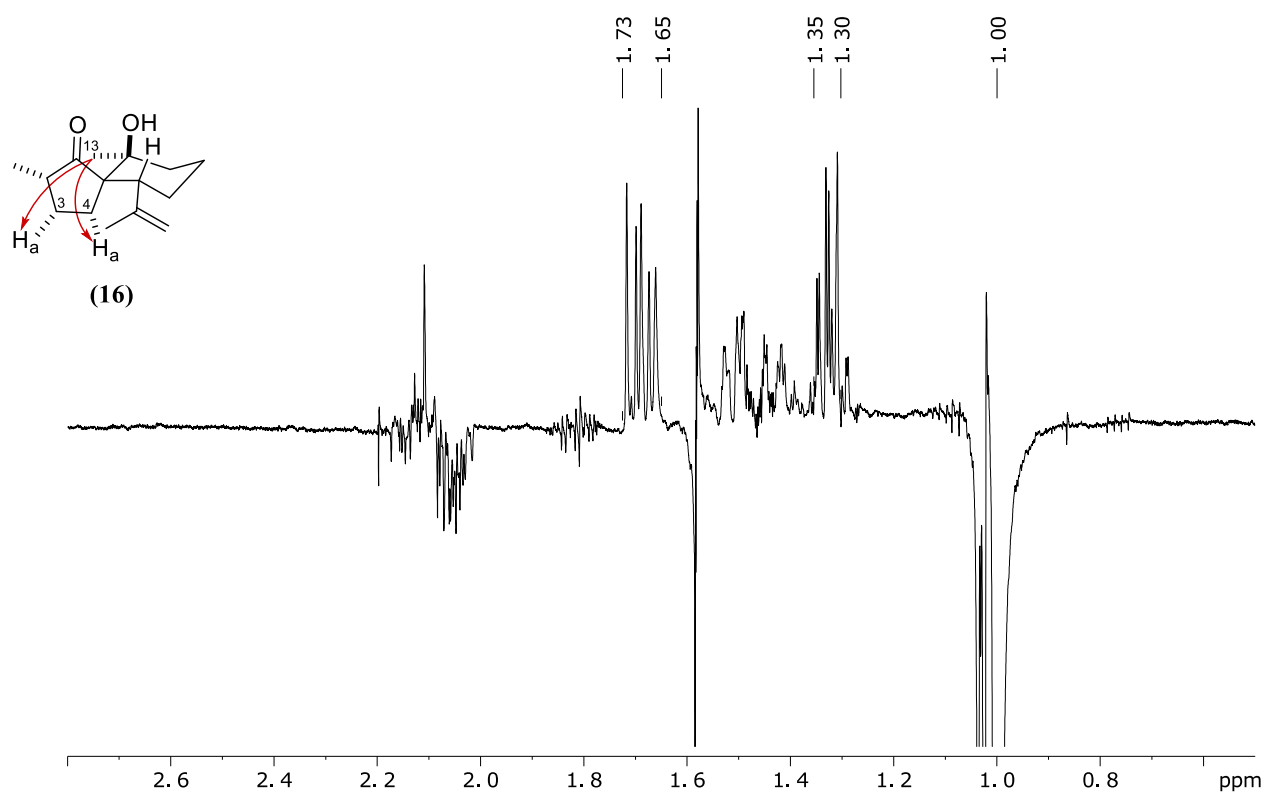
(7)



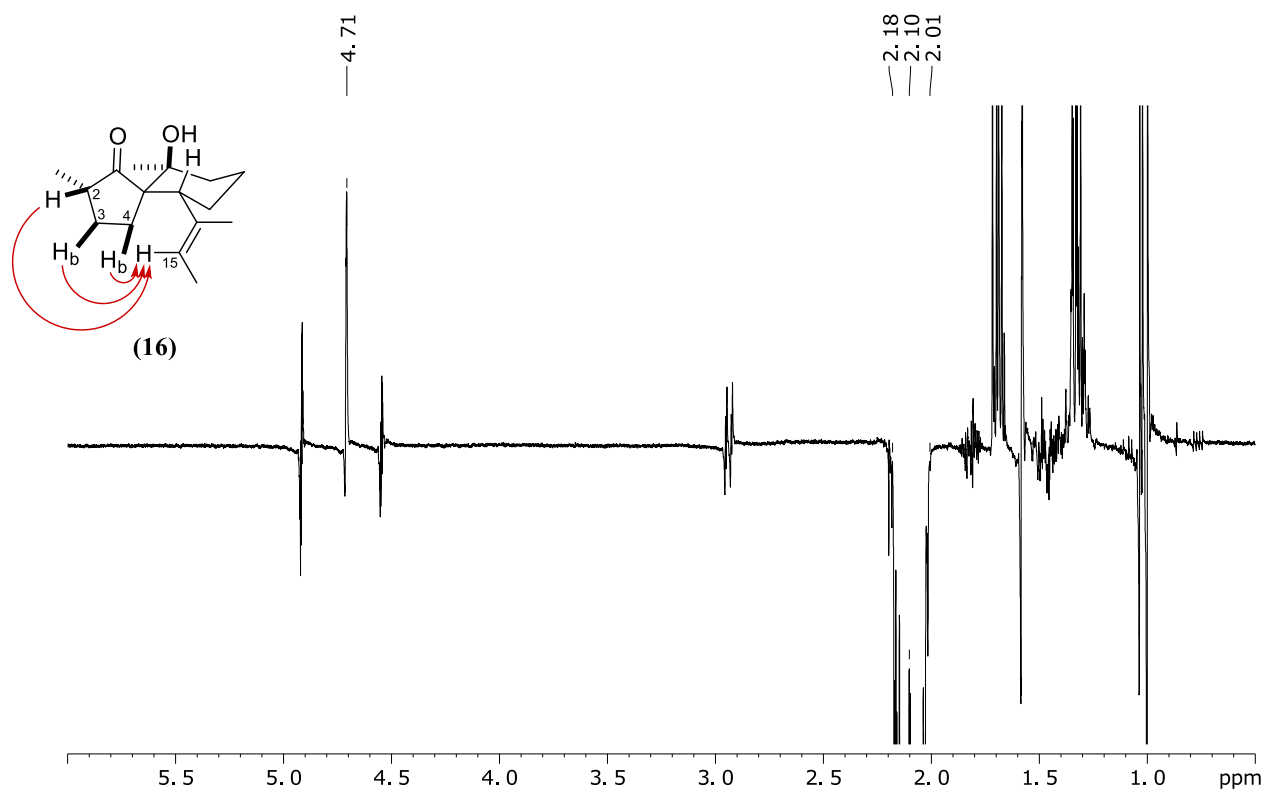




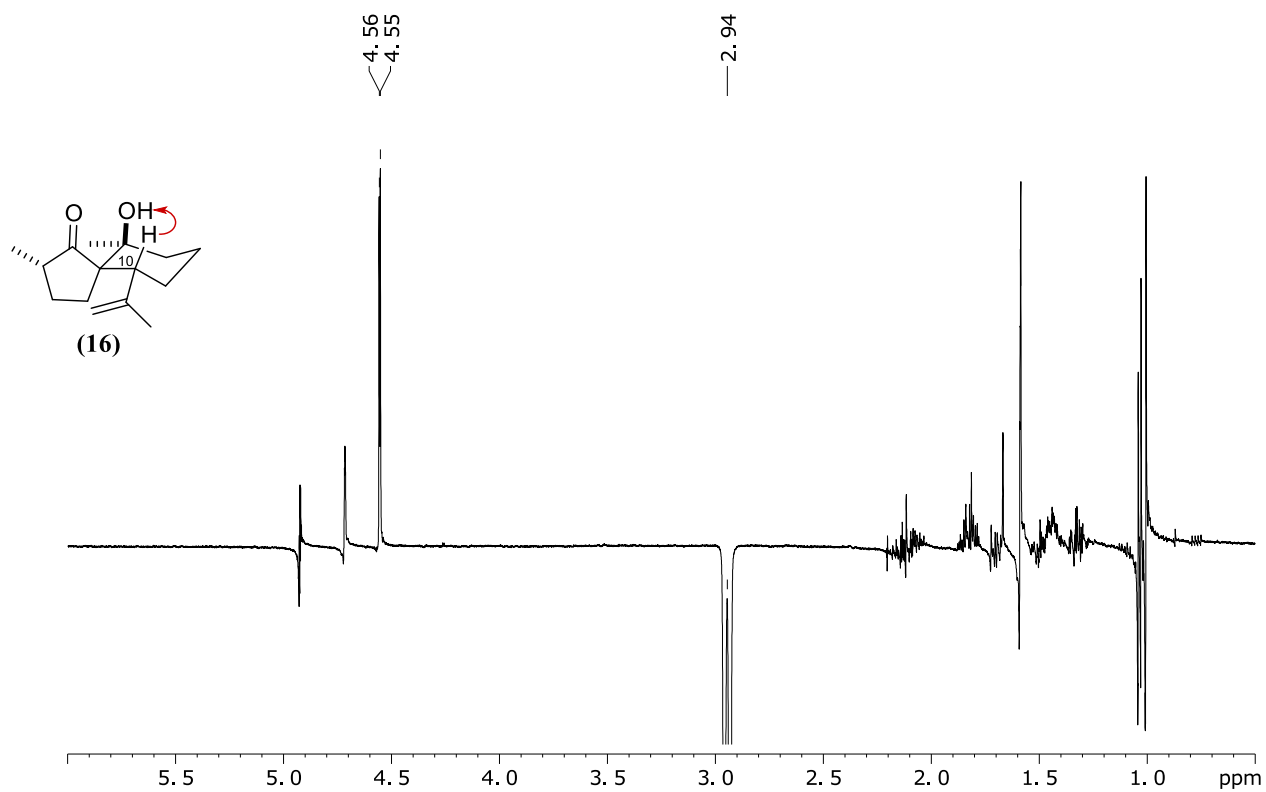




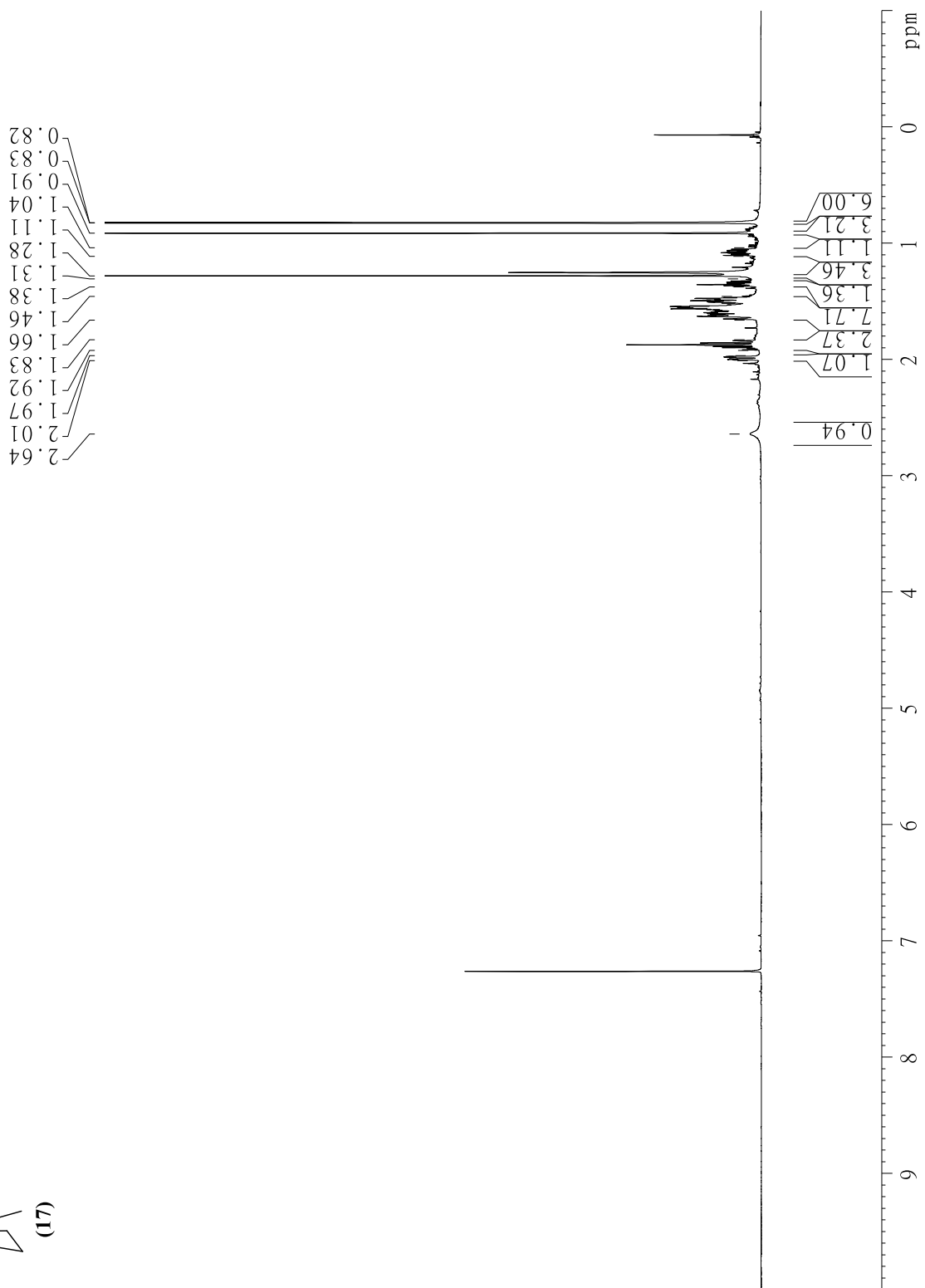
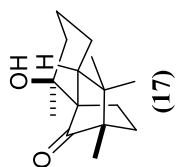
NOE response of **(16)** after irradiation at 1.00 ppm (CH_3 -13); spectrum measured in $CDCl_3$ at 500 MHz.

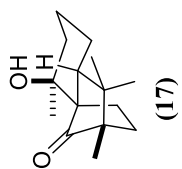


NOE response of **(16)** after irradiation at 2.10 ppm (CH -2, CH_2 -3b and CH_2 -4b); the saturated multiplet (2.18–2.01 ppm) corresponds to all three protons. No distinction was possible due to strong overlap of the signals. Spectrum measured in $CDCl_3$ at 500 MHz.



NOE response of (16) after irradiation at 2.94 ppm (CH-10); spectrum measured in CDCl₃ at 500 MHz.

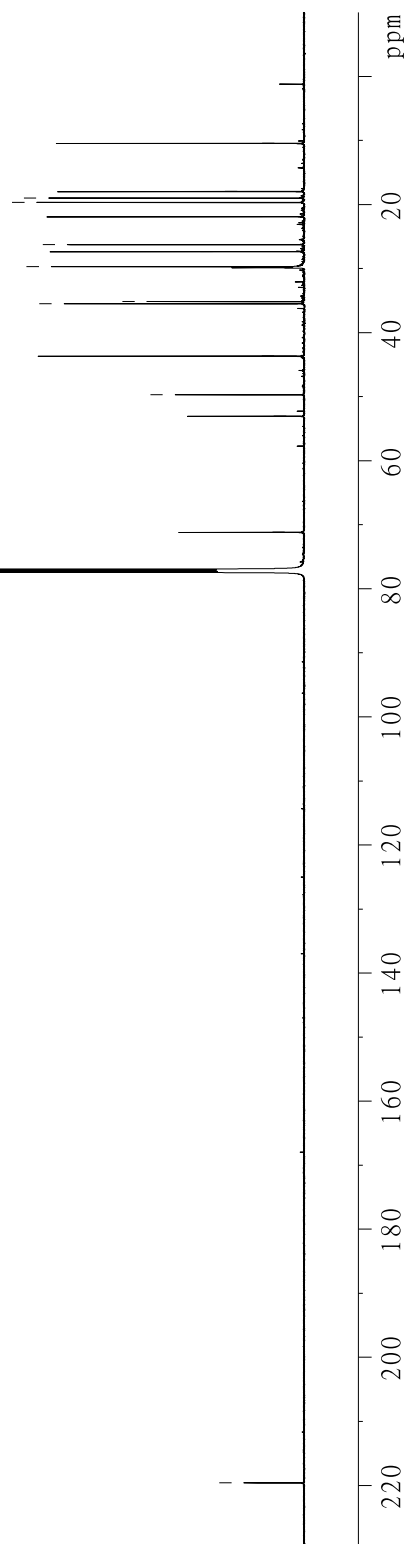


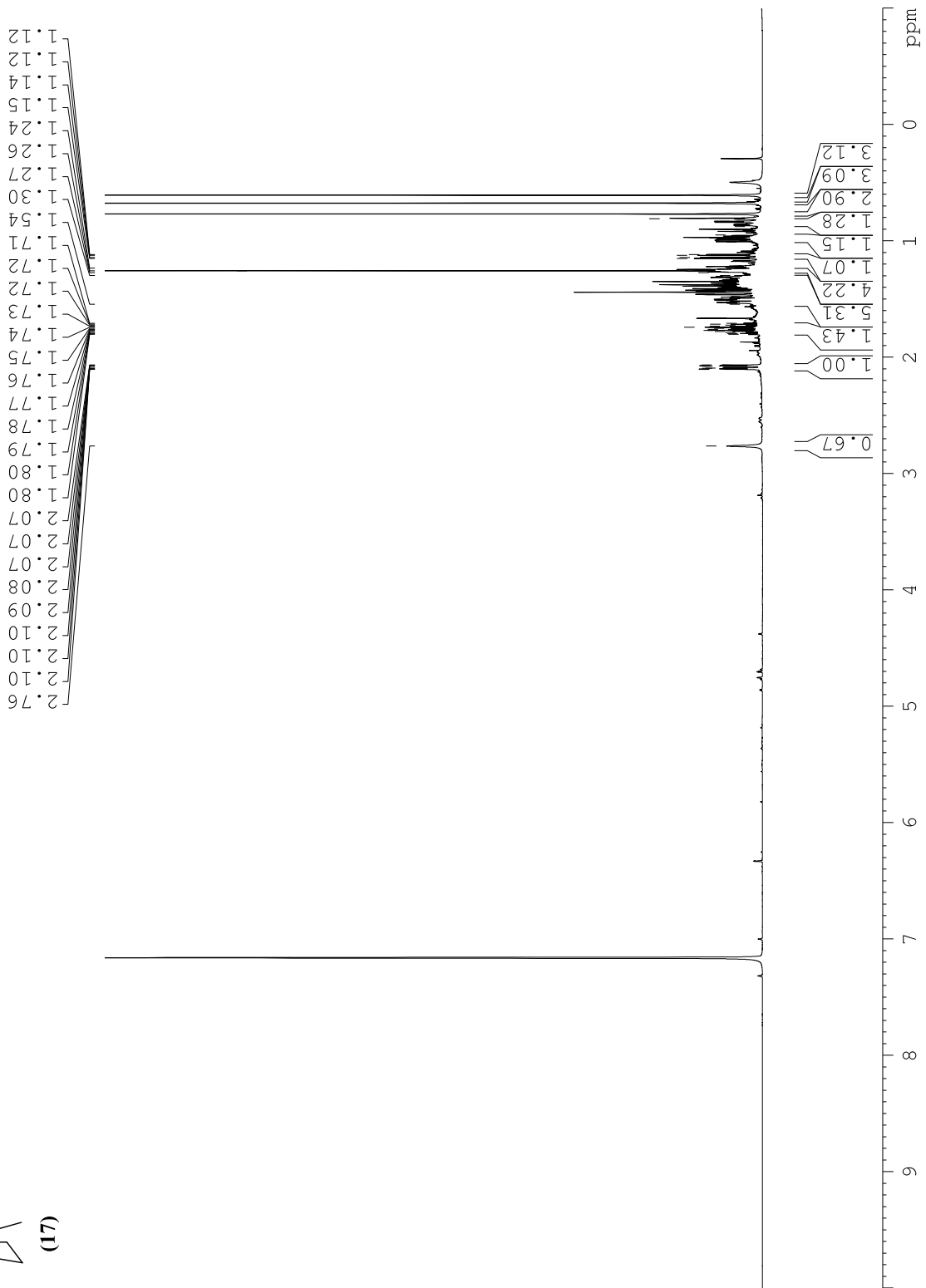
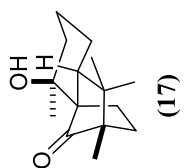


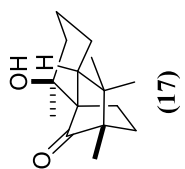
— 219.6

53.1
49.7
43.7
35.5
35.1
29.7
27.3
26.3
21.9
19.7
19.0
18.0
10.5

— 71.2

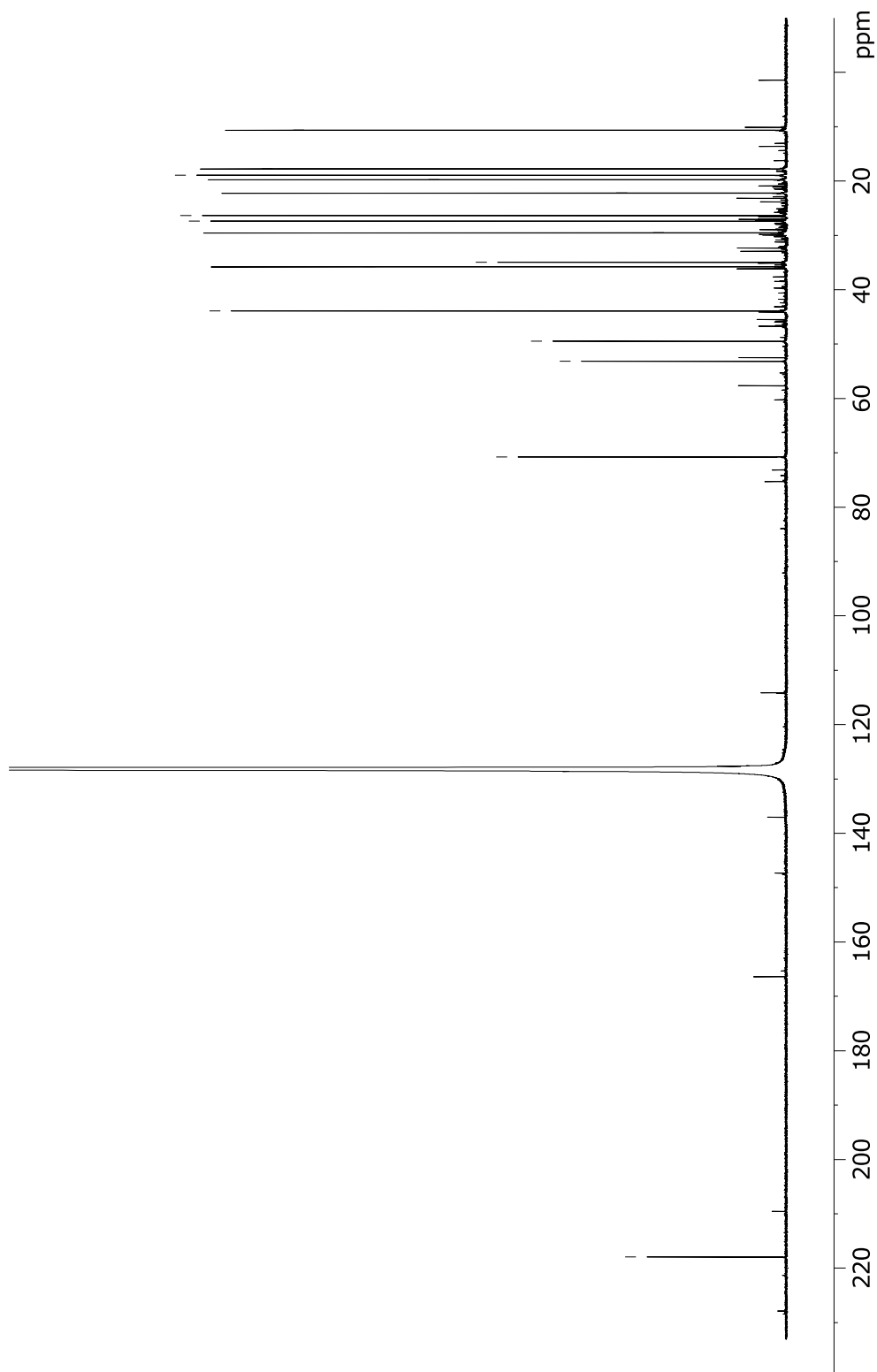


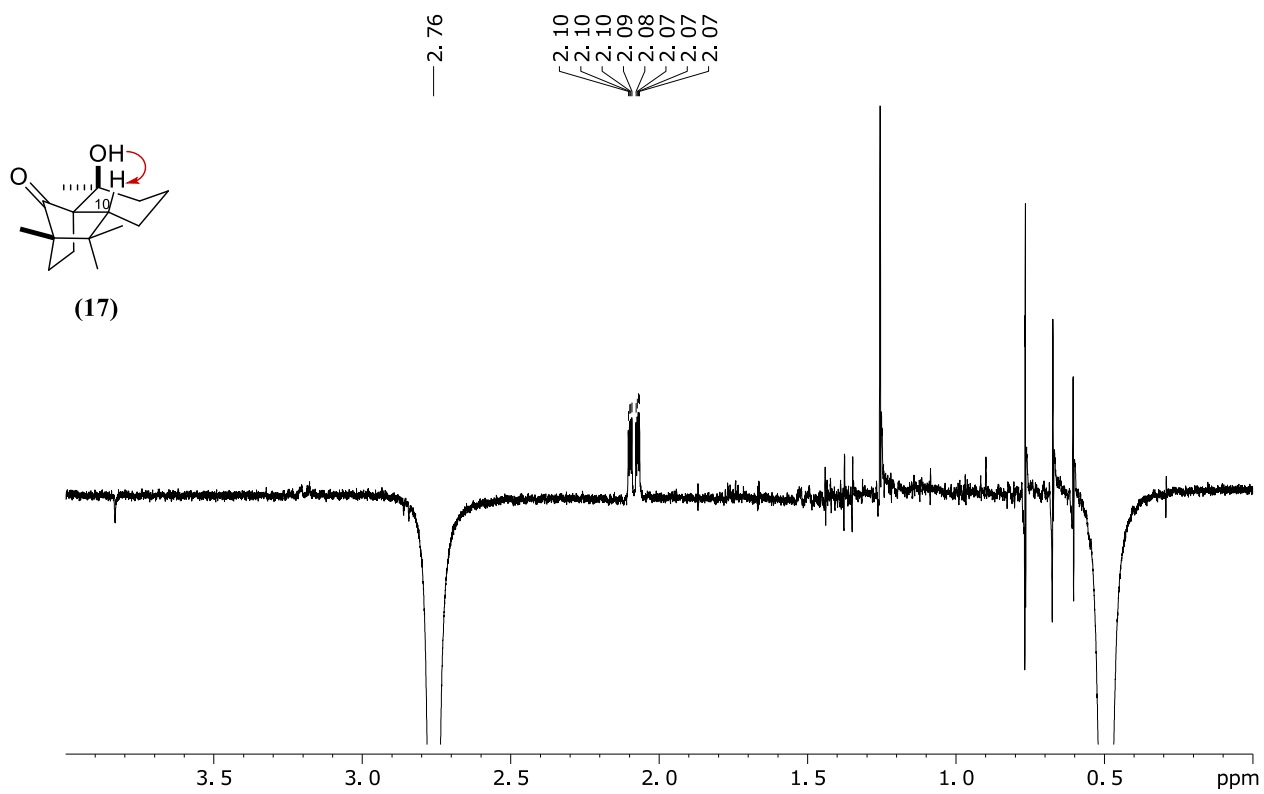




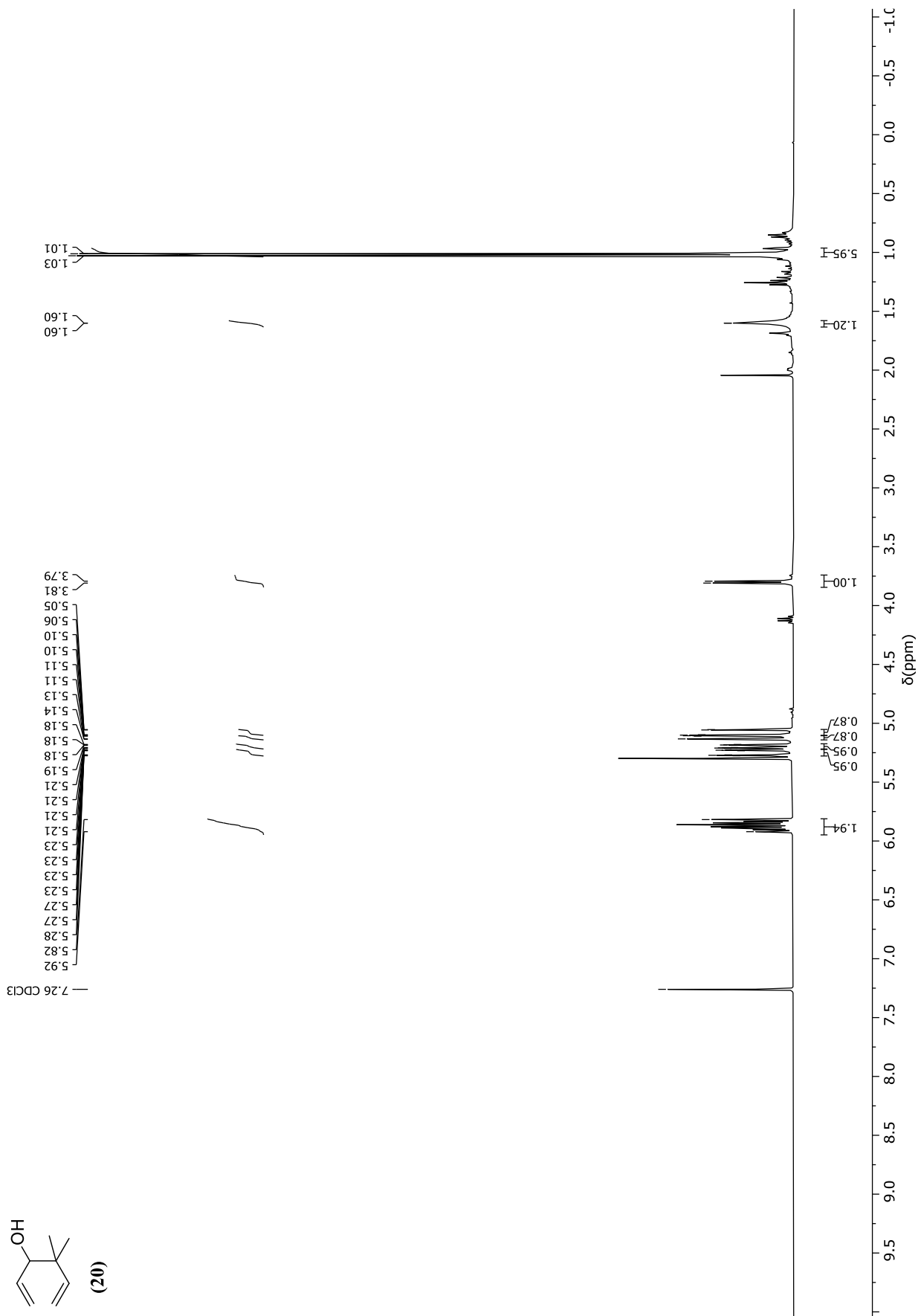
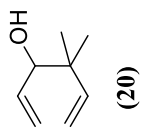
— 217.9

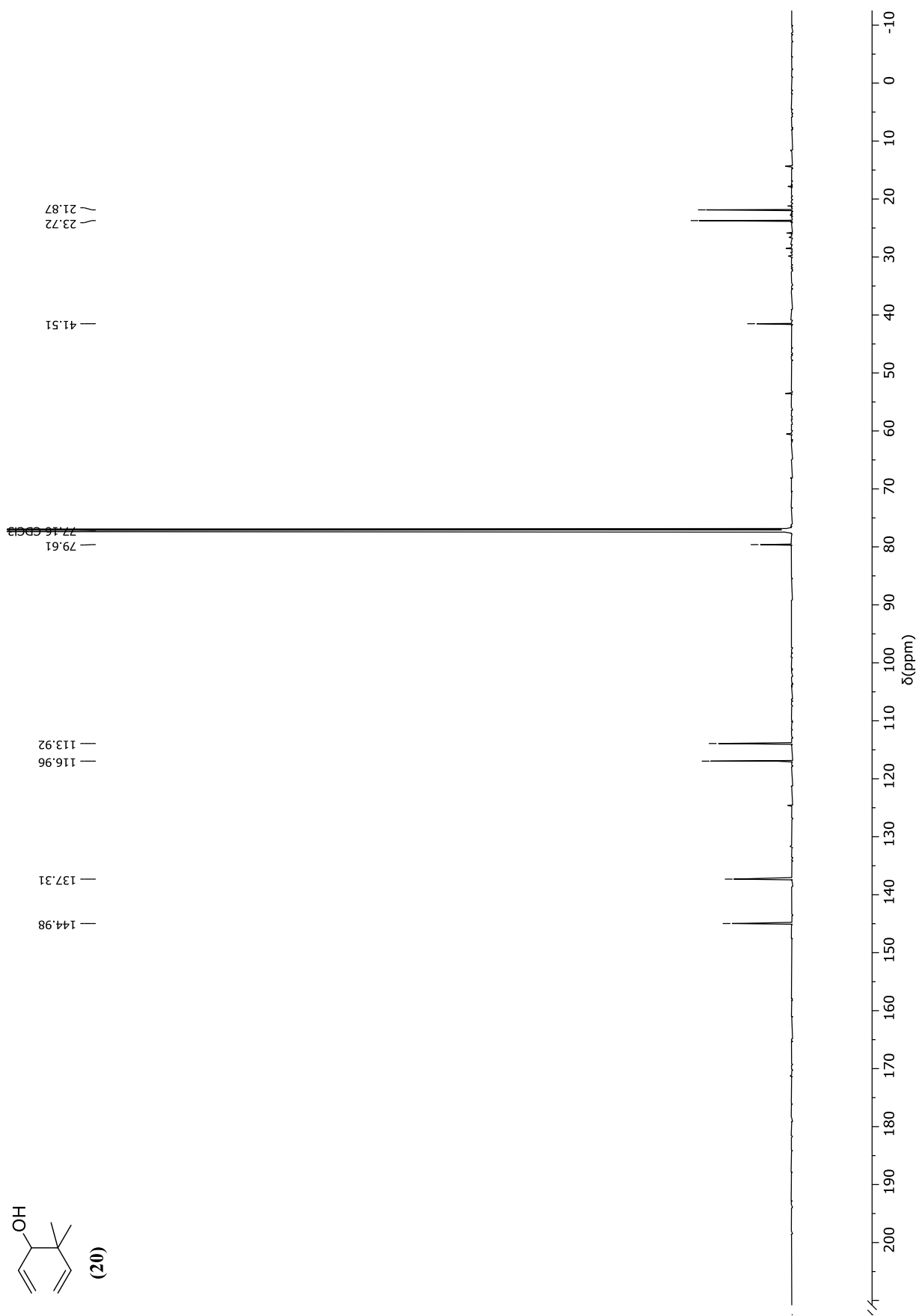
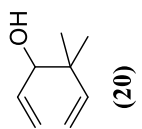
53.1
49.5
43.9
35.8
34.9
29.5
27.3
26.3
22.2
19.7
18.9
17.7
10.6

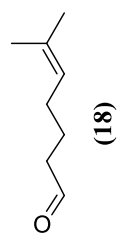




NOE response of (17) after irradiation at 2.76 ppm (OH); spectrum measured in C₆D₆ at 500 MHz.



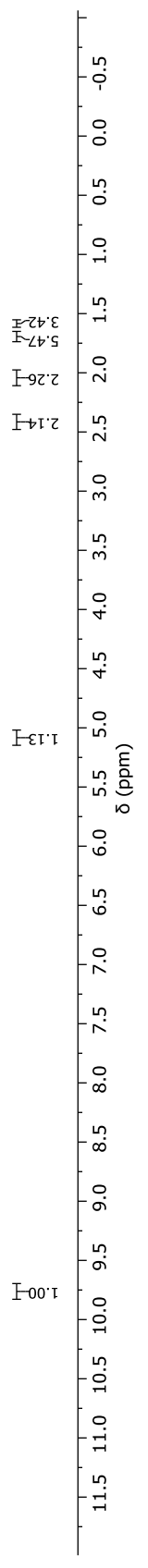


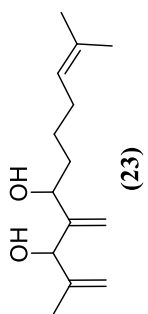


7.26 CDCl₃

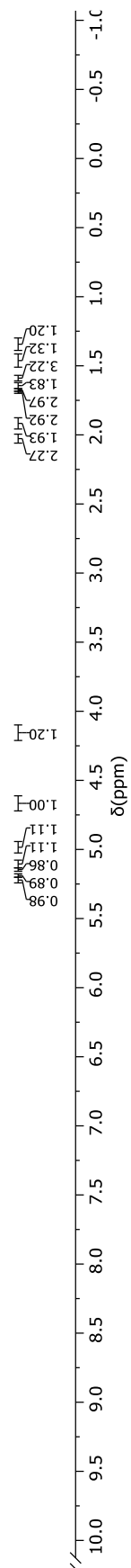
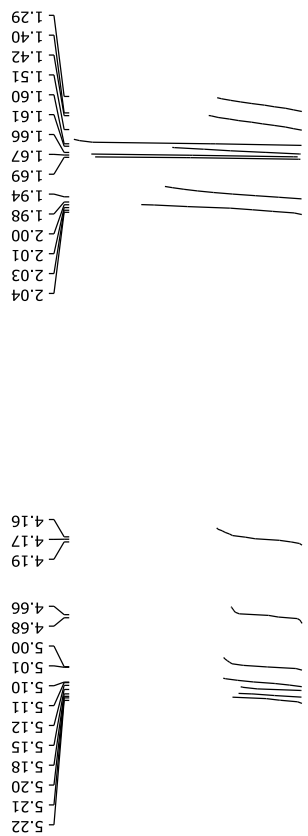
5.10
5.09
5.09
5.08
5.08
5.07
5.07
5.06
5.06

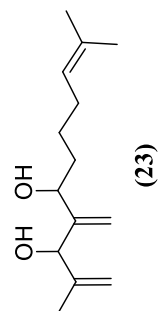
2.43
2.42
2.41
2.41
2.39
2.39
2.05
2.03
2.01
2.00
1.71
1.69
1.69
1.68
1.67
1.65
1.59



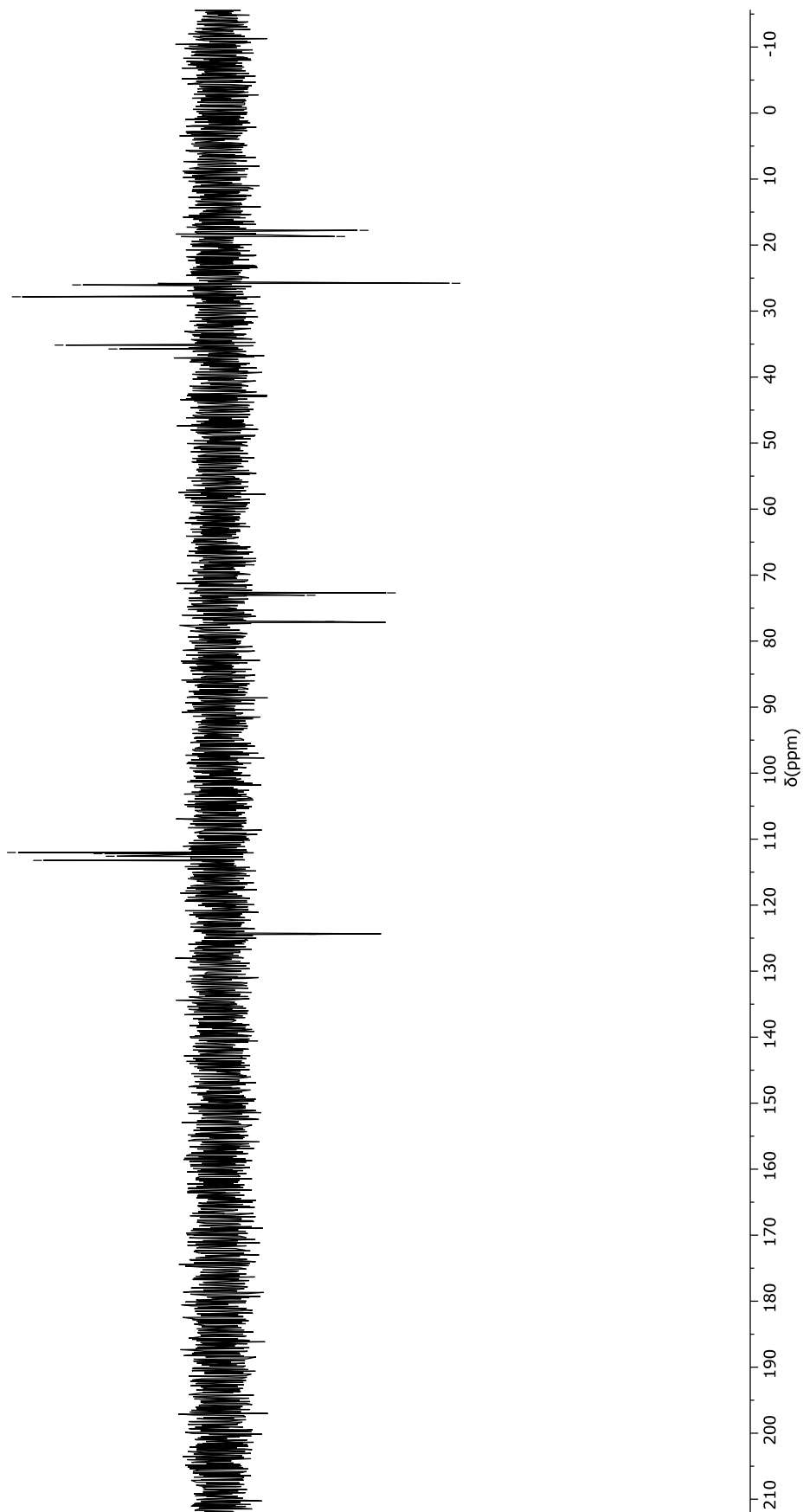


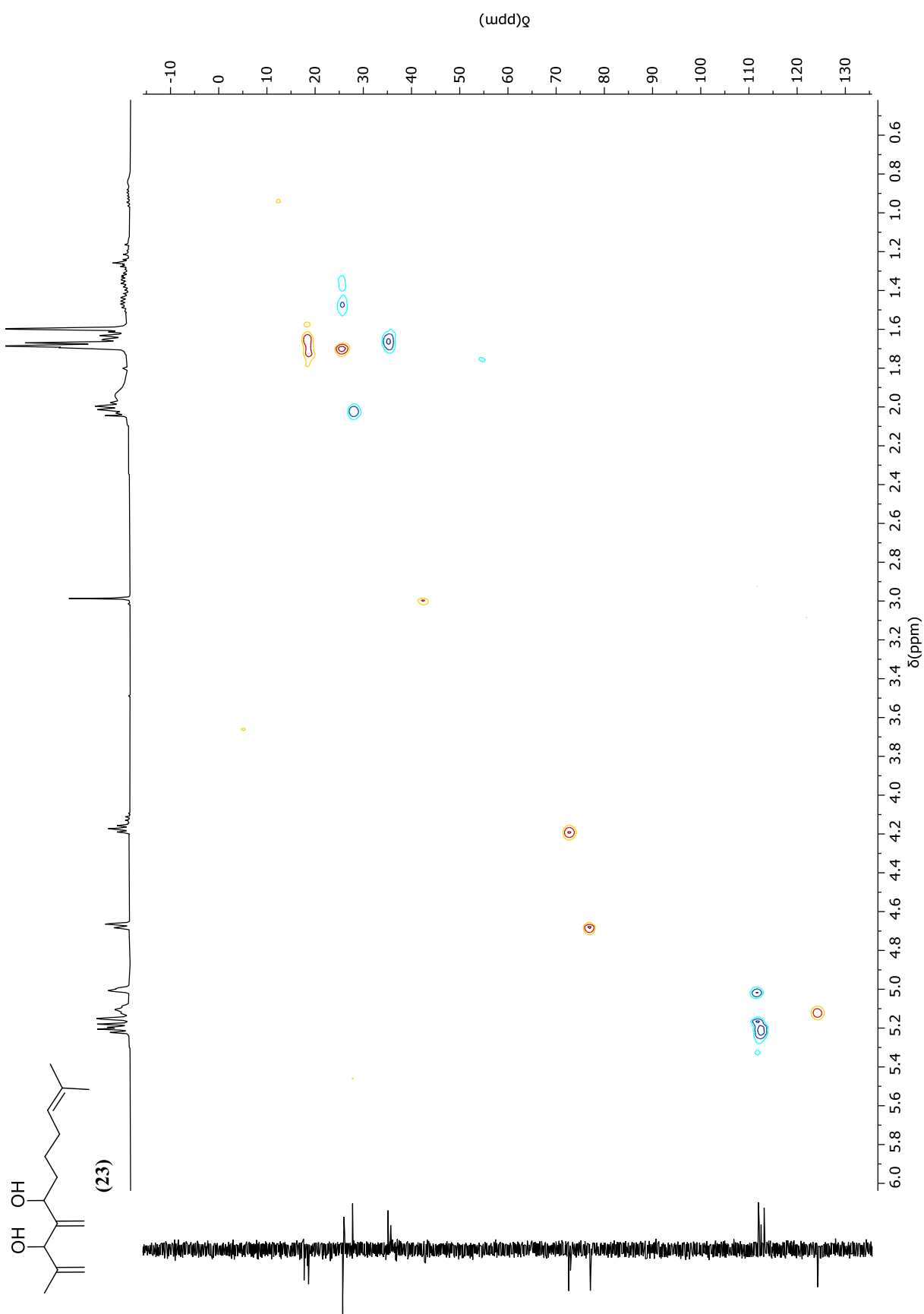
7.26 CDCl₃

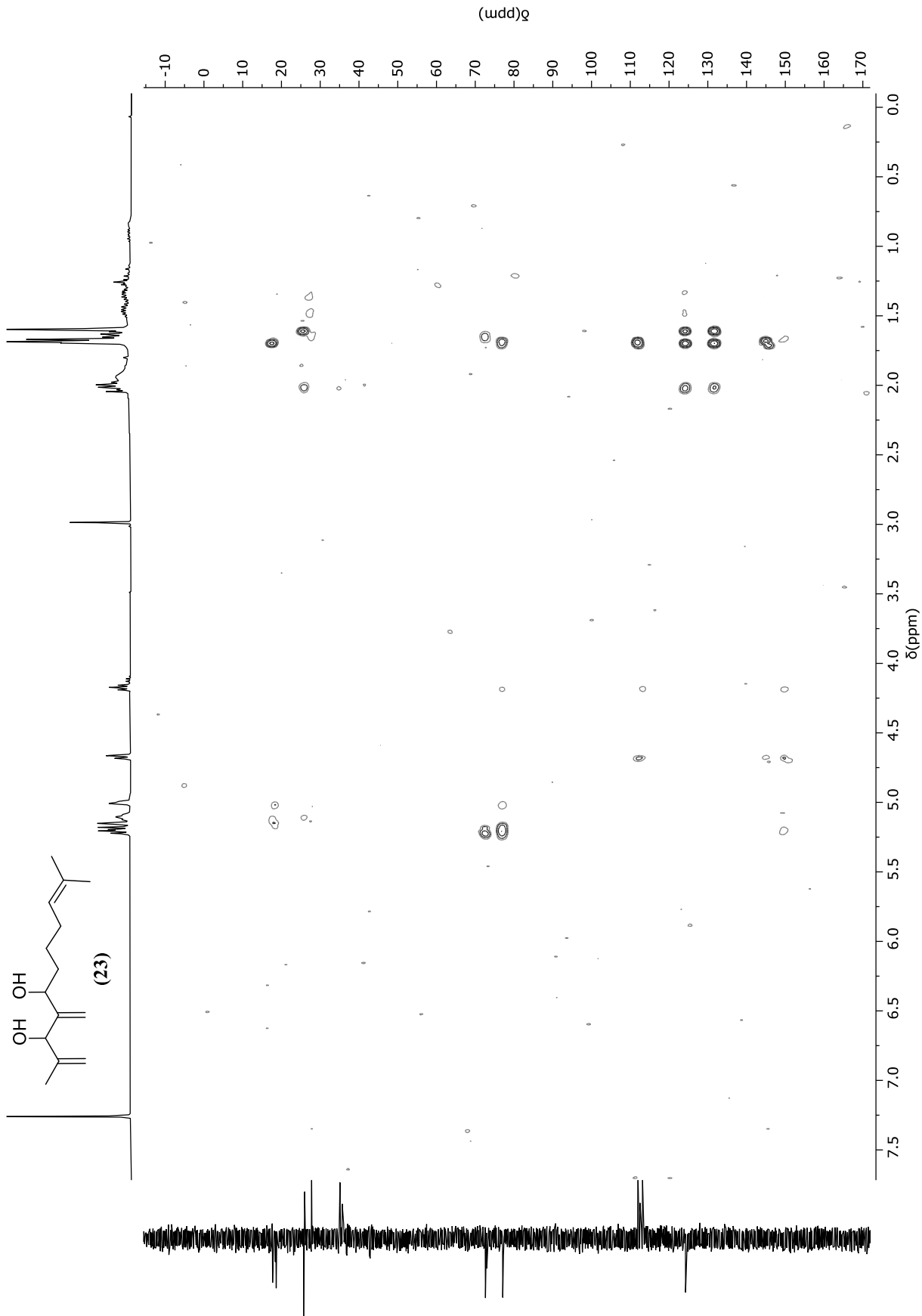


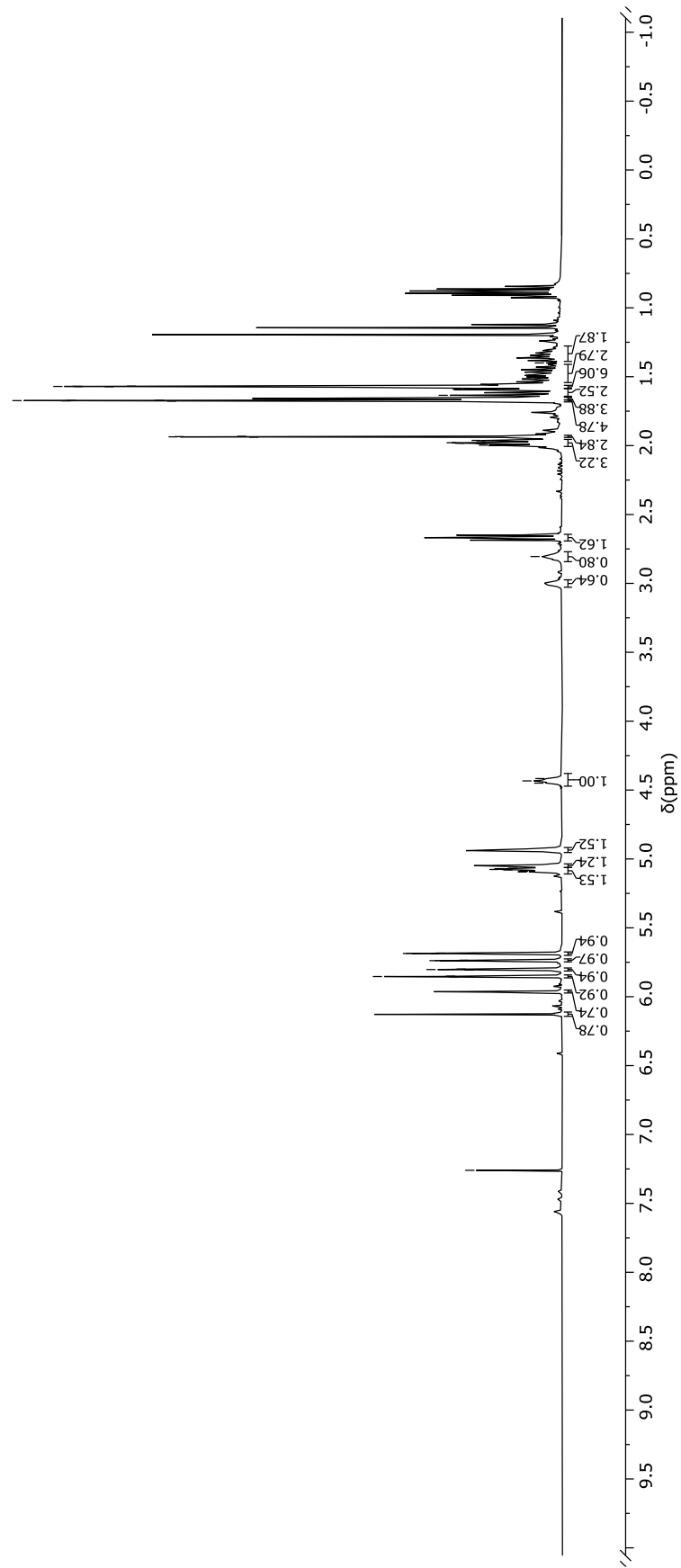
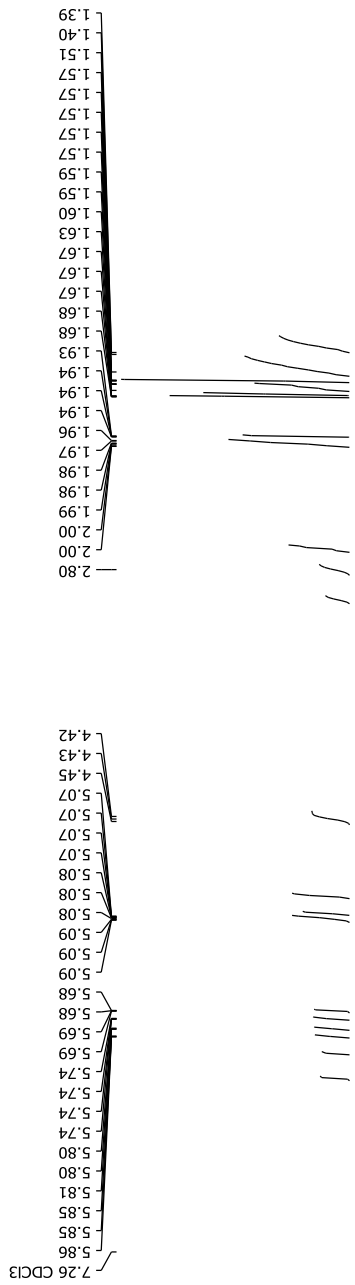
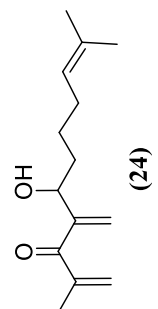


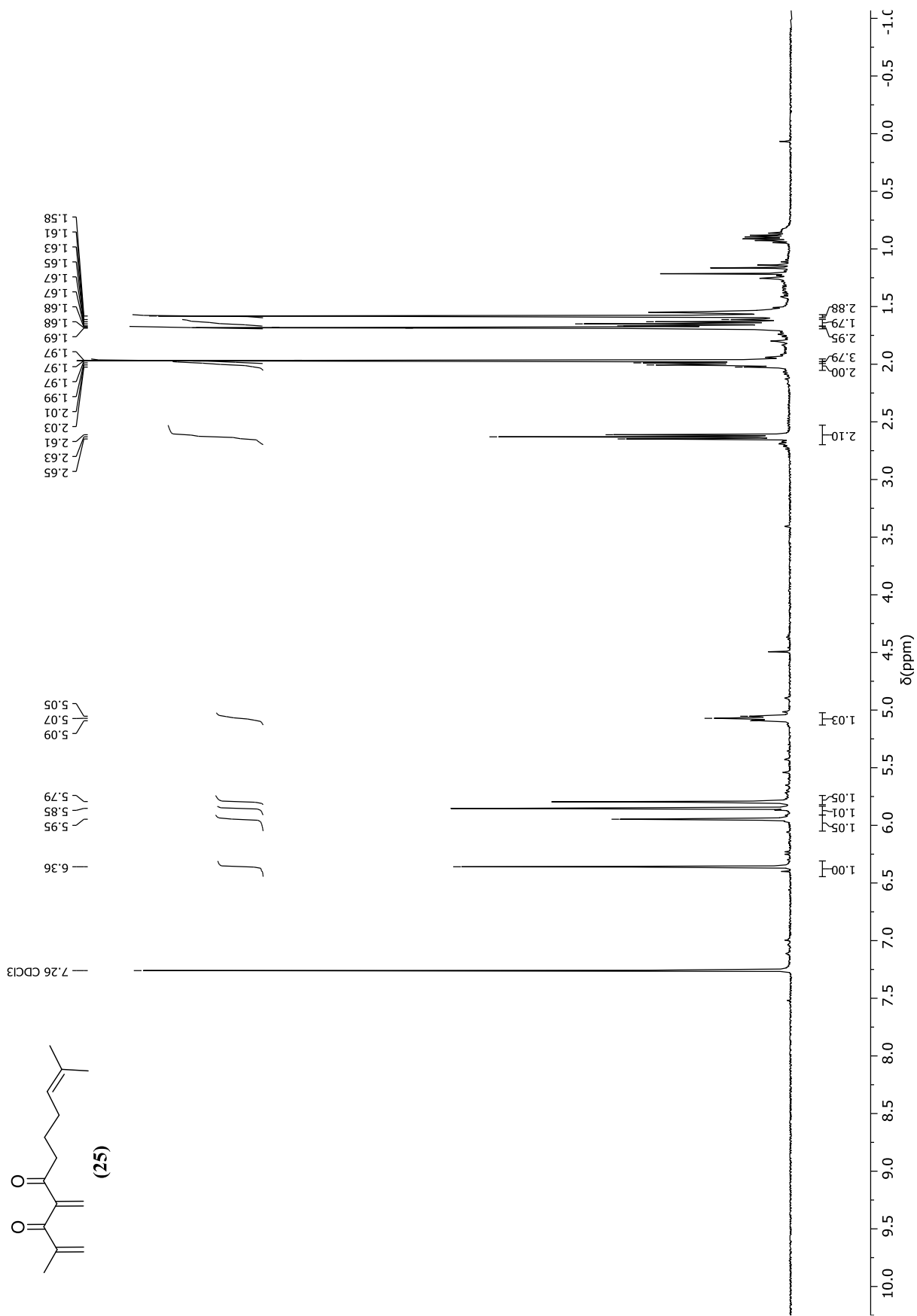
124.41
124.33
113.22
112.59
112.19
112.02
77.16 CDCl₃
77.05
73.04
72.70
35.74
35.15
27.83
26.03
25.79
18.70
17.77

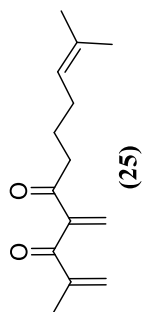










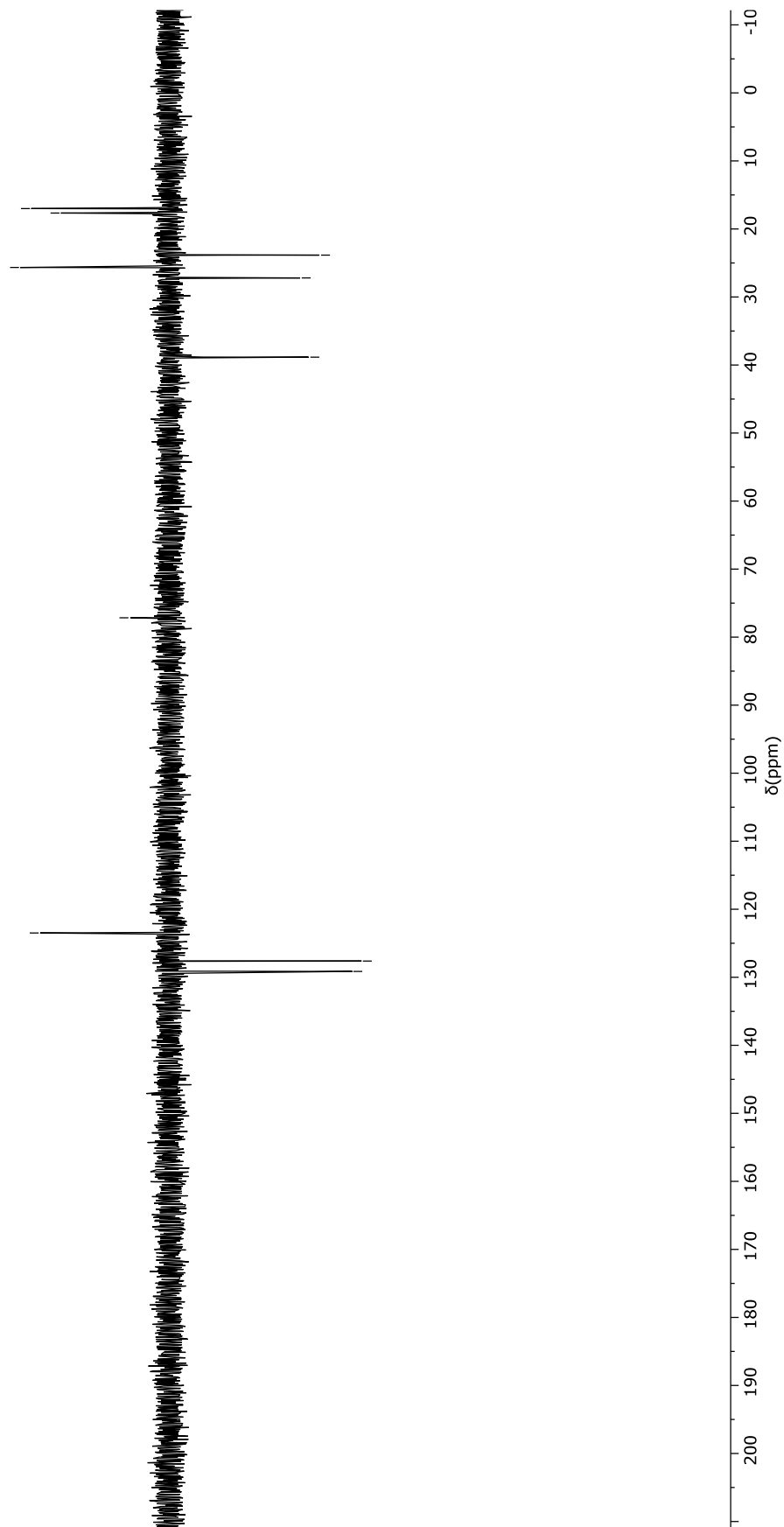


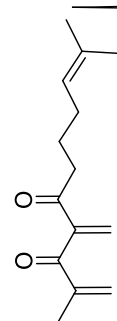
132.49
129.14
127.62
123.49

77.16 CDCl₃

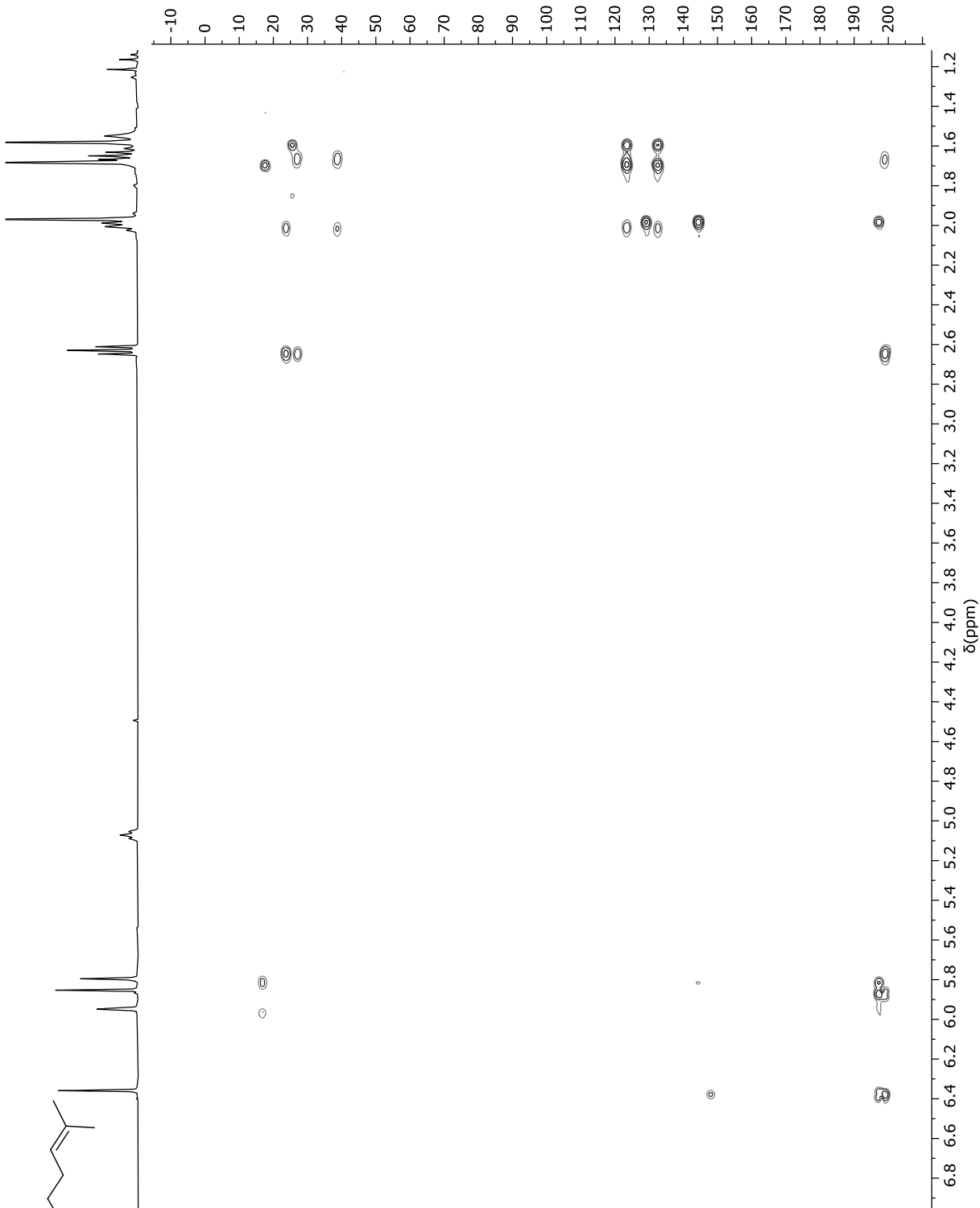
38.85

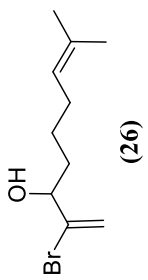
27.20
25.66
23.85
17.66
17.01





(25)





7.26 CDCl₃

2.04
2.02
2.00
1.98
1.87
1.85
1.69
1.67
1.63
1.60
1.45
1.32

4.11
4.09
4.08
4.06

5.87
5.86
5.56
5.55
5.12
5.10
5.09

2.83
1.01
3.64
2.17
3.30
2.07

0.98

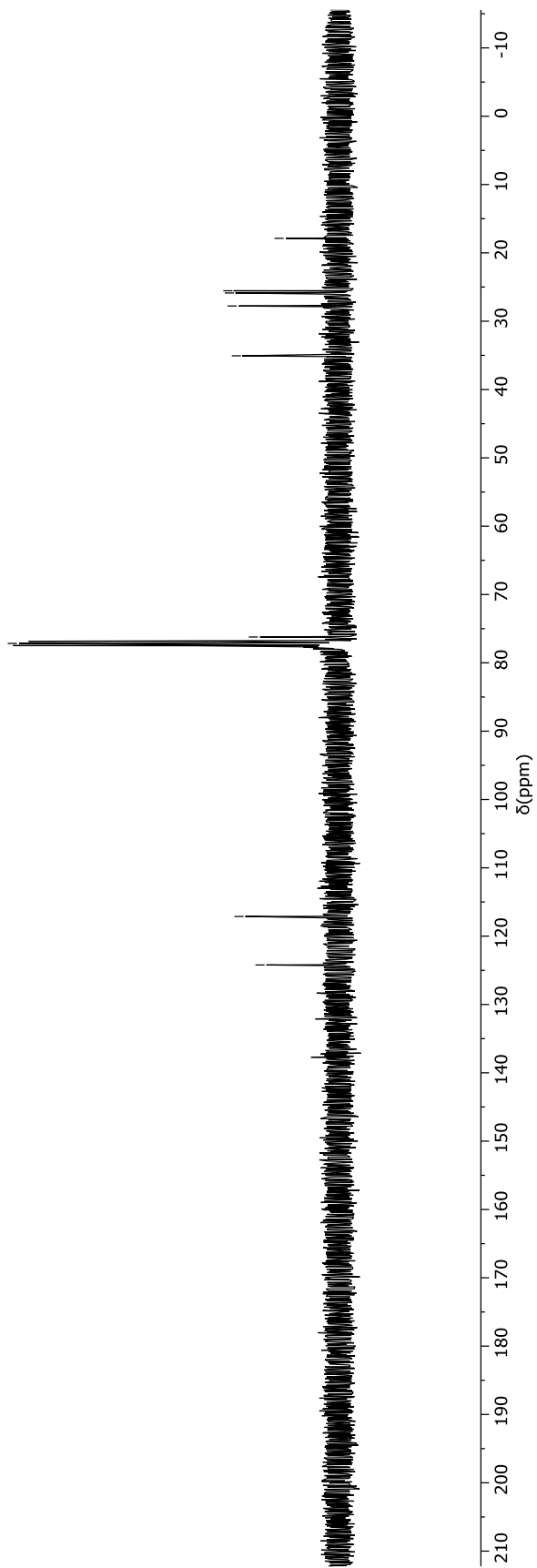
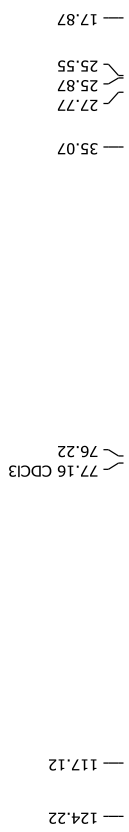
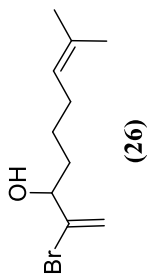
1.39

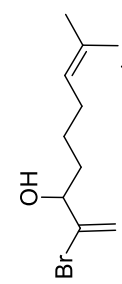
1.02

1.02

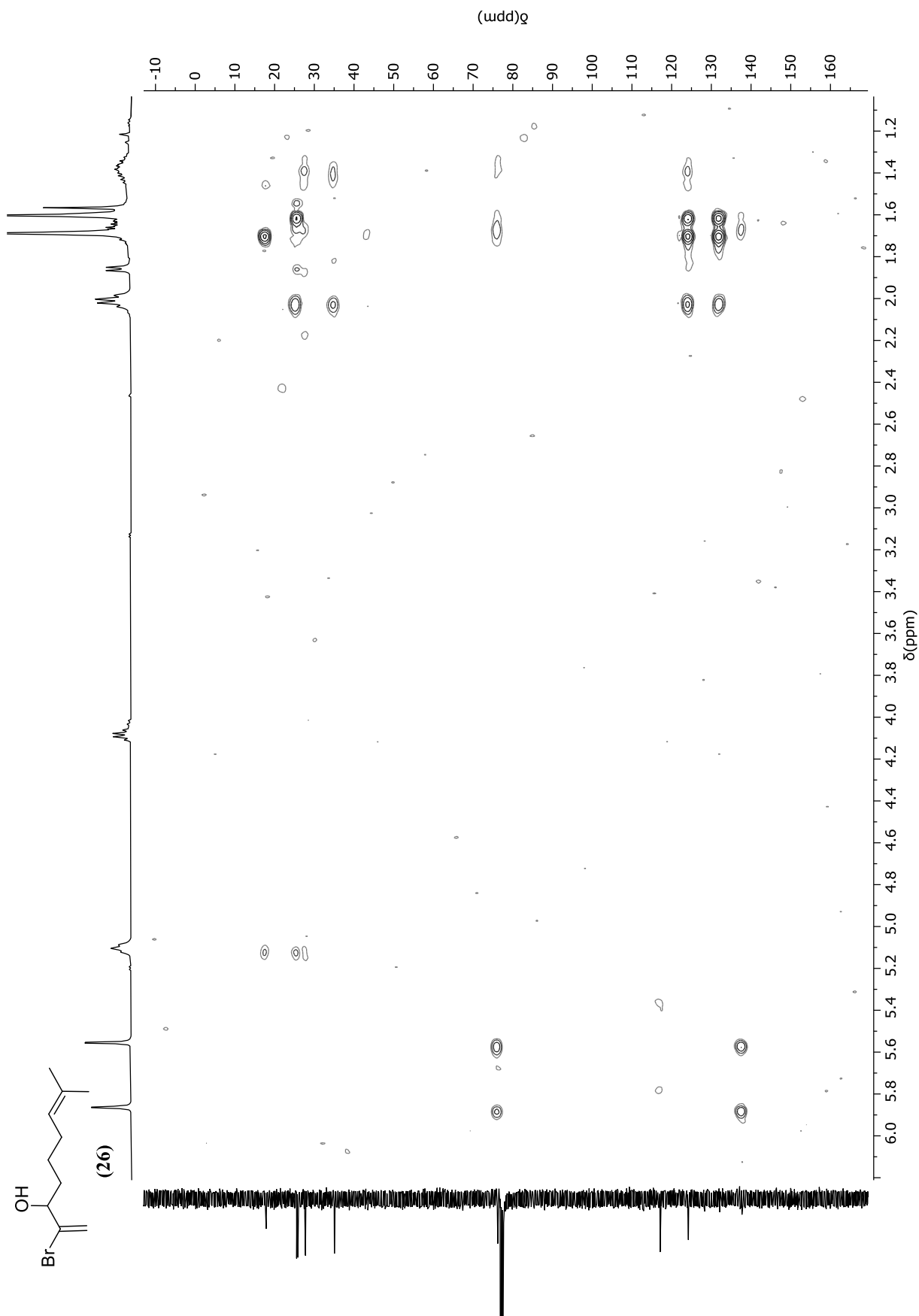
δ(ppm)

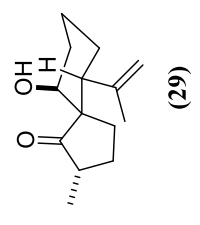
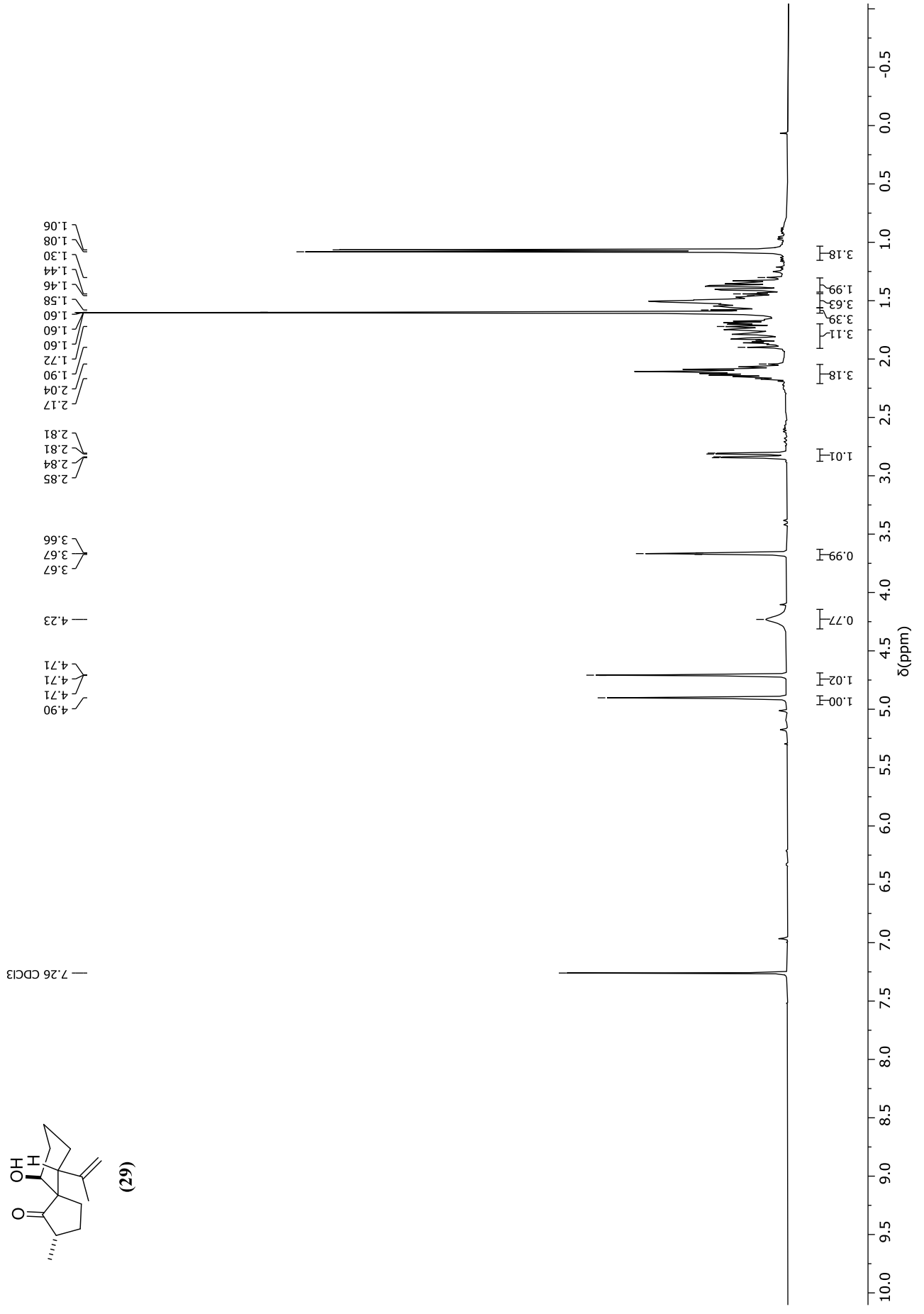
10.0 9.5 9.0 8.5 8.0 7.5 7.0 6.5 6.0 5.5 5.0 4.5 4.0 3.5 3.0 2.5 2.0 1.5 1.0 0.5 0.0 -0.5 -1.0

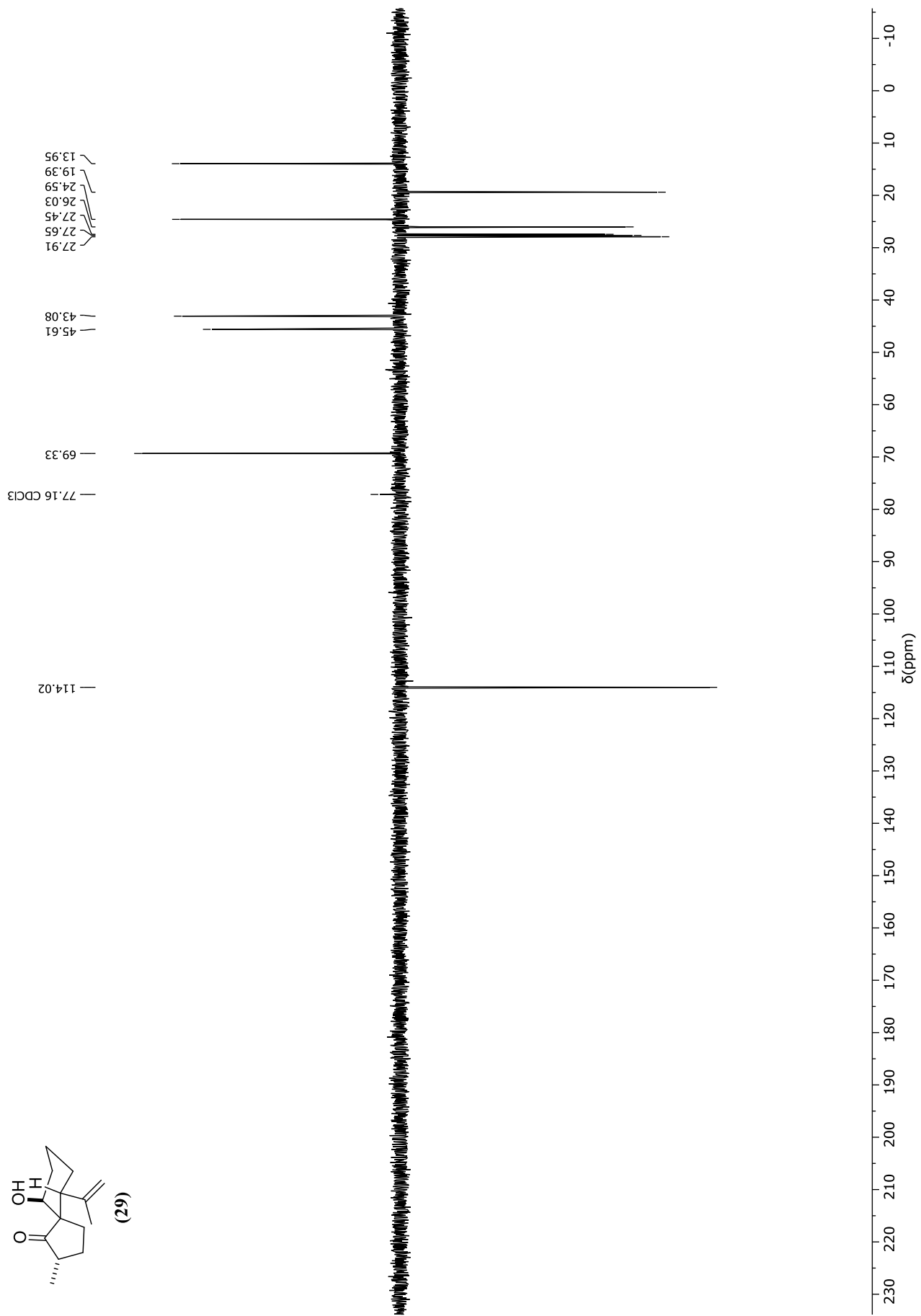
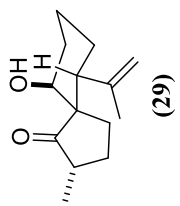


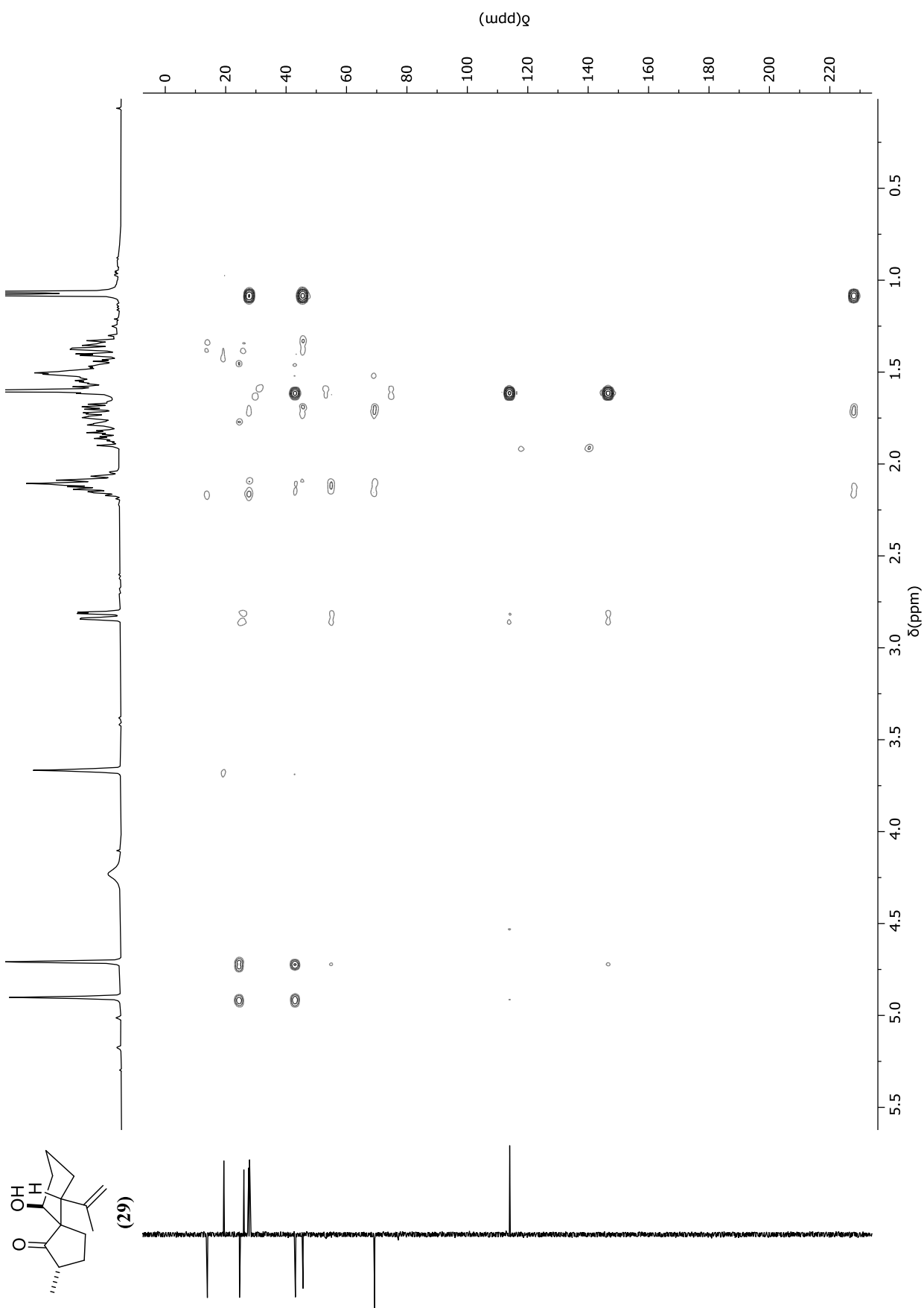


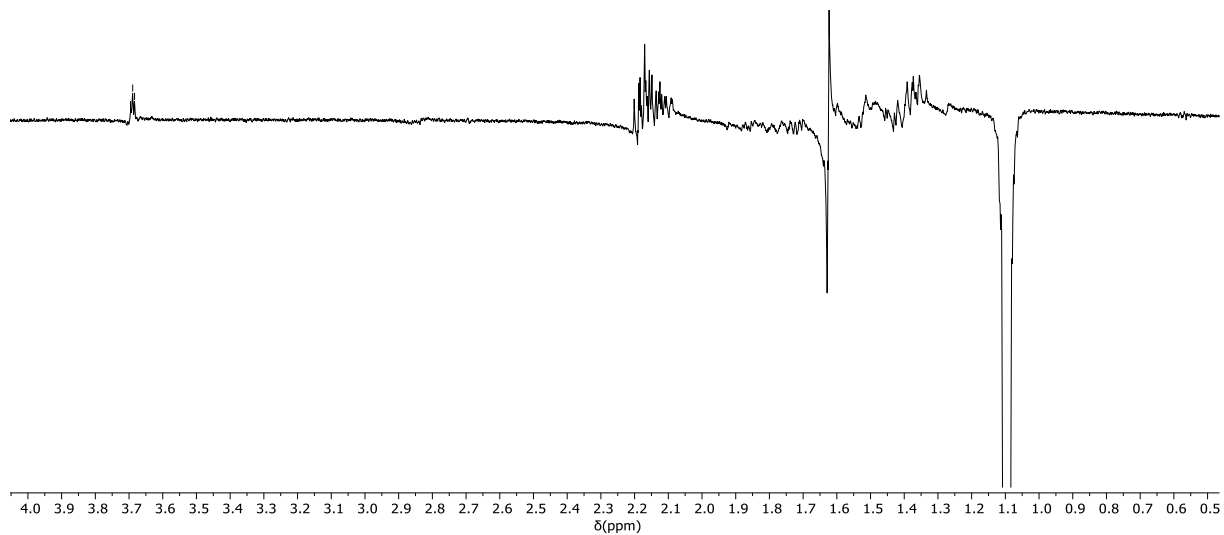
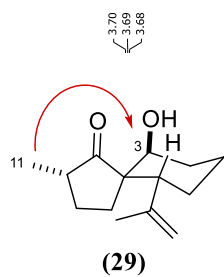
(26)



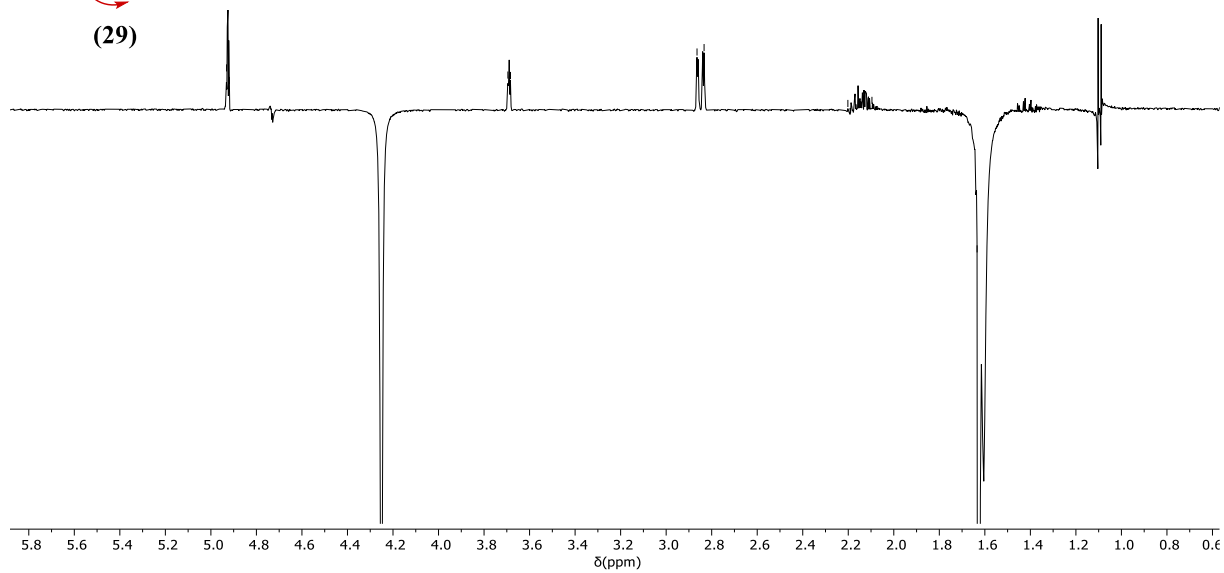
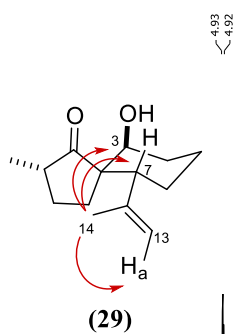




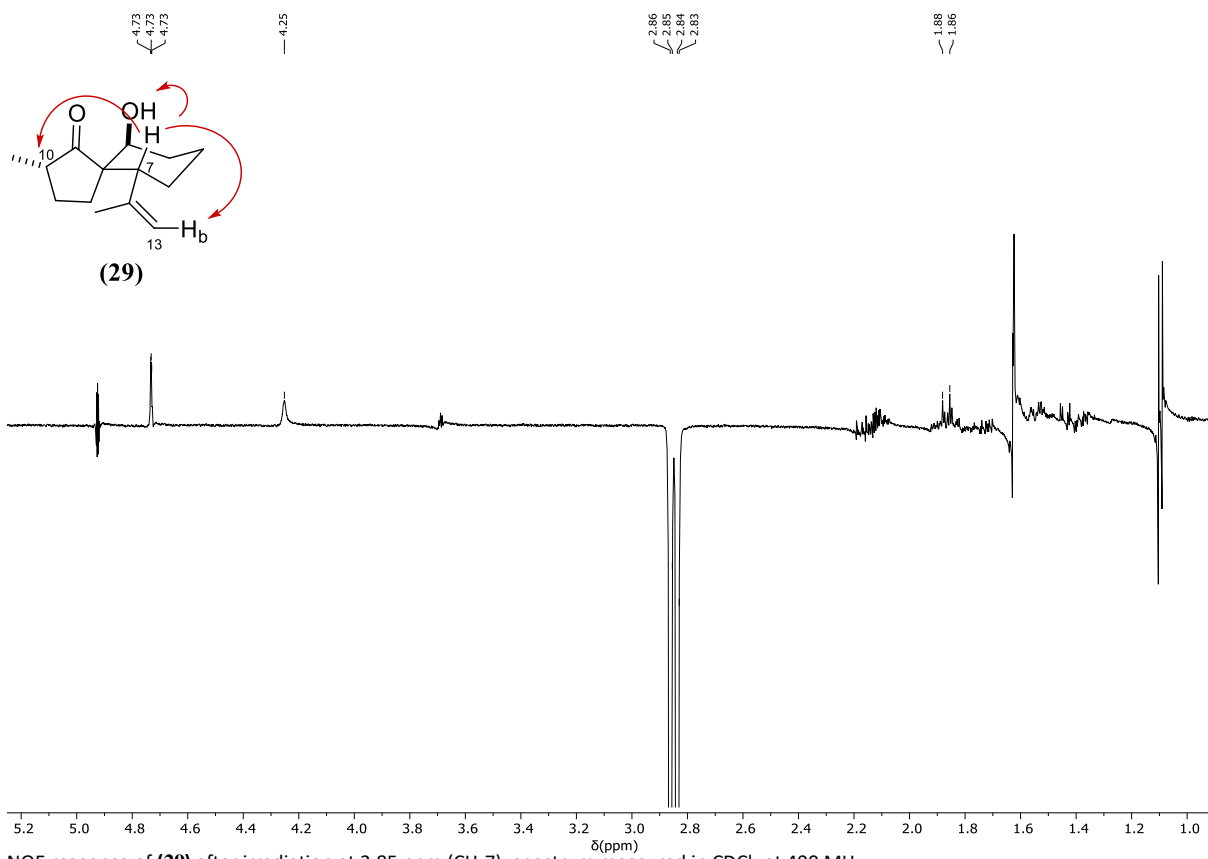




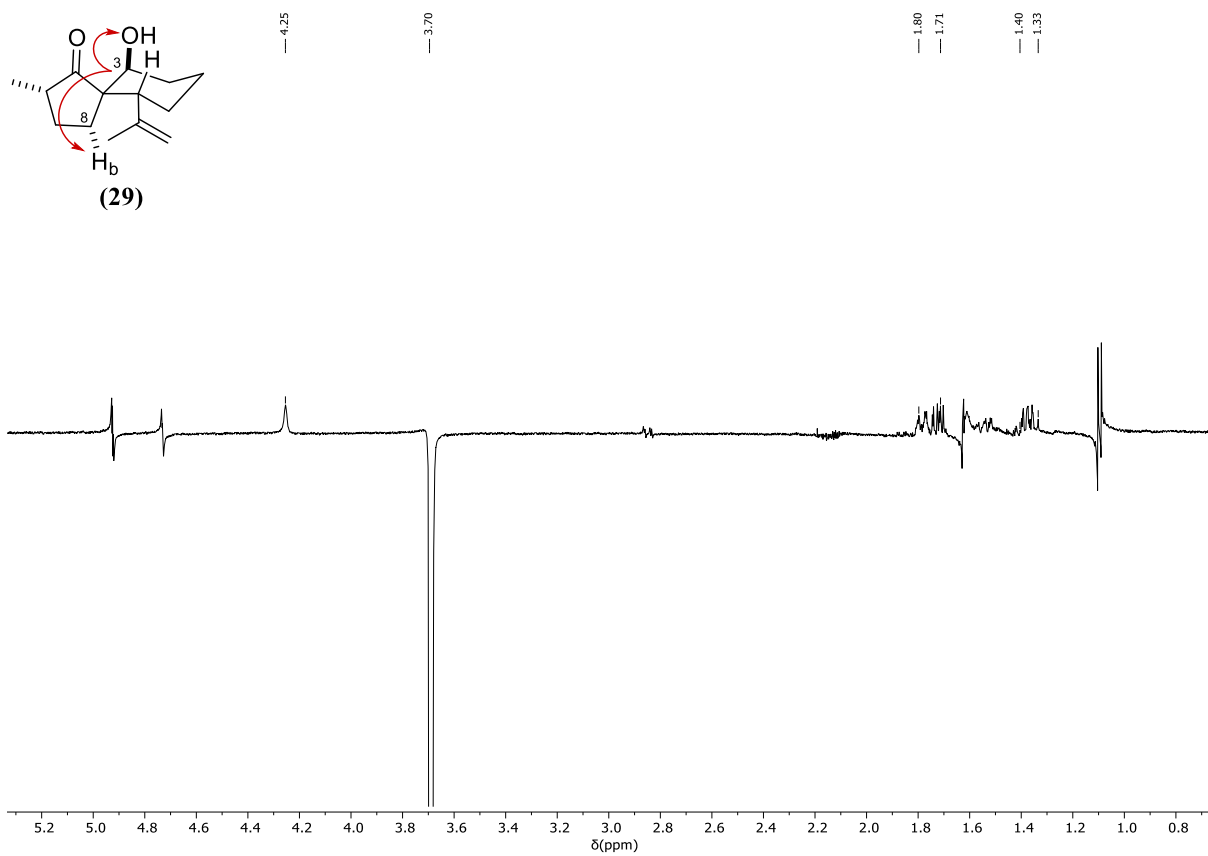
NOE response of (29) after irradiation at 1.10 ppm (CH₃-11); spectrum measured in CDCl₃ at 400 MHz.



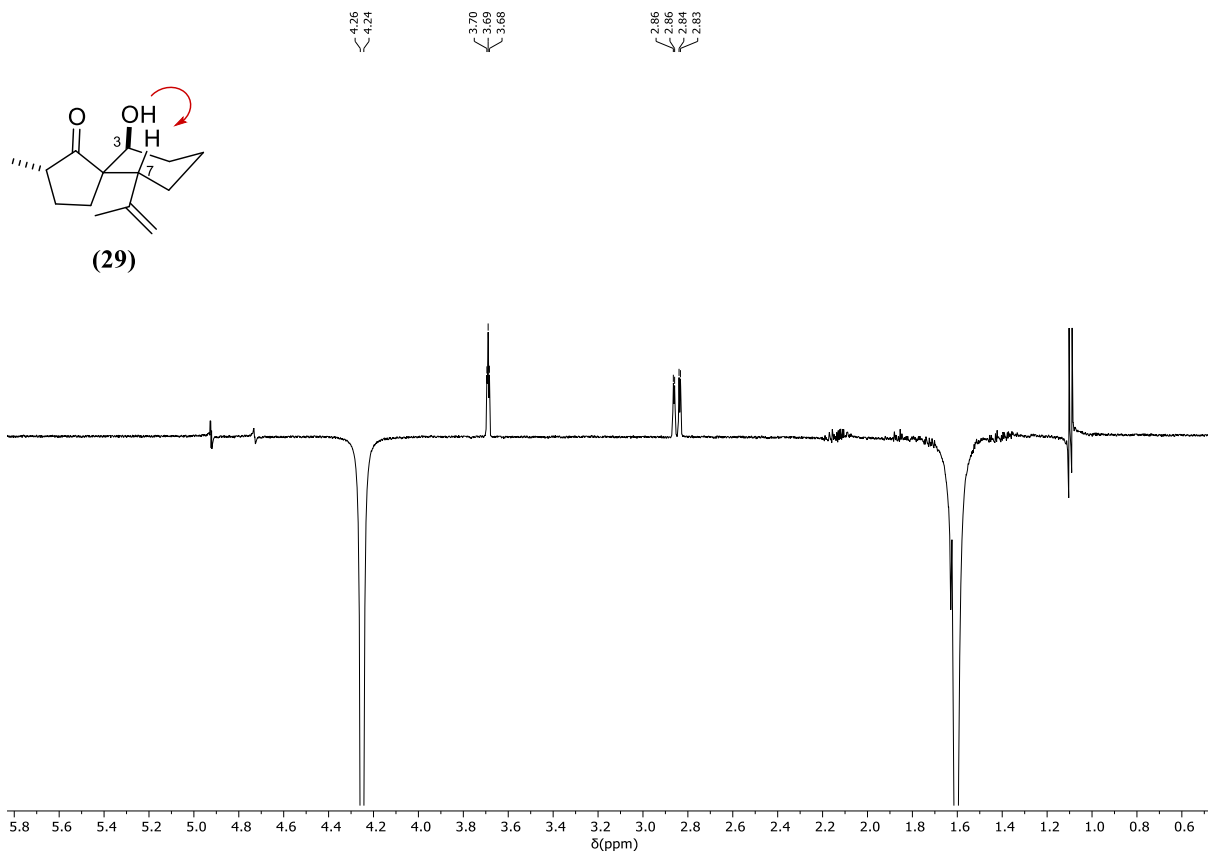
NOE response of (29) after irradiation at 1.63 ppm (CH₃-14); spectrum measured in CDCl₃ at 400 MHz.



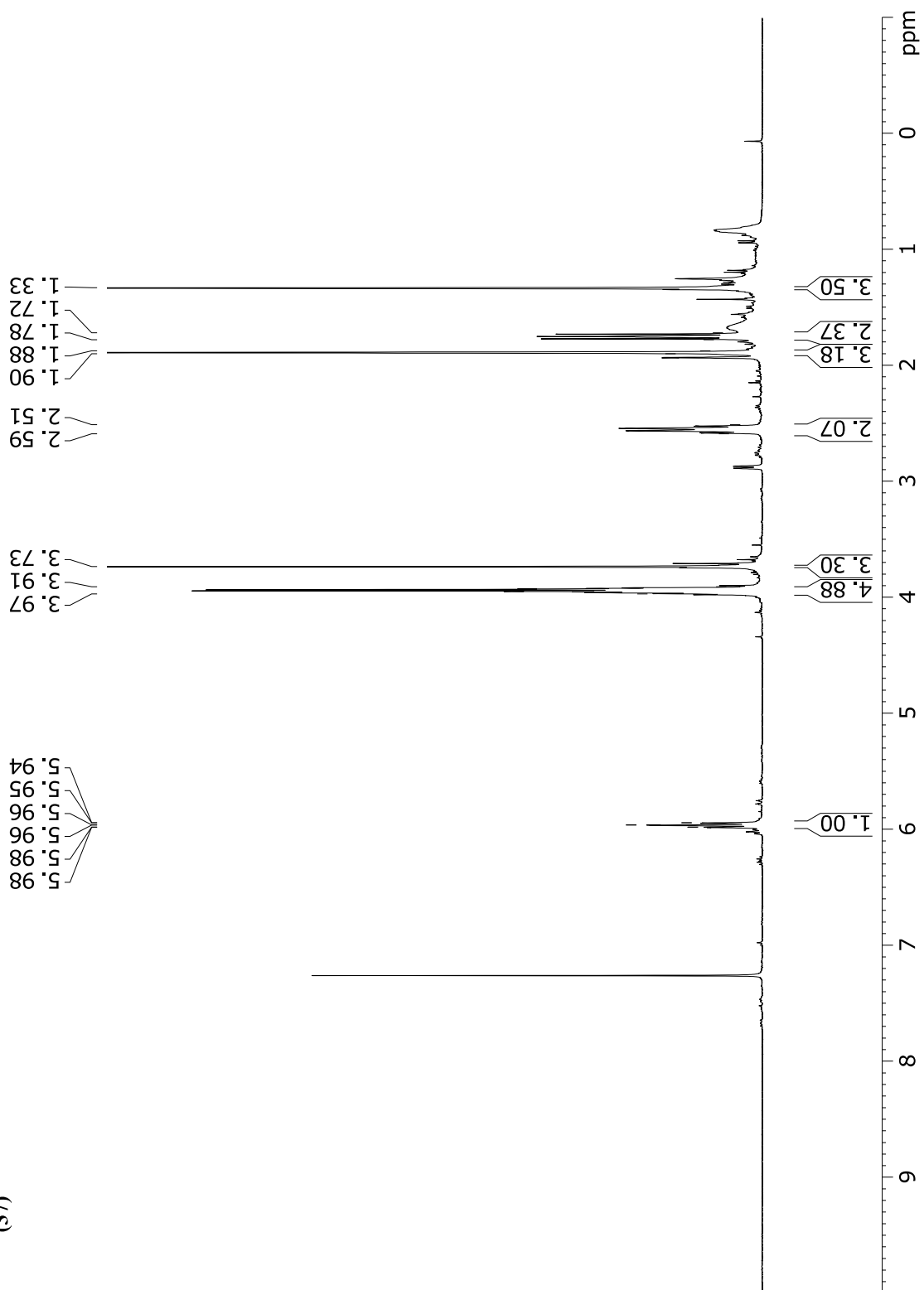
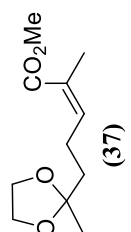
NOE response of (29) after irradiation at 2.85 ppm (CH-7); spectrum measured in CDCl₃ at 400 MHz.

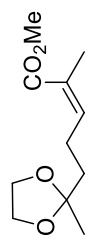


NOE response of (29) after irradiation at 2.85 ppm (CH-3); spectrum measured in CDCl₃ at 400 MHz.

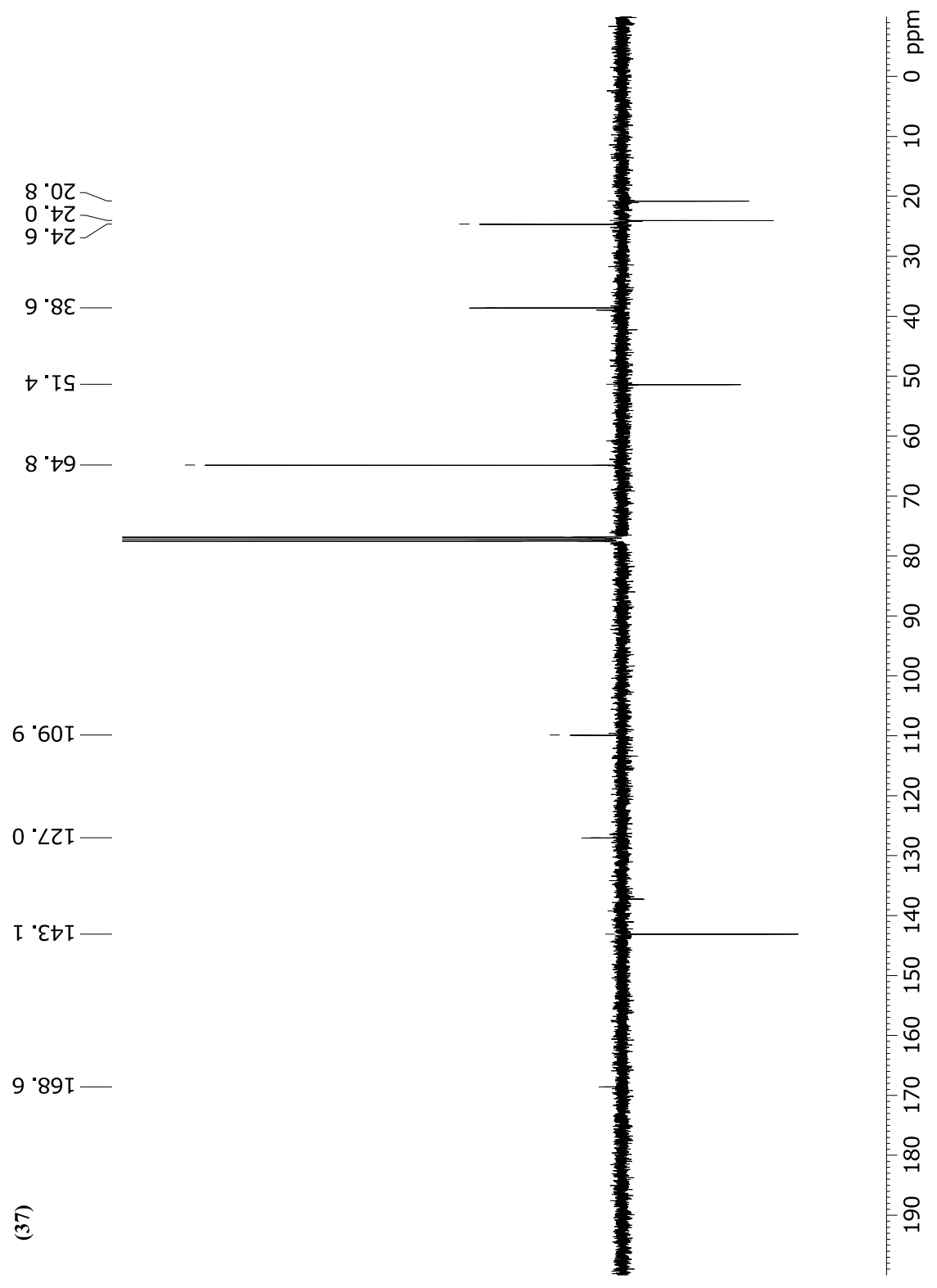


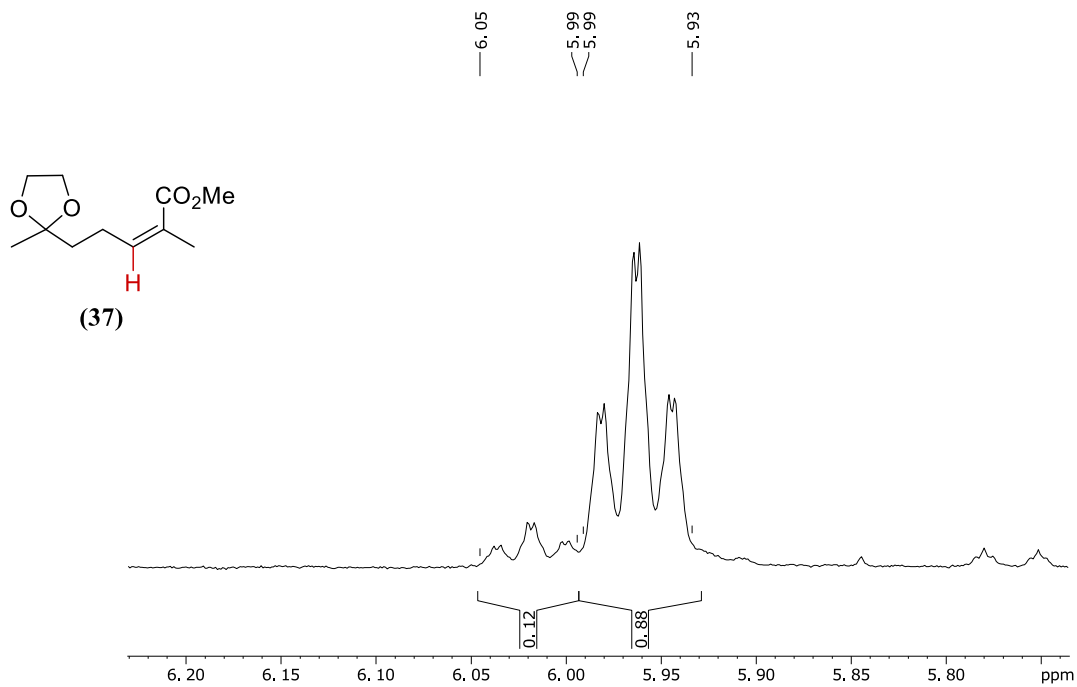
NOE response of (29) after irradiation at 4.25 ppm (OH); spectrum measured in CDCl_3 at 400 MHz.



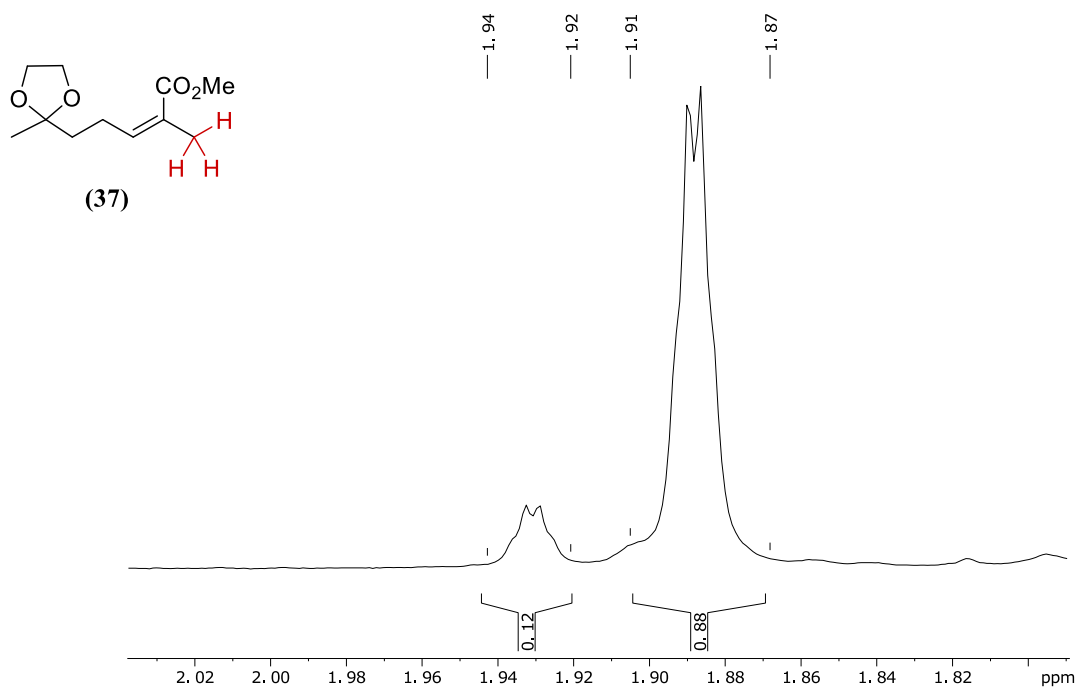


(37)

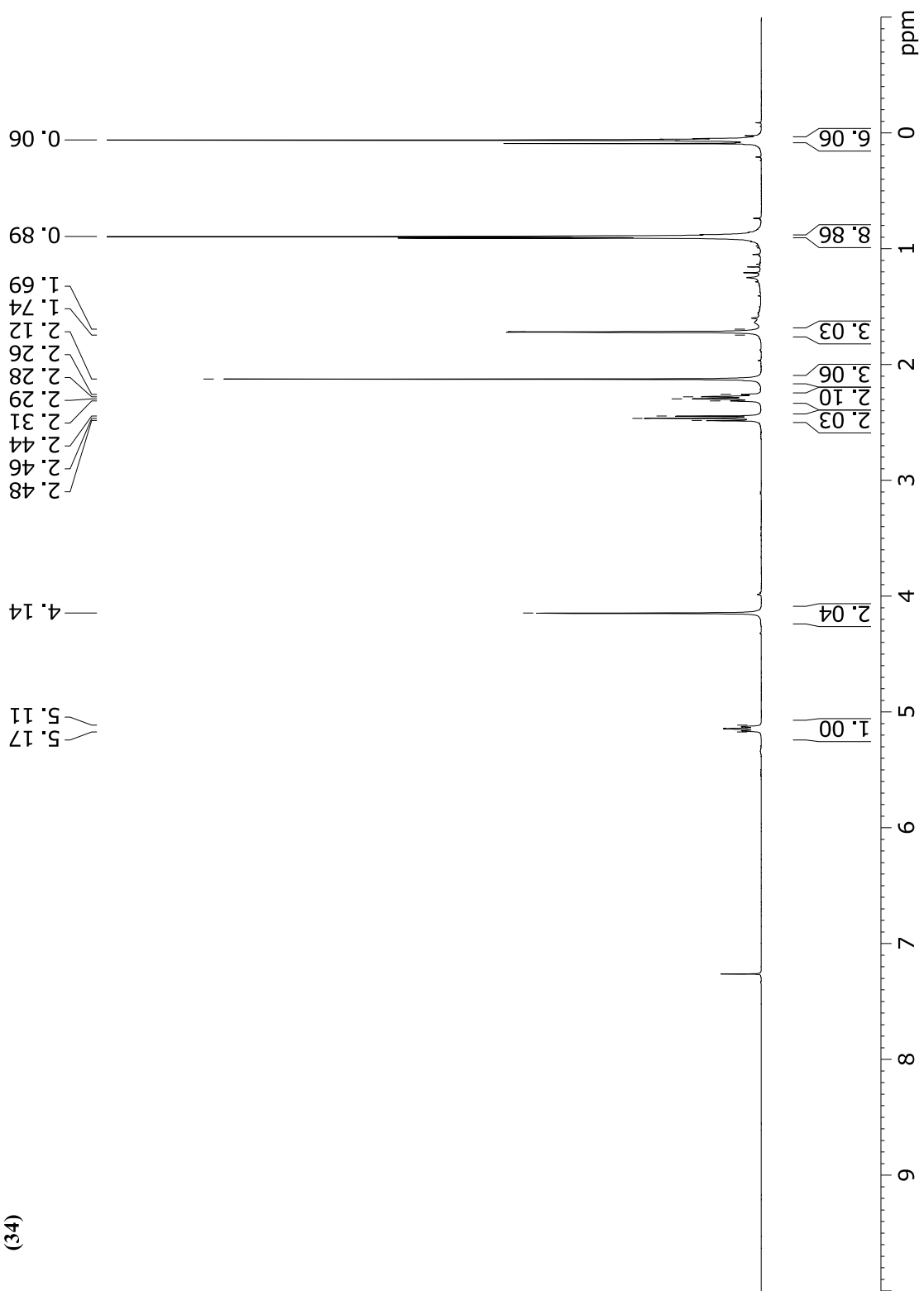
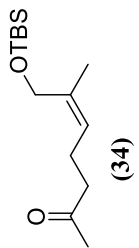


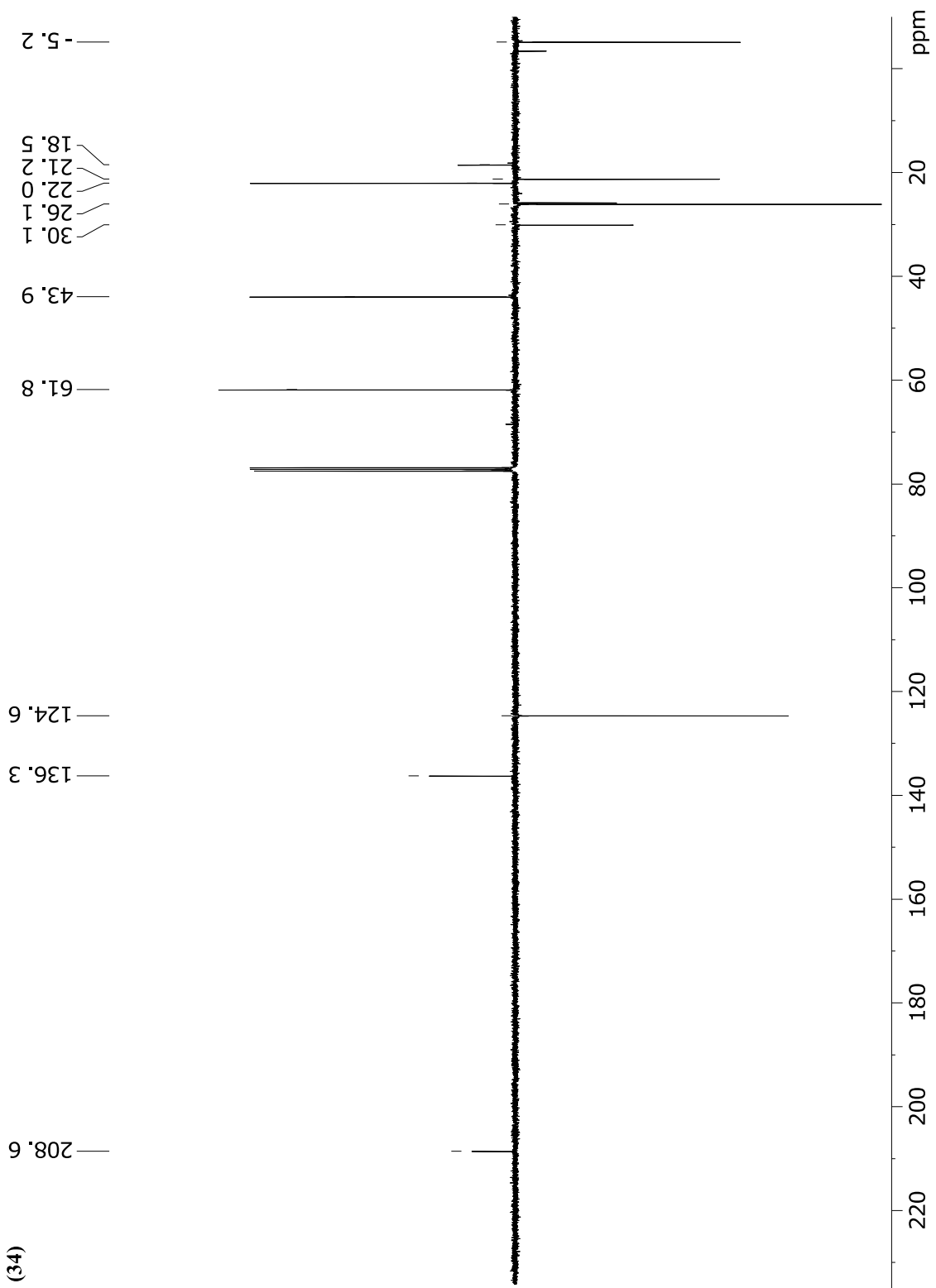
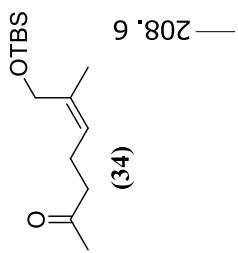


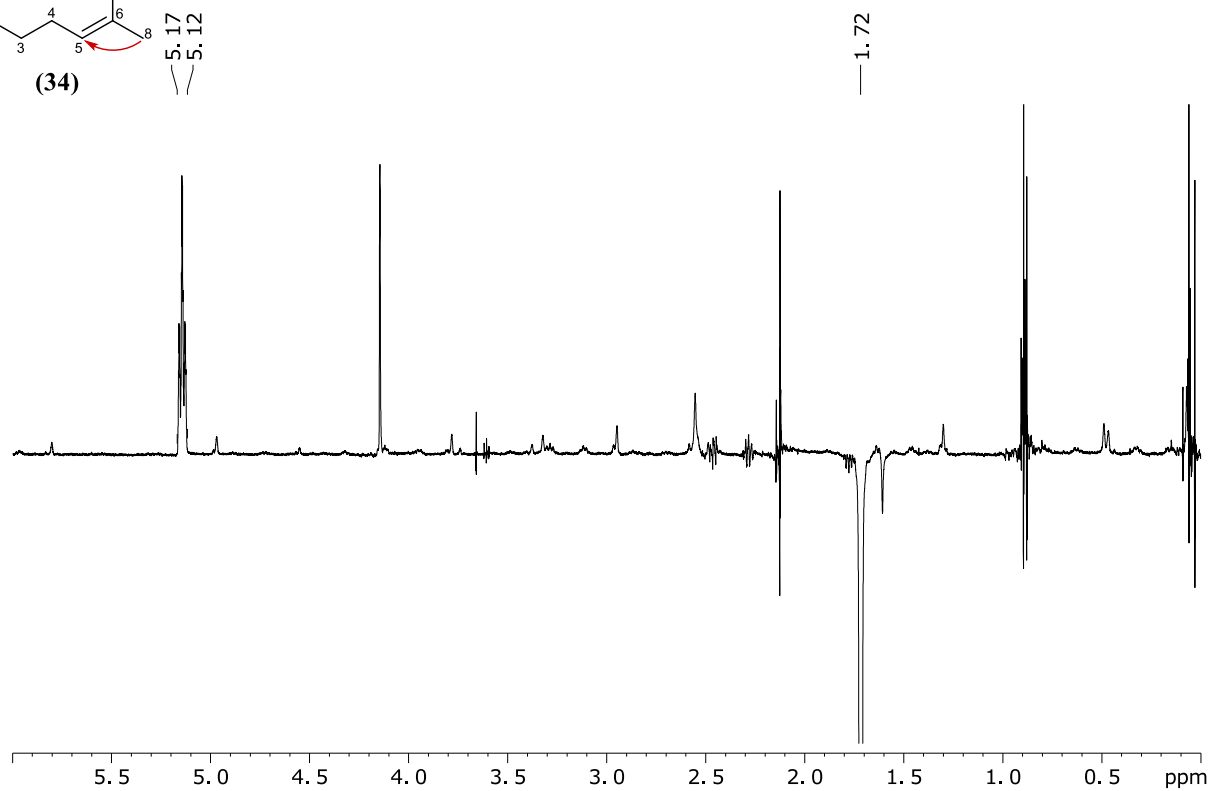
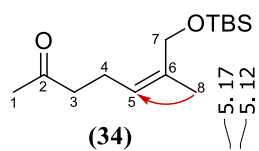
Enhancement of (37) ¹H-NMR spectrum for determination of the (*E*)/(*Z*)-ratio. The corresponding protons are marked for the major (*Z*)-isomer.



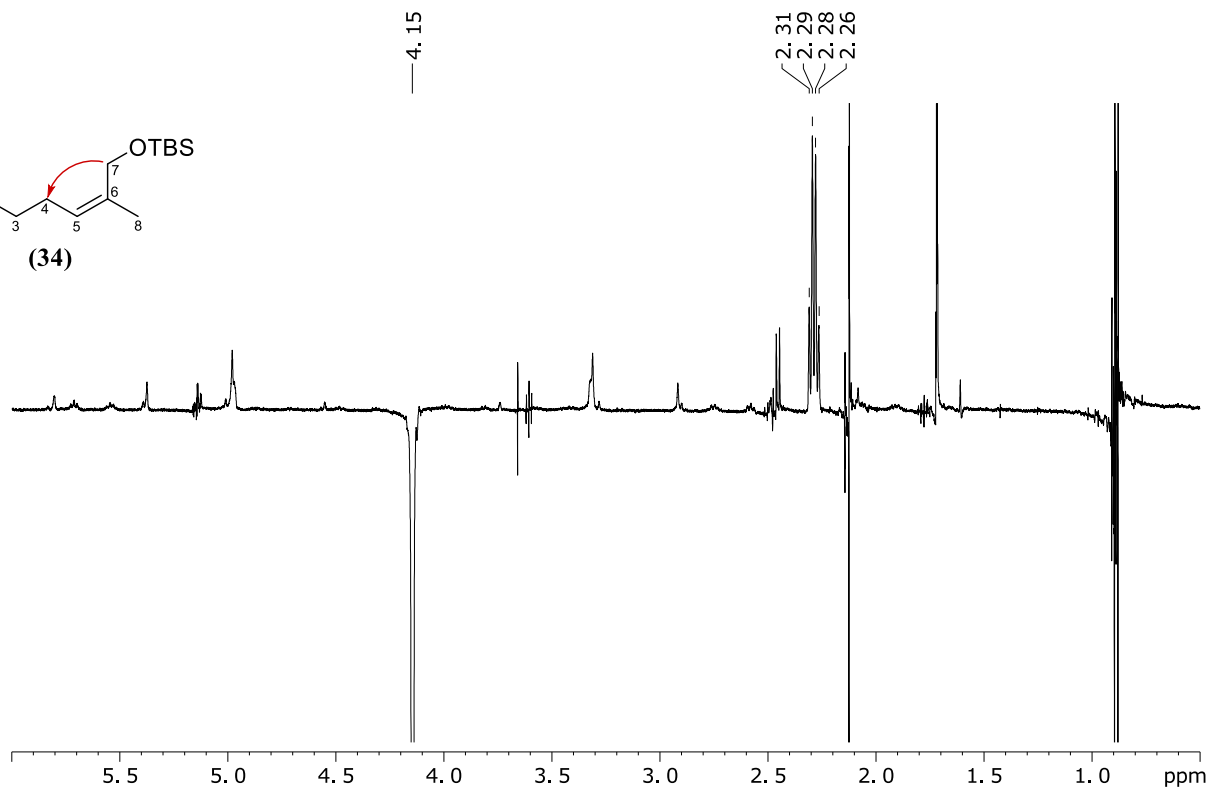
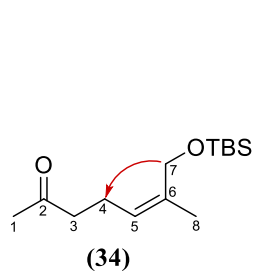
Enhancement of (37) ¹H-NMR spectrum for determination of the (*E*)/(*Z*)-ratio. The corresponding protons are marked for the major (*Z*)-isomer.



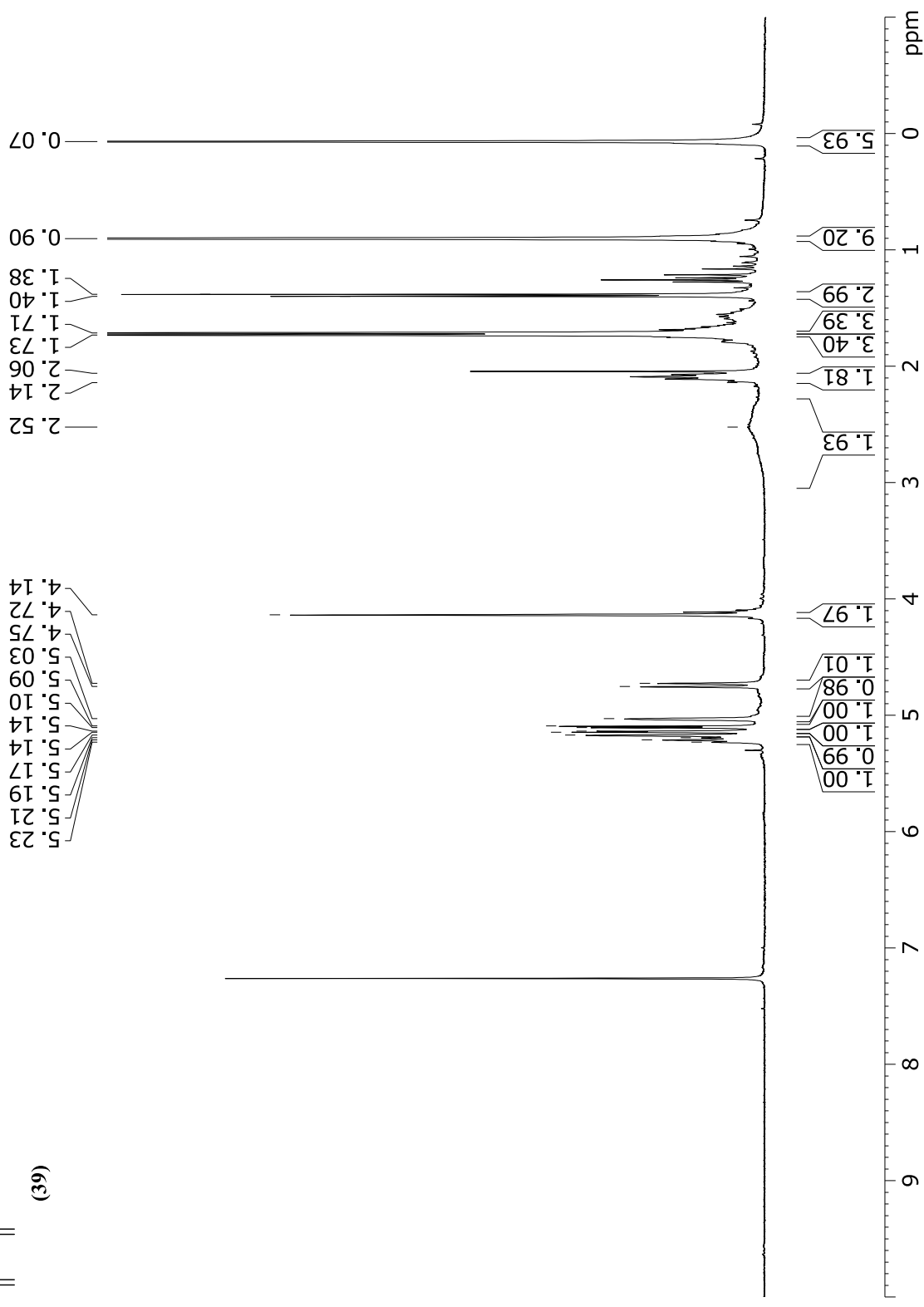
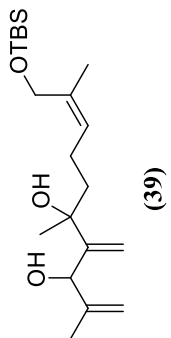


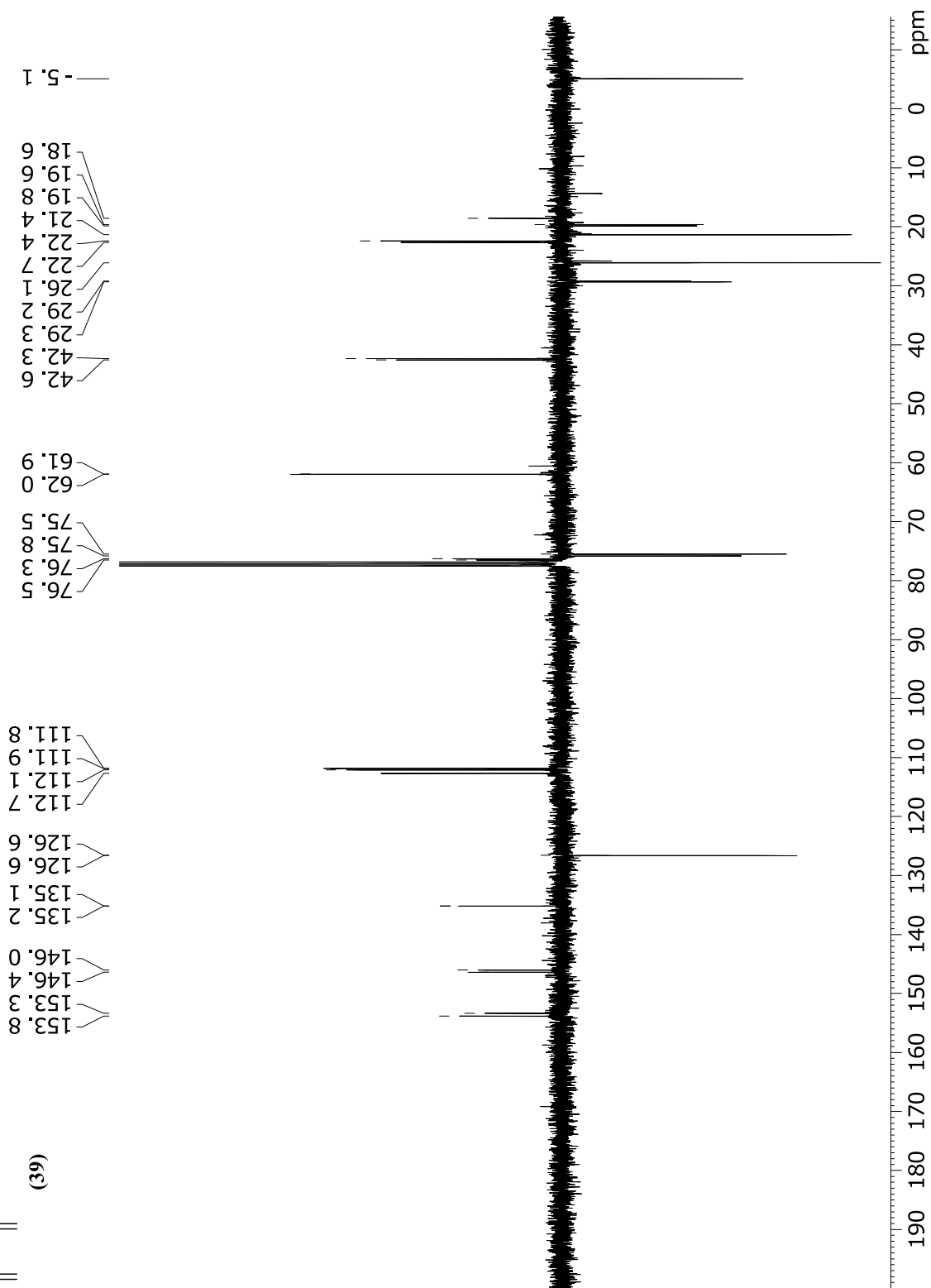
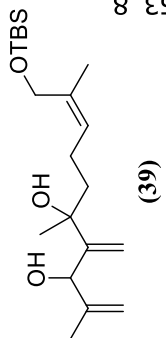


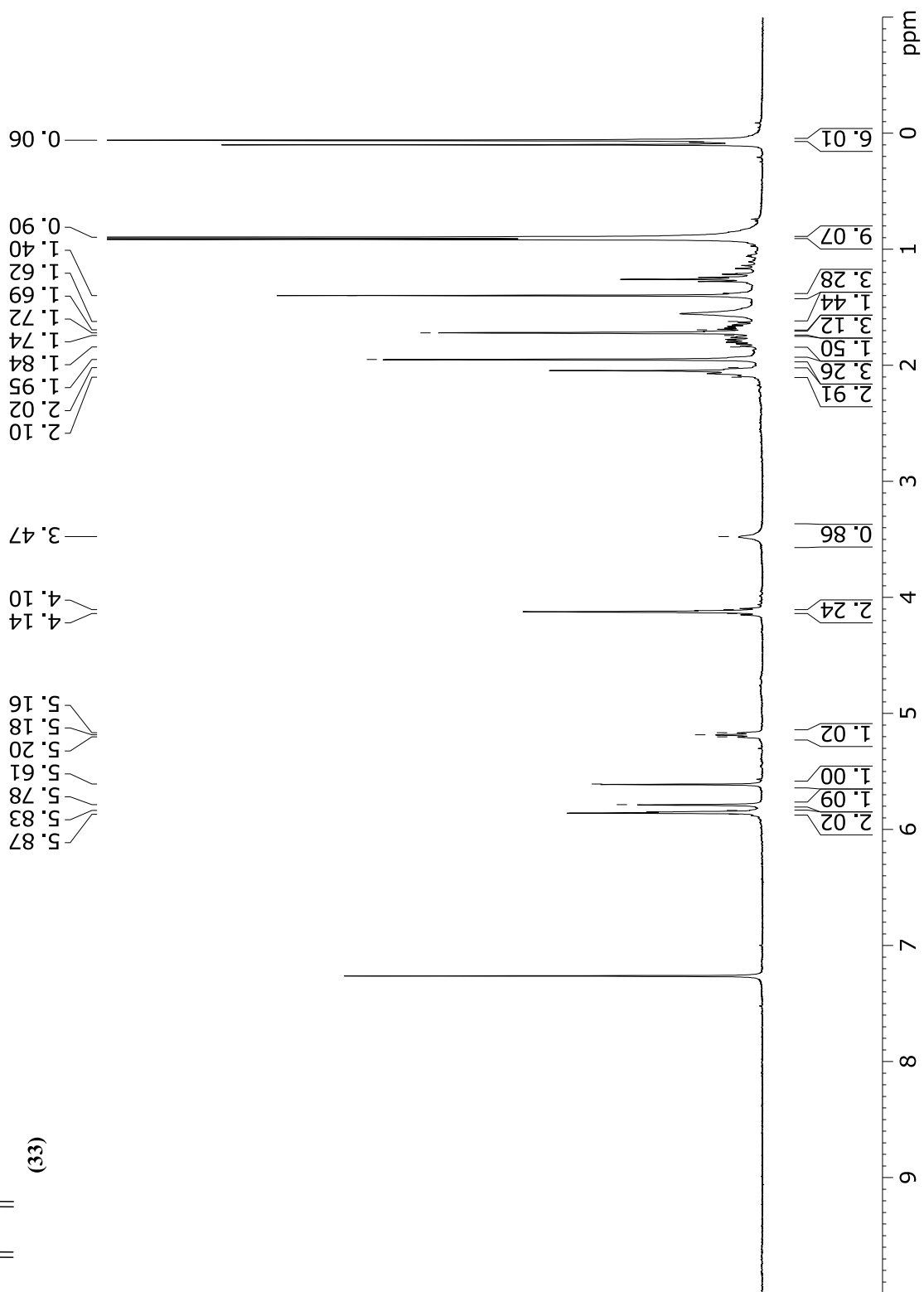
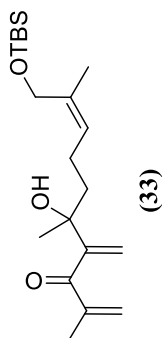
NOE response of (34) after irradiation at 1.72 ppm (CH₃-8). Spectrum measured in CDCl₃ at 400 MHz.

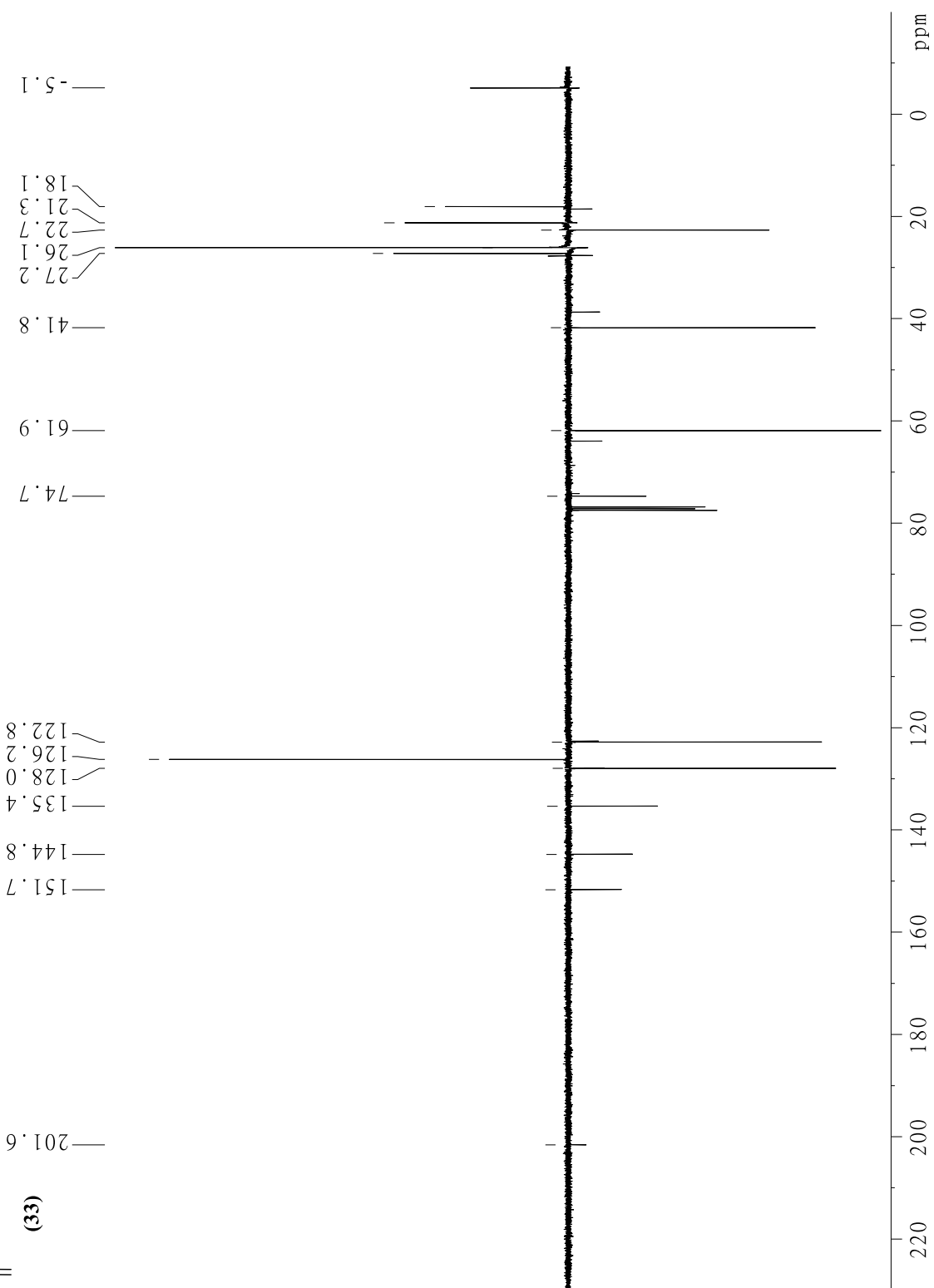
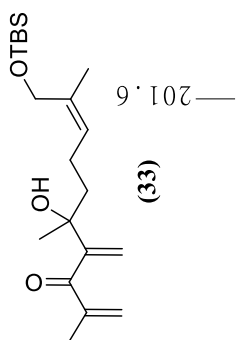


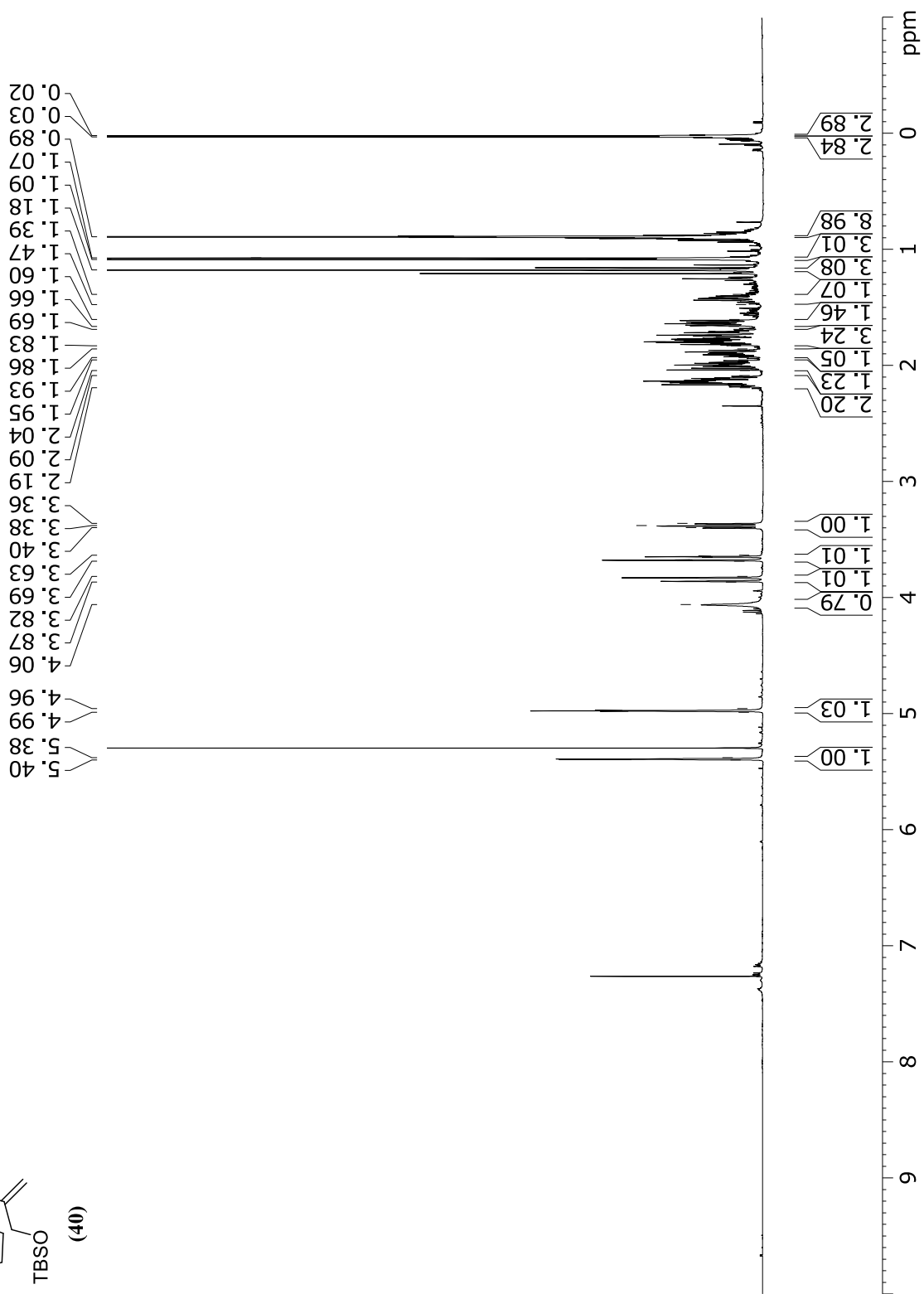
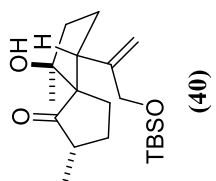
NOE response of (34) after irradiation at 4.15 ppm (CH₂-7). Spectrum measured in CDCl₃ at 400 MHz.

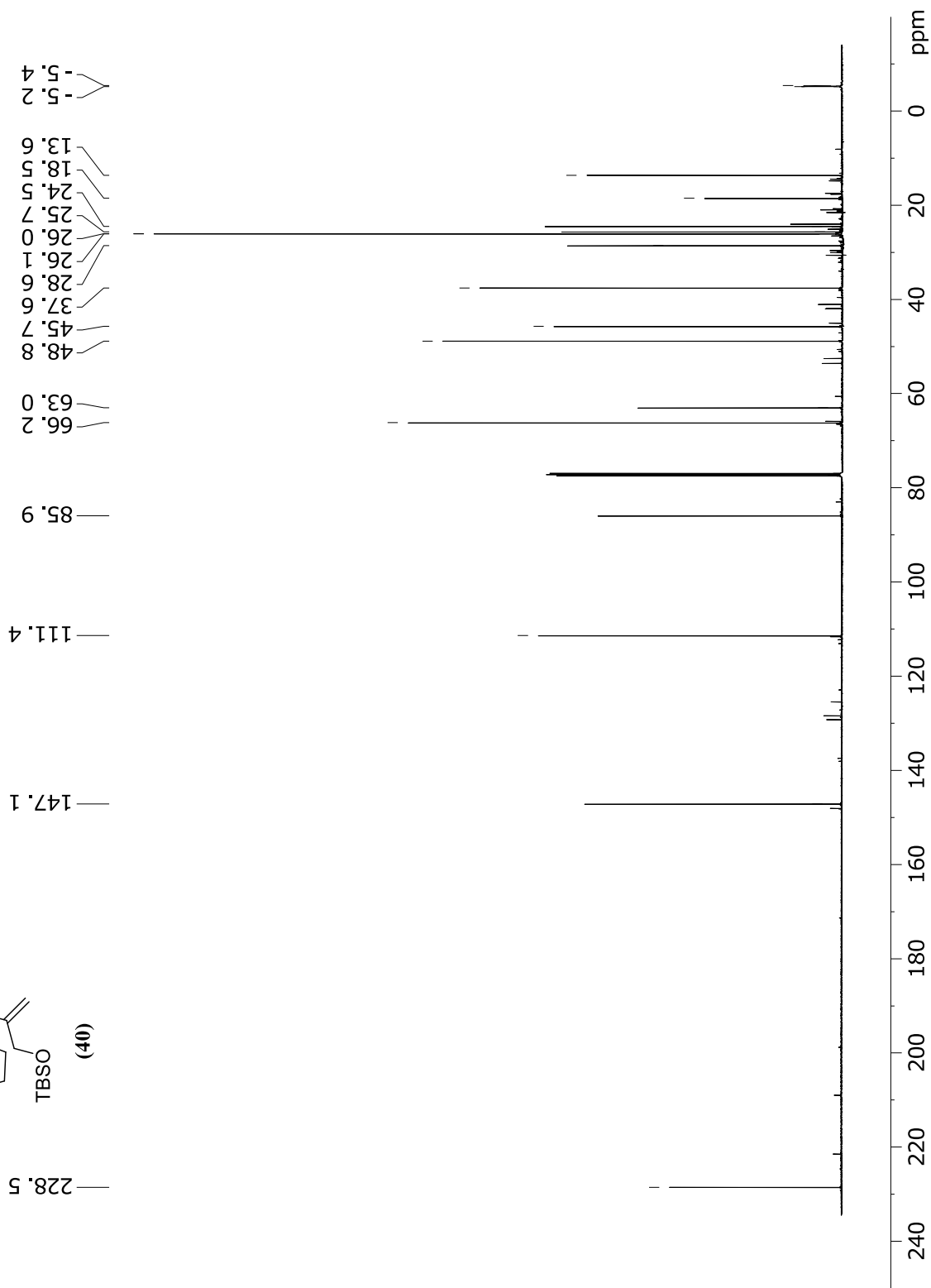
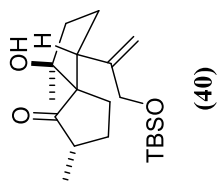


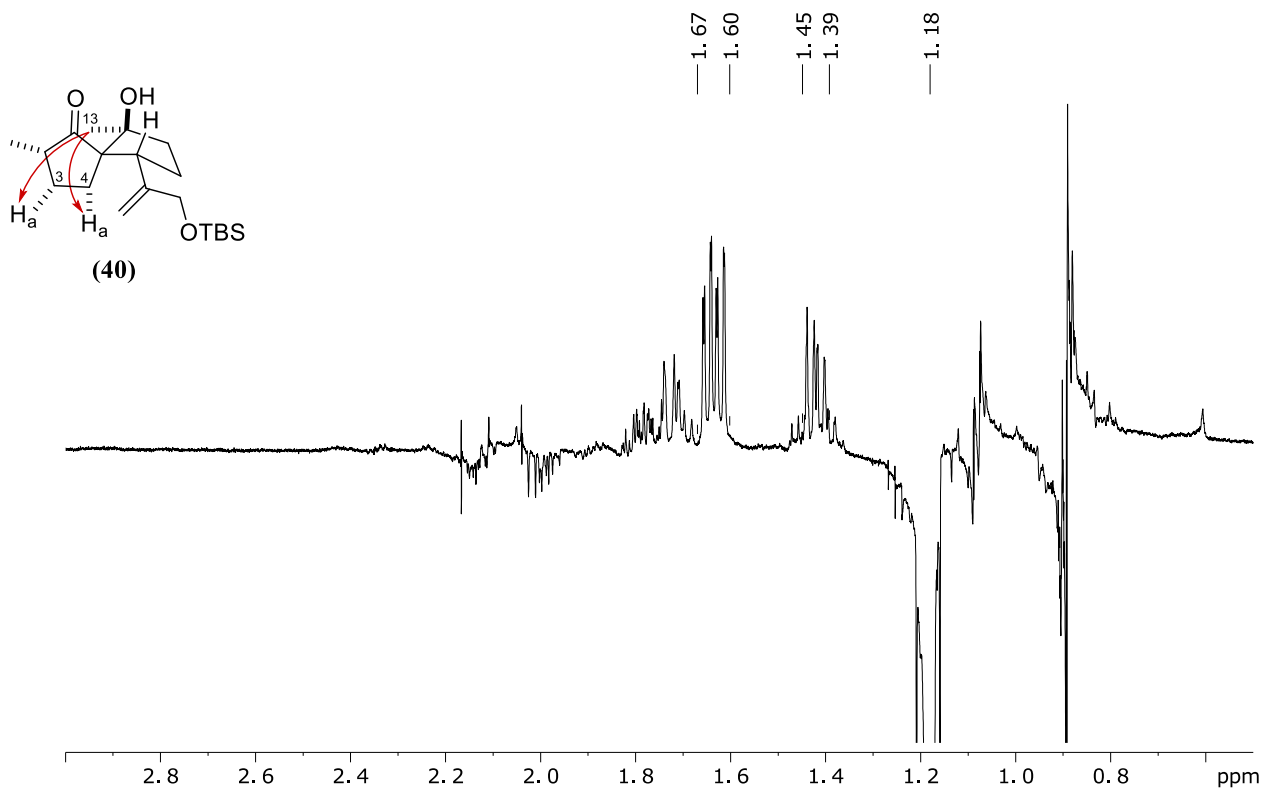




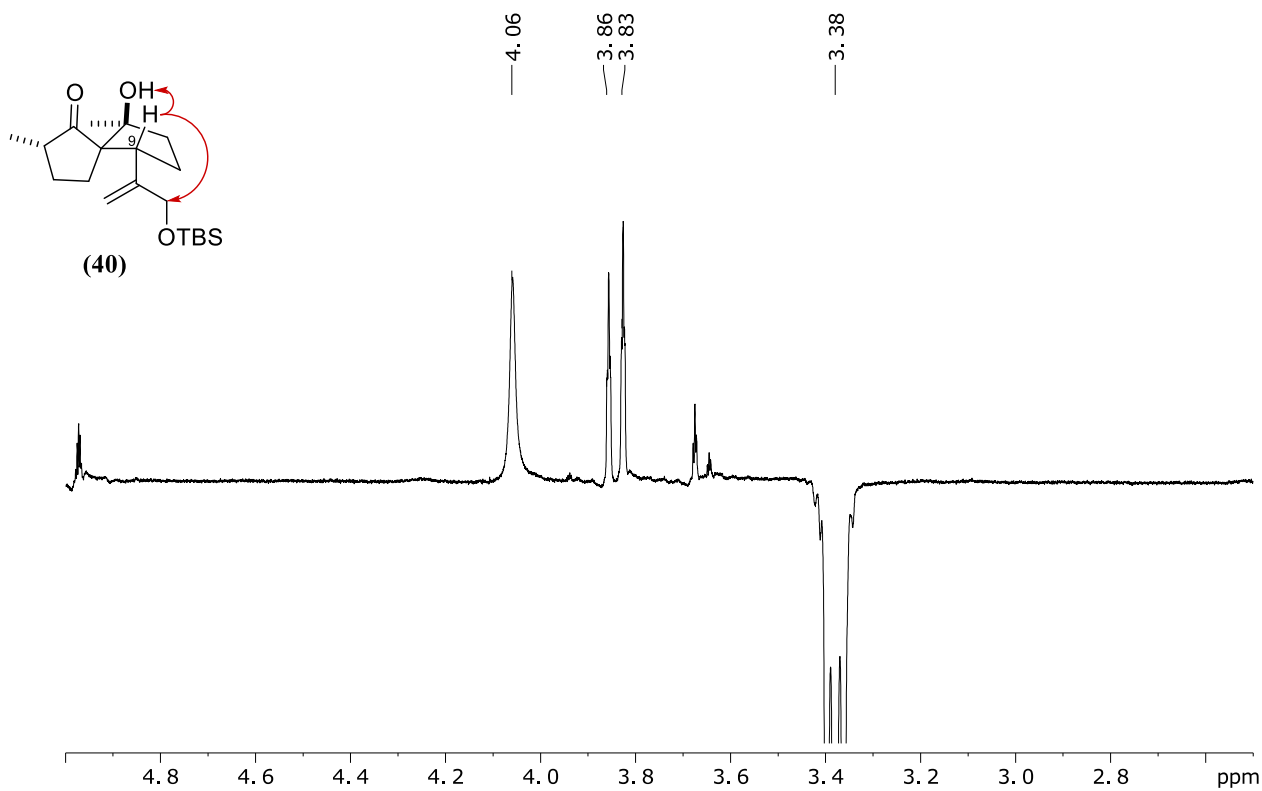




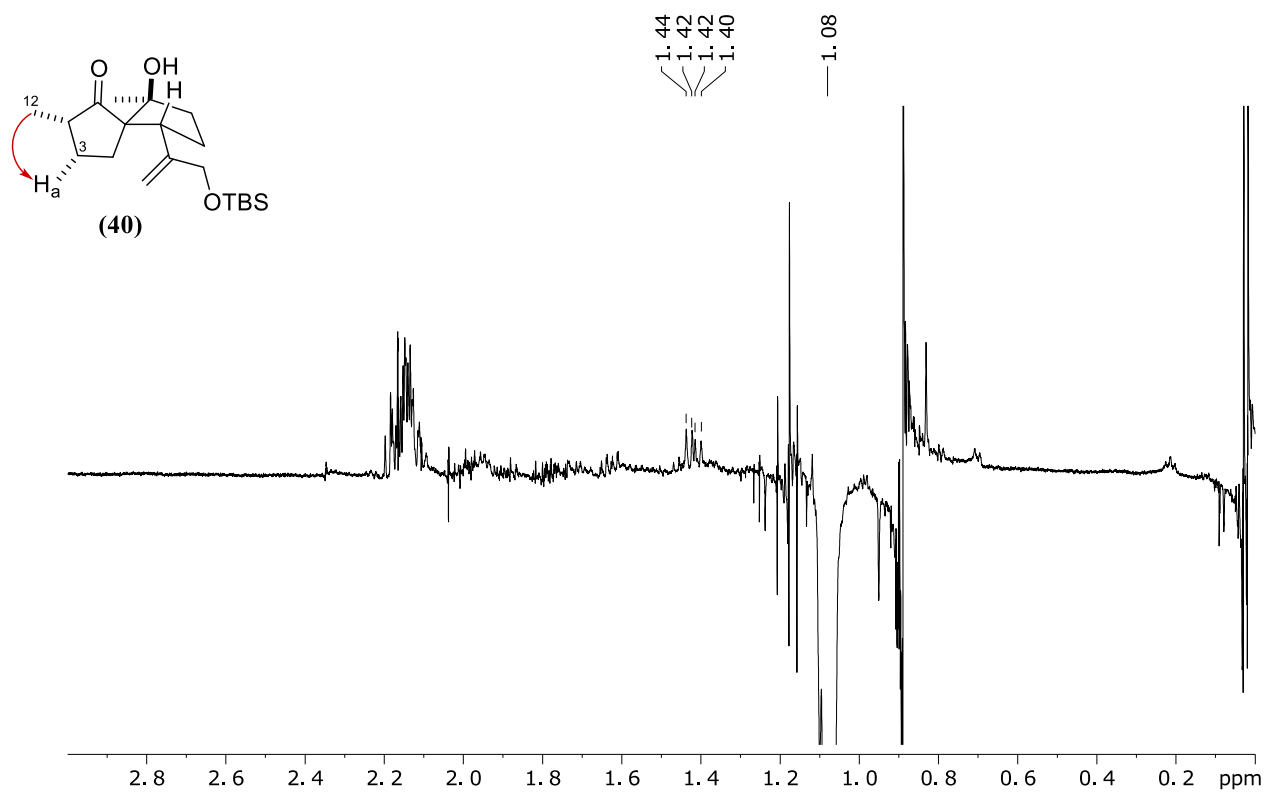




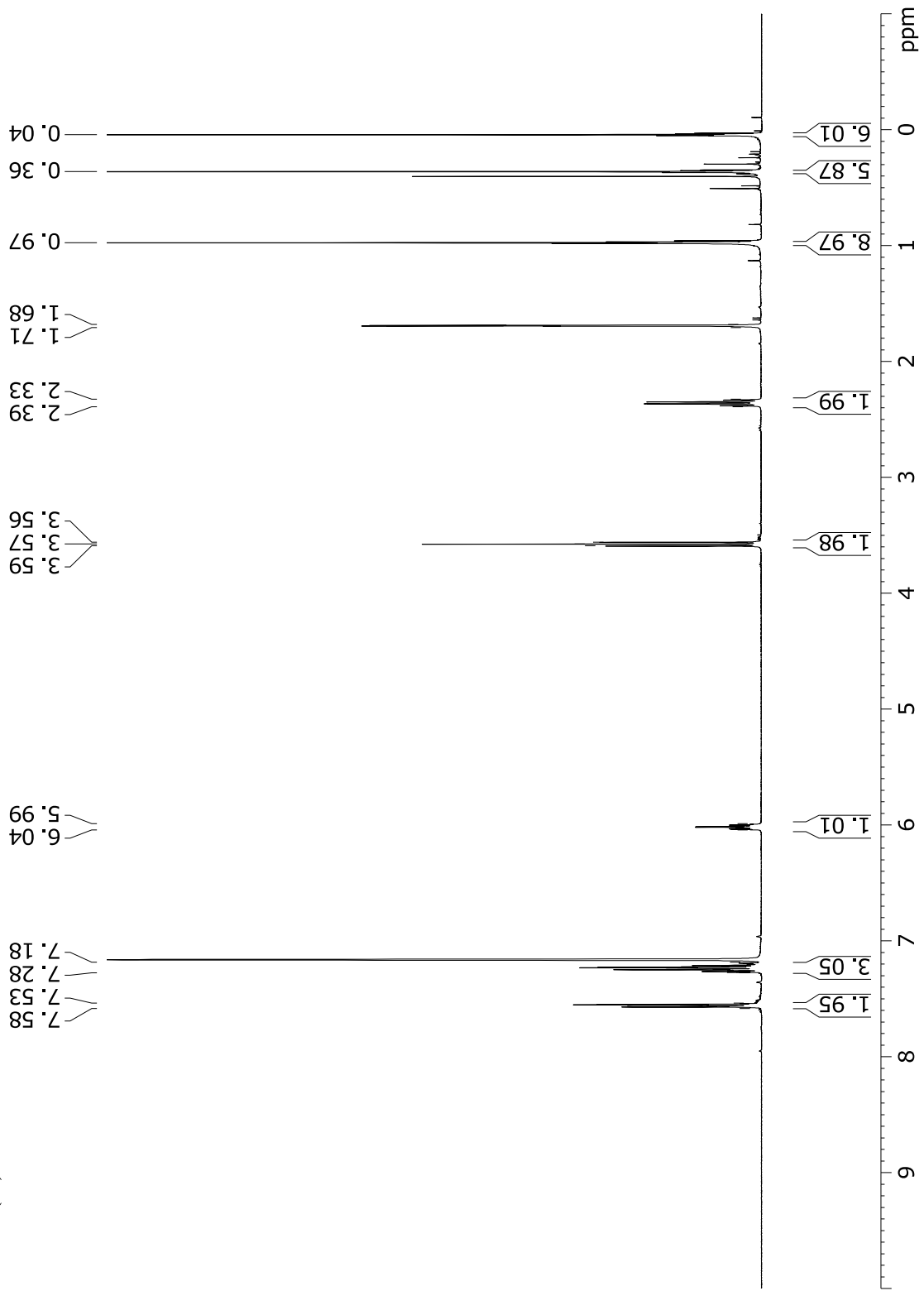
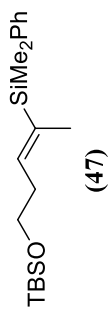
NOE response of **(40)** after irradiation at 1.18 ppm (CH_3 -13). Spectrum measured in $CDCl_3$ at 500 MHz.

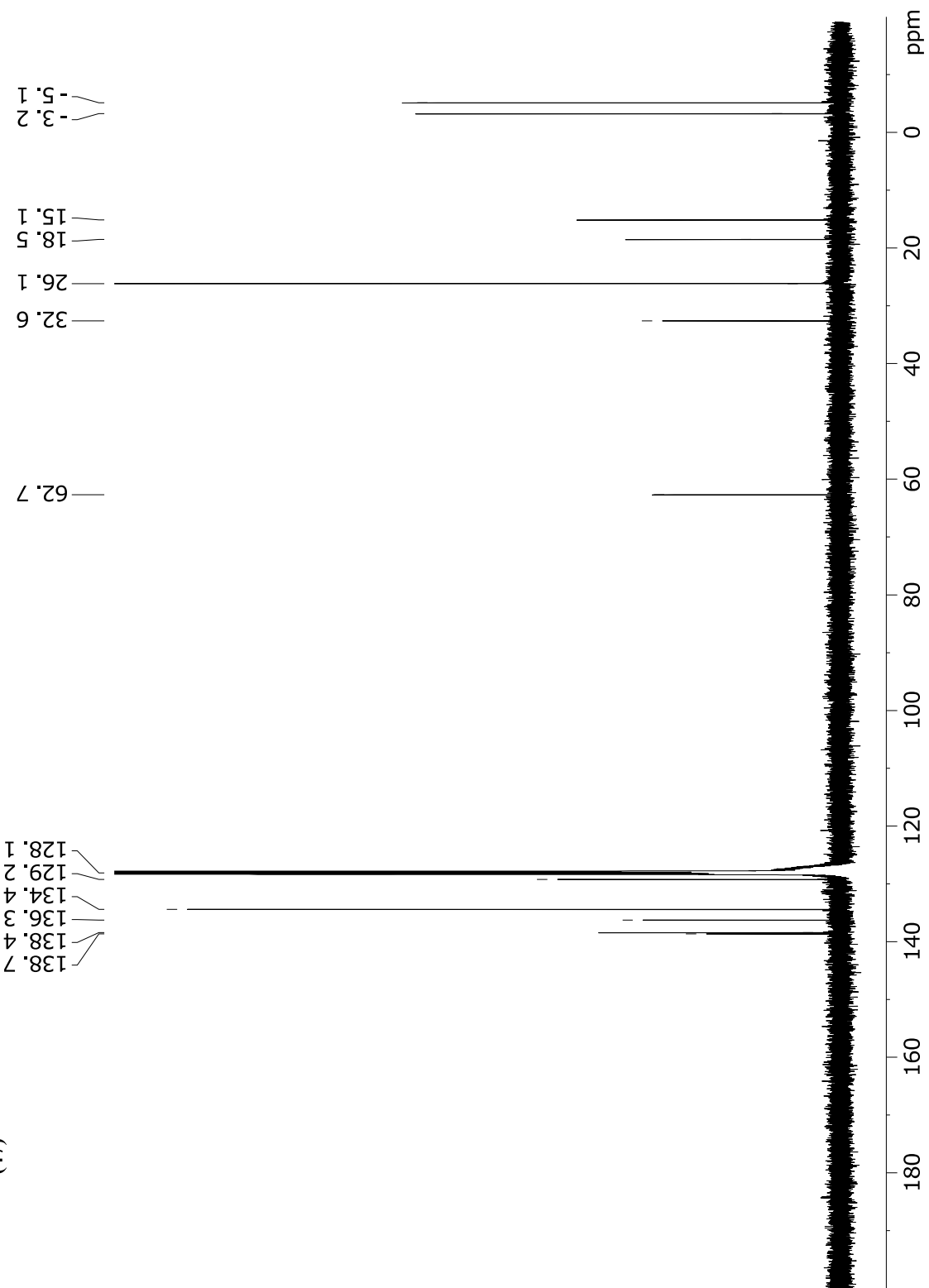
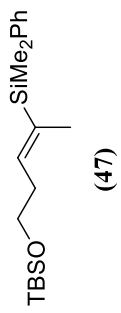


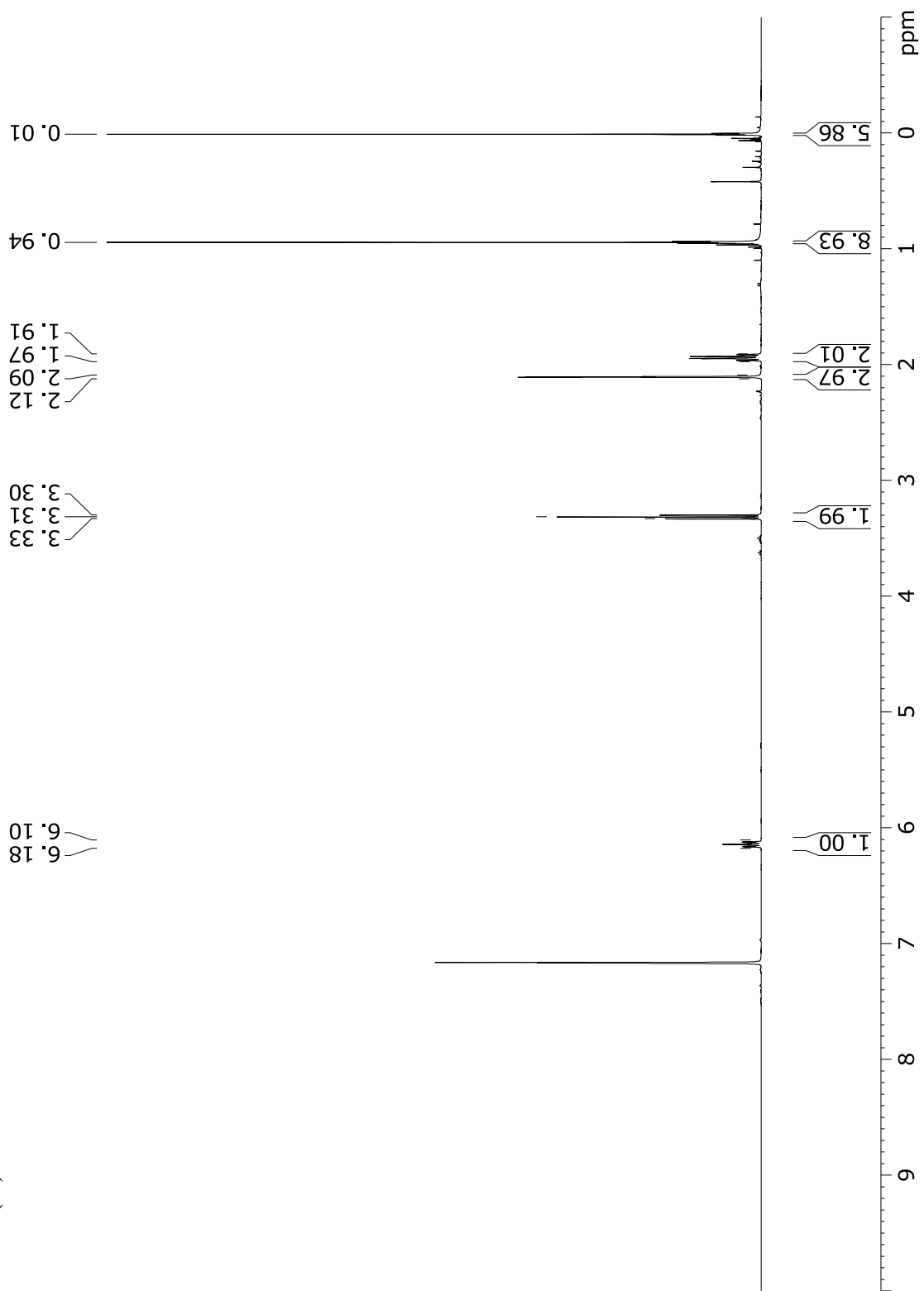
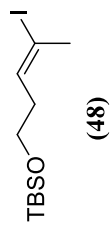
NOE response of **(40)** after irradiation at 3.38 ppm (CH-9). Spectrum measured in $CDCl_3$ at 500 MHz.

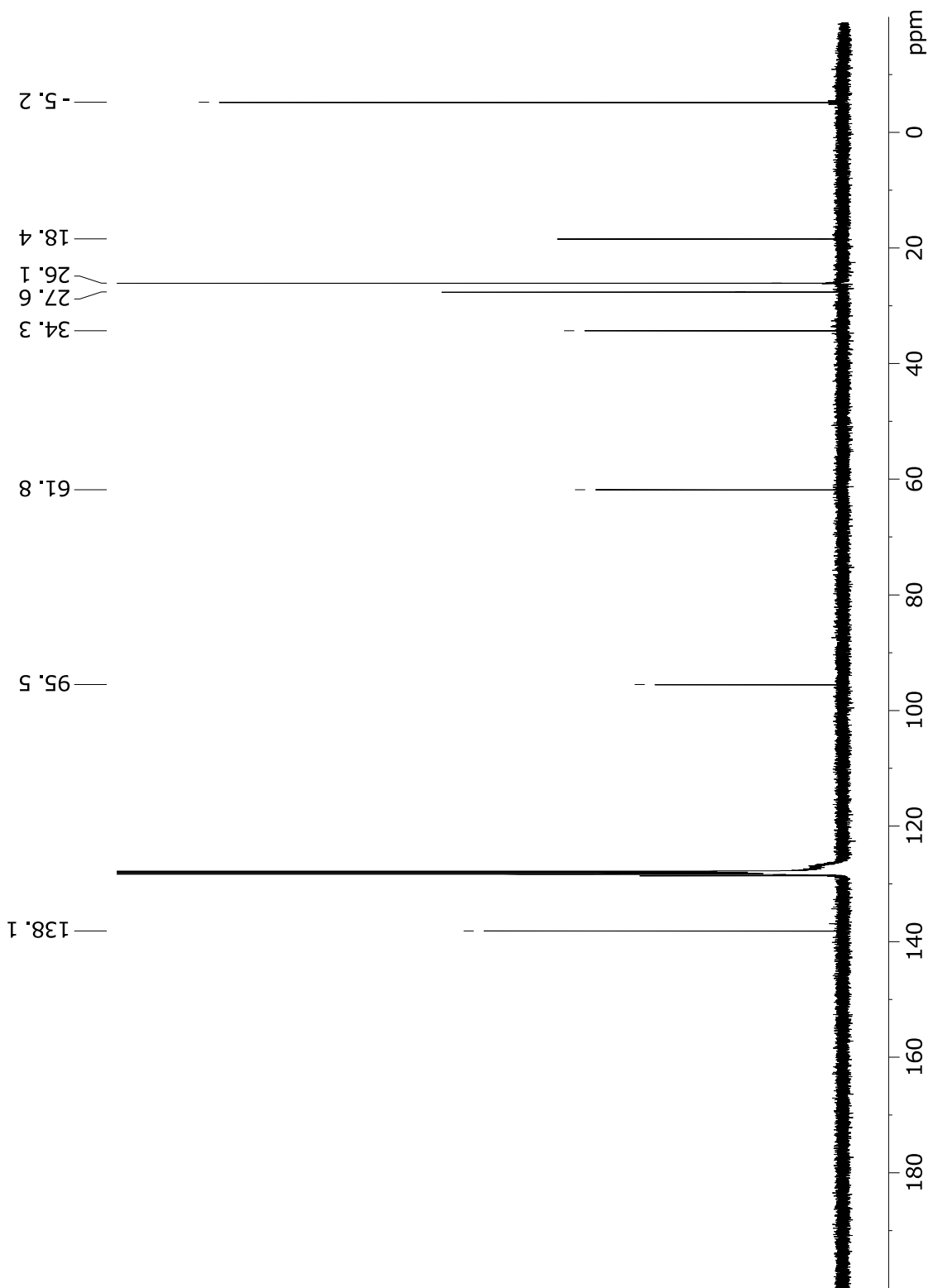
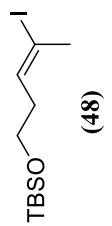


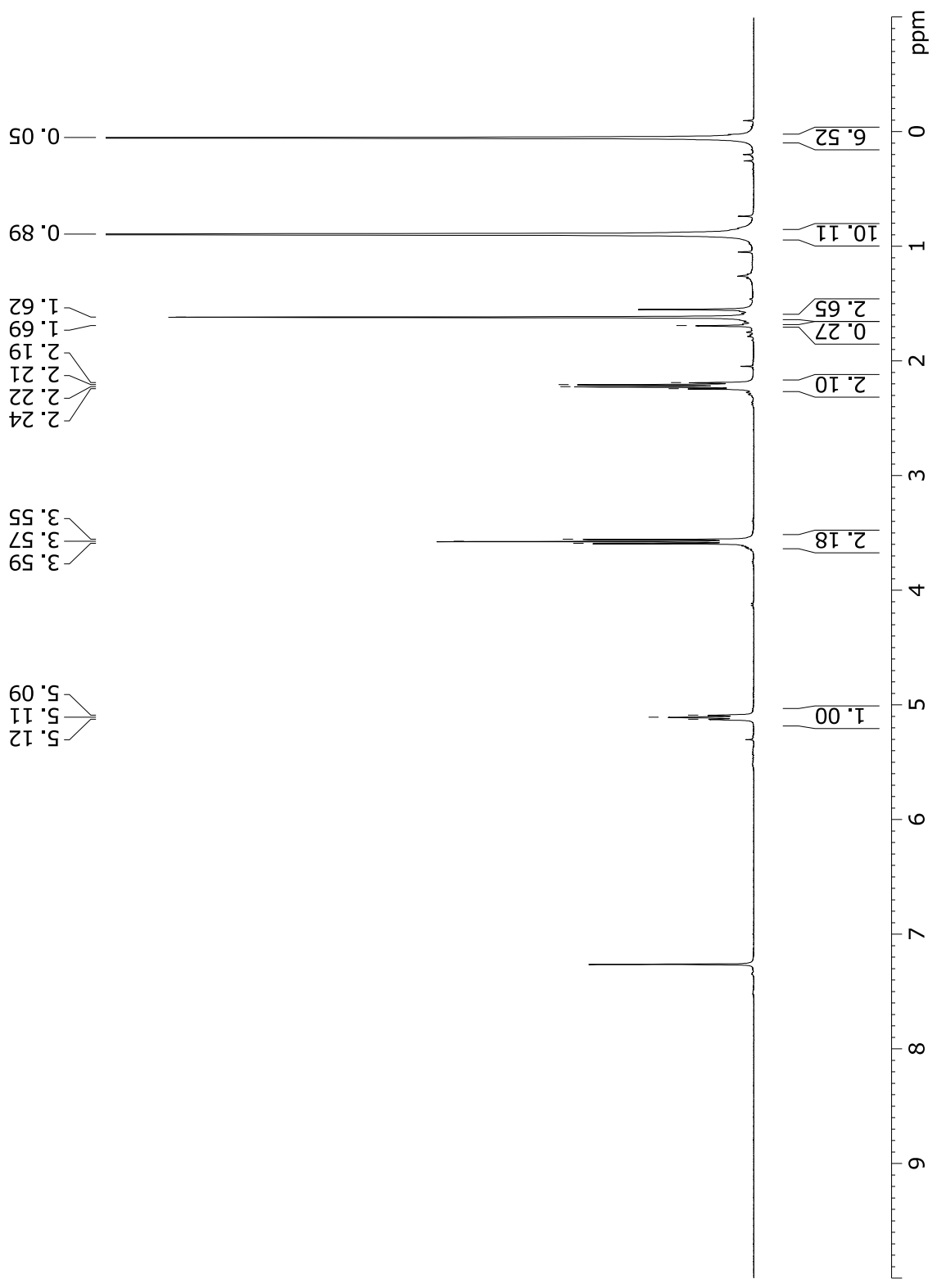
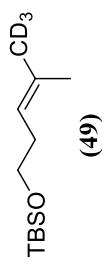
NOE response of (40) after irradiation at 1.08 ppm (CH_3 -12). Spectrum measured in $CDCl_3$ at 500 MHz.

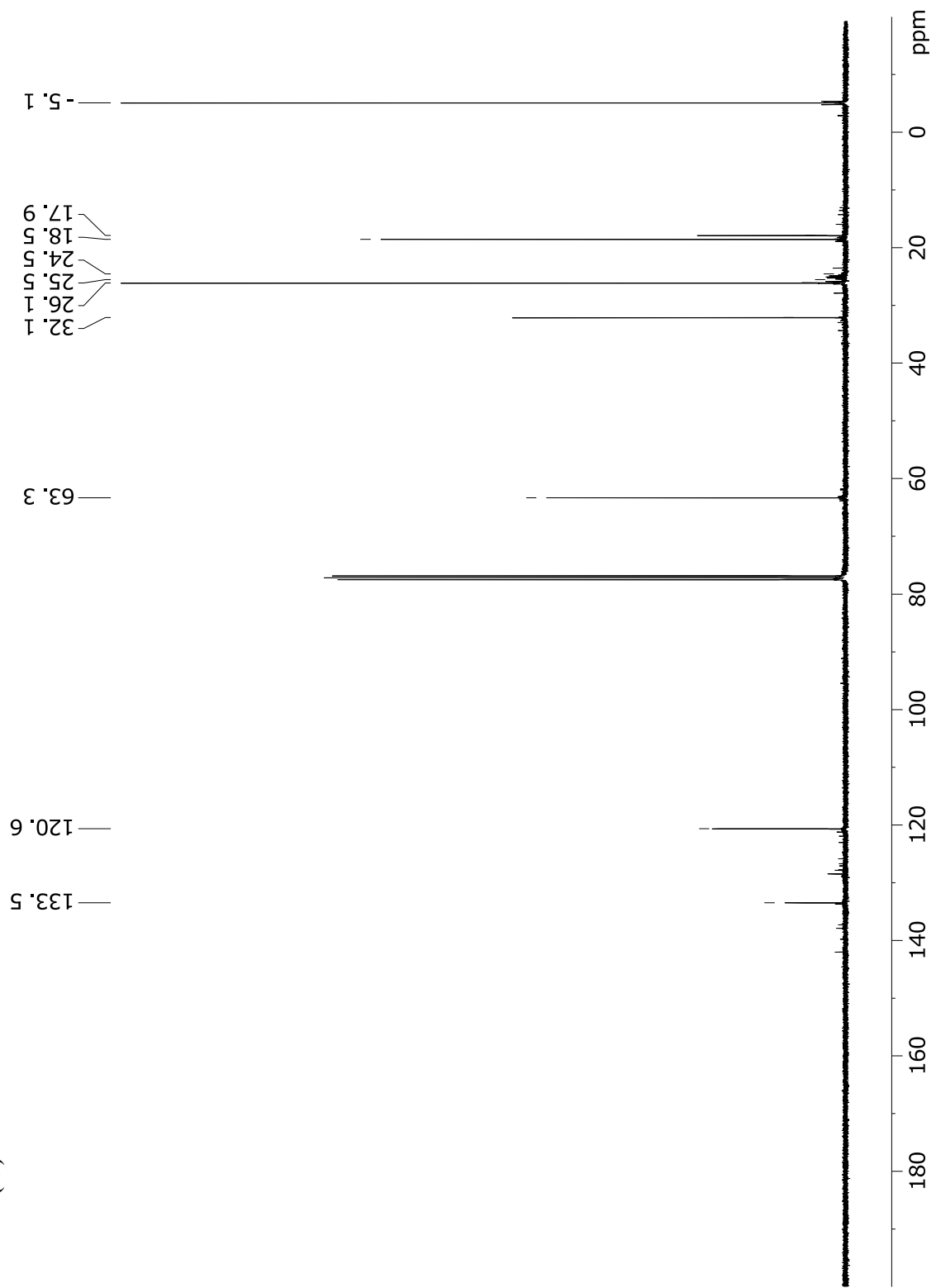
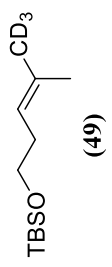


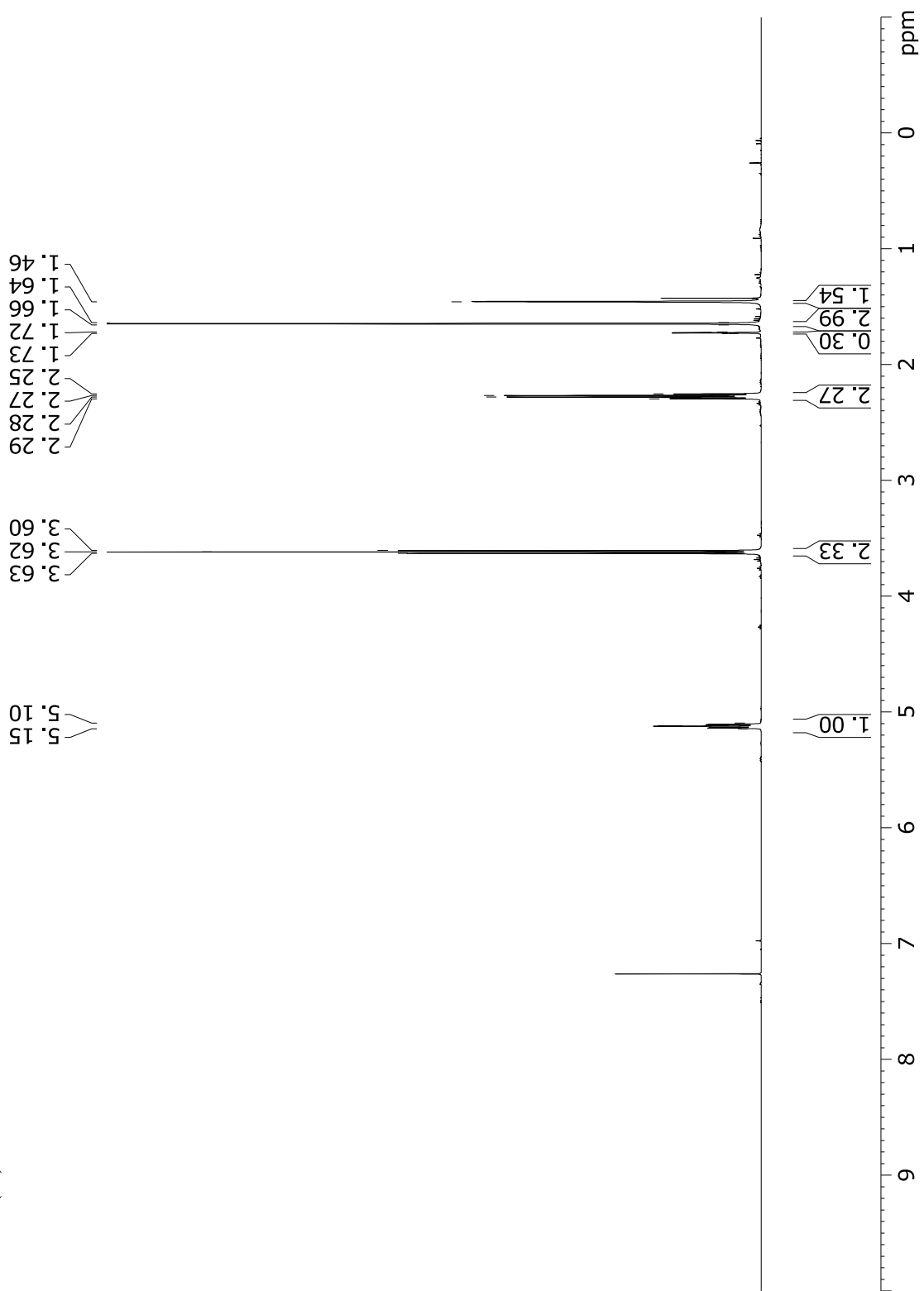
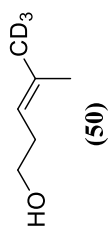


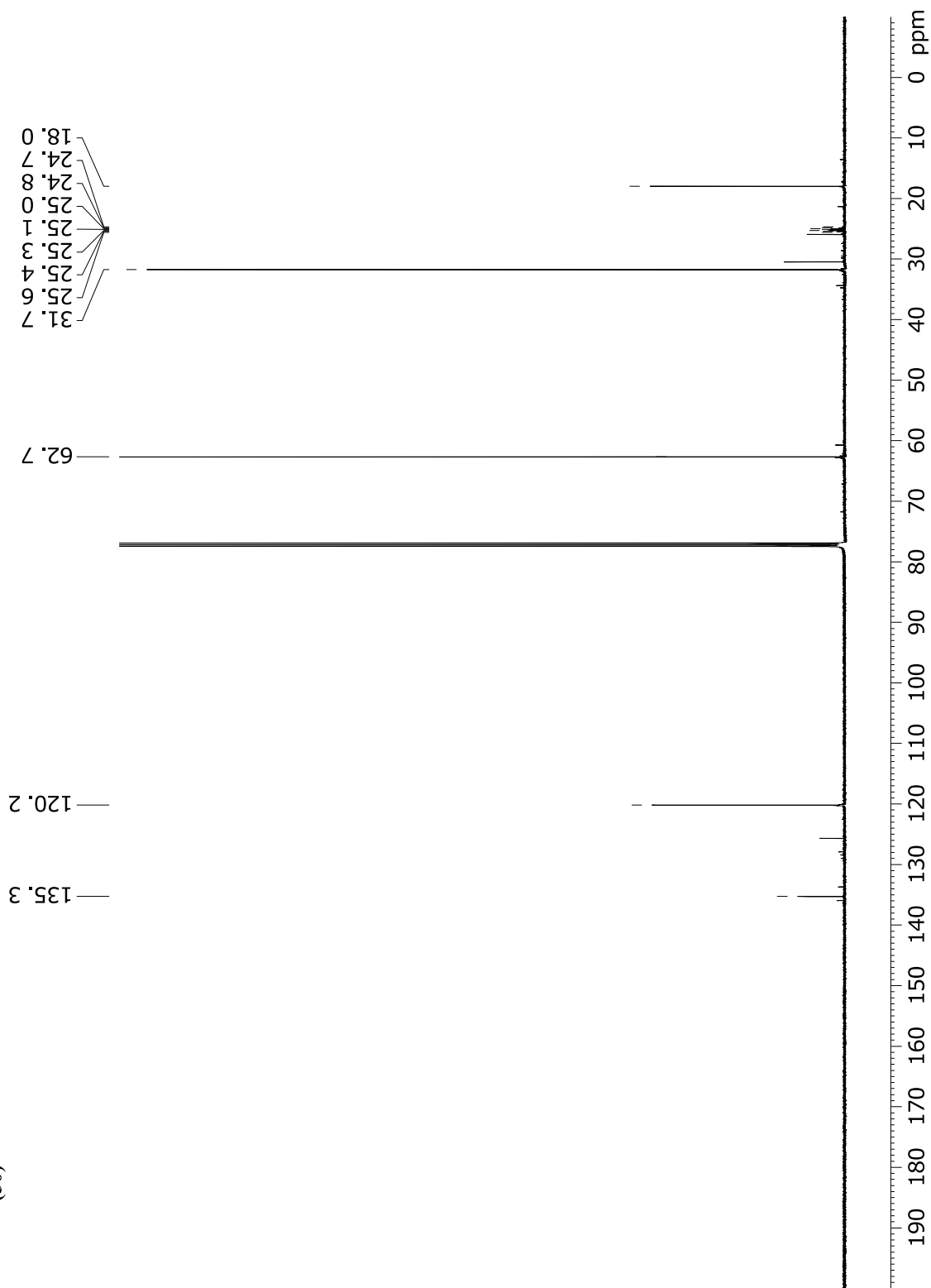
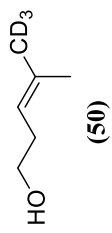


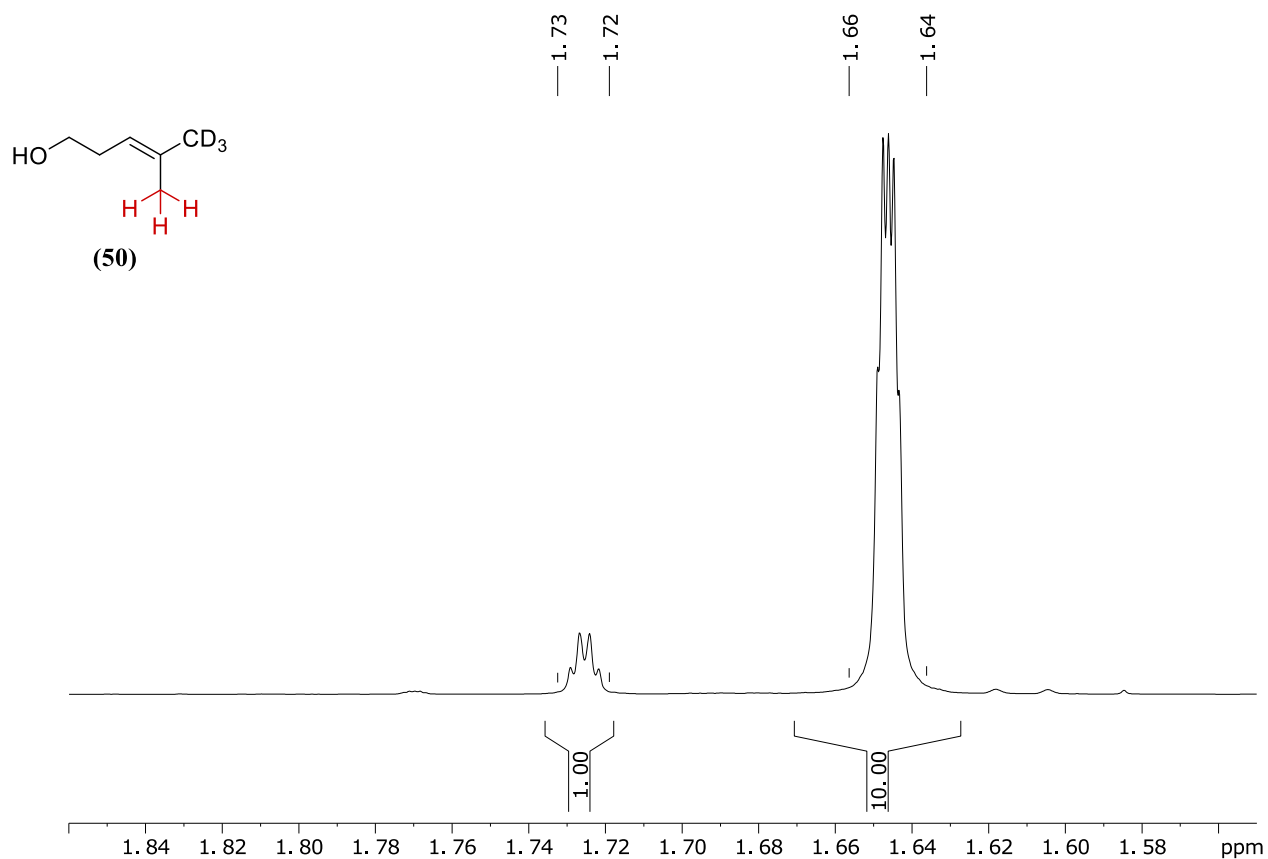




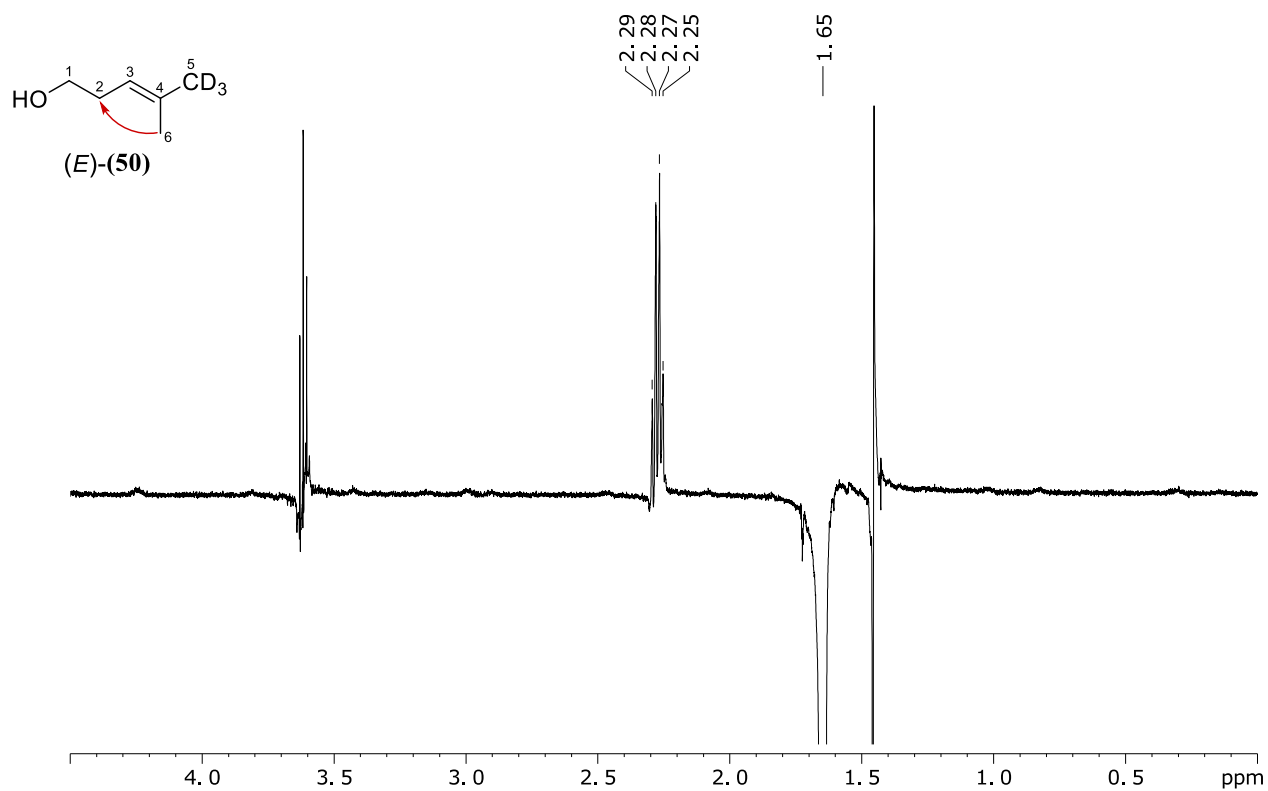




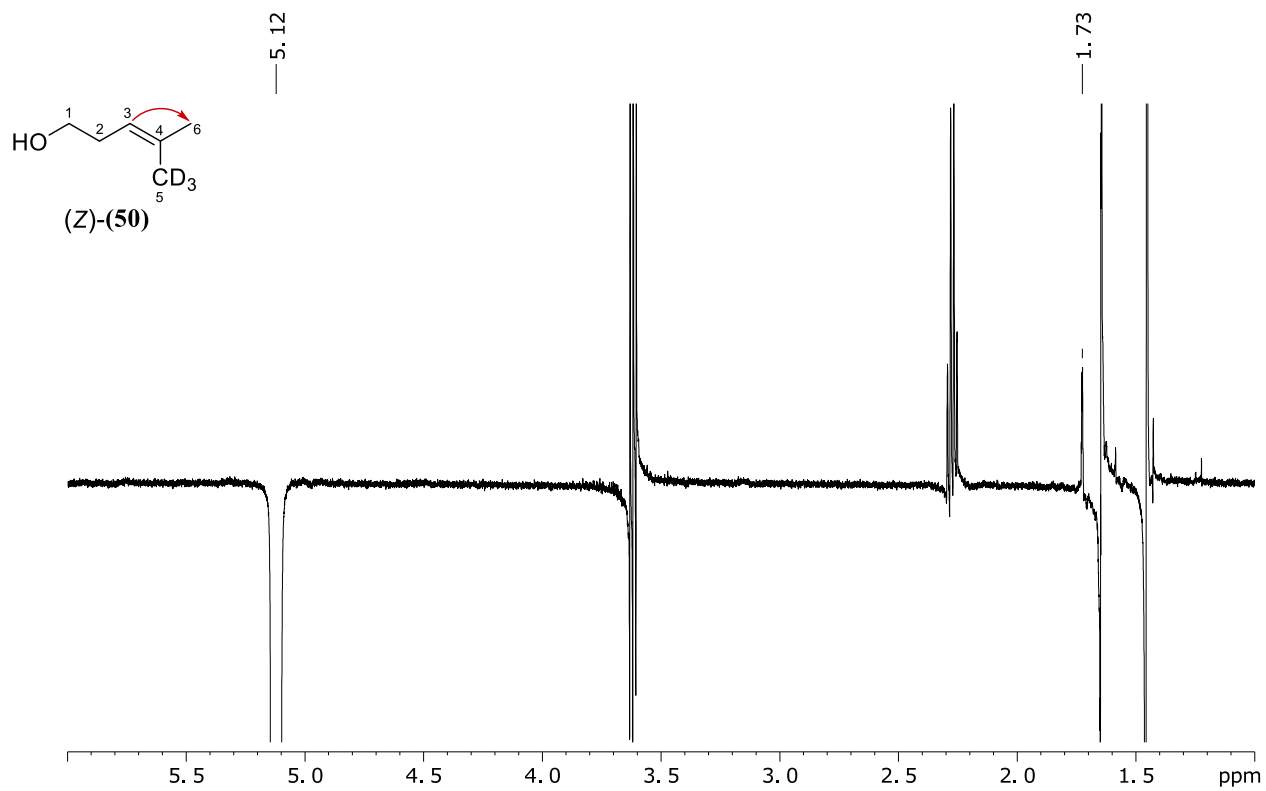




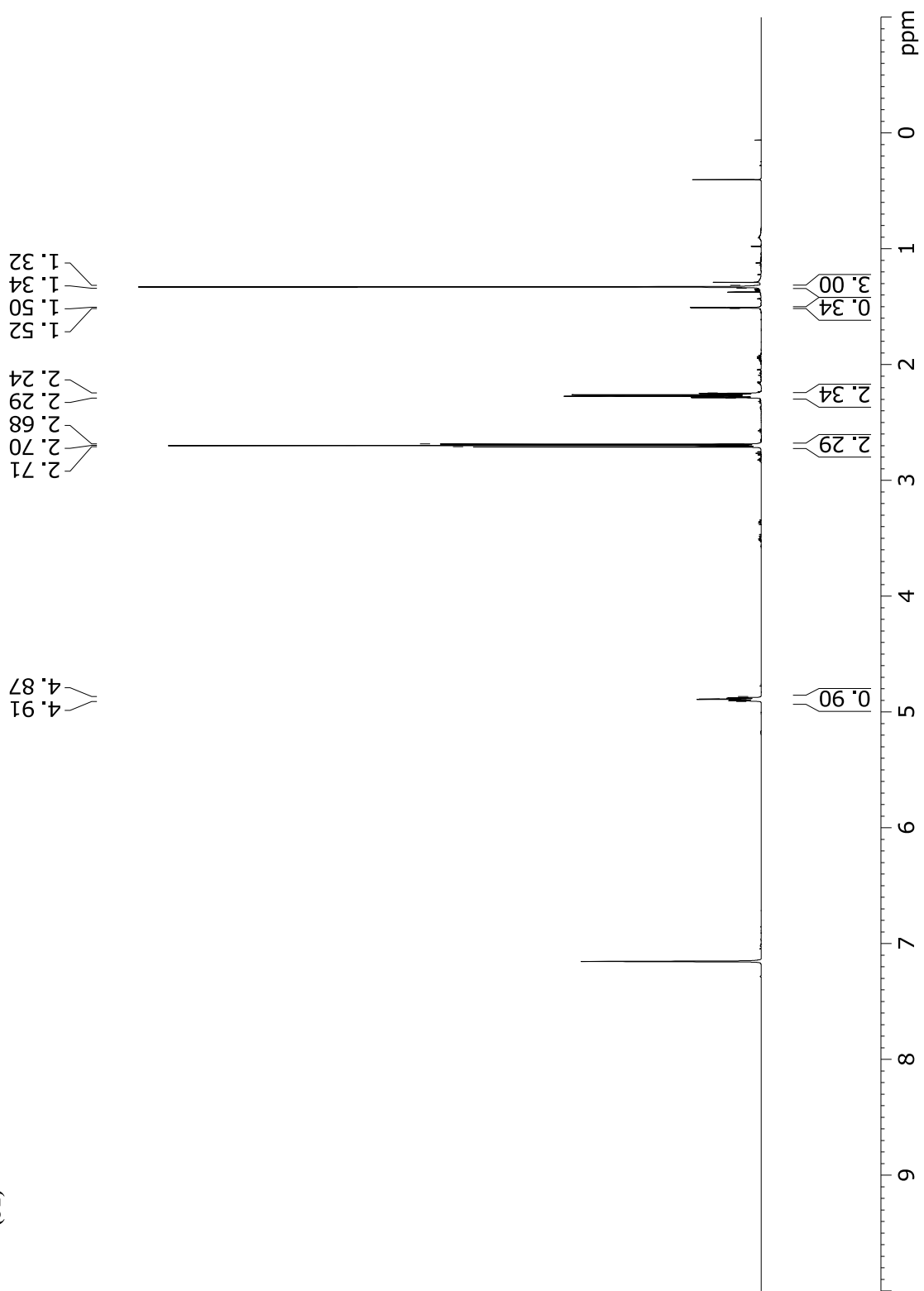
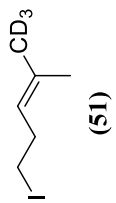
Enhancement of (50) ¹H-NMR spectrum for determination of the (*E*)/(*Z*)-ratio. The protons corresponding to depicted signal are marked in red; (*E*)-isomer is the major isomer.

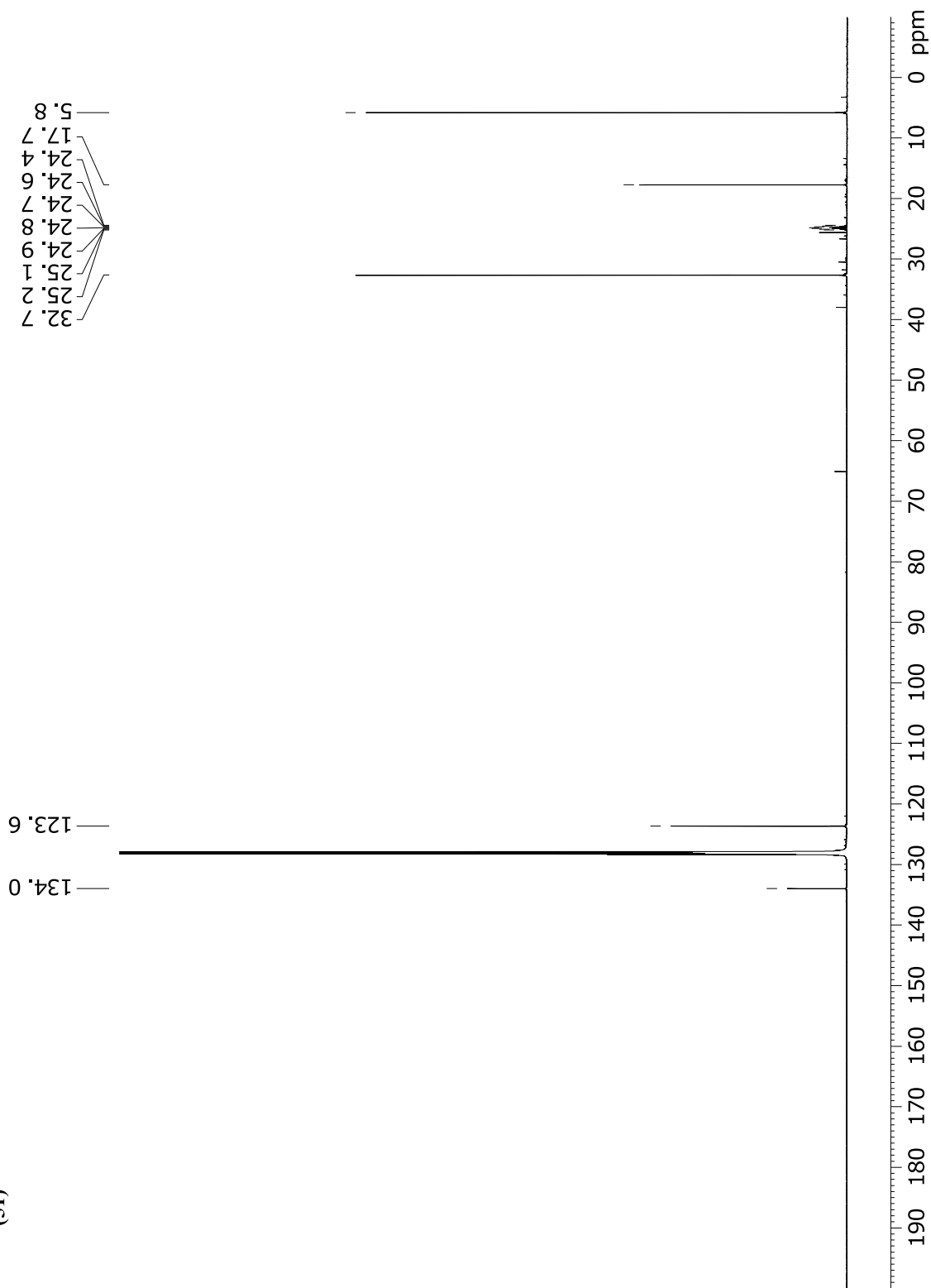
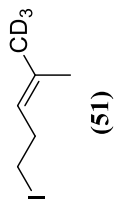


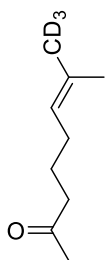
NOE response of (50) after irradiation at 1.65 ppm (CH₃-6, (*E*)-isomer); confirmation of the major isomer's double bond geometry via NOE correlation between methyl group CH₃-6 and methylene CH₂-2. Spectrum measured in CDCl₃ at 400 MHz.



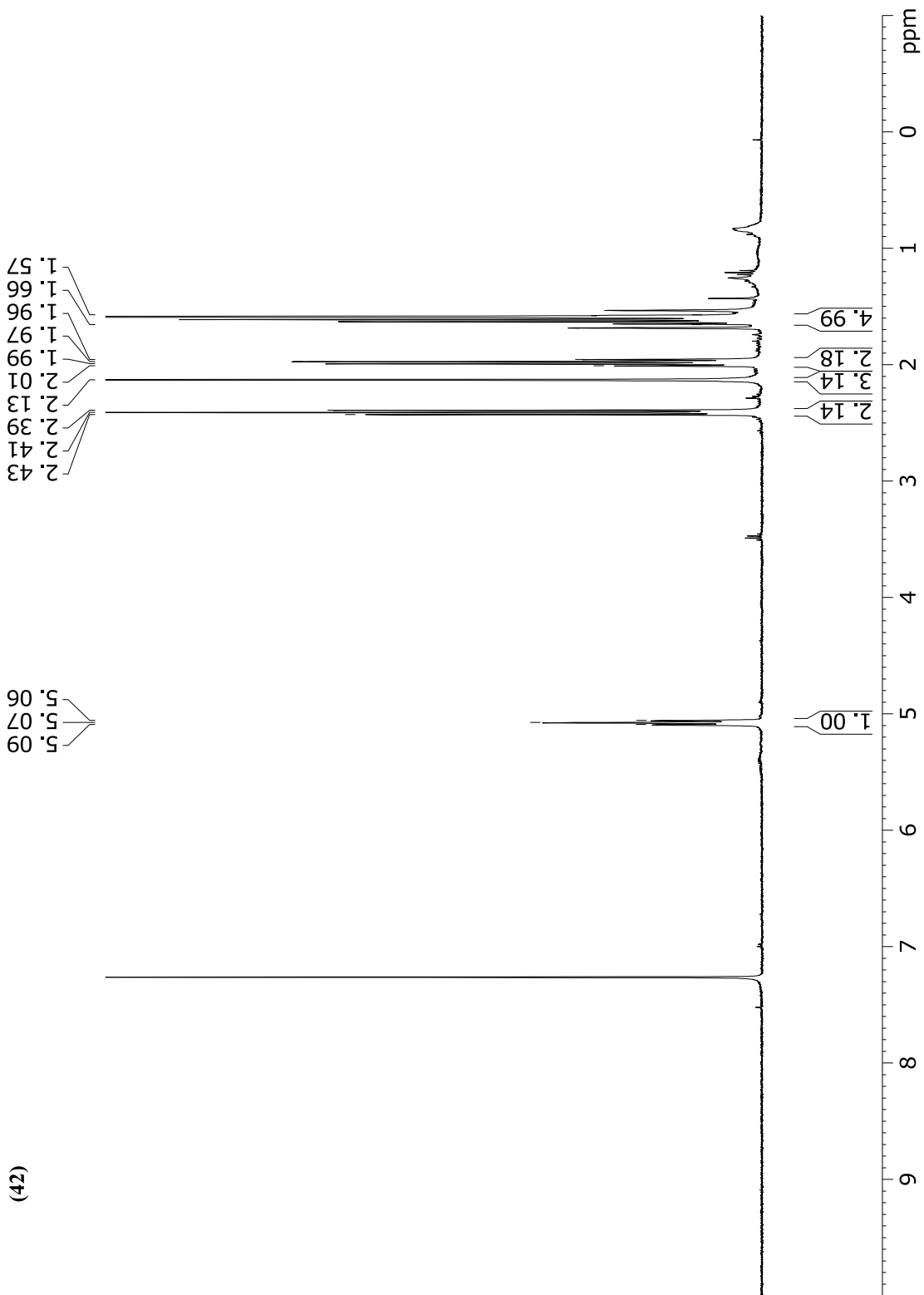
NOE response of **(50)** after irradiation at 1.73 ppm (CH₃-6, (Z)-isomer); confirmation of the minor isomer's double bond geometry *via* NOE correlation between olefinic methine proton CH-3 and methyl group CH₃-6. Spectrum measured in CDCl₃ at 400 MHz.

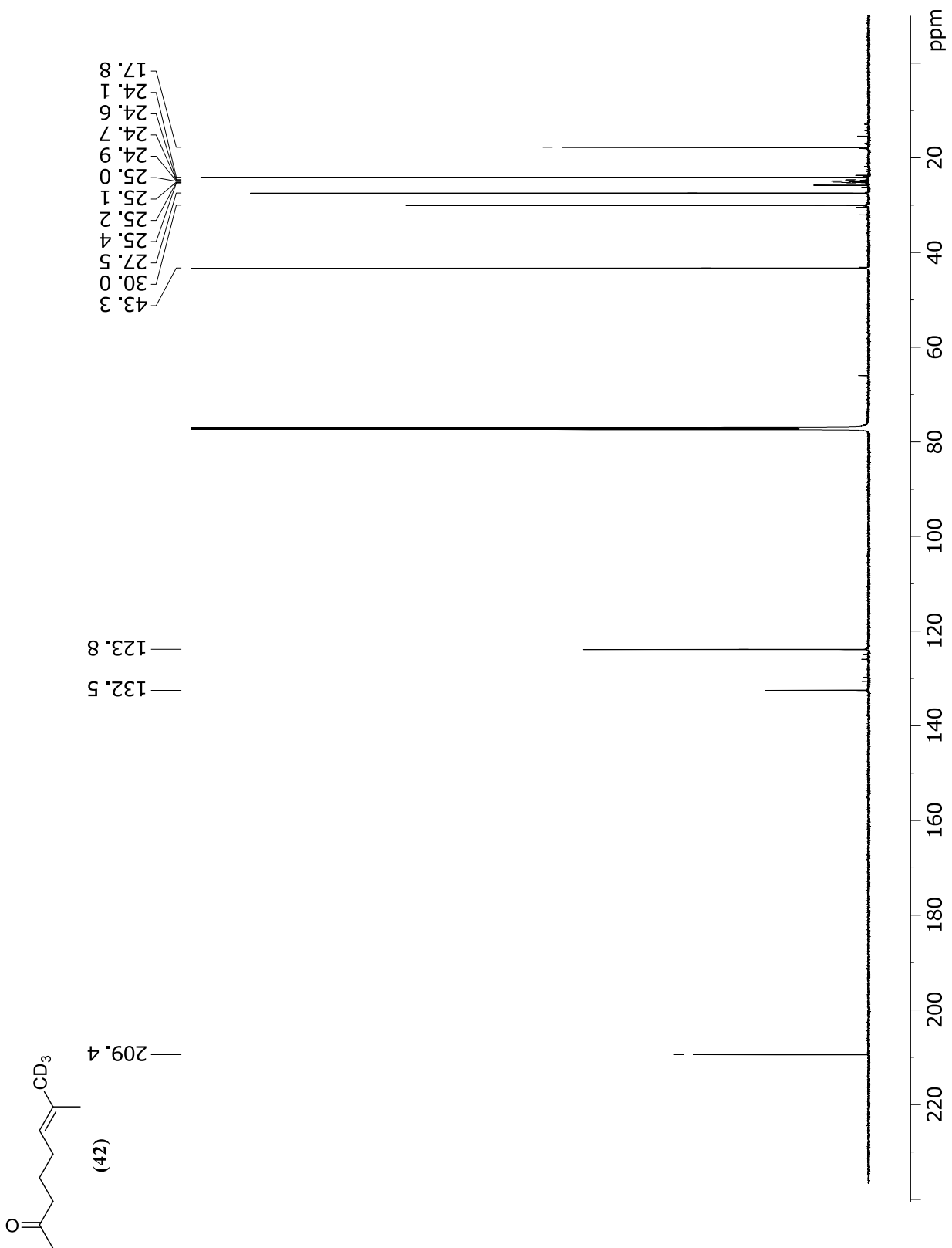


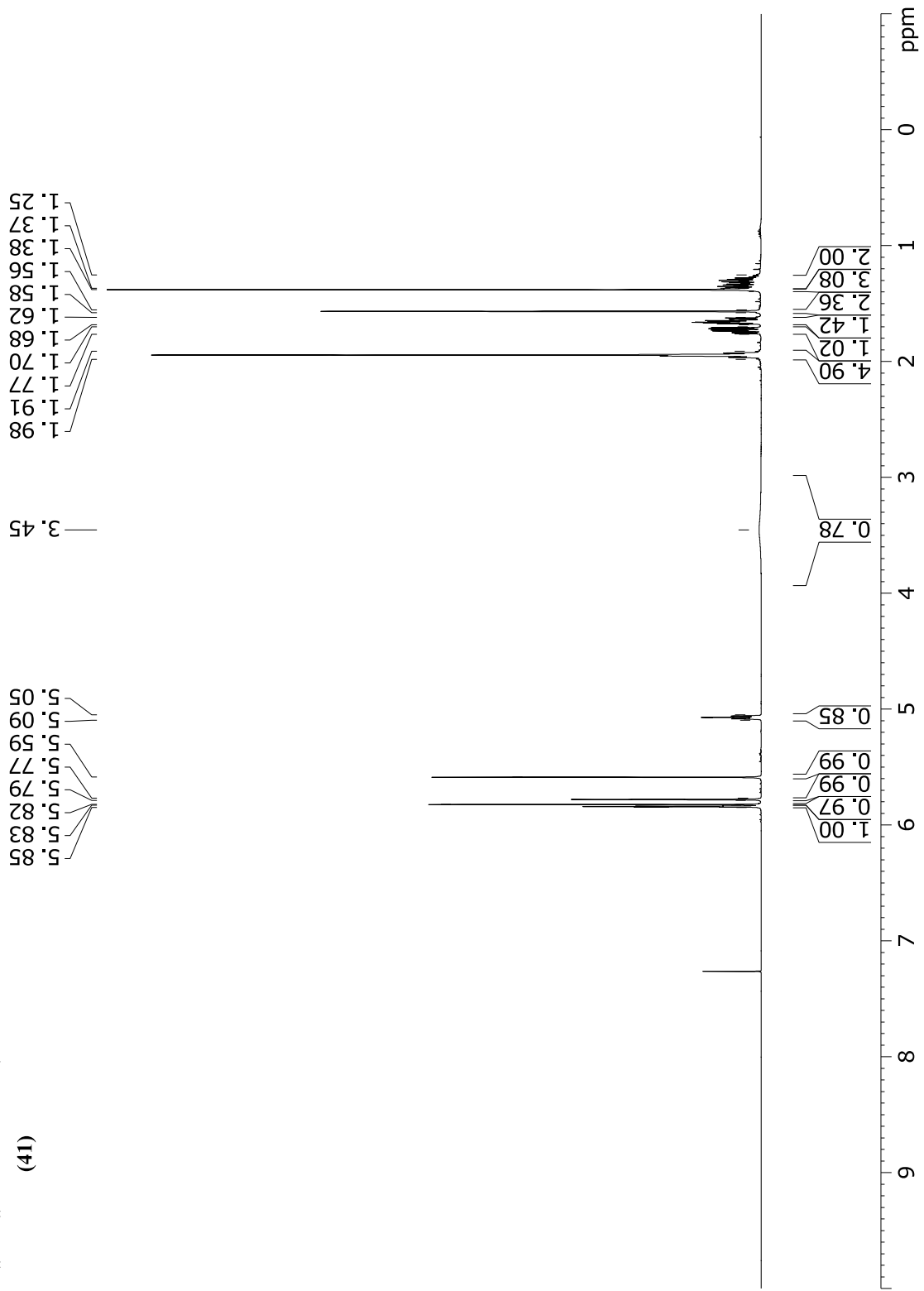
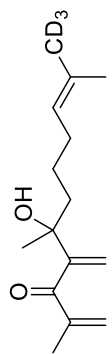


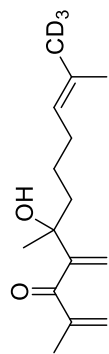


(42)









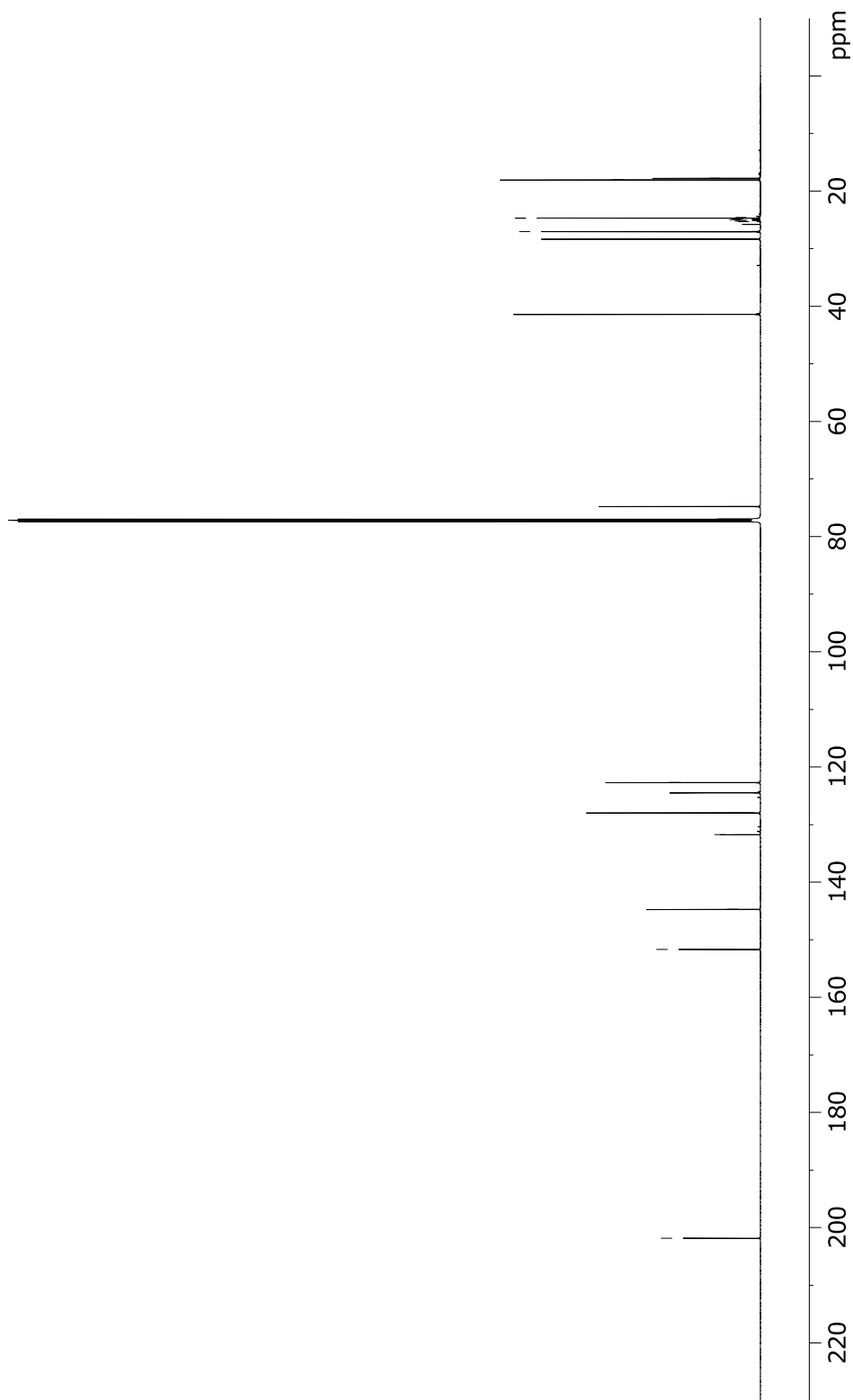
201.8

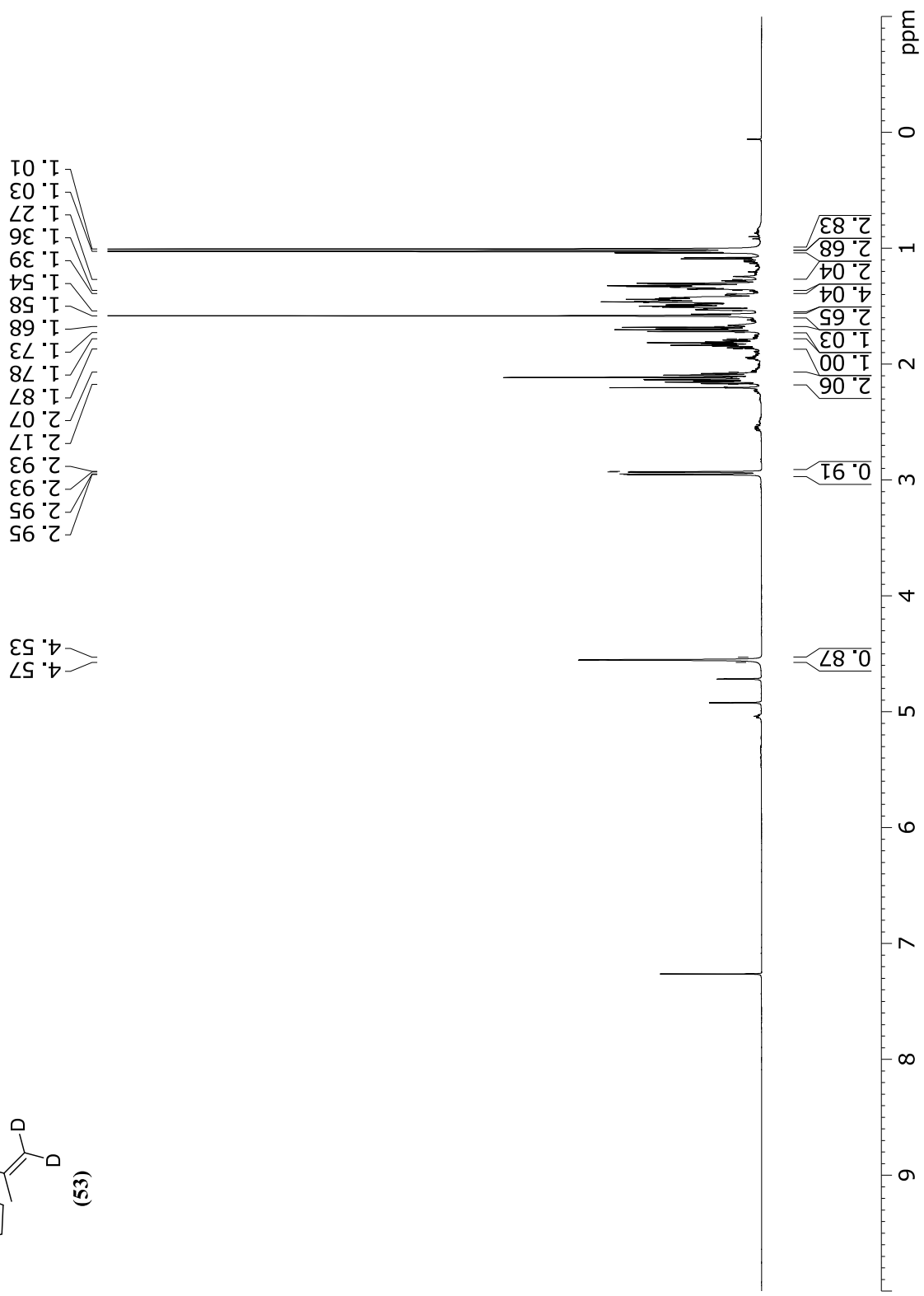
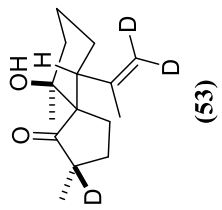
151.7
144.7

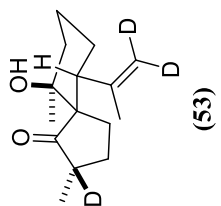
131.7
128.0
124.5
122.7

74.8

41.4
28.3
27.0
25.3
25.2
25.1
25.0
24.8
24.7
24.7
24.6
18.1
17.8







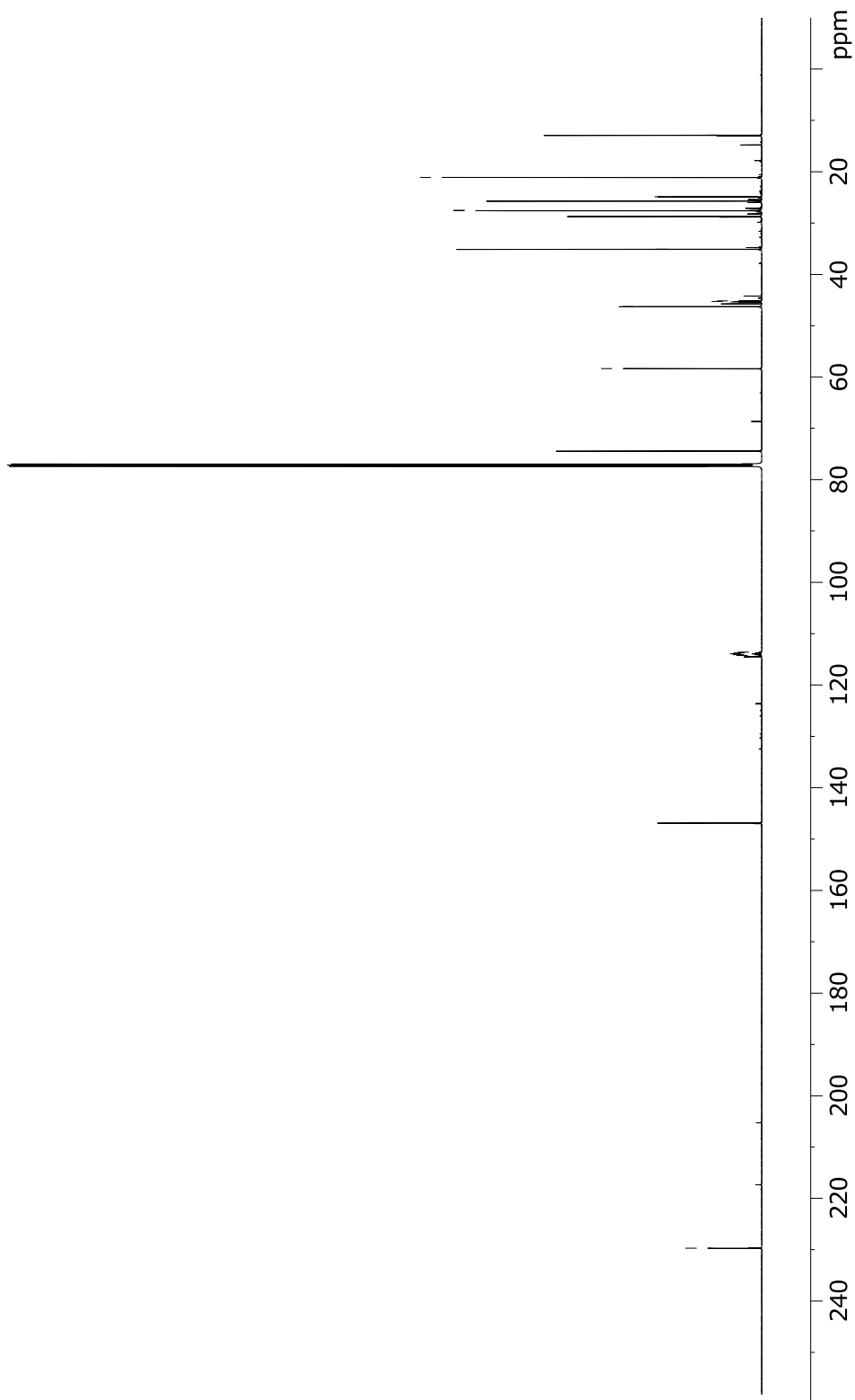
— 229.7

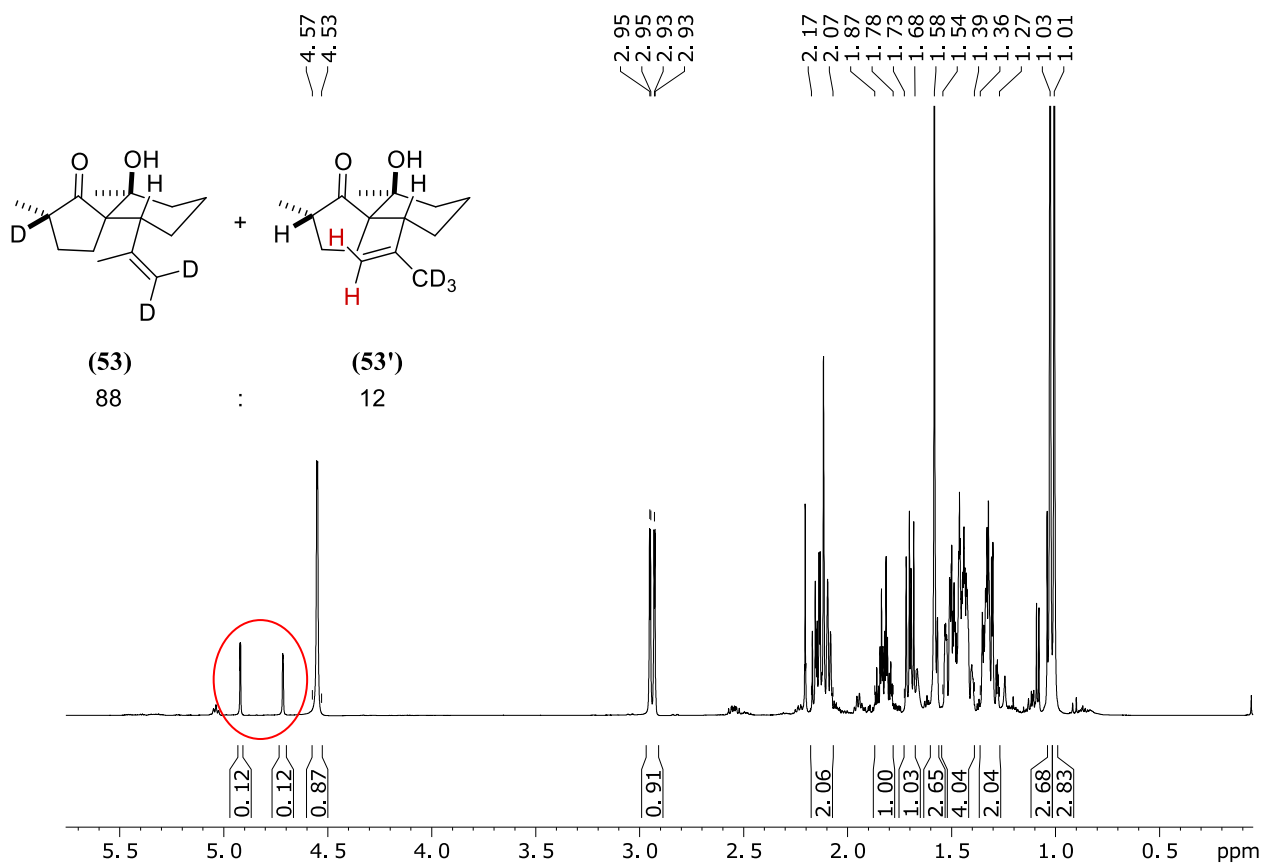
— 146.9

114.2
114.1
113.9
113.8
113.6

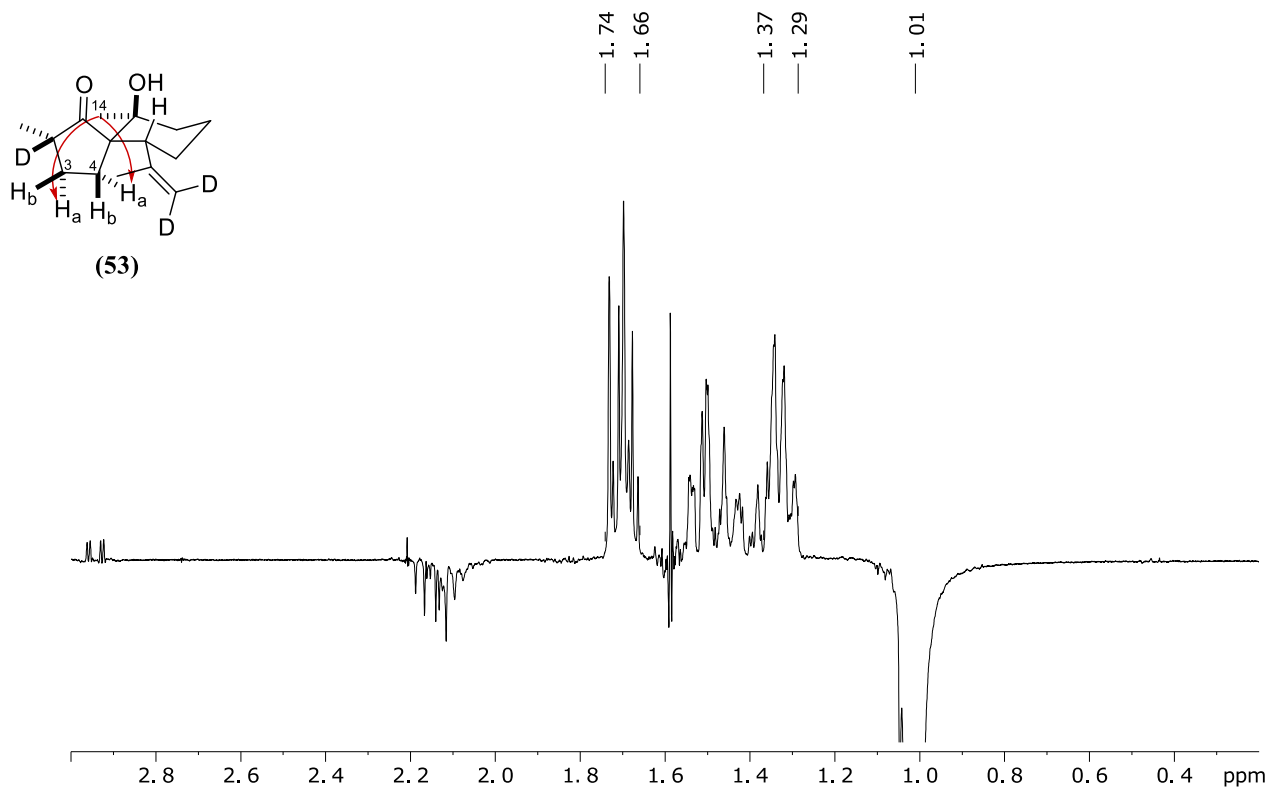
— 74.4

58.4
46.3
45.4
45.3
45.1
35.1
28.7
27.6
27.6
25.7
24.9
21.1
12.9

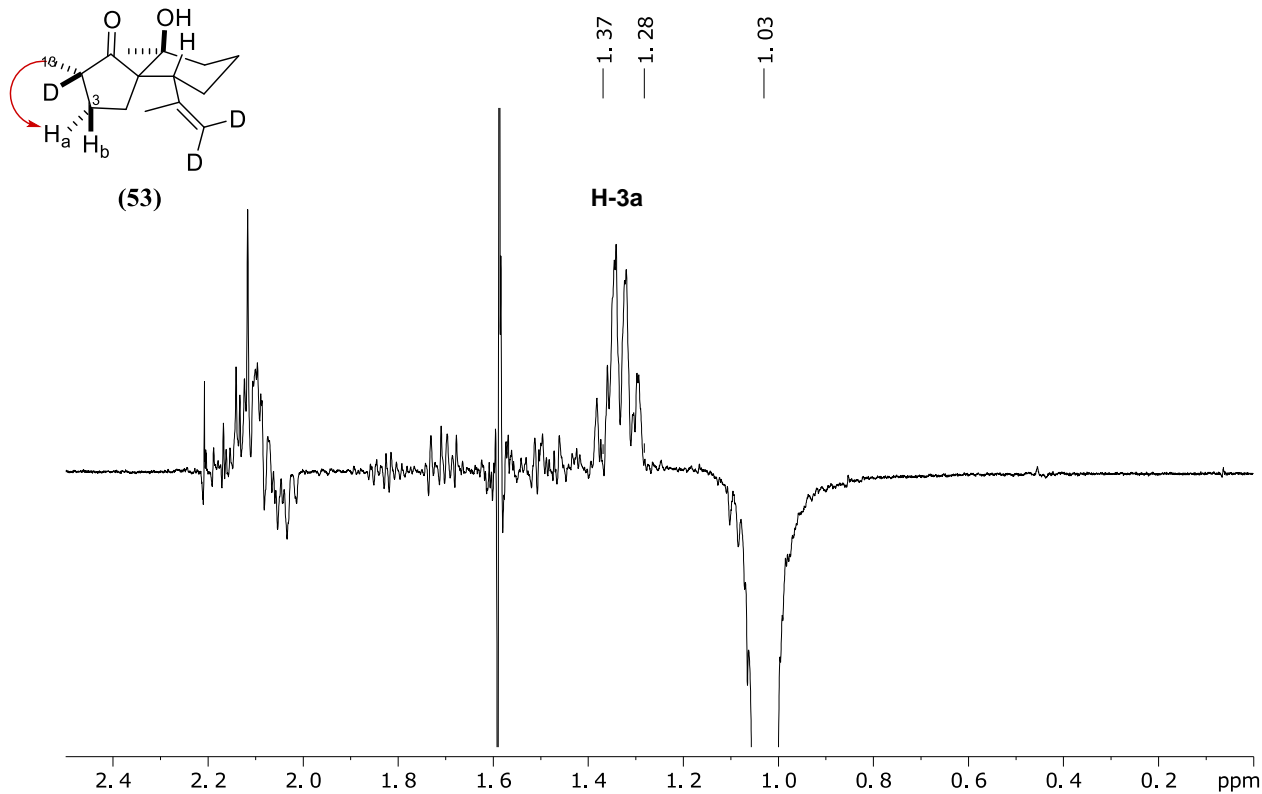




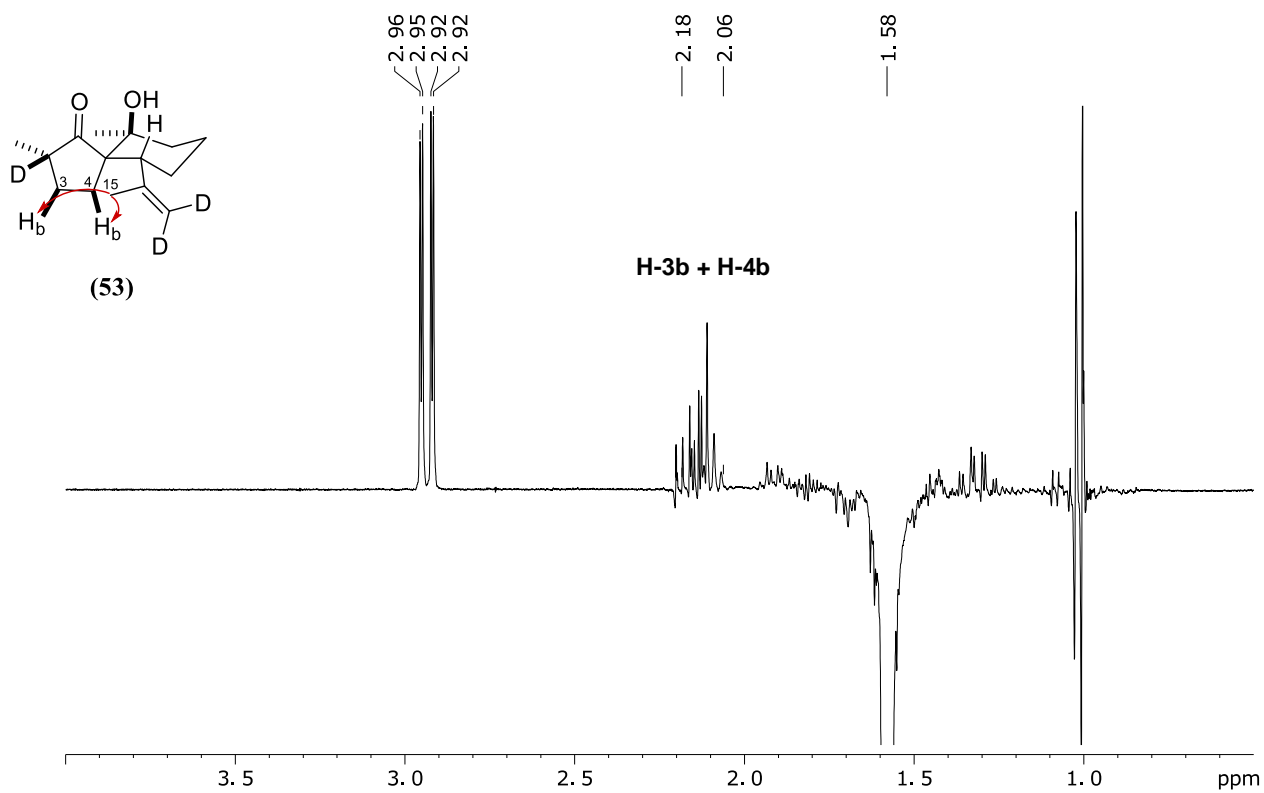
Integrated ¹H spectrum for determination of the ratio between the two obtained isomers **(53)** and **(53')**. The clearly distinguishable olefinic signals of **(53')** are marked. The aliphatic signals were used as reference for the determination, since their integrals showed the greatest consistency. The ratio **(53)**:**(53')** = 88:12, was determined based on the assumption, that multiplet at 1.87–1.78 ppm (1H) corresponds to the H-8 signals of both isomers (hence, 100% reference). Spectrum measured in CDCl₃ at 600 MHz.



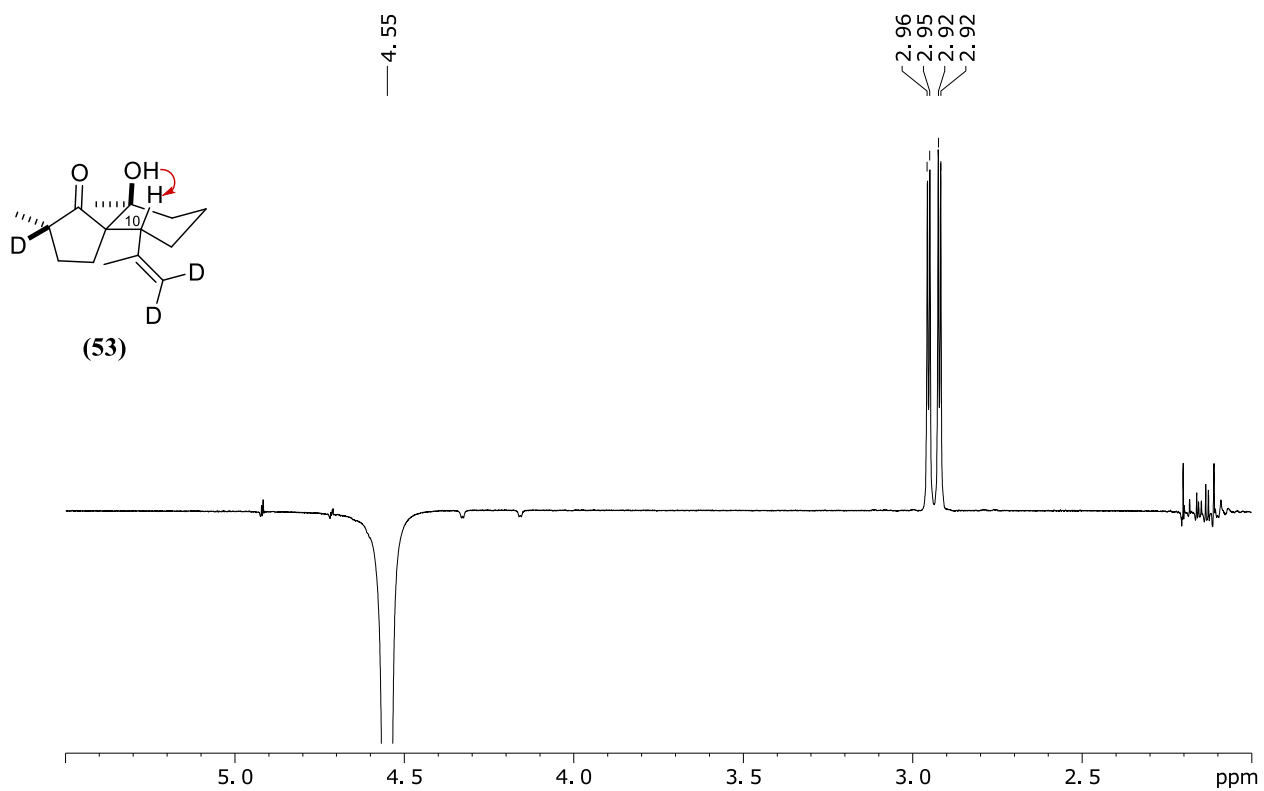
NOE response of (53) after irradiation at 1.01 ppm (CH₃-14). Spectrum measured in CDCl₃ at 400 MHz.



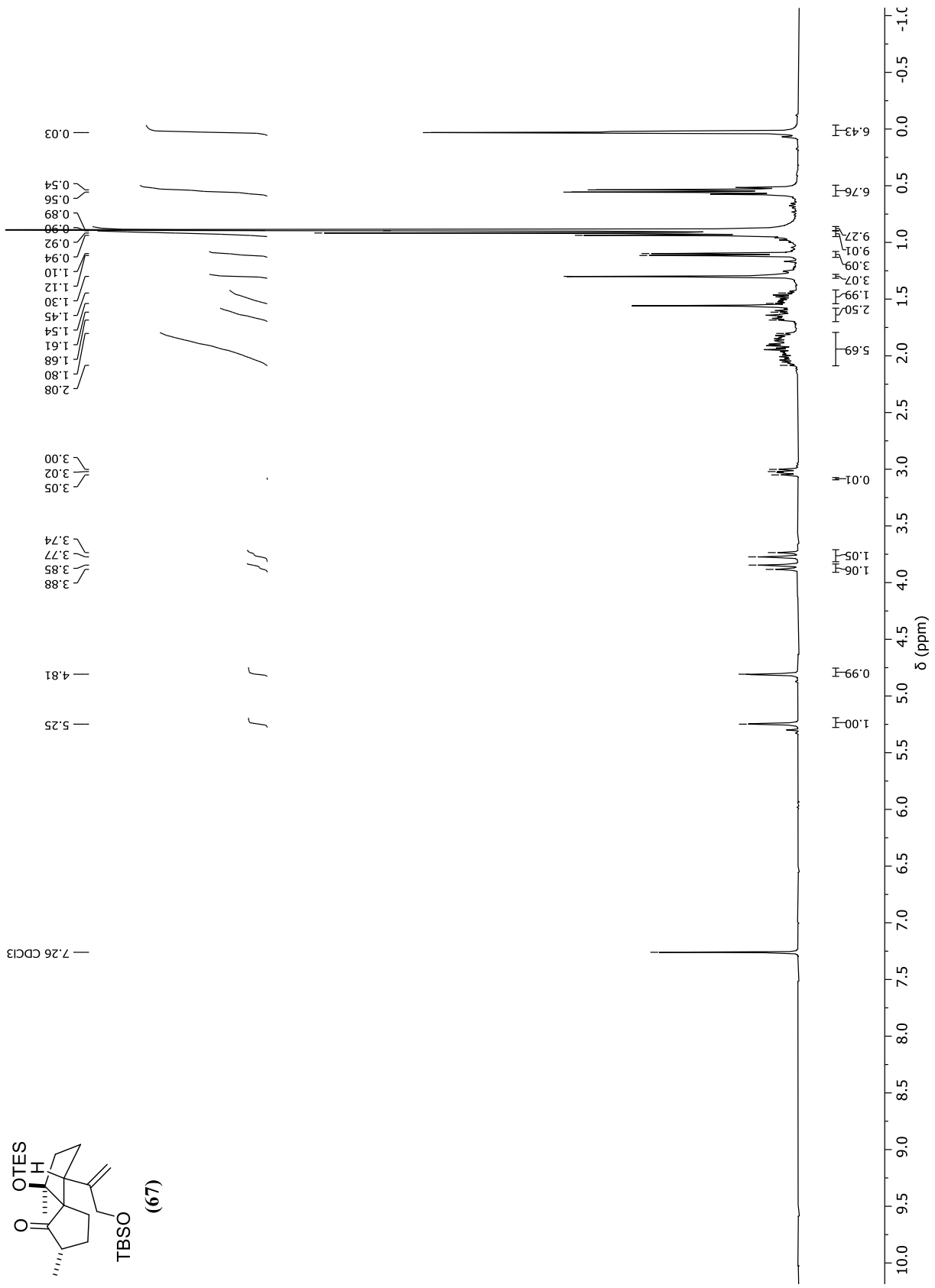
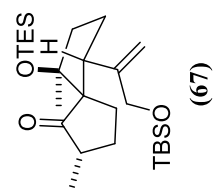
NOE response of (53) after irradiation at 1.03 ppm (CH₃-13). Spectrum measured in CDCl₃ at 400 MHz.

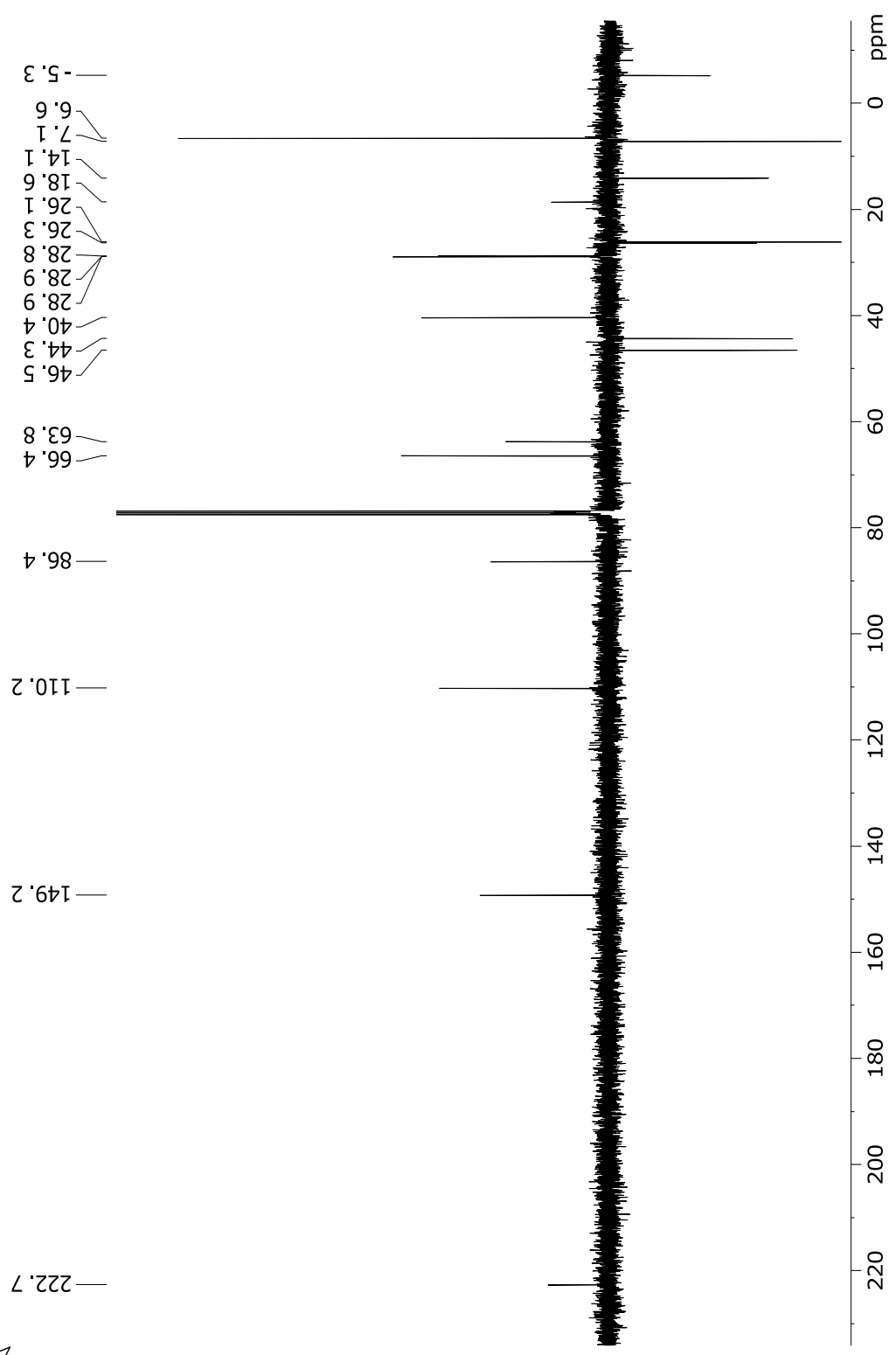
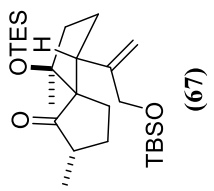


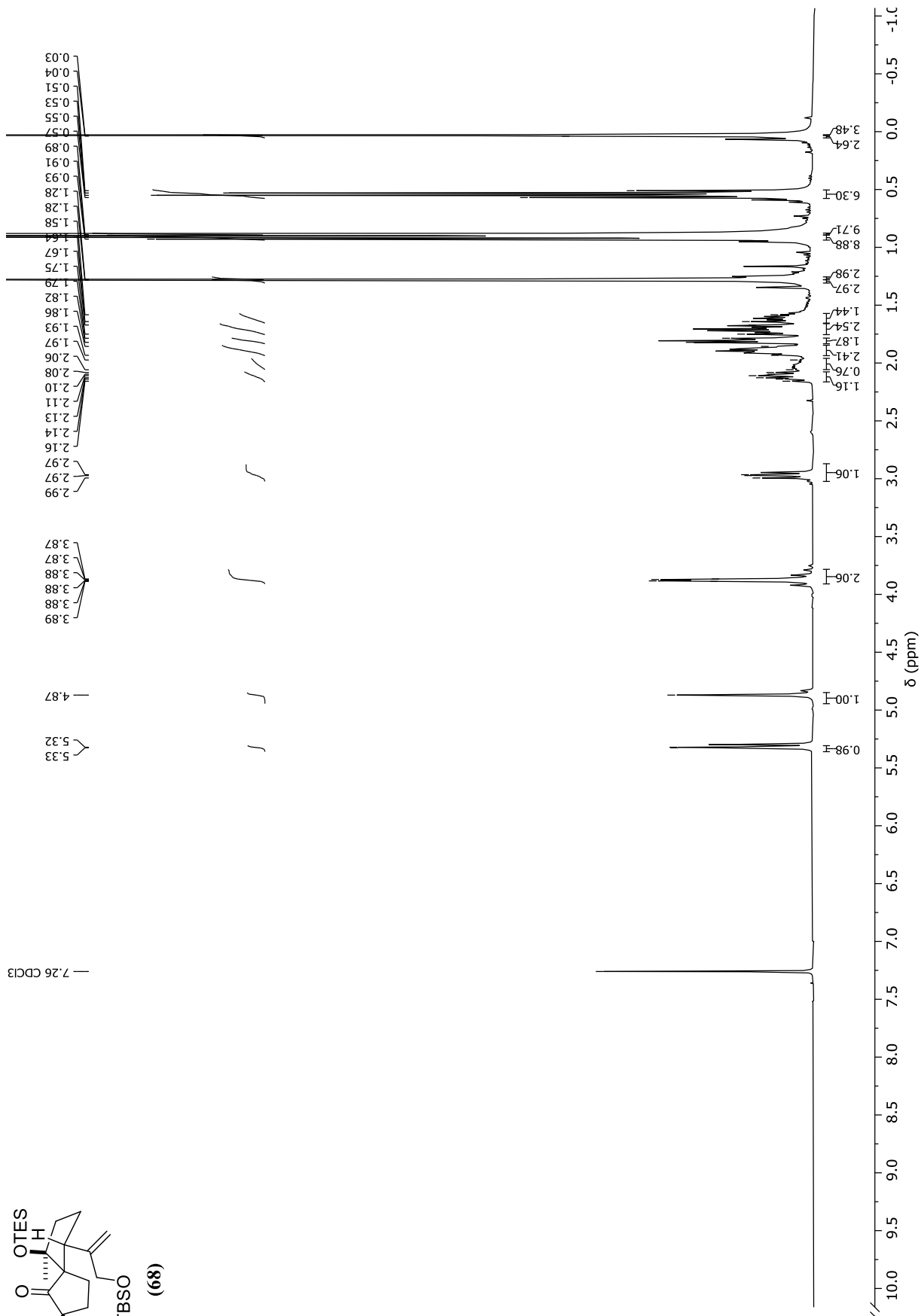
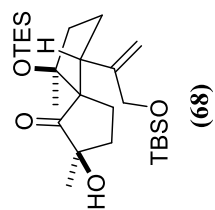
NOE response of (53) after irradiation at 1.58 ppm (CH_3 -15). Spectrum measured in CDCl_3 at 400 MHz.

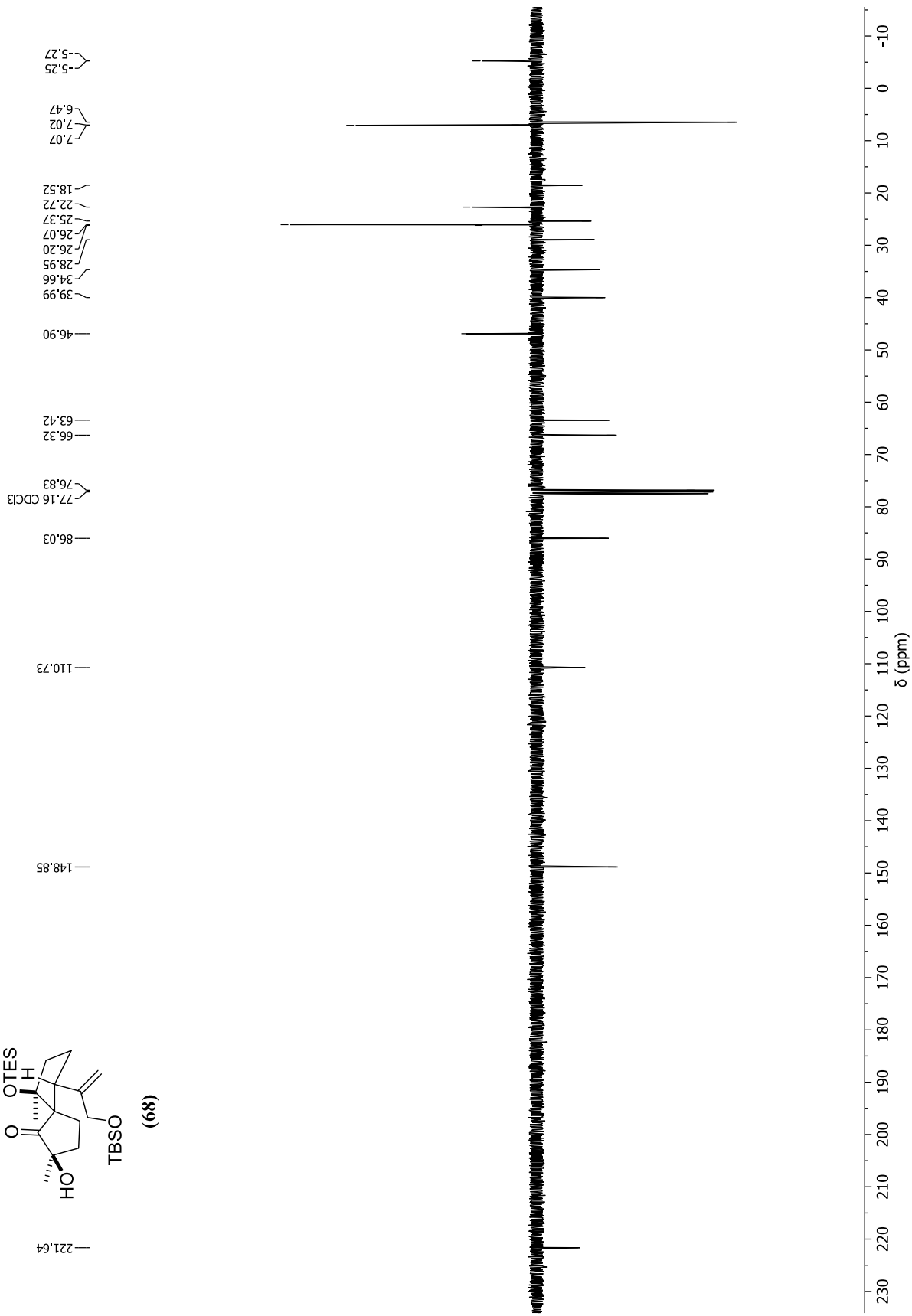
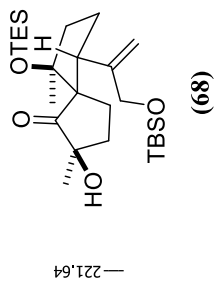


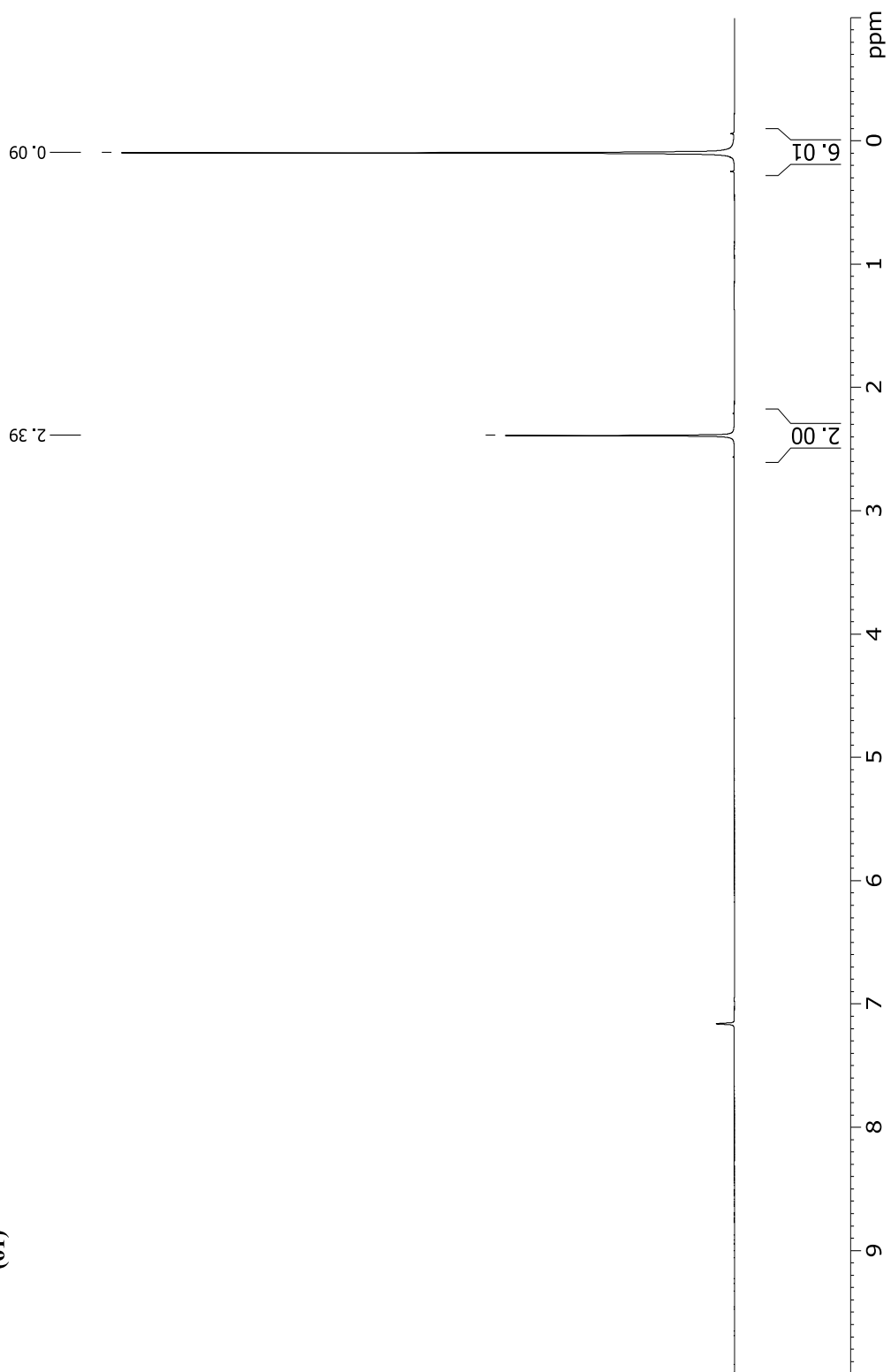
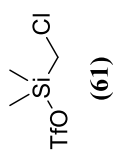
NOE response of (53) after irradiation at 4.55 ppm (OH). Spectrum measured in CDCl_3 at 400 MHz.

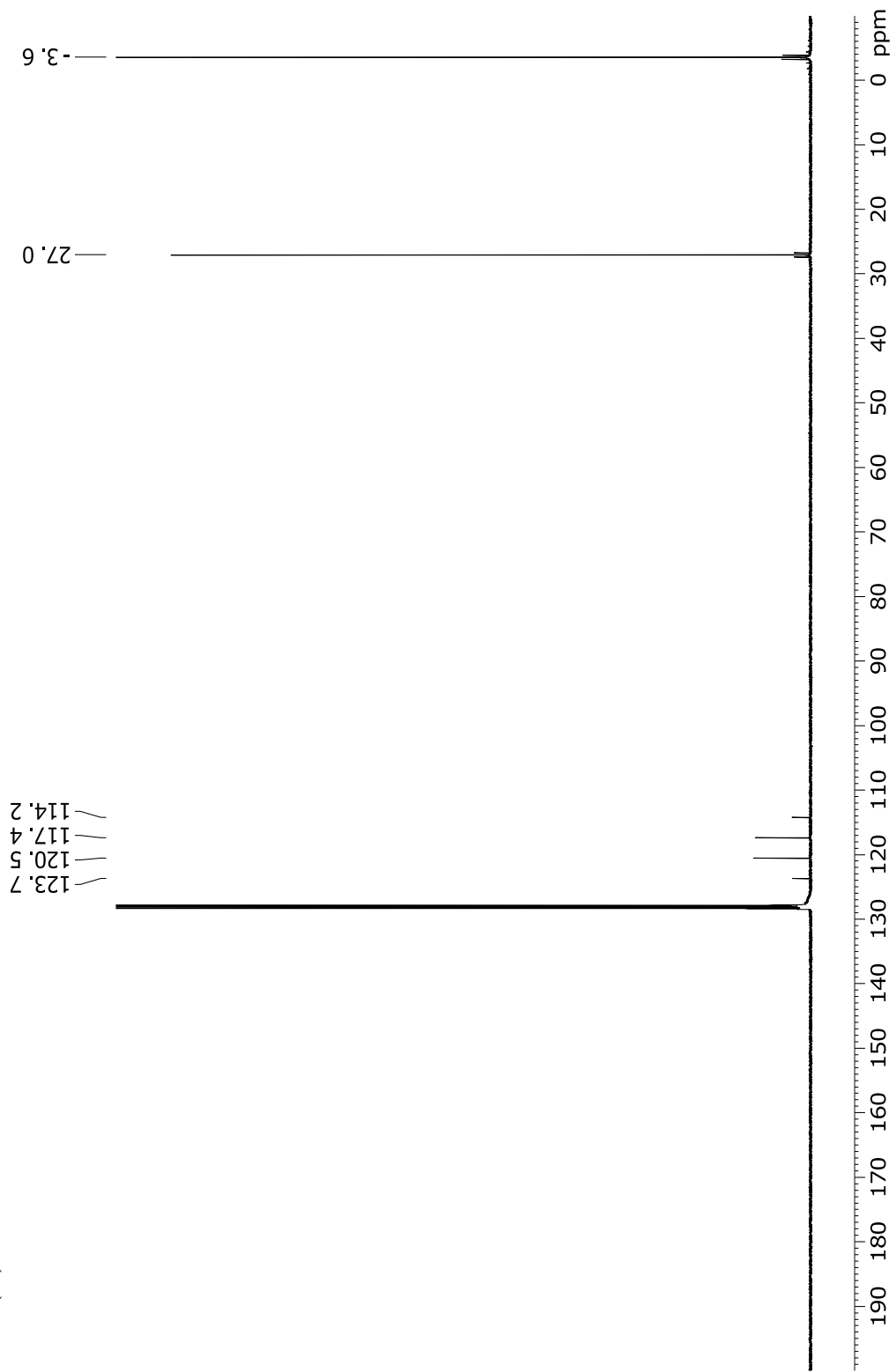
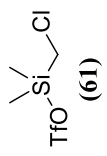


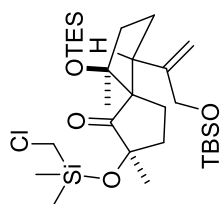




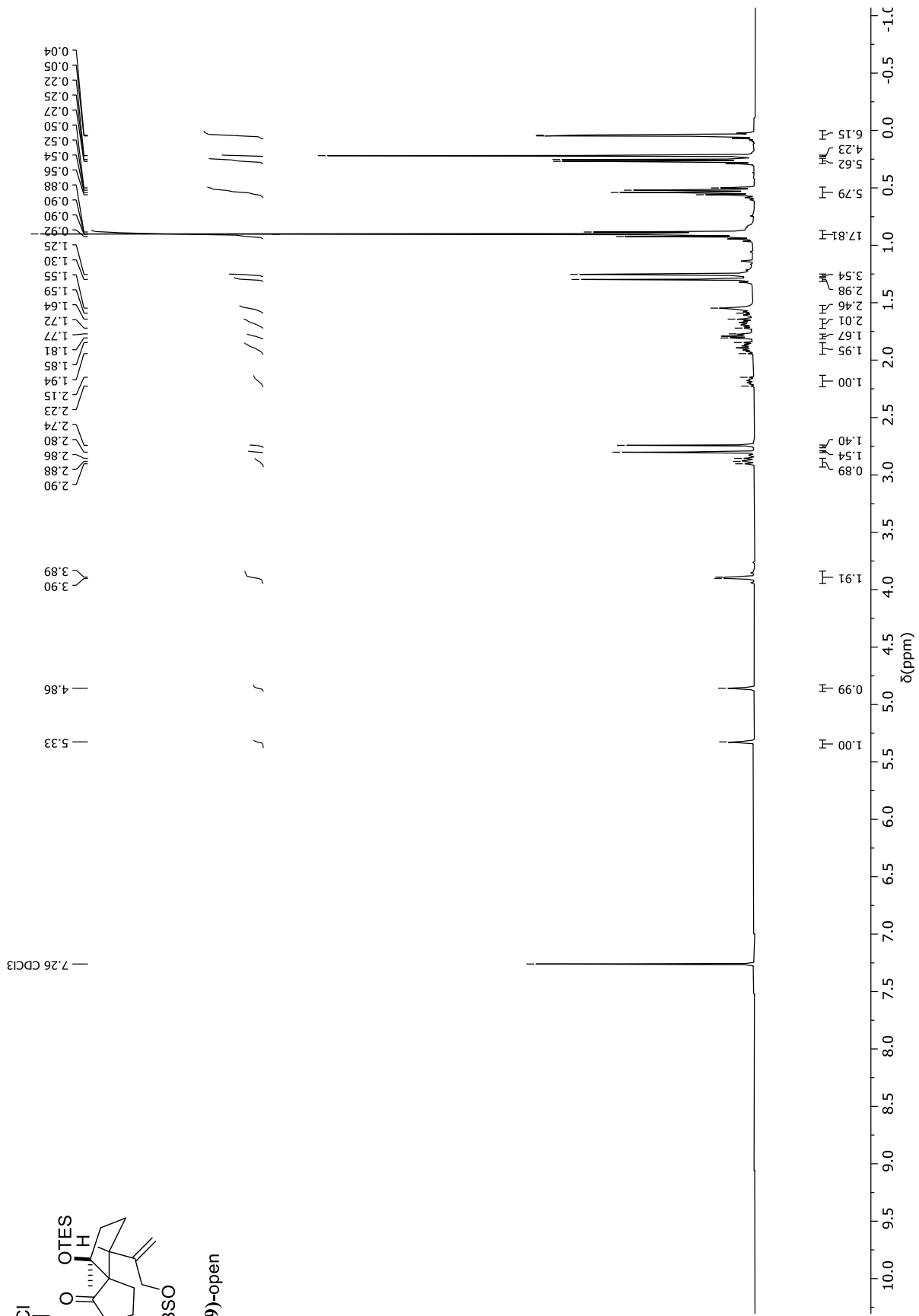


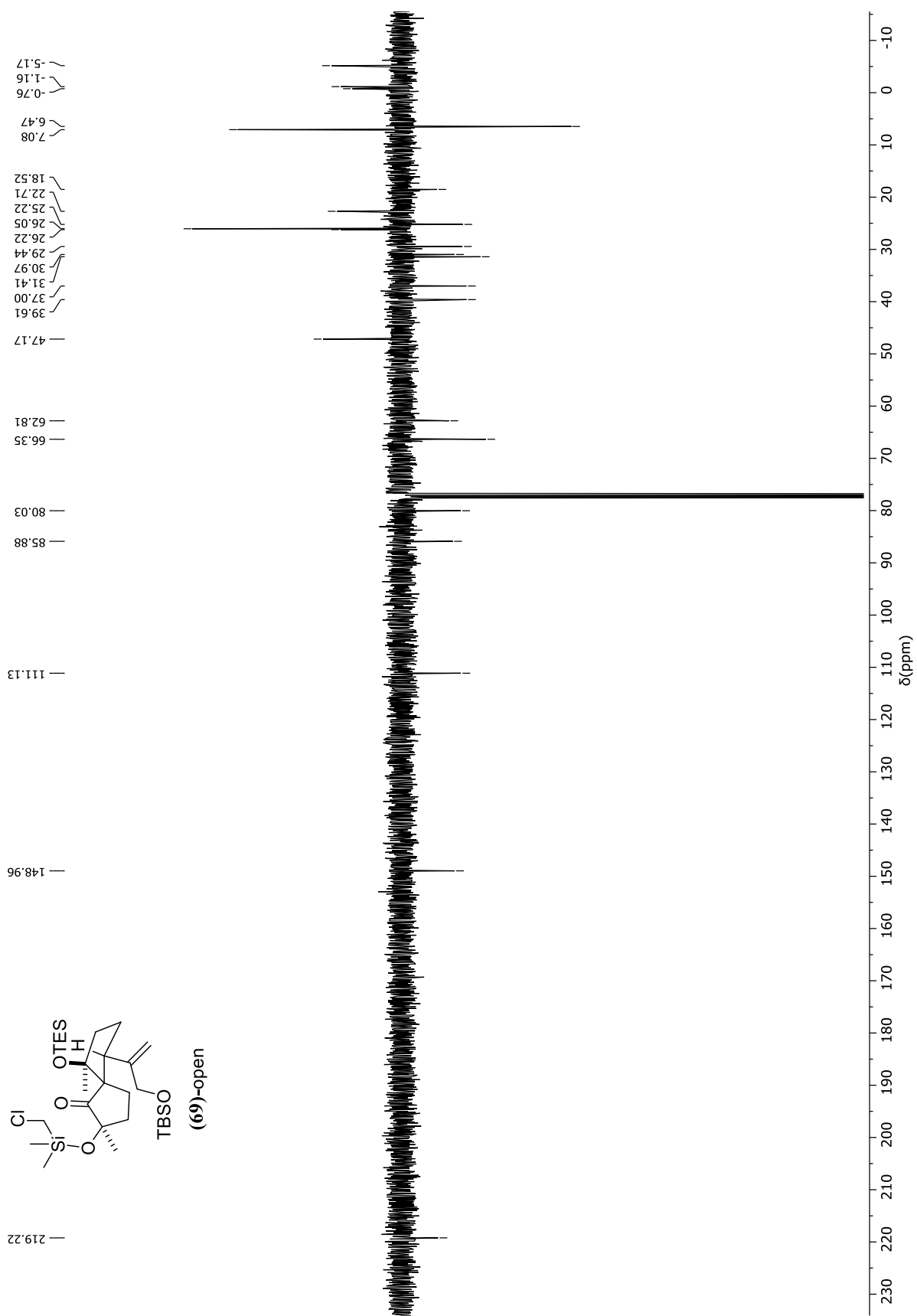
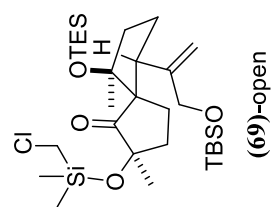


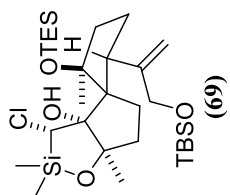




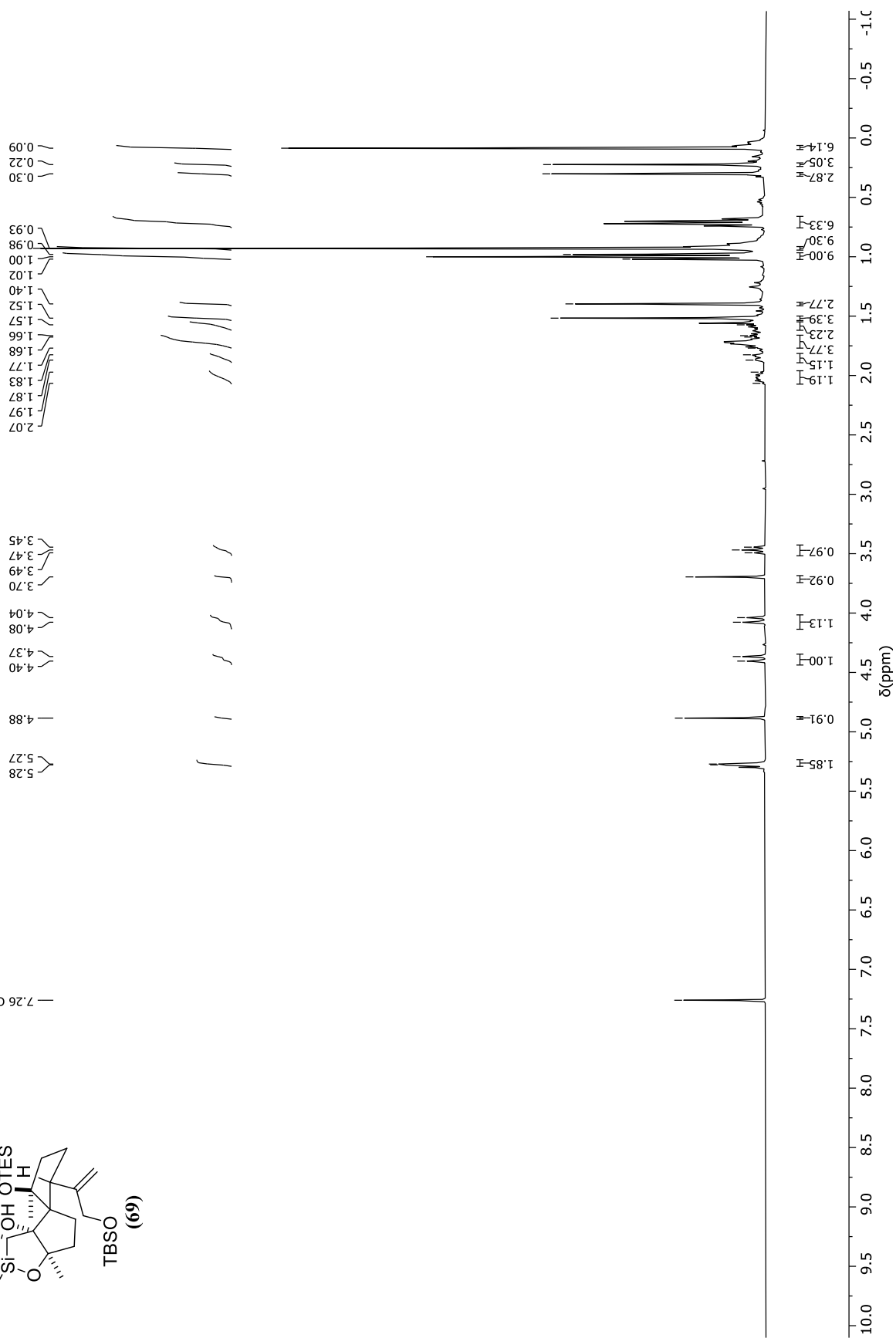
(69)-open

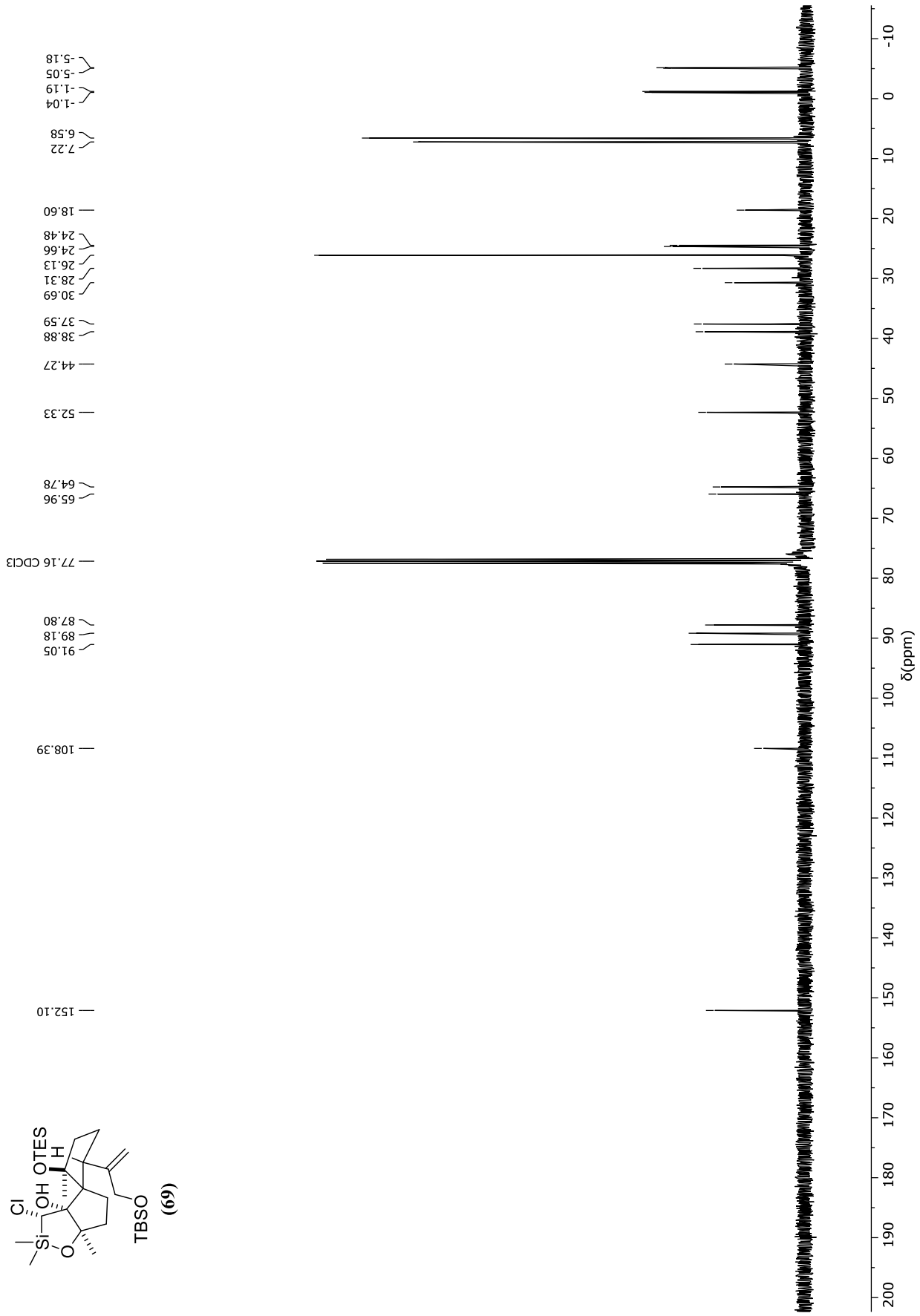
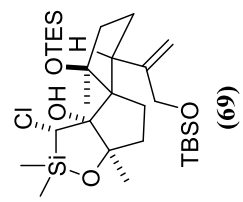


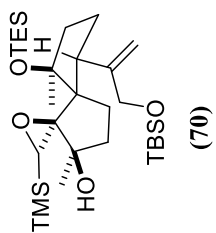




— 7.26 CDCl₃



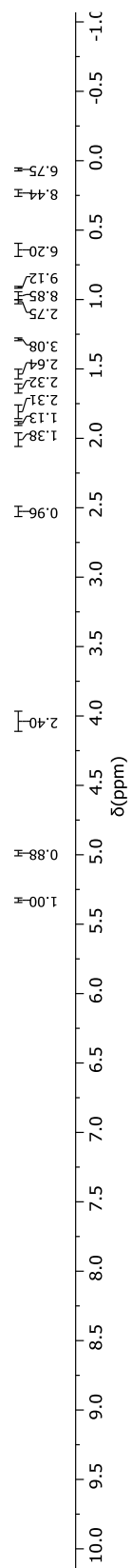


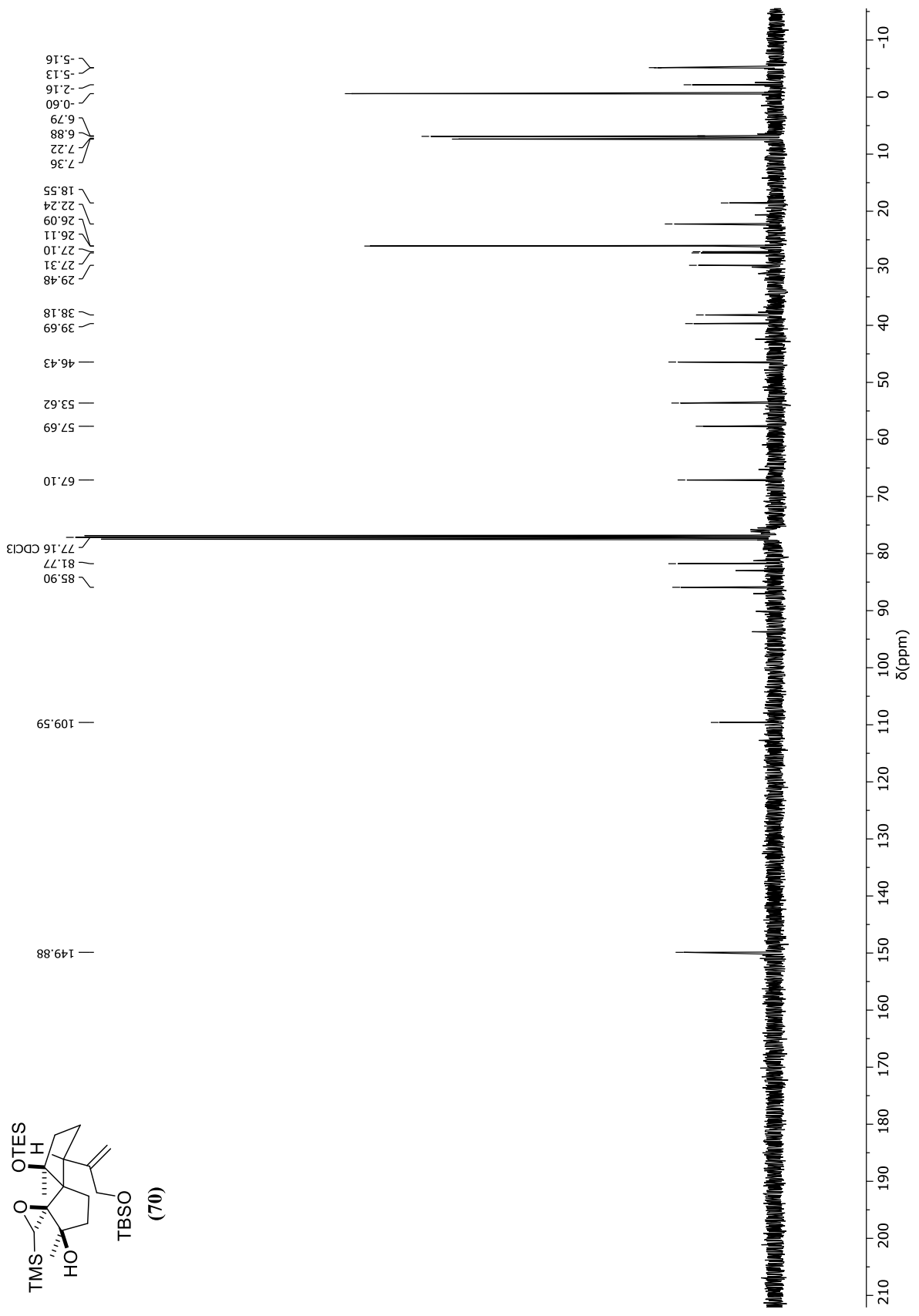
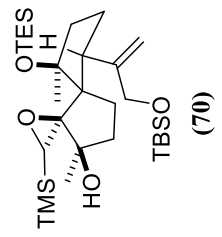


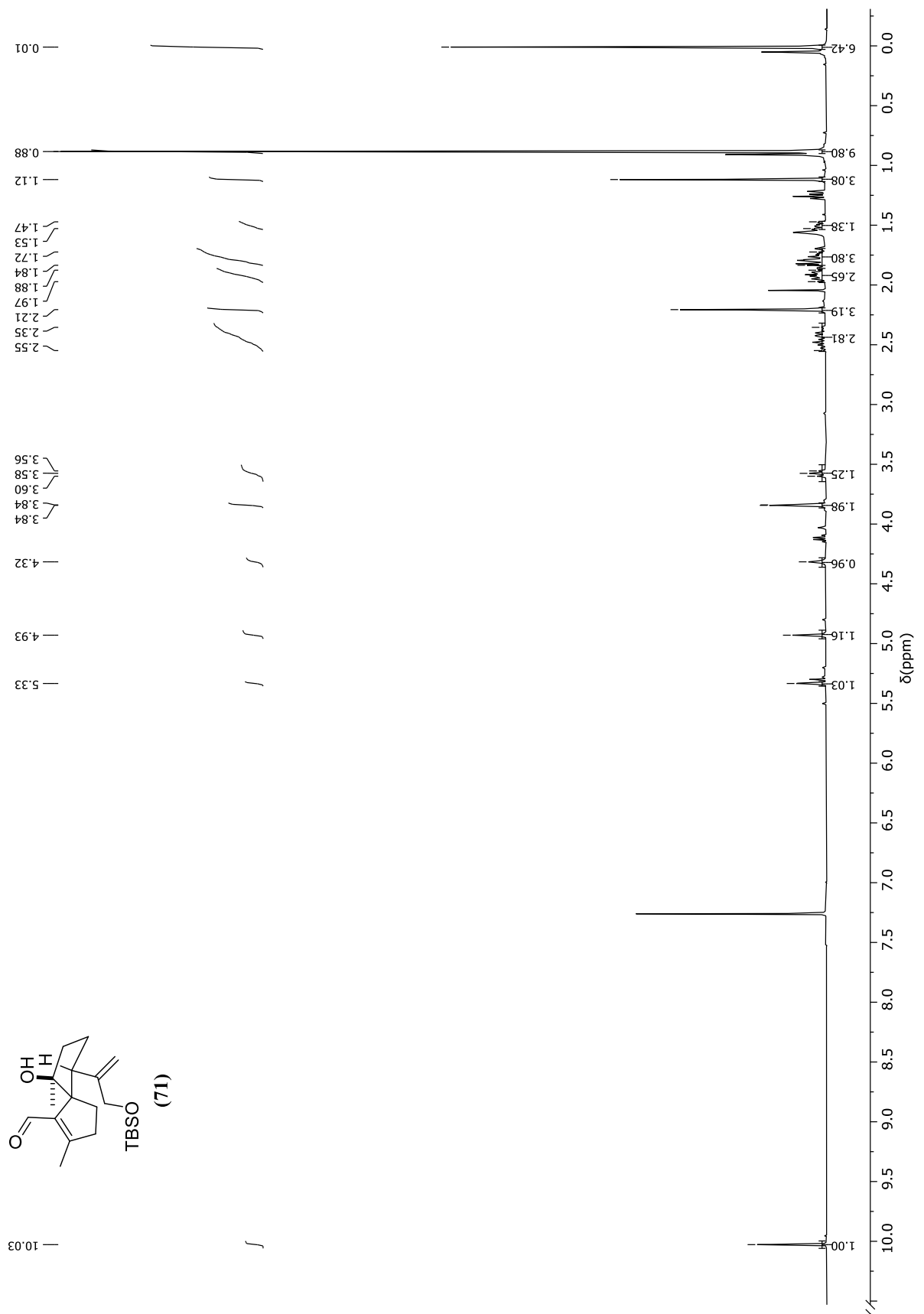
— 7.26 CDCl₃

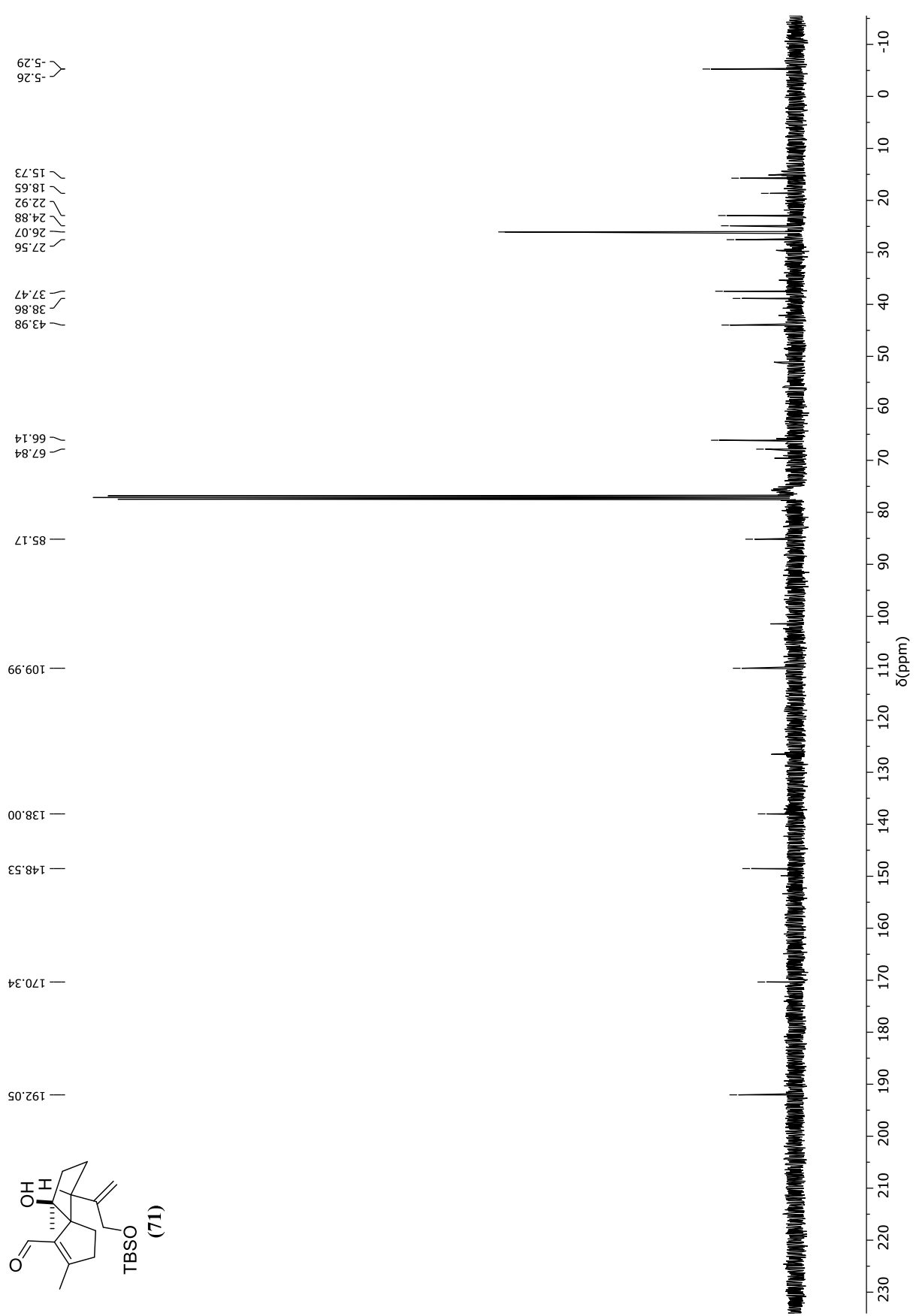
2.55
 2.52
 2.50
 2.05
 1.97
 1.90
 1.85
 1.78
 1.67
 1.62
 1.55
 1.51
 1.28
 1.01
 0.99
 0.97
 0.95
 0.91
 0.67
 0.63
 0.61
 0.23
 0.07
 0.06

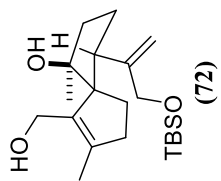
5.33
 5.00
 4.10
 3.98





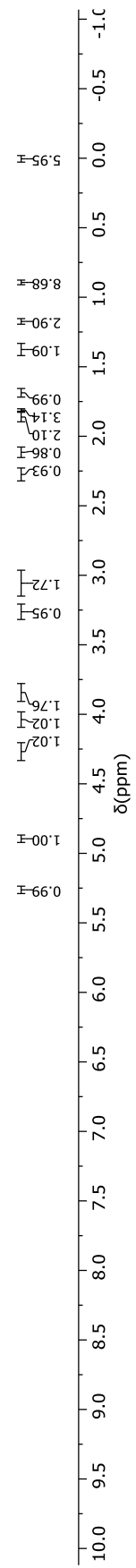


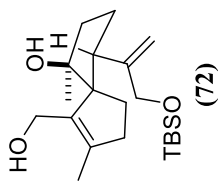




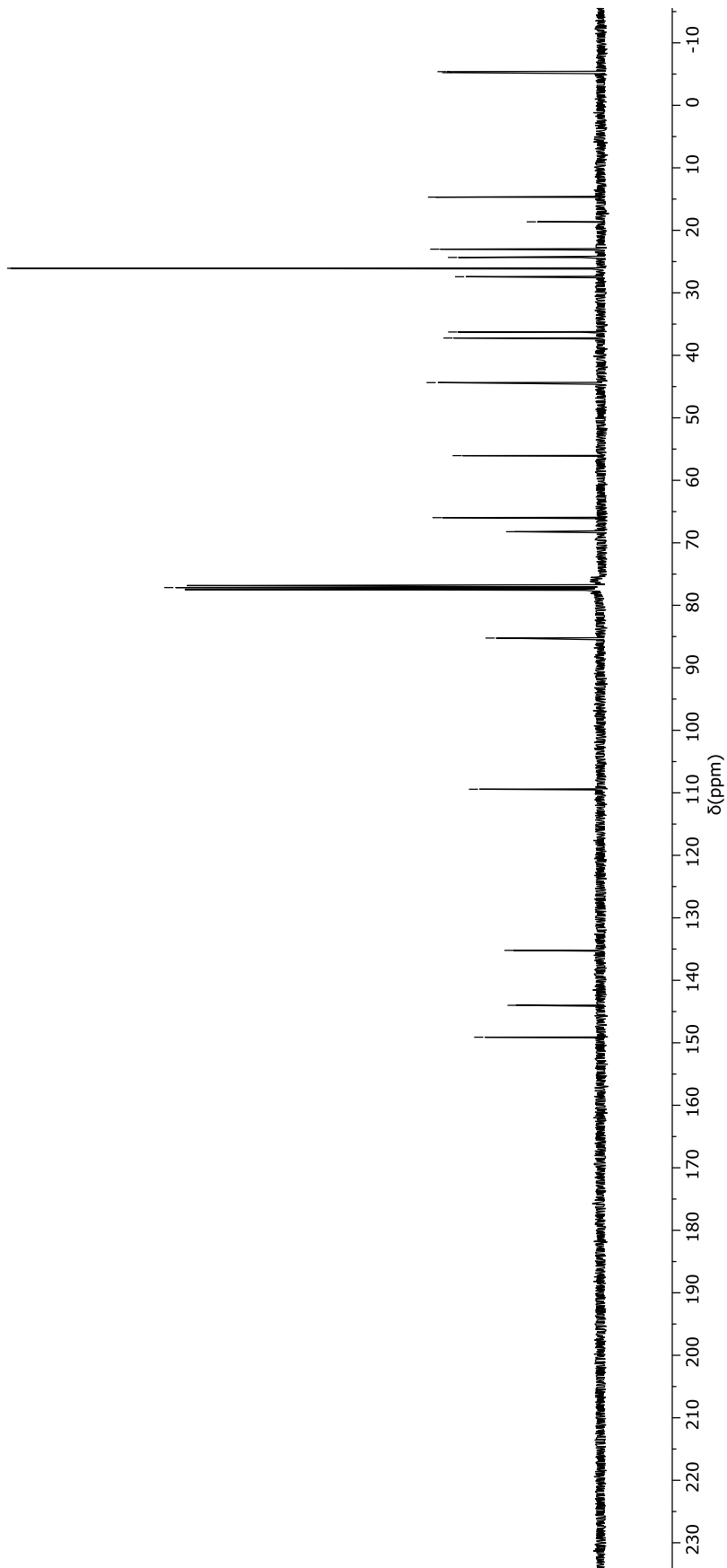
— 7.26 CDCl₃

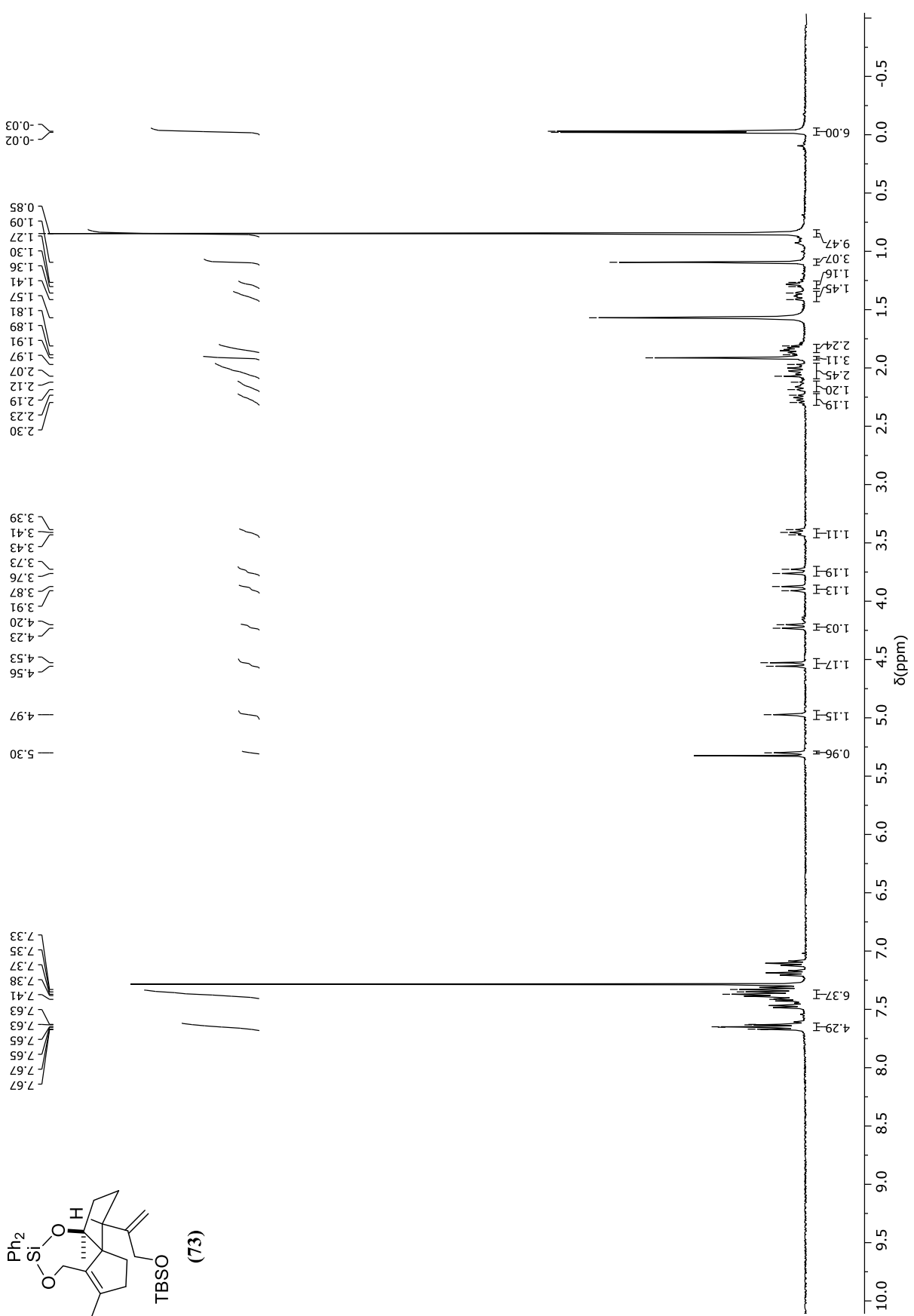
— 5.27
 — 4.90
 4.29
 4.26
 4.03
 4.00
 3.90
 3.86
 3.81
 3.77
 3.26
 3.23
 3.21
 3.06
 2.29
 2.22
 2.13
 2.07
 1.89
 1.84
 1.81
 1.80
 1.76
 1.72
 1.64
 1.40
 1.34
 1.17
 0.88
 0.01

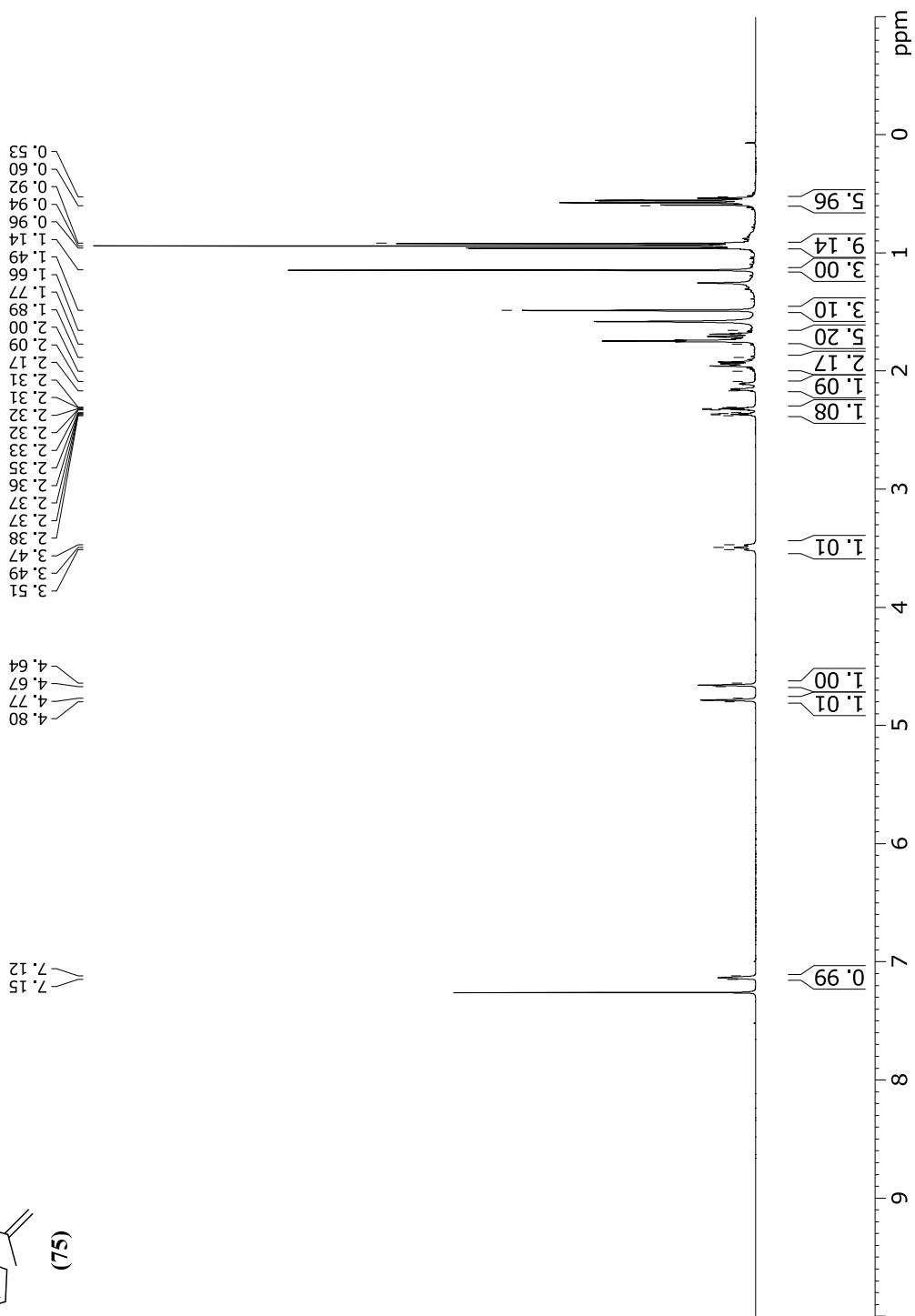
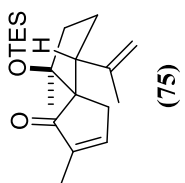


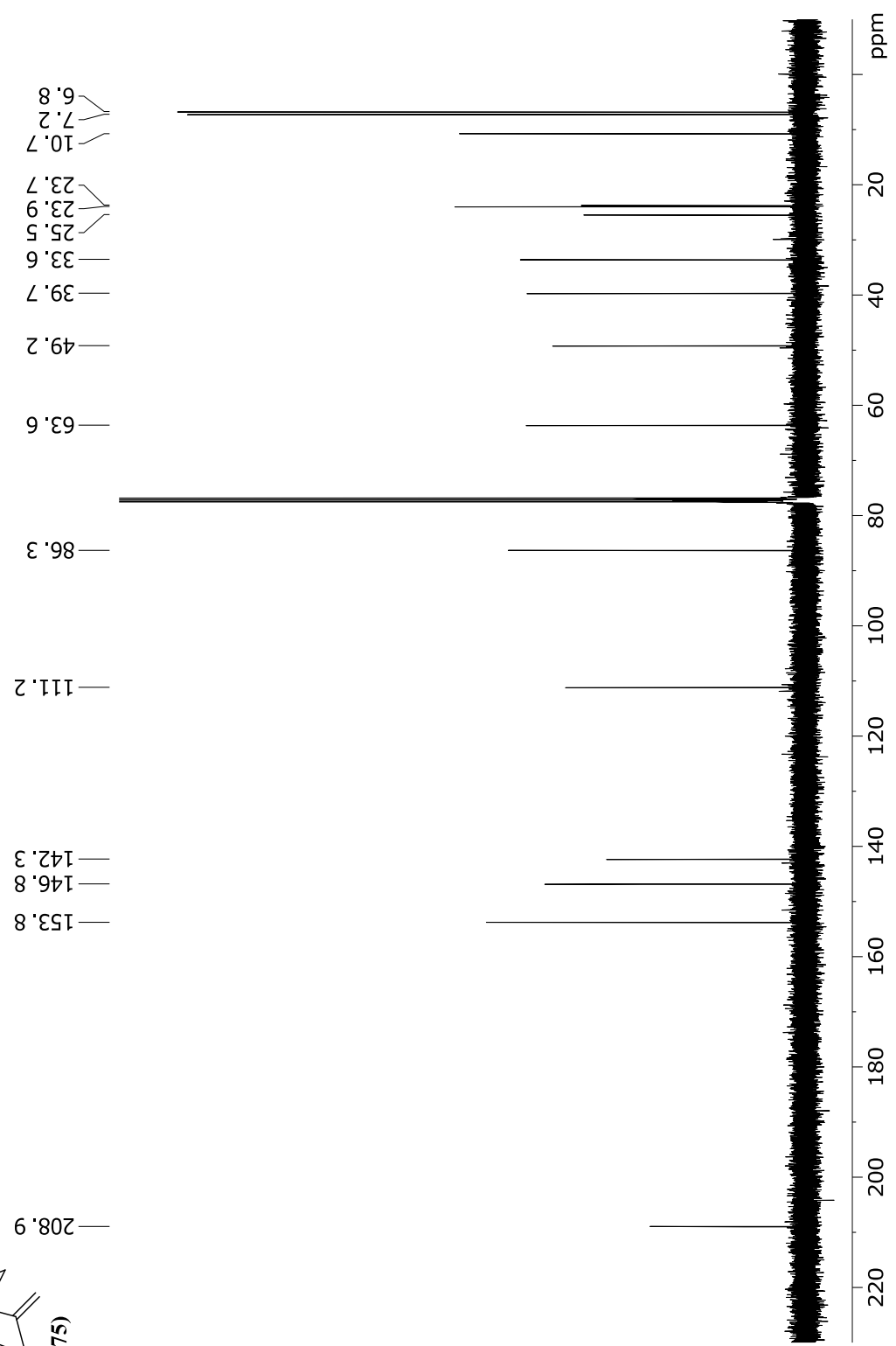
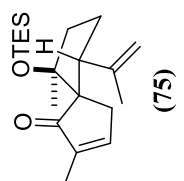


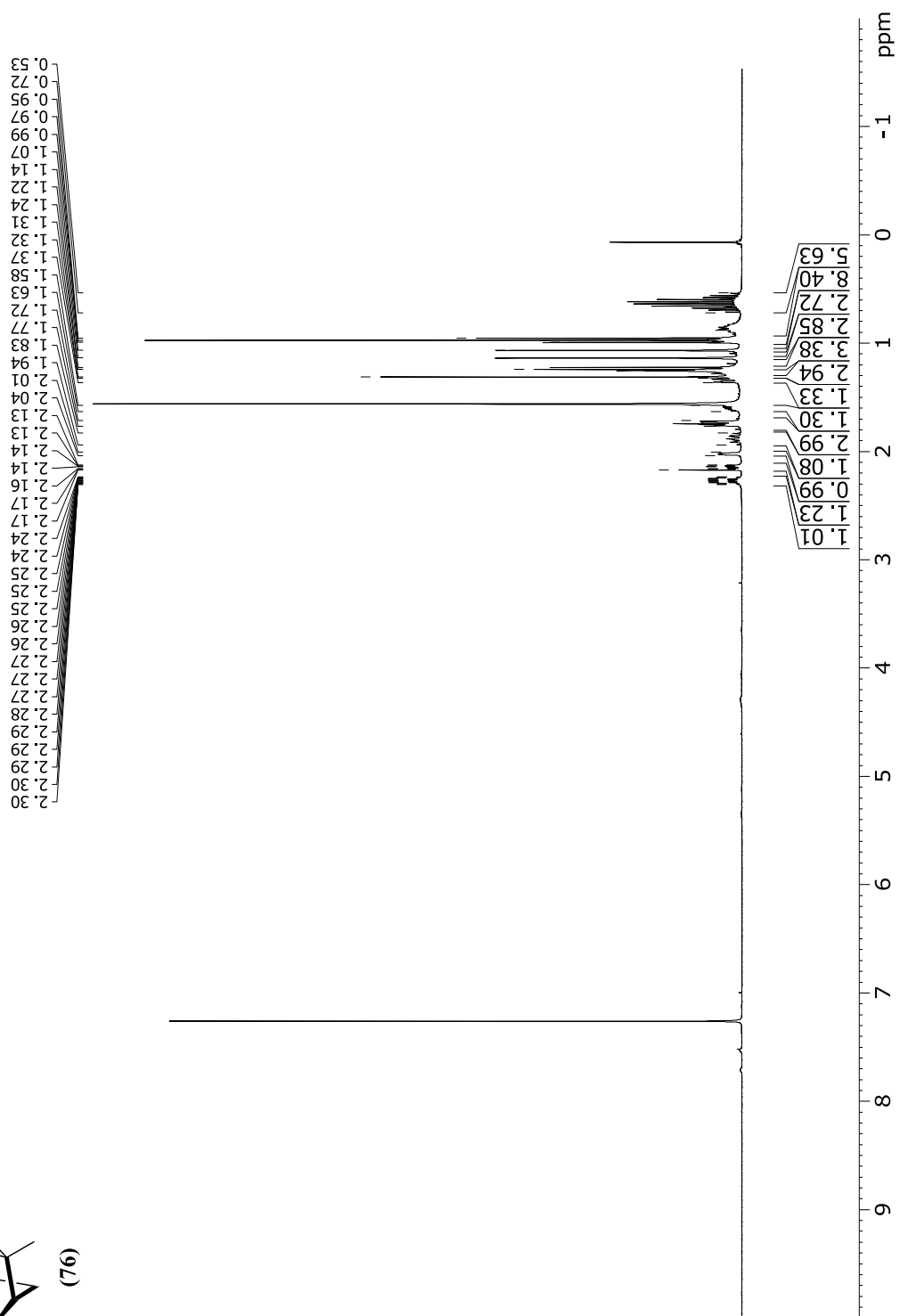
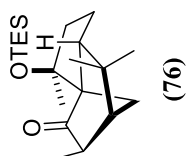
149.10
 144.00
 135.21
 109.43
 85.24
 77.16 CDCl₃
 68.22
 65.97
 56.05
 44.36
 37.23
 36.27
 27.42
 26.07
 24.34
 23.01
 18.64
 14.69
 -5.23
 -5.39

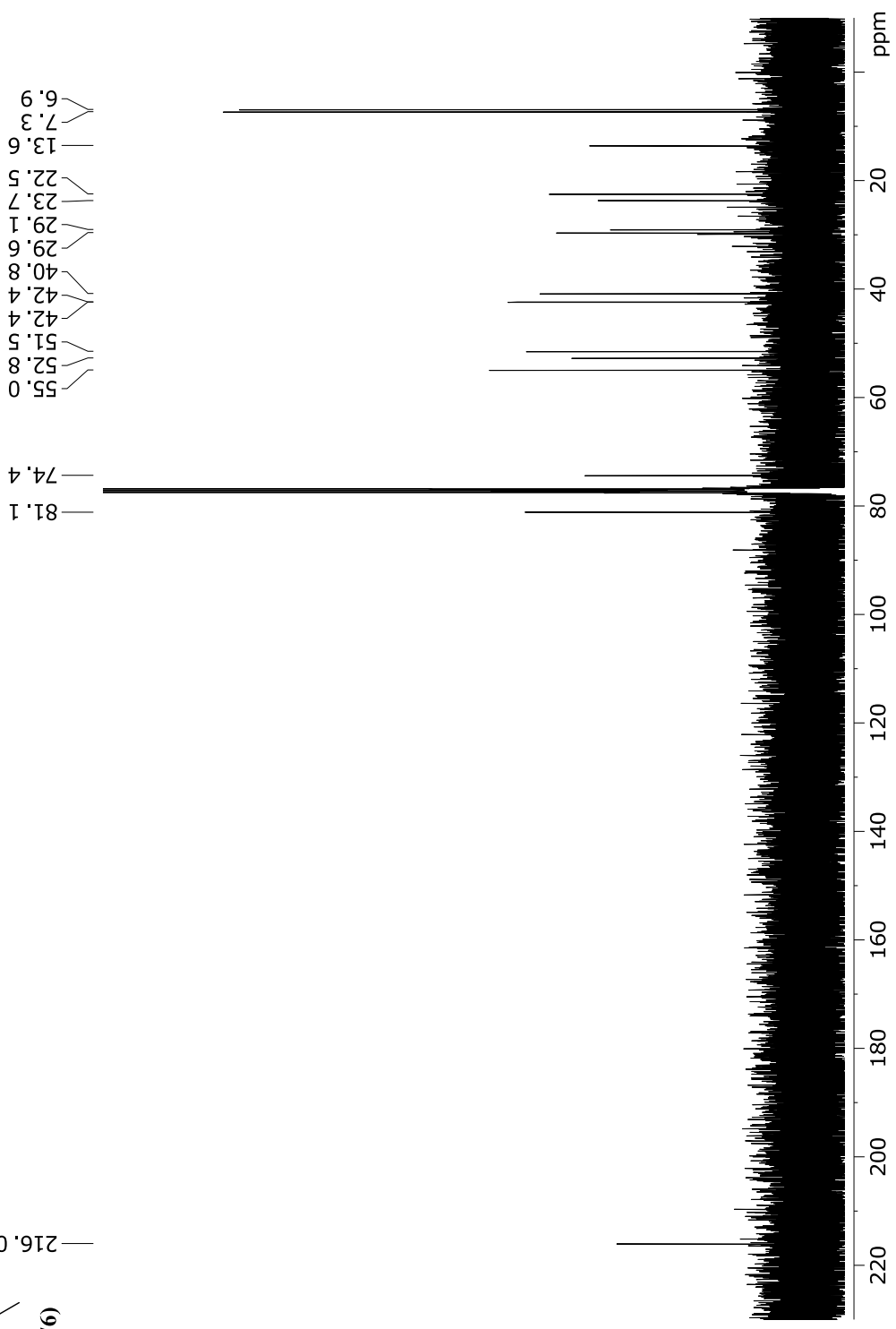
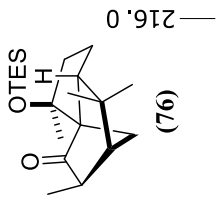


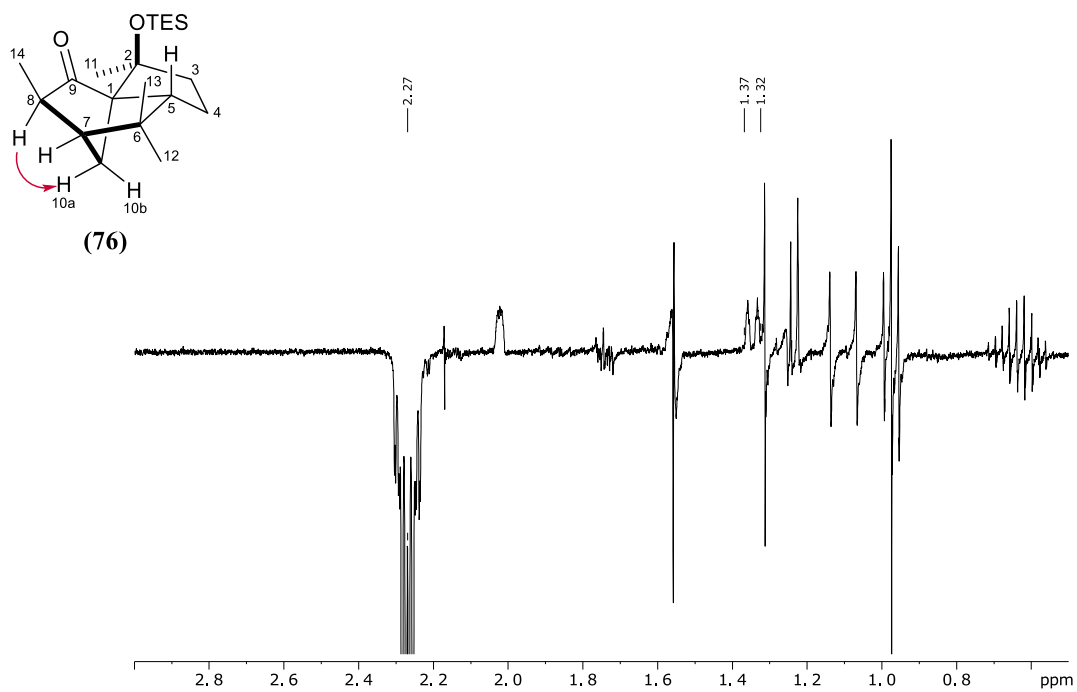




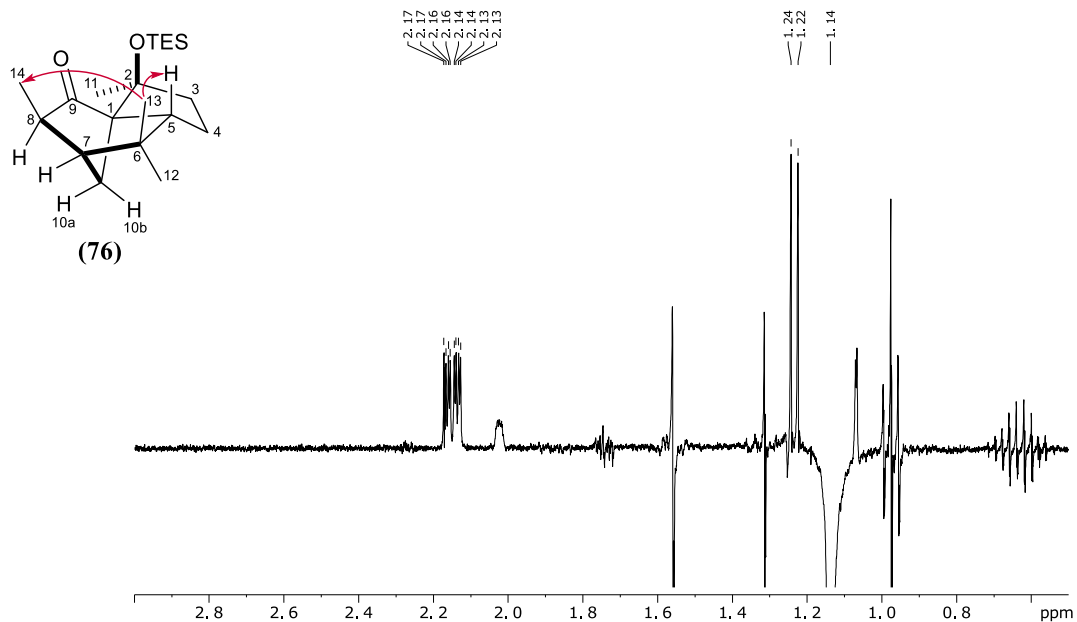




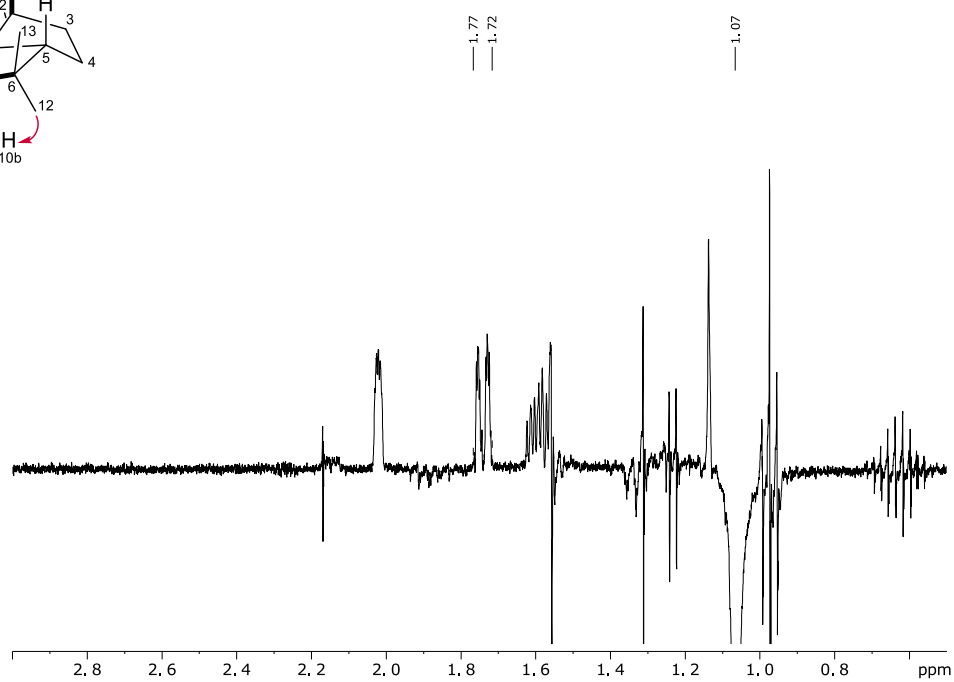
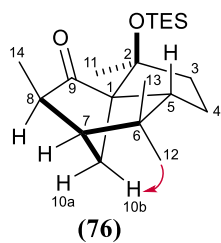




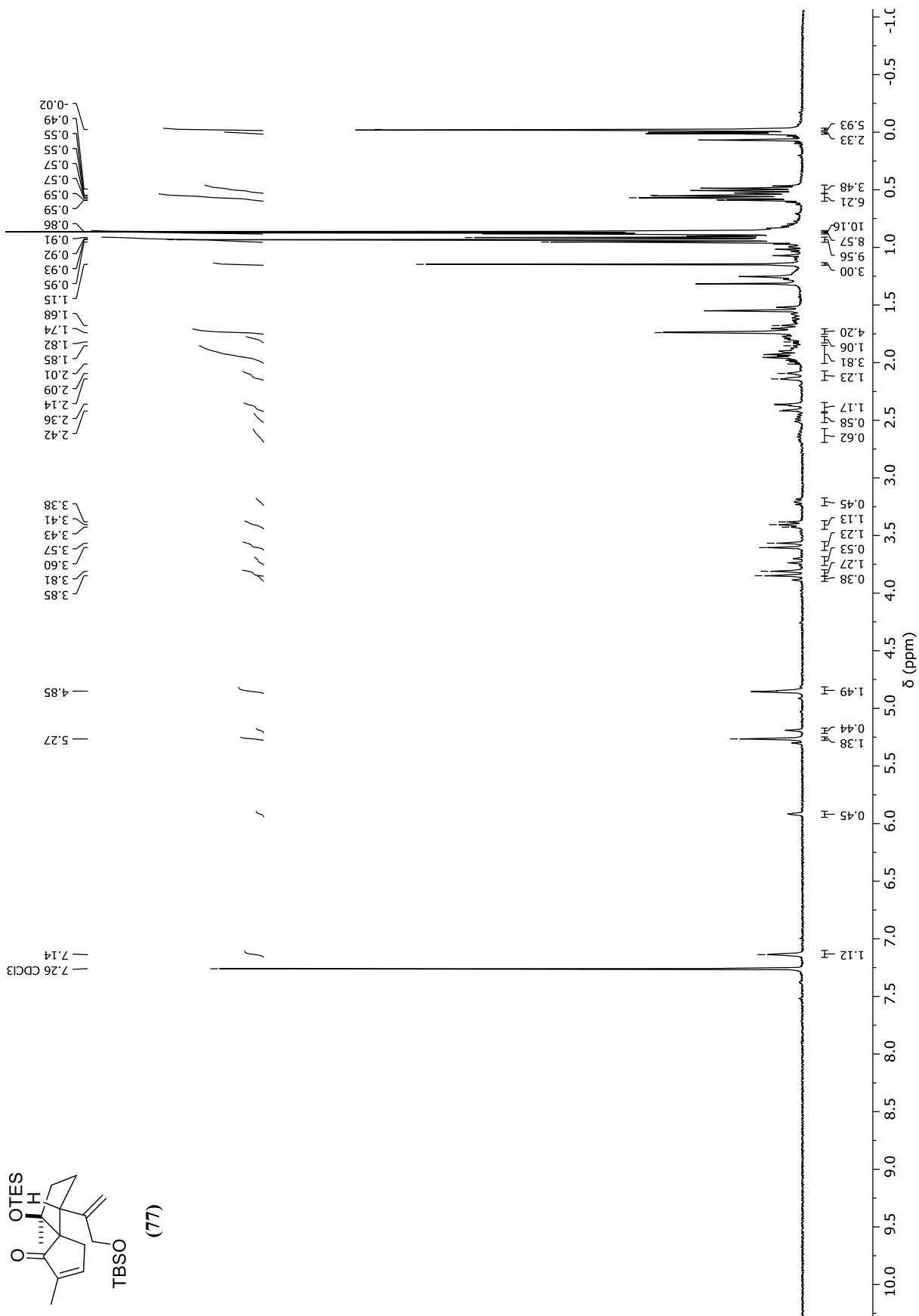
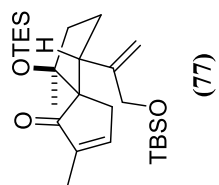
NOE response of tricyclic (76) after irradiation at 2.27 ppm (CH-8), measured in CDCl₃ at 400 MHz.

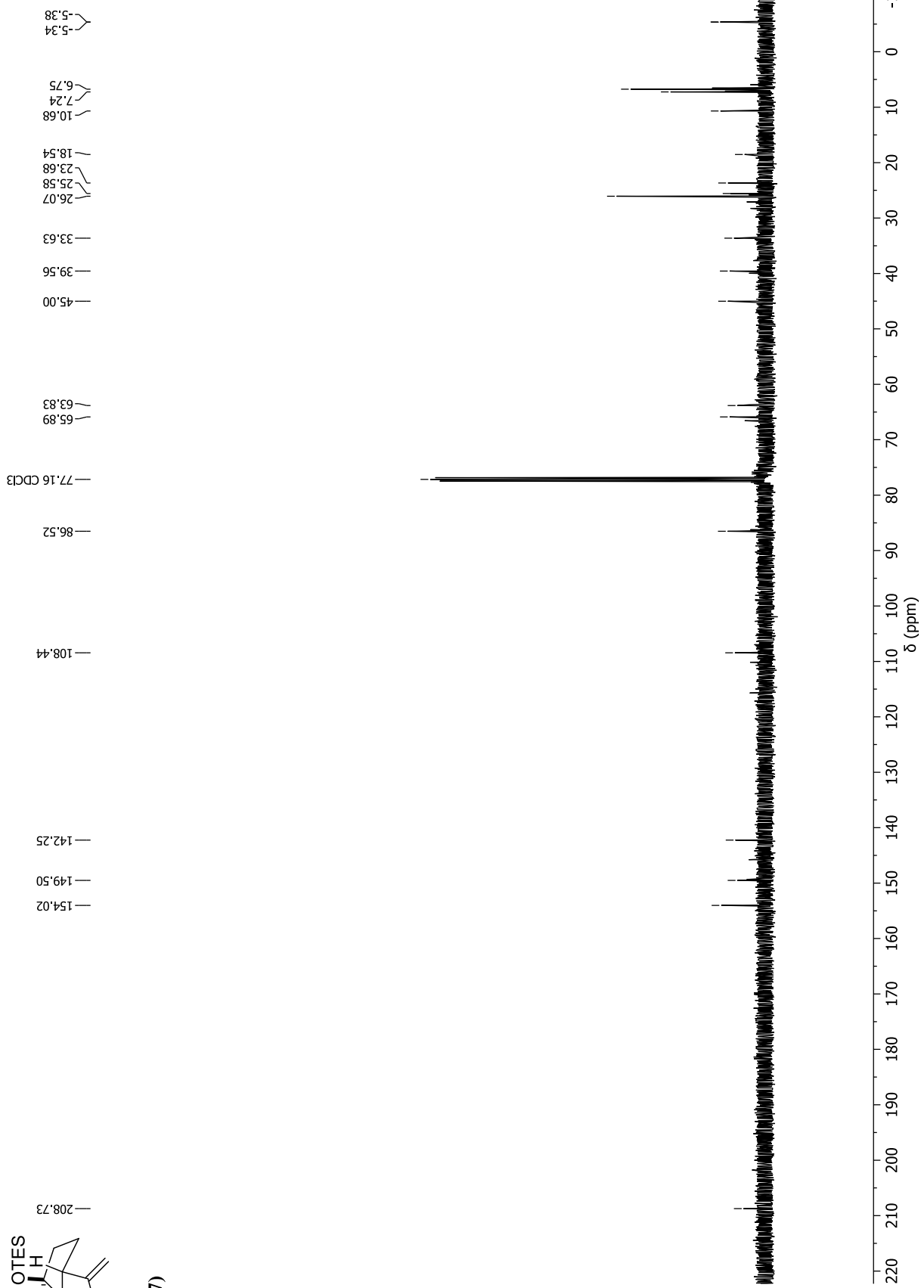
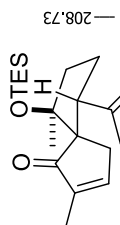


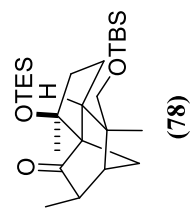
NOE response of tricyclic (76) after irradiation at 1.14 ppm (CH₃-13), measured in CDCl₃ at 400 MHz.



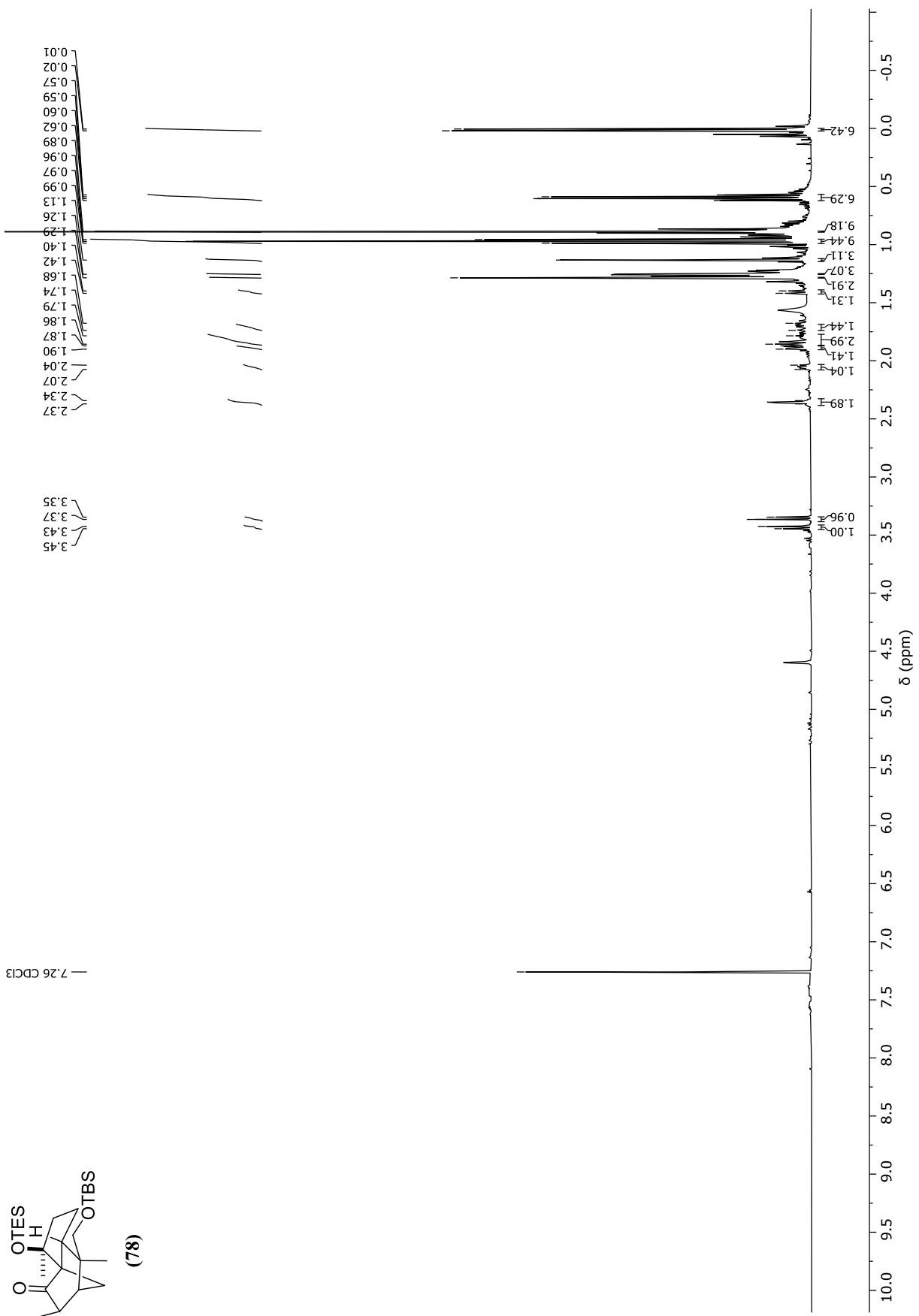
NOE response of tricycle **(76)** after irradiation at 1.07 ppm (CH₃-12), measured in CDCl₃ at 400 MHz.

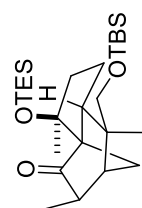




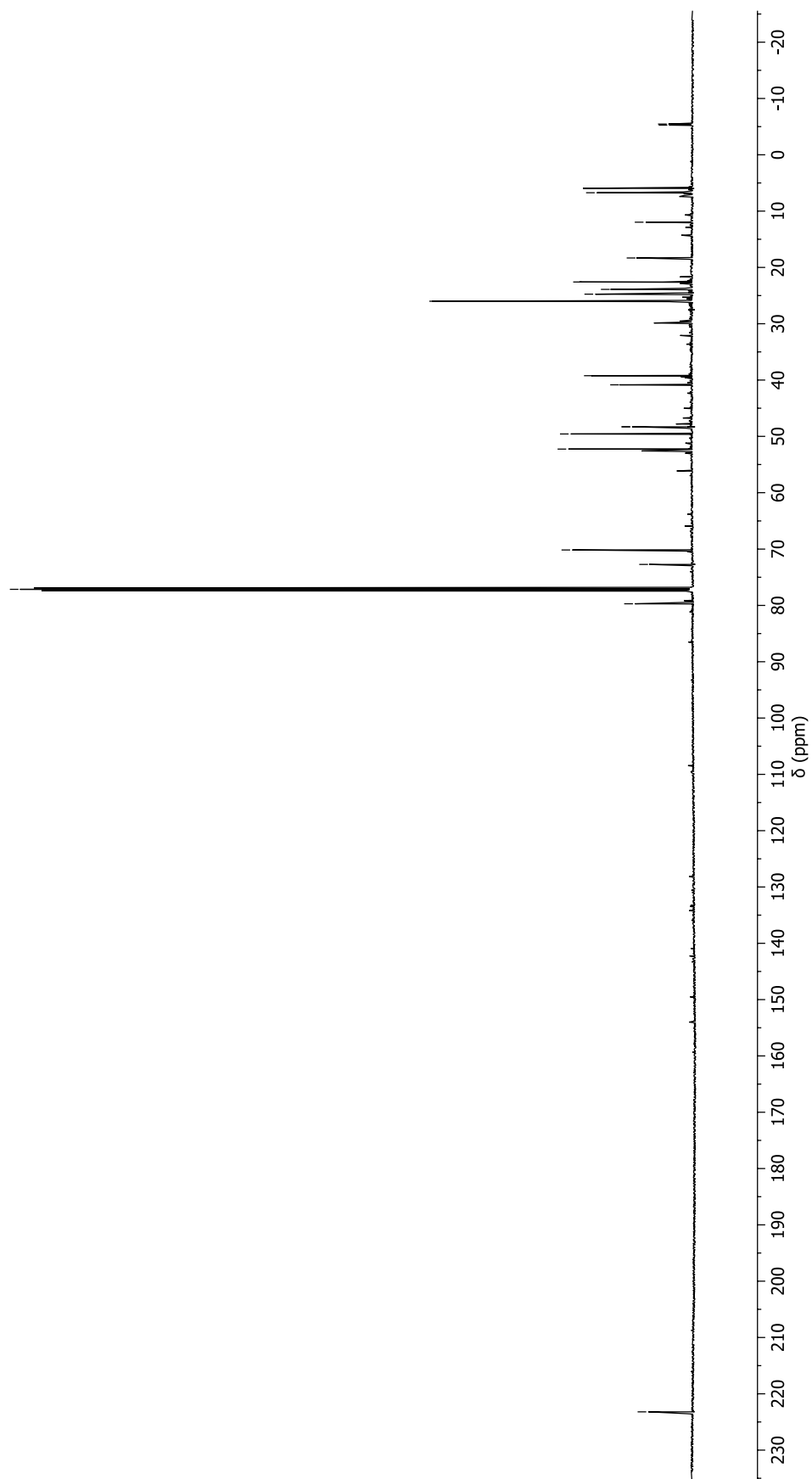
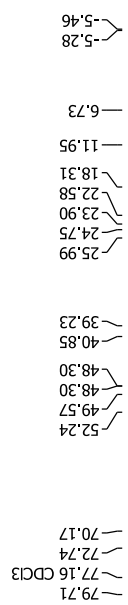


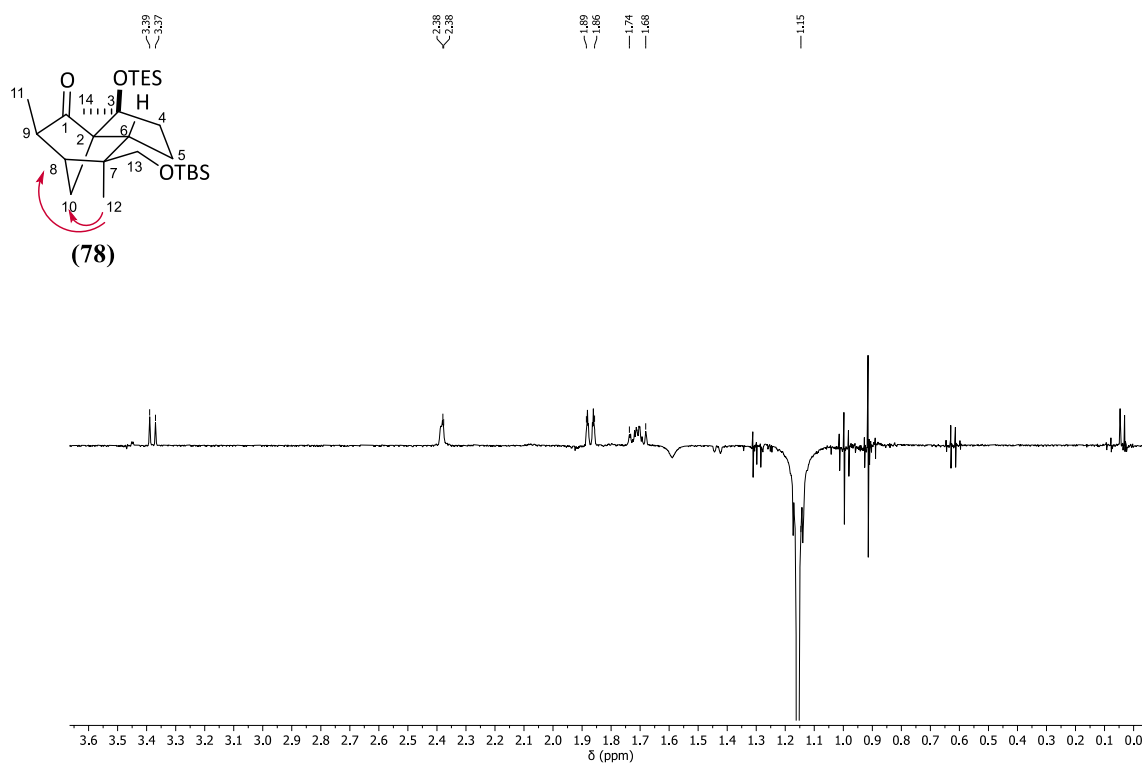
— 7.26 CDCl₃



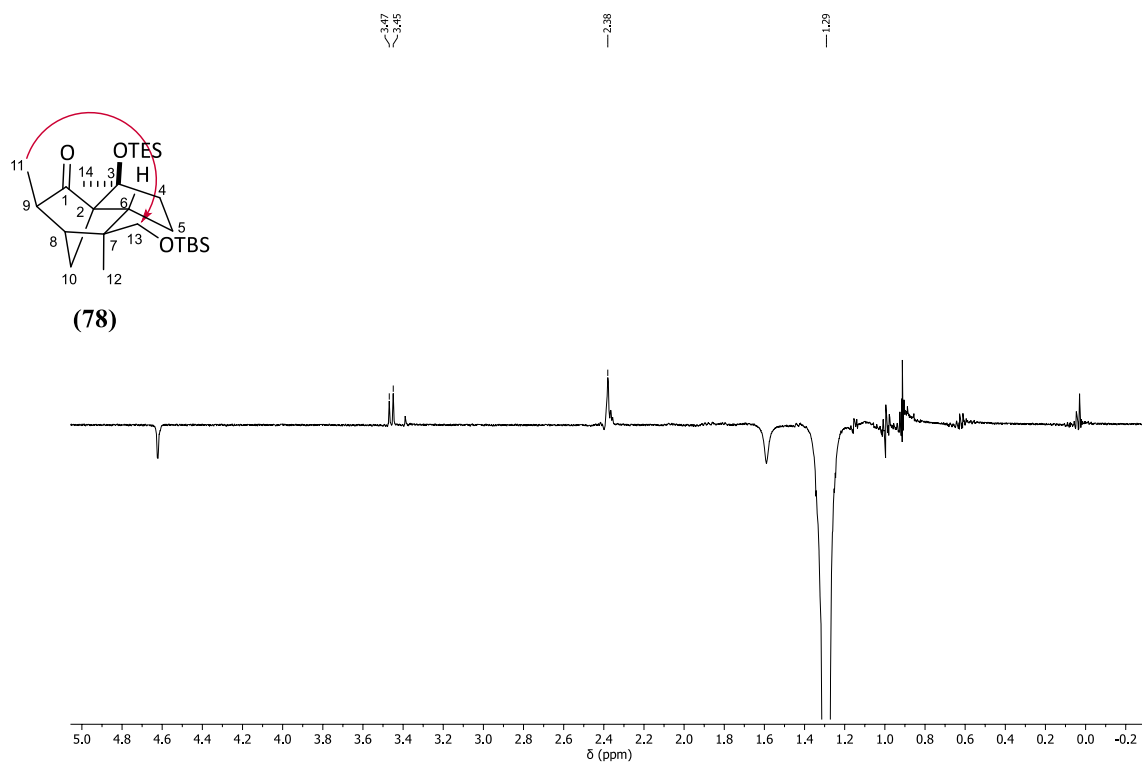


(78)

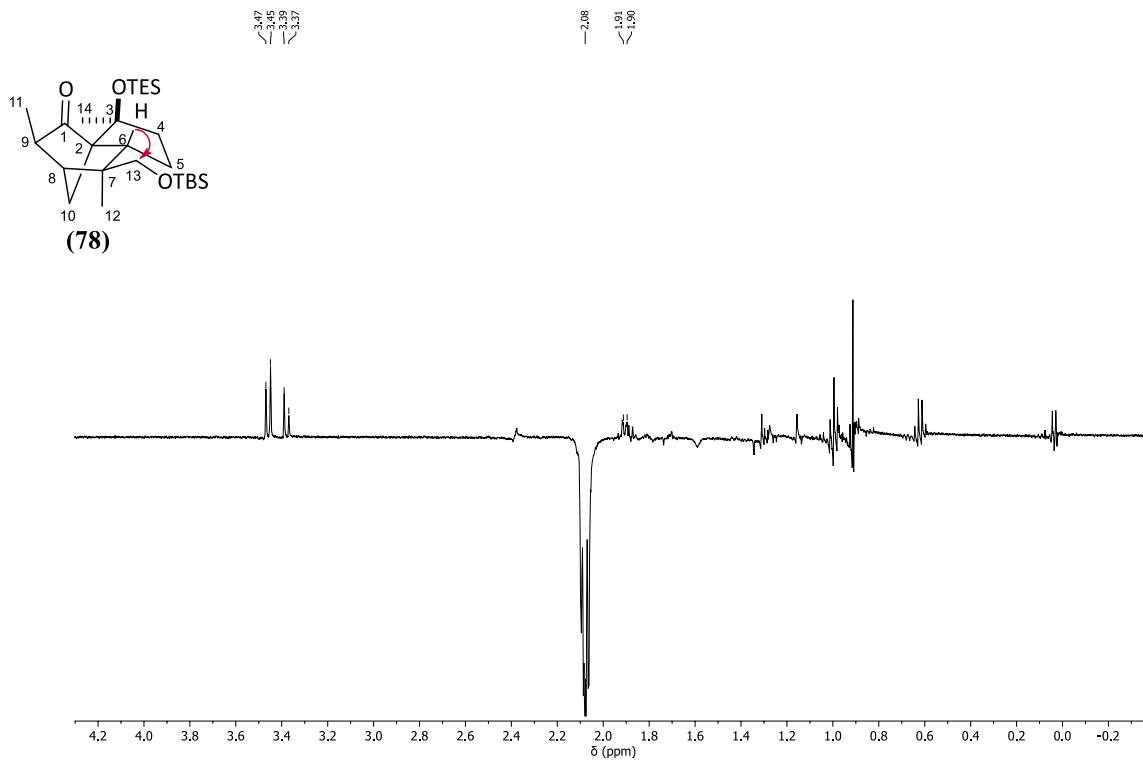




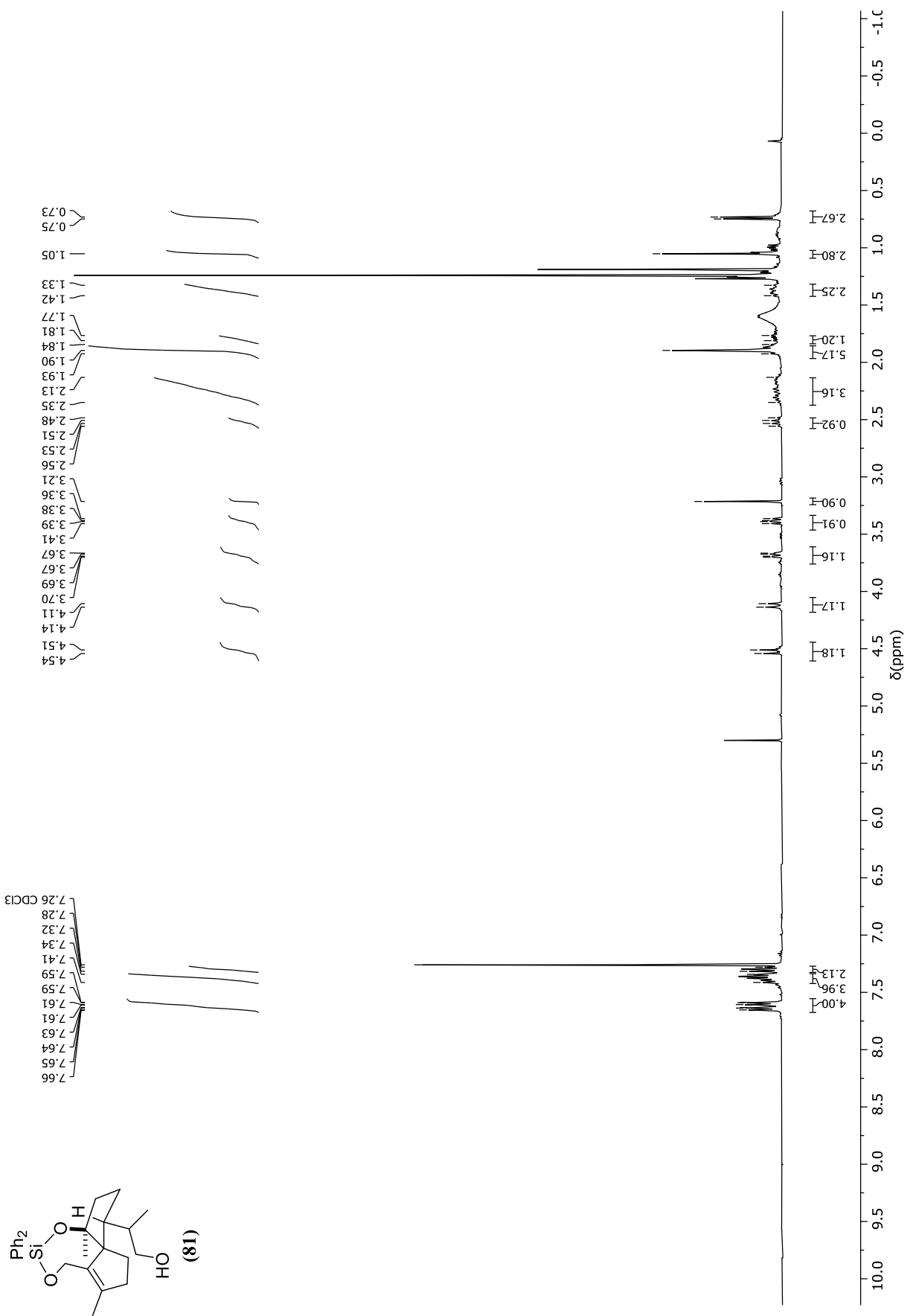
NOE response of tricyclic **(78)** (OTBS derivative) after irradiation at 1.15 ppm (CH₂-12) measured in CDCl₃ at 400 MHz.

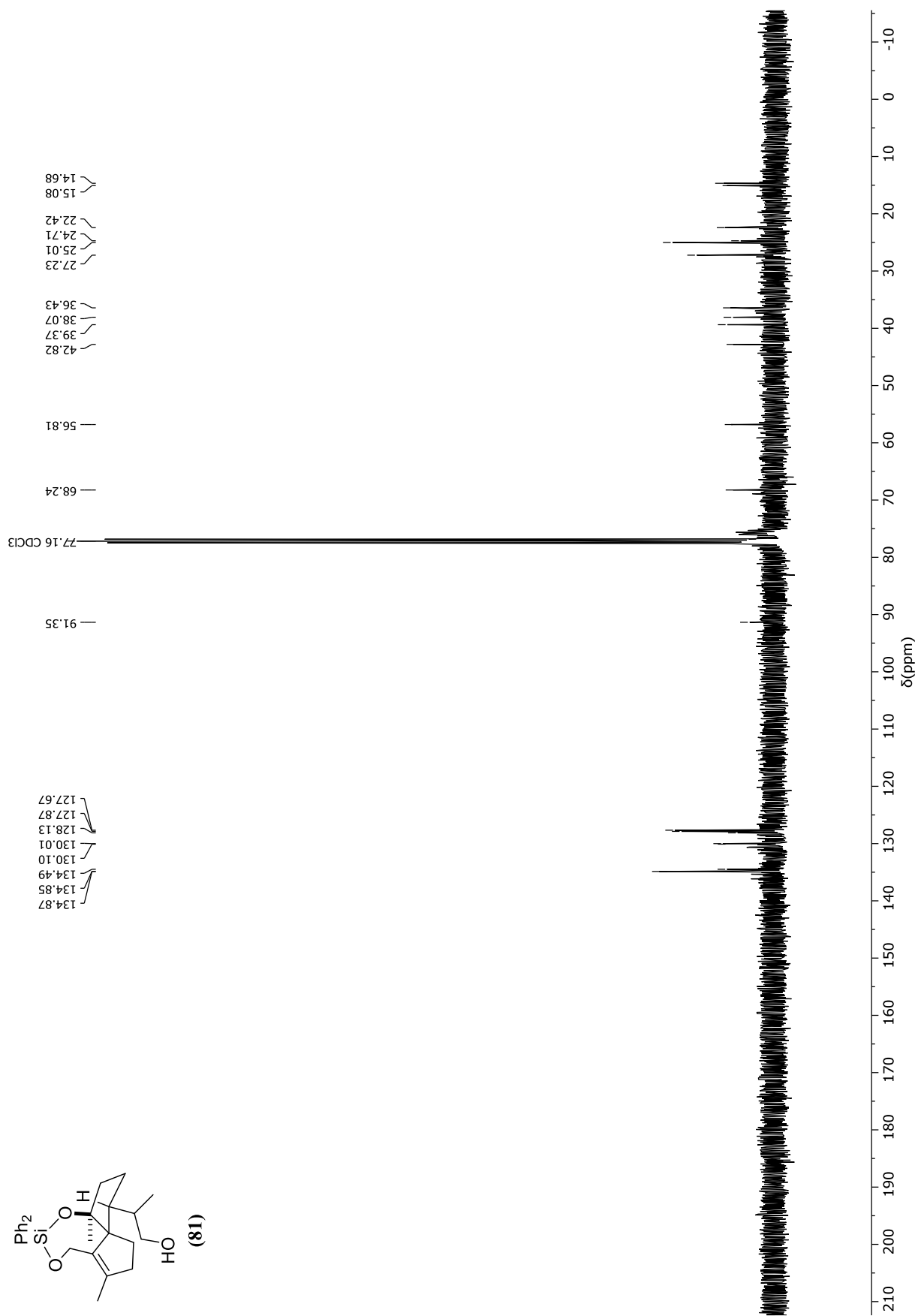
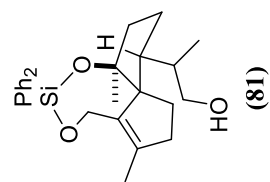


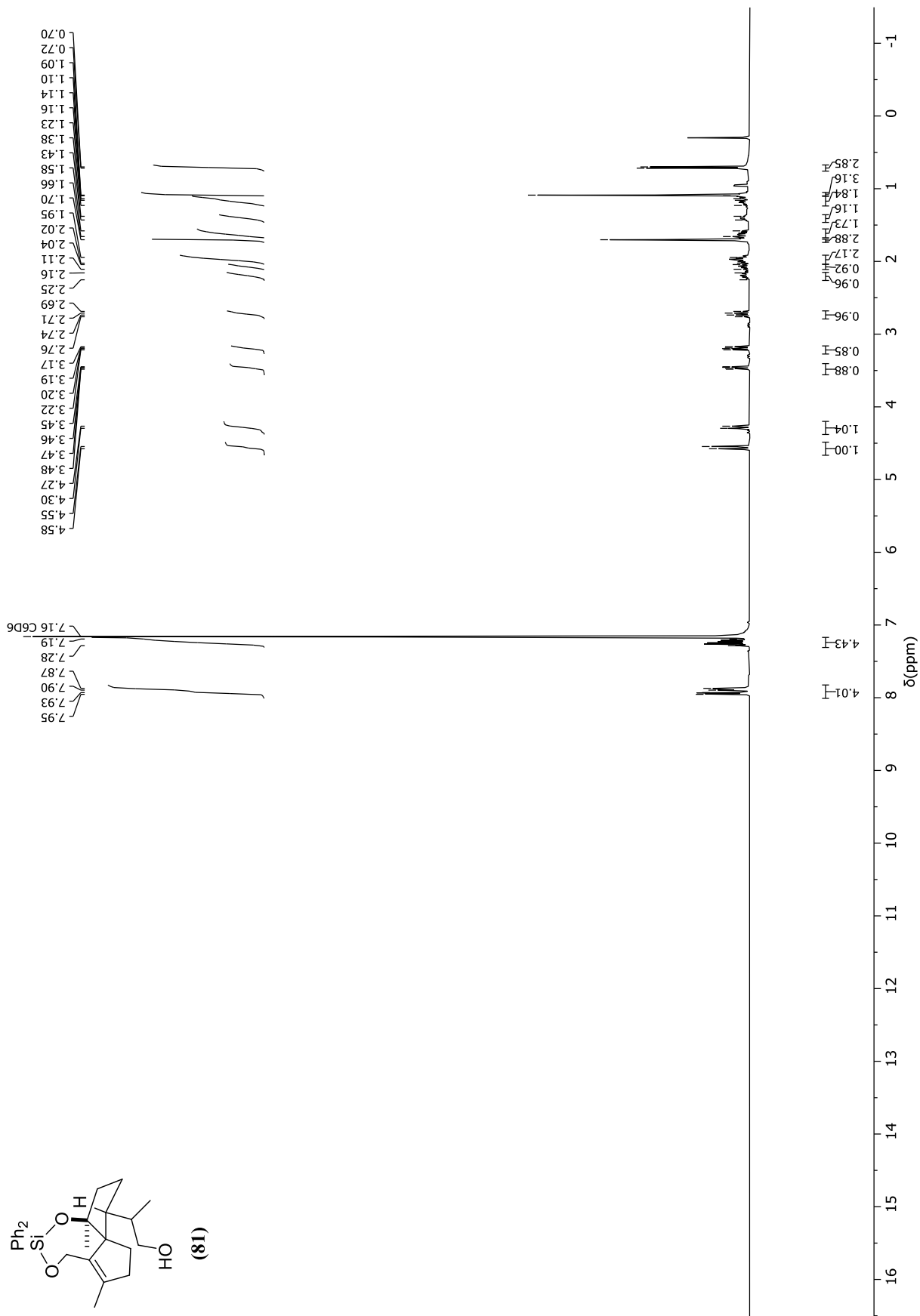
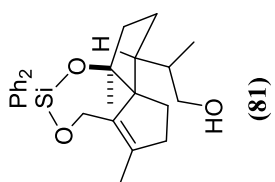
NOE response of tricyclic **(78)** (OTBS derivative) after irradiation at 1.29 ppm (CH₂-11) measured in CDCl₃ at 400 MHz.

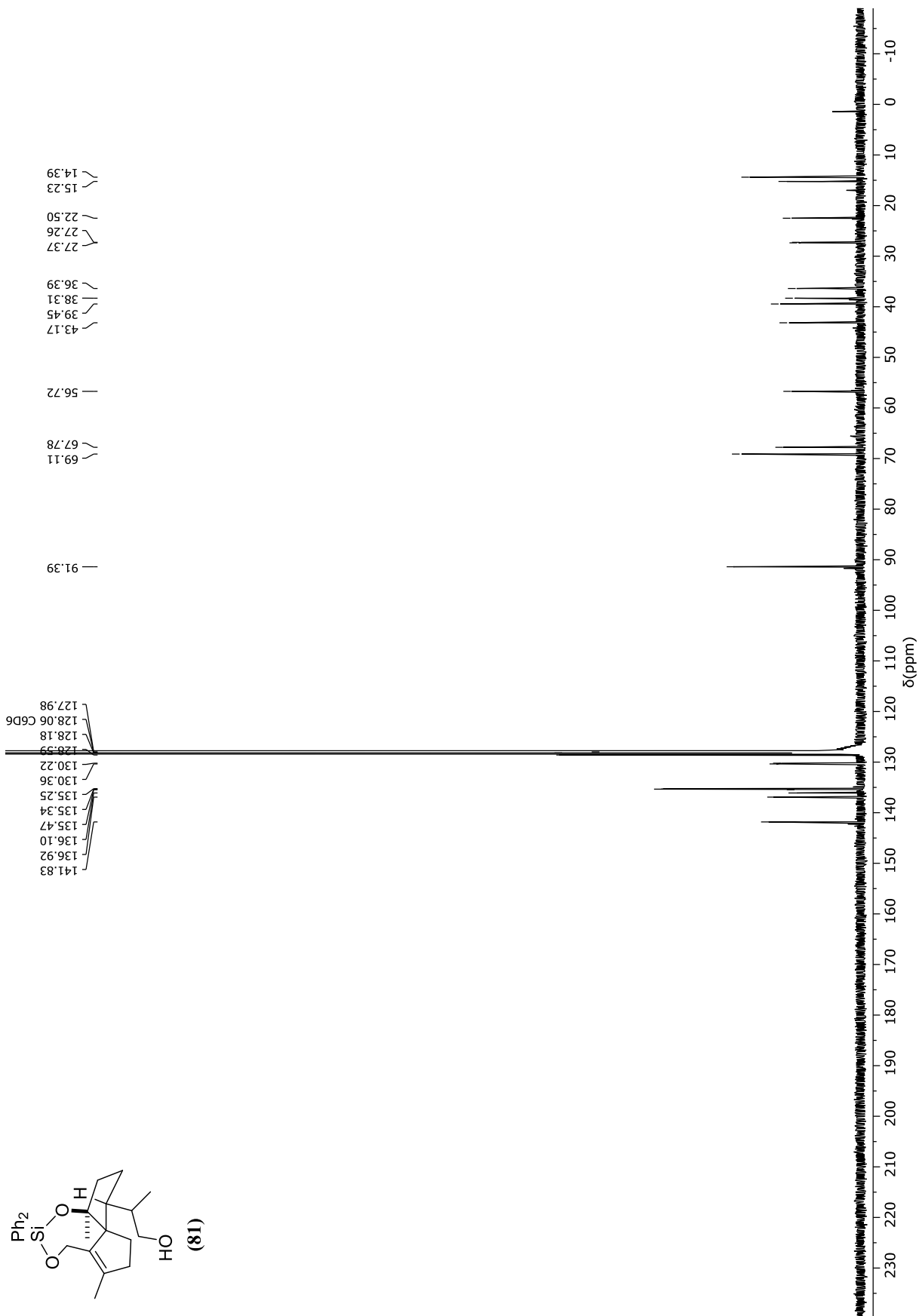
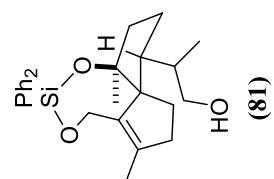


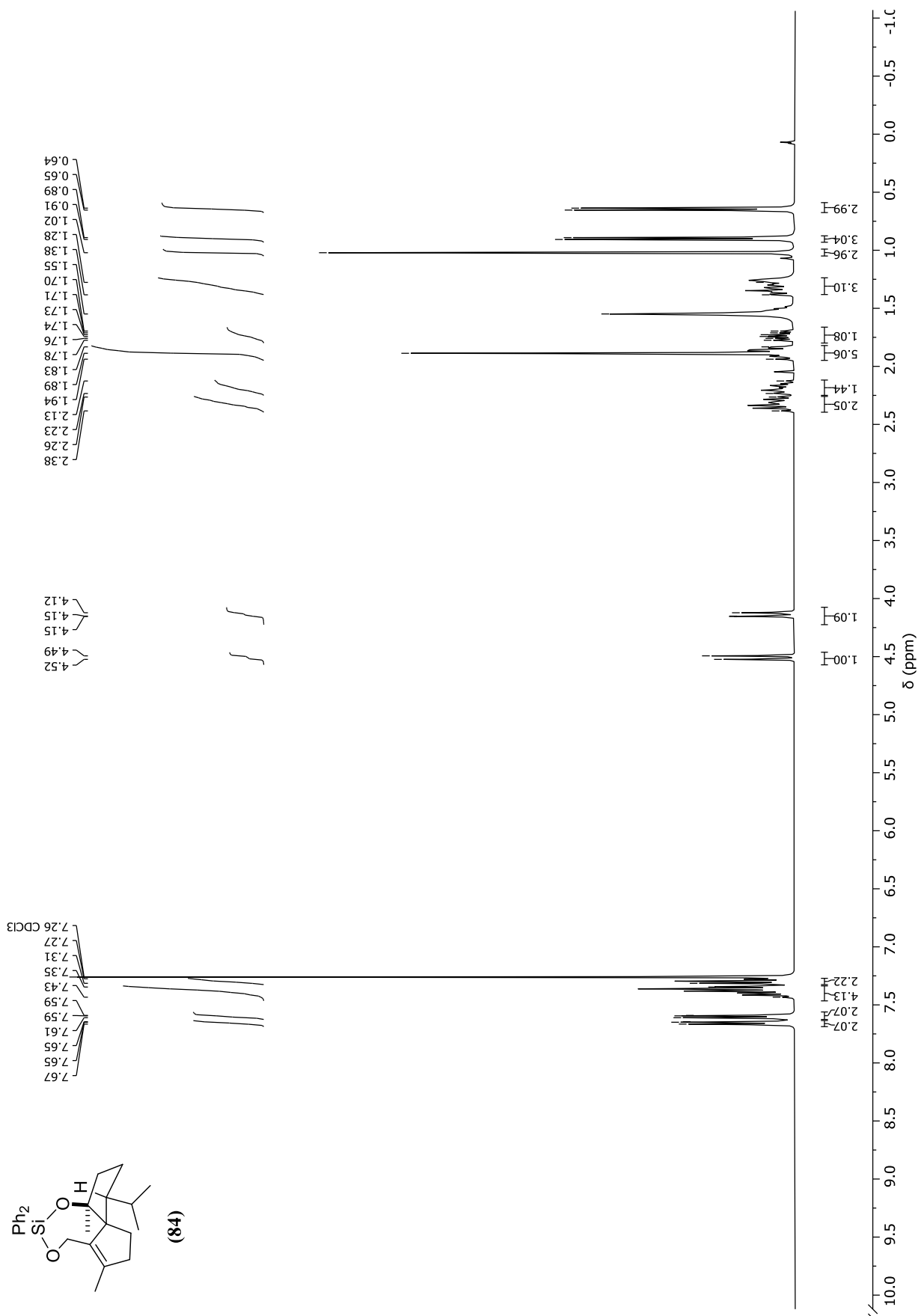
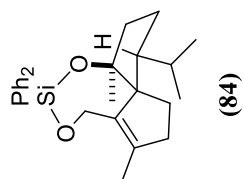
NOE response of tricycle **(78)** (OTBS derivative) after irradiation at 2.08 ppm (CH-6) measured in CDCl_3 at 400 MHz.

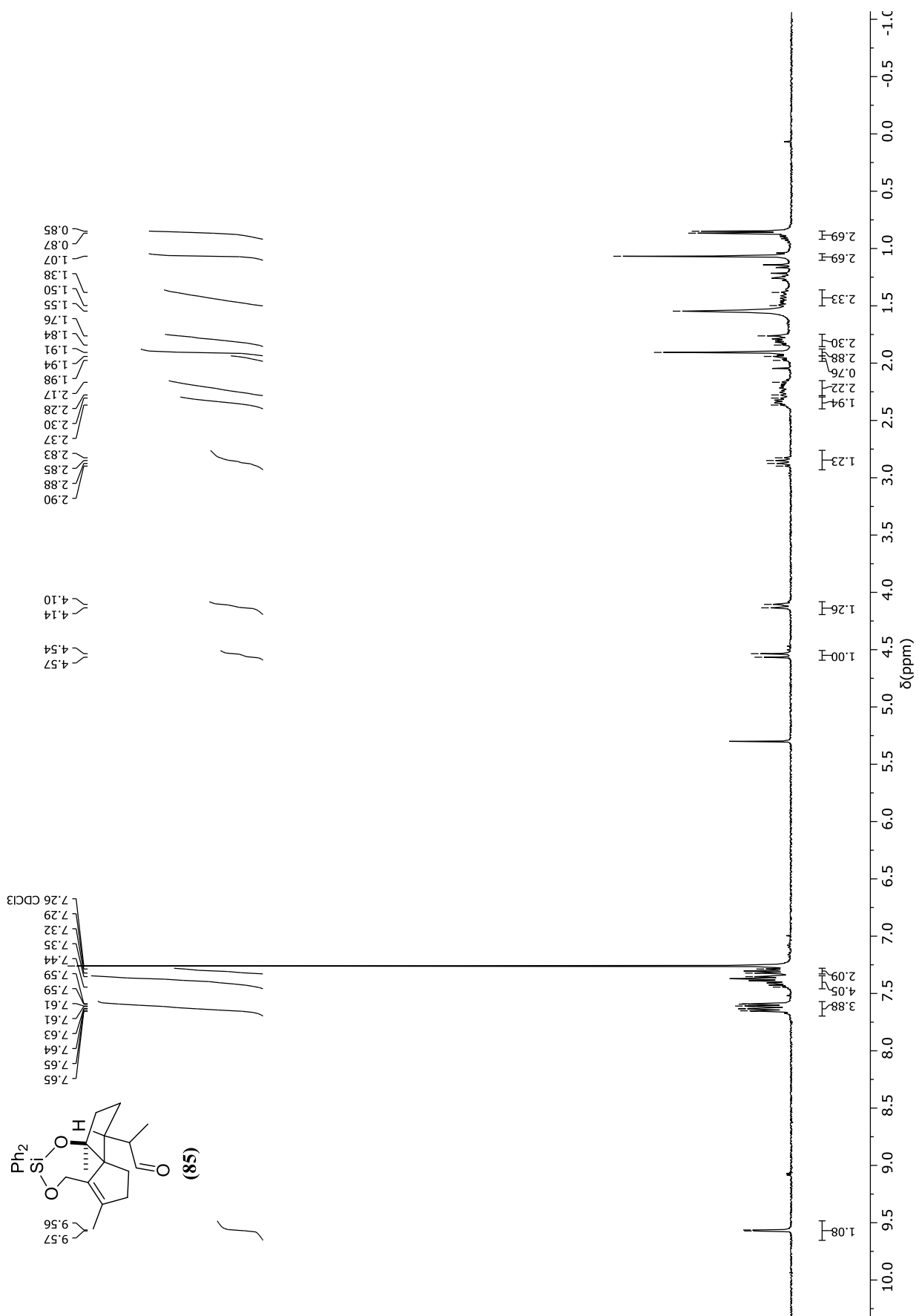


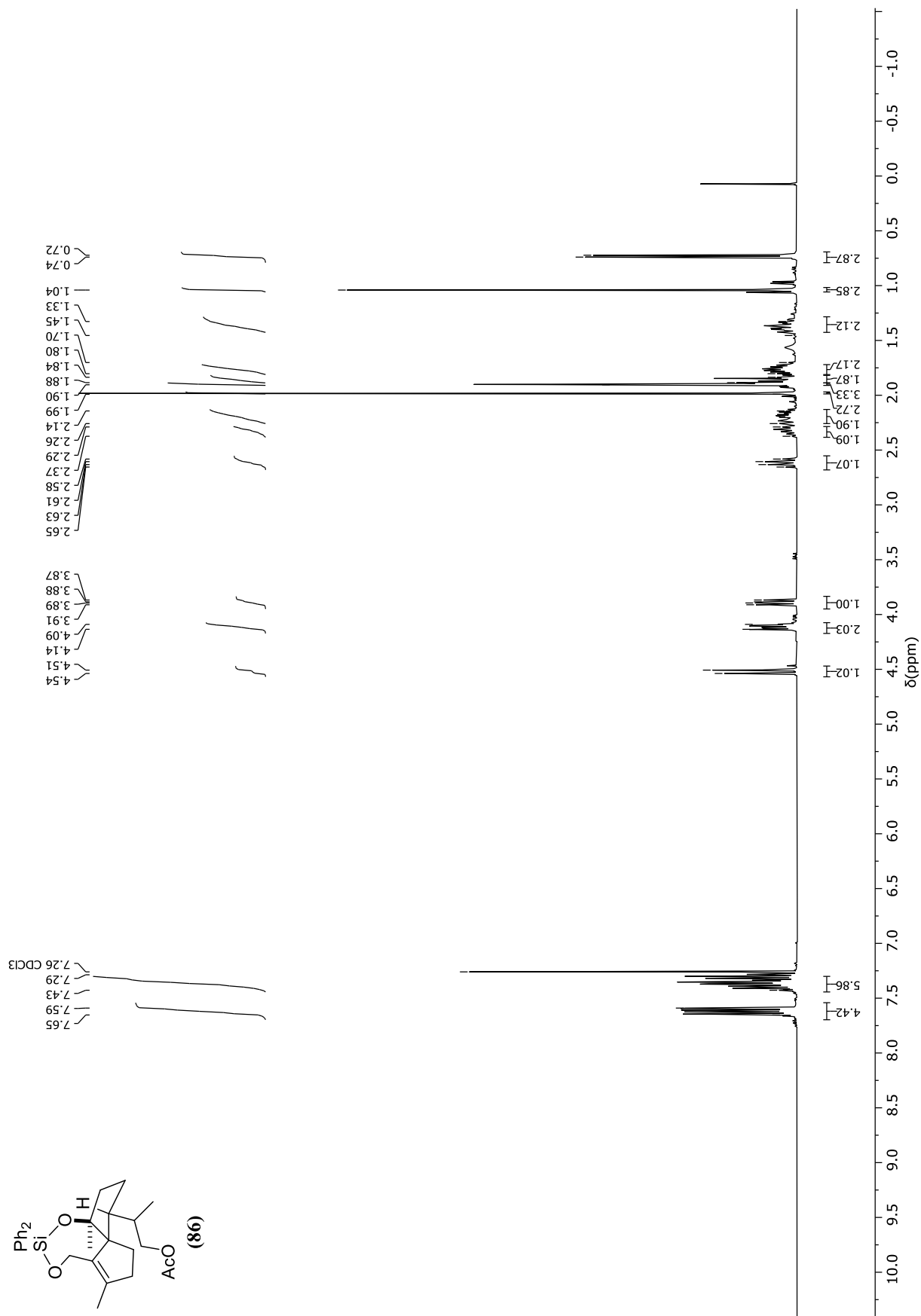
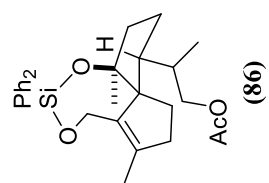


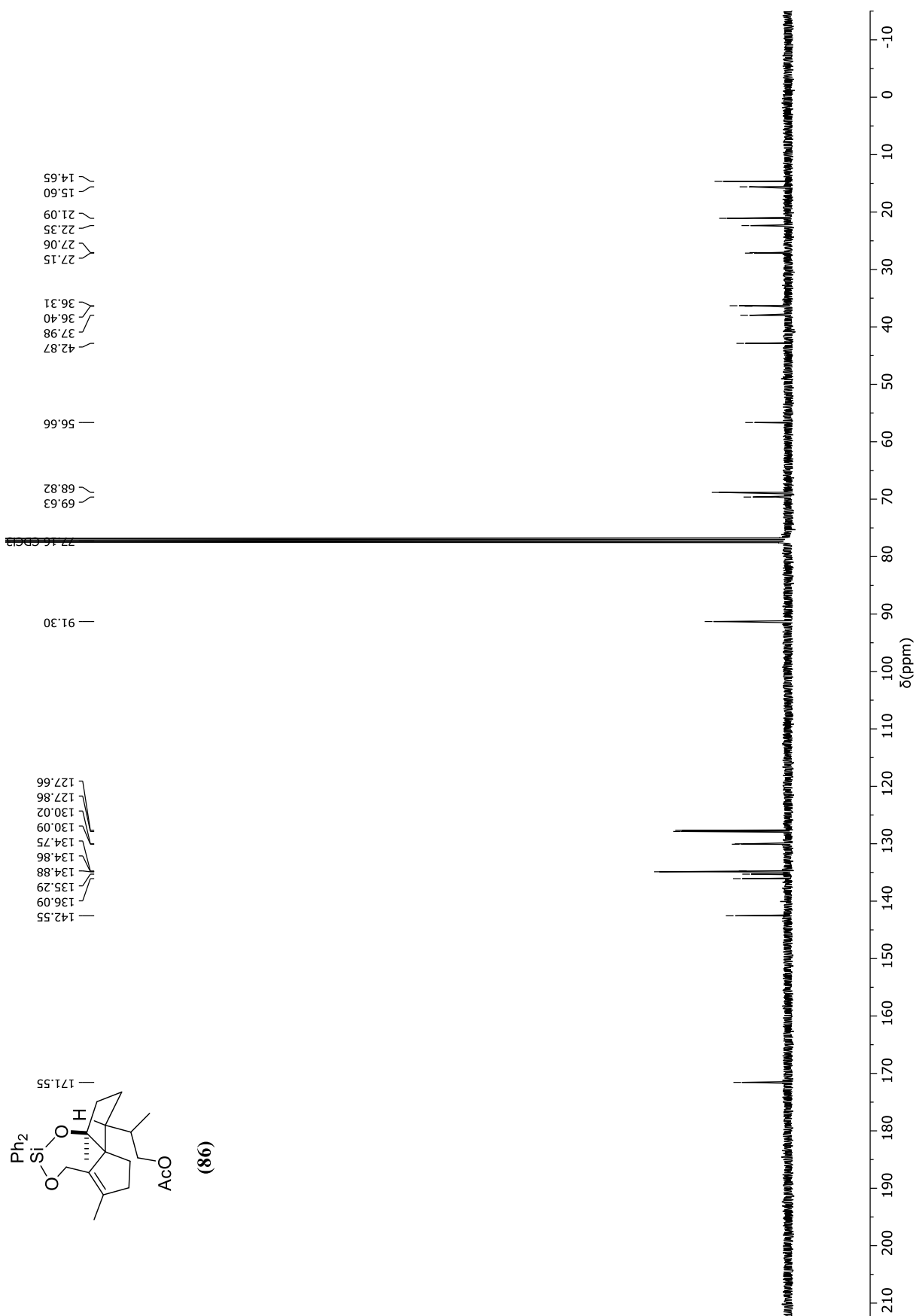


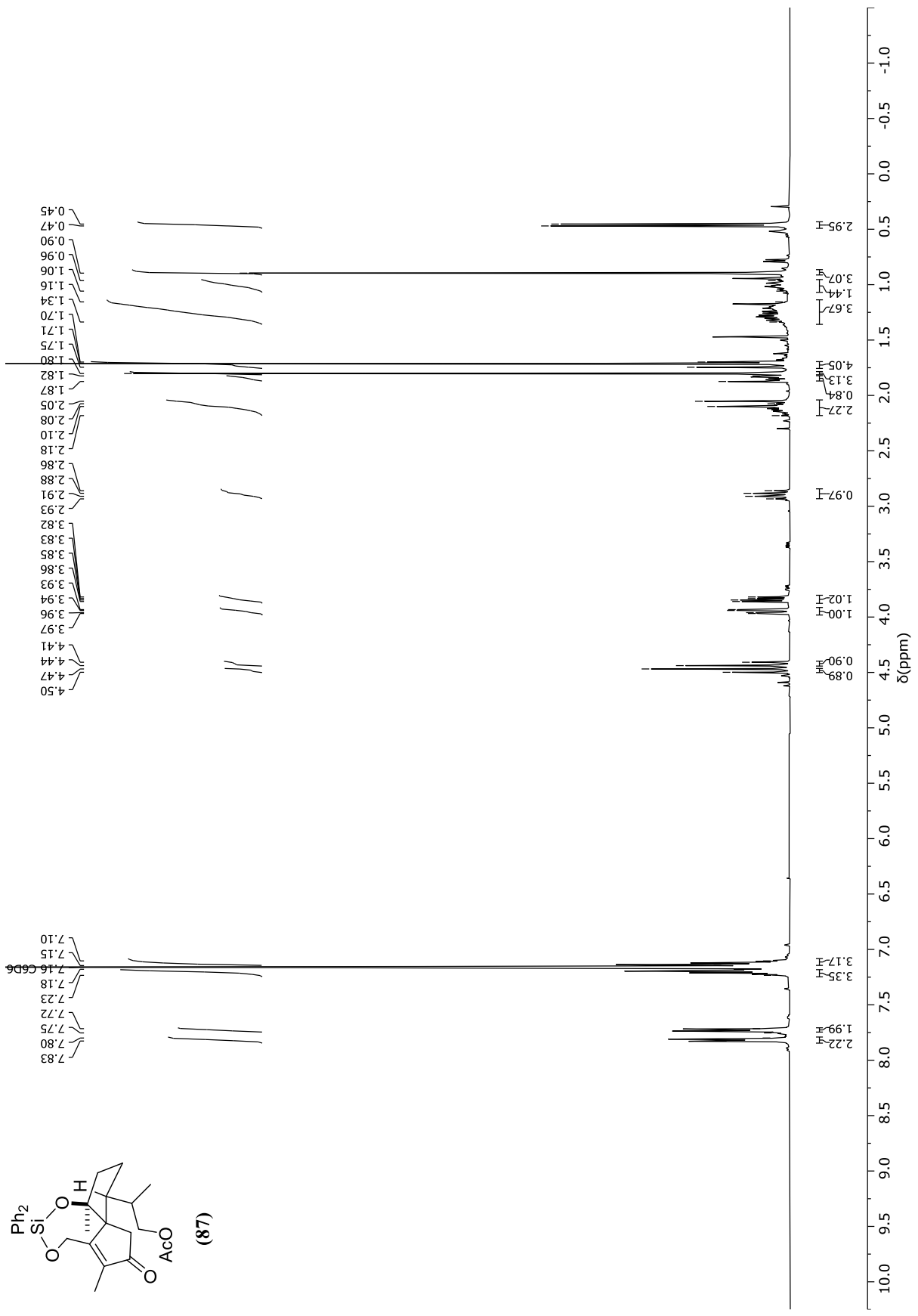
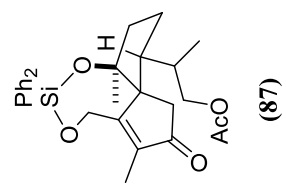


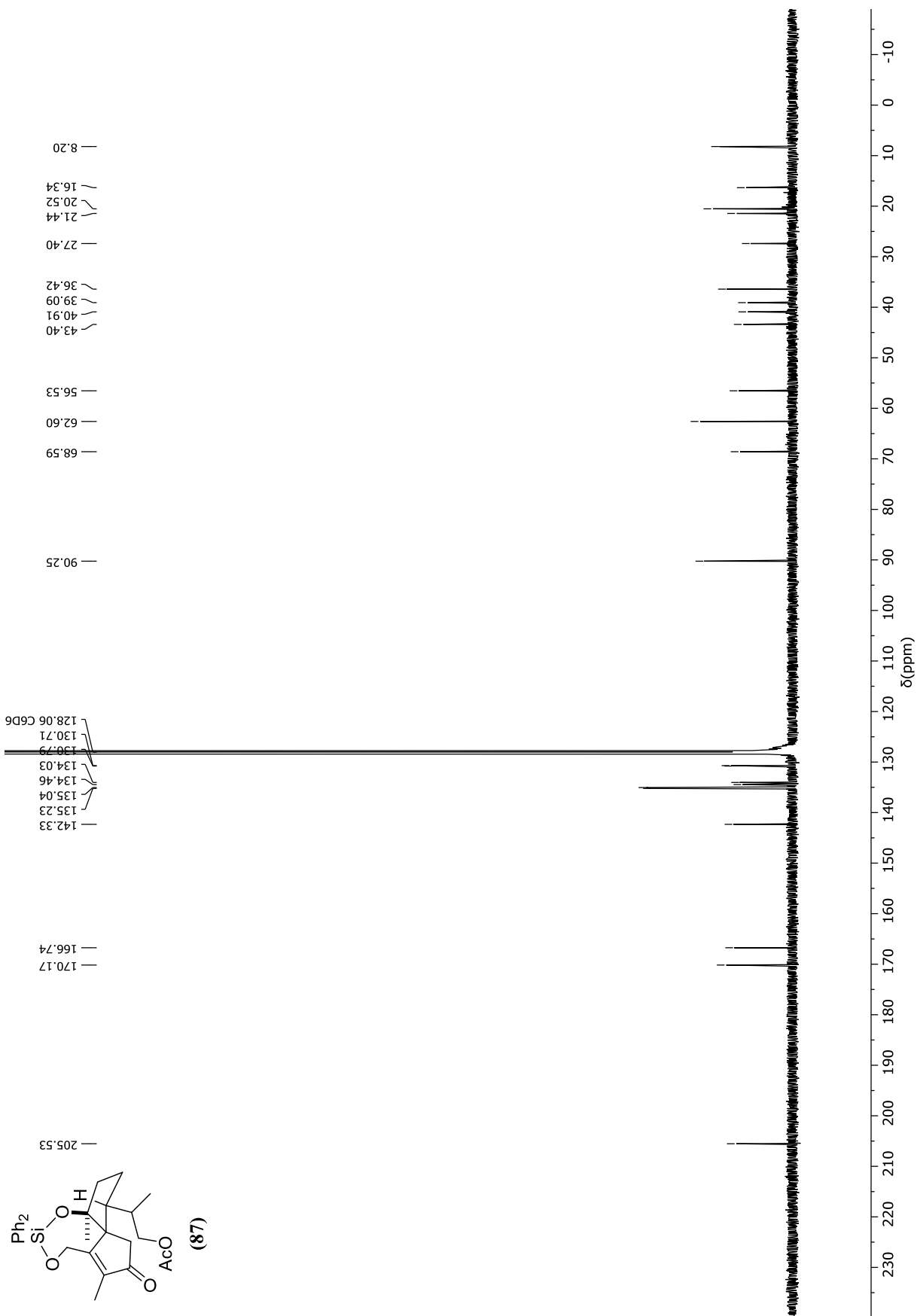


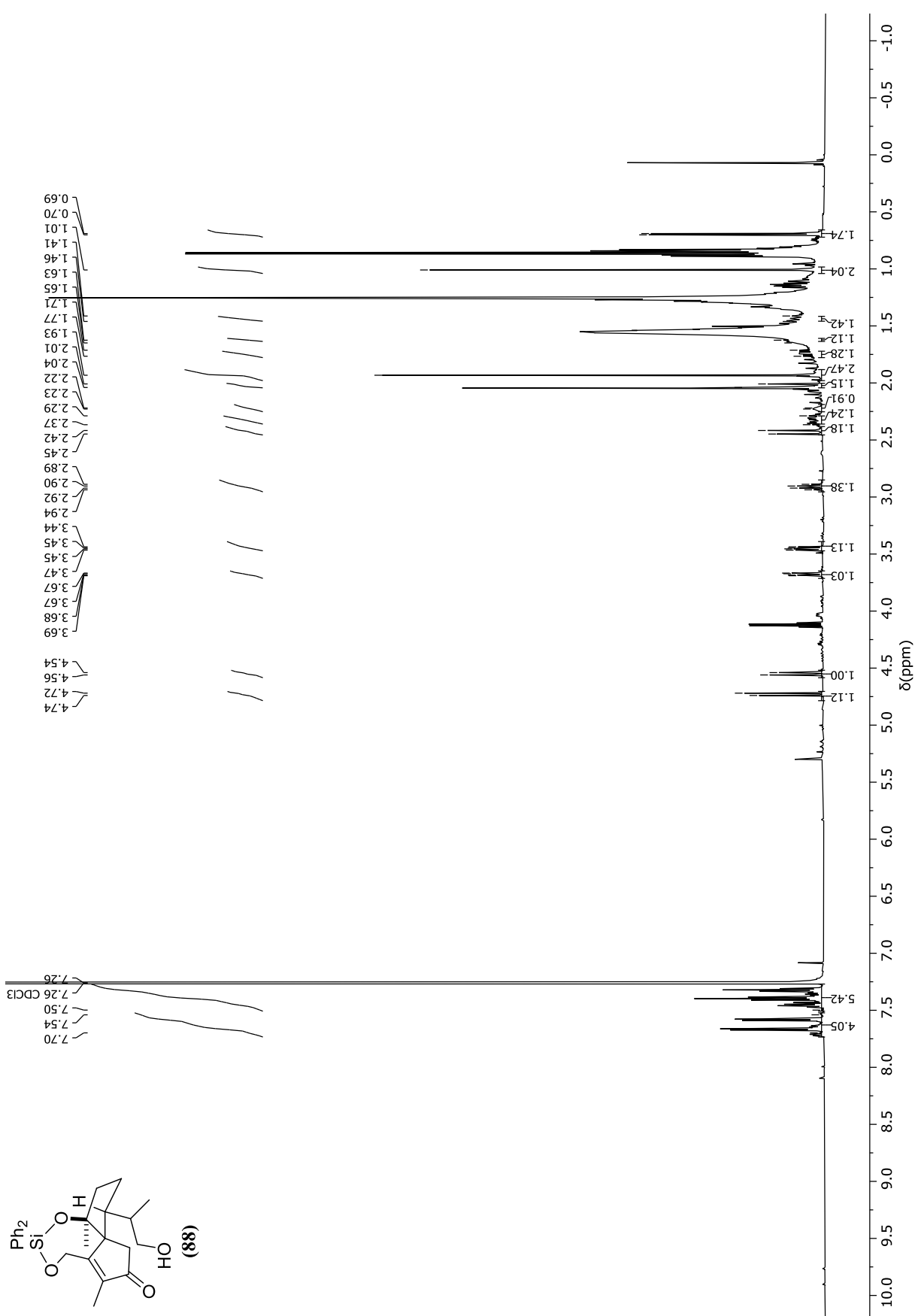


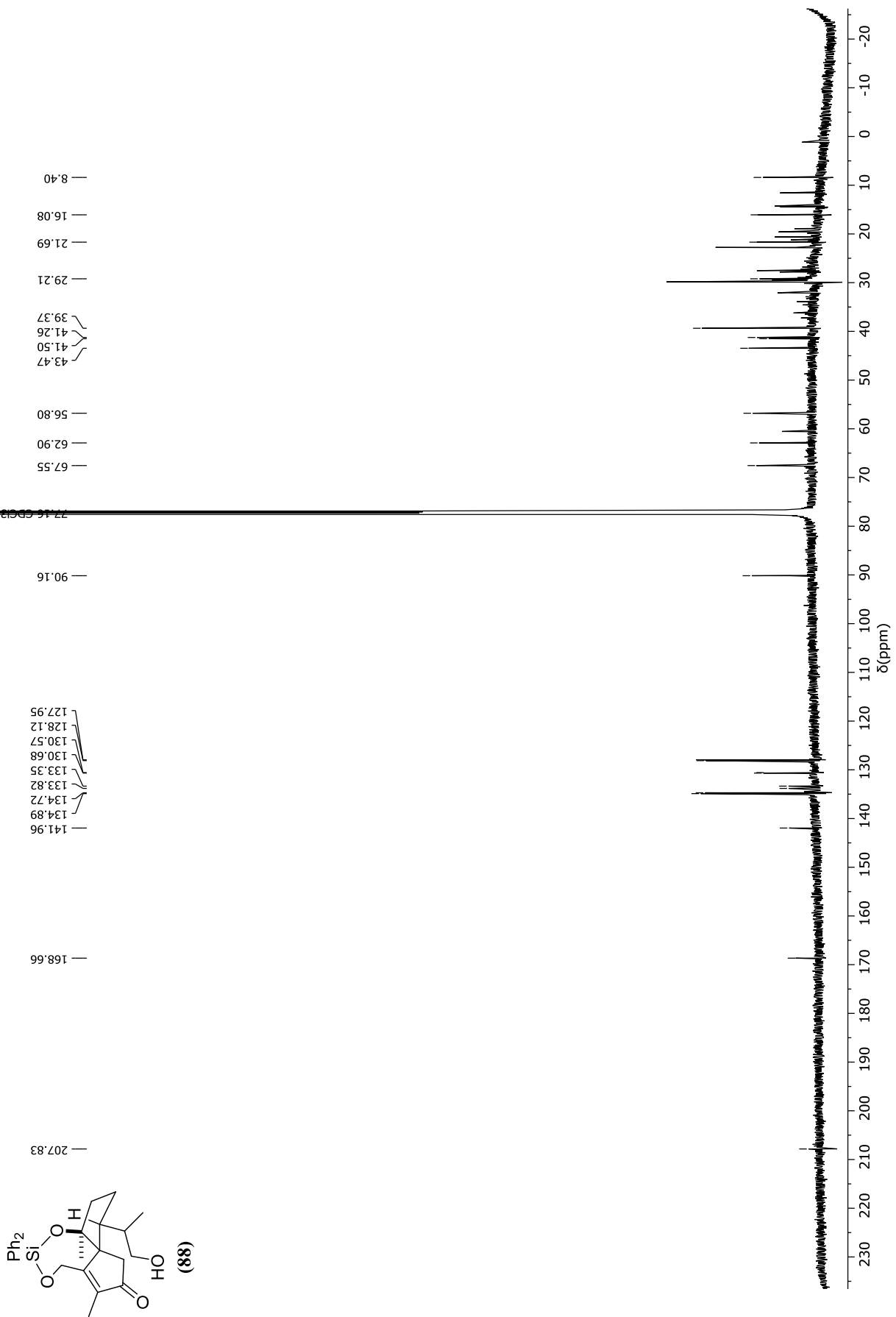


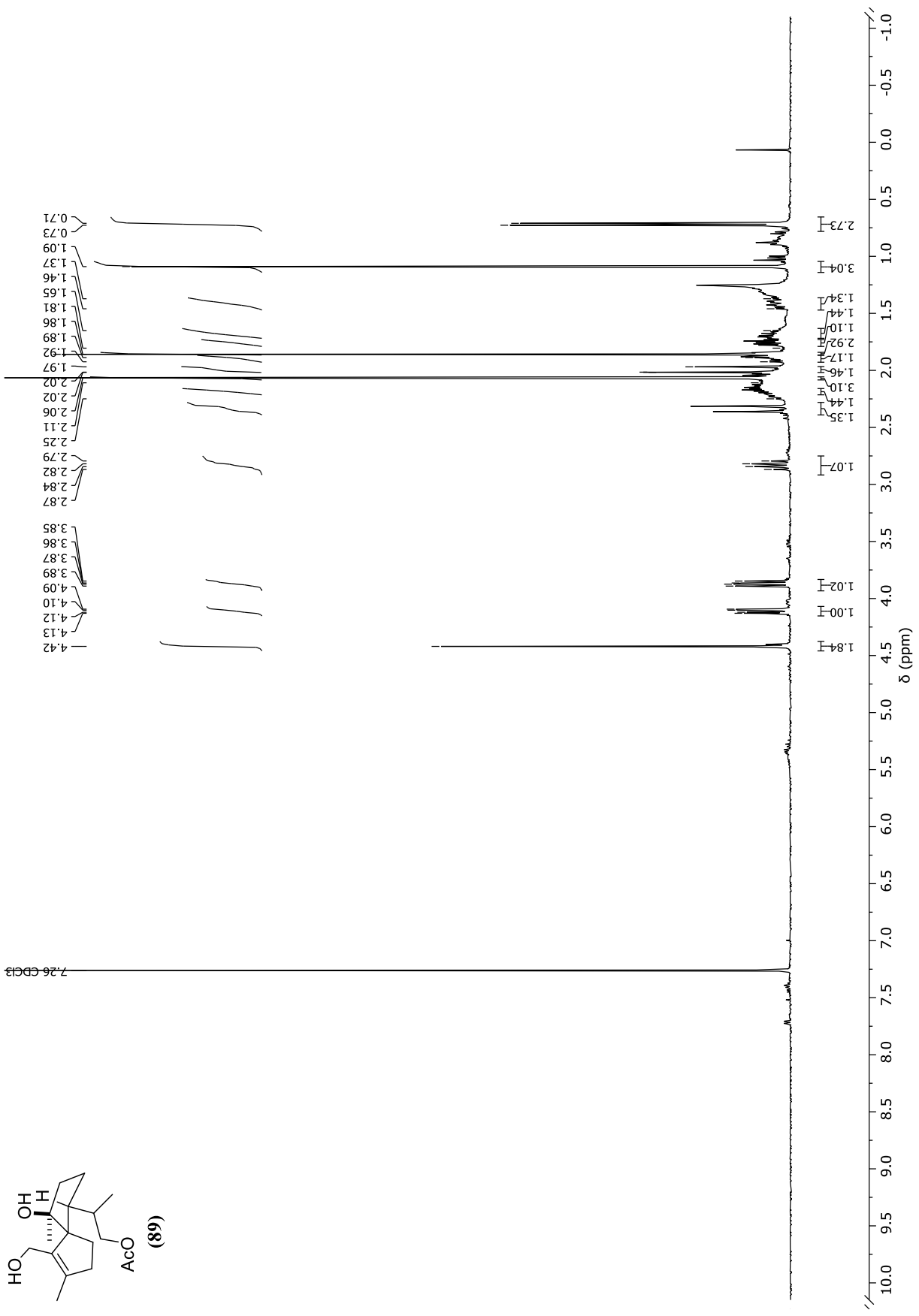
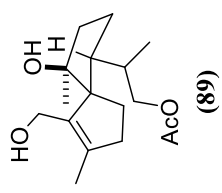


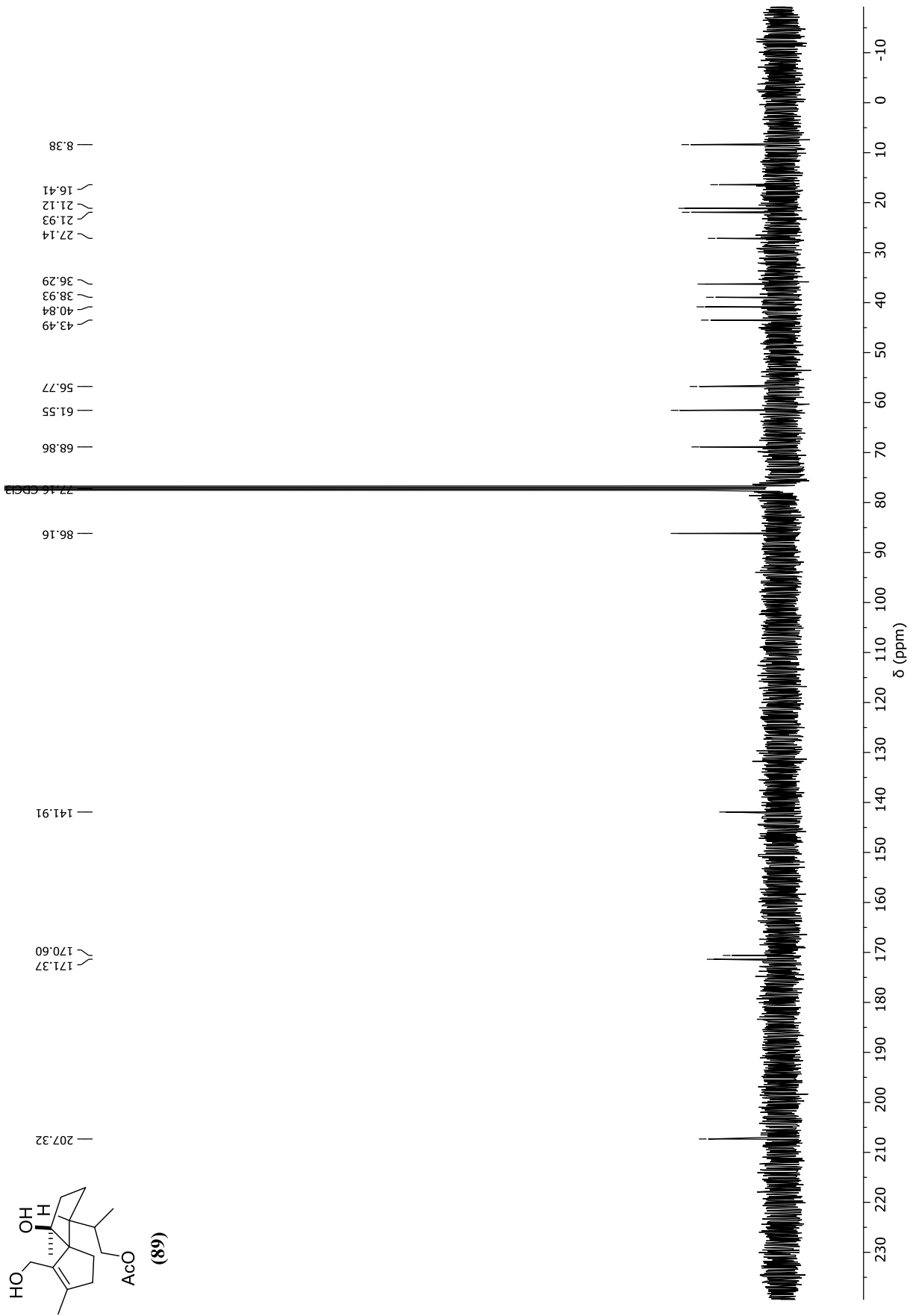


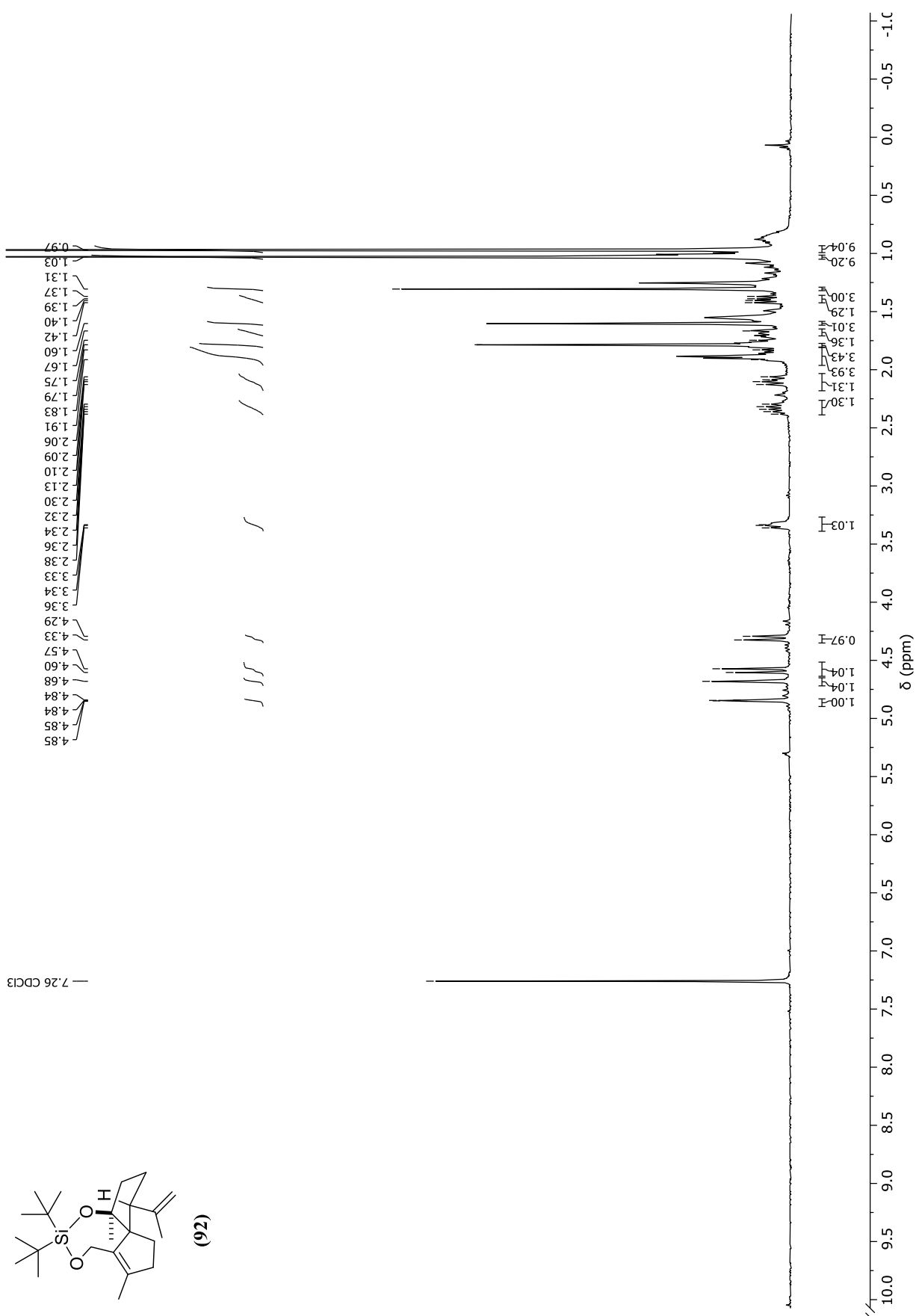


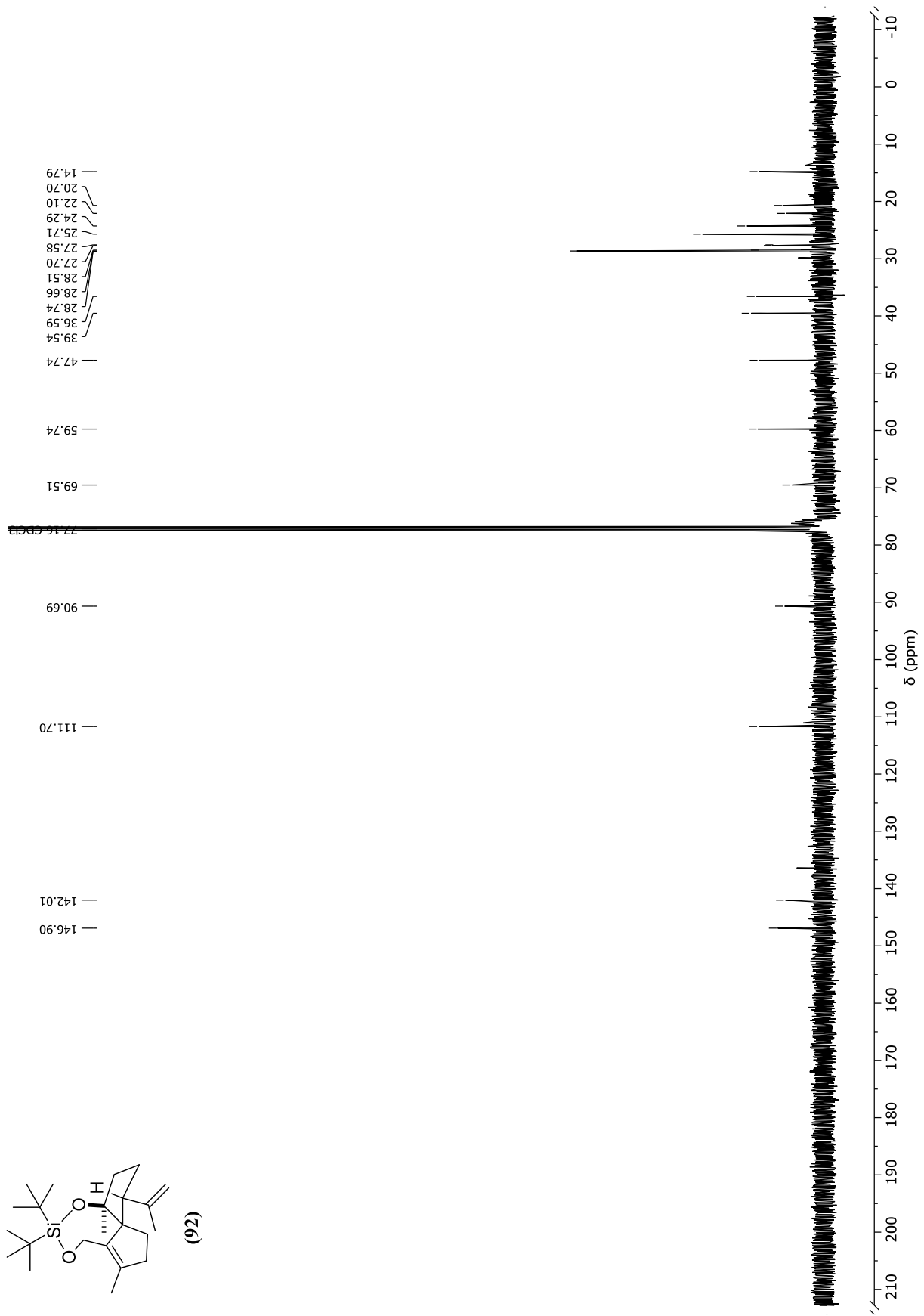


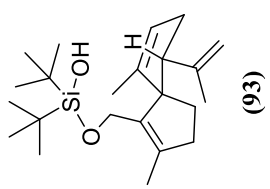
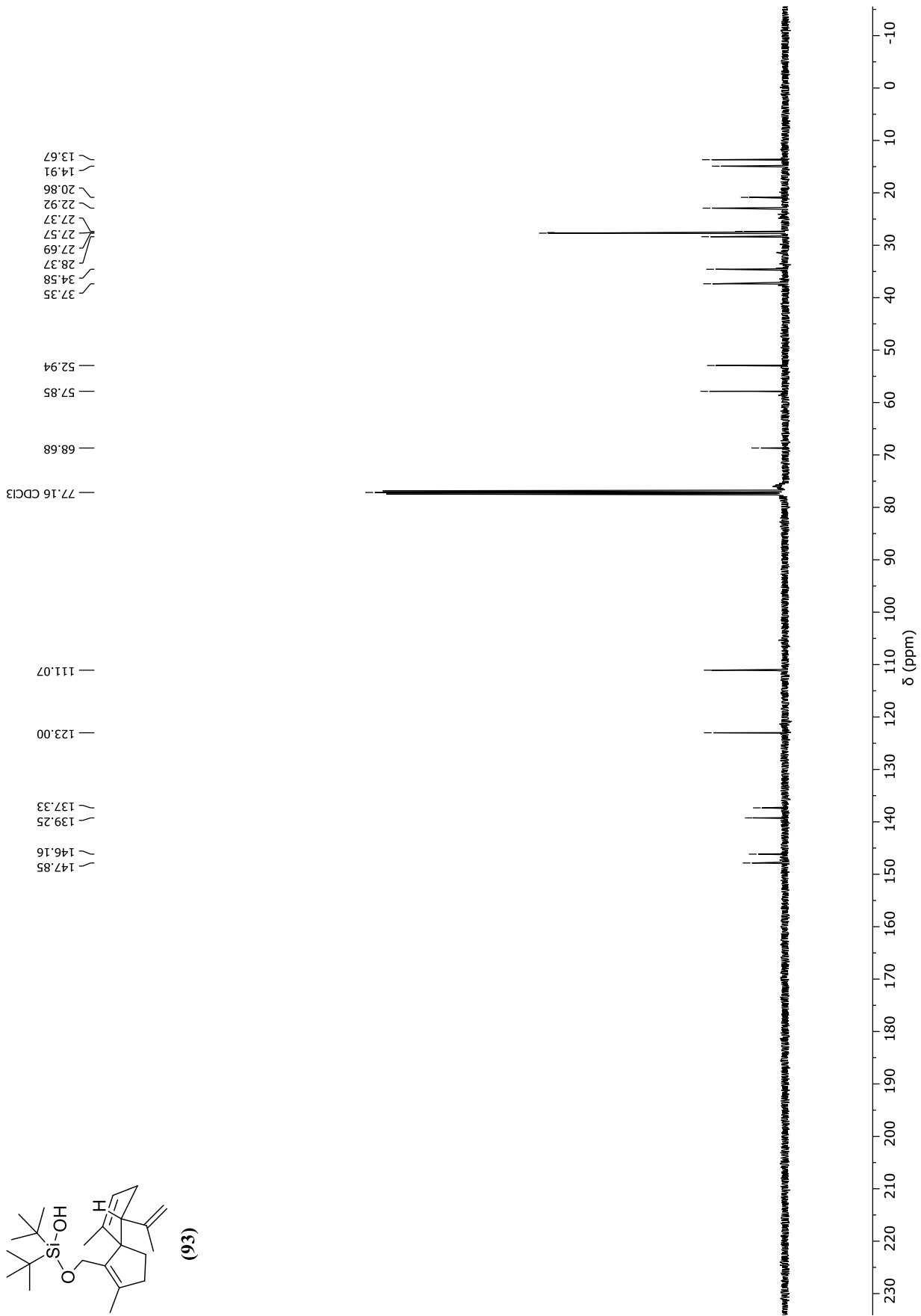


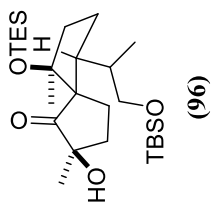




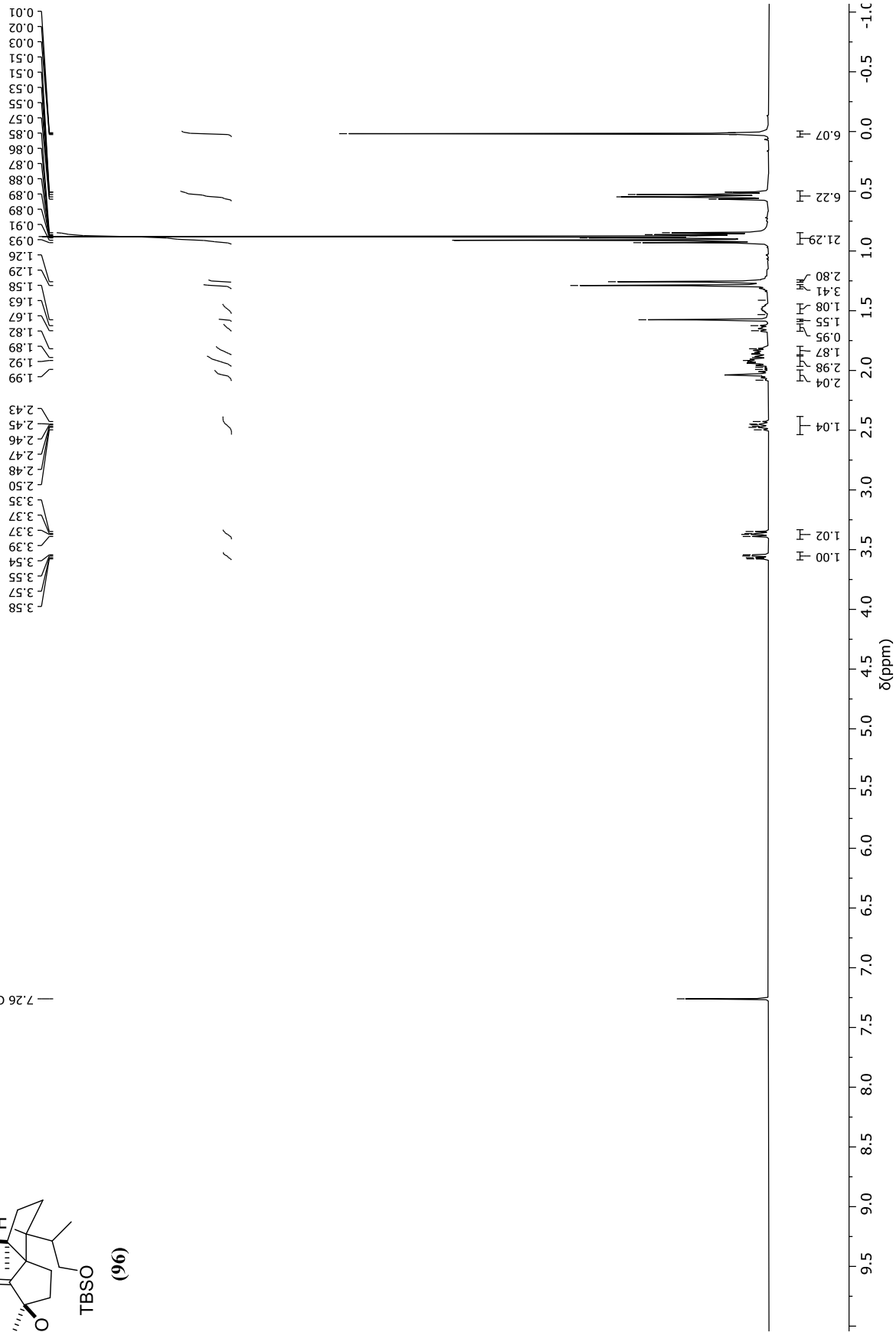


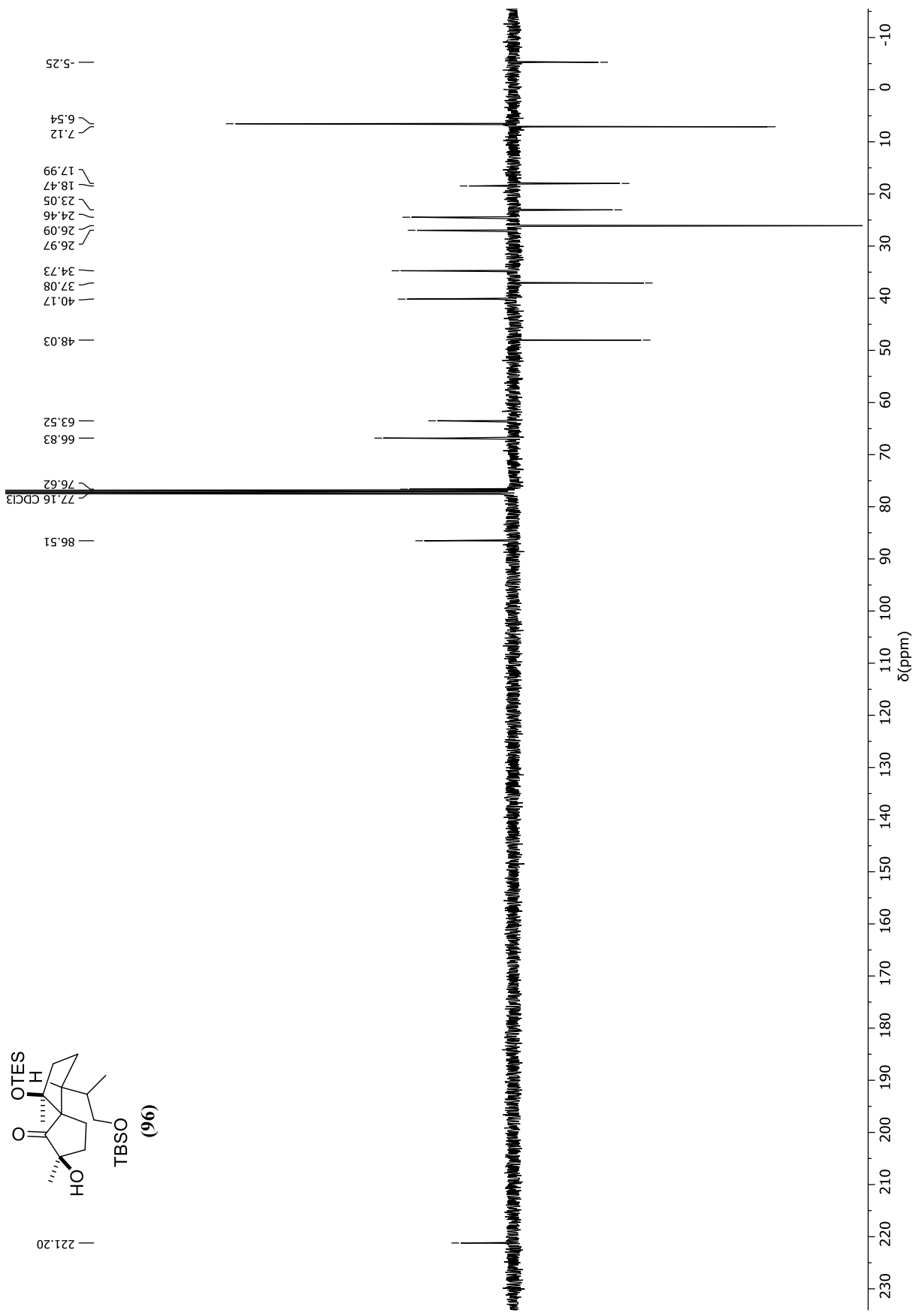
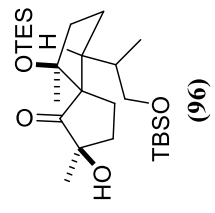


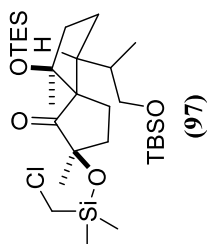




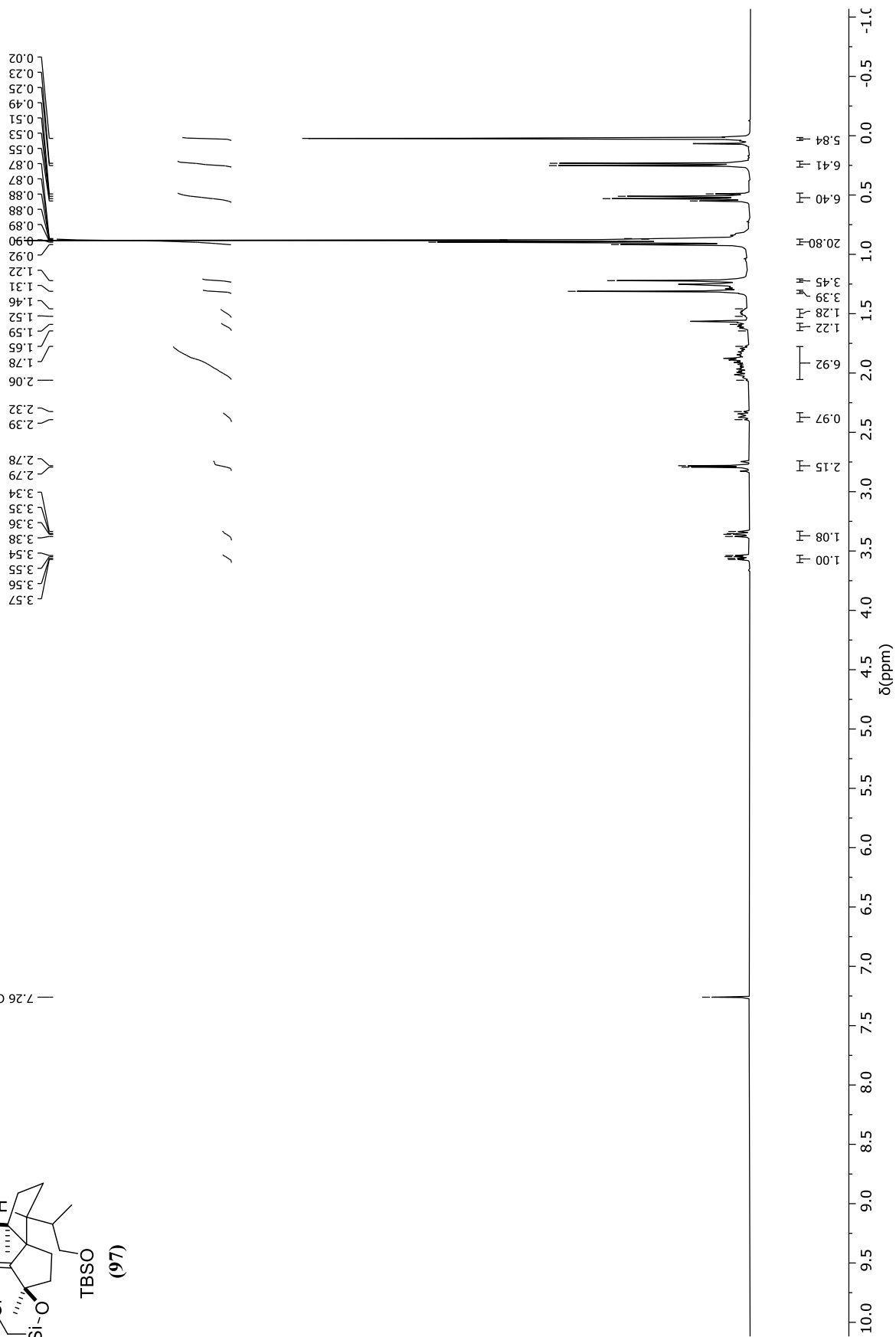
— 7.26 CDCl₃

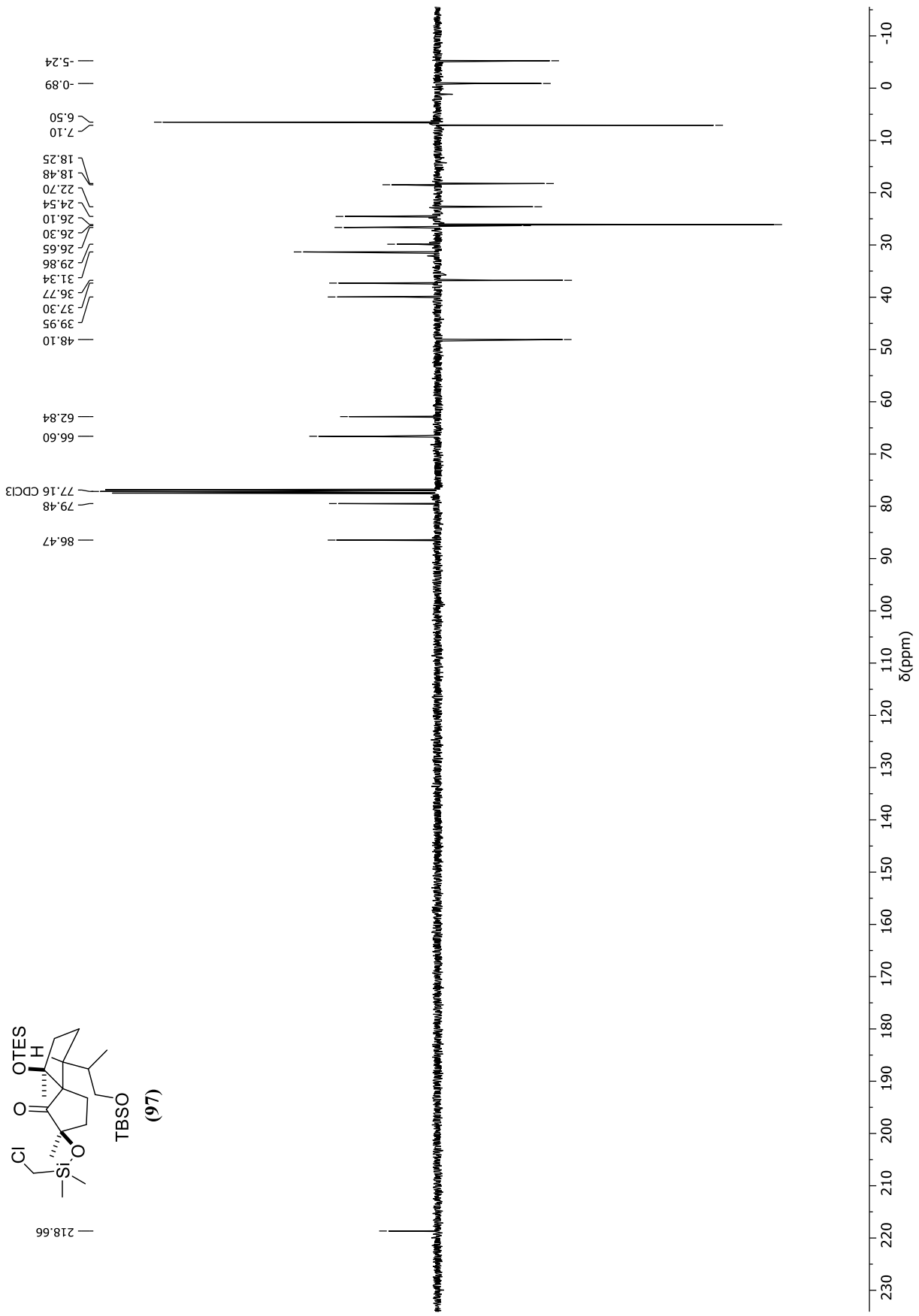
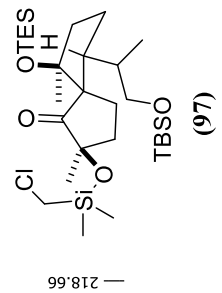


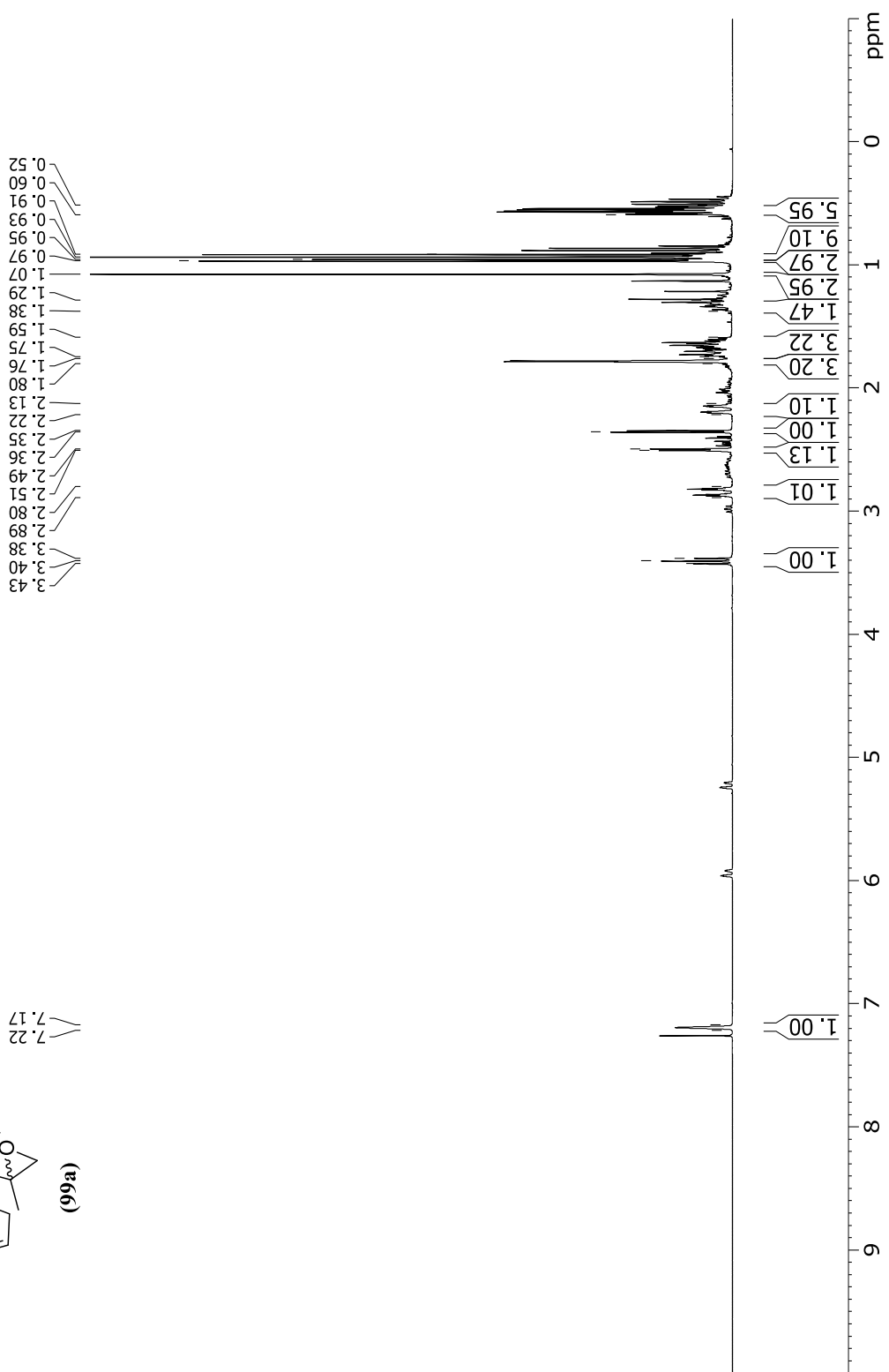
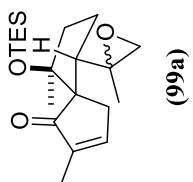


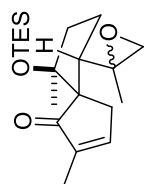


— 7.26 CDCl₃









—207.9

—153.6

—142.5

—87.1

—63.8

—56.8

—51.4

—46.0

—39.6

—34.6

—22.3

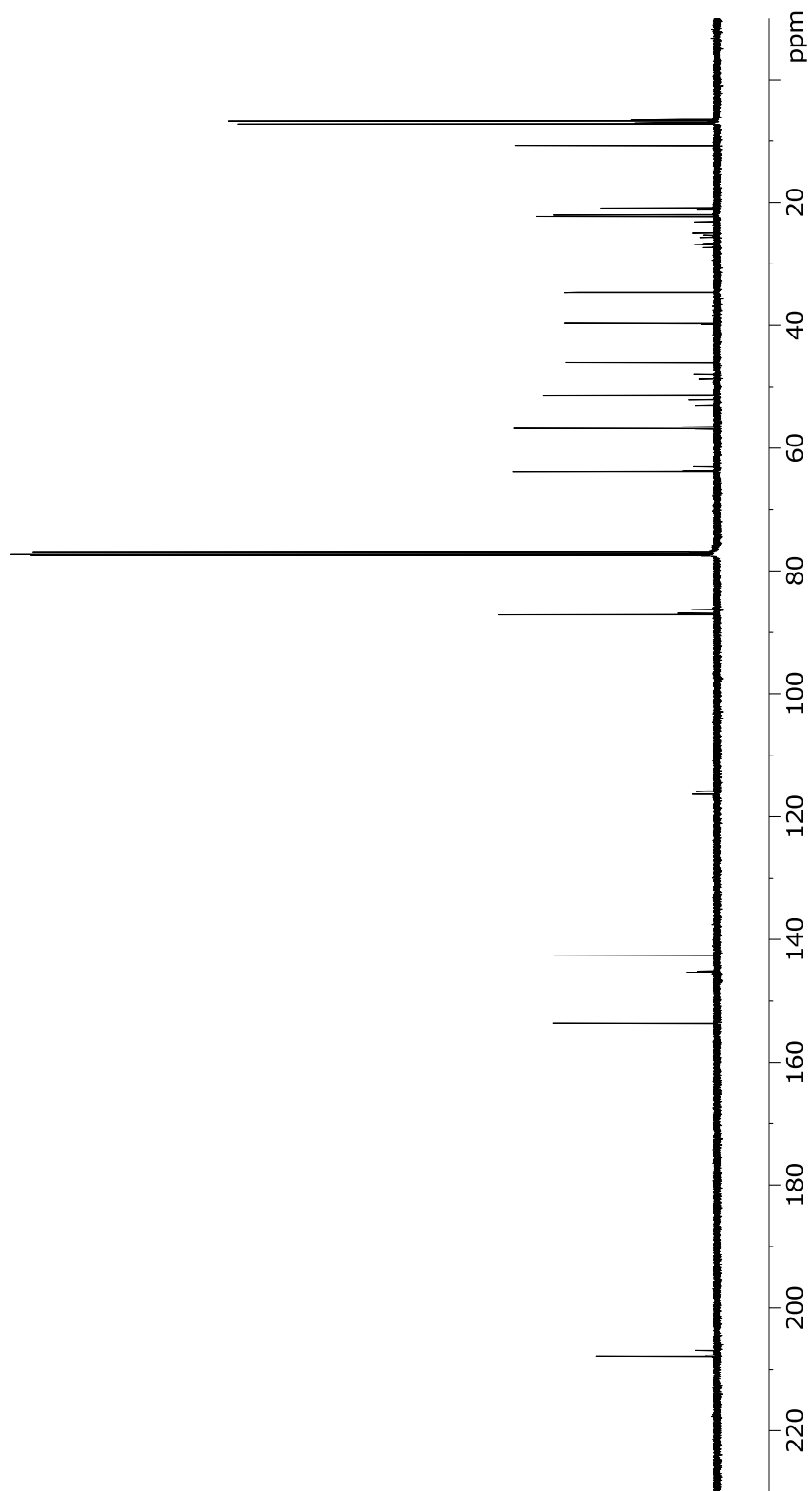
—22.0

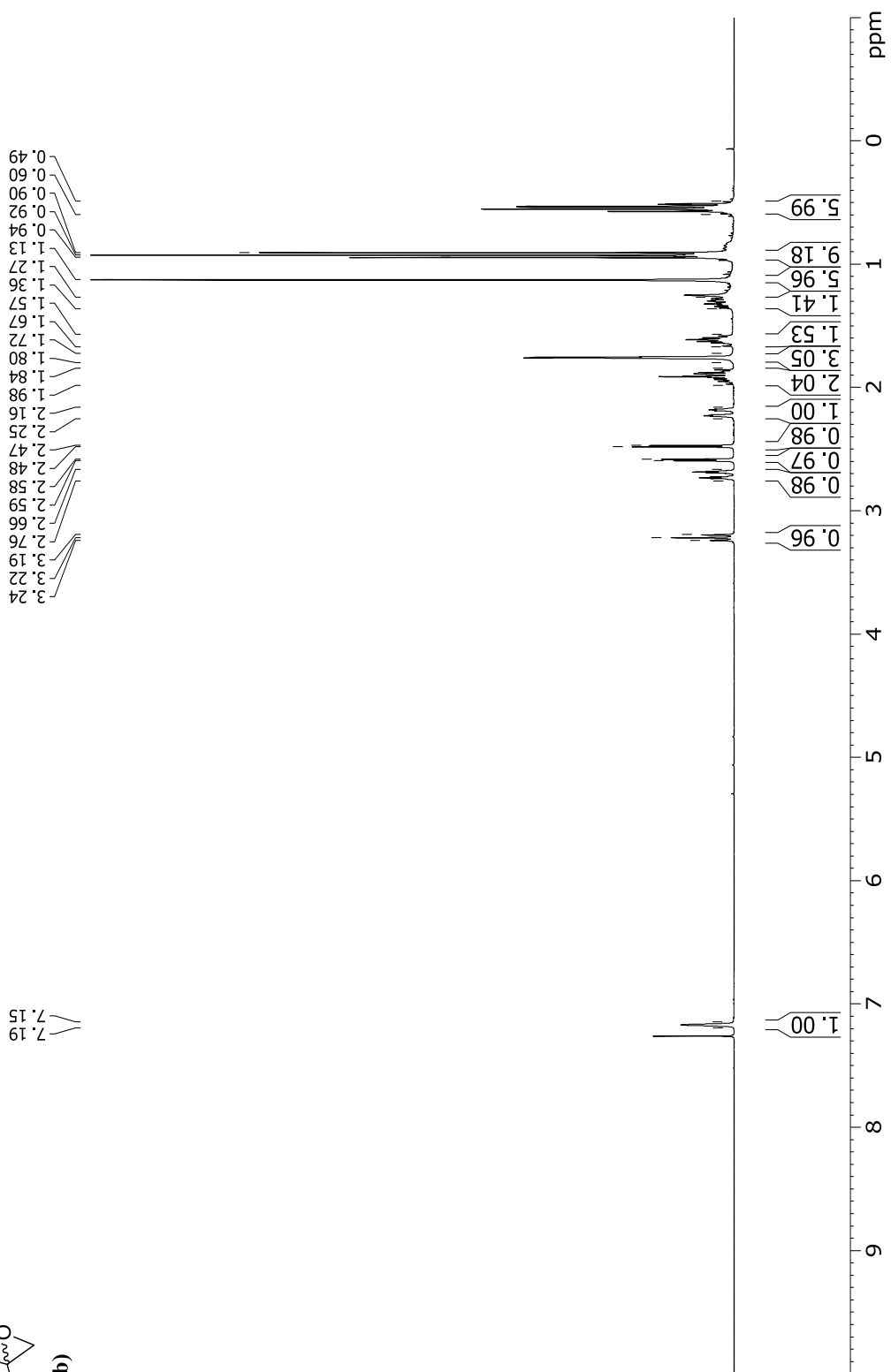
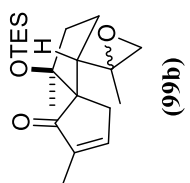
—20.8

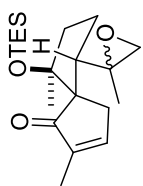
—10.7

—7.3

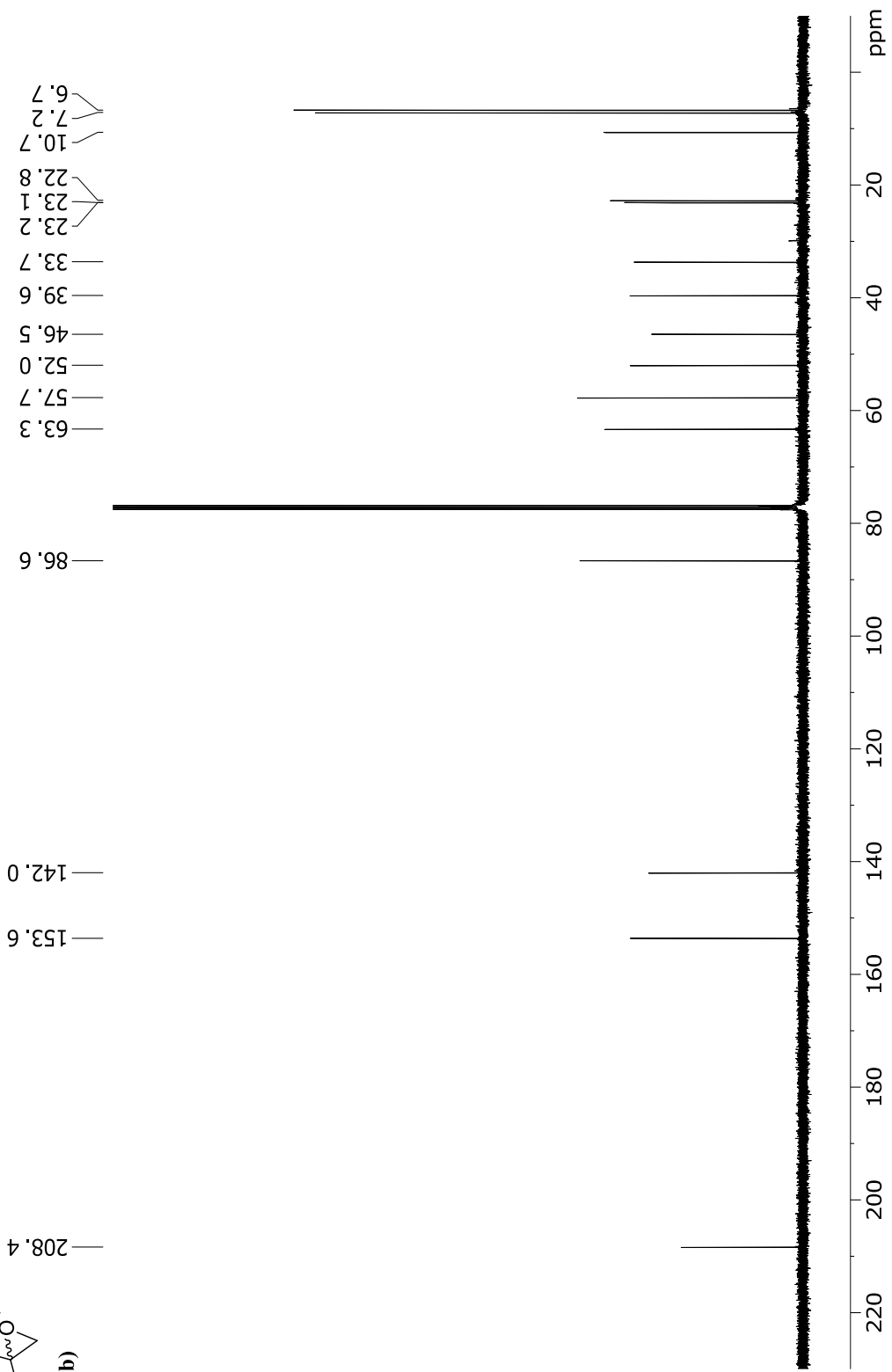
—6.8

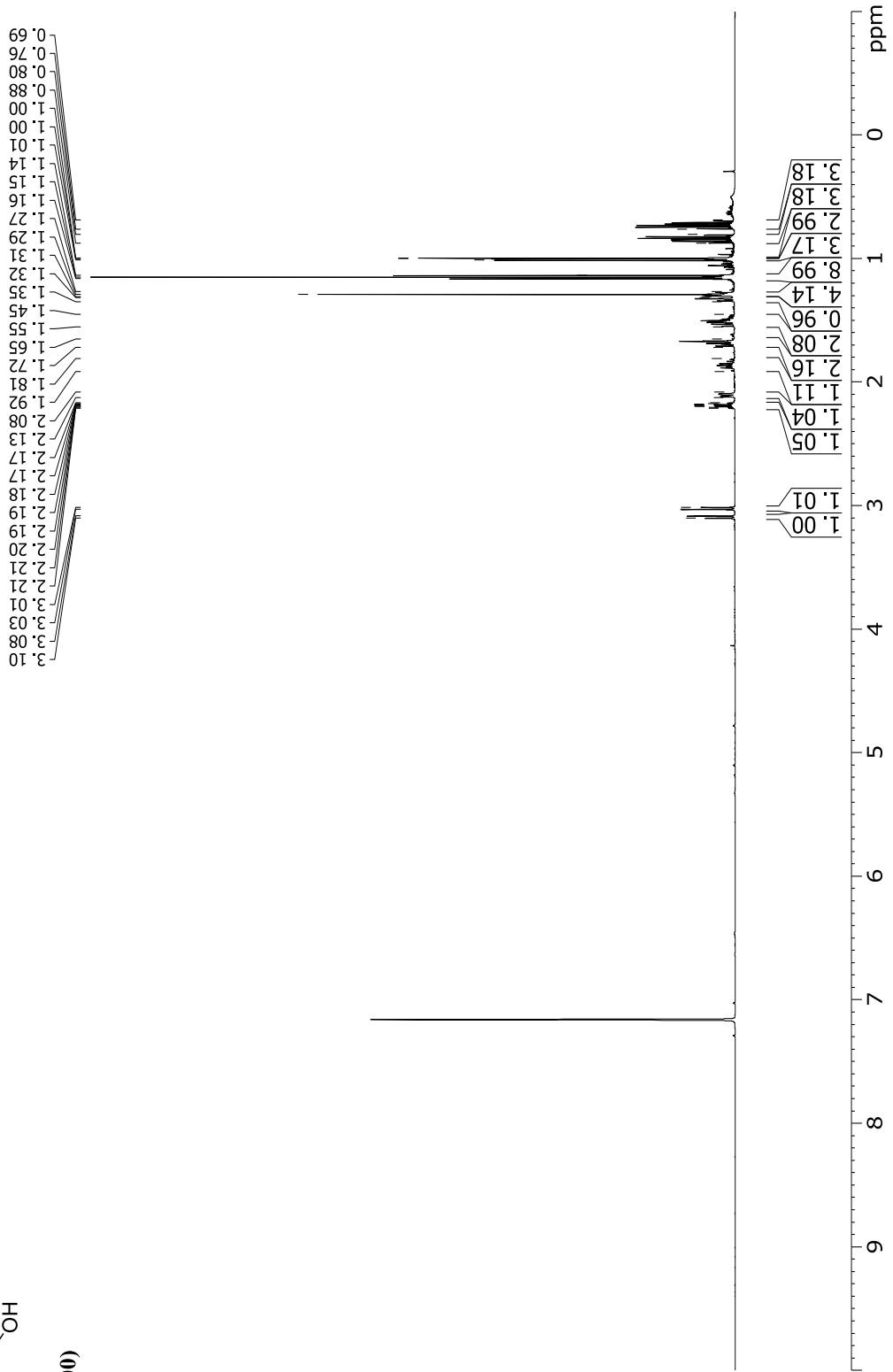
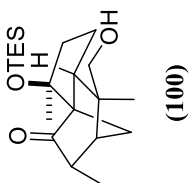


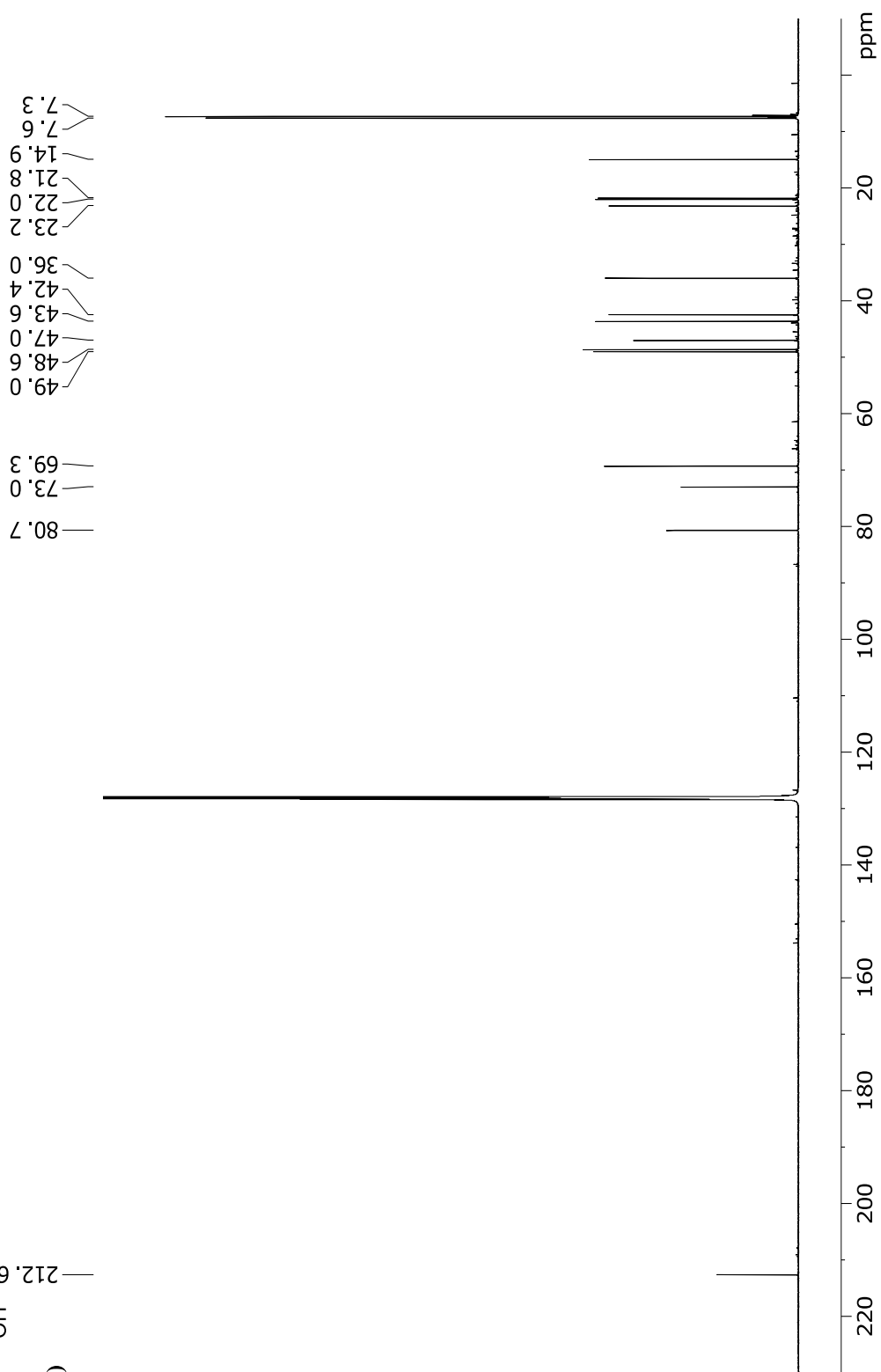
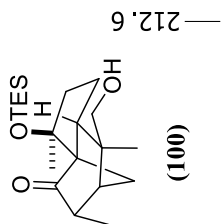


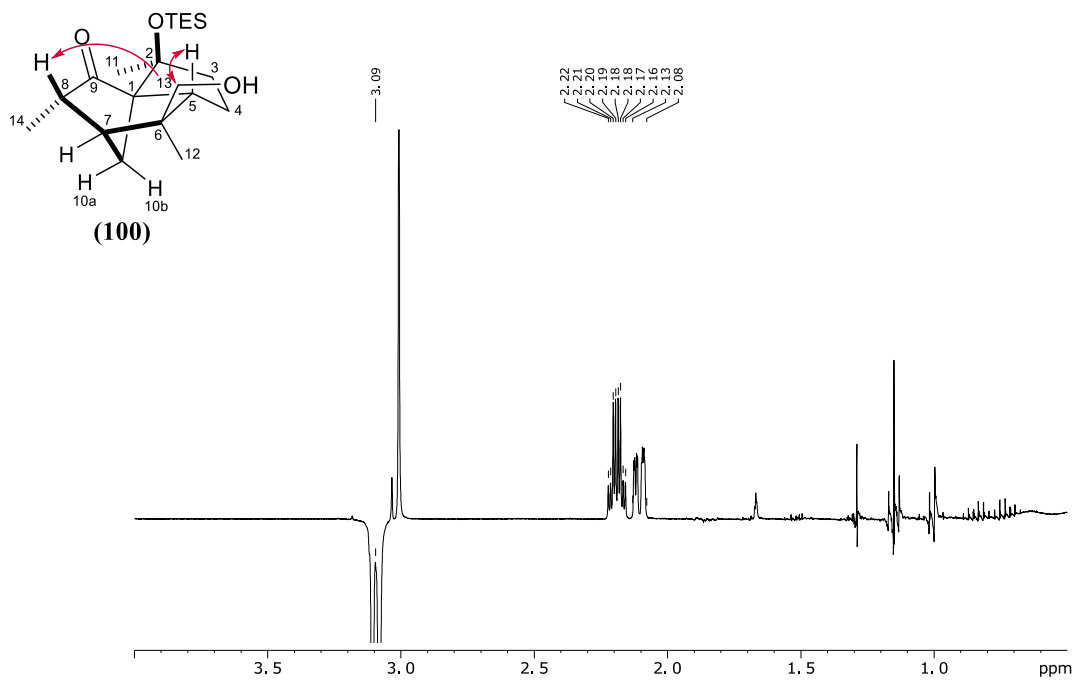


(966)

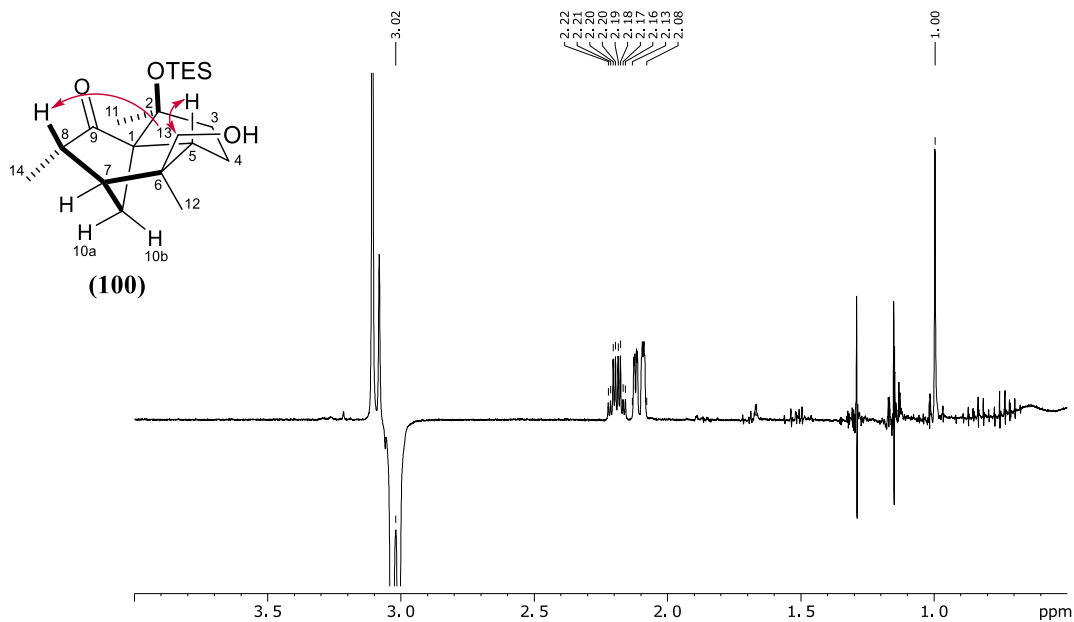




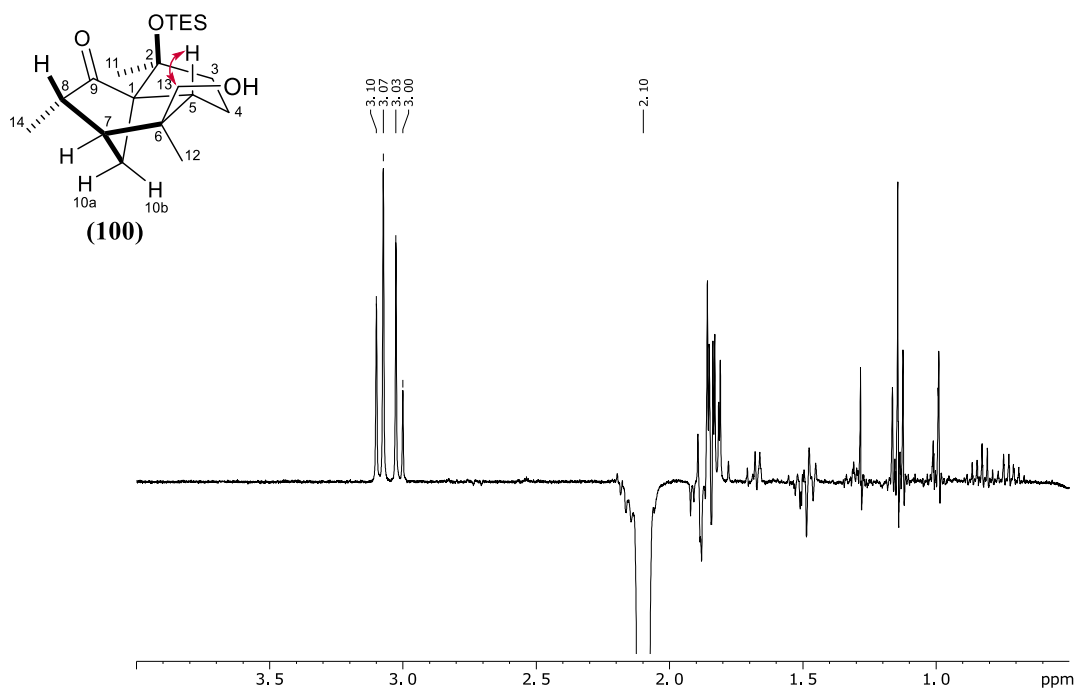




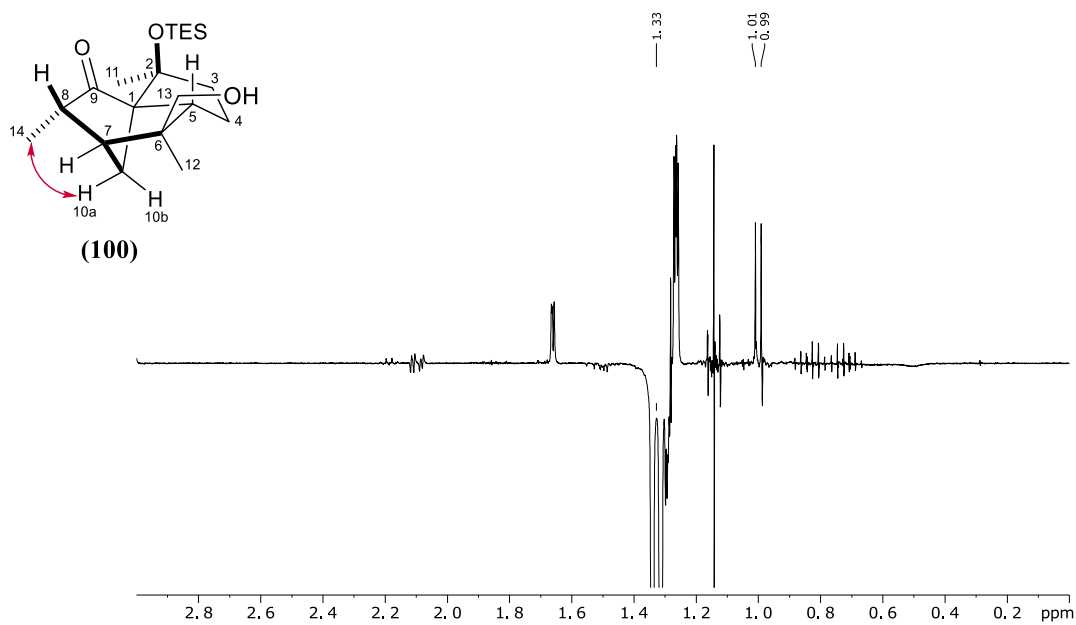
NOE response of cyclization product **(100)** after irradiation at 3.09 ppm (CH₂-13a) measured in C₆D₆ at 400 MHz.



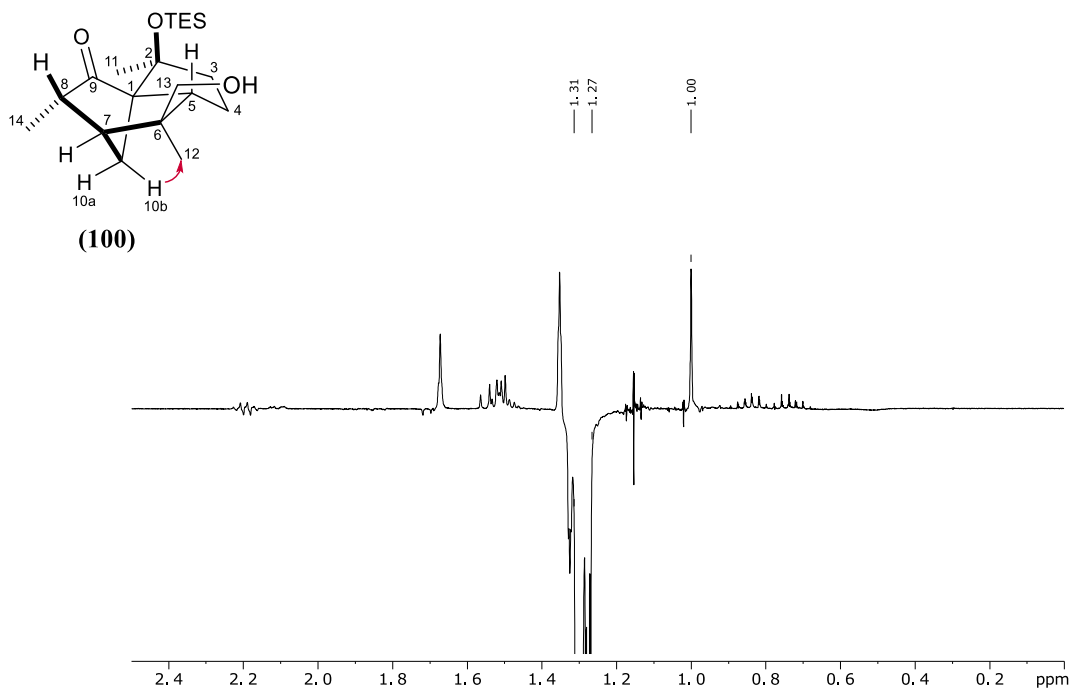
NOE response of cyclization product **(100)** after irradiation at 3.02 ppm (CH₂-13b) measured in C₆D₆ at 400 MHz.



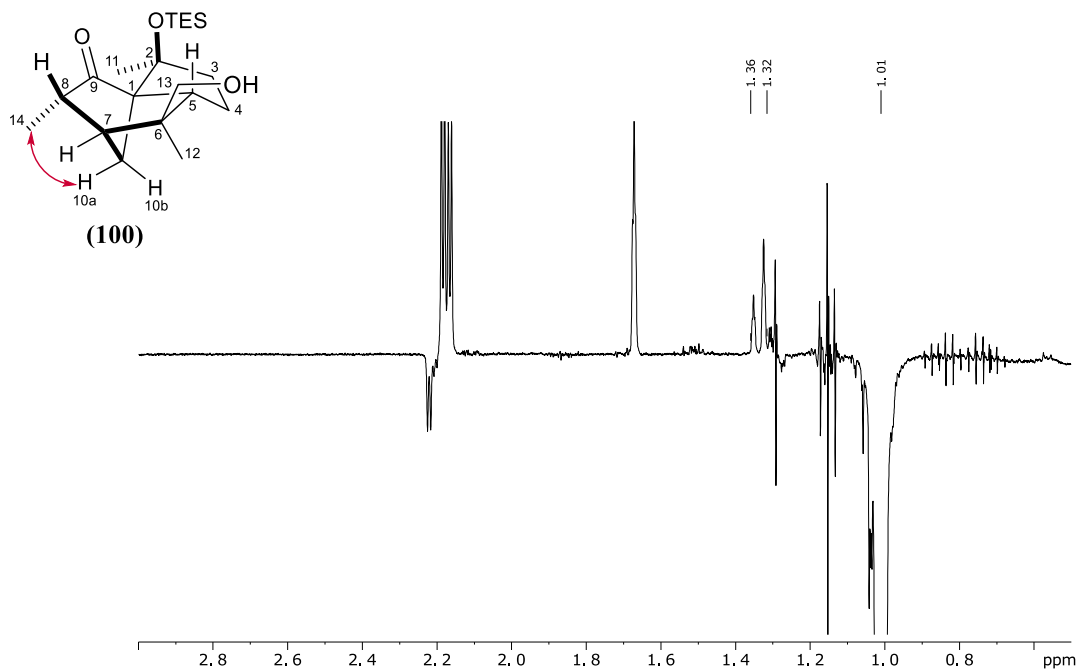
NOE response of cyclization product **(100)** after irradiation at 2.10 ppm (CH-5) measured in C_6D_6 at 400 MHz.



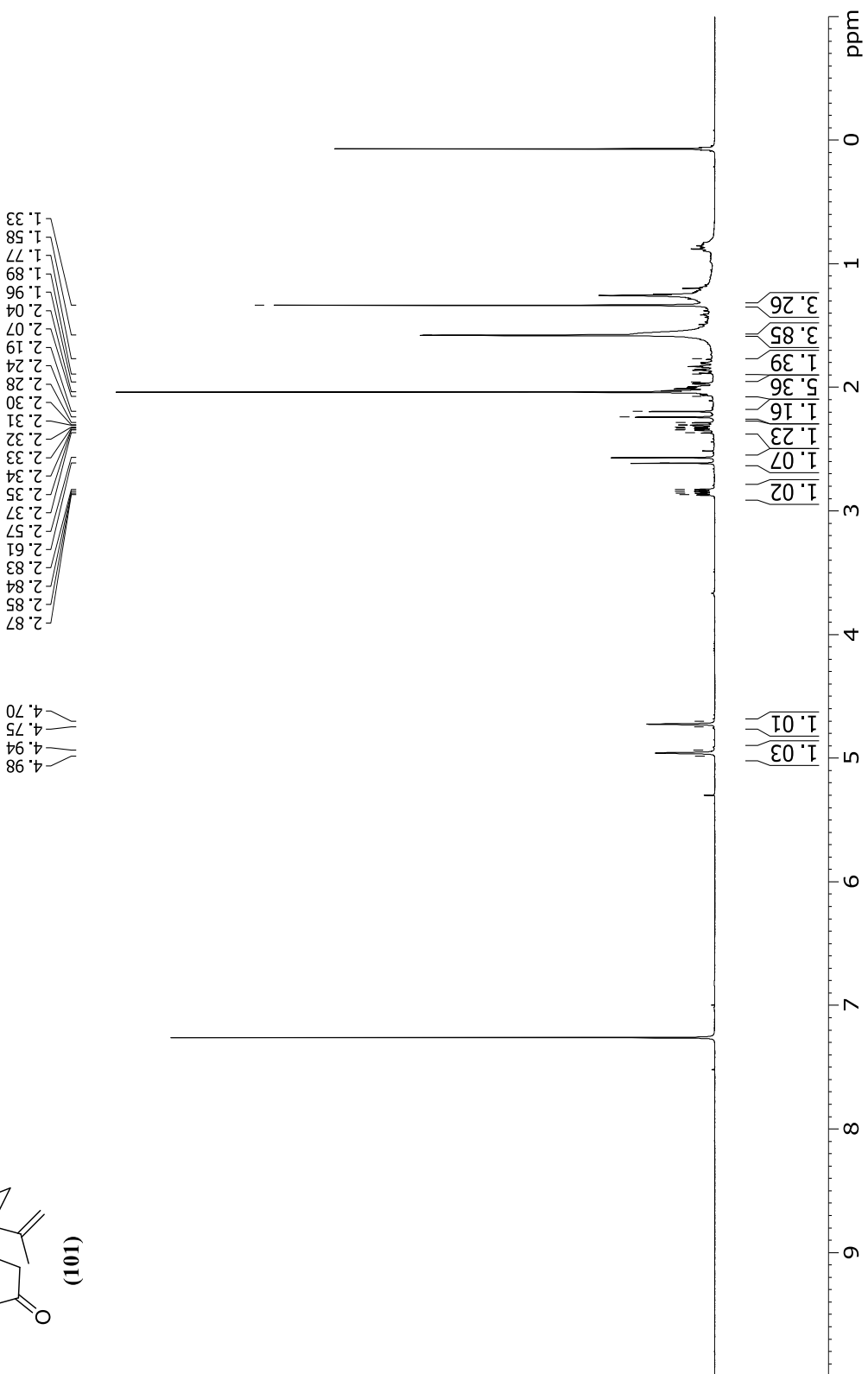
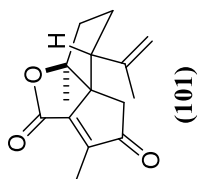
NOE response of cyclization product **(100)** after irradiation at 1.33 ppm (CH₂-10a) measured in C_6D_6 at 400 MHz.

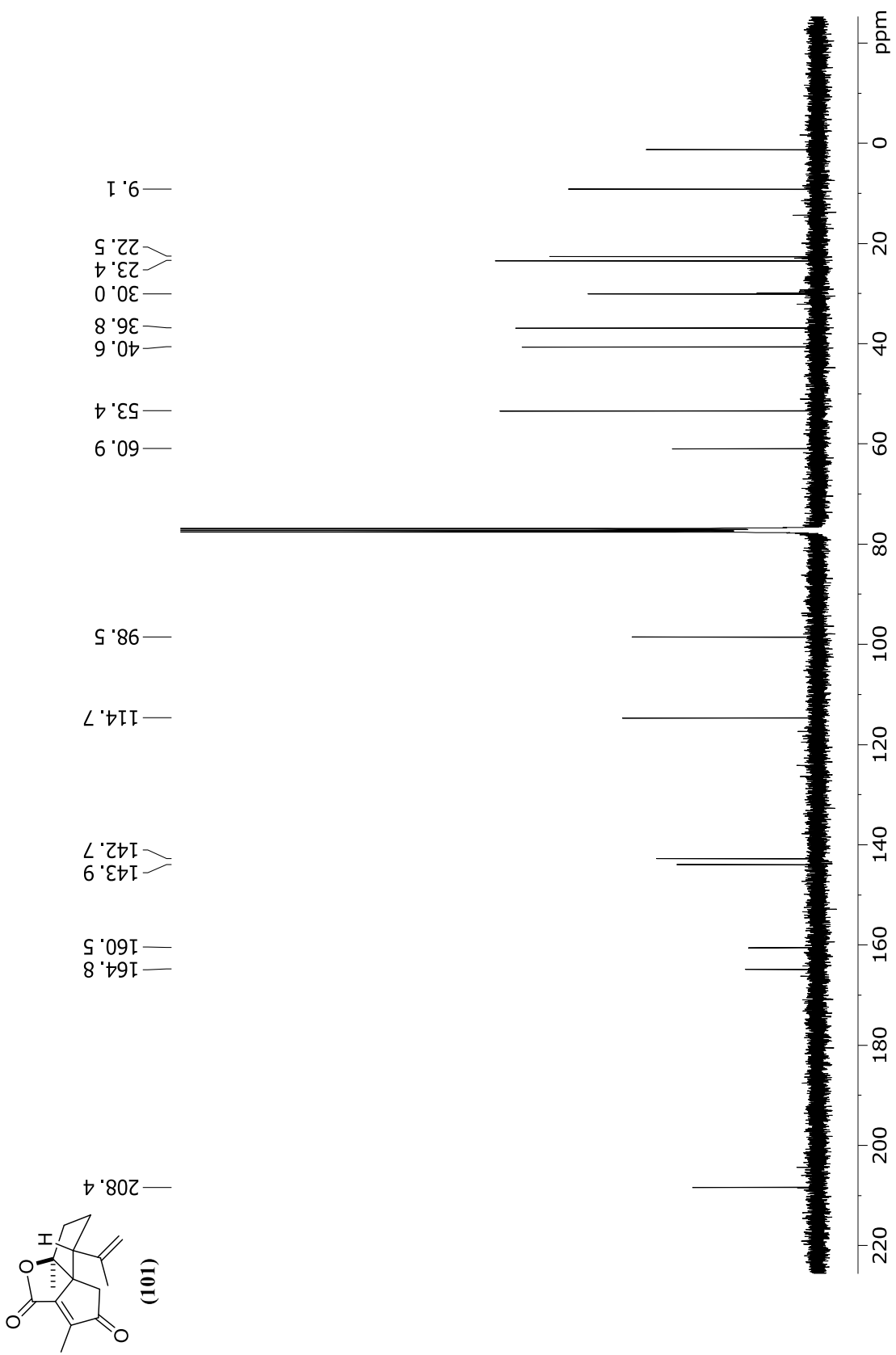


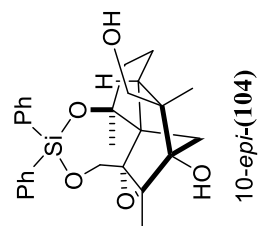
NOE response of cyclization product **(100)** after irradiation at 1.27 ppm (CH₂-10b) measured in C₆D₆ at 400 MHz.



NOE response of cyclization product **(100)** after irradiation at 1.01 ppm (CH₃-14) measured in C₆D₆ at 400 MHz.

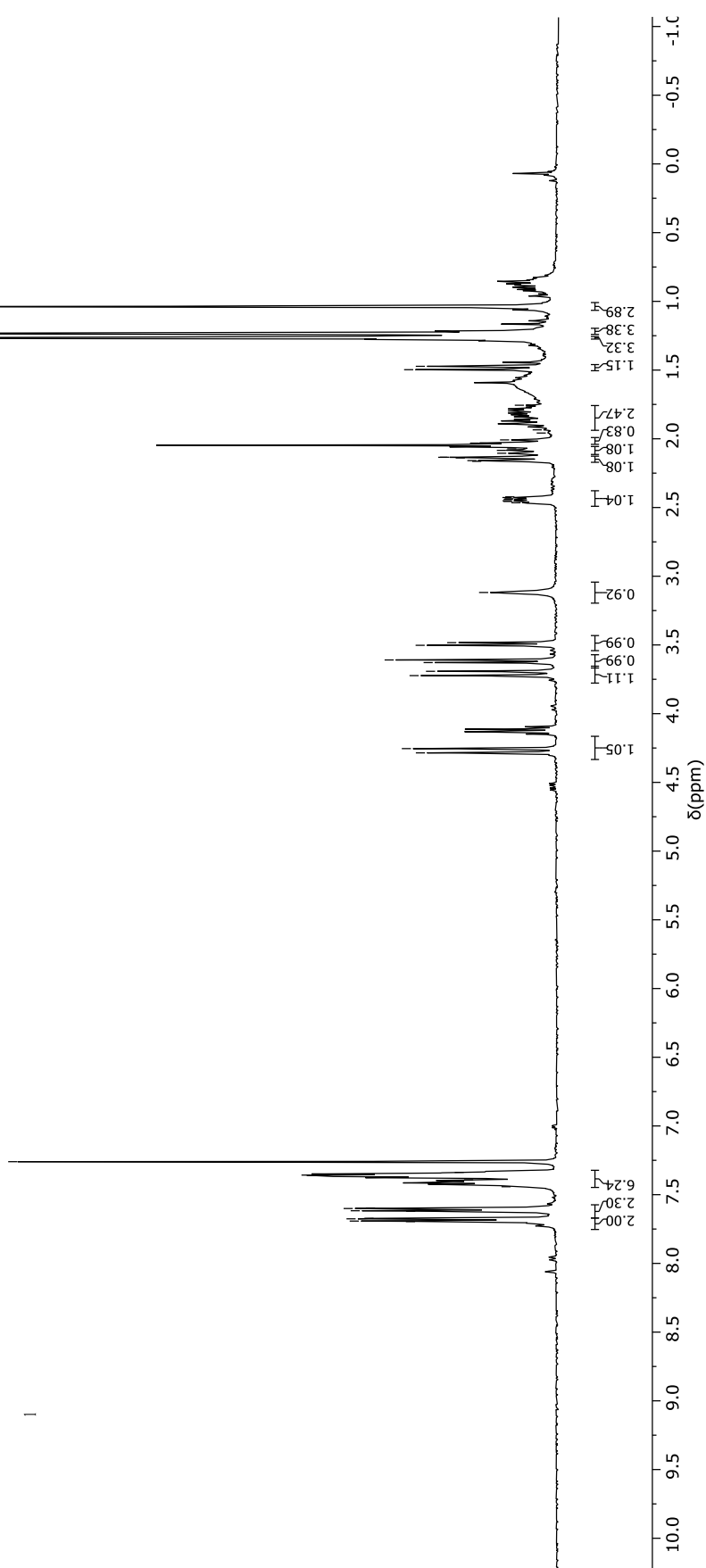


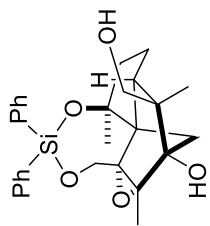




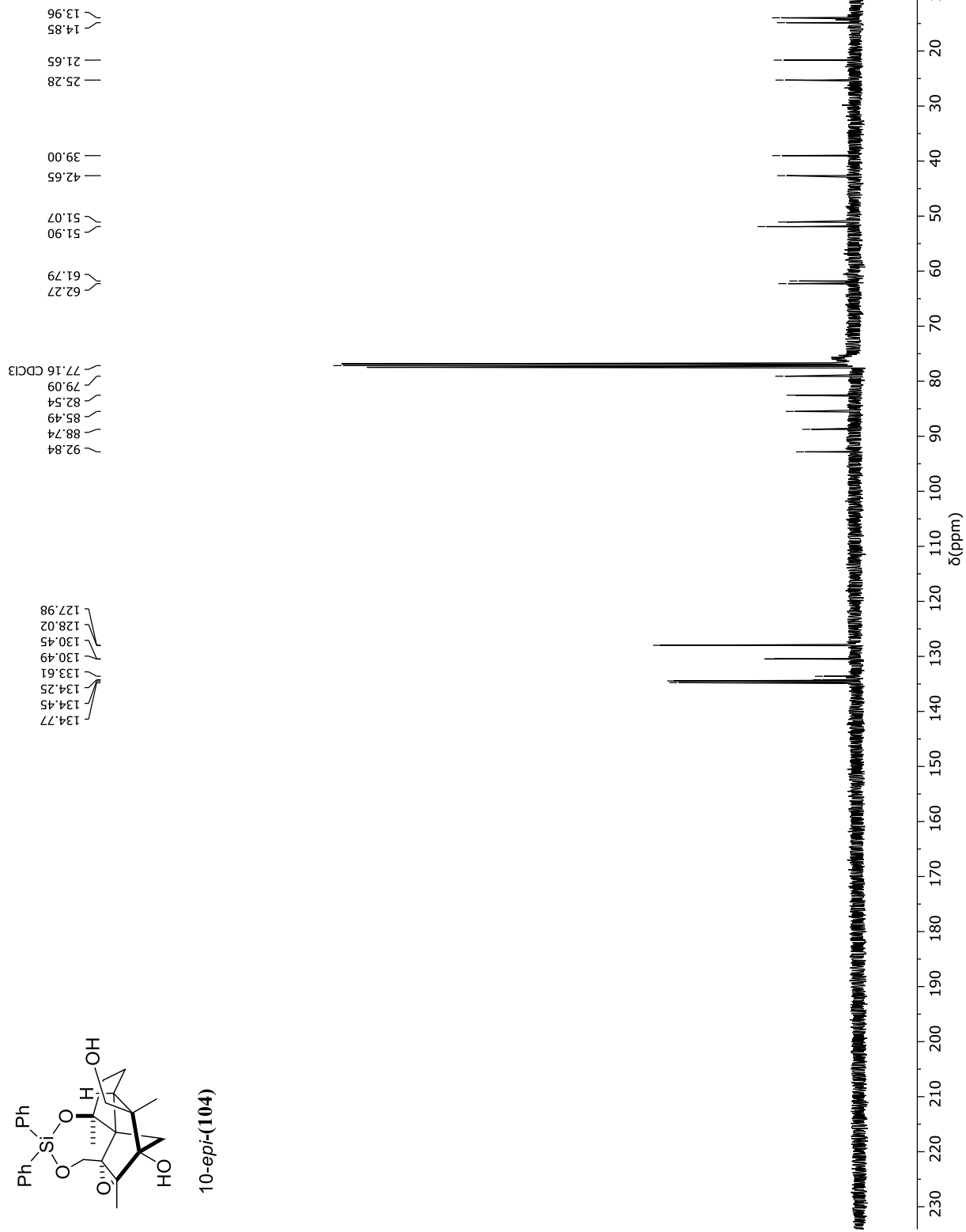
7.26 CDCl₃
 7.34
 7.36
 7.39
 7.41
 7.44
 7.60
 7.60
 7.62
 7.62
 7.67
 7.68
 7.69
 7.70

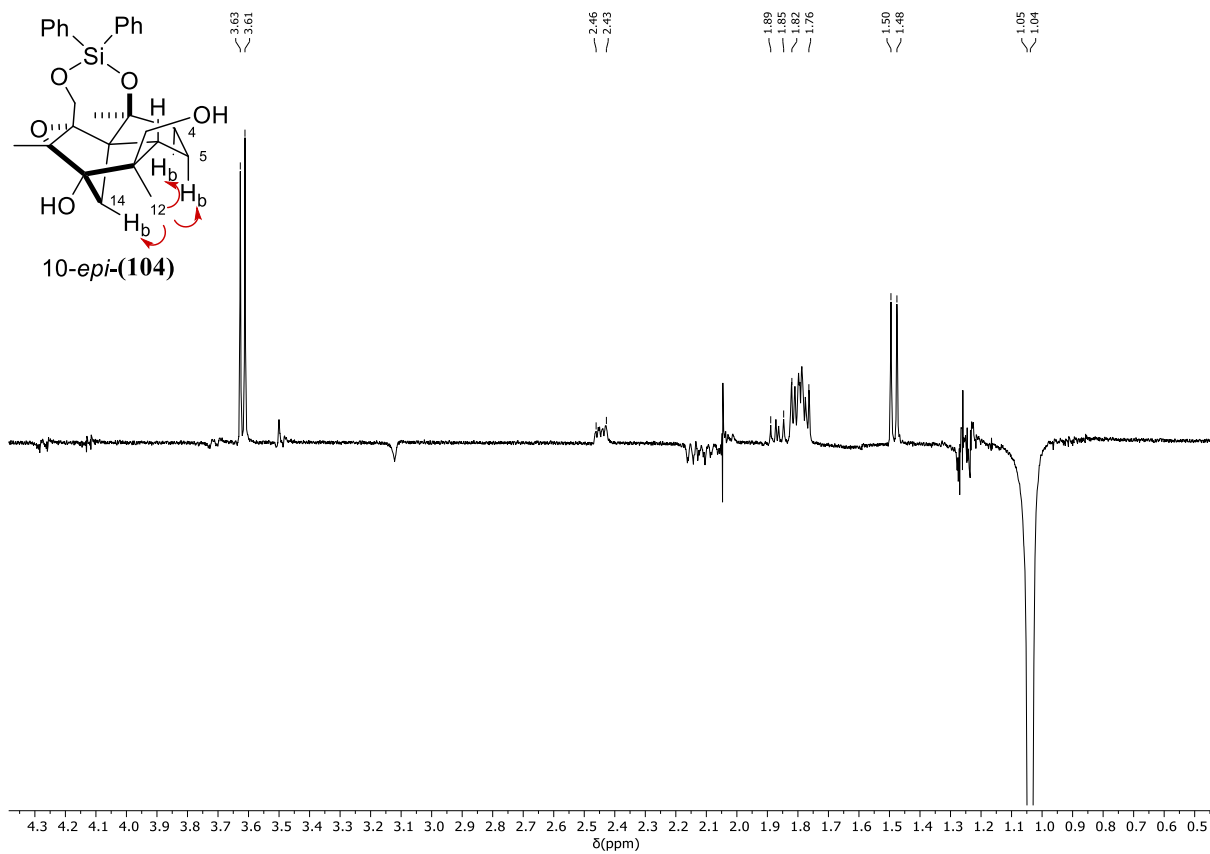
4.25
 4.29
 3.72
 3.69
 3.63
 3.61
 3.50
 3.48
 3.12
 2.47
 2.46
 2.45
 2.44
 2.44
 2.43
 2.42
 2.16
 2.14
 2.13
 2.13
 2.11
 2.08
 2.07
 2.03
 2.01
 1.96
 1.93
 1.76
 1.50
 1.47
 1.27
 1.23
 1.04



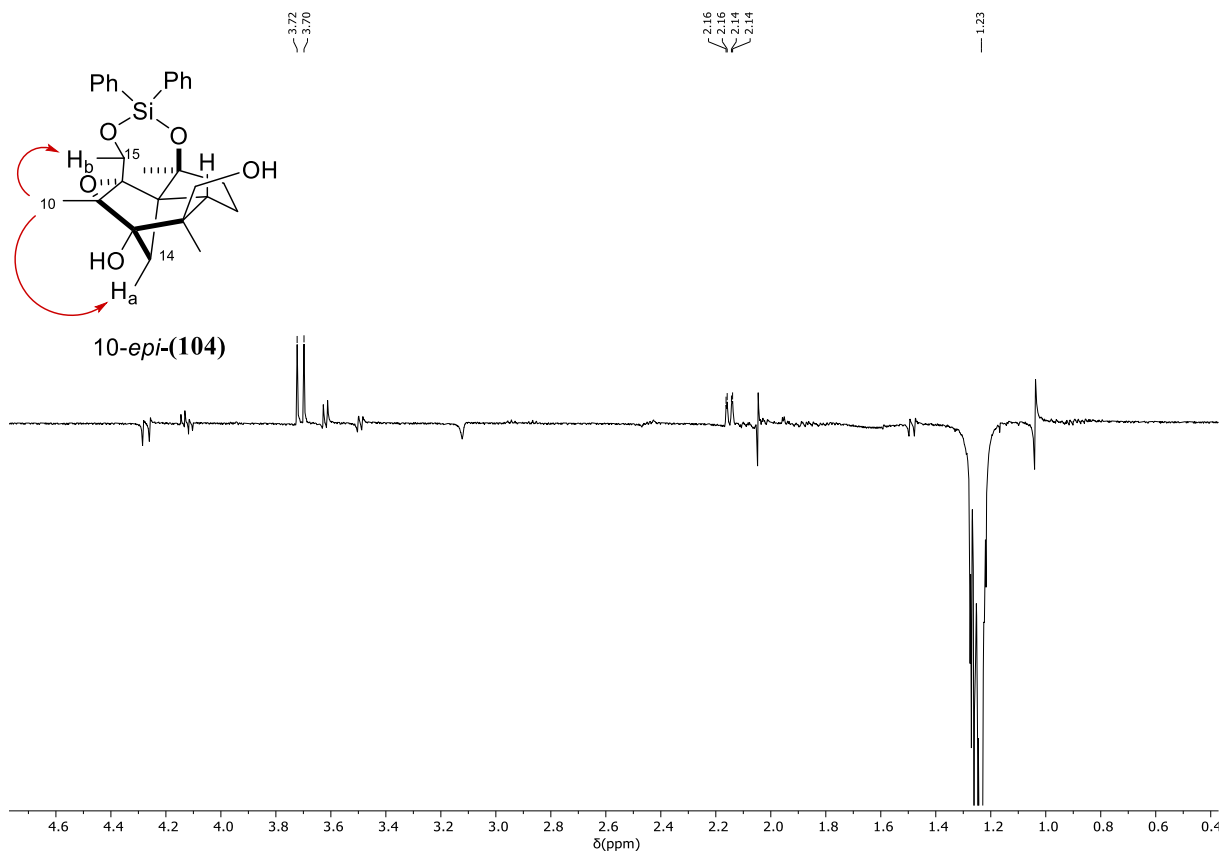


10-epi-(104)

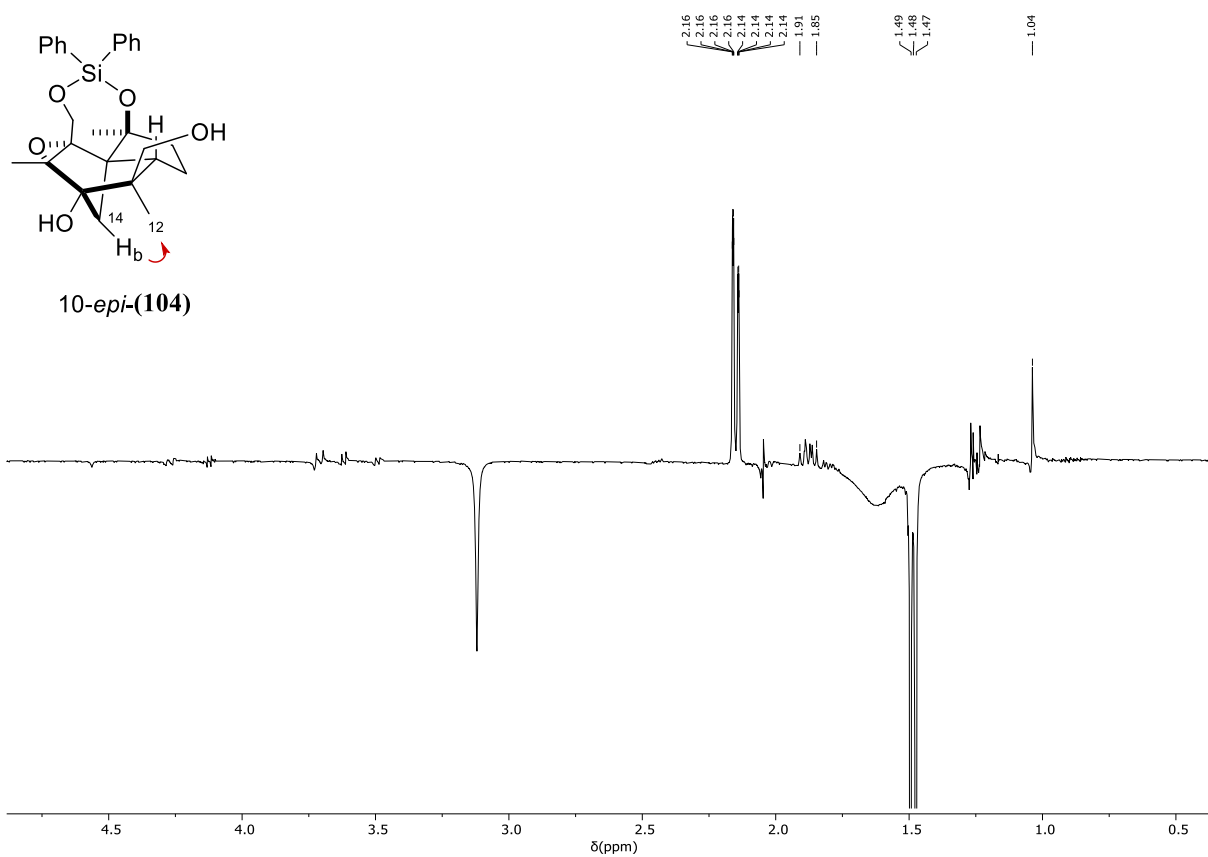




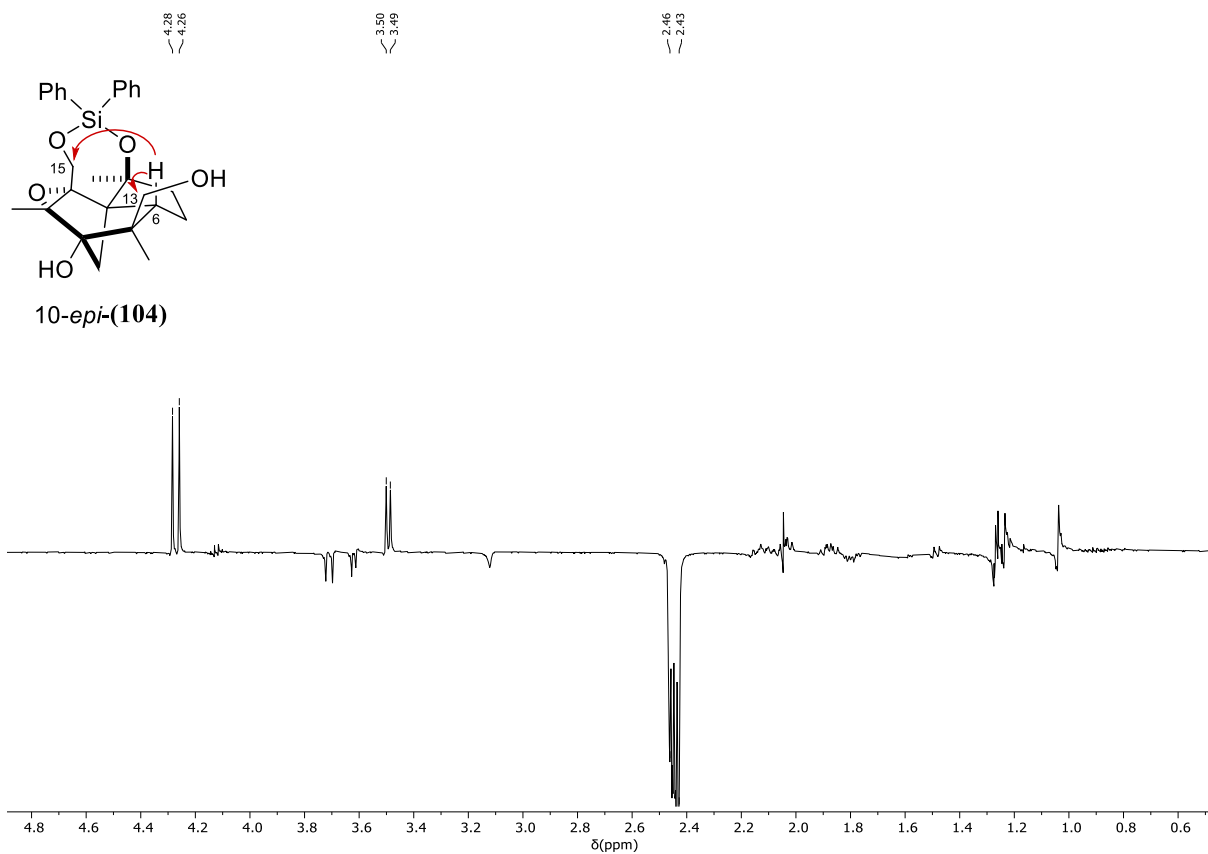
NOE response of **10-epi-(104)** after irradiation at 1.04 ppm (CH_3 -12). Spectrum measured in $CDCl_3$ at 400 MHz.



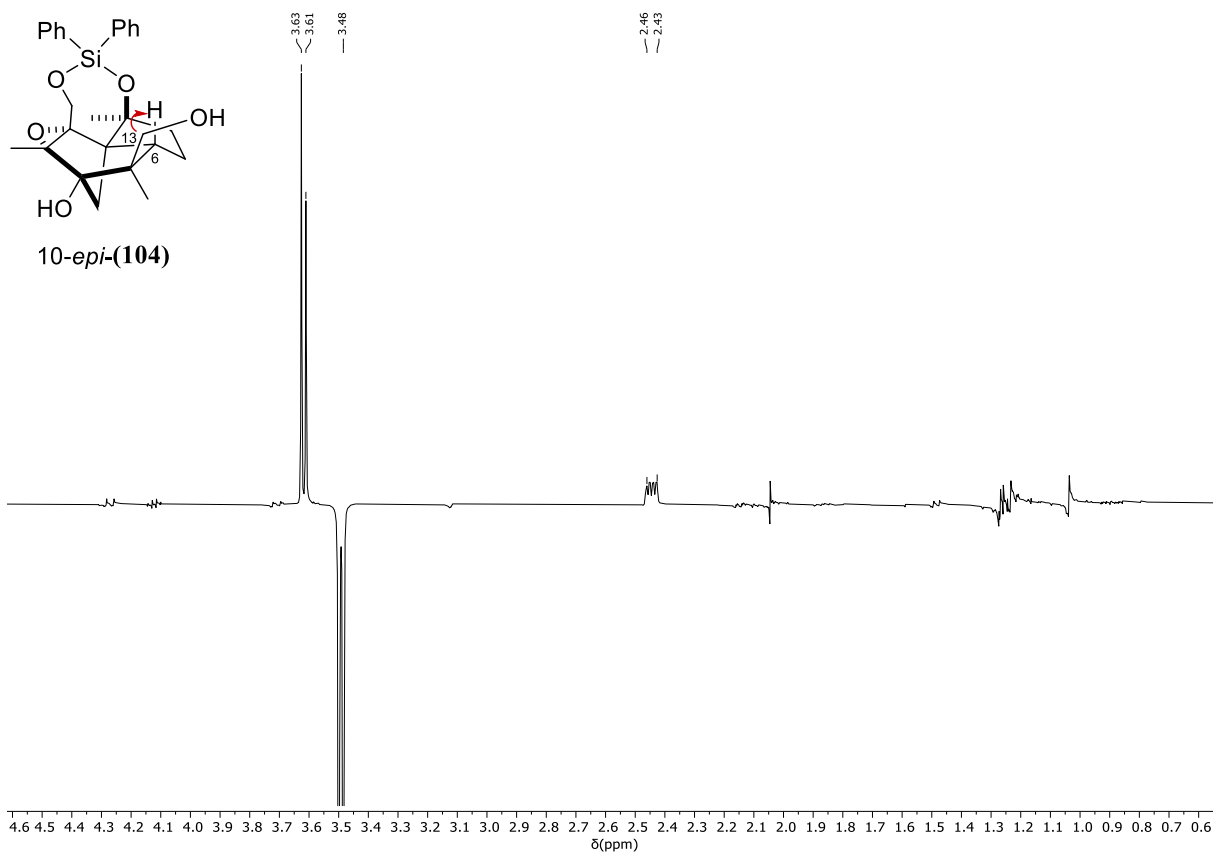
NOE response of **10-epi-(104)** after irradiation at 1.23 ppm (CH_3 -10). Spectrum measured in $CDCl_3$ at 400 MHz.



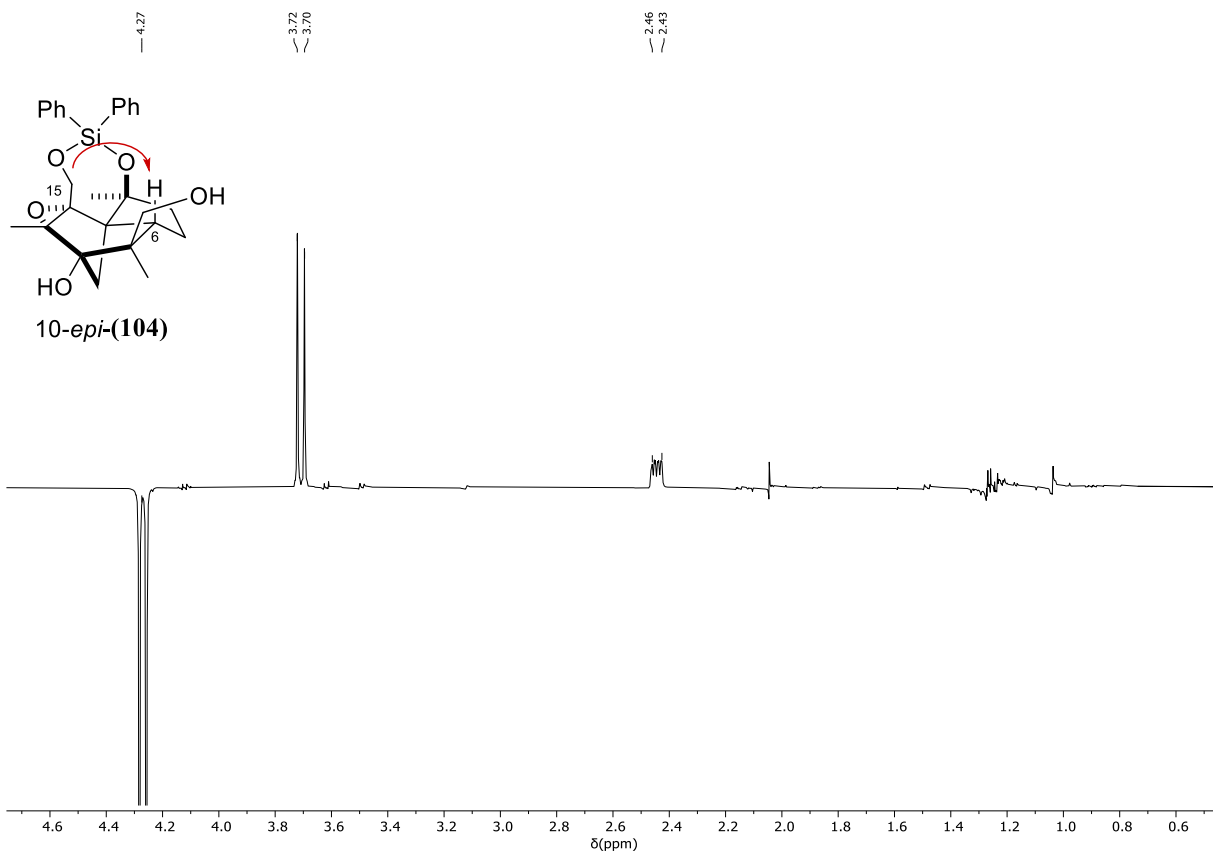
NOE response of **10-*epi*-(104)** after irradiation at 1.48 ppm (CH₂-14b). Spectrum measured in CDCl₃ at 400 MHz.



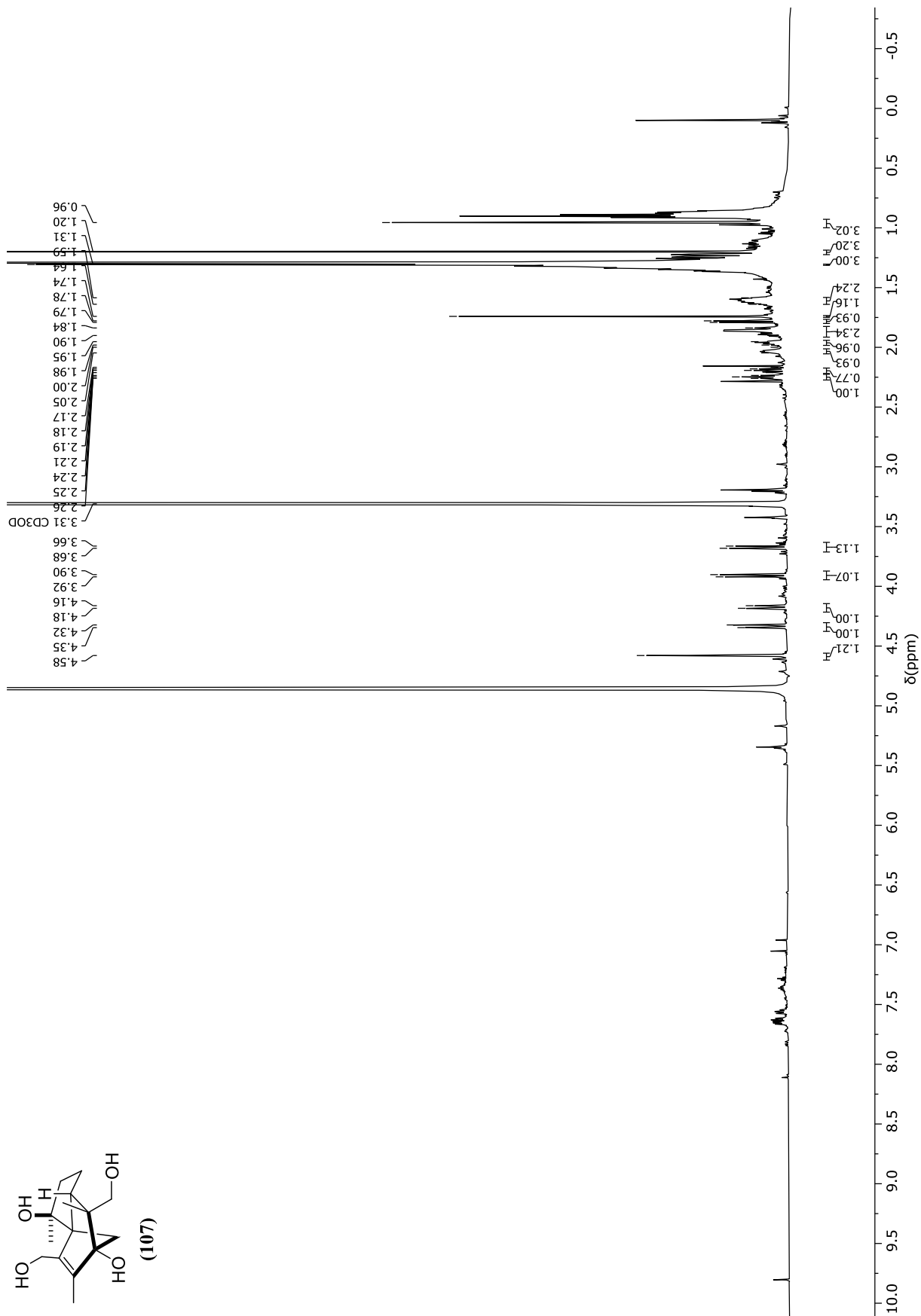
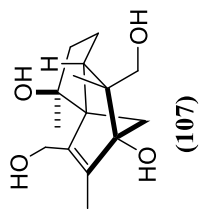
NOE response of **10-*epi*-(104)** after irradiation at 2.44 ppm (CH-6). Spectrum measured in CDCl₃ at 400 MHz.

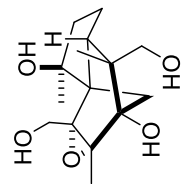


NOE response of **10-*epi*-(104)** after irradiation at 3.48 ppm (CH_2 -13b). Spectrum measured in CDCl_3 at 400 MHz.



NOE response of **10-*epi*-(104)** after irradiation at 4.27 ppm (CH_2 -15a). Spectrum measured in CDCl_3 at 400 MHz.

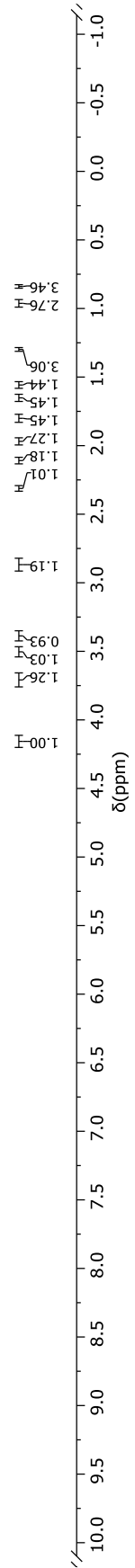


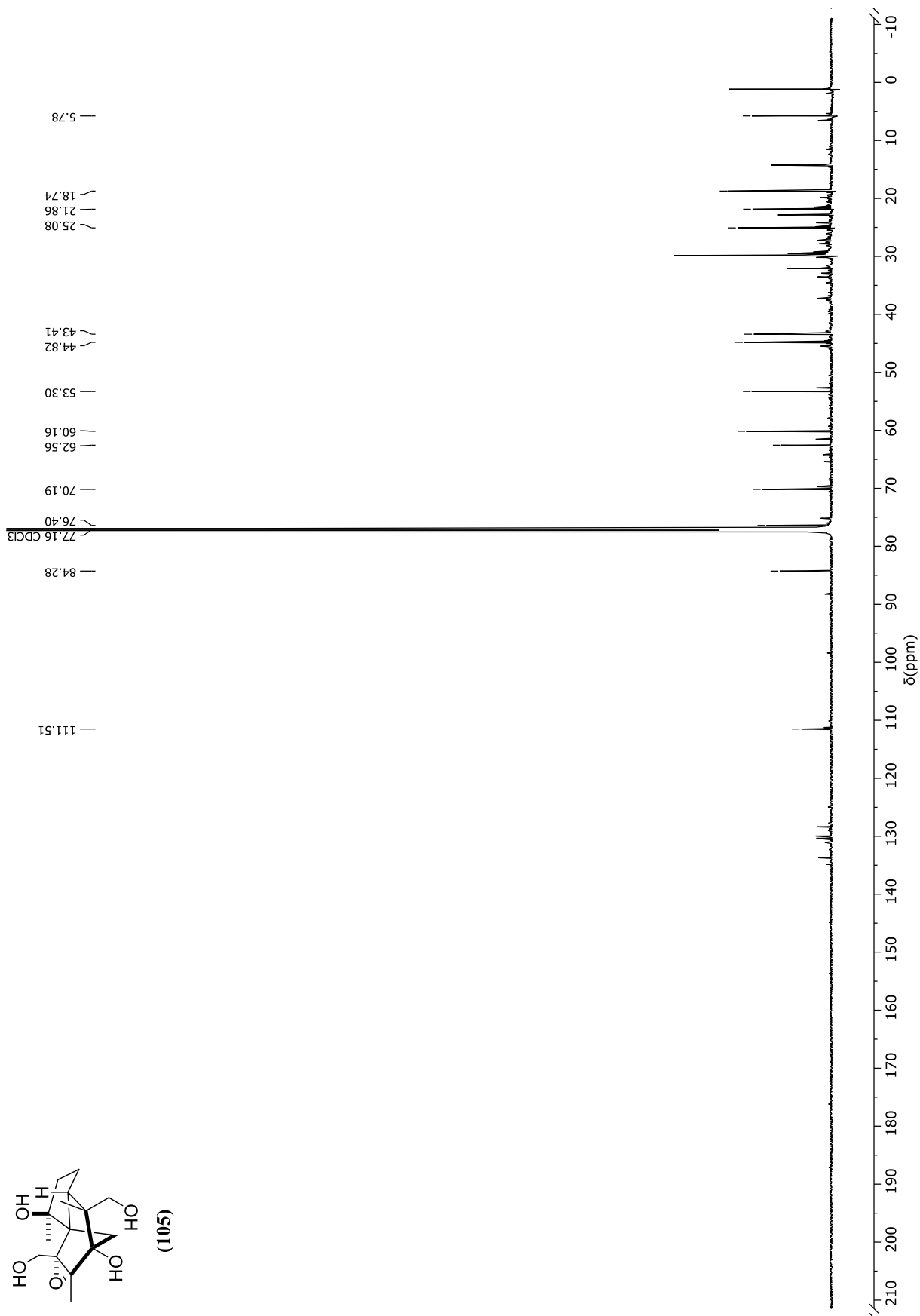
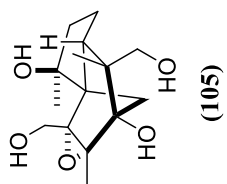


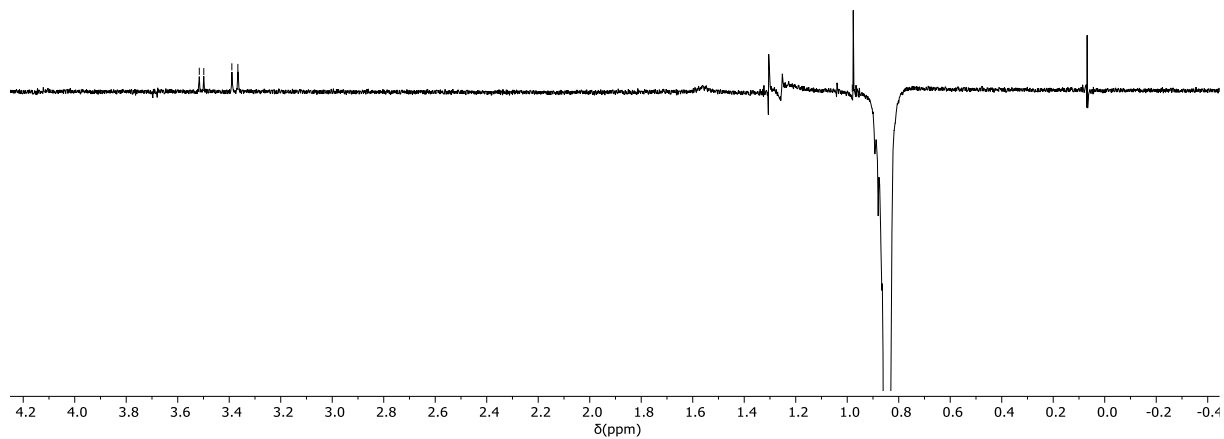
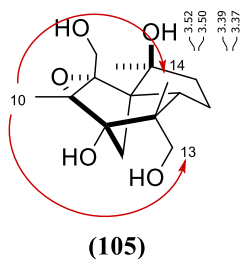
(105)

7.26 CDCl₃

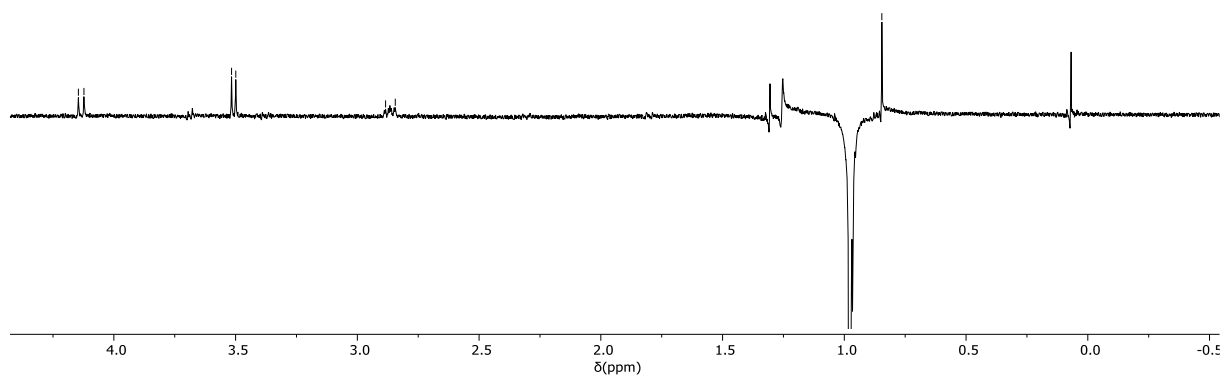
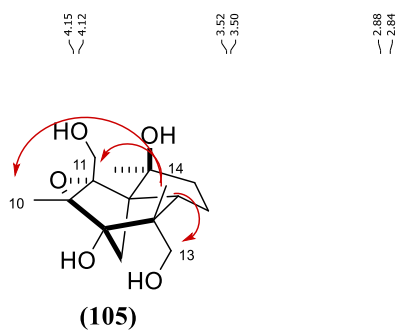
4.14
4.12
3.69
3.68
3.51
3.50
3.39
3.39
3.37
3.37
2.88
2.88
2.87
2.87
2.86
2.86
2.85
2.85
2.32
2.30
2.14
2.10
1.99
1.96
1.81
1.79
1.68
1.62
1.58
1.51
1.30
0.98
0.85



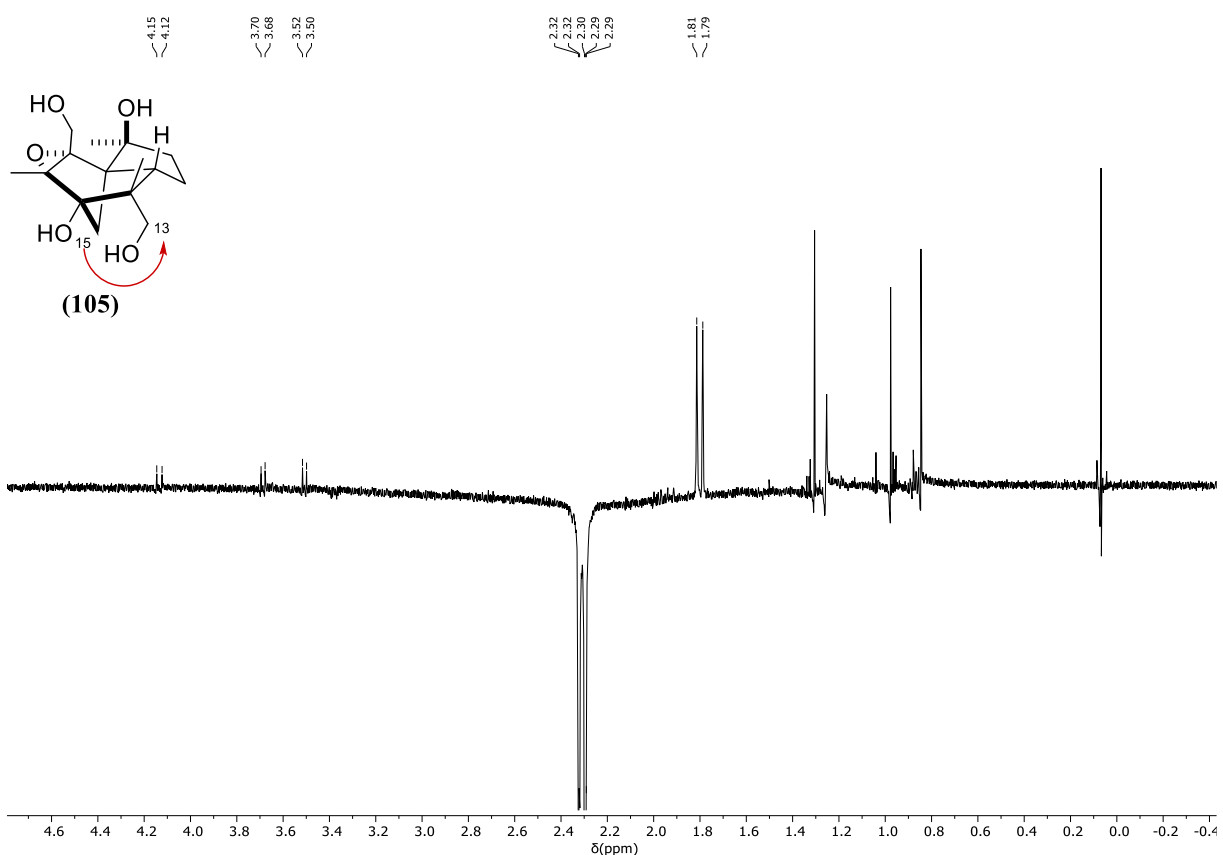
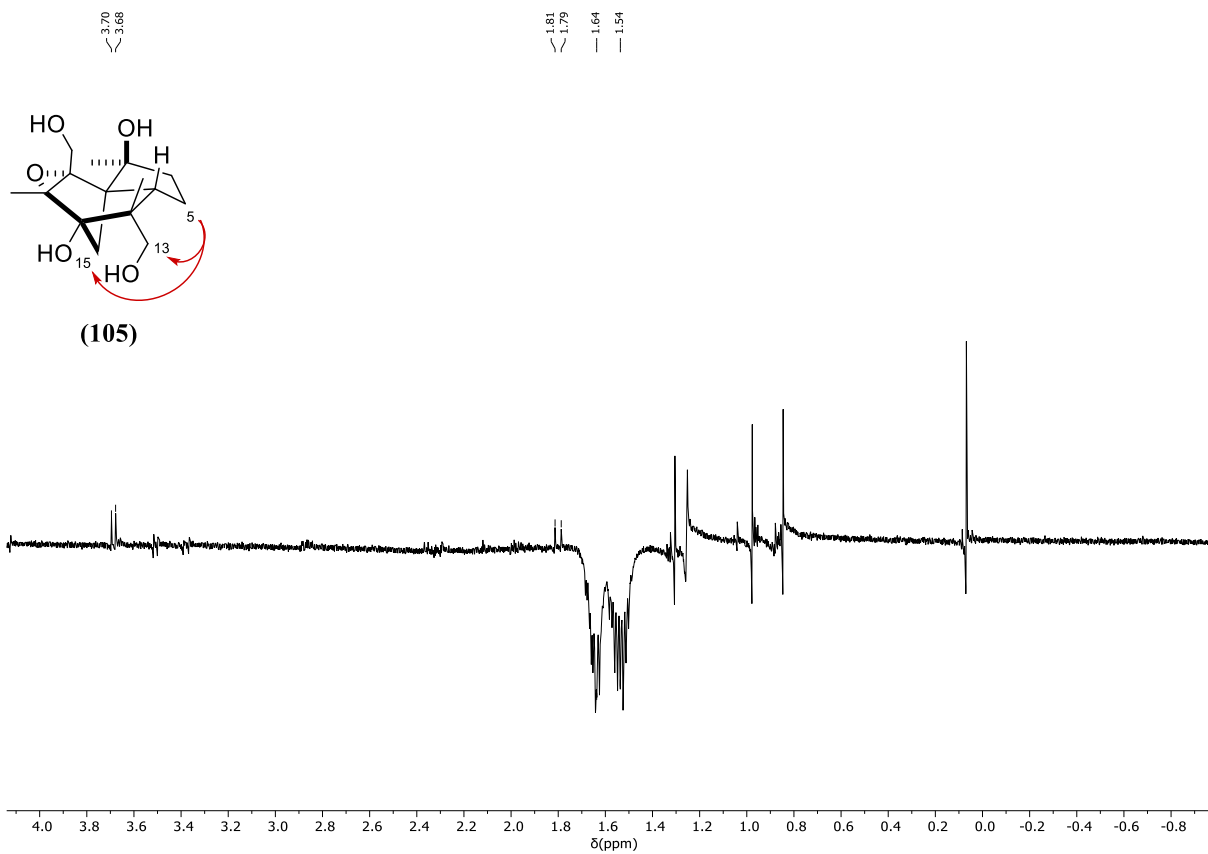


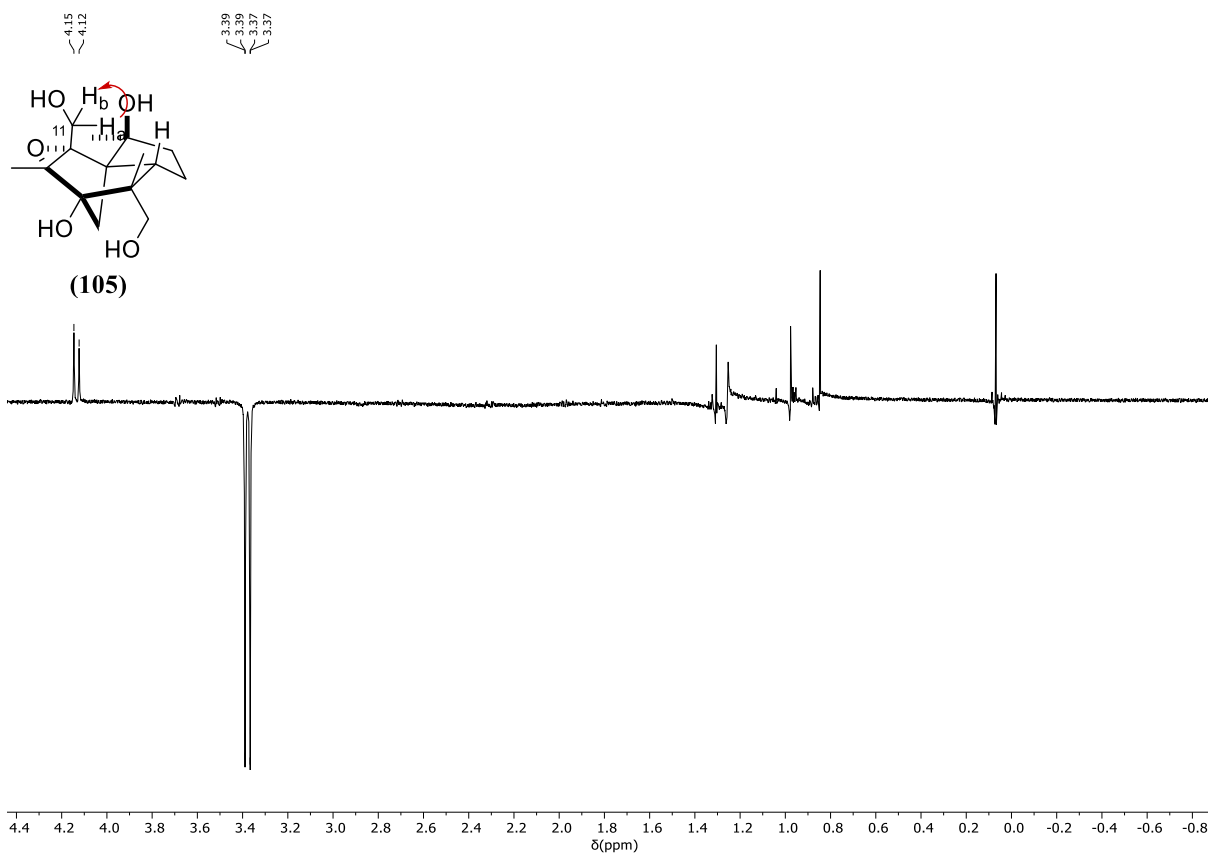
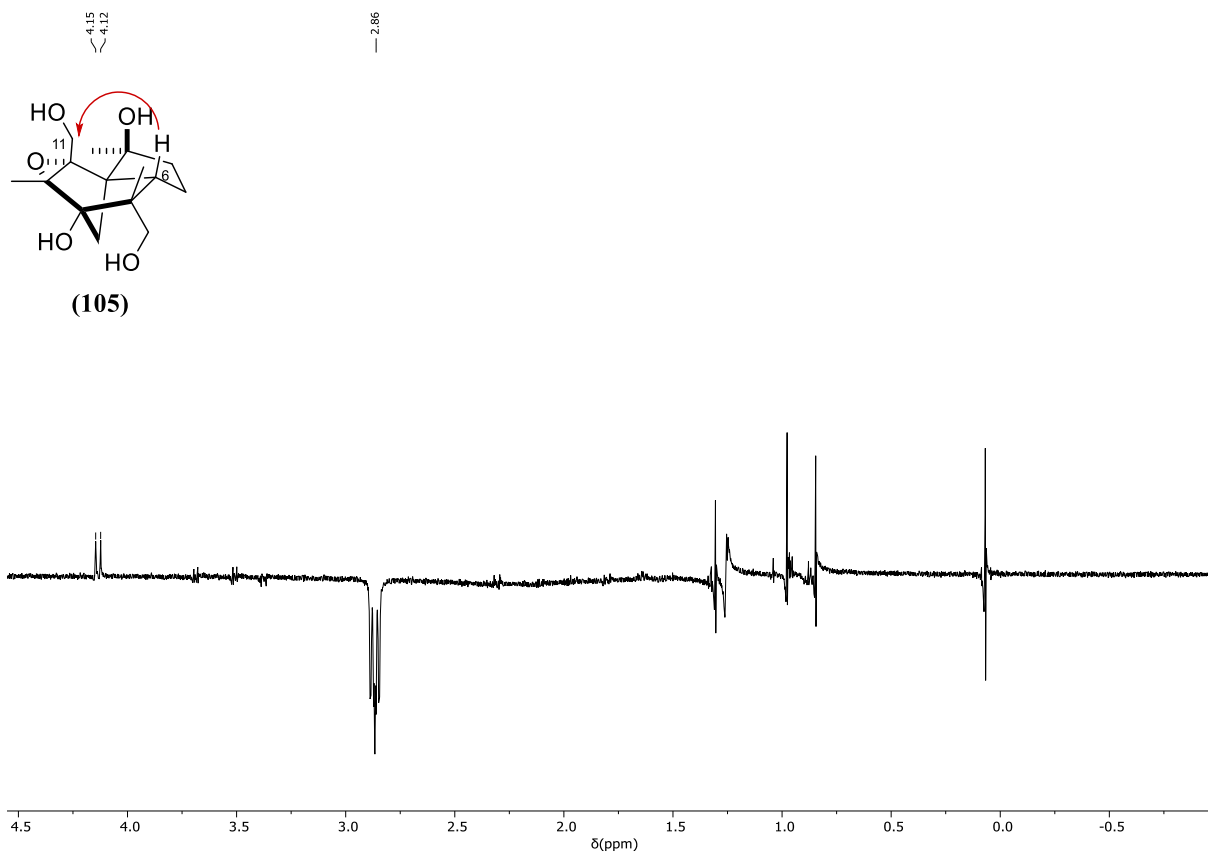


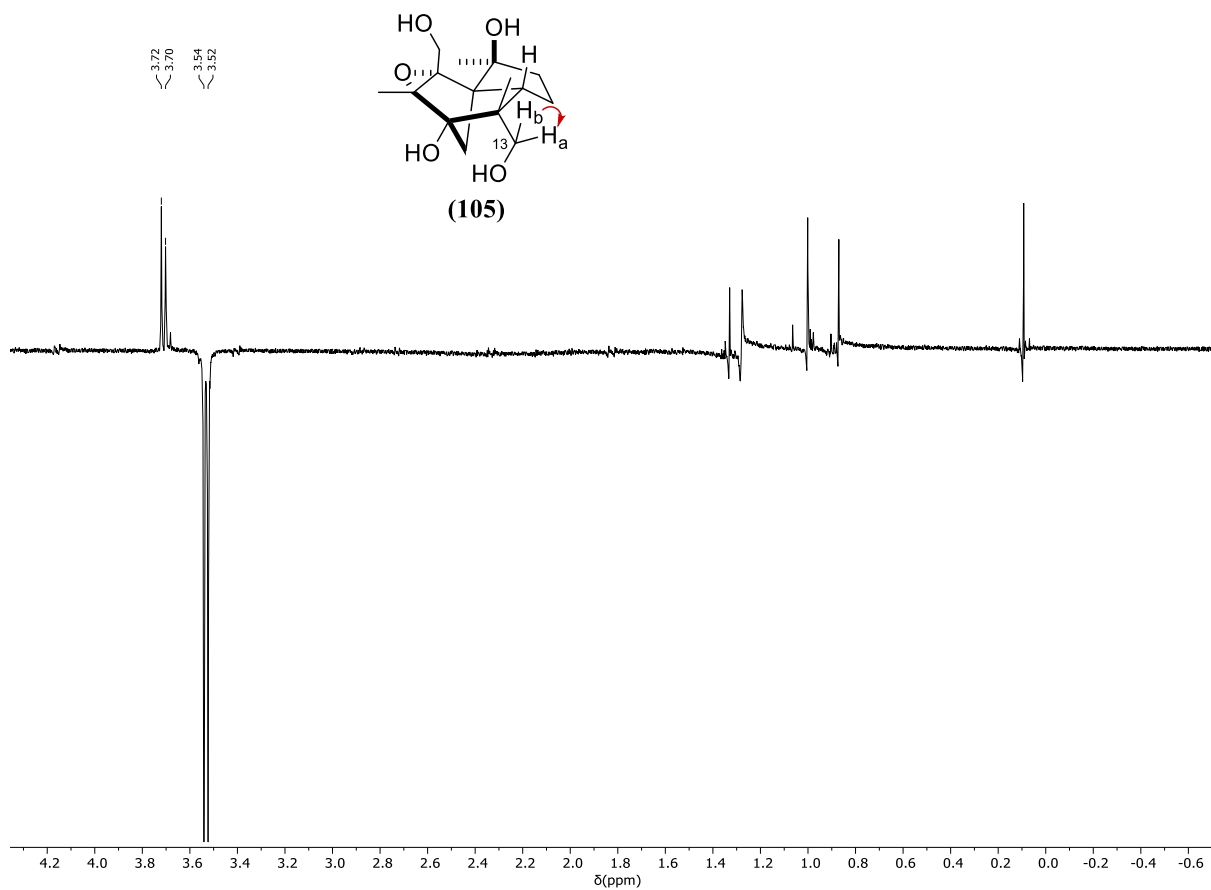
NOE response of epoxytetraol (**105**) after irradiation at 0.86 ppm (CH₃-10). Spectrum measured in CDCl₃ at 400 MHz.



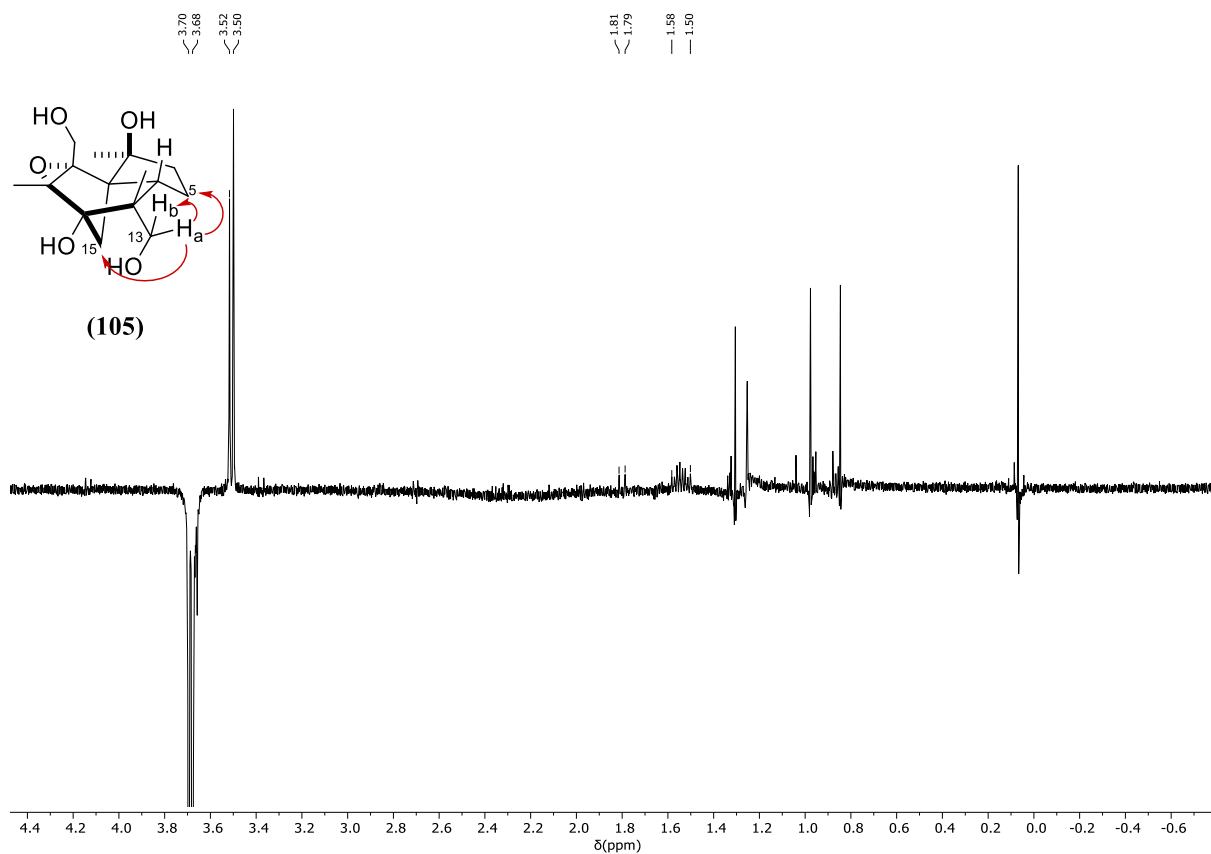
NOE response of epoxytetraol (**105**) after irradiation at 0.98 ppm (CH₃-14). Spectrum measured in CDCl₃ at 400 MHz.



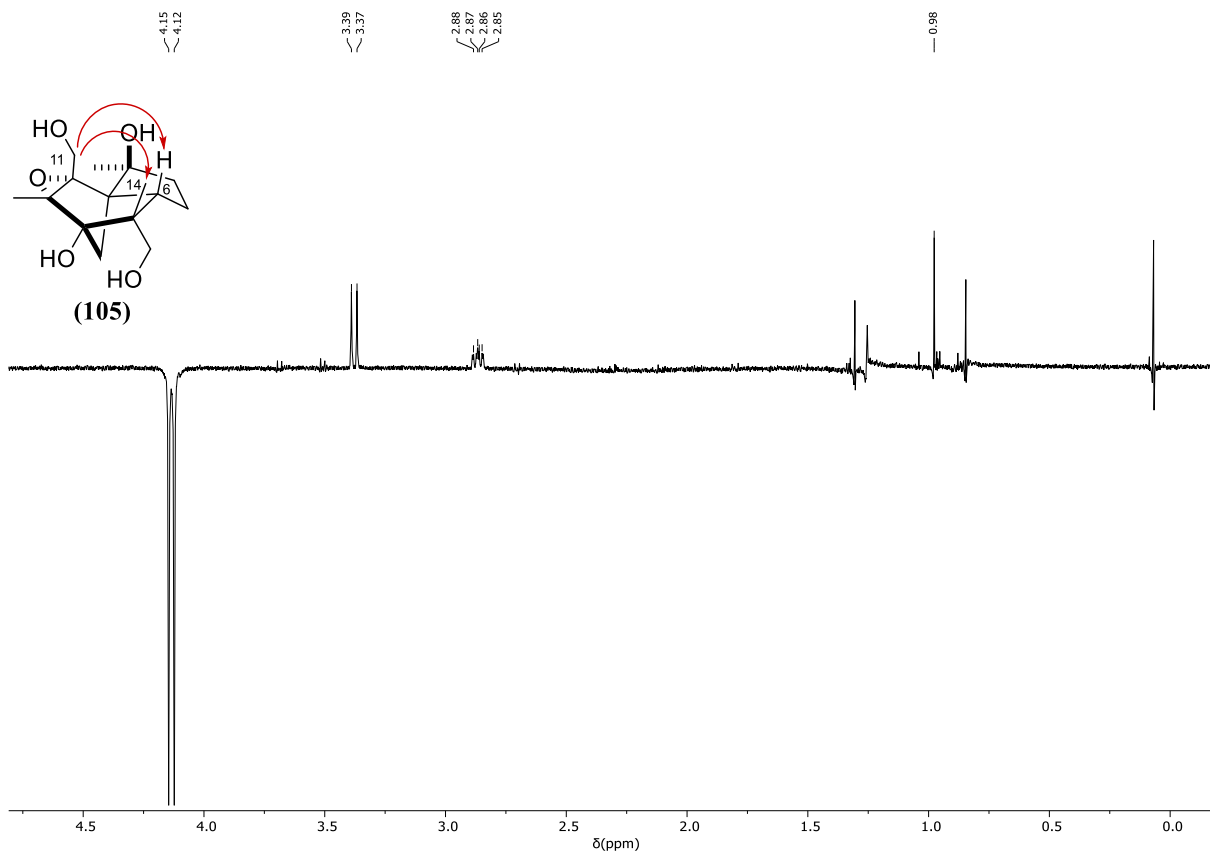




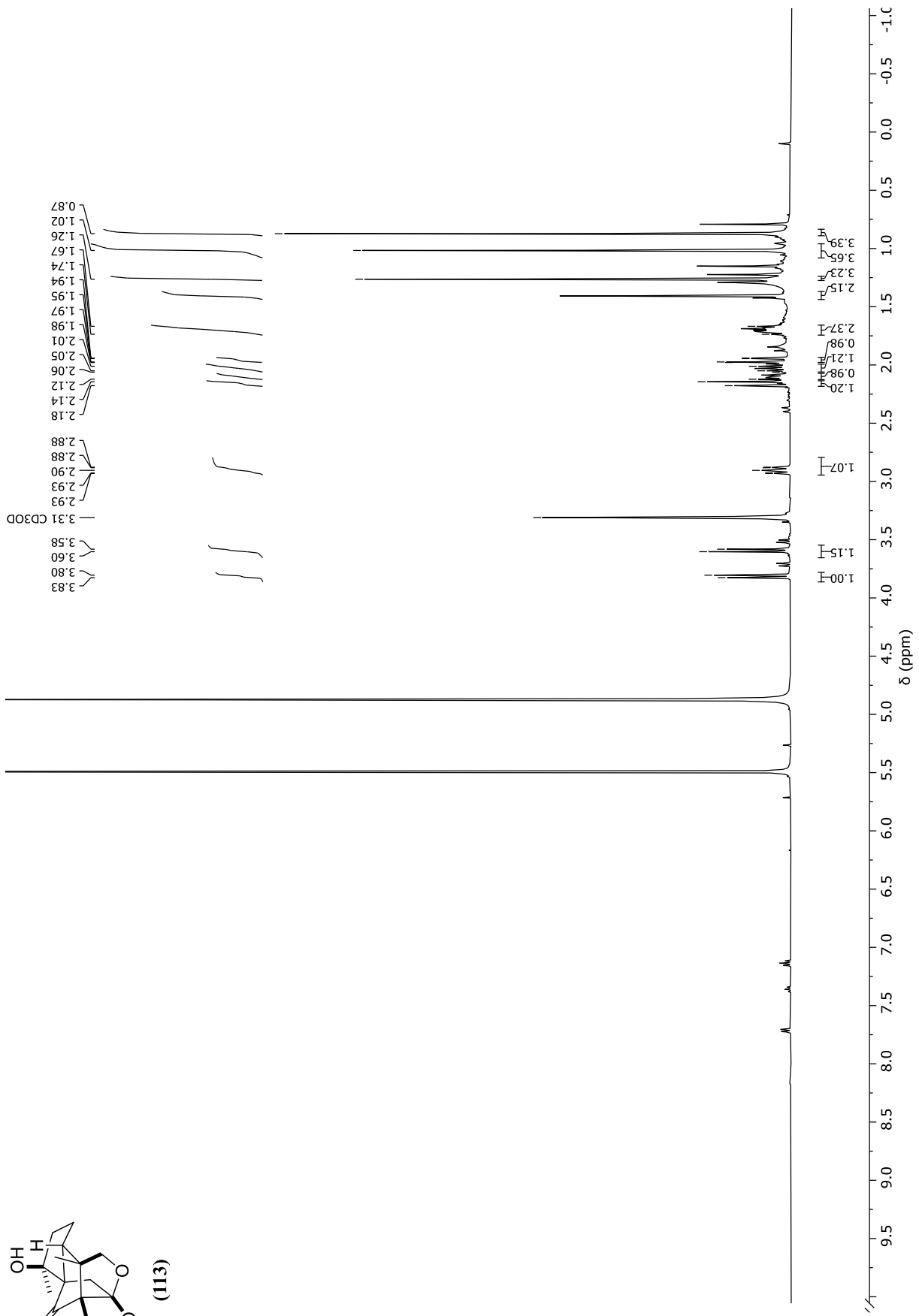
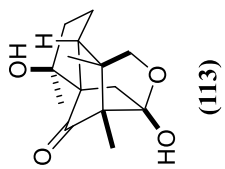
NOE response of epoxytetraol (**105**) after irradiation at 3.53 ppm (CH₂-13b). Spectrum measured in CDCl₃ at 400 MHz.

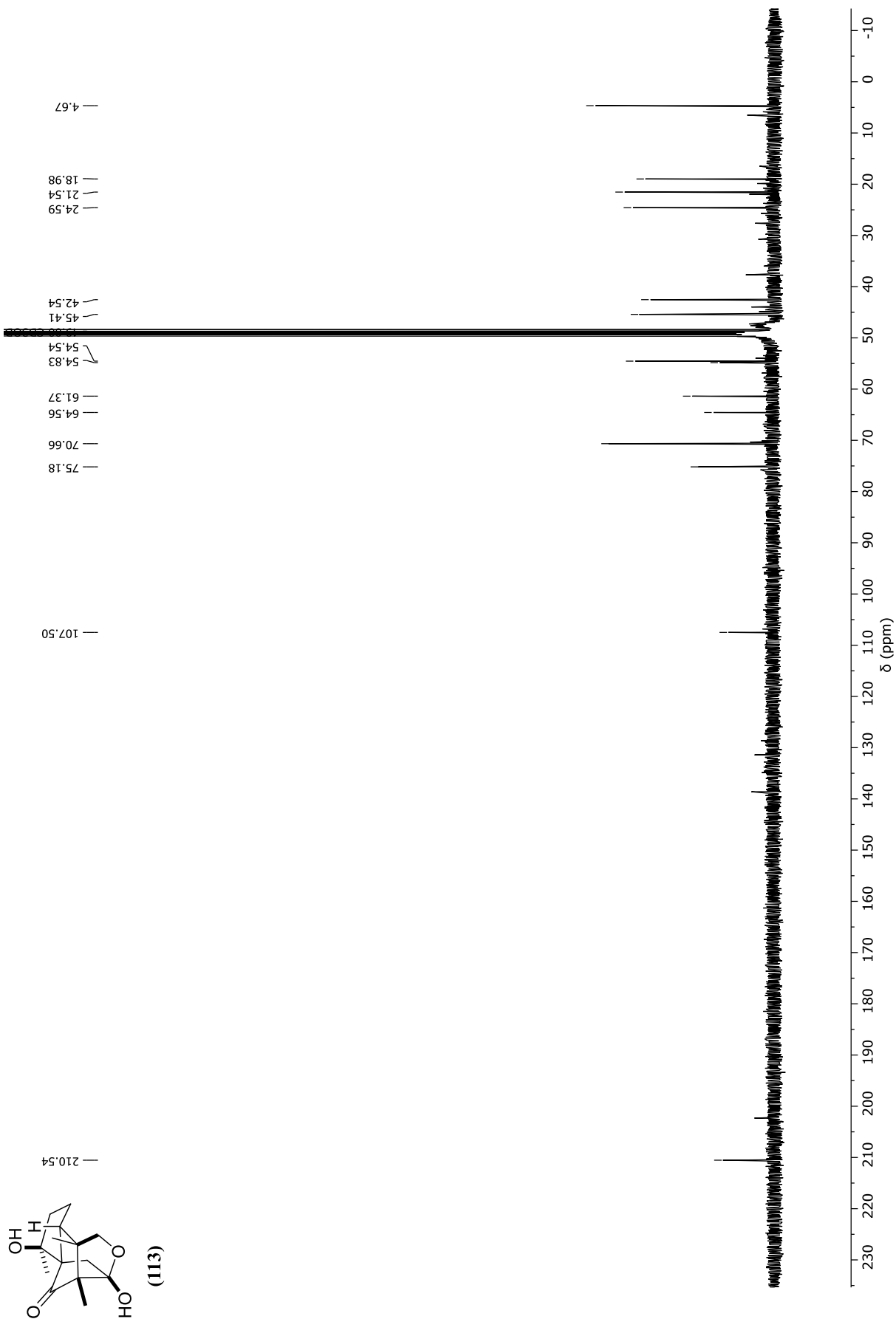


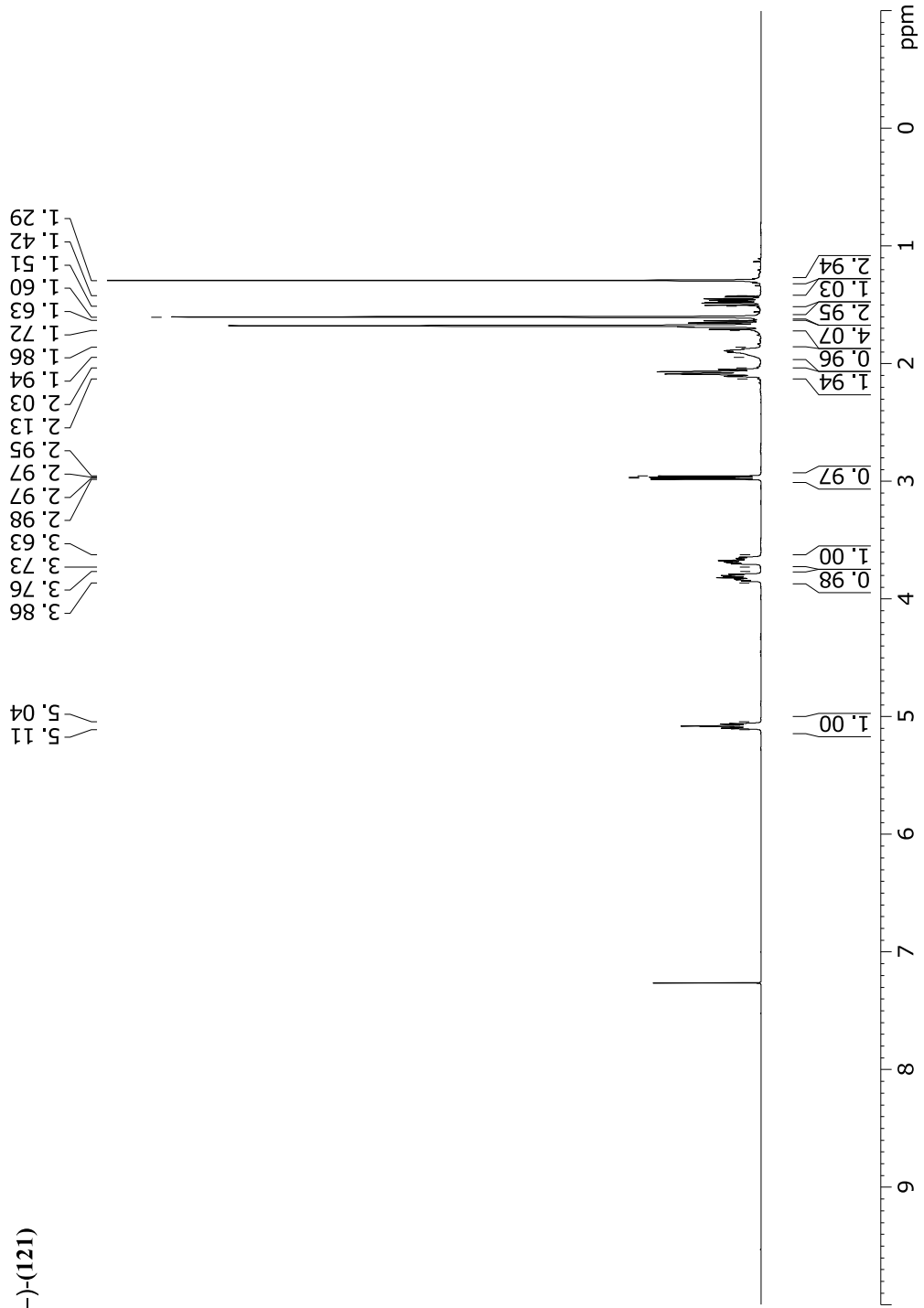
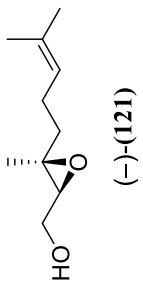
NOE response of epoxytetraol (**105**) after irradiation at 3.69 ppm (CH₂-13a). Spectrum measured in CDCl₃ at 400 MHz.

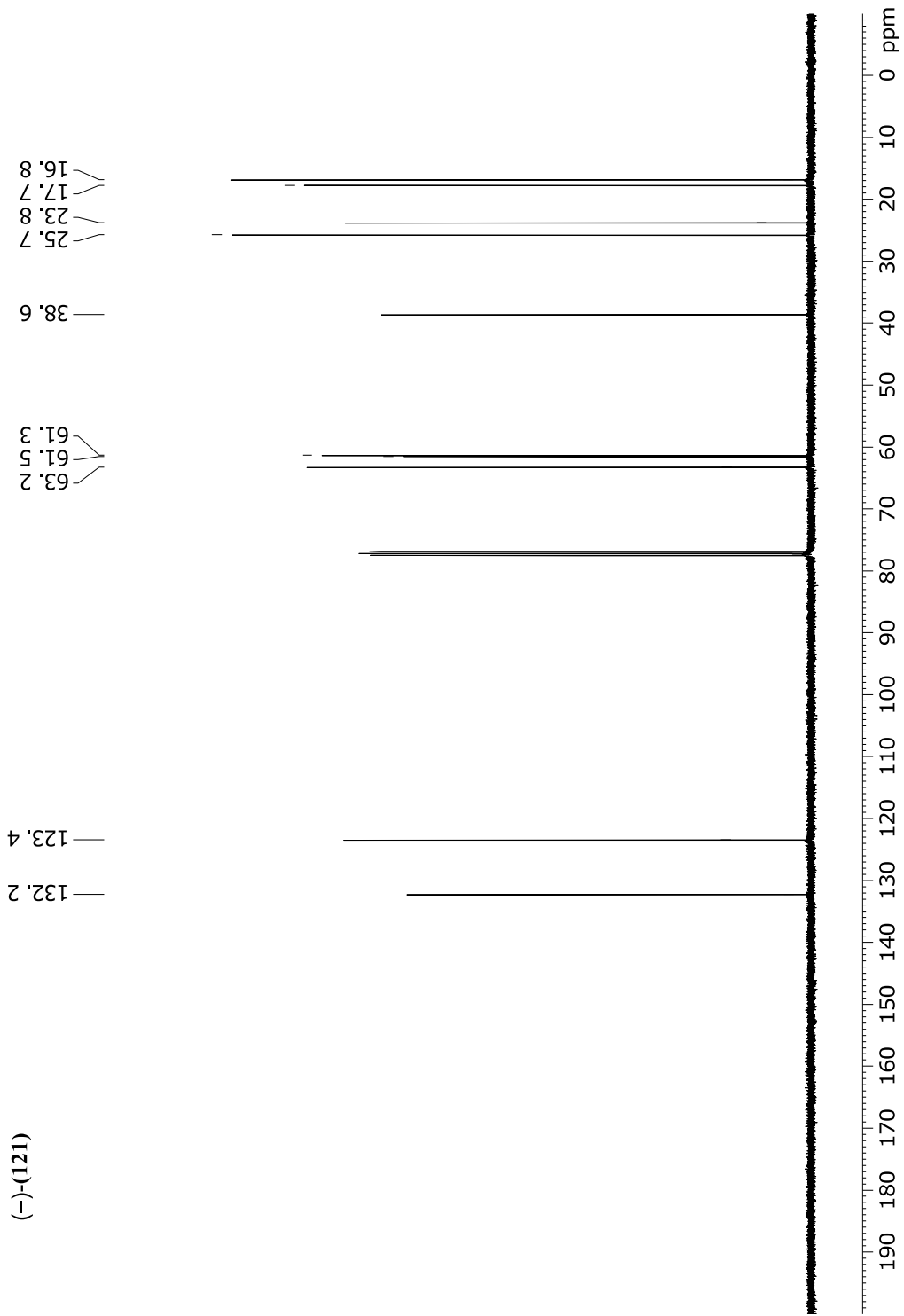
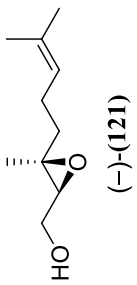


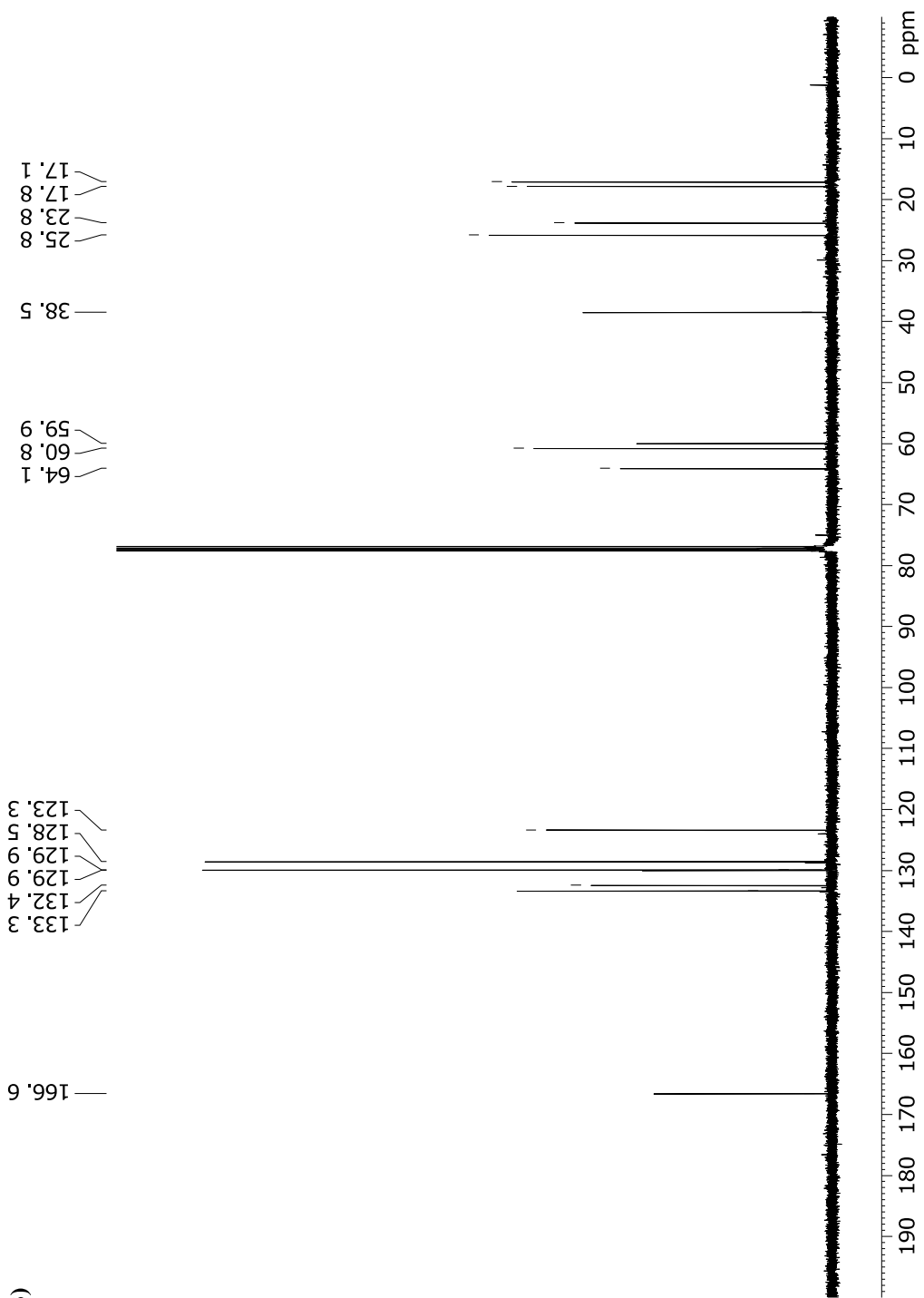
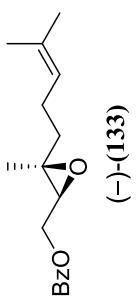
NOE response of epoxytetraol (**105**) after irradiation at 3.14 ppm (CH₂-11a). Spectrum measured in CDCl₃ at 400 MHz.

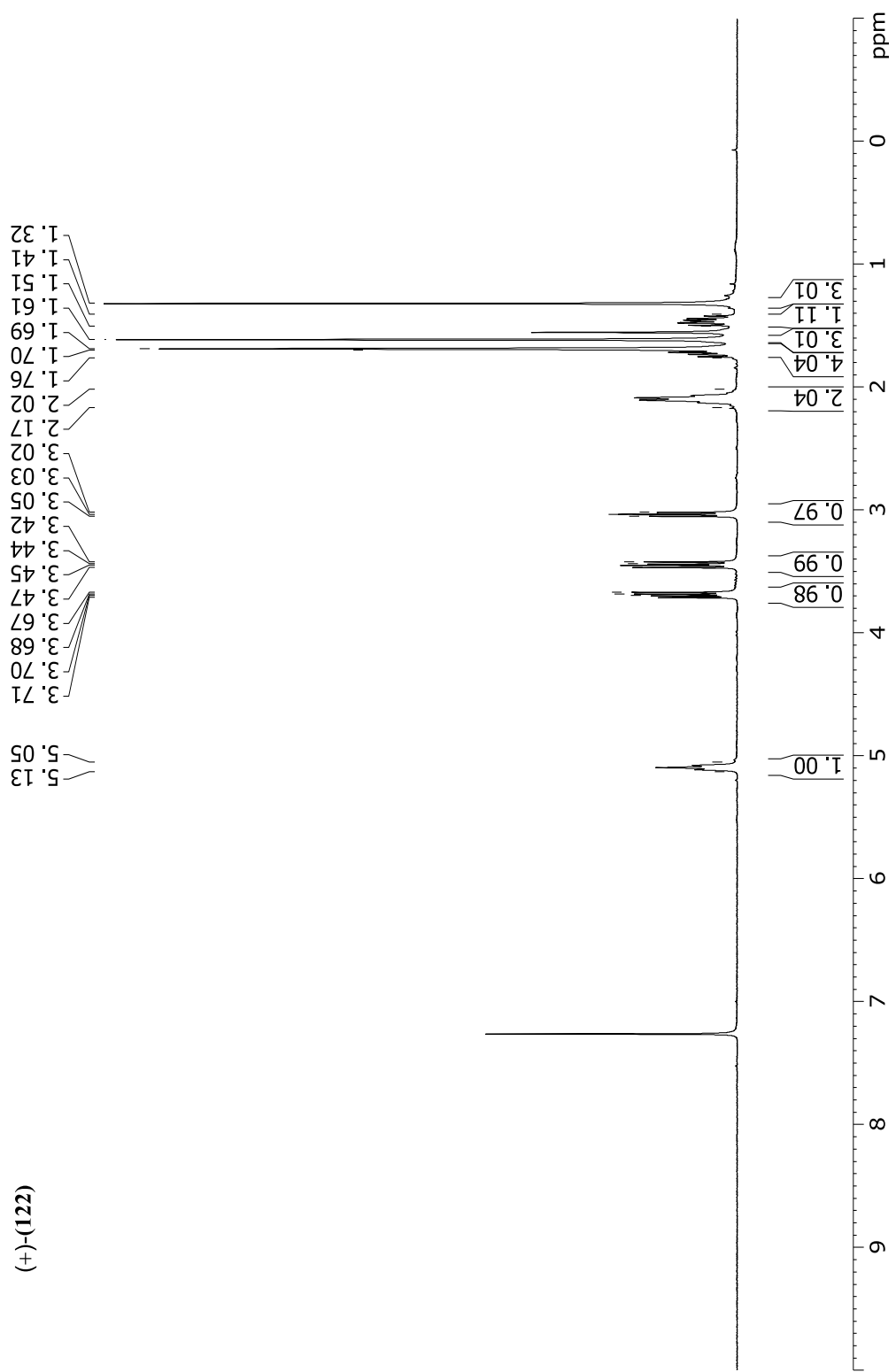
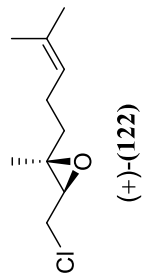


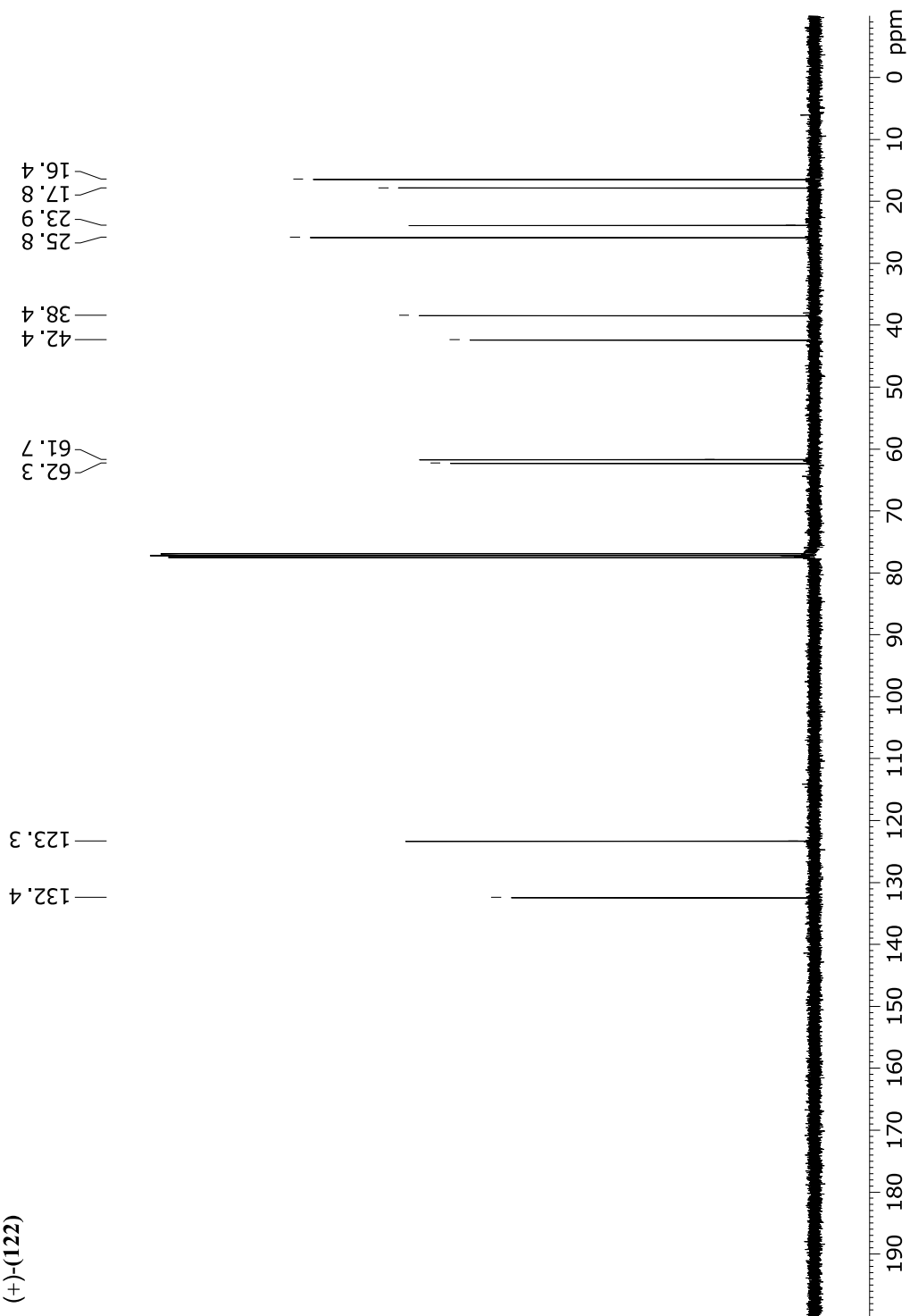
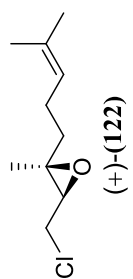


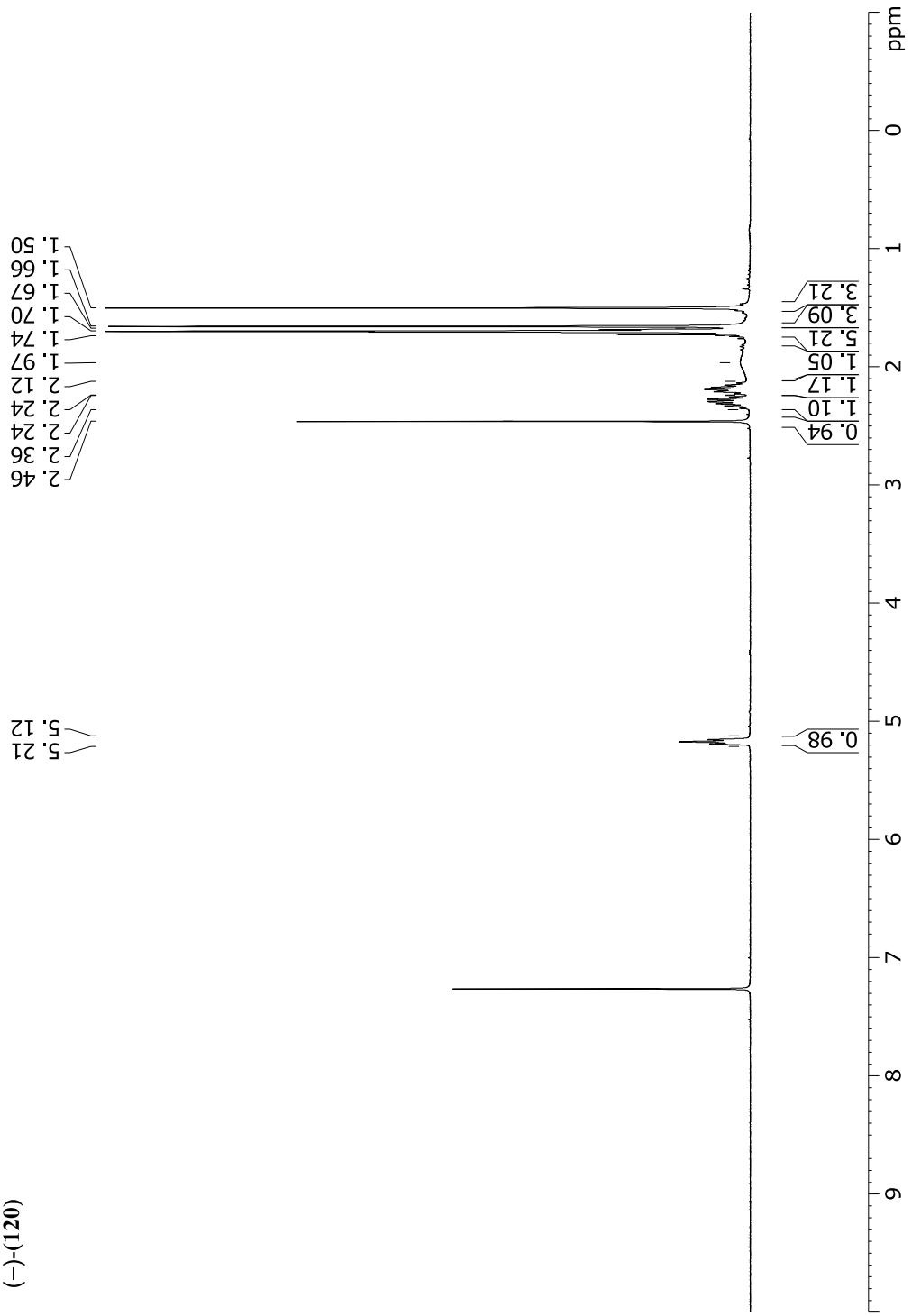
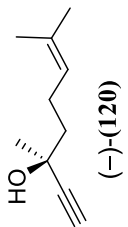


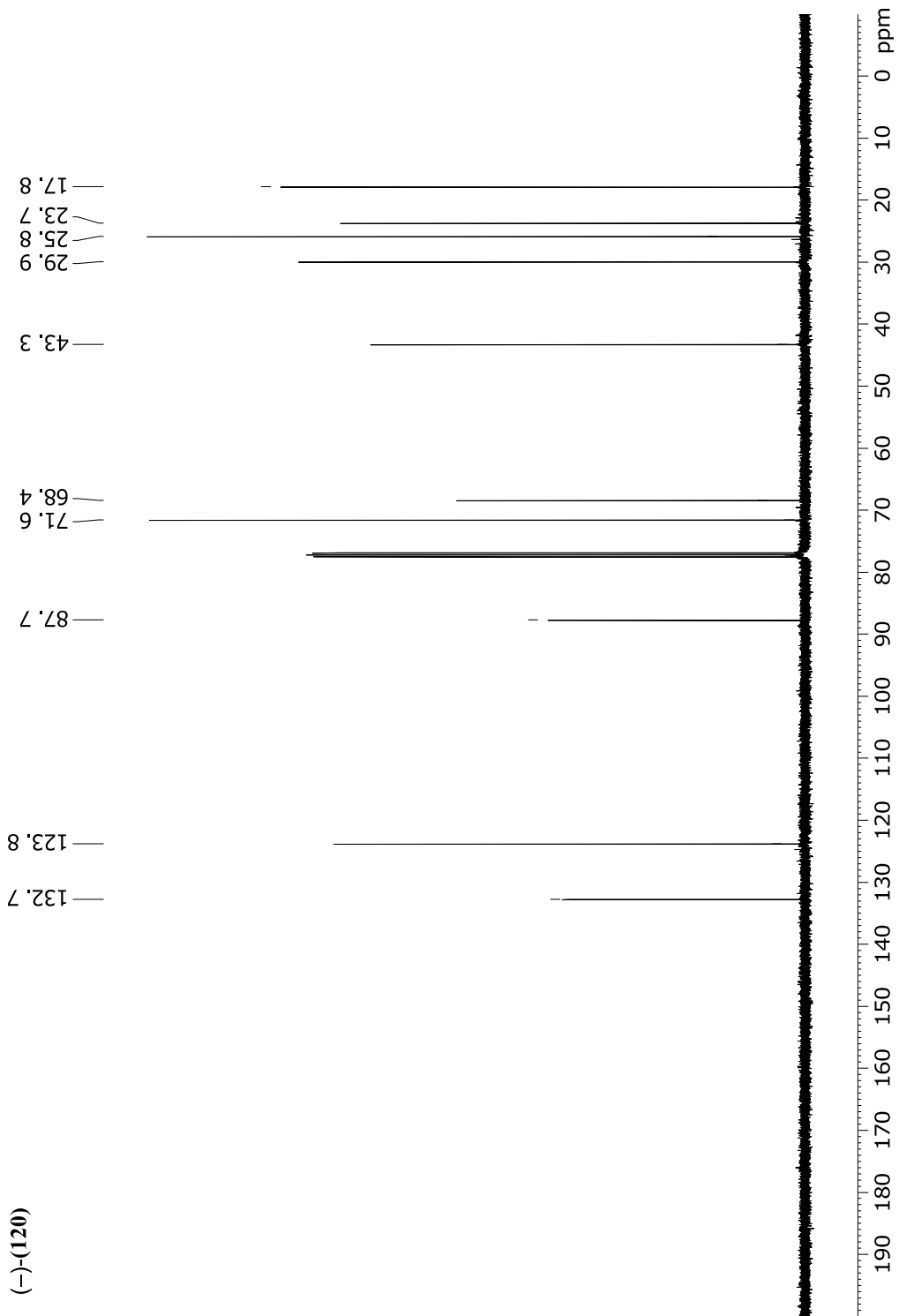
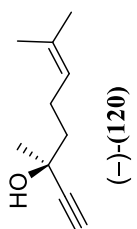


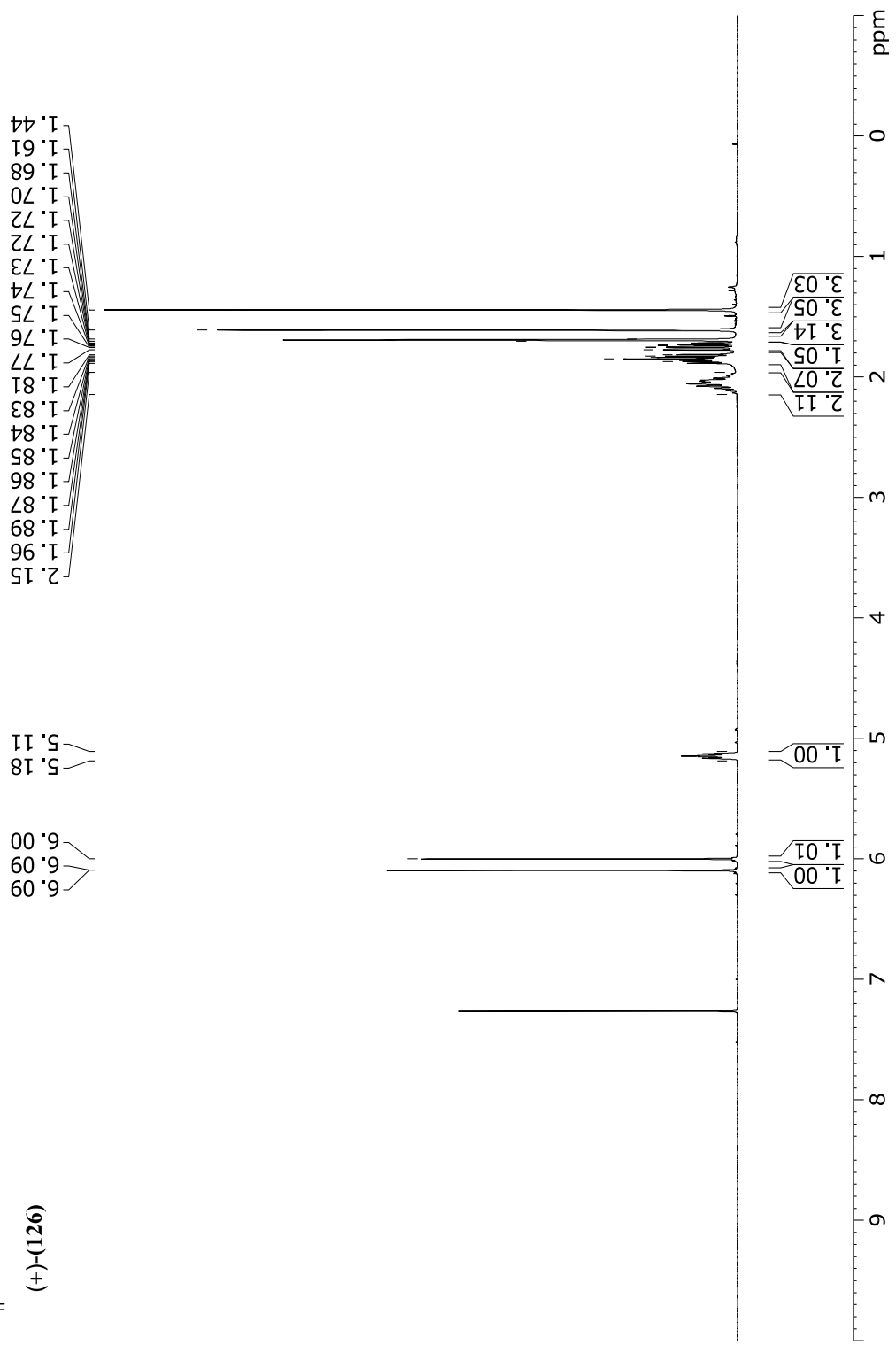
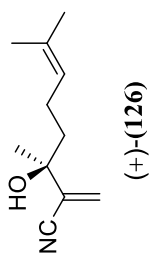


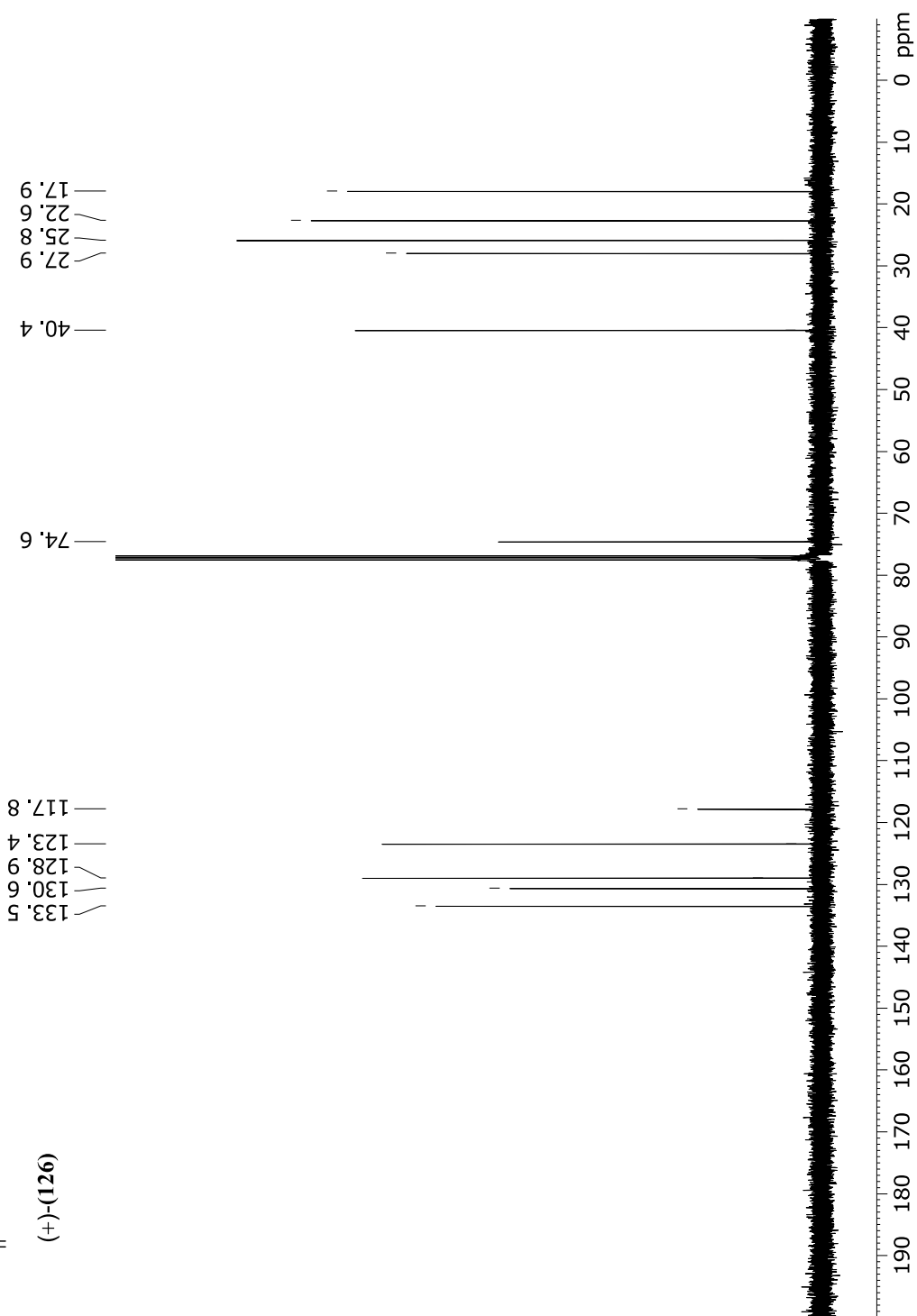
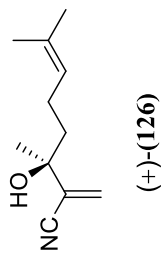


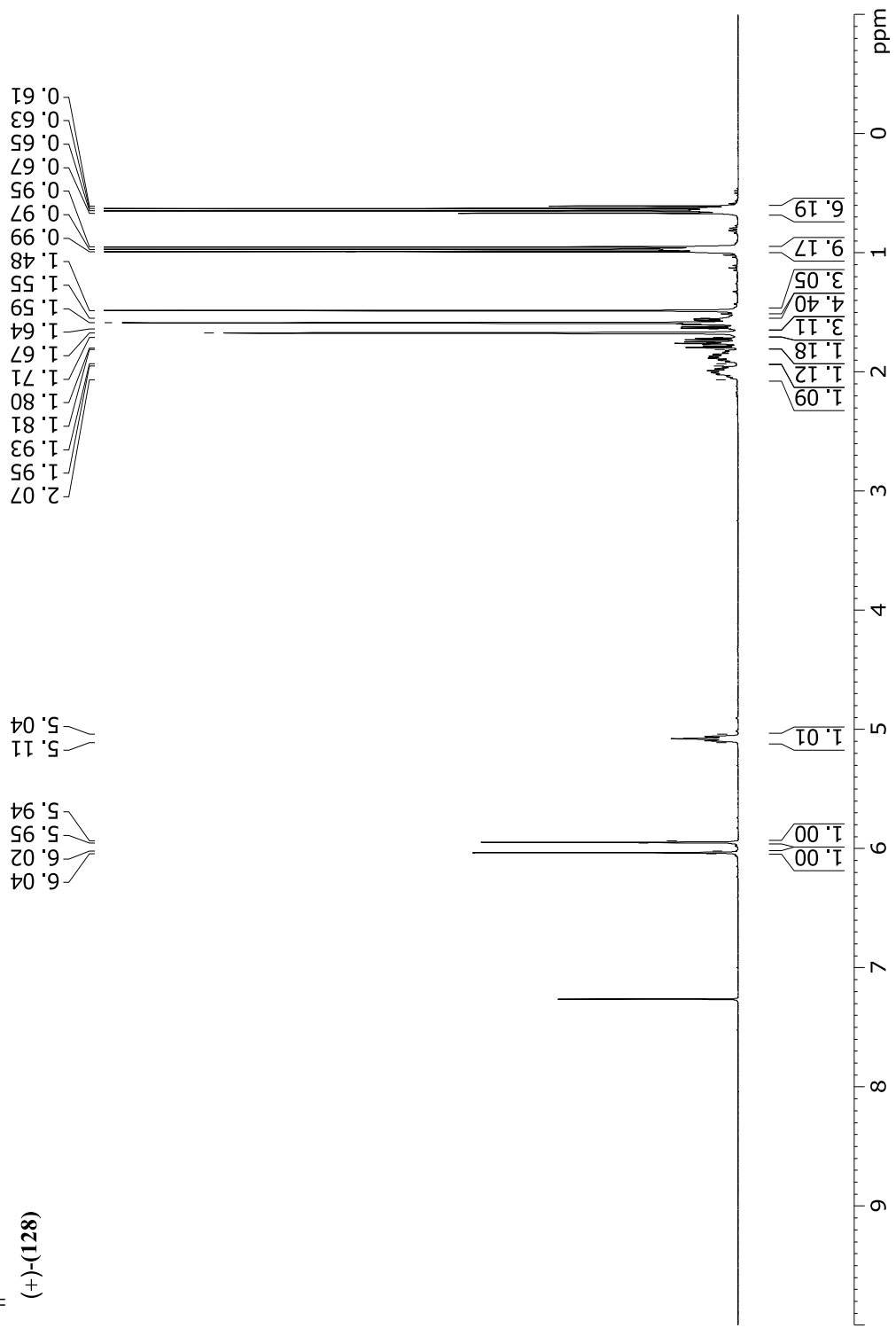
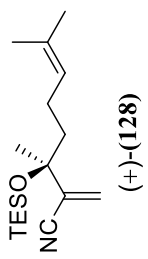


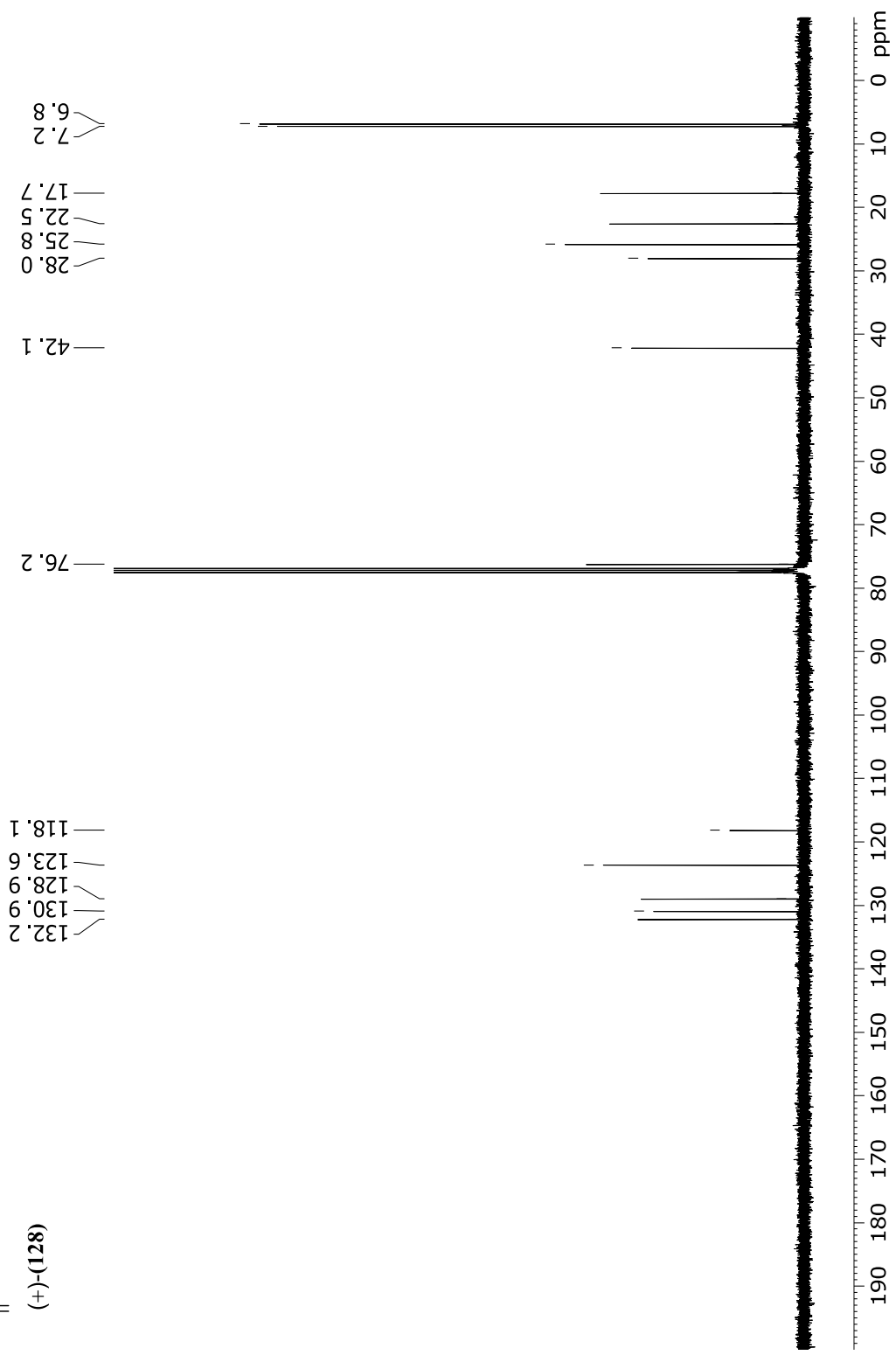
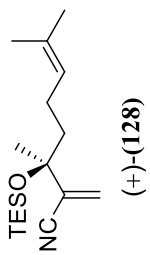


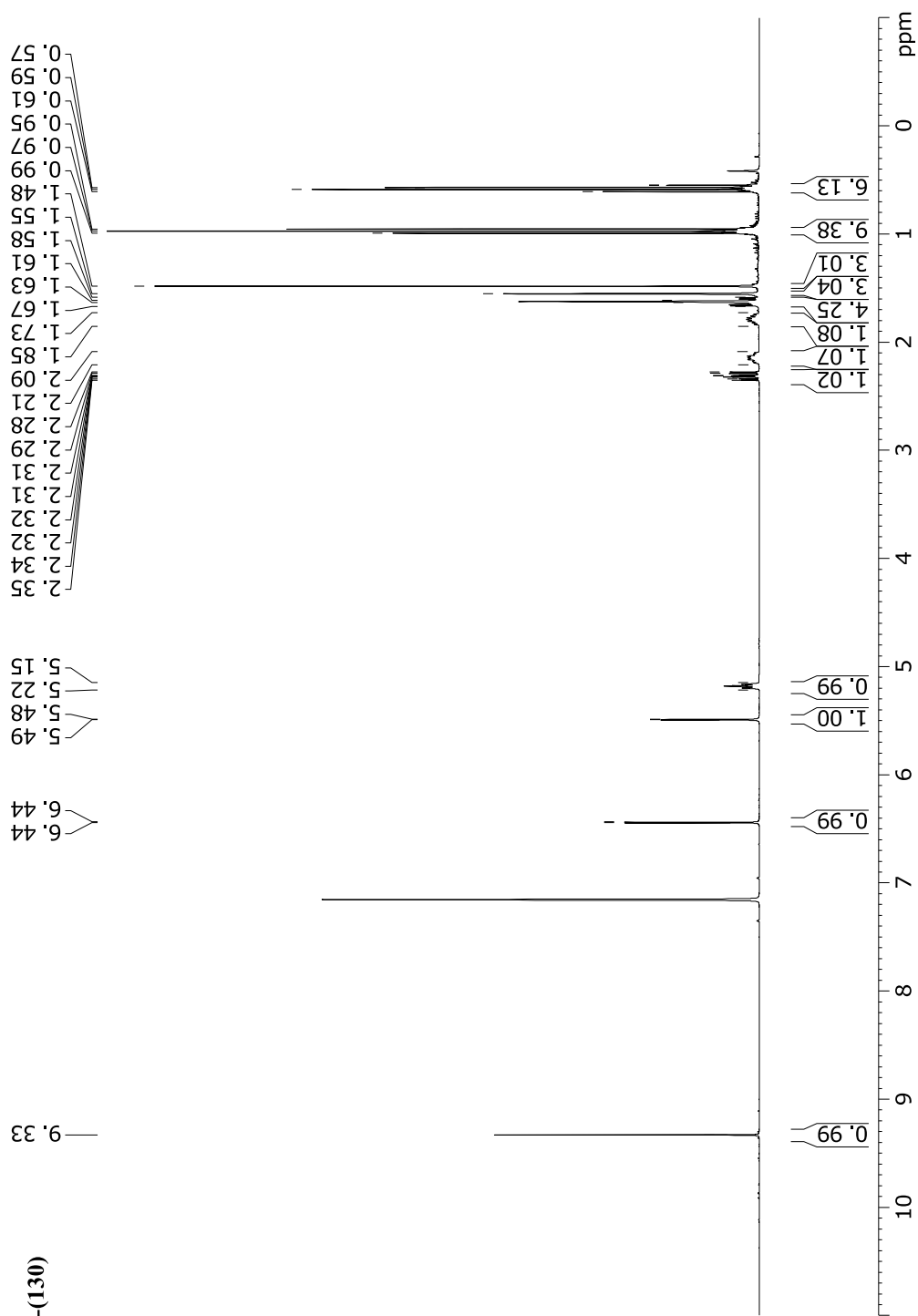
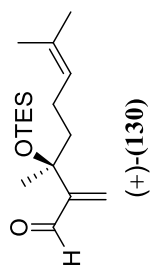


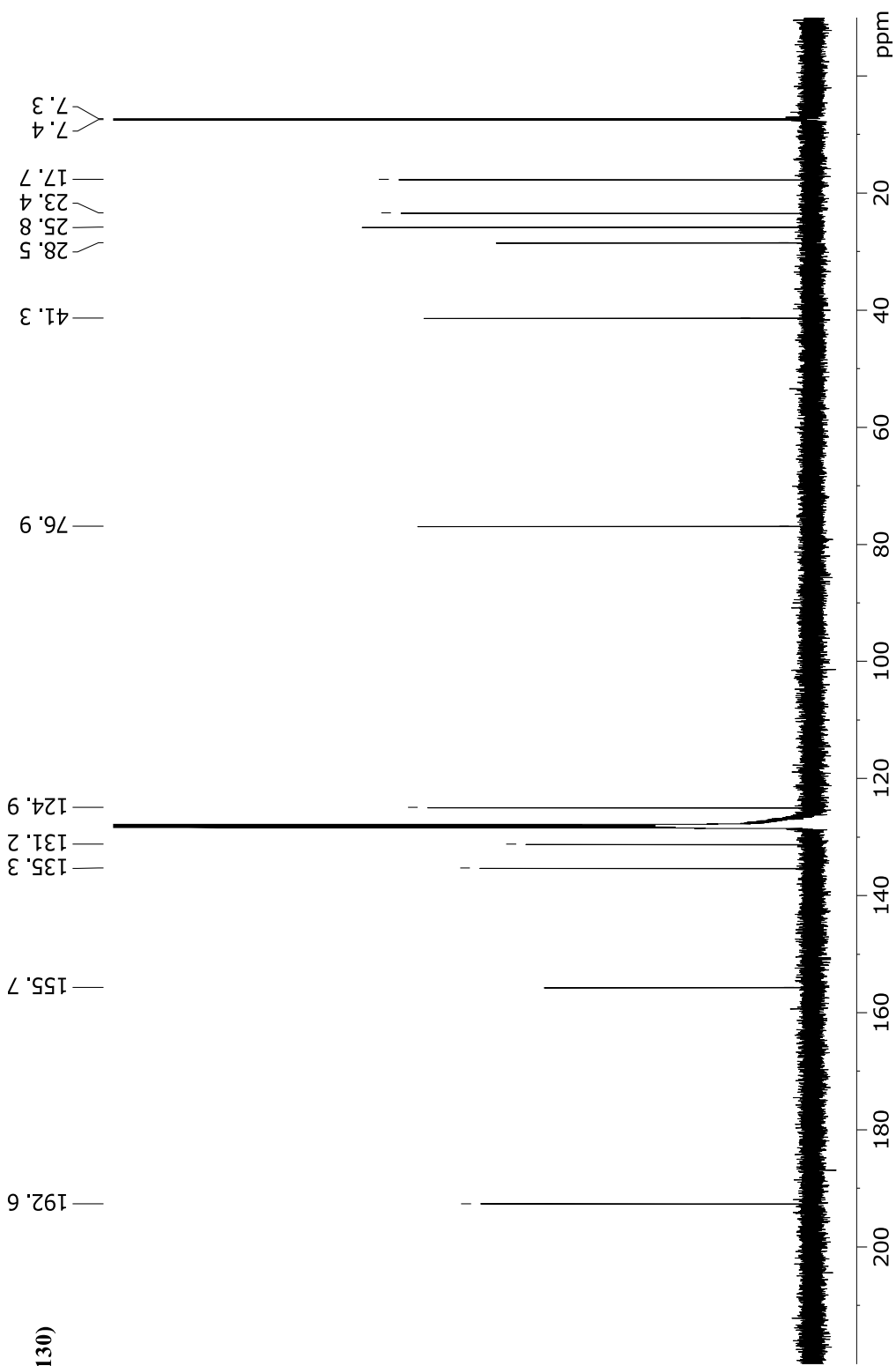
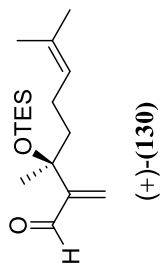


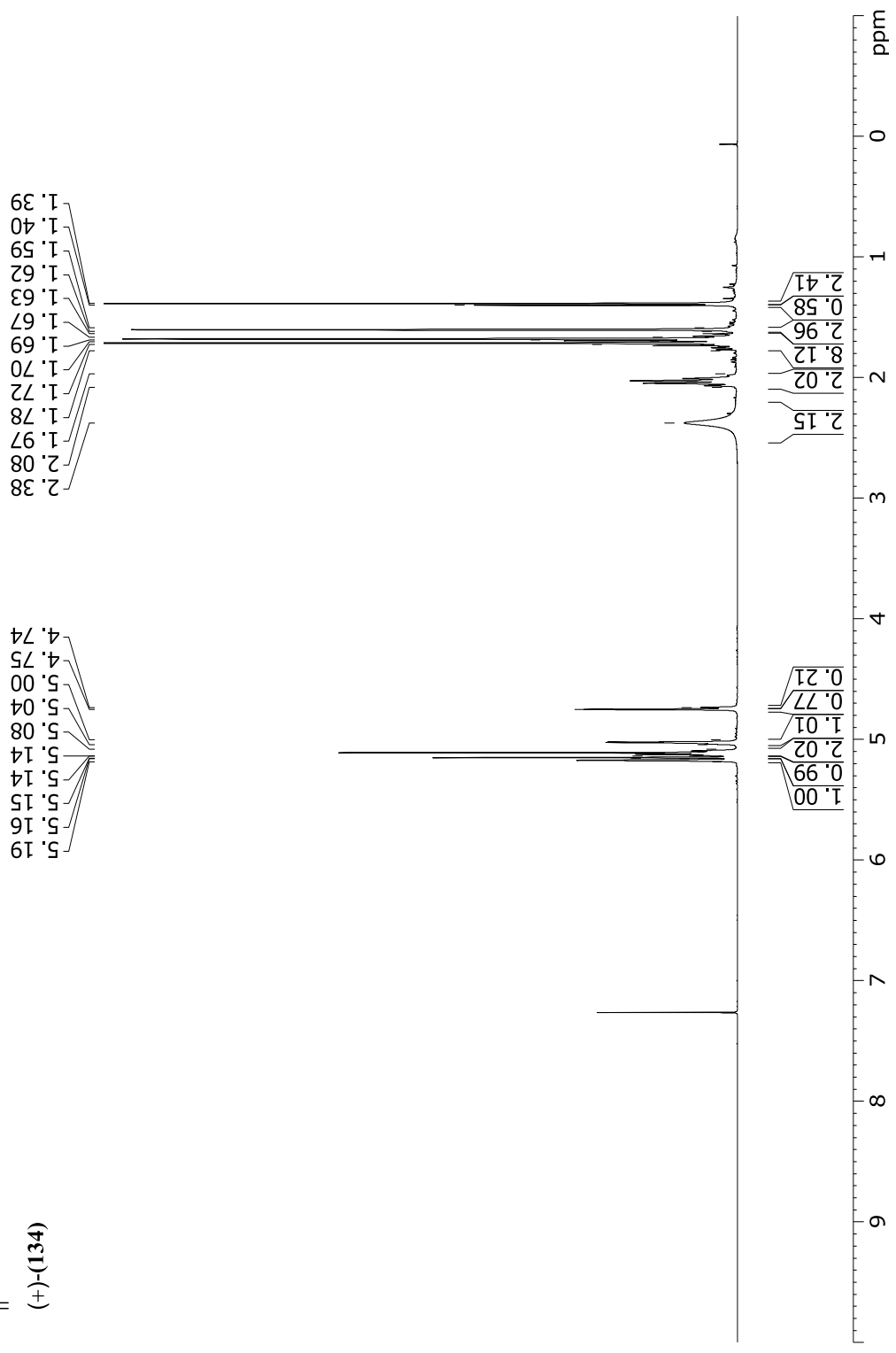
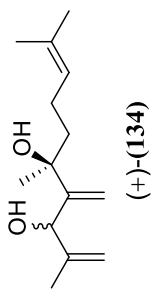


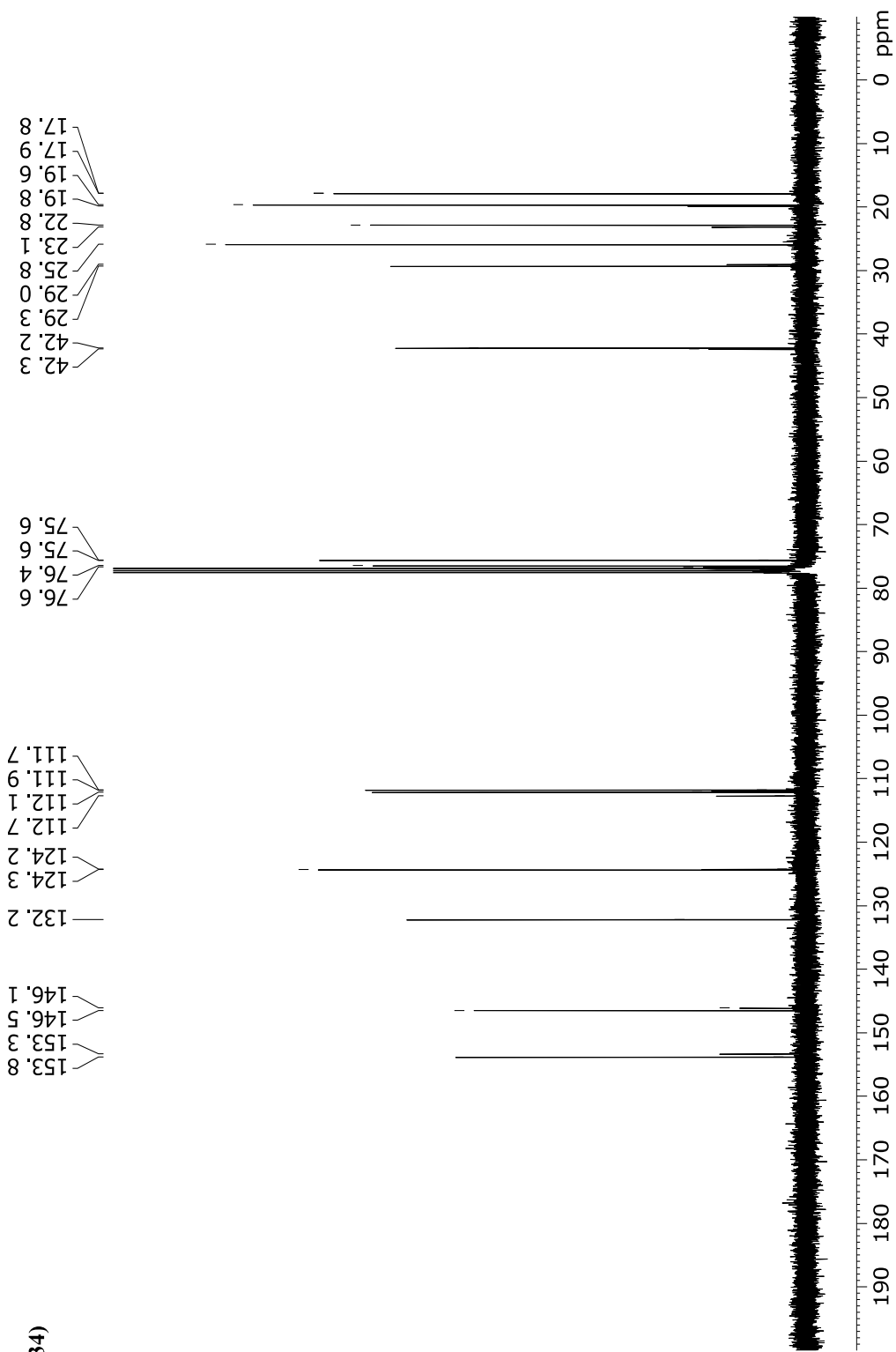
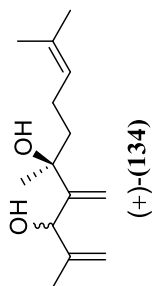


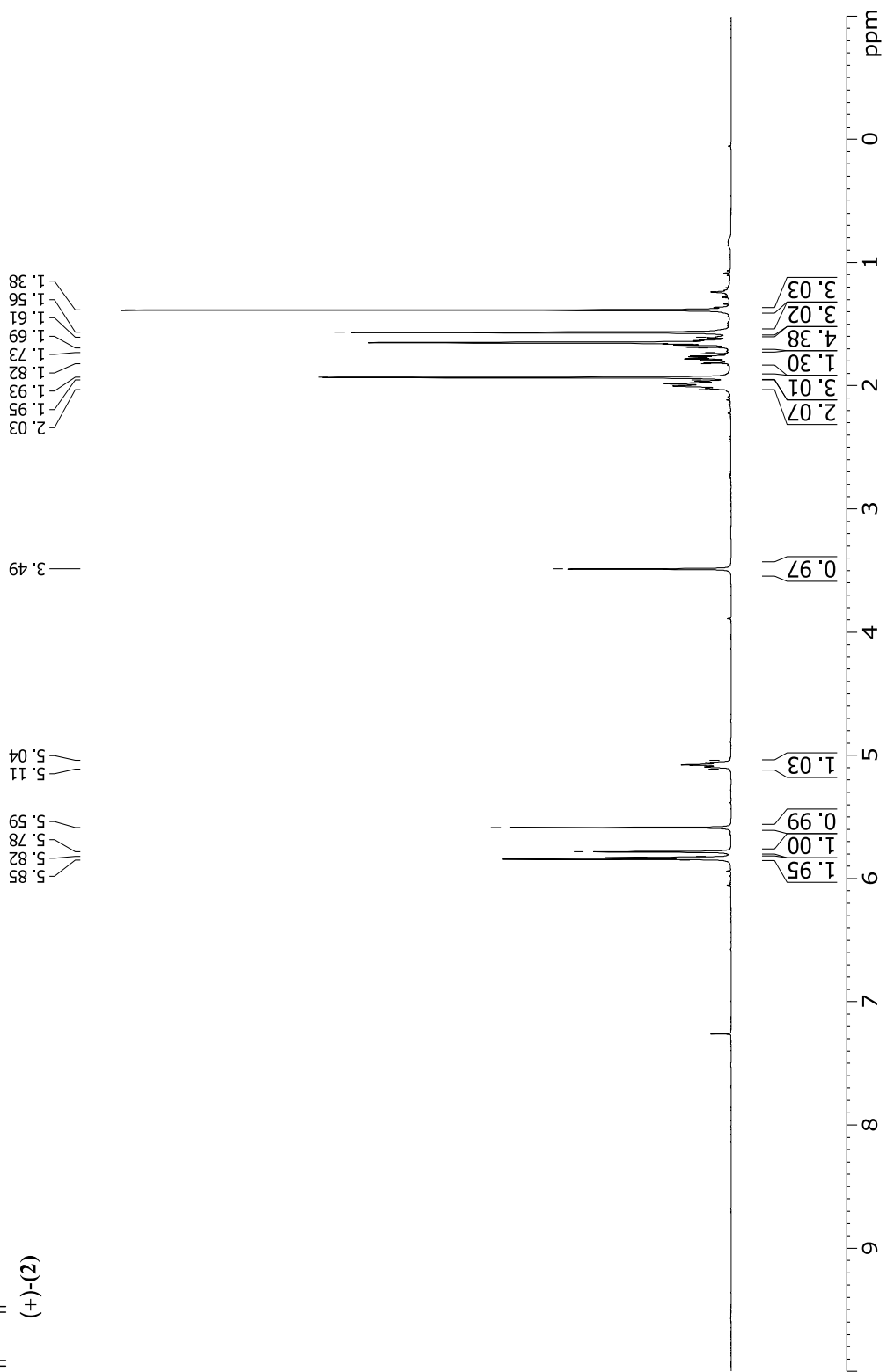
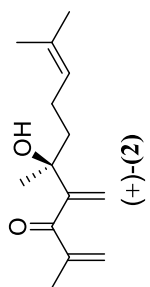


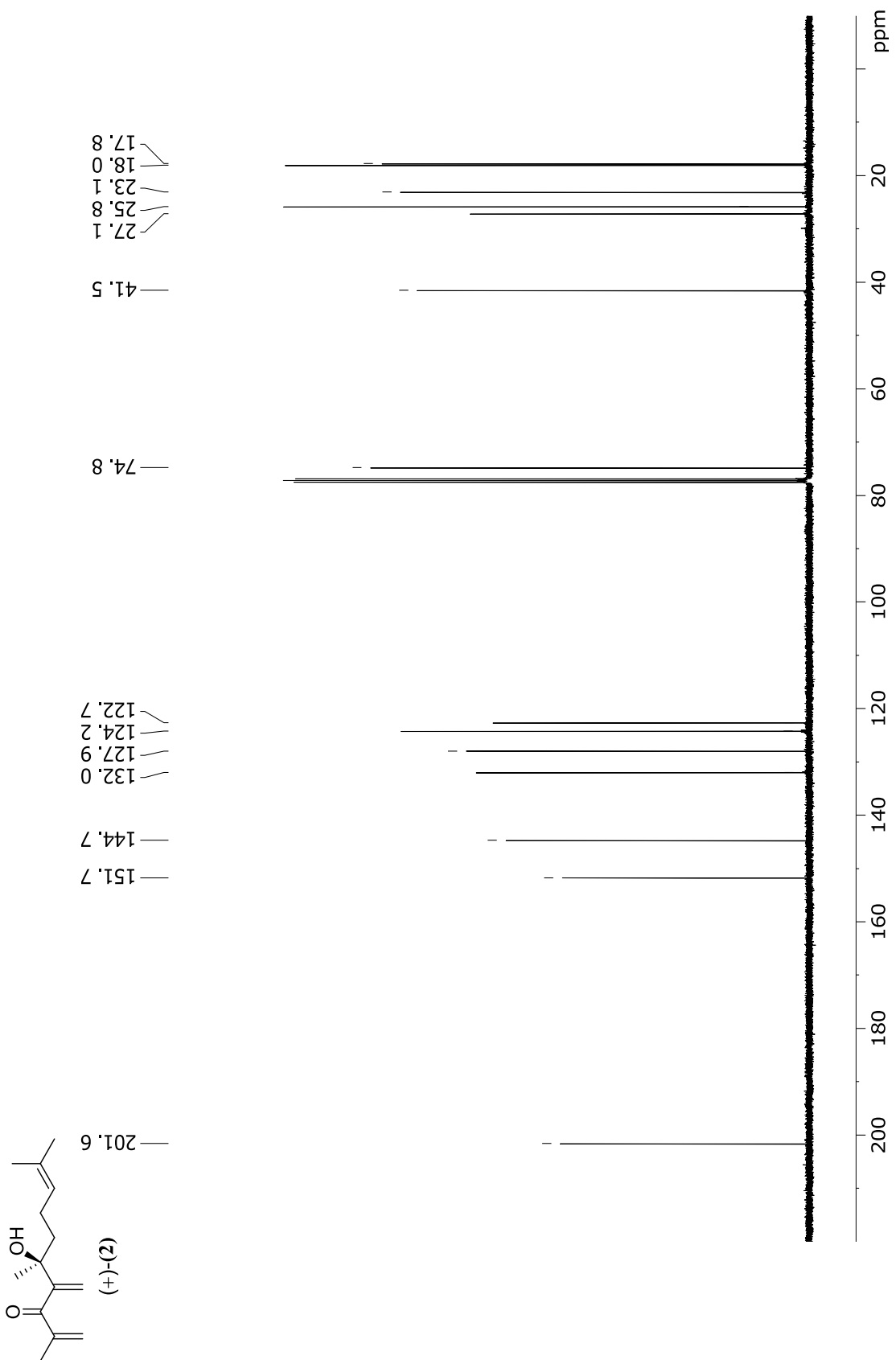


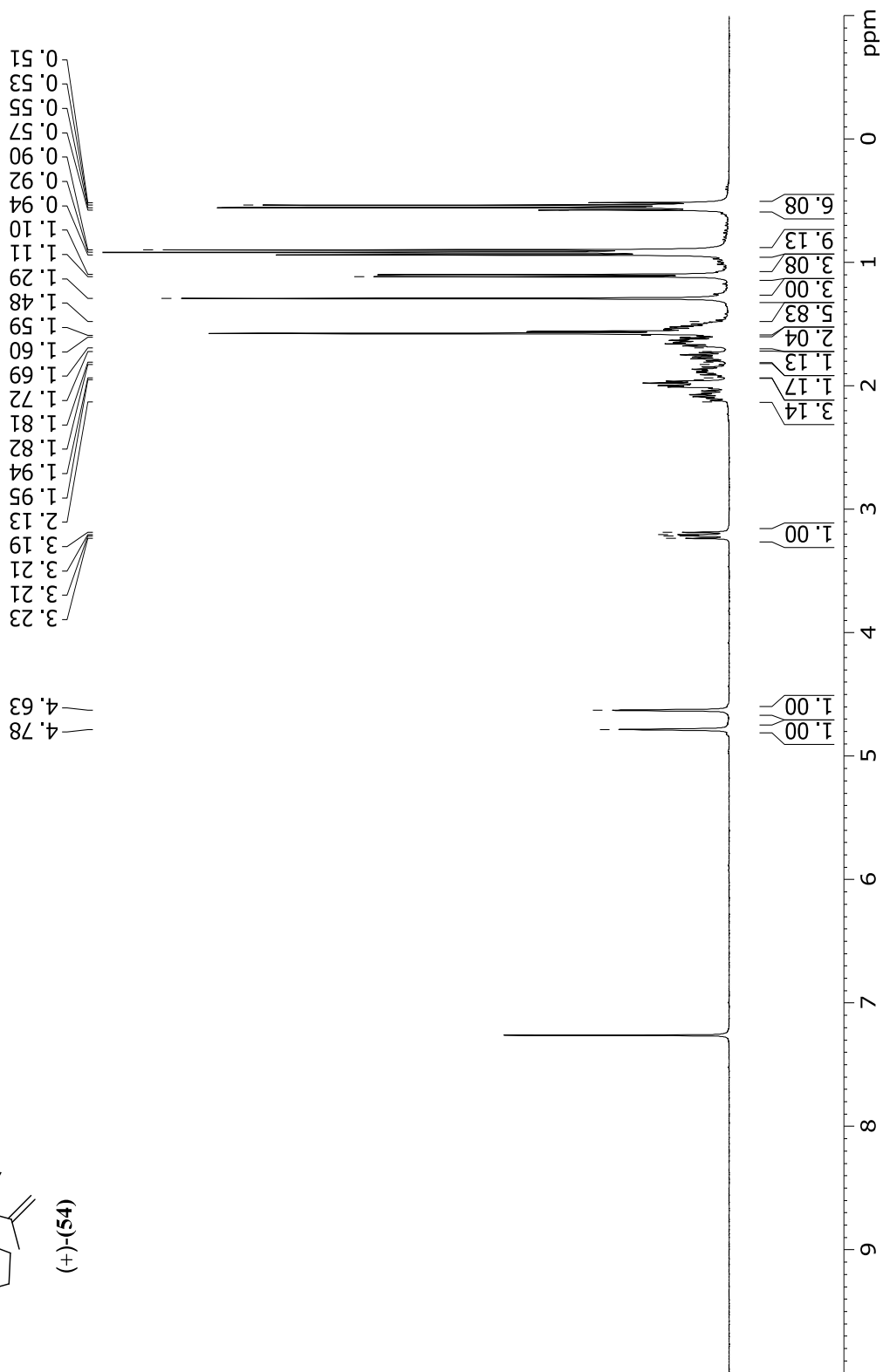
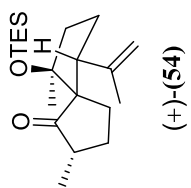


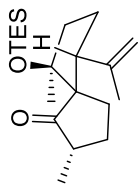












222.8

146.1

113.3

86.2

63.8

51.6

44.2

40.4

28.9

28.1

27.8

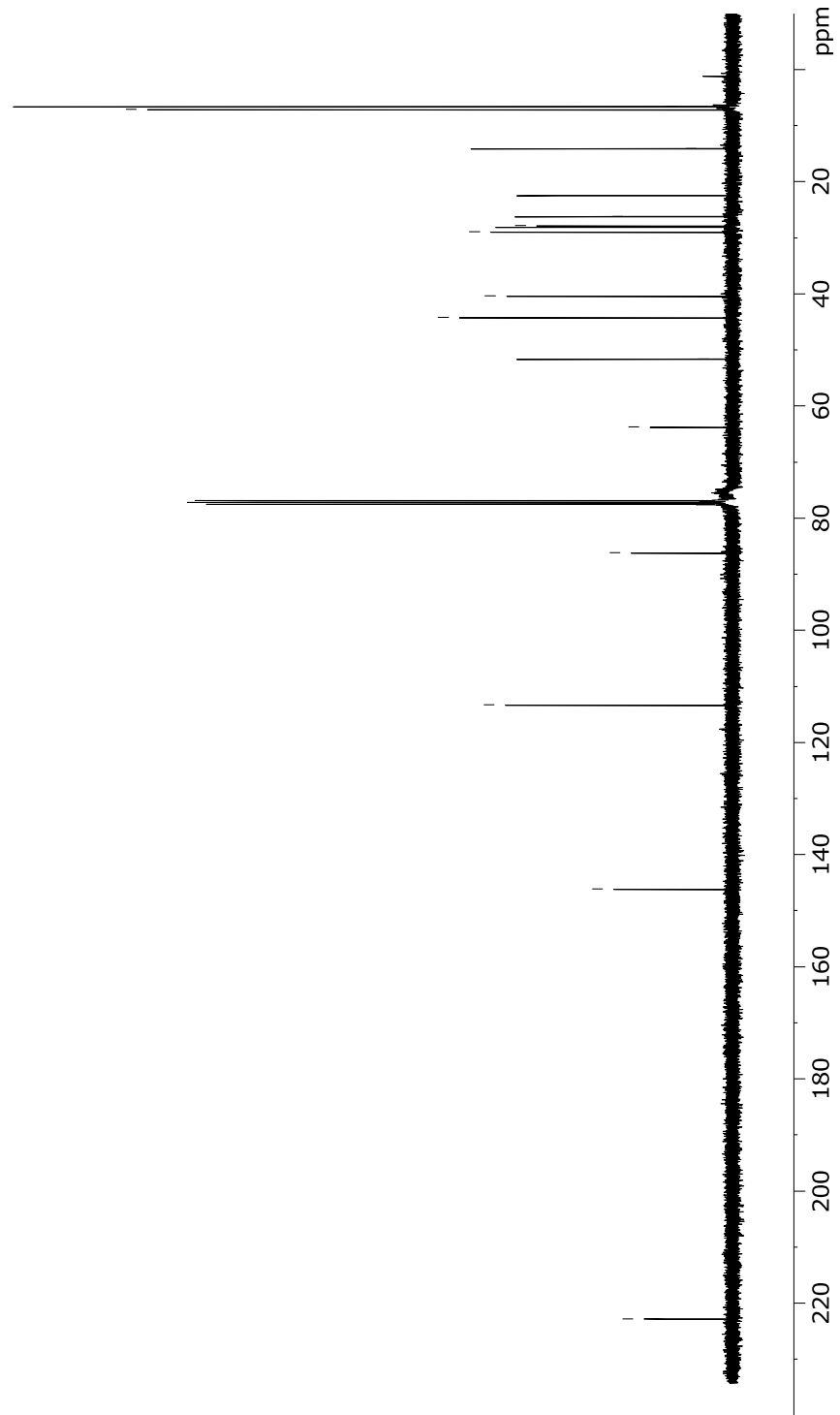
26.2

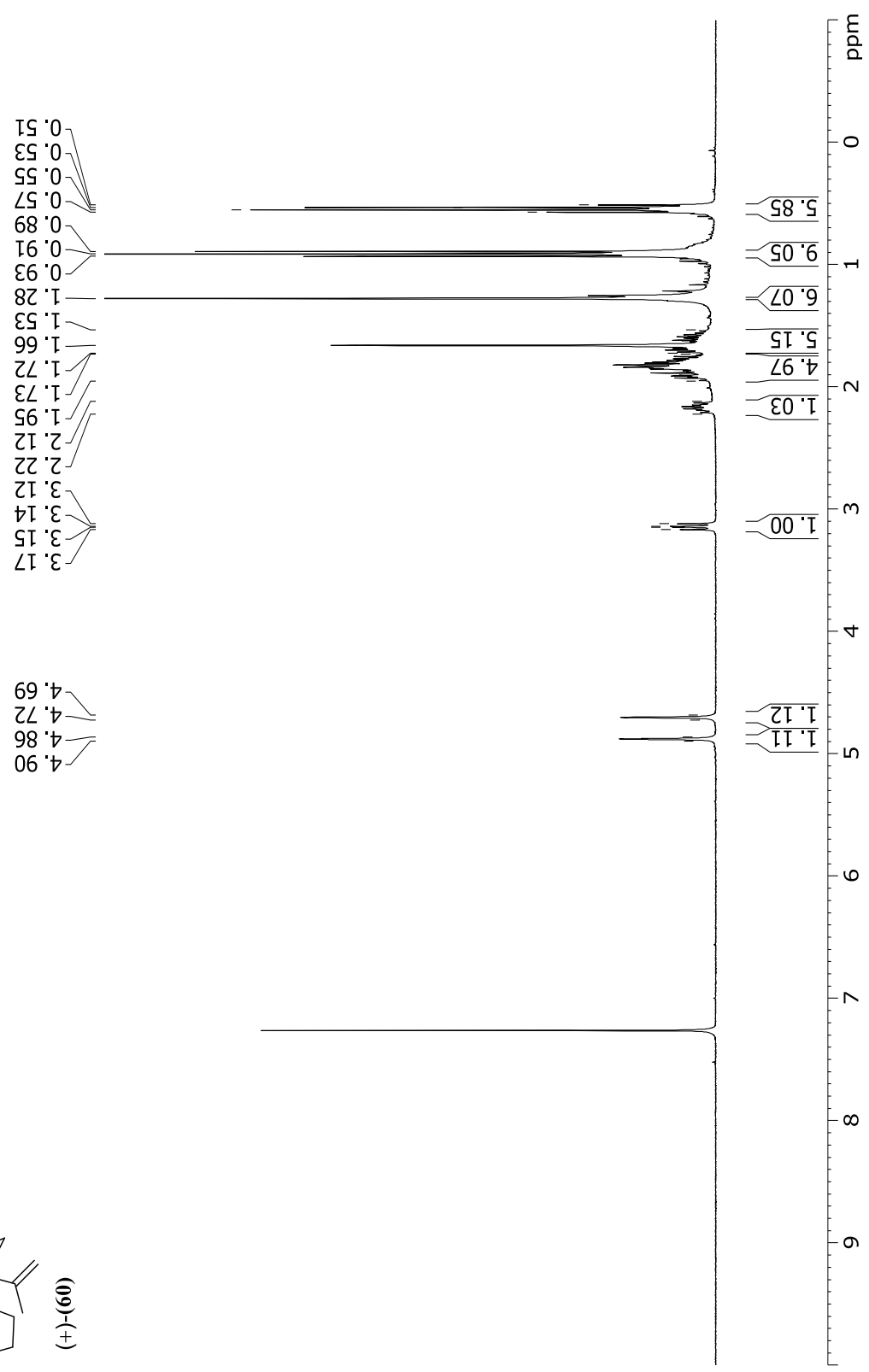
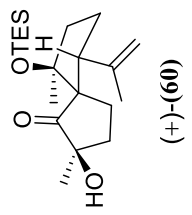
22.4

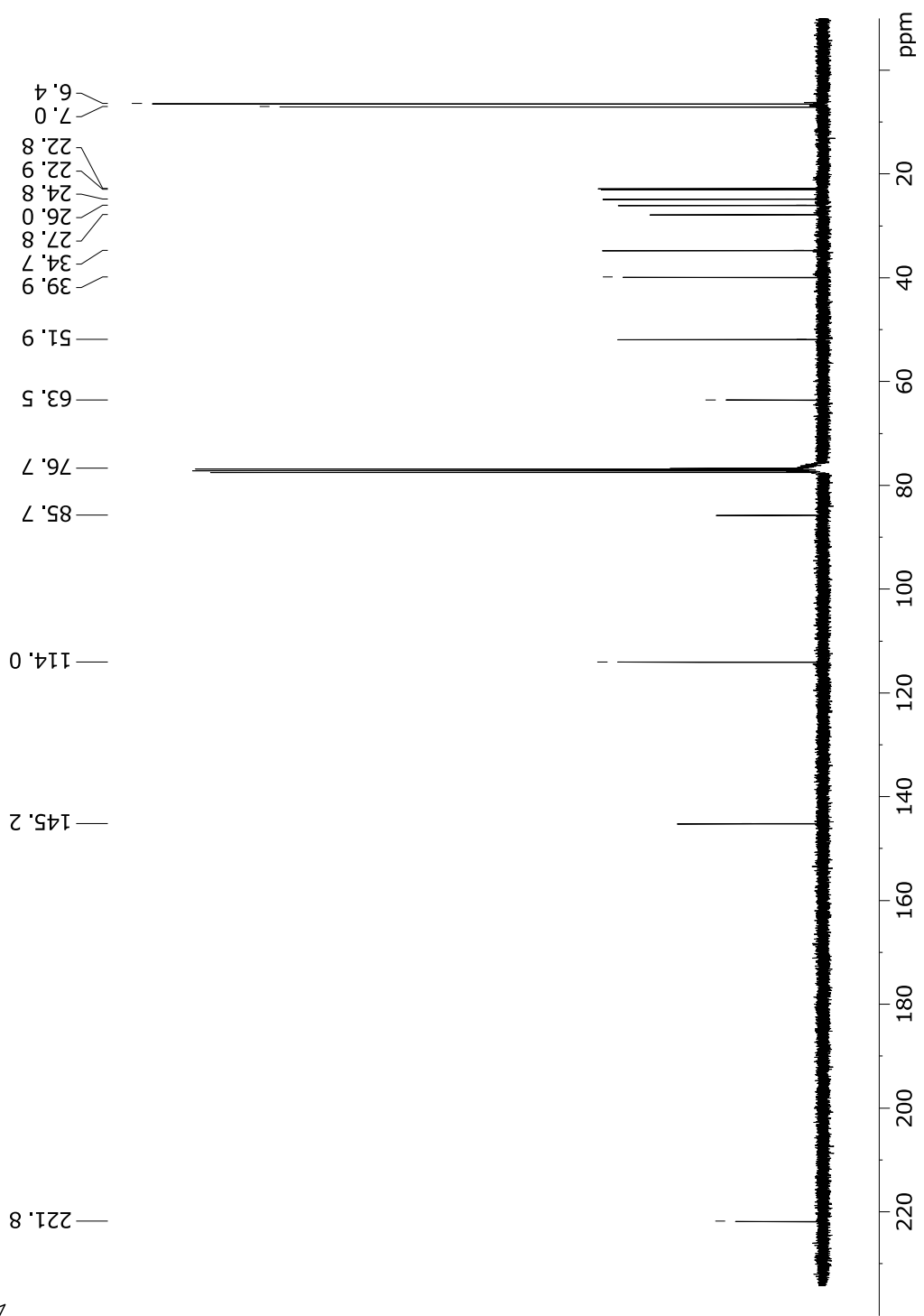
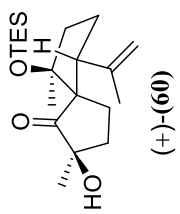
14.1

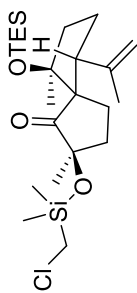
7.1

6.6



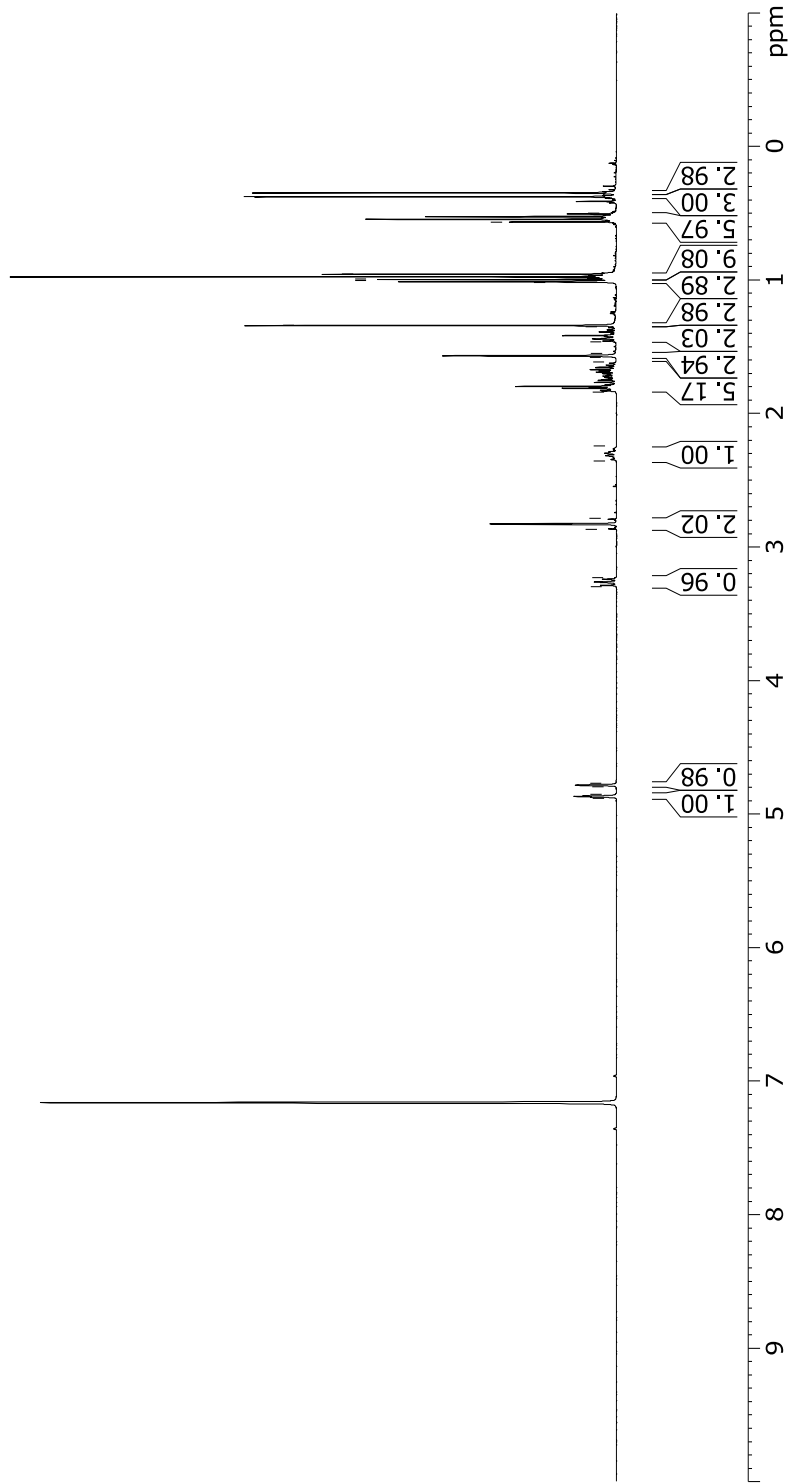


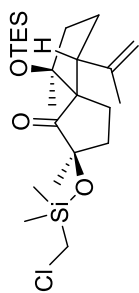




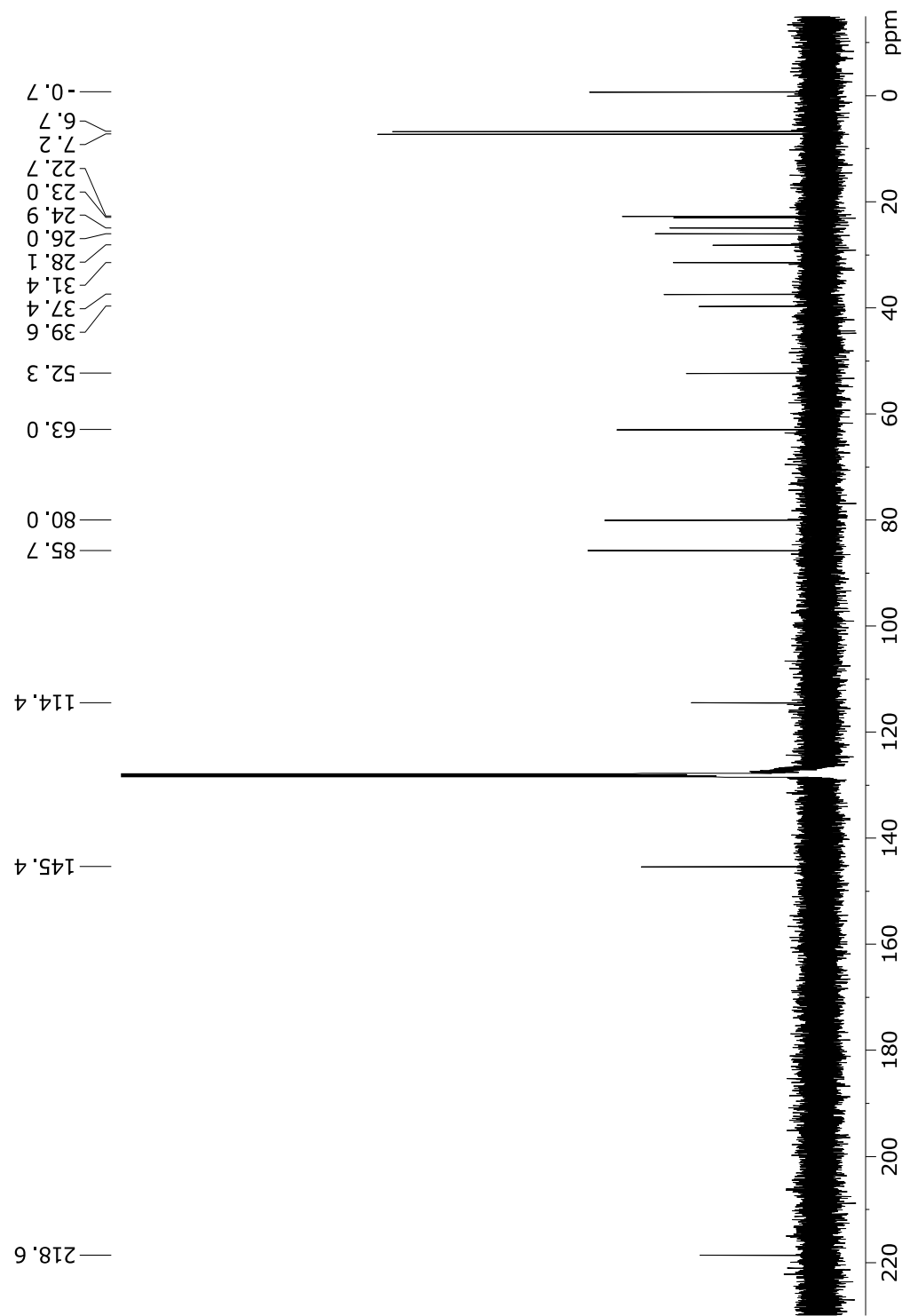
(62)

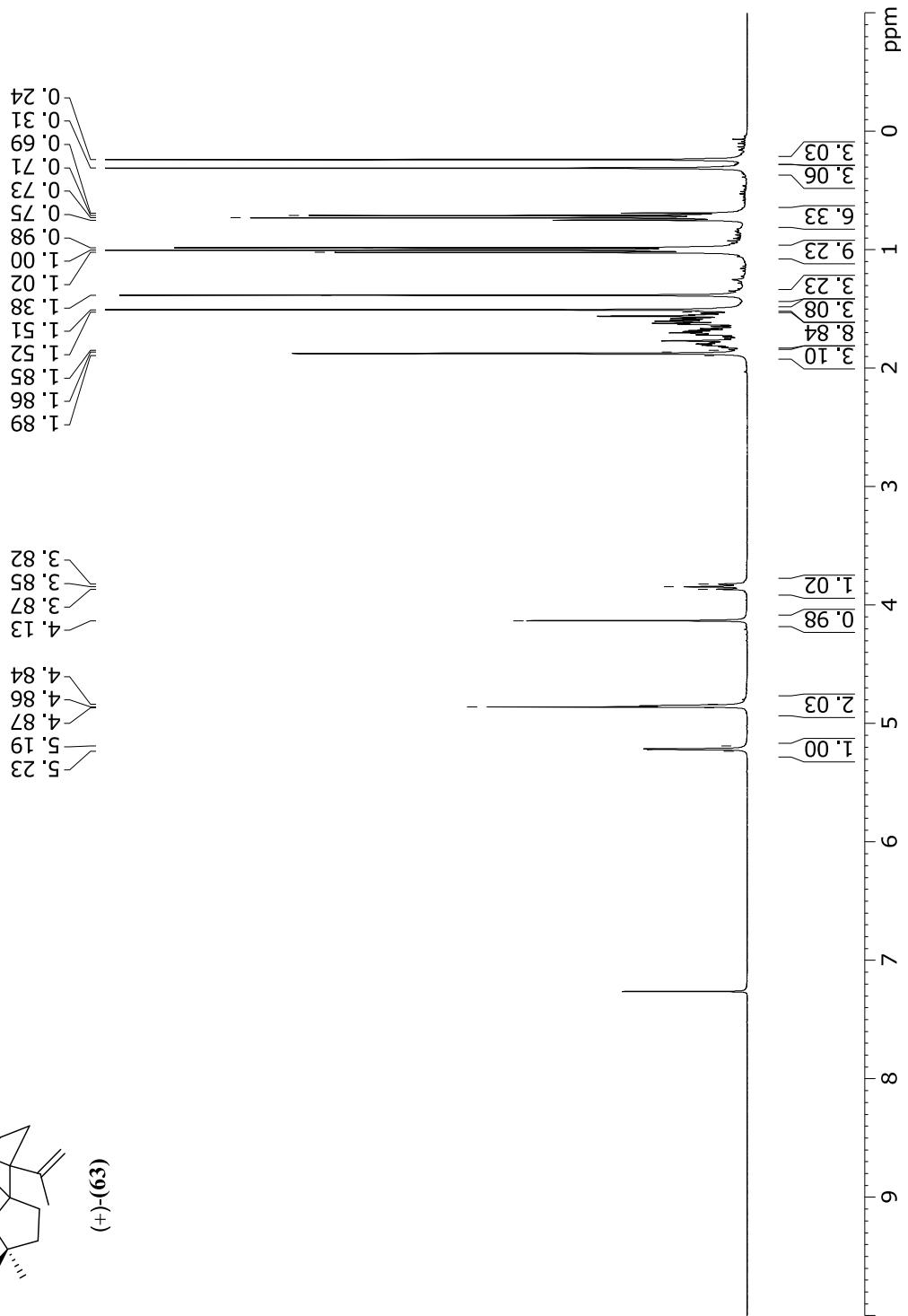
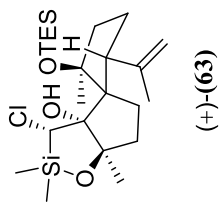
4.88
4.85
4.80
4.77
3.30
3.23
2.87
2.79
2.36
2.24
1.84
1.61
1.58
1.55
1.46
1.35
1.34
1.02
1.00
0.99
0.97
0.95
0.57
0.50
0.37
0.35

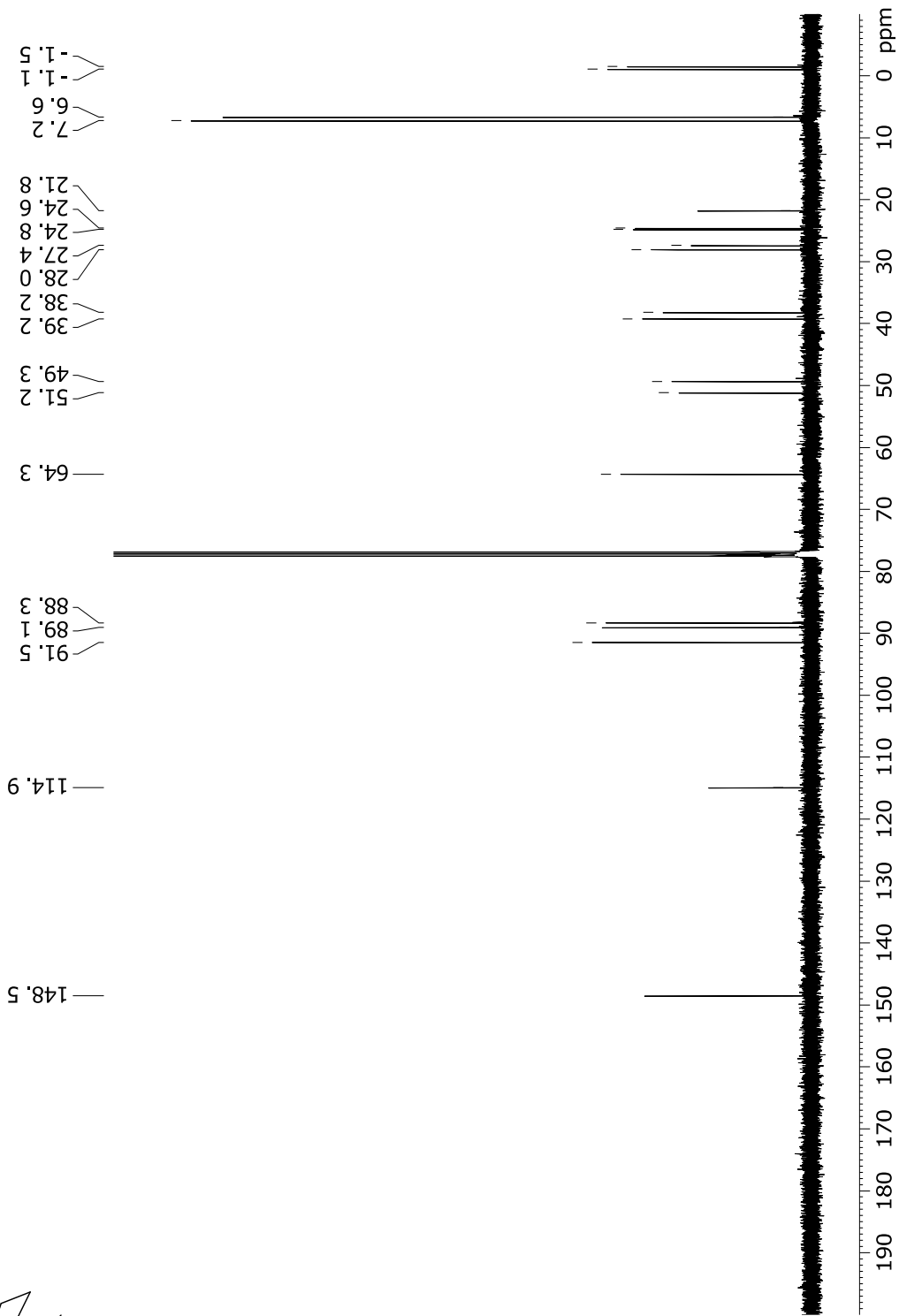
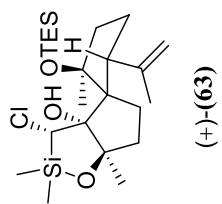


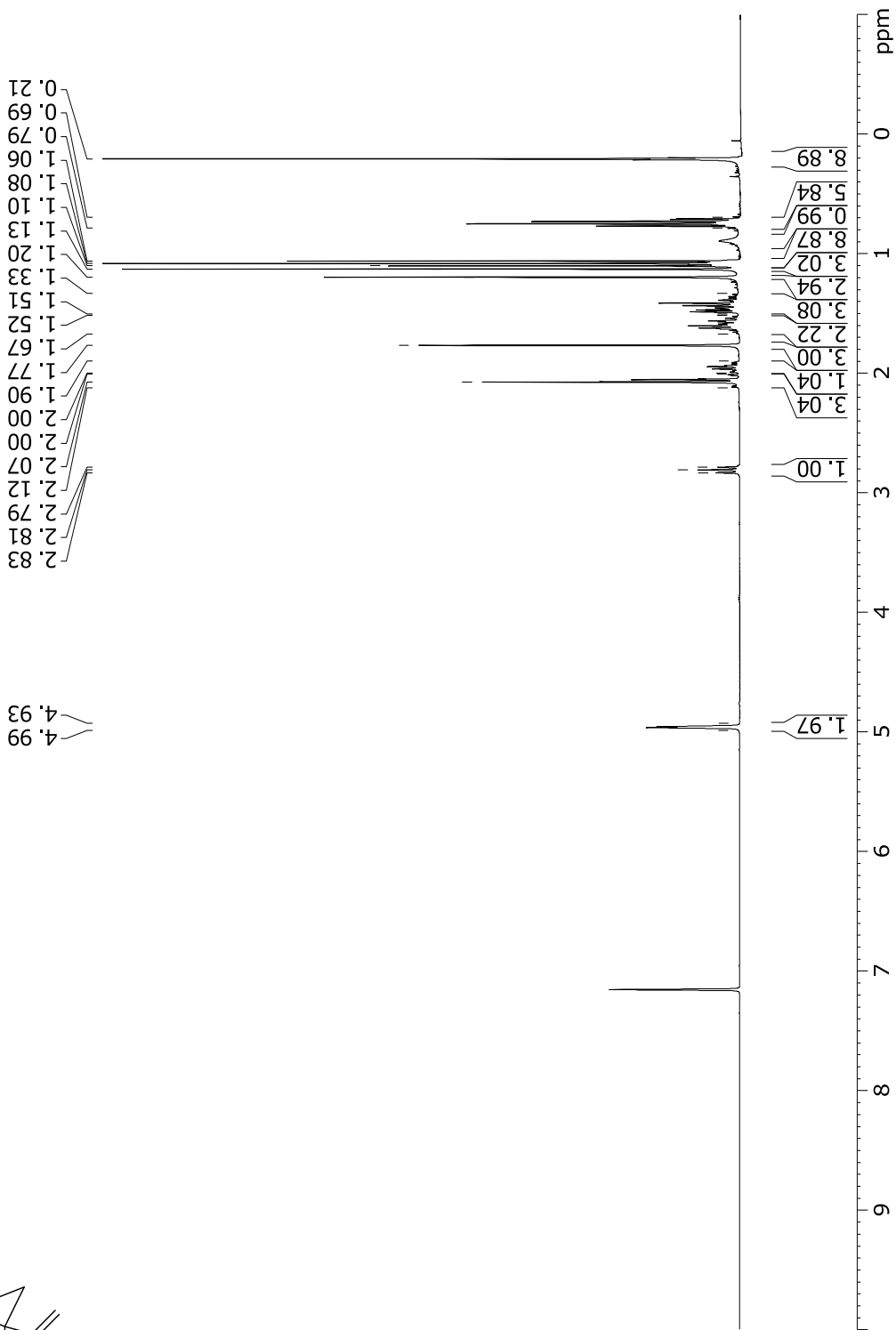
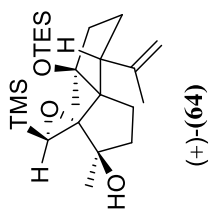


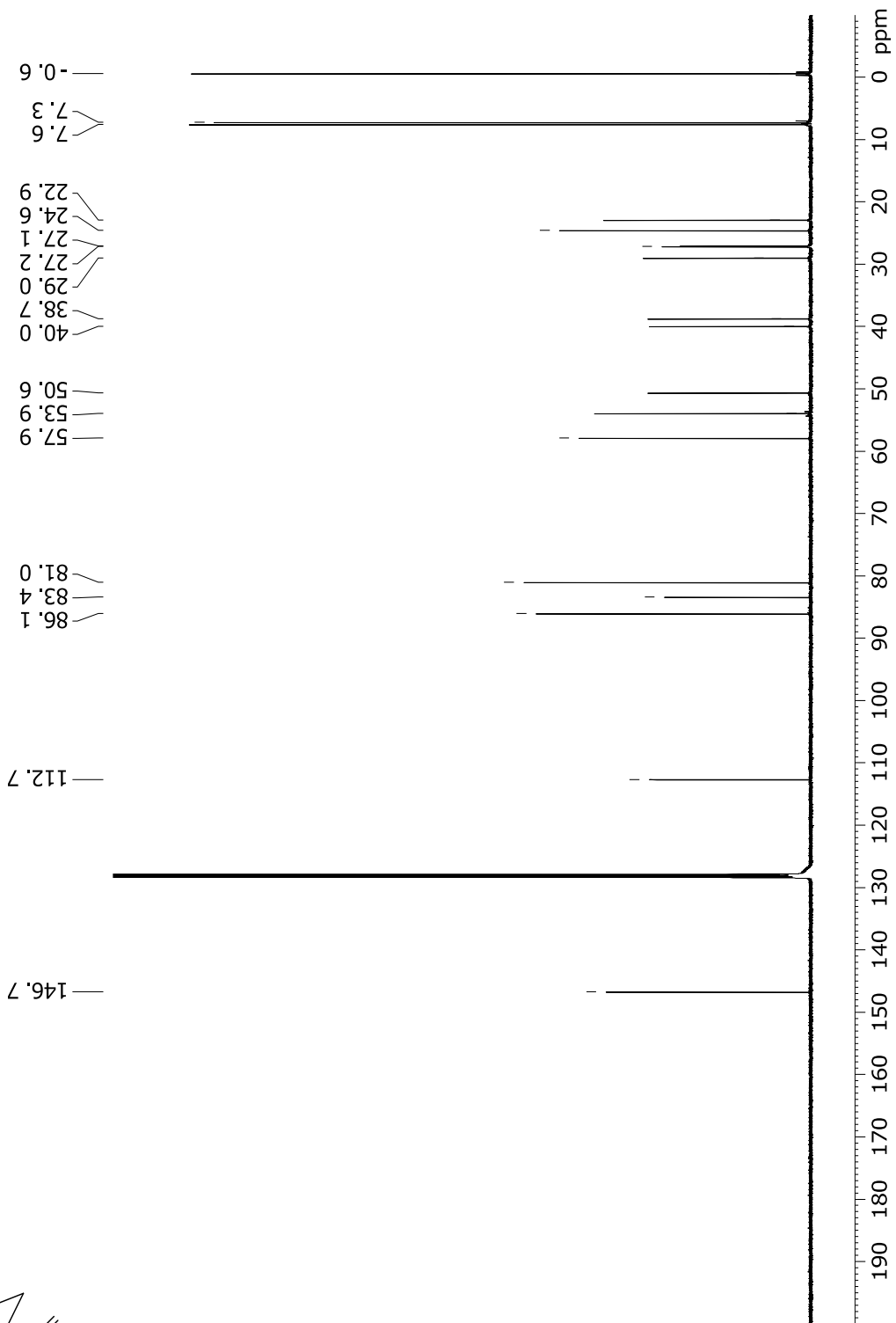
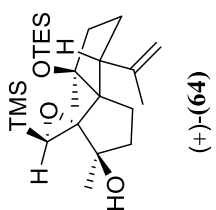
(29)

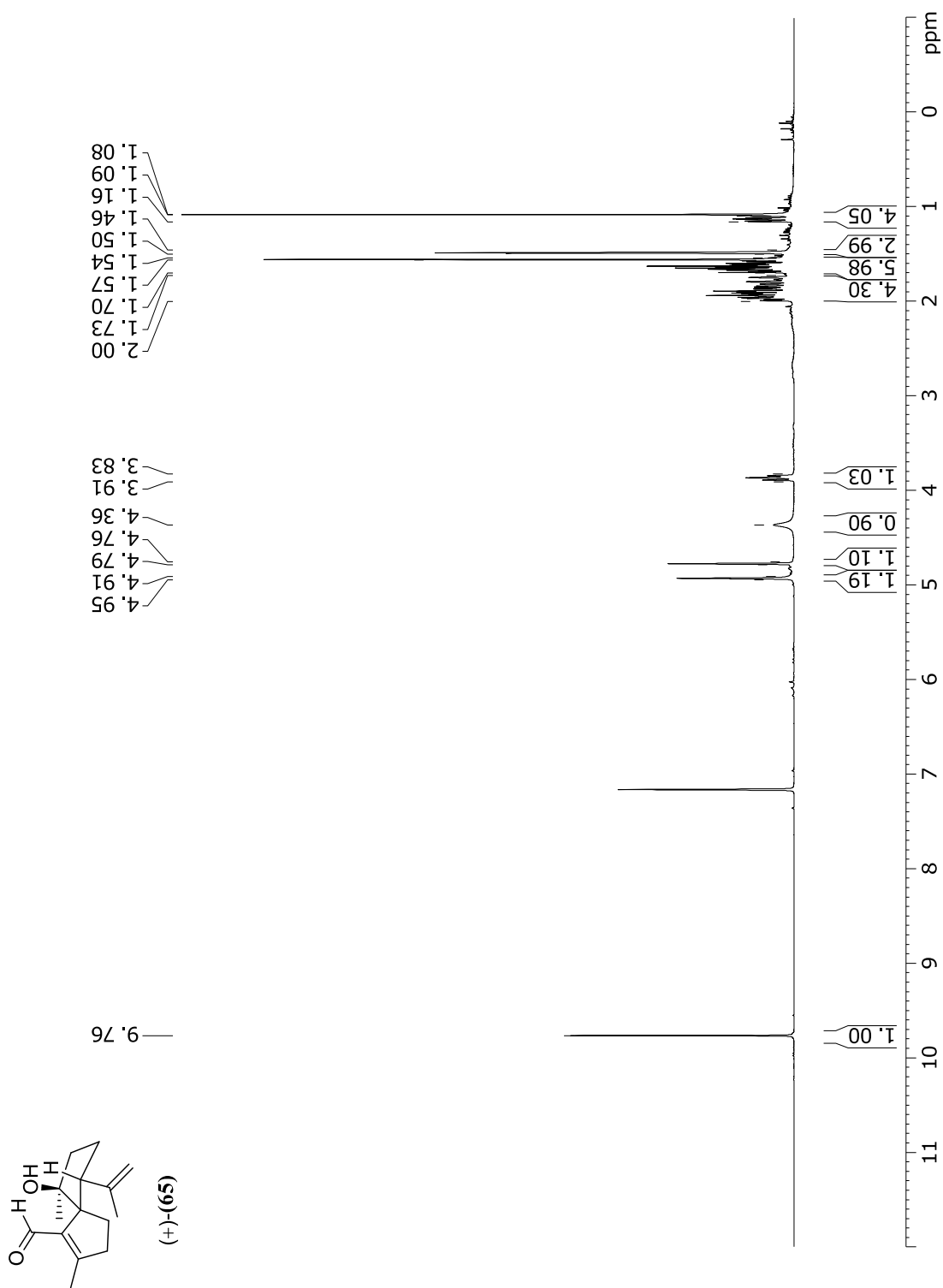


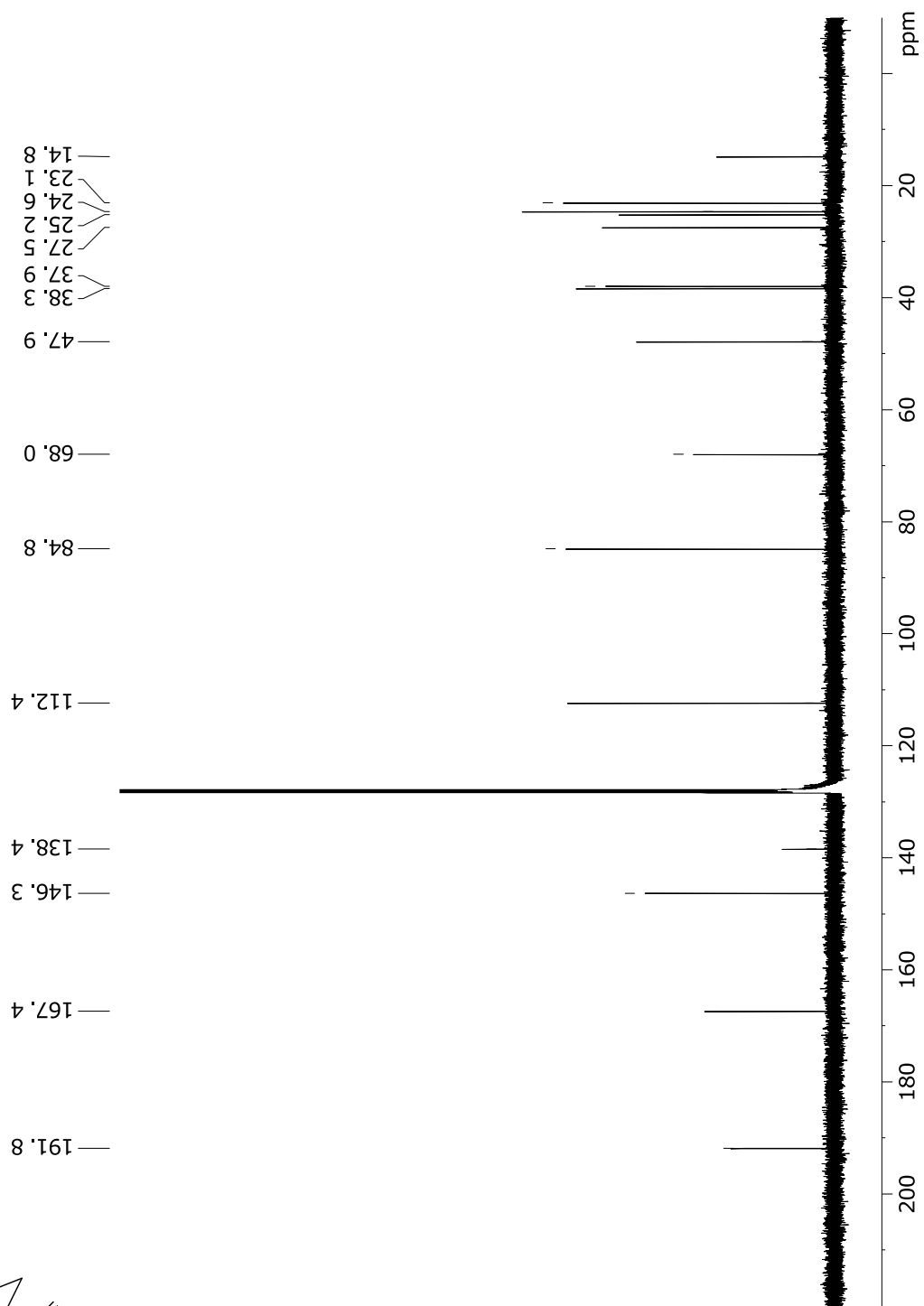
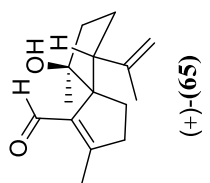


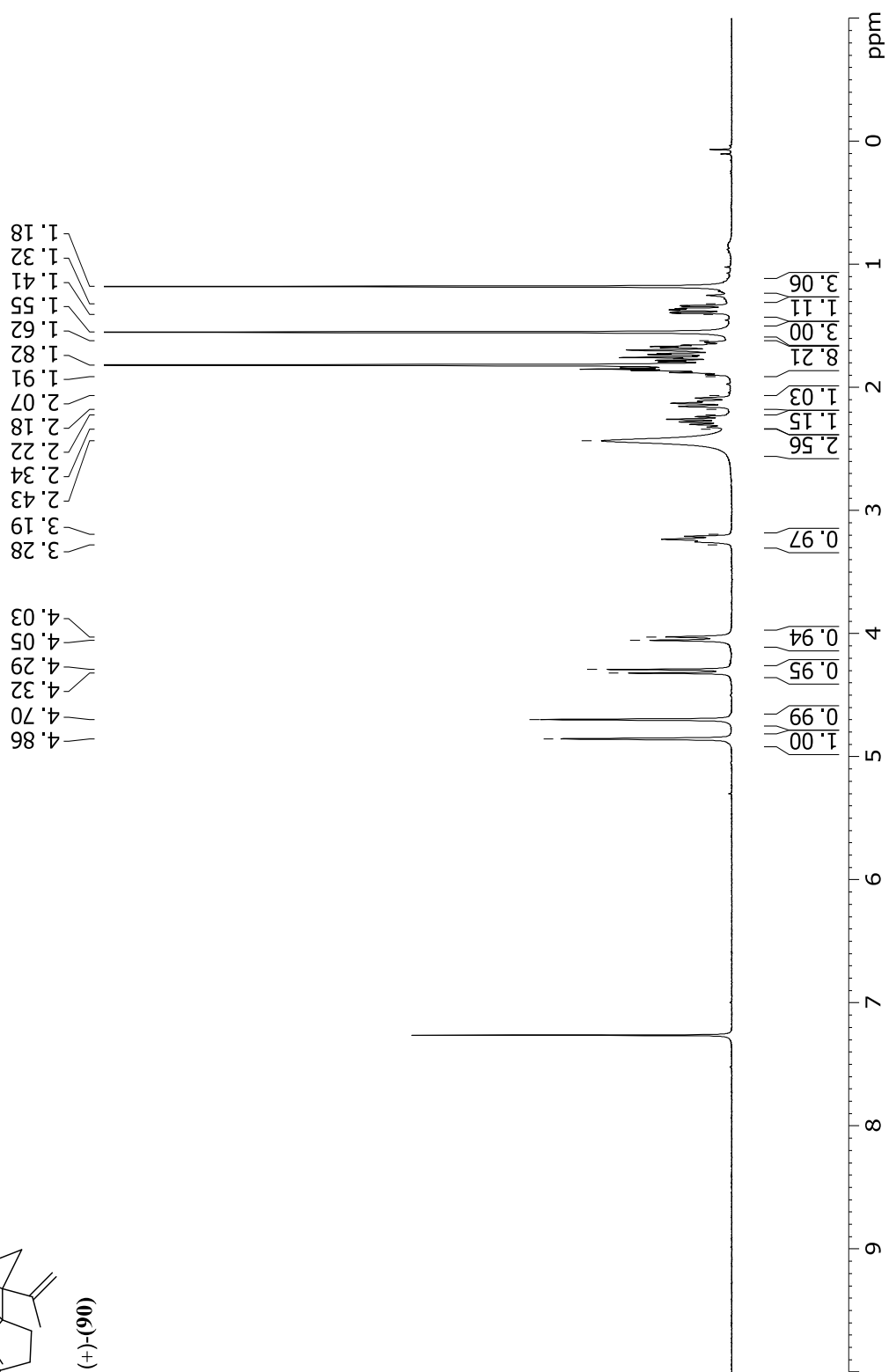
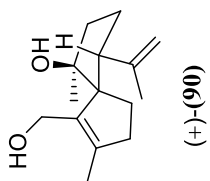


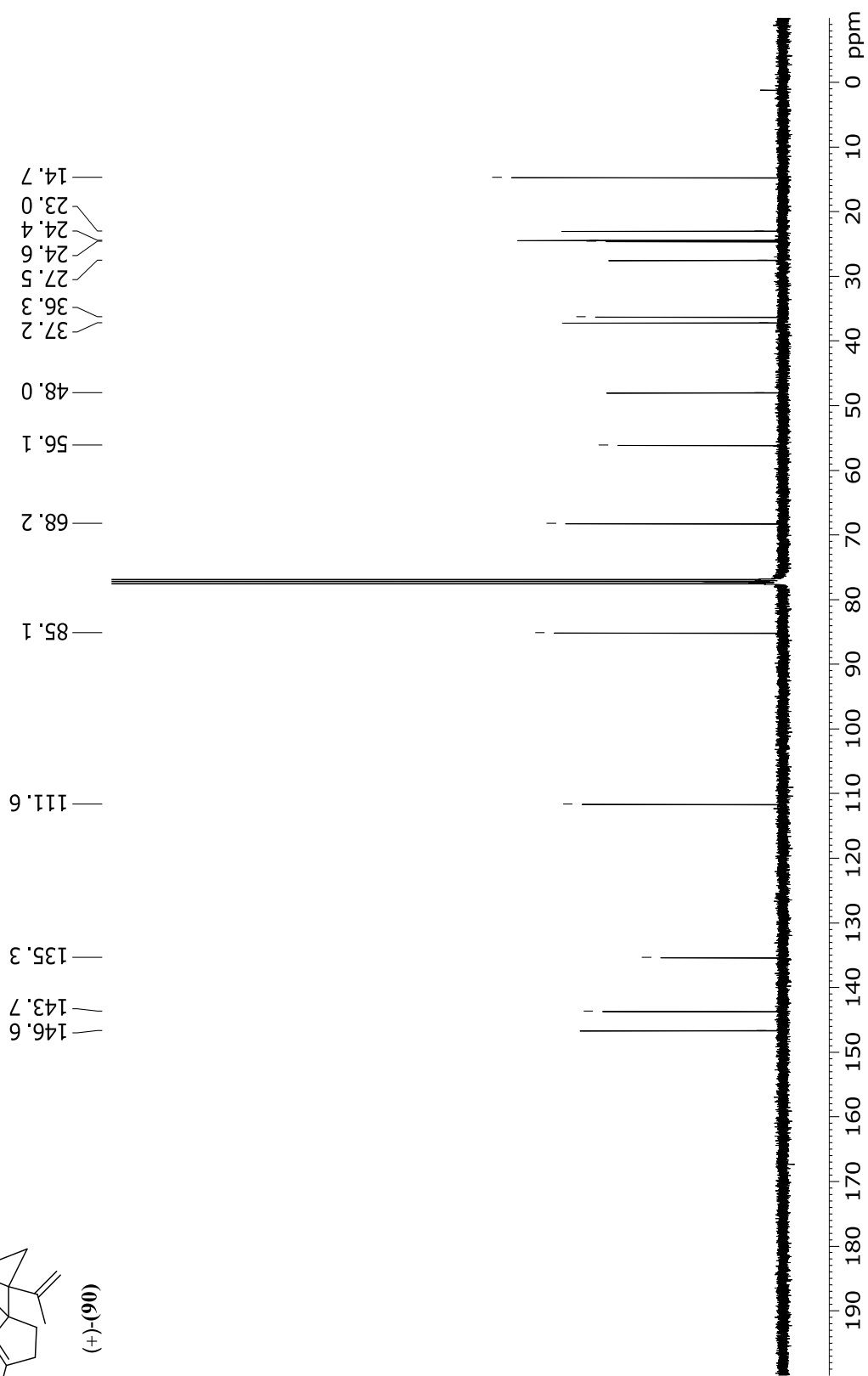
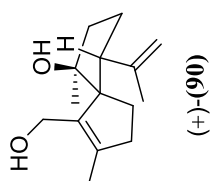


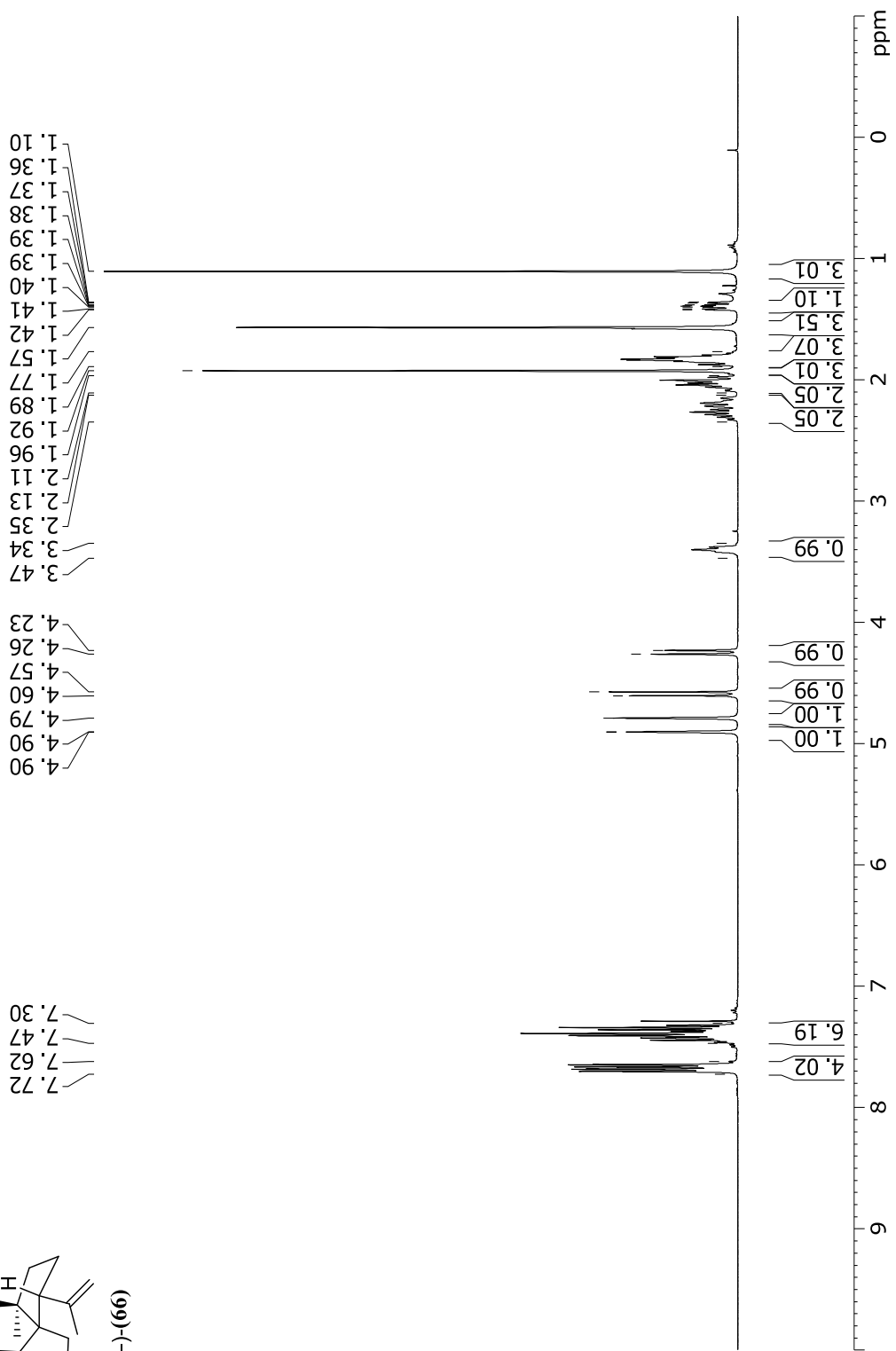
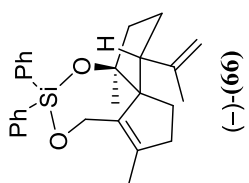


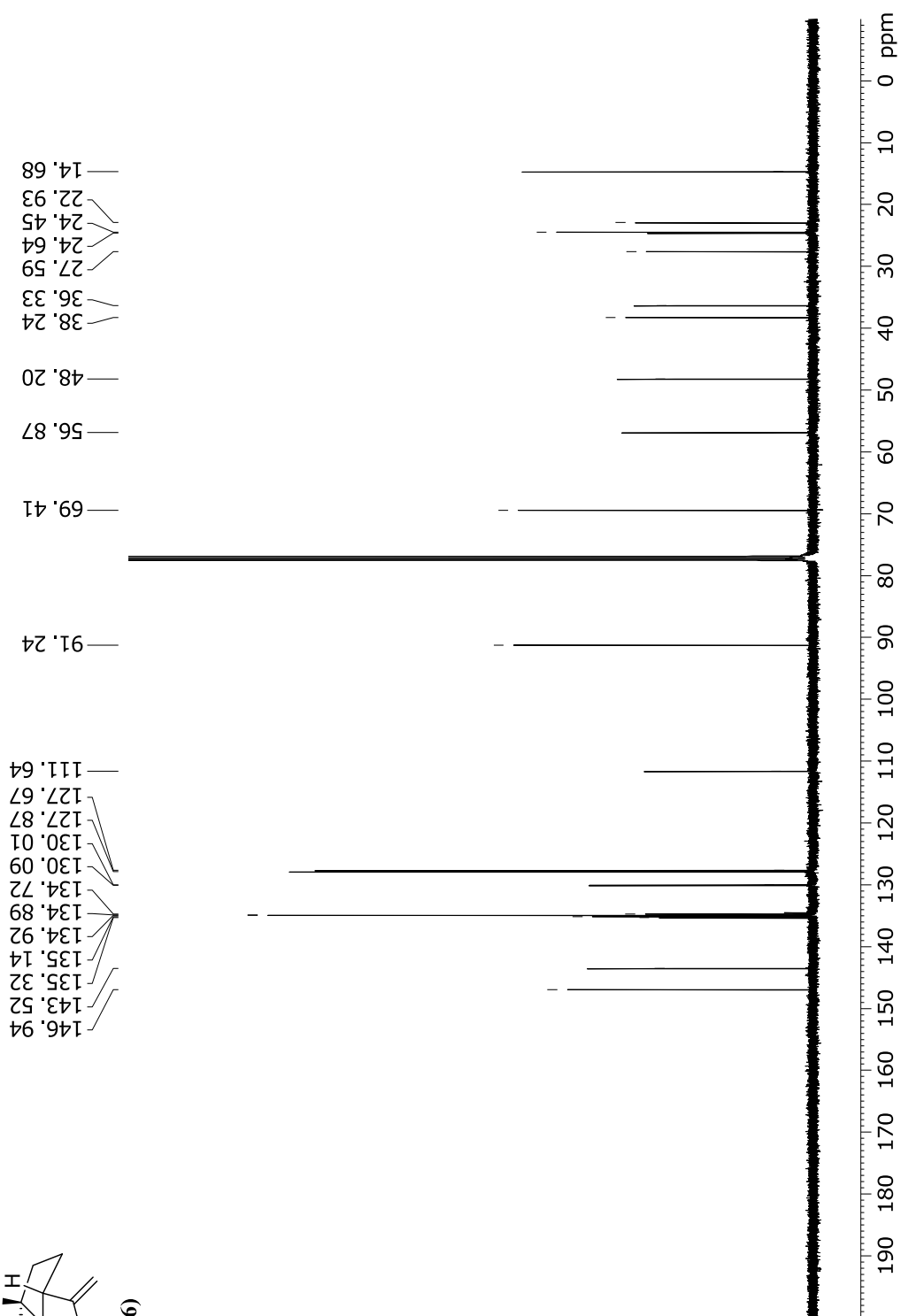
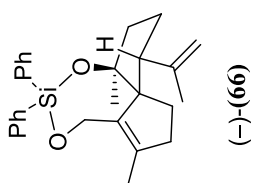


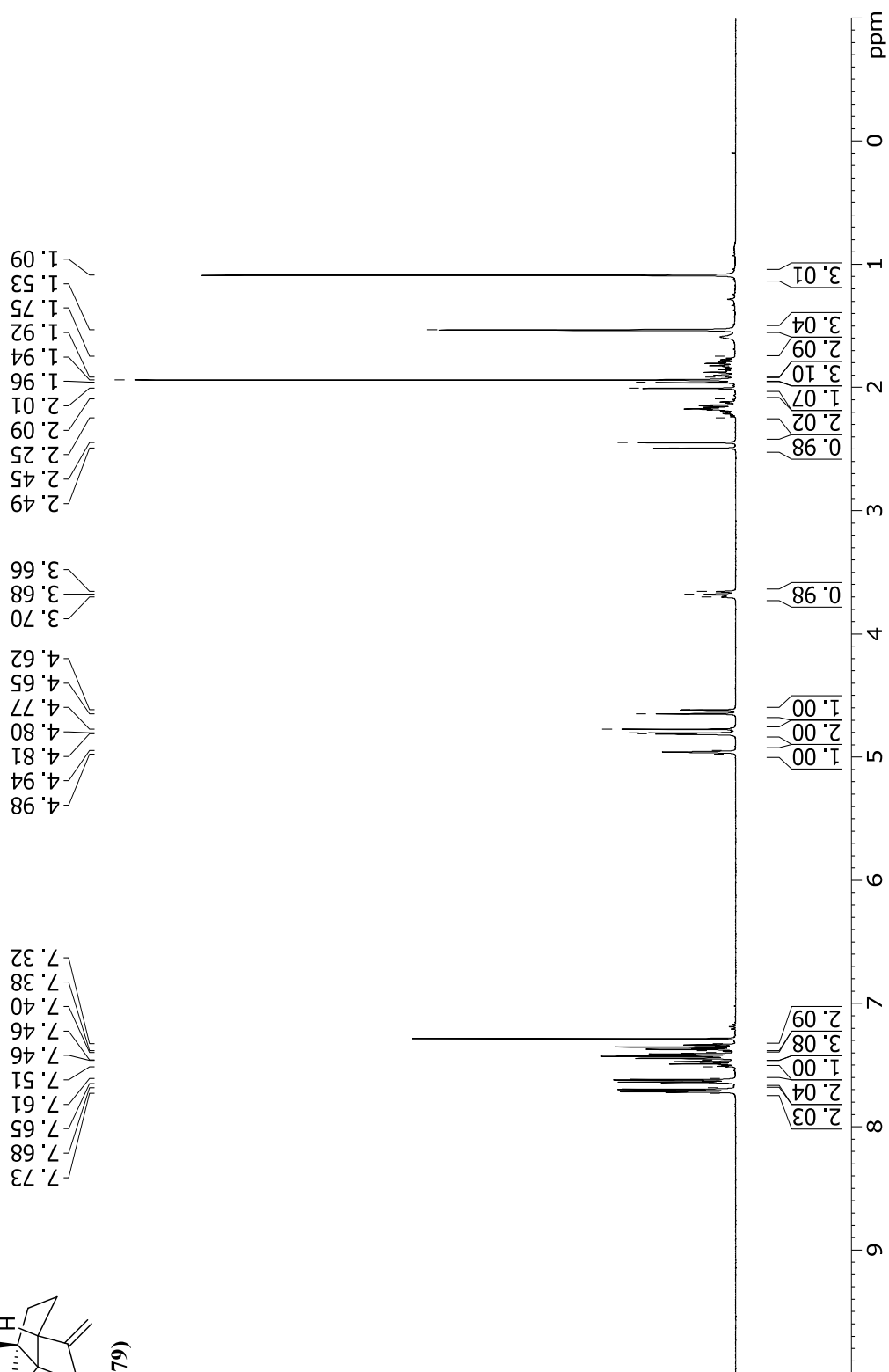
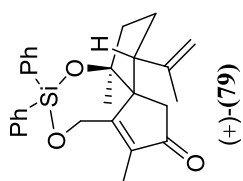


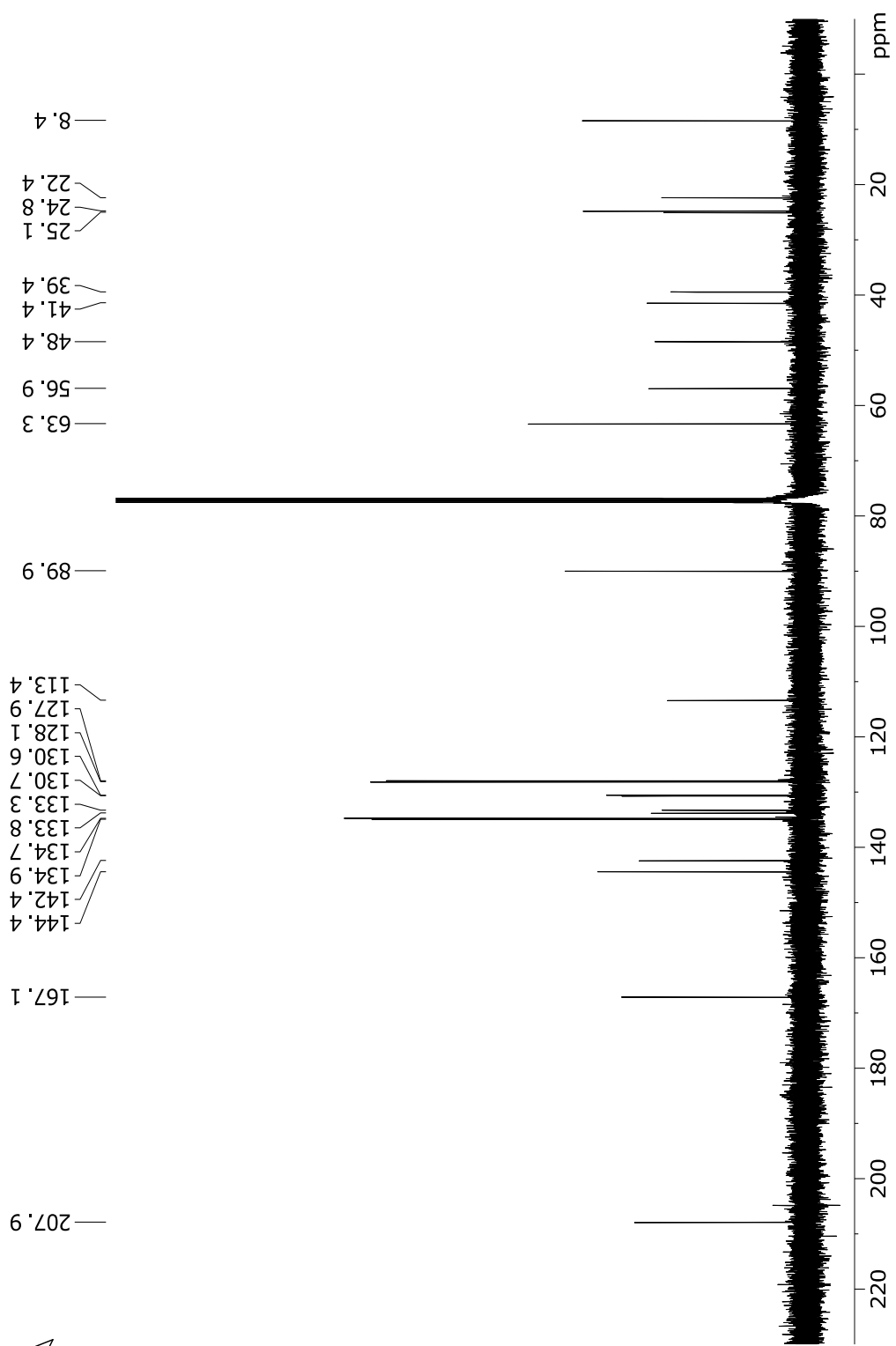
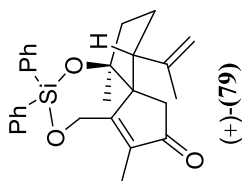


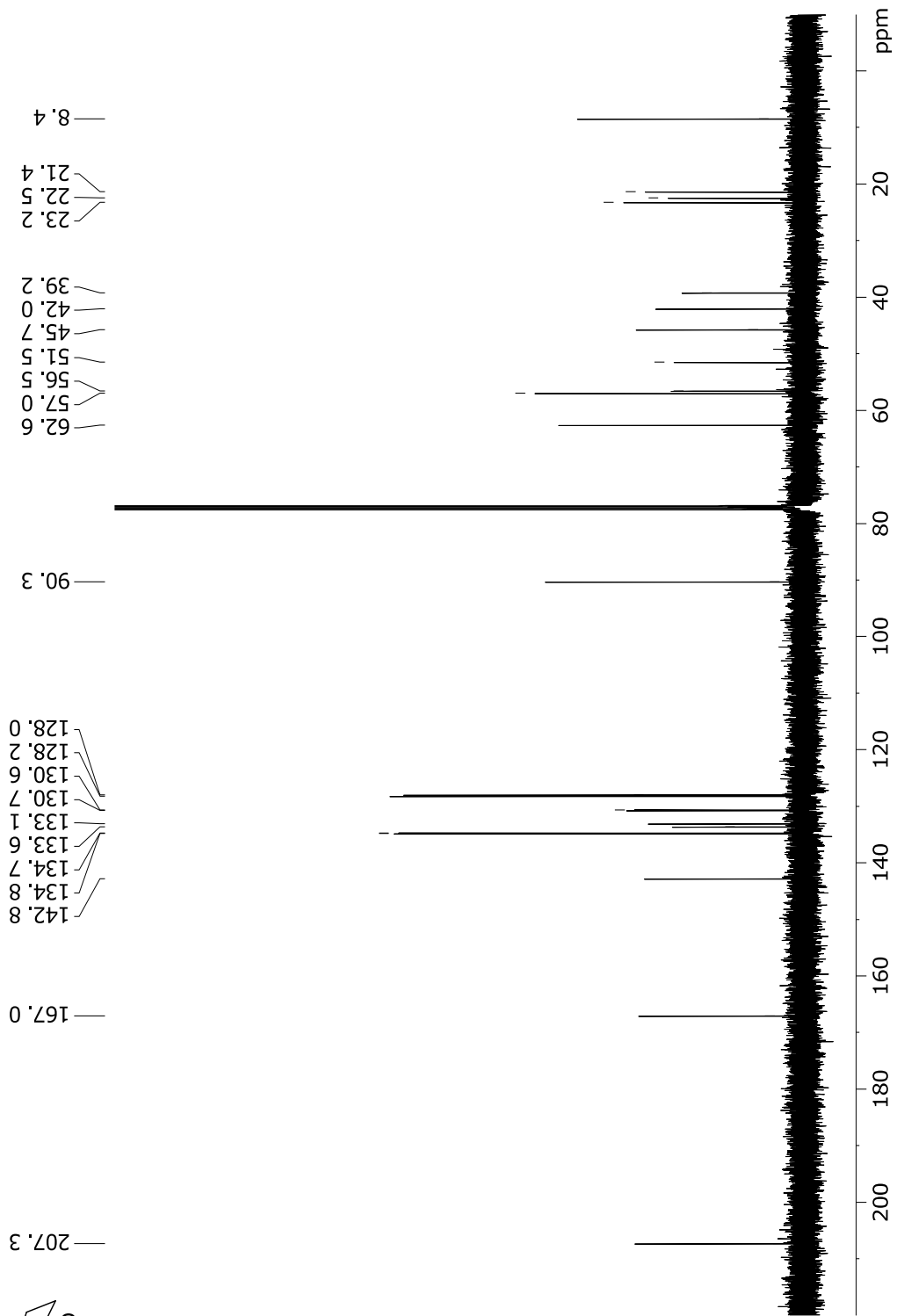
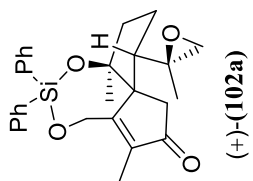


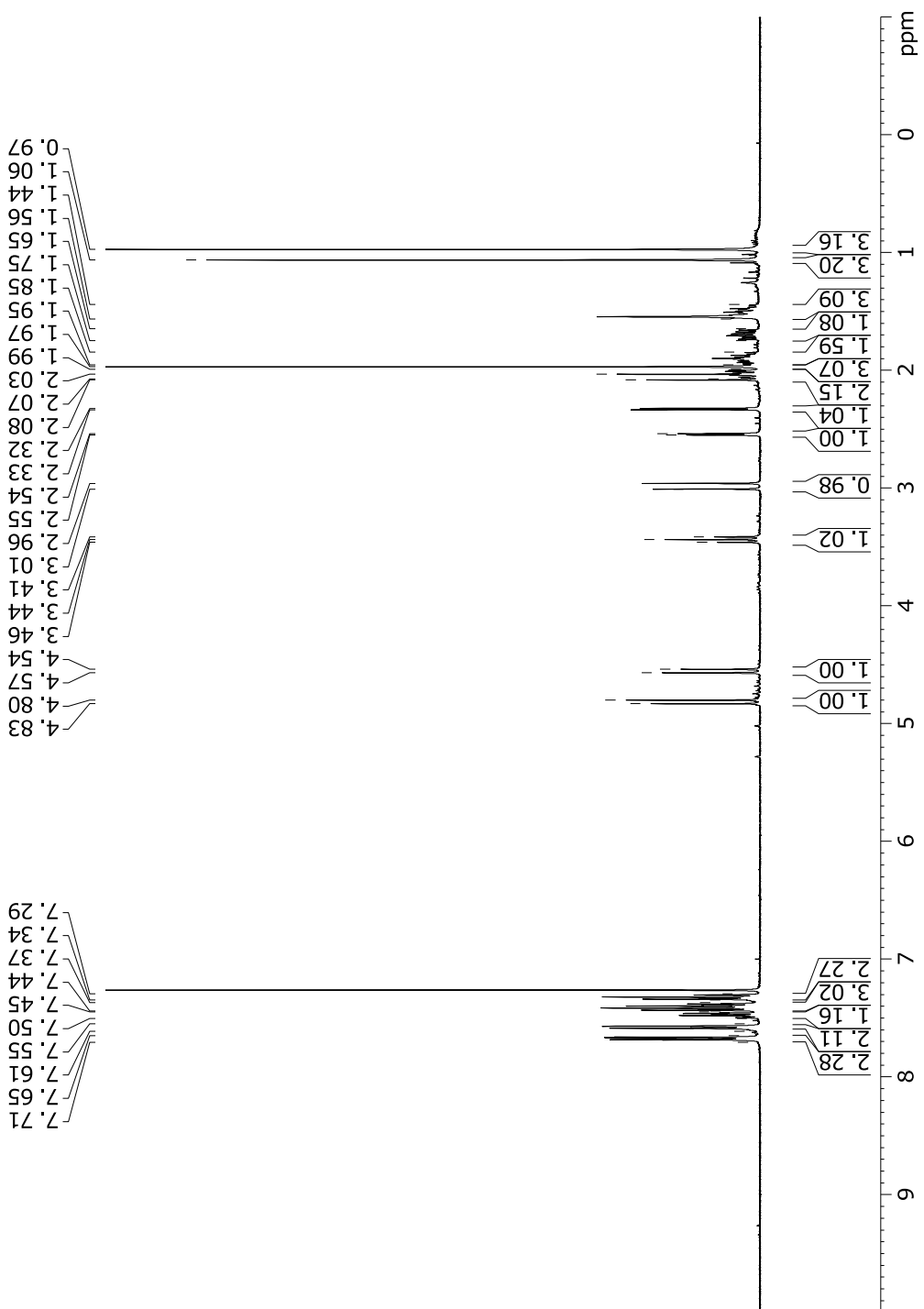
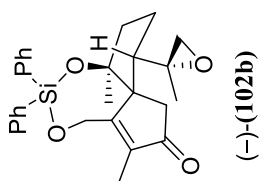


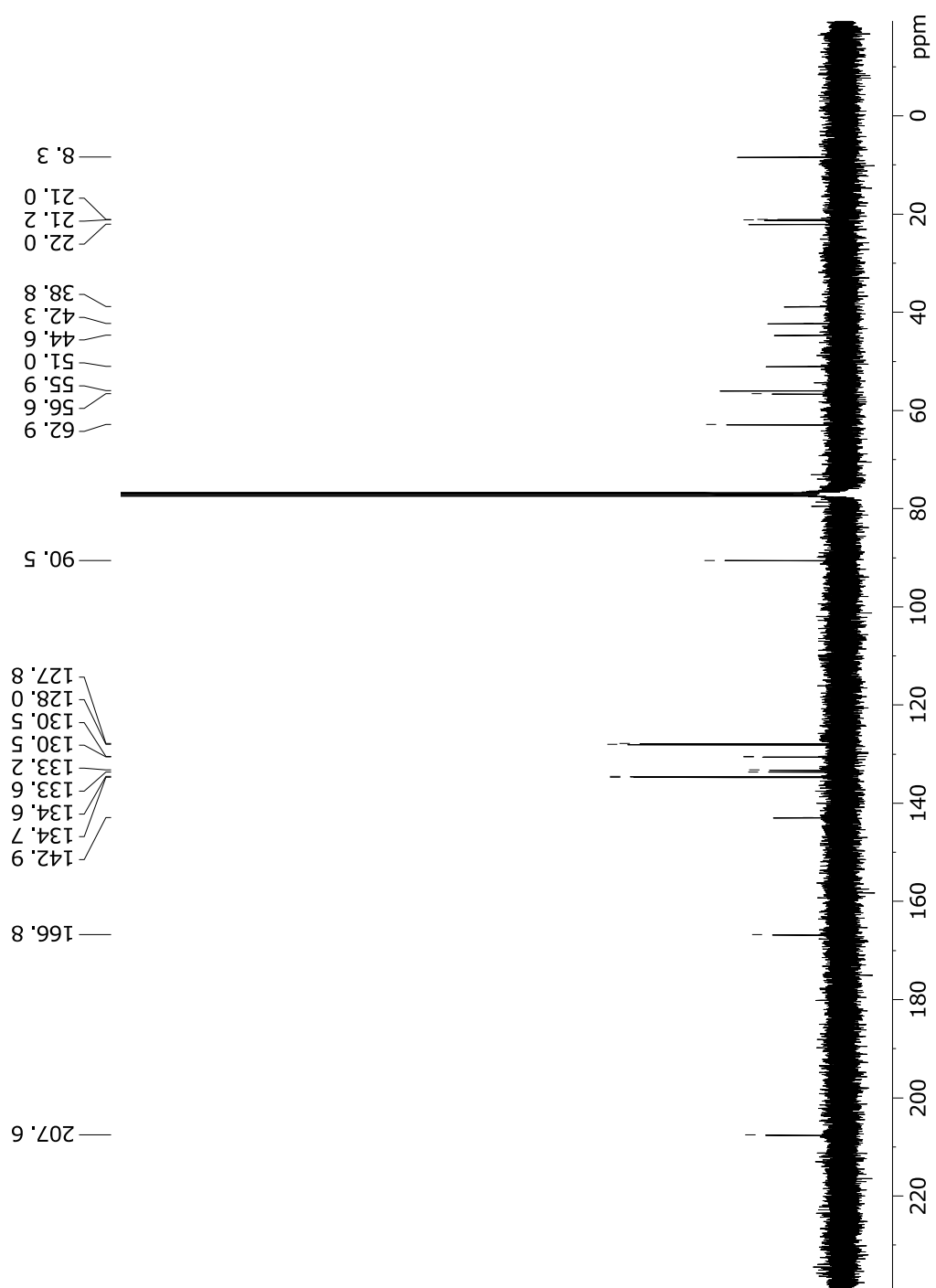
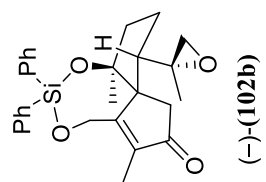


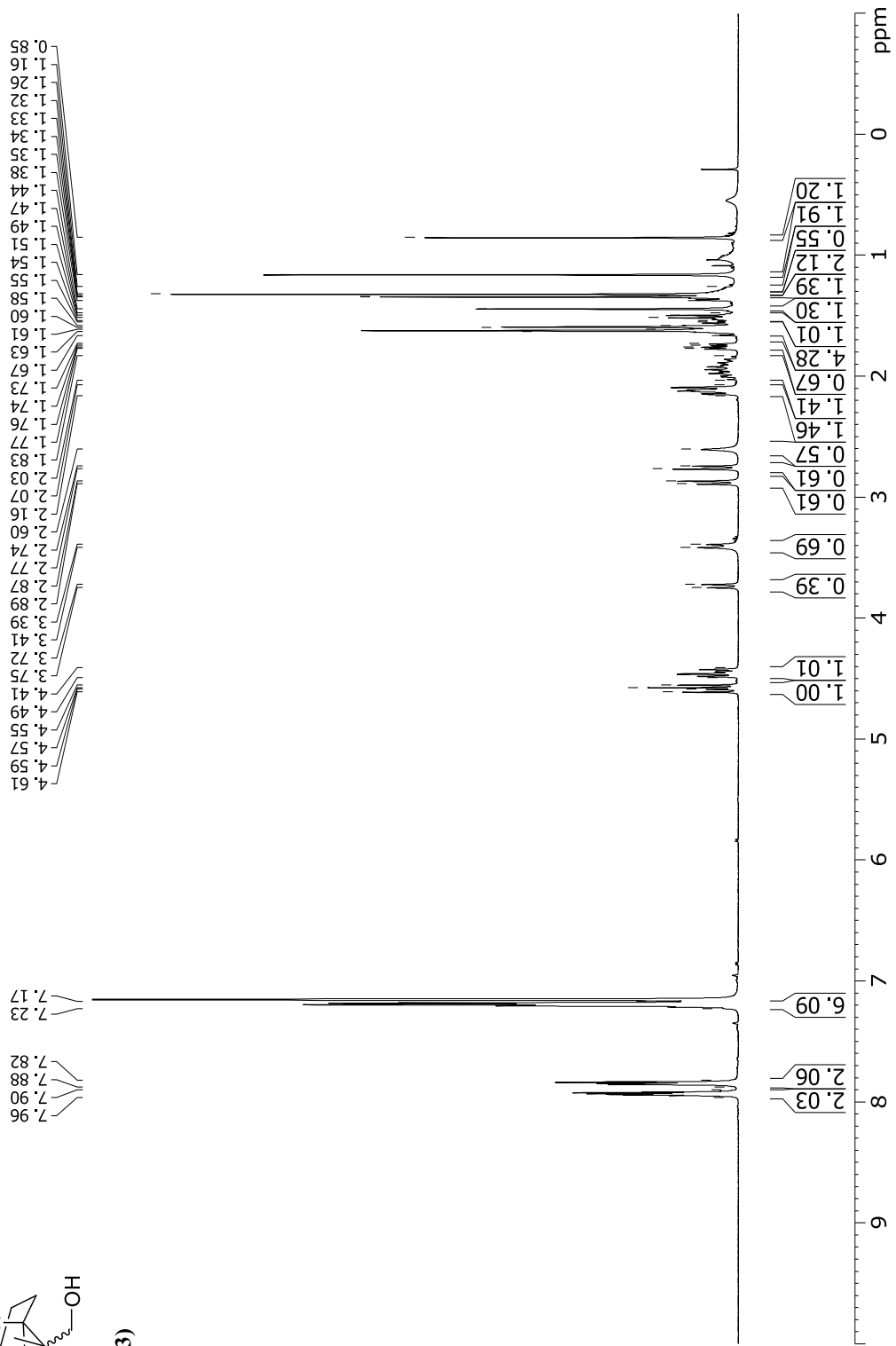
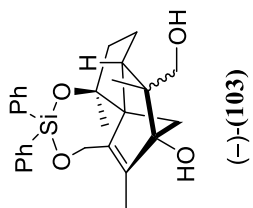


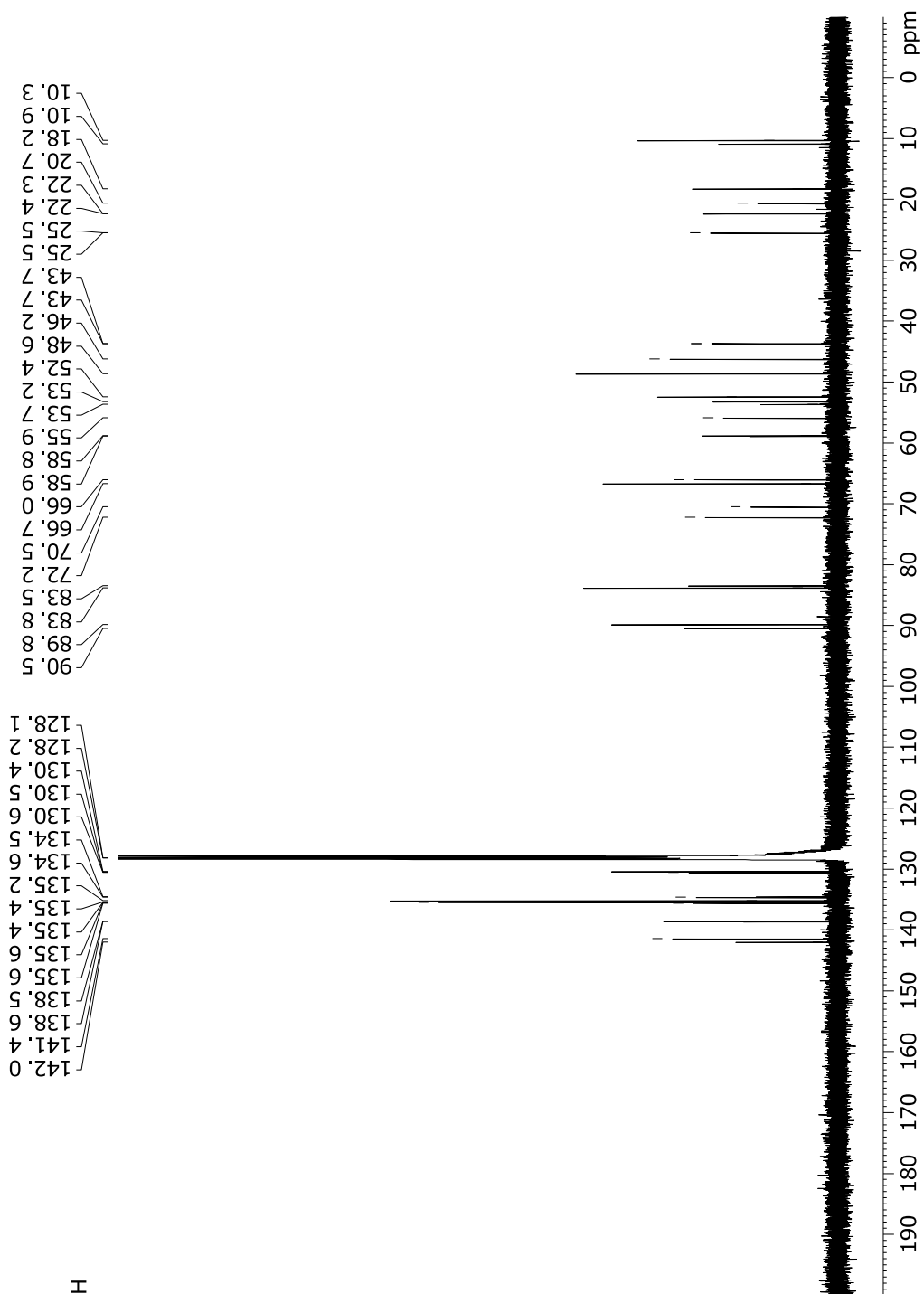
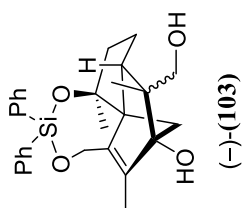


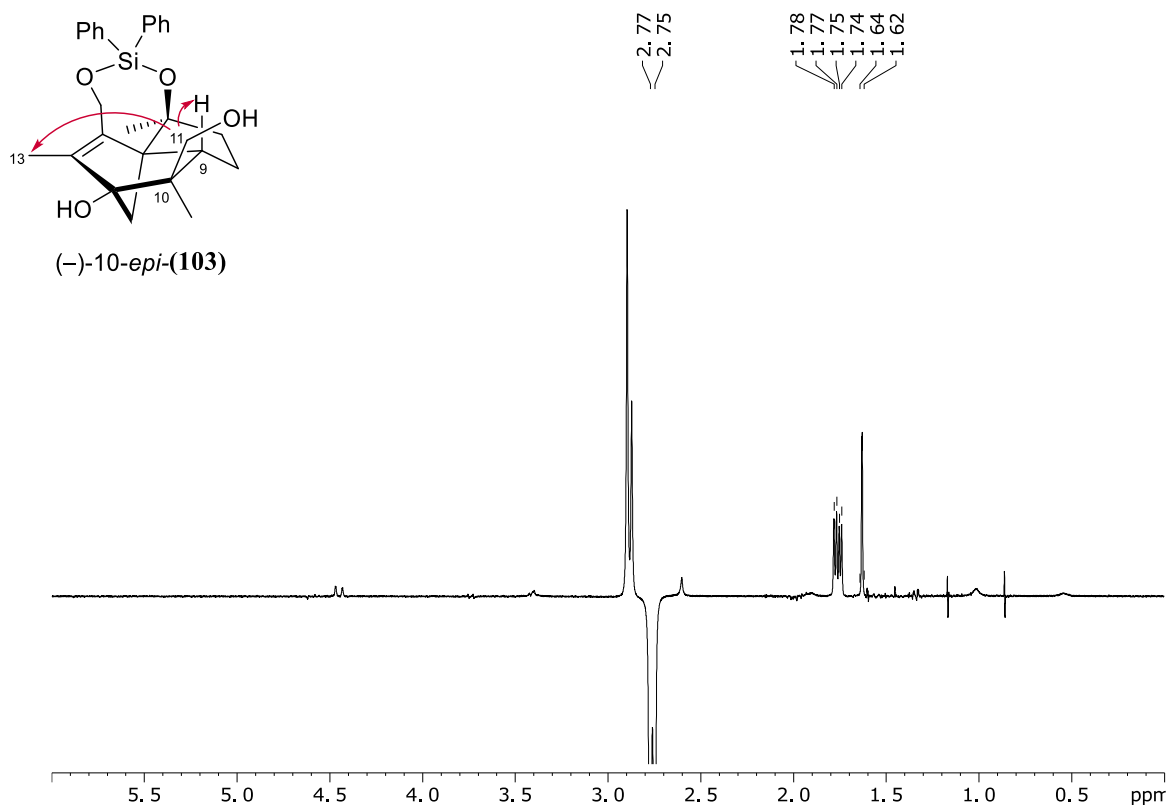




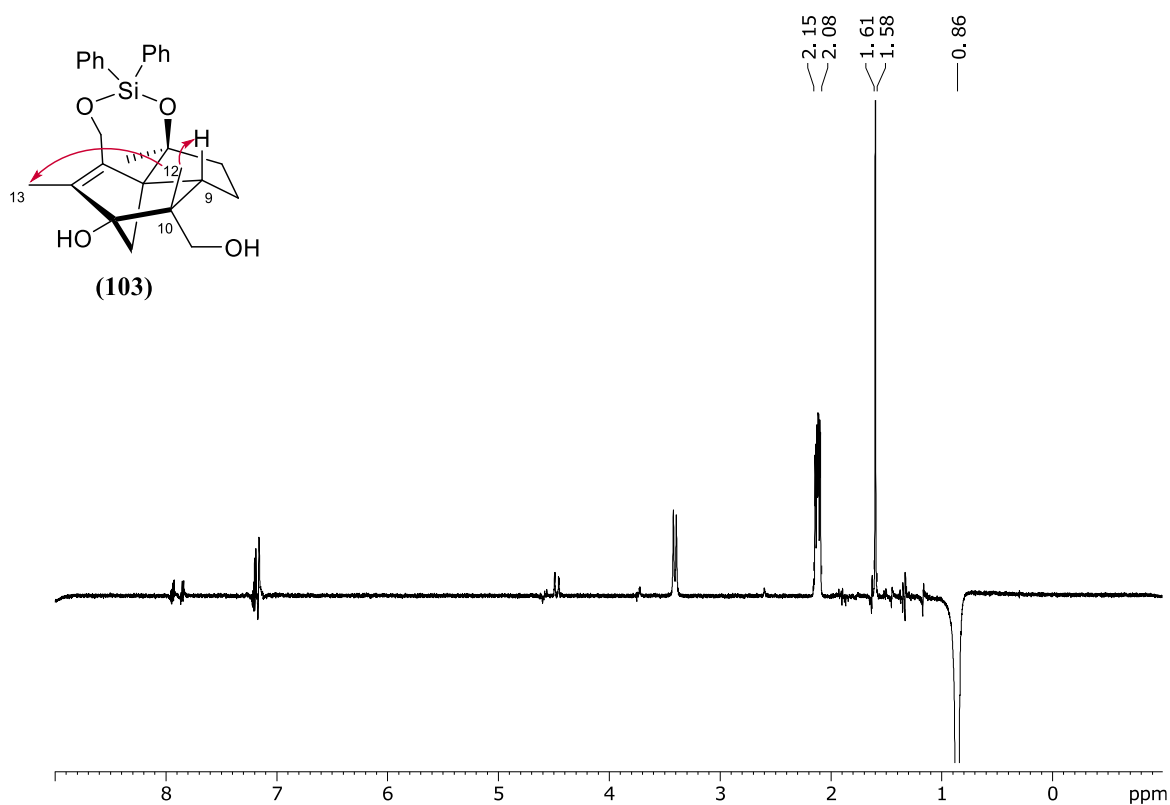




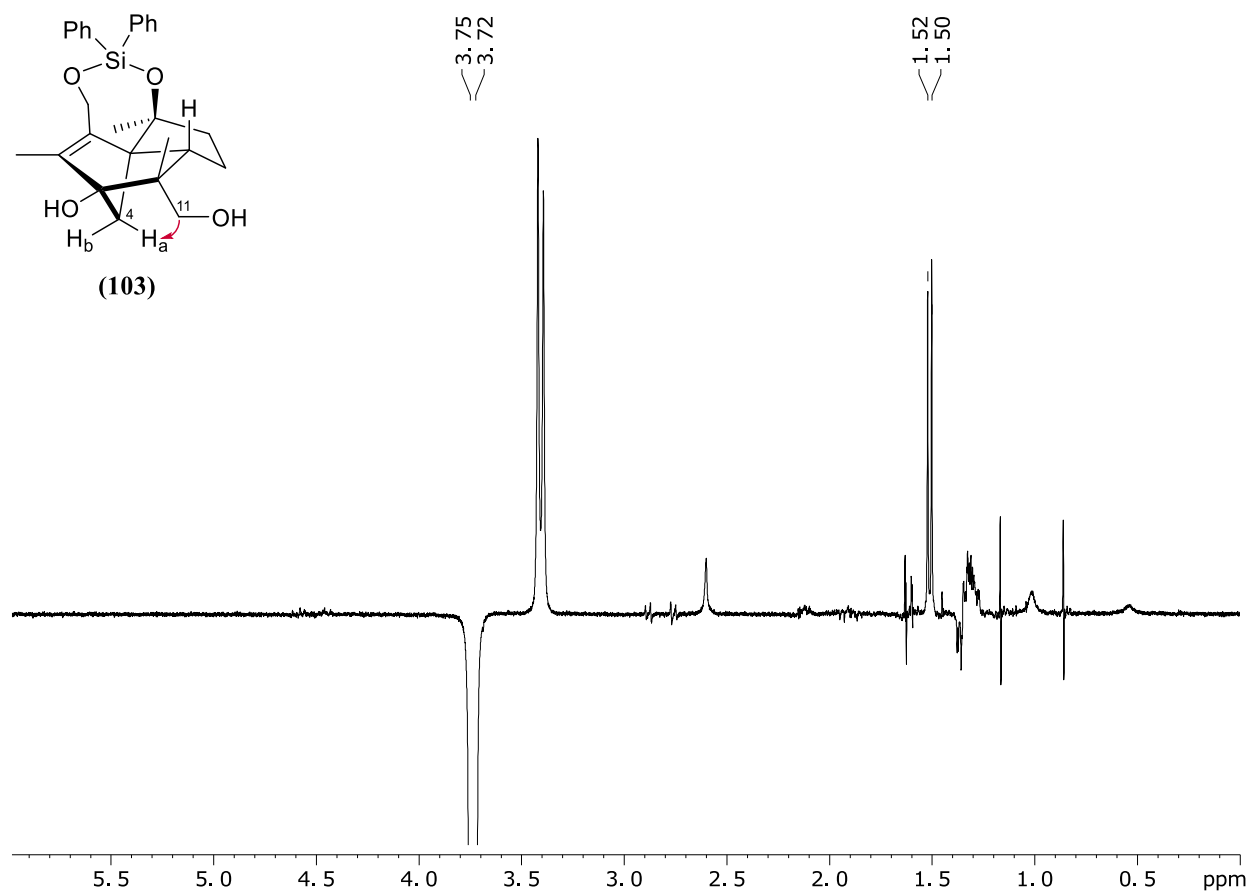
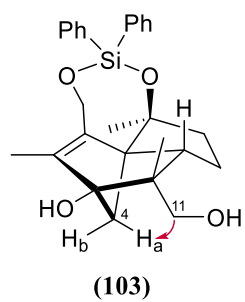




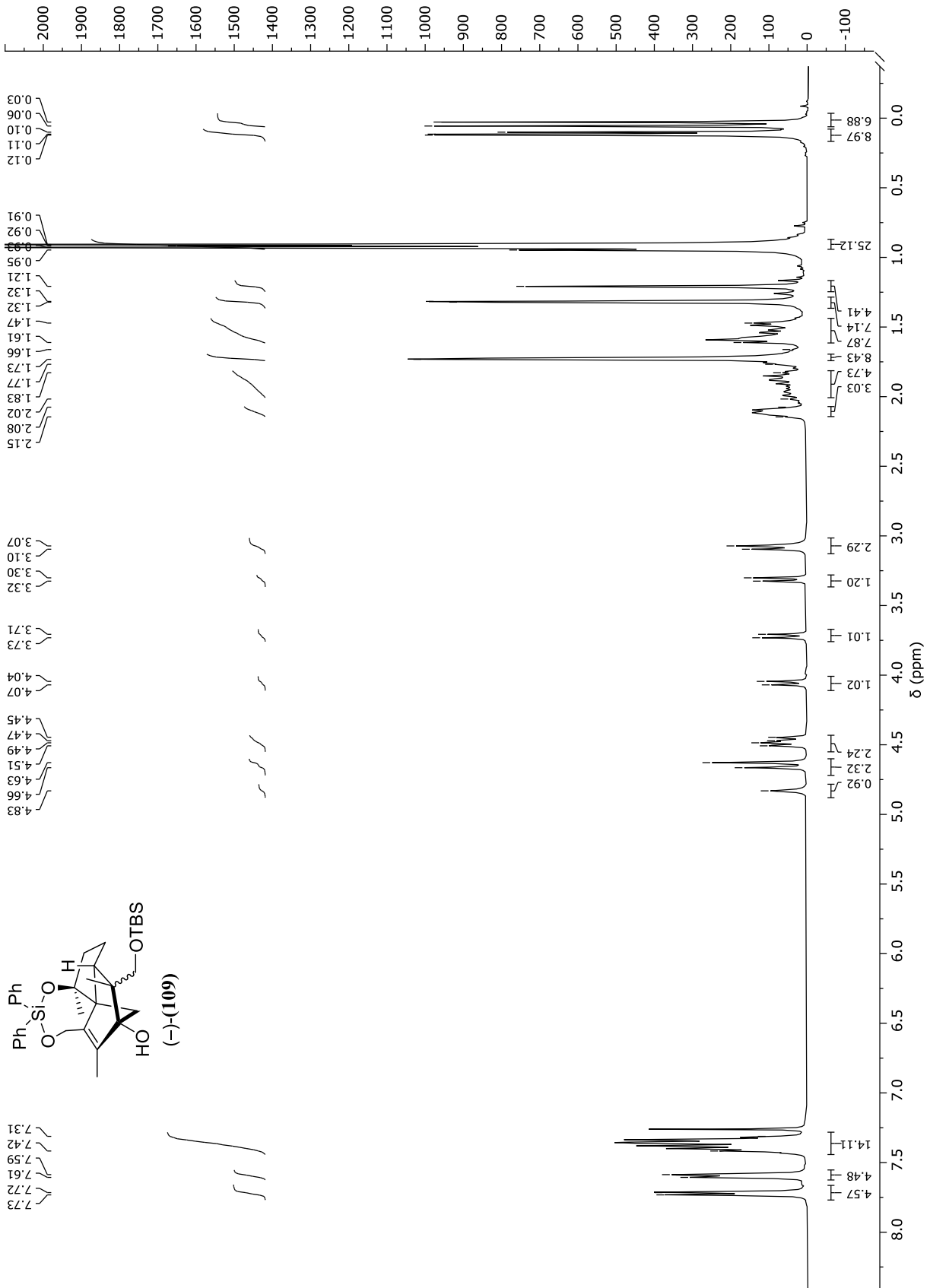
NOE response of cyclization product 10-epi-(103) (diastereomeric mixture) after irradiation at 2.75 ppm (major H-11b), showing the diagnostic correlations for the proposed stereoconfiguration of the major diastereomer. Spectrum measured in C_6D_6 at 400 MHz.

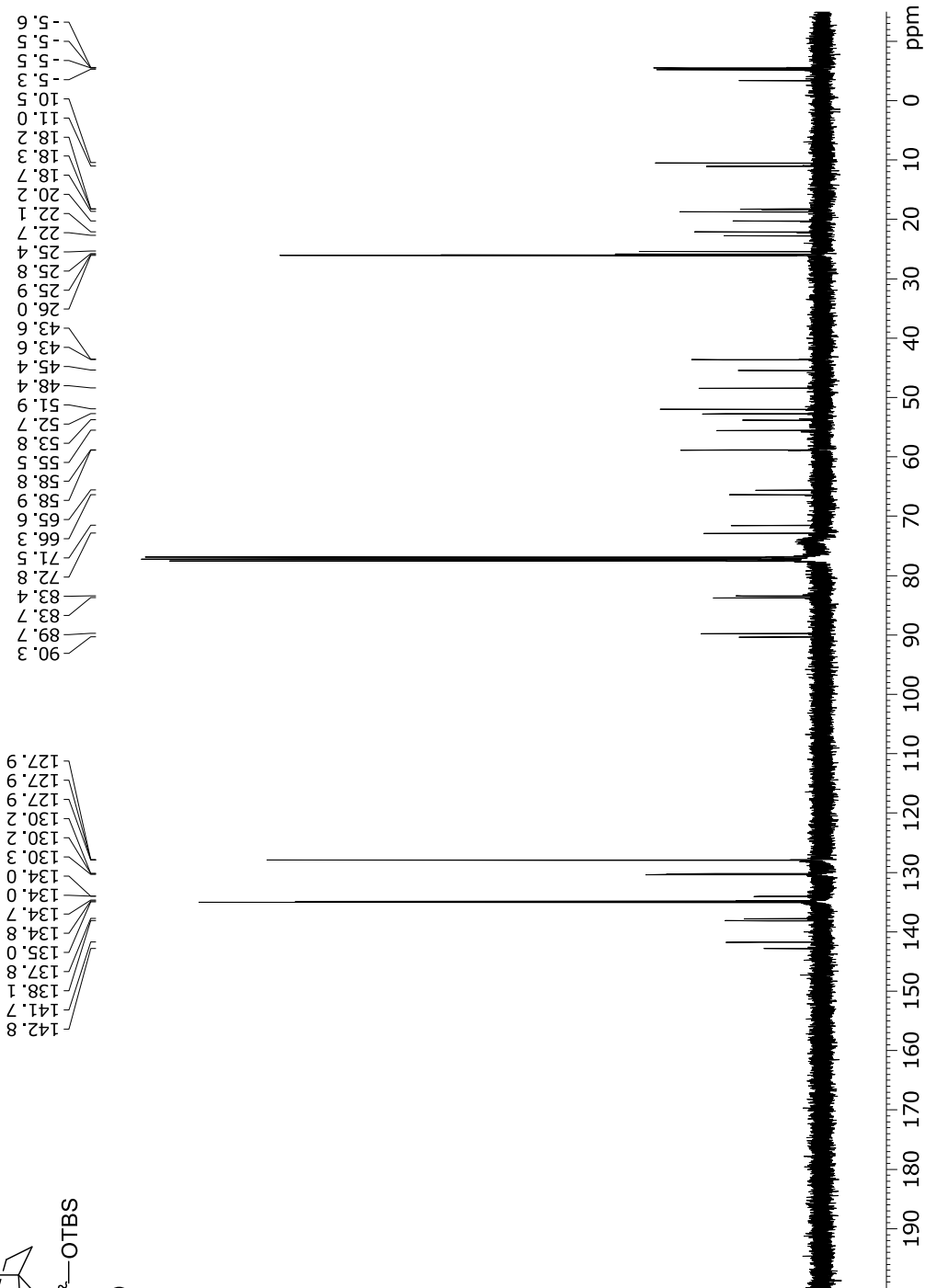
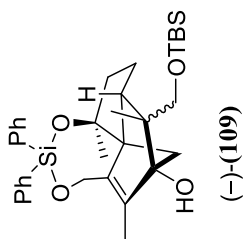


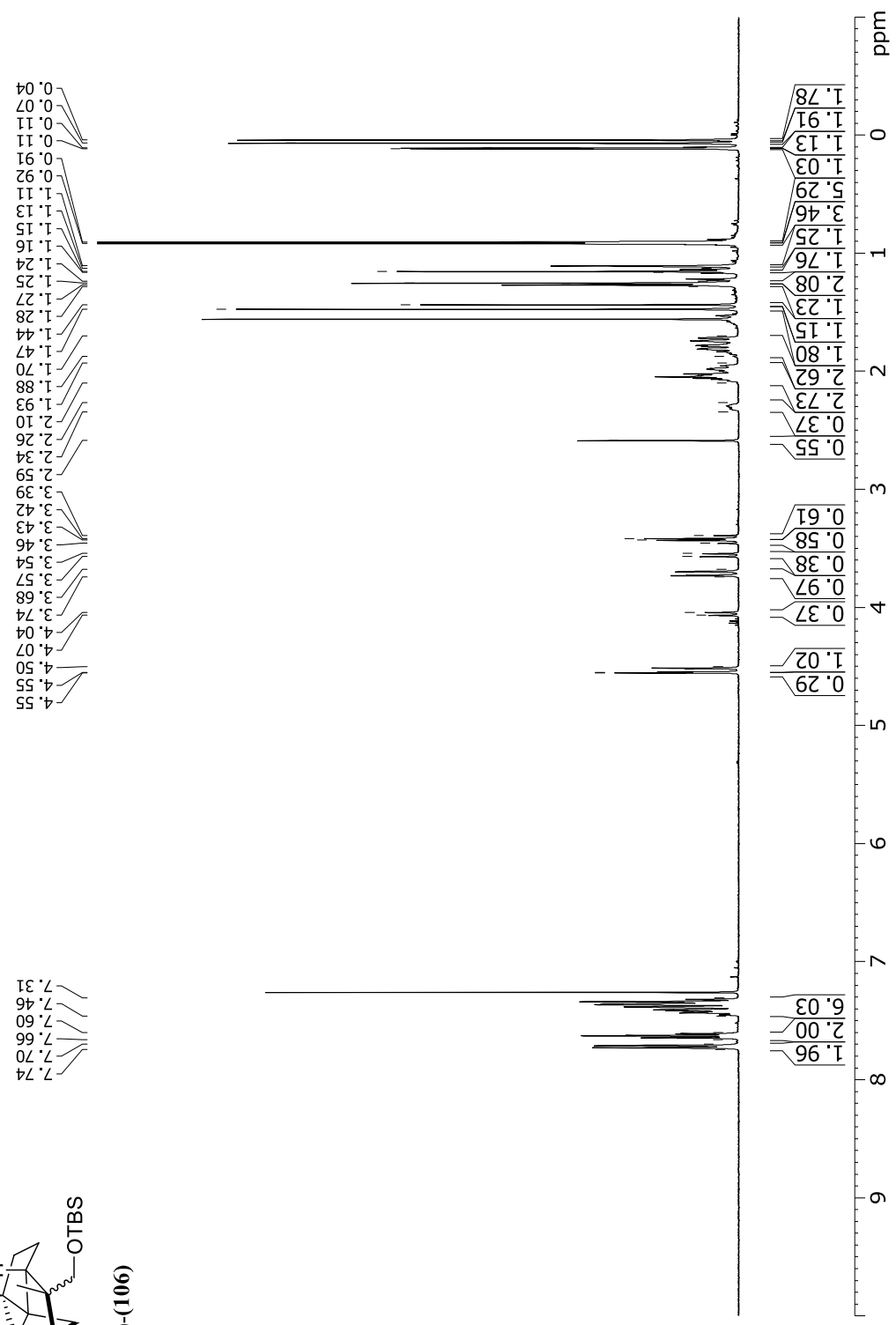
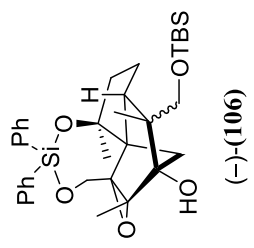
NOE response of cyclization product (103) (diastereomeric mixture) after irradiation at 0.86 ppm (minor CH_3 -12), showing the diagnostic correlations for the proposed stereoconfiguration of the minor diastereomer. Spectrum measured in C_6D_6 at 400 MHz.

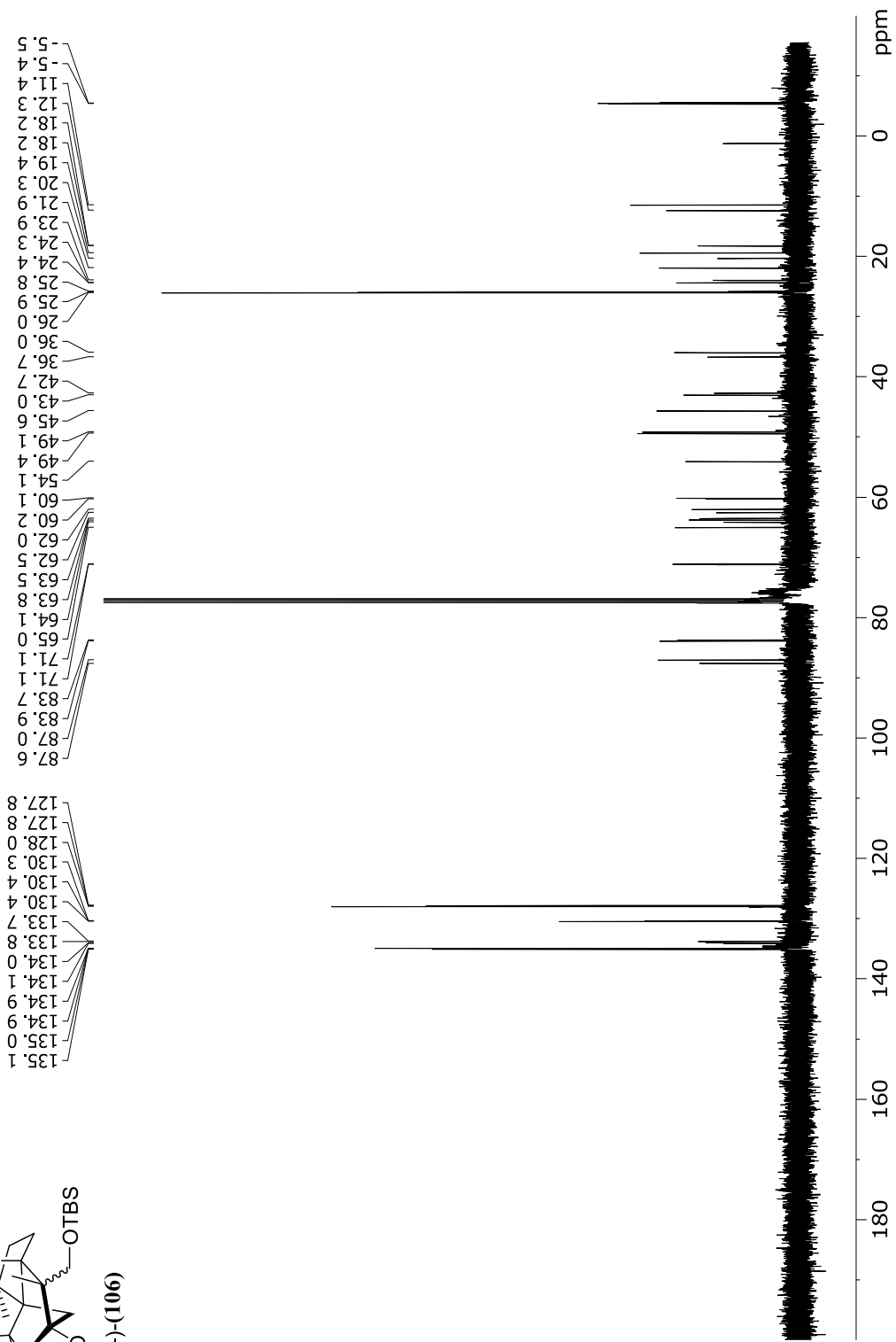
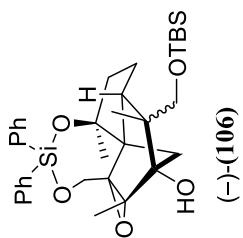


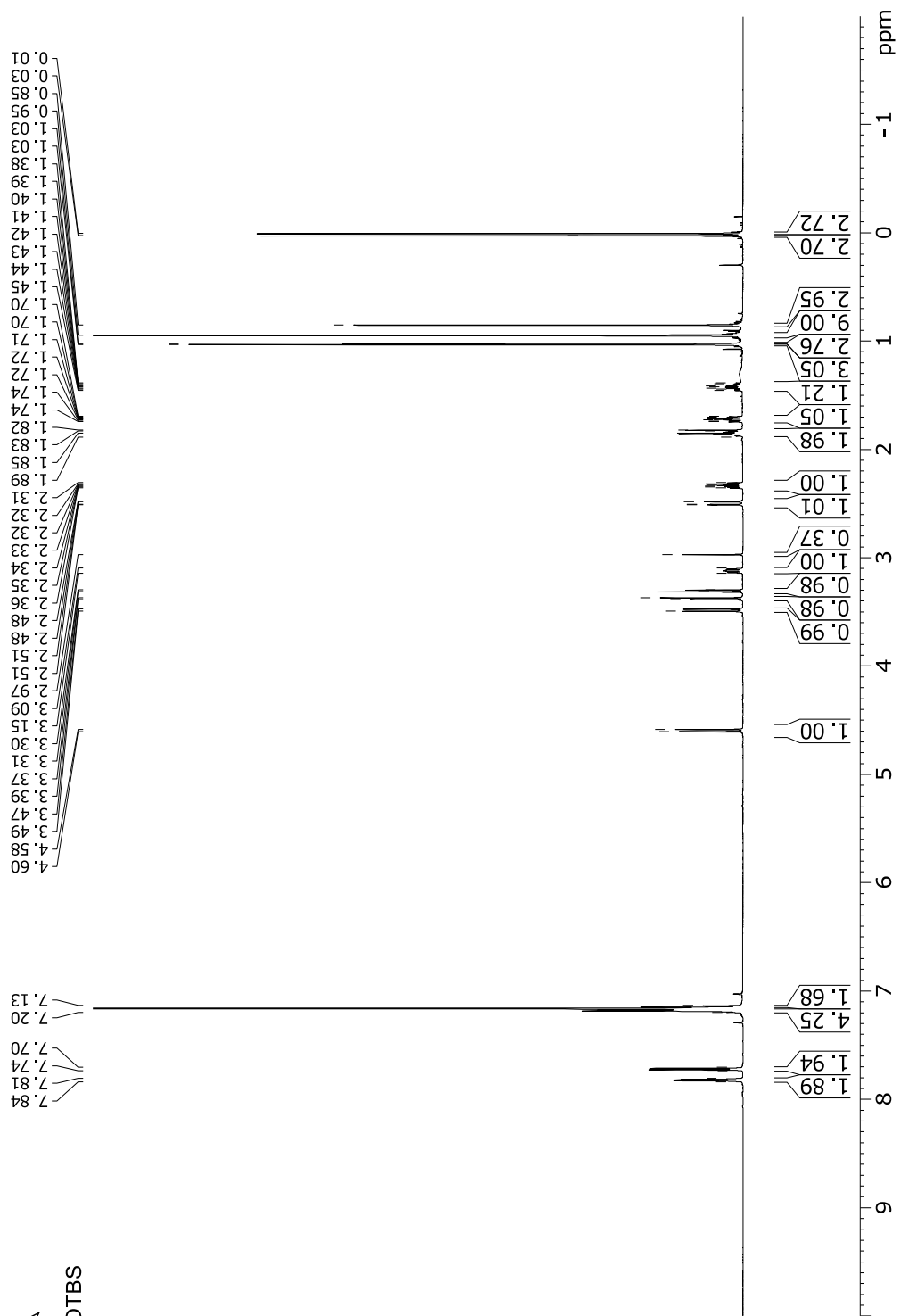
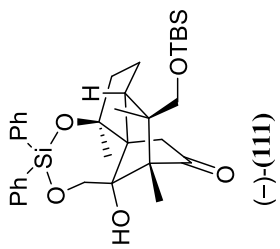
NOE response of cyclization product **(103)** (diastereomeric mixture) after irradiation at 3.73 ppm (minor H-11a), showing the diagnostic correlations for the proposed stereoconfiguration of the minor diastereomer. Spectrum measured in C_6D_6 at 400 MHz.

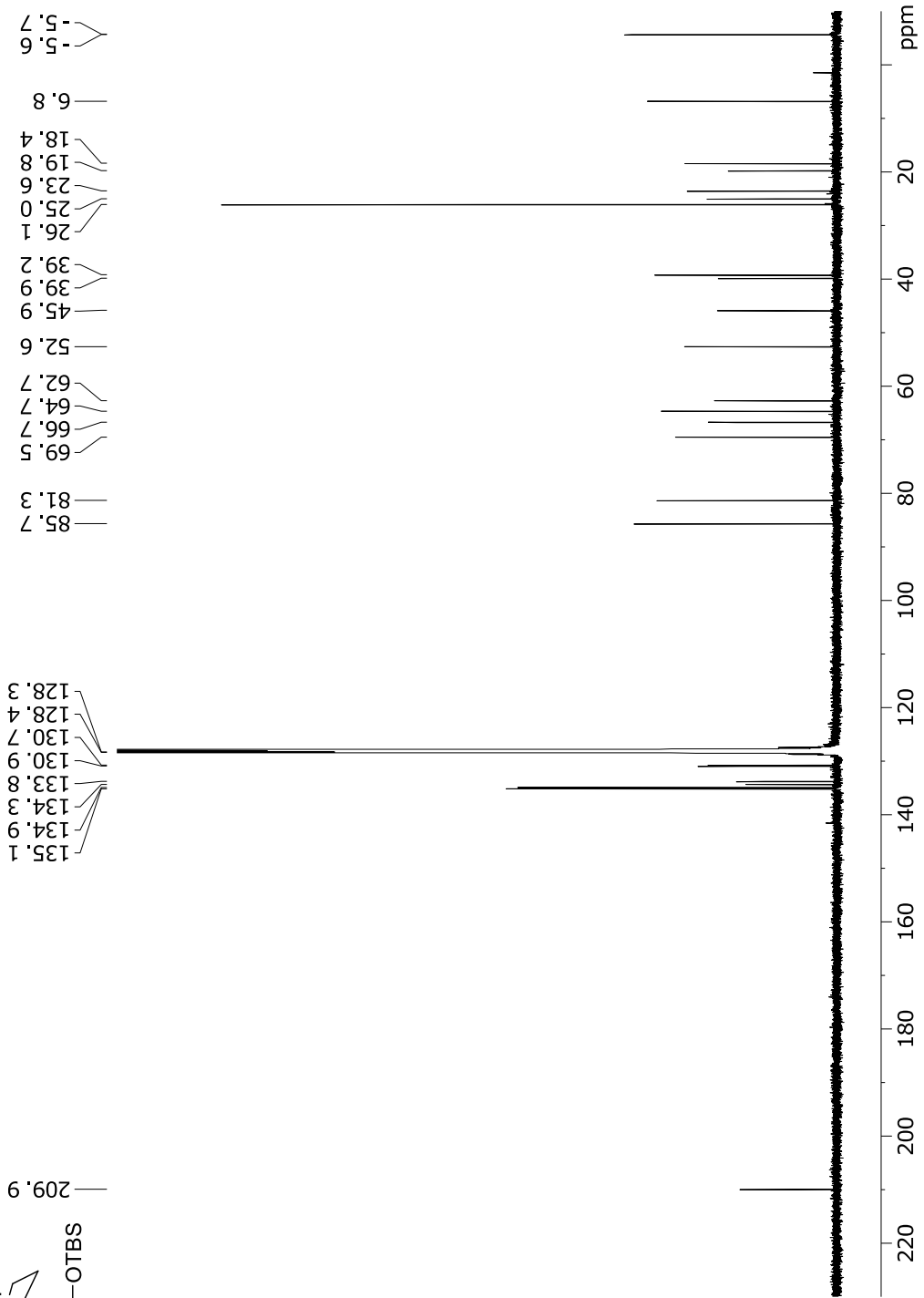
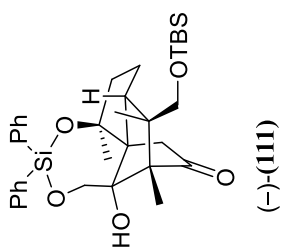


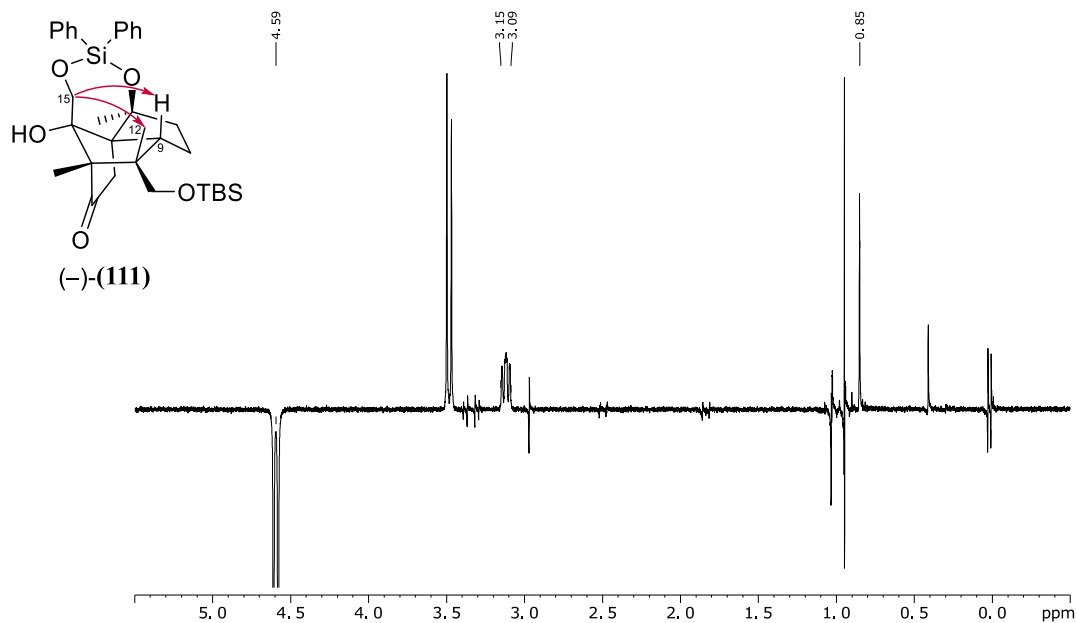




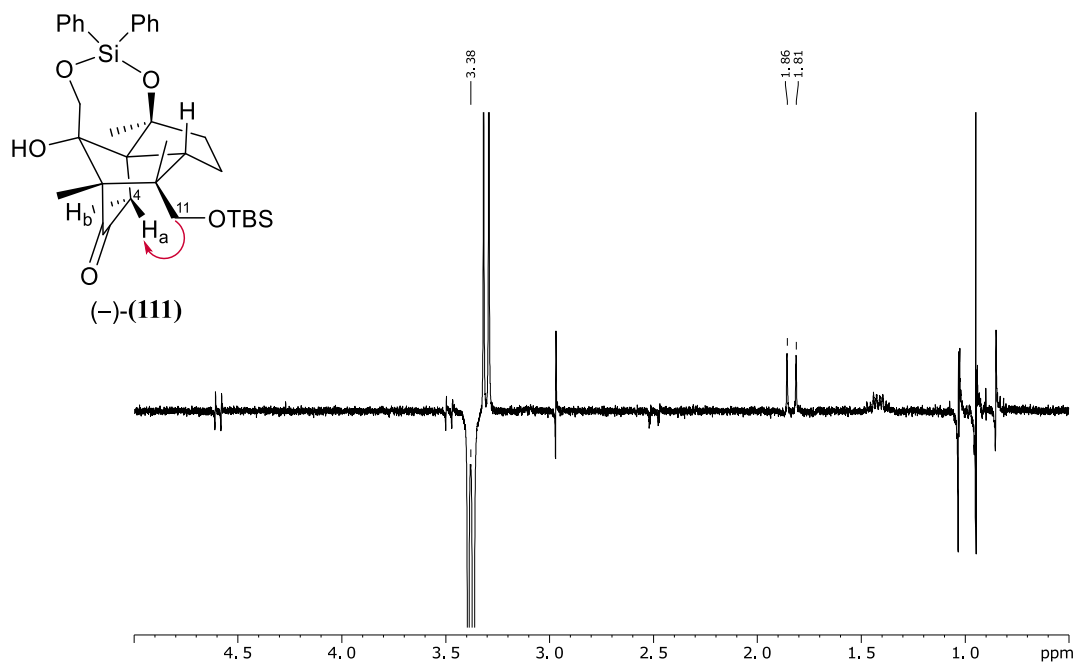




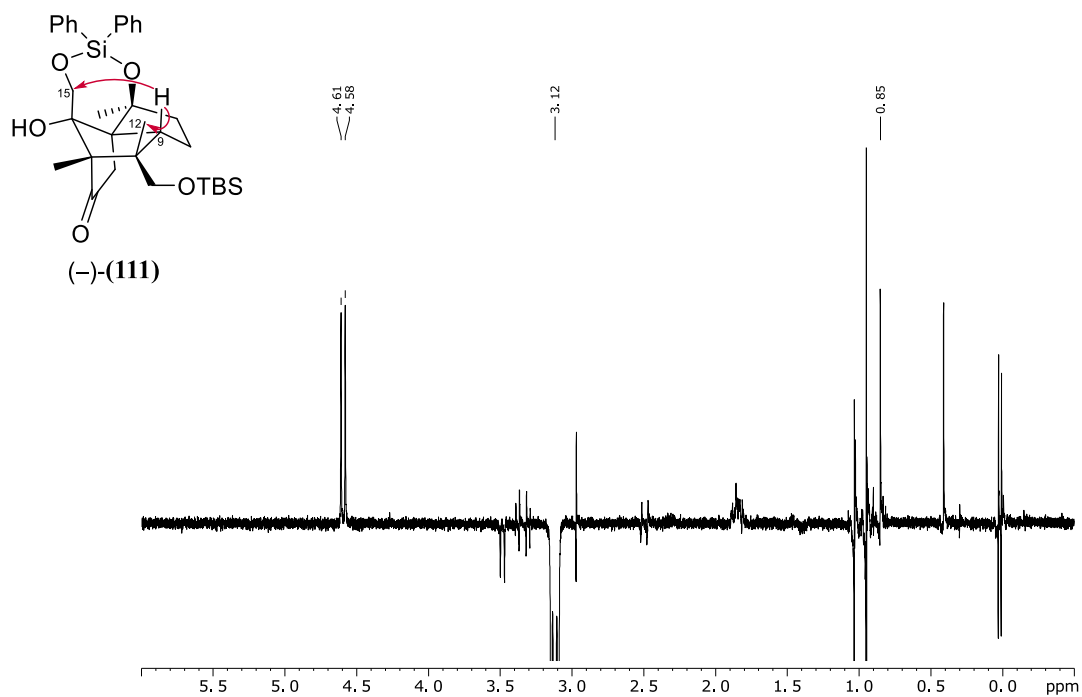




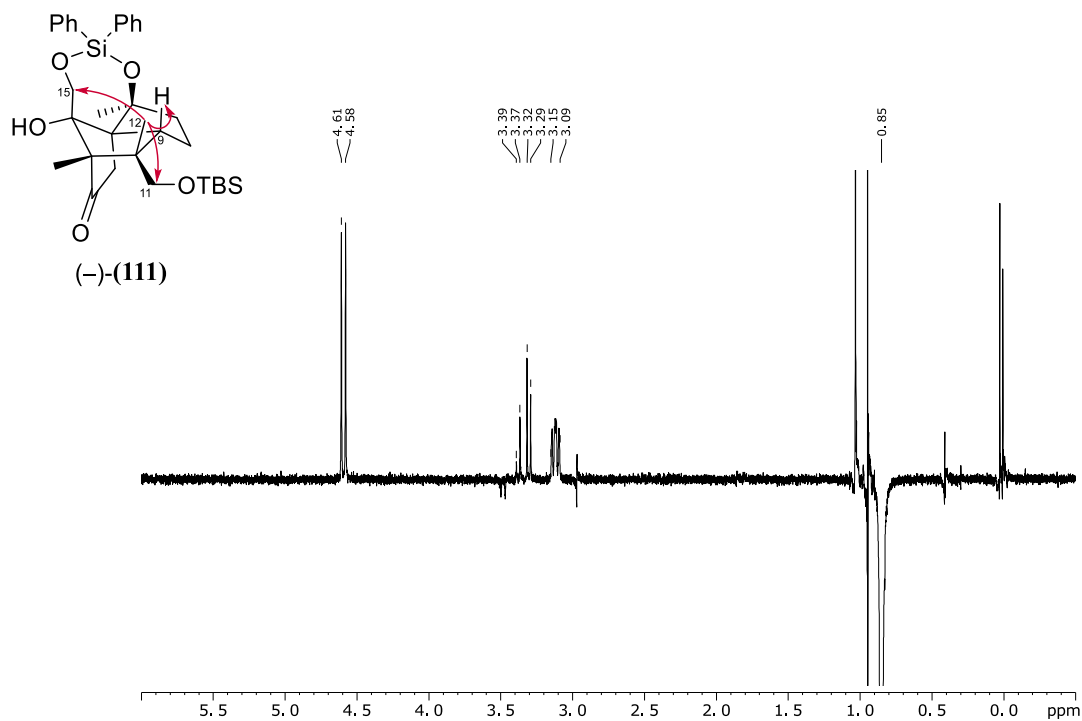
NOE response of semipinacol rearrangement product **(111)** after irradiation at 4.59 ppm (CH₂-15a), measured in C₆D₆ at 400 MHz.



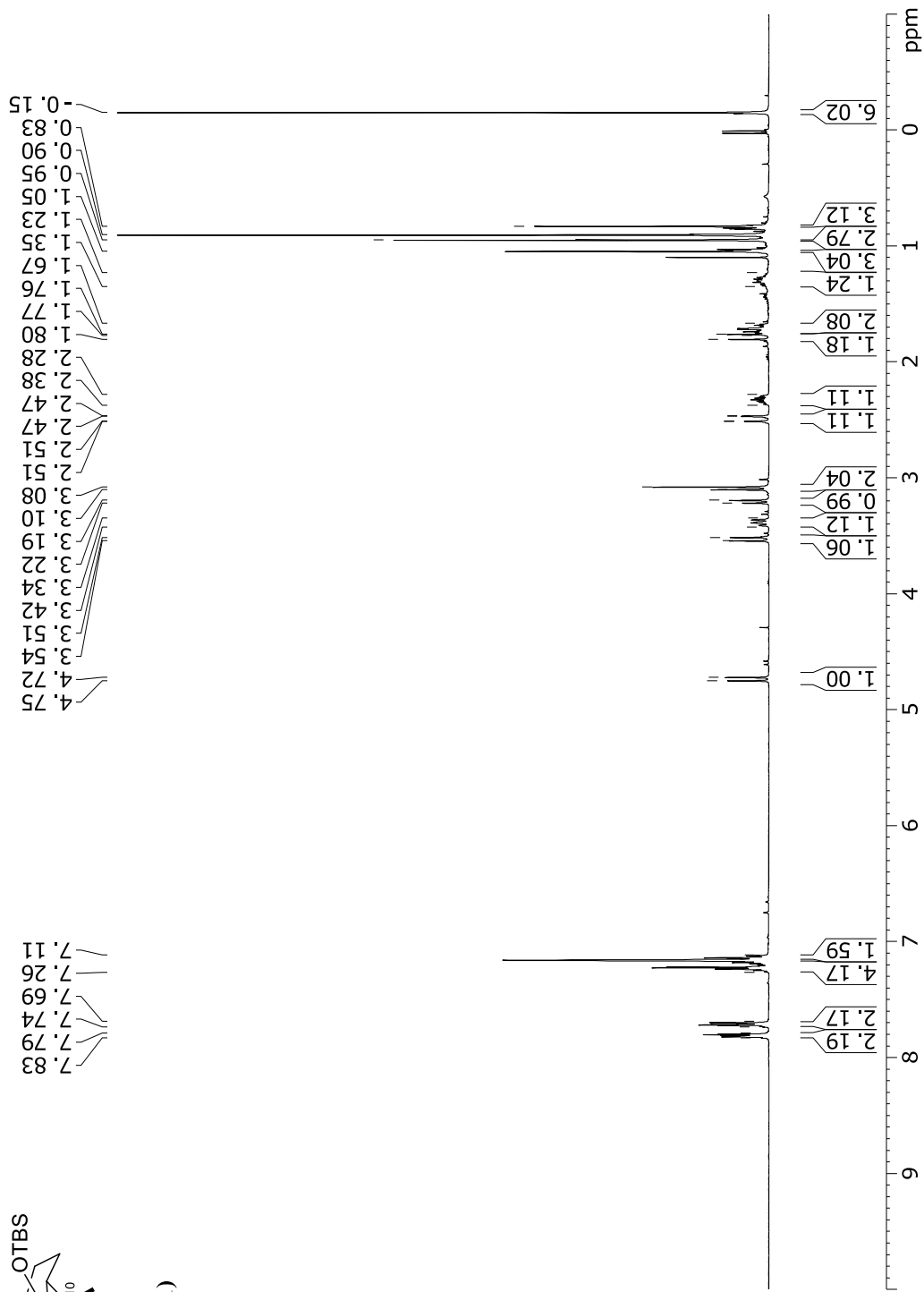
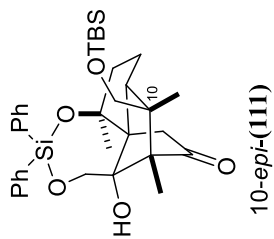
NOE response of semipinacol rearrangement product **(111)** after irradiation at 3.38 ppm (CH₂-11a), measured in C₆D₆ at 400 MHz.

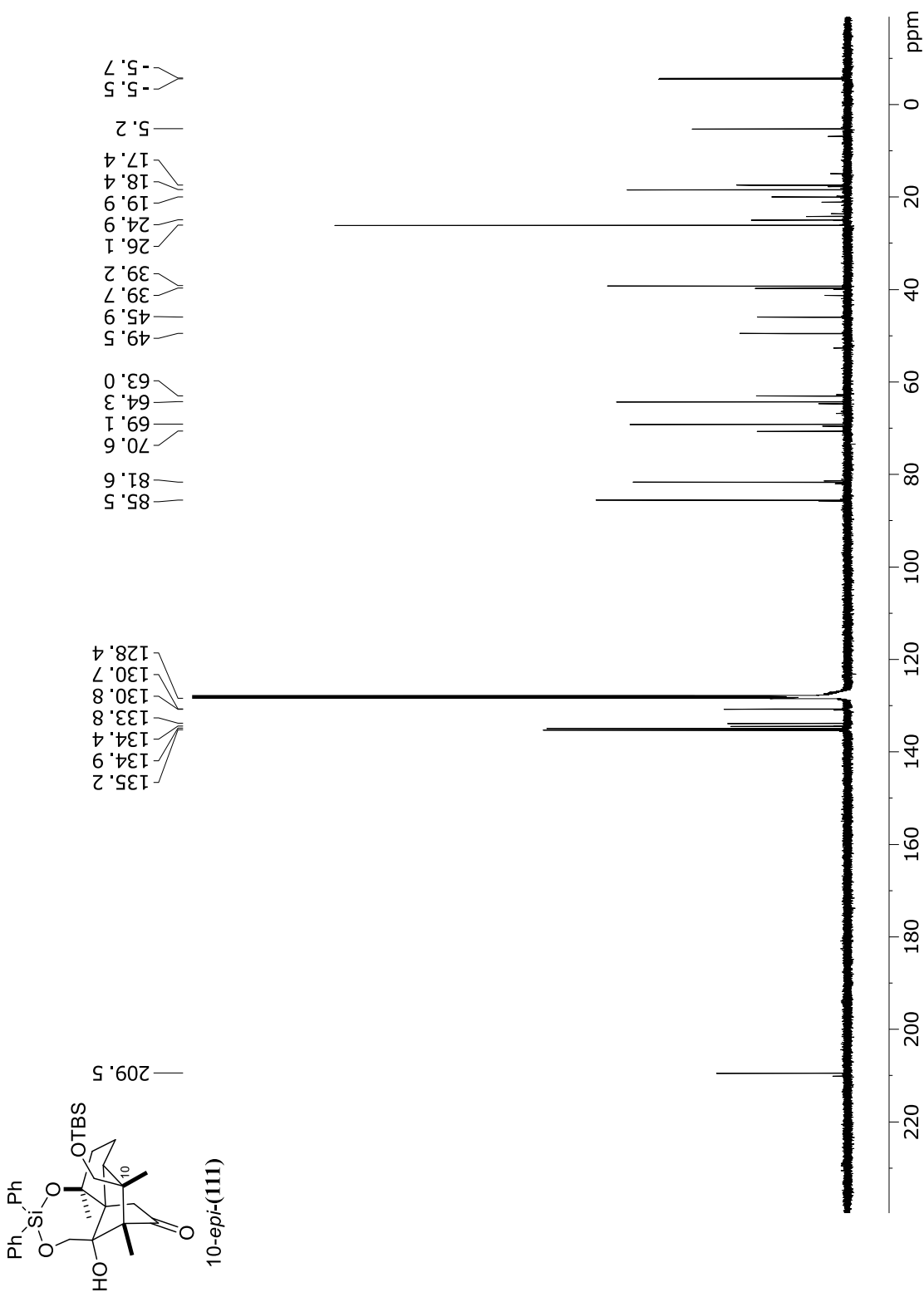


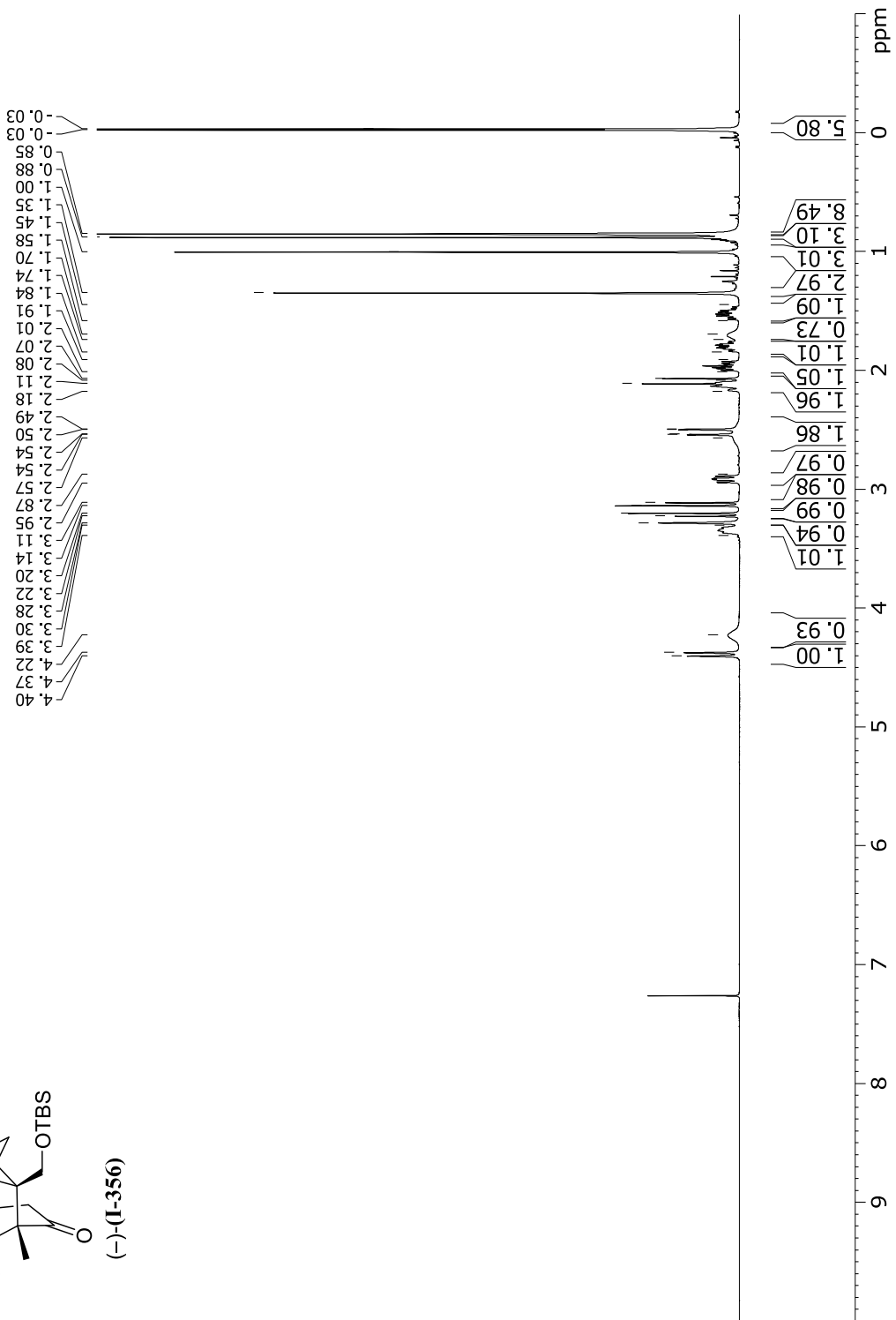
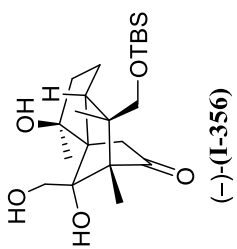
NOE response of semipinacol rearrangement product **(111)** after irradiation at 3.12 ppm (CH-9), measured in C₆D₆ at 400 MHz.

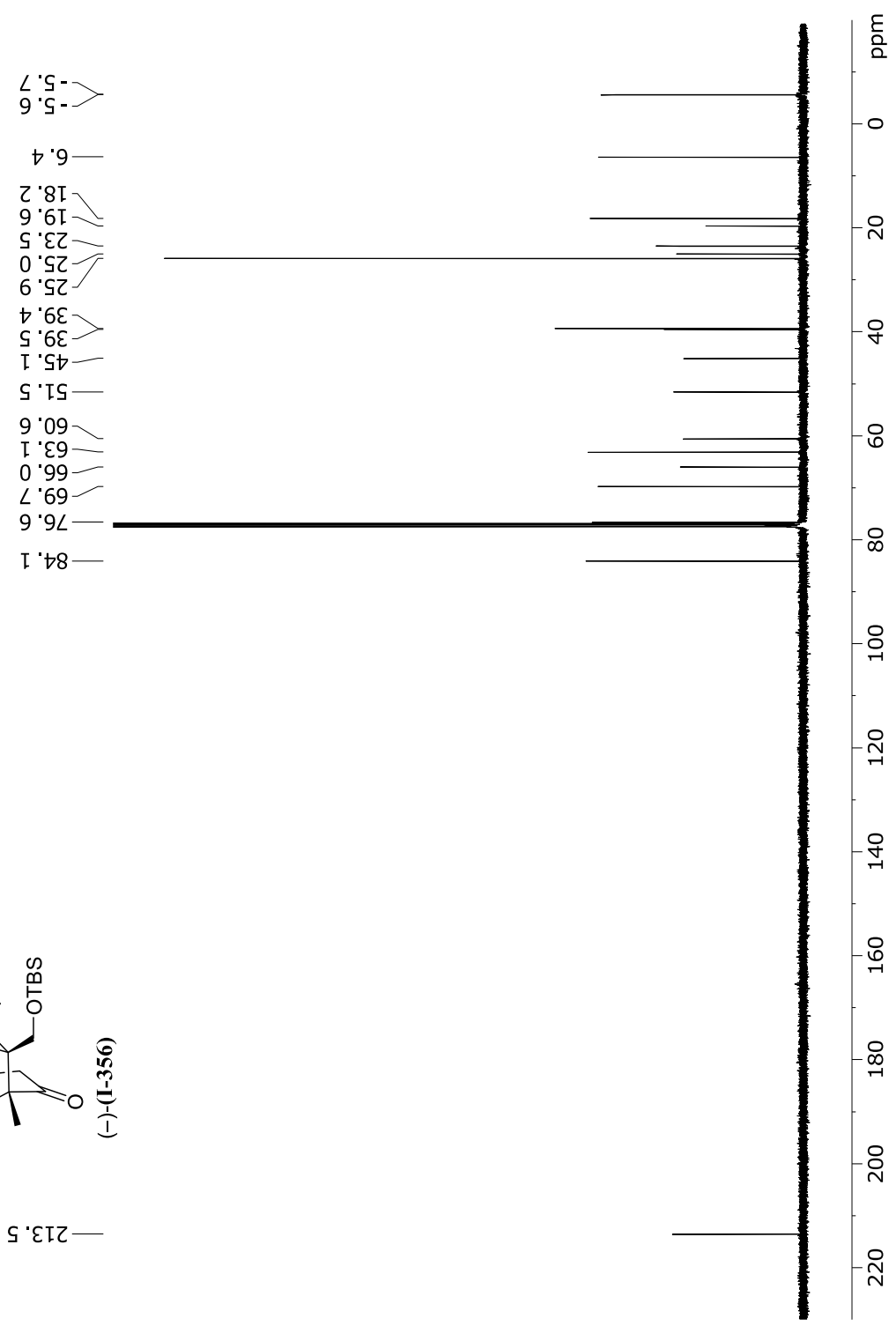
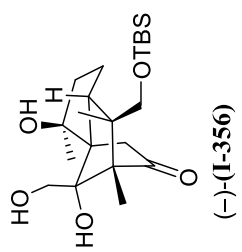


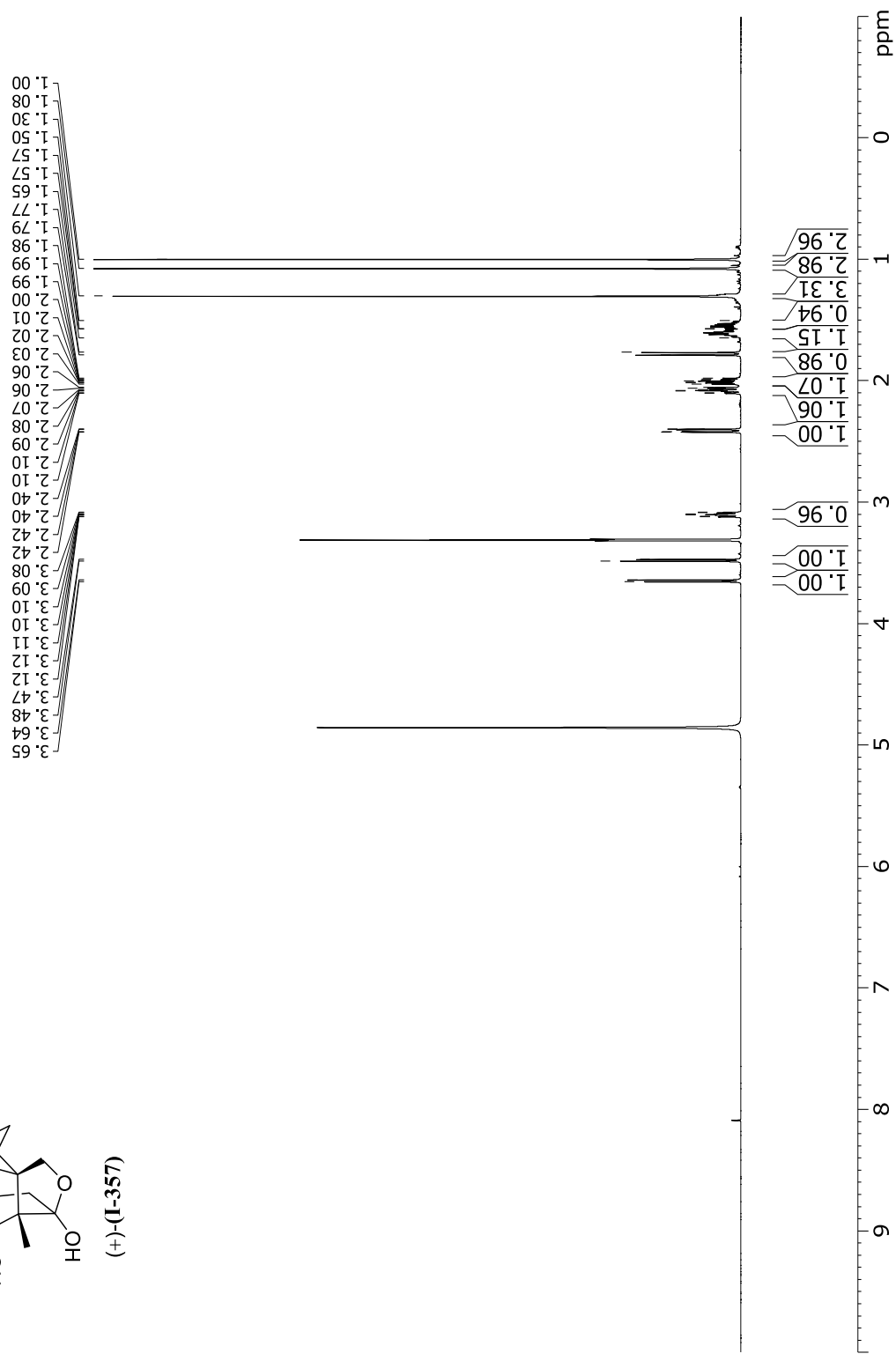
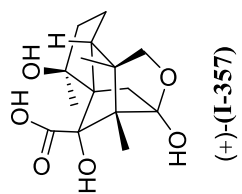
NOE response of semipinacol rearrangement product **(111)** after irradiation at 0.85 ppm (CH₃-12), measured in C₆D₆ at 400 MHz.

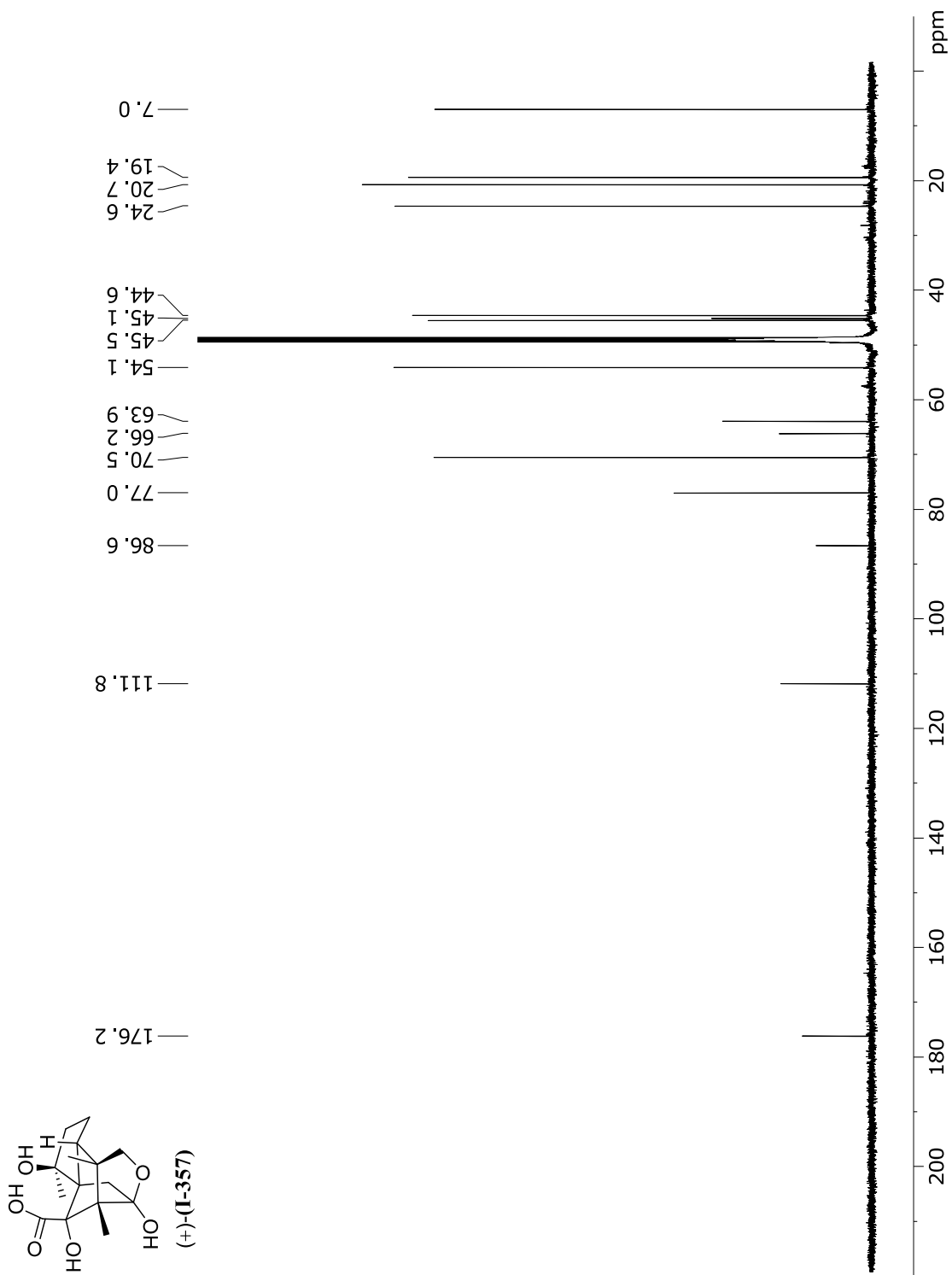


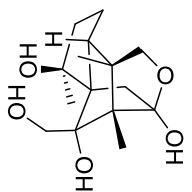




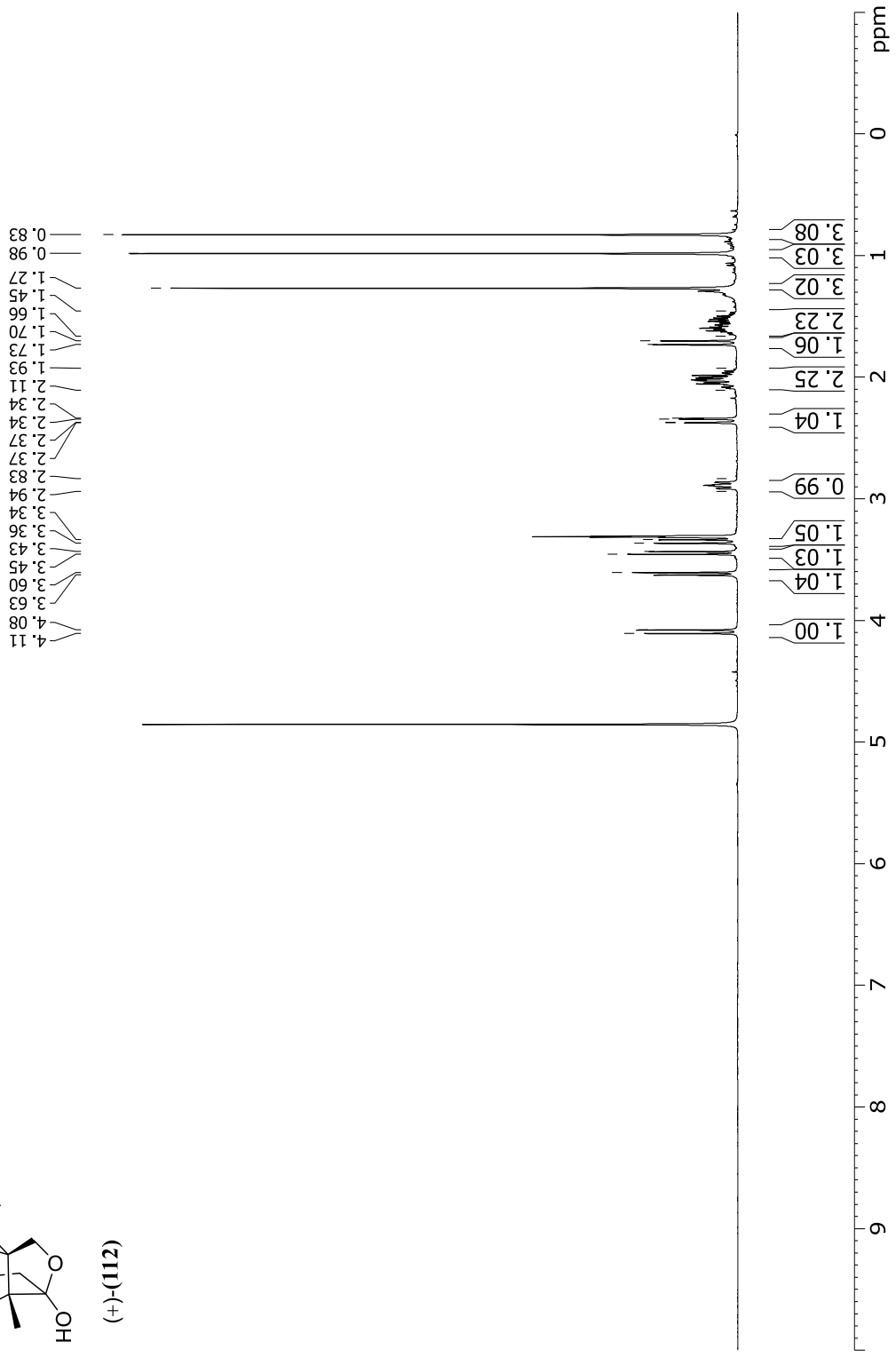


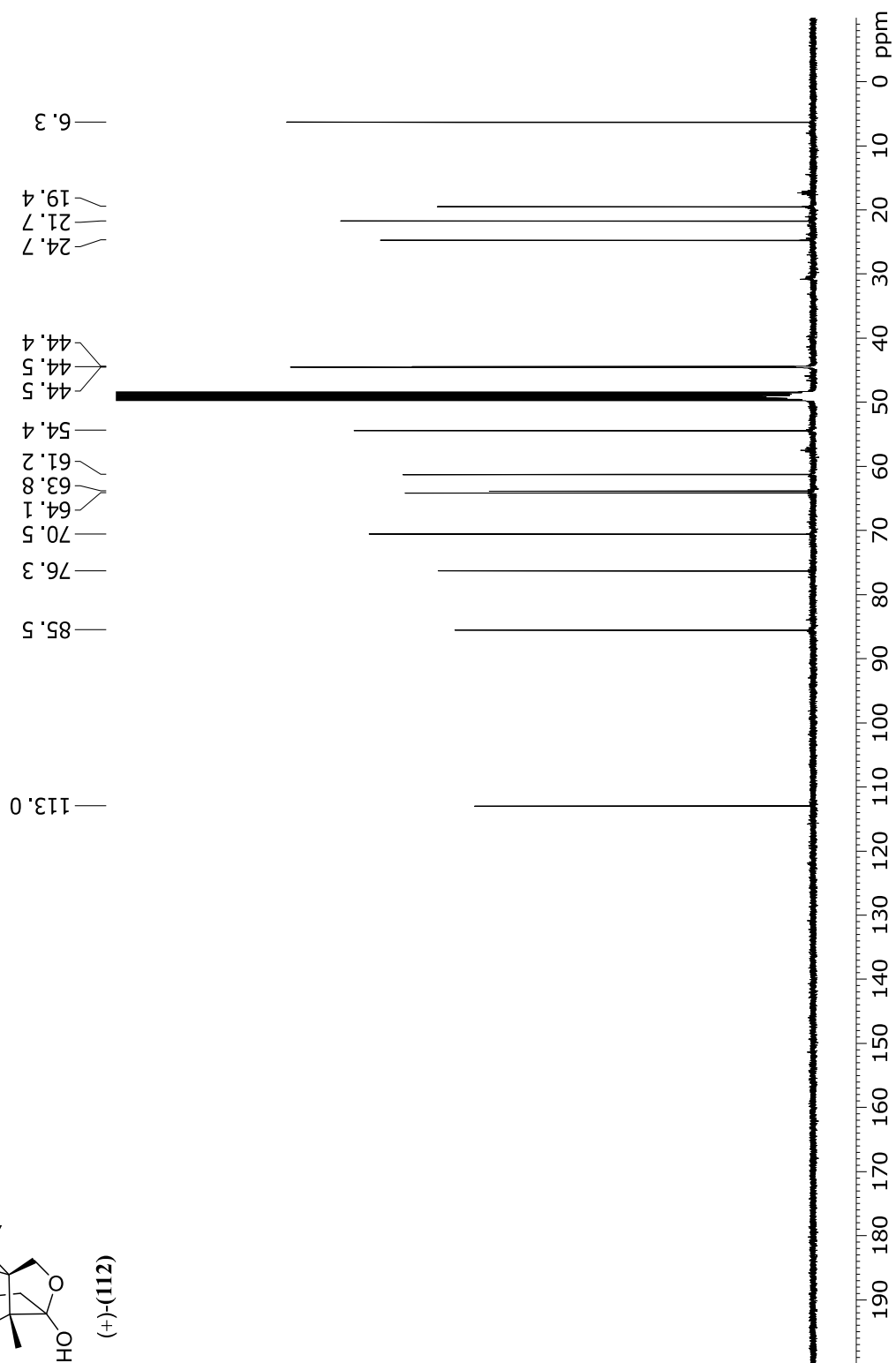
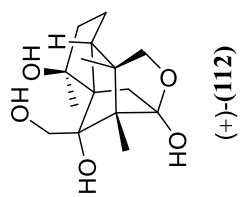


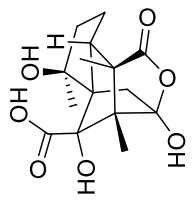




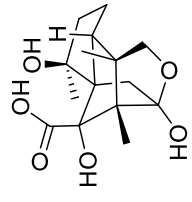
(+)-(112)



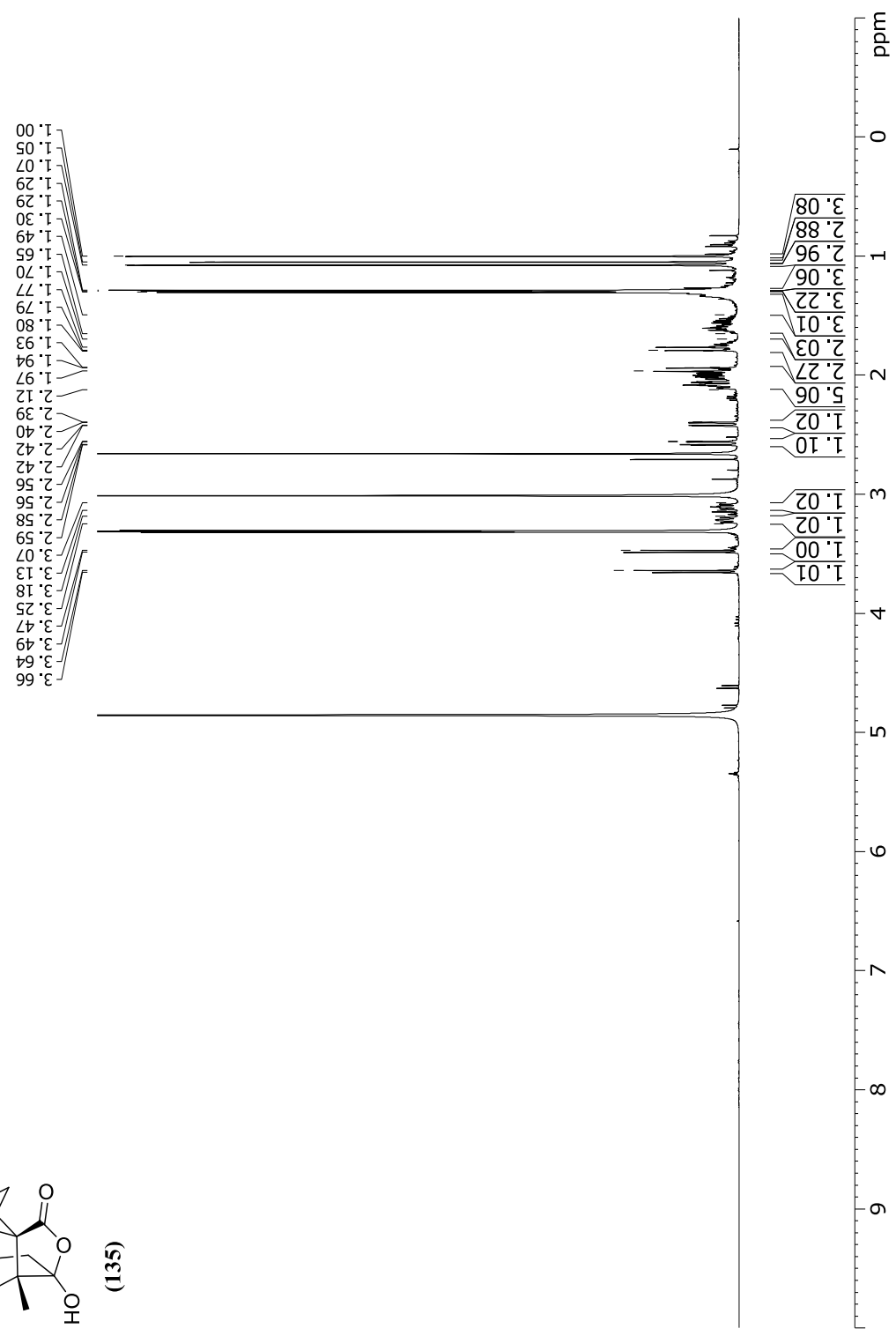


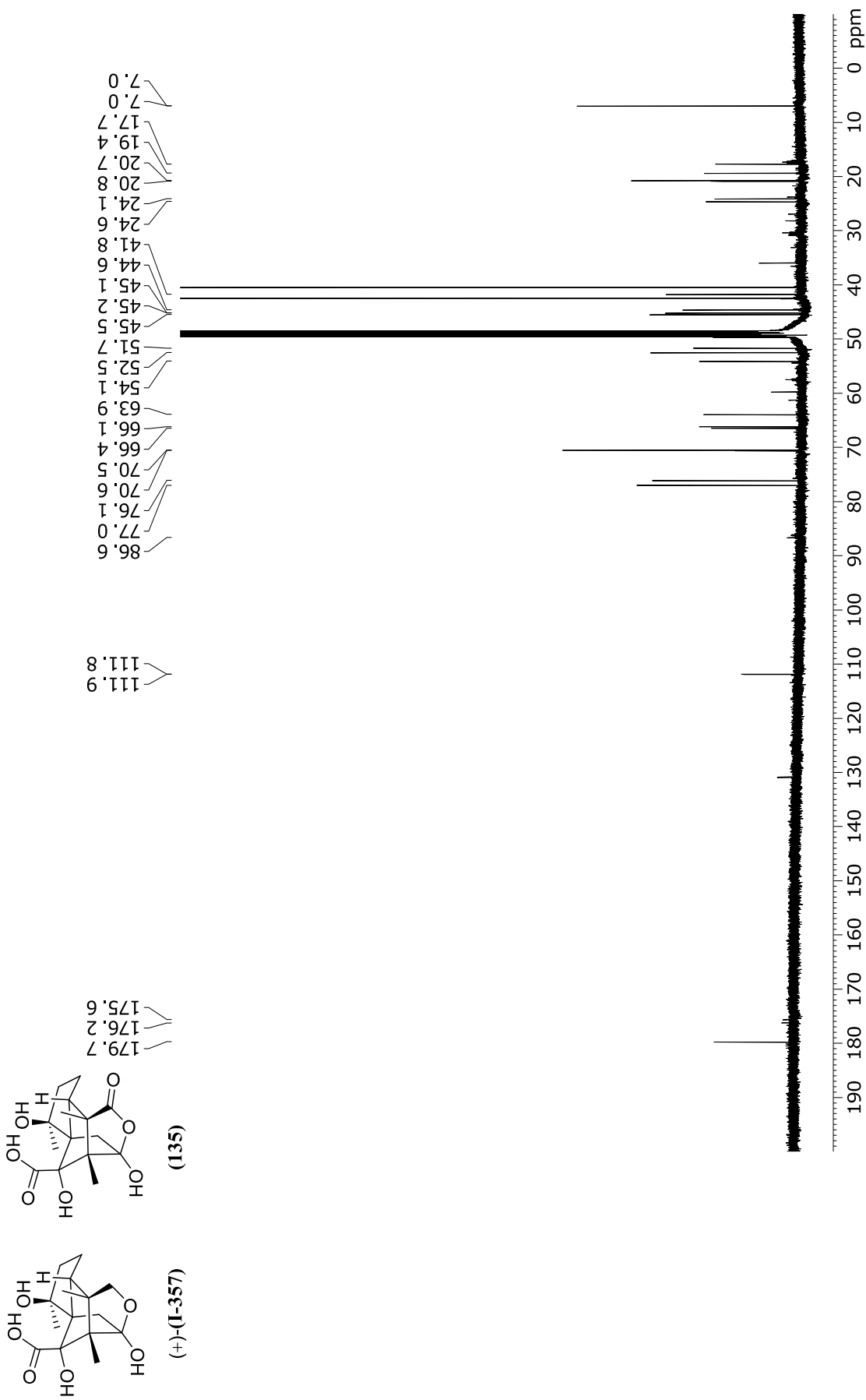


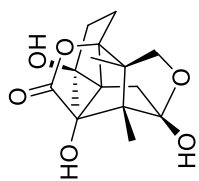
(135)



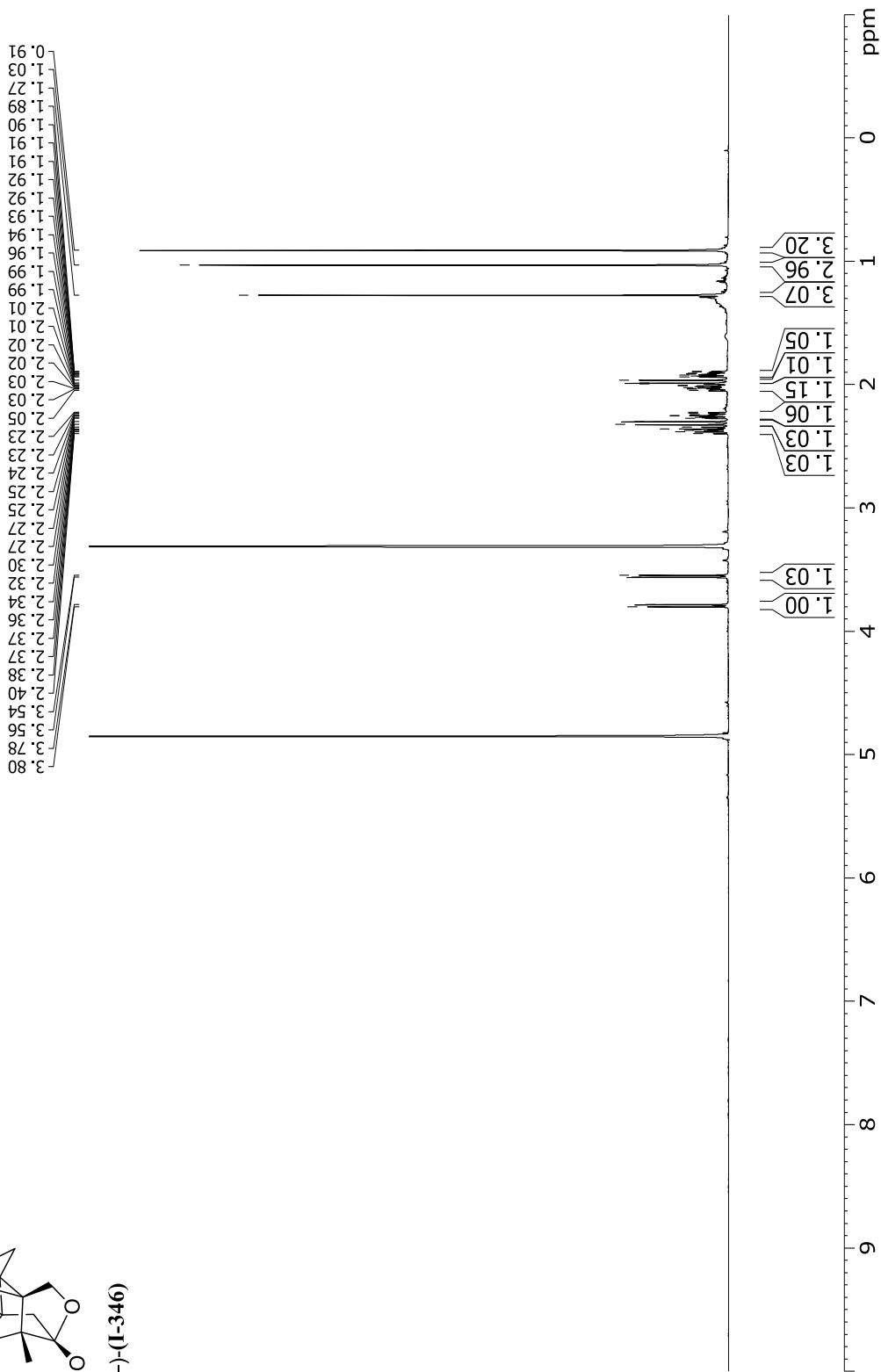
(+)-(1-357)

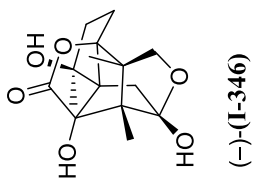






(-)-(1-346)





— 177.6

— 111.5

— 104.9

— 88.4

— 76.7

— 71.0

— 69.7

— 63.9

— 52.8

— 46.5

— 39.1

— 28.1

— 23.1

— 16.7

— 5.9



Curriculum Vitae

GIADA TEDESCO

Dott. ssa Mag. in Chimica
Università degli Studi dell'Insubria

2019 – 2023

Ph. D. student at Gottfried Wilhelm Leibniz University - Hannover

Supervisor: Prof. Dr. rer. nat. Markus Kalesse
Thesis topic: Studies on Nazarov/ene tandem cyclizations and their application in the total synthesis of (-)-illisimonin A

2017 – 2019

Master student (Stud. ssa Magistrale) at Università degli Studi dell'Insubria – Como

Grade: 110/110 *cum laude*
Thesis Supervisor: Prof. Dr. rer. nat. Gianluigi Brogginì
Thesis topic: Anaferine and Withaferin A as leads in total synthesis

2014 – 2017

Bachelor student (Stud. ssa Triennale) at Università degli Studi dell'Insubria – Como

Grade: 110/110 *cum laude*
Thesis Supervisor: Prof. Dr. rer. nat. Angelo Maspero
Thesis topic: Sintesi, caratterizzazione e reattività dei 5-pentafluorofeniltetrazolato complessi di Ag(I) e Zn(II)

2009– 2014

Student at Liceo Scientifico Paolo Giovio – Como

Grade: 100/100

Scientific Contributions

Presentations

- 2022 Poster presentation at ORCHEM 2022, Münster – Germany
“A New Tool for the Construction of Contiguous Stereocenters: the Nazarov/ene cyclization”
- 2022 Poster presentation at BOSS 2022, Namur – Belgium
“A New Tool for the Construction of Contiguous Stereocenters: the Nazarov/ene cyclization”
- 2022 OCI presentation at OCI Hannover – Germany
“Towards the Total Synthesis of Illisimonin A – a Nazarov approach”
- 2019 Poster presentation at ISSNP 2019 Napoli – Italy
“Total Synthesis of (-)-anaferine: a Piperidine Alkaloid from *Withania somnifera*”

Publications

- 2023 Asymmetric Total Synthesis of Illisimonin A.
Tedesco, G.*; Etling, C.*; Di Marco, A.; Kalesse, M. *J. Am. Chem. Soc.*, **2023**, *145*, 12.
* equal contribution
- 2021 A Nazarov-Ene Tandem Reaction for the Stereoselective Construction of Spiro Compounds.
Tedesco, G.*; Etling, C.*; Kalesse, M. *Chem. Eur. J.* **2021**, *27*, 9257.
* equal contribution
- 2020 Total Synthesis of (-)-Anaferine: A Further Ramification in a Diversity-Oriented Approach.
Bonandi, E; Tedesco, G.; Perdicchi, D.; Passarella, D. *Molecules* **2020**, *25*(5), 1057.